

SERI/PR-211-3483  
UC Category: 270  
DE89000898

SERI/PR--211-3483  
DE89 000898

## Annual Report

### Photovoltaic Program Branch

FY 1988

This report was prepared as an account of work sponsored by an agency of the United States Government. Neither the United States Government nor any agency thereof, nor any of their employees, makes any warranty, express or implied, or assumes any legal liability or responsibility for the accuracy, completeness, or usefulness of any information, apparatus, product, or process disclosed, or represents that its use would not infringe privately owned rights. Reference herein to any specific commercial product, process, or service by trade name, trademark, manufacturer, or otherwise does not necessarily constitute or imply its endorsement, recommendation, or favoring by the United States Government or any agency thereof. The views and opinions of authors expressed herein do not necessarily state or reflect those of the United States Government or any agency thereof.

### DISCLAIMER

March 1989

Prepared under Task No. PV840101

**Solar Energy Research Institute**  
A Division of Midwest Research Institute

1617 Cole Boulevard  
Golden, Colorado 80401-3393

Prepared for the  
**U.S. Department of Energy**  
Contract No. DE-AC02-83CH10093

DISTRIBUTION OF THIS DOCUMENT IS UNLIMITED

AP  
M

## **DISCLAIMER**

**This report was prepared as an account of work sponsored by an agency of the United States Government. Neither the United States Government nor any agency thereof, nor any of their employees, makes any warranty, express or implied, or assumes any legal liability or responsibility for the accuracy, completeness, or usefulness of any information, apparatus, product, or process disclosed, or represents that its use would not infringe privately owned rights. Reference herein to any specific commercial product, process, or service by trade name, trademark, manufacturer, or otherwise does not necessarily constitute or imply its endorsement, recommendation, or favoring by the United States Government or any agency thereof. The views and opinions of authors expressed herein do not necessarily state or reflect those of the United States Government or any agency thereof.**

---

## **DISCLAIMER**

**Portions of this document may be illegible in electronic image products. Images are produced from the best available original document.**

## NOTICE

This report was prepared as an account of work sponsored by an agency of the United States government. Neither the United States government nor any agency thereof, nor any of their employees, makes any warranty, express or implied, or assumes any legal liability or responsibility for the accuracy, completeness, or usefulness of any information, apparatus, product, or process disclosed, or represents that its use would not infringe privately owned rights. Reference herein to any specific commercial product, process, or service by trade name, trademark, manufacturer, or otherwise does not necessarily constitute or imply its endorsement, recommendation, or favoring by the United States government or any agency thereof. The views and opinions of authors expressed herein do not necessarily state or reflect those of the United States government or any agency thereof.

Printed in the United States of America  
Available from:  
National Technical Information Service  
U.S. Department of Commerce  
5285 Port Royal Road  
Springfield, VA 22161

Price: Microfiche A01  
Printed Copy A14

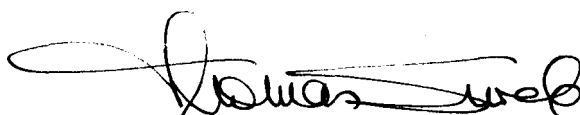
Codes are used for pricing all publications. The code is determined by the number of pages in the publication. Information pertaining to the pricing codes can be found in the current issue of the following publications which are generally available in most libraries: *Energy Research Abstracts (ERA)*; *Government Reports Announcements and Index (GRA and I)*; *Scientific and Technical Abstract Reports (STAR)*; and publication NTIS-PR-360 available from NTIS at the above address.

## PREFACE

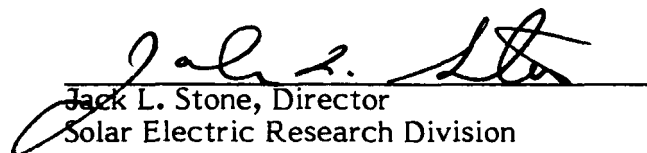
This report summarizes the progress of the Photovoltaic (PV) Program Branch of the Solar Energy Research Institute (SERI) from October 1, 1987, through September 30, 1988. The branch is responsible for the management of the subcontracted portion of SERI's PV Advanced Research and Development Project. In fiscal year (FY) 1988, this included more than 55 subcontracts with a total annualized funding of approximately \$13.5 million. Approximately two-thirds of the subcontracts were with universities, at a total funding of nearly \$4.7 million. The six technical sections of the report cover the main areas of the subcontracted program: the Amorphous Silicon Research Project, Polycrystalline Thin Films, Crystalline Silicon Materials Research, High-Efficiency Concepts, the New Ideas Program, and the University Participation Program. Technical summaries of each of the subcontracted programs provide a discussion of approaches, major accomplishments in FY 1988, and future research directions.

Approved for

SOLAR ENERGY RESEARCH INSTITUTE



\_\_\_\_\_  
Thomas Surek, Manager  
Photovoltaic Program Branch



\_\_\_\_\_  
Jack L. Stone, Director  
Solar Electric Research Division

## SUMMARY

The PV Program Branch of the Solar Energy Research Institute (SERI) is responsible for managing the subcontracted portion of SERI's Photovoltaic Advanced Research and Development (PV AR&D) Project. In fiscal year (FY) 1988, this included more than 55 subcontracts, with a total annualized funding of approximately \$13.5 million. Research was conducted in the following task areas: the Amorphous Silicon Research Project, Polycrystalline Thin Films, Crystalline Silicon Materials Research, High-Efficiency Concepts, the New Ideas Program, and the University Participation Program. The major portion of FY 1988's subcontracted research resulted from awards under six competitive solicitations initiated in FY 1986.

### Amorphous Silicon Research Project

The objectives of research in amorphous silicon are to improve and understand the opto-electronic properties of amorphous-silicon-based alloy materials and to improve the conversion efficiency and stability of single-junction and multijunction solar cells and submodules. The research is directed toward achieving FY 1990 goals, which are 10% efficiency for single-junction and 13% efficiency for multijunction submodules 900 cm<sup>2</sup> in area.

The technical plan of the Amorphous Silicon Research Project (ASRP) is divided into two principal activities: (1) multidisciplinary research activities and (2) fundamental research activities. Multidisciplinary activities involve government/industry cost-shared programs made up of broad-based research teams, located at individual companies' facilities, performing directed research that covers starting materials to demonstrations of proof-of-concept cells and submodules. Fundamental research activities involve basic, higher-risk, and supporting research at universities and research laboratories that aids industry in advancing the technology base. Cost-shared multidisciplinary programs address issues concerning single-junction and multijunction cells. Research is also performed to advance the conversion efficiency and the stability of small-area cells and of larger submodules, with areas of at least 900 cm<sup>2</sup>, fabricated by plasma-enhanced chemical vapor deposition. Stability issues encompass both intrinsic aspects, such as light-induced effects, and extrinsic aspects, such as diffusion or corrosion as a result of the environment. Efficiency improvement involves work on better light trapping, higher conductivity of interconnectors, and minimizing area losses due to interconnections.

### Polycrystalline Thin Films

The objective of the Polycrystalline Thin Film Program is to develop thin-film cells, flat-plate modules that meet DOE's long-term goals of reasonable efficiencies (15%-20%), very low cost (near \$50/m<sup>2</sup>), and long-term reliability (30 years). The approach relies on developing solar cells based on highly light-absorbing compound semiconductors such as CuInSe<sub>2</sub> and CdTe and their alloys. These semiconductors are fabricated as thin-film cells (1-3  $\mu$ m thick) with minimal material and processing costs.

Polycrystalline cells require continued development to achieve 15%-20% conversion efficiencies. Two strategies are being used: development of single-junction cells and innovative work on two-junction cascade cells. Improvement of the single-junction technologies has been steady and reliable. This strategy remains the major focus of the task. Potentially achievable efficiencies approach 20%, and projections indicate the likelihood of fabricating modules of more than 15% efficiency. Developing two-junction, CuInSe<sub>2</sub>-based cascade cells permits even more ambitious long-term efficiency goals. Combining two well-matched single-junction modules into a cascade design could lead to

module efficiencies of better than 20% at costs under \$60/m<sup>2</sup>. The materials being investigated for the top cells include CdTe and ZnTe alloyed with Mn, Mg, Zn, and Hg.

Developing scalable, low-cost fabrication methods is important in providing industry with a foundation for future large-area, high-throughput commercial processes. Research methods for fabricating polycrystalline cells include, for CuInSe<sub>2</sub>, an electrochemical/selenization method, a reactive-sputtering and hybrid sputtering/evaporation method, and evaporation; for CdTe, close-spaced sublimation, evaporation, electrodeposition, metal-organic chemical vapor deposition, and proprietary methods.

### Crystalline Silicon Materials Research

At present, crystalline silicon photovoltaic technology has not been surpassed by the newer thin-film approaches in module efficiency, long-term stability, or produced energy cost. Yet, in spite of the technology's relative maturity, continued research is expected to yield improvements in performance and production cost. This program supports research in universities and coordinates the transfer of sample materials and information among universities, industry research groups, and SERI. The objective of this project is to improve our fundamental understanding of electrically active defects in various forms of crystalline and polycrystalline silicon.

During FY 1988, three university teams were selected from a public competition to perform three-year research efforts investigating structural and chemical defects in silicon. In particular, they will investigate the interactions of carbon and oxygen at local defects and along dislocations. The mechanisms under which atomic hydrogen treatments passivate certain defects will also be identified. The investigations will utilize samples provided by the photovoltaic industry as well as materials with specific carbon or oxygen concentrations, or both, provided by SERI. In the coming year, these efforts will be complemented by additional, unique characterization capabilities provided through two smaller subcontracts with the Georgia Institute of Technology (impurity and structural characterization) and the University of Southern California (electrical characterization).

### High-Efficiency Concepts

The objective of the High-Efficiency Concepts Task is to evaluate and develop advanced photovoltaic technologies capable of energy conversion efficiencies in excess of 20% for flat-plate configurations and 30% for concentrator systems. Because of the demonstrated performance of crystalline III-V semiconductors, the task has become synonymous with III-V compound semiconductor research.

Research in gallium arsenide (GaAs) and related compounds emphasizes the control of heteroepitaxial growth. This work supports the eventual development of two photovoltaic technologies. First, heteroepitaxy will be essential in any low-cost, single-crystal, thin-film photovoltaic technology. This area emphasizes research in the growth of the binary compound GaAs in the novel regimes required to meet flat-plate module cost goals. Specifically, this requires heteroepitaxial growth on significantly dissimilar substrates, such as silicon or various crystalline interfacial layers, or lateral epitaxial growth over amorphous or polycrystalline substrates. Second, multijunction cells by their very design will require heteroepitaxy. The key topic in this area is the heteroepitaxial growth of ternary and quaternary alloys of III-V compounds. The alloys of study include AlGaAs, GaInAs, AlGaInAs, GaAsP, GaAsSb, and AlGaAsSb. Each of these alloys is quite different from GaAs in that the properties of a given alloy change significantly even with relatively small changes in the composition of that alloy. The emphasis of the research is to identify and control the key mechanisms affecting film quality.

### New Ideas Program

The objective of the New Ideas Task is to identify new photovoltaic materials, device configurations, and concepts and to conduct preliminary research and development in the areas that show the most promise. Subcontracted research in this task that shows significant potential is transferred into the appropriate major task area within the DOE Photovoltaic Program for continued support.

The New Ideas Task provides public solicitations for new and innovative research ideas that are relevant under the Photovoltaic Advanced Research and Development Project's guidelines to perform high-risk, long-term, and potentially high-payoff research and development. These solicitations for new and innovative research ideas are submitted by universities, business, and nonprofit organizations. Subcontracts are awarded to study the most promising concepts associated with these solicitations. These subcontracts are reviewed, and successful concepts are selected for renewal with a second year of funding.

### University Participation Program

The objective of this program is to maximize the contribution of universities to the future of photovoltaic technology by focusing on the traditional needs and strengths of that community. Thus, it provides a forum in which the university researchers identify research topics critical to the advancement of photovoltaic technology with minimal influence from the current programmatic interests. The selected participants are then permitted to pursue the proposed basic and applied research ideas in an environment designed to foster creativity by limiting requirements for delivery of reports and samples and achievement of specific goals. Reporting is limited to annual reports and journal publications. Research symposia organized by the participant are held periodically and are open to all students, program participants, and outside researchers. The intent of the initiative is to provide continuity of funding over a minimum three-year period, which will allow universities to build and support interdisciplinary teams with specialized expertise that can be applied to furthering the technology base of photovoltaics. Such a program is expected to attract the most highly qualified university research teams to the DOE National Photovoltaics Program. The University Participation Program also supports the photovoltaic industry through the technology transfer that occurs not only by publishing research results in the technical literature, but also by enhancing students' awareness of photovoltaic technology and educating future professionals.

### Technology Transfer

The prompt, effective transfer of research results is a key element in the PV Program Branch's strategy. In addition to close working relationships with industrial and academic communities through subcontracts, such as the unique government/industry partnerships in amorphous silicon, the primary means of information transfer are through subcontractor reports and review meetings. These reports are made available to the entire PV community, and the review meetings are open to all relevant outside interests as well as to subcontractors.

During FY 1988, branch personnel and subcontractors contributed to two major photovoltaic conferences: the 8th Photovoltaic Advanced Research and Development Conference (November 1987), sponsored by SERI, and the 20th IEEE PV Specialists Conference (September 1988). In addition, the program sponsored seven workshops and university photovoltaic symposia, focusing on topics such as safety, chemical vapor deposition of

amorphous silicon, and ion/photon-assisted deposition and doping. Collectively, these were attended by more than 300 students and professionals. Subcontractors' research results were widely disseminated to the PV community in more than 25 technical subcontractor reports and in numerous journal and conference papers.

## TABLE OF CONTENTS

	<u>Page</u>
1.0 Introduction .....	1
Background .....	1
Key Accomplishments .....	3
Technology Transfer .....	7
Conclusions .....	7
2.0 Amorphous Silicon Research Project .....	9
Research on High-Efficiency, Multiple-Gap, Multi-Junction Amorphous Silicon-Based Alloy Thin Film Solar Cells; <i>Energy Conversion Devices, Inc.</i> .....	11
Research on Stable, High Efficiency, Large Area, Amorphous Silicon Based Submodules; <i>Solarex Thin Film Division</i> .....	13
Research on Stable, High-Efficiency, Large Area, Amorphous Silicon Based Submodules; <i>Chronar Corporation</i> .....	15
Research on Amorphous Silicon-Based Thin Film Photovoltaic Devices; <i>ARCO Solar, Inc.</i> .....	21
Structural and Electronic Properties of Defects in Amorphous Silicon; <i>Xerox PARC</i> .....	26
Investigations of the Origins of Light-Induced Changes in Hydrogenated Amorphous Silicon; <i>University of Oregon</i> .....	32
Effect of Charge Defects on Photovoltaic Properties of Hydrogenated Amorphous Silicon; <i>University of North Carolina</i> .....	36
Photo-CVD of Amorphous Silicon Alloy Materials and Devices; <i>Institute of Energy Conversion</i> .....	39
Research on Amorphous Silicon-Germanium Alloys for Tandem Solar Cells; <i>Harvard University</i> .....	45
Structure of Amorphous Silicon Alloy Films; <i>Washington University</i> .....	47
Deposition, Characterization and Optimization of Optically Transparent Films; <i>Harvard University</i> .....	53
Research on Material Properties of Device Quality Amorphous Silicon Deposited at High Deposition Rates Using Higher Order Silanes; <i>Glasstech Solar, Inc.</i> .....	56
Amorphous Silicon Photovoltaic Devices Prepared by Chemical and Photo-Chemical Vapor Deposition of Higher Order Silanes; <i>Chronar Corporation</i> .....	60

## TABLE OF CONTENTS (Continued)

	<u>Page</u>
Diagnostics of Glow Discharges Used to Produce Hydrogenated Amorphous Silicon Films; <i>National Institute of Standards and Technology</i> .....	66
Study of Thermal and Light Induced Changes in Amorphous Silicon Alloy Materials; <i>North Carolina A&amp;T State University</i> .....	70
Study of Large Area Amorphous Silicon Films by Photo-CVD; <i>Hughes Aircraft Company</i> .....	72
Improvement of Small Area Amorphous Silicon Thin Film Photovoltaics on Polymer Substrate; <i>3M Company</i> .....	73
Hydrogenated Amorphous Silicon Device Modeling; <i>University of Florida</i> .....	75
Investigations of Stable Contact to Amorphous Silicon Thin Films; <i>California Institute of Technology</i> .....	84
Hydrogenated Amorphous Silicon Films Prepared by Glow Discharge of Disilane; <i>UHT Corporation</i> .....	86
Amorphous Silicon Deposition Research with In Situ Diagnostics; <i>Jet Propulsion Laboratory</i> .....	94
<b>3.0 Polycrystalline Thin Films .....</b>	<b>100</b>
High-Efficiency Copper Ternary Thin-Film Solar Cells; <i>International Solar Electric Technology</i> .....	102
High Efficiency CuInSe <sub>2</sub> and CuInGaSe <sub>2</sub> Based Cells and Materials Research; <i>Boeing Electronics</i> .....	105
Material Analysis and Device Optimization of CuInSe <sub>2</sub> Solar Cells; <i>Institute of Energy Conversion</i> .....	109
Analysis of Loss Mechanisms in Polycrystalline Thin Film Solar Cells; <i>Colorado State University</i> .....	115
Alternative Fabrication Techniques for High-Efficiency CuInSe <sub>2</sub> and CuInSe <sub>2</sub> -Alloy Films and Cells; <i>University of Illinois</i> .....	119
Novel Thin-Film CuInSe <sub>2</sub> Fabrication; <i>University of Arkansas</i> .....	122
Polycrystalline Thin-Film Cadmium Telluride Solar Cells; <i>Ametek Applied Materials Laboratory</i> .....	126
High-Efficiency Large-Area CdTe Panels; <i>Photon Energy, Inc.</i> .....	129

## TABLE OF CONTENTS (Continued)

	<u>Page</u>
Thin Film Cadmium Telluride Solar Cells; <i>Southern Methodist University</i> .....	134
High Efficiency Cadmium and Zinc Telluride Based Thin Film Solar Cells; <i>Georgia Institute of Technology</i> .....	136
Wide Bandgap II-VI Window and Photon Absorber Materials for Cascaded Cells; <i>Jet Propulsion Laboratory</i> .....	141
CuInSe <sub>2</sub> Based Cascade Solar Cells; <i>Institute of Energy Conversion</i> .....	147
<b>4.0 Crystalline Silicon Materials Research</b> .....	<b>153</b>
The Effectiveness and Stability of Impurity/Defect Interactions and their Impact on Minority Carrier Lifetime; <i>North Carolina State University</i> .....	154
Basic Studies of Point Defects and their Influence on Solar Cell Related Electronic Properties of Crystalline Silicon; <i>Duke University</i> .....	160
Passivation and Gettering Studies in Solar Cell Silicon; <i>The University at Albany, Albany, New York</i> .....	163
<b>5.0 High-Efficiency Concepts</b> .....	<b>170</b>
Basic Studies of III-V High-Efficiency Cell Components; <i>Purdue University</i> .....	171
Research on Semiconductors for High-Efficiency Solar Cells; <i>Rensselaer Polytechnic Institute</i> .....	175
High Efficiency Thin Film GaAs and Ternary III-V Solar Cells; <i>Kopin Corporation</i> .....	178
Gallium Arsenide Based Ternary Compounds and Multibandgap Solar Cell Research; <i>Spire Corporation</i> .....	184
Advanced High-Efficiency Concentrator Cells; <i>Varian Research Center</i> .....	188
Research on Large Scale MOCVD Deposition; <i>Spire Corporation</i> .....	192
<b>6.0 New Ideas Program</b> .....	<b>196</b>
New Concepts for High Efficiency Energy Conversion: The Avalanche Heterostructure and Superlattice Solar Cells; <i>Georgia Tech Research Institute</i> .....	197

## TABLE OF CONTENTS (Concluded)

	<u>Page</u>
Low Cost Technique for Producing CdZnTe Devices for Cascade Cell Application; <i>International Solar Electric Technology</i> .....	200
Hydrogen Radical Enhanced Growth of Solar Cells; <i>Rensselaer Polytechnic Institute</i> .....	206
High Efficiency Flat-Plate Silicon Solar Cells; <i>Stanford Electronics Laboratories</i> .....	210
Performance of MBE Solar Cells; <i>Howard University</i> .....	215
7.0 University Participation Program .....	217
Low Temperature MOCVD Processes for High Efficiency Solar Cells; <i>University of Southern California</i> .....	218
Improvement of Bulk and Epitaxial III-V Semiconductors for Solar Cells by Creation of Denuded Recombination Zones; <i>Carnegie Mellon University</i> .....	221
Electronic Processes in Thin Film PV Materials; <i>University of Utah</i> .....	226
Defects and Photocarrier Processes in Hydrogenated Amorphous Silicon Germanium Alloys; <i>Syracuse University</i> .....	232
Ion-Assisted Deposition Doping of p-CdTe; <i>Stanford University</i> .....	238
Rapid Liquid Phase Epitaxy of Gallium Arsenide Photovoltaic Devices; <i>Brown University</i> .....	241
New Approaches for High Efficiency Solar Cell: Role of Strained Layer Superlattices; <i>North Carolina State University</i> .....	245
8.0 List of Active Subcontracts .....	251
9.0 Bibliography .....	259
Subcontractor Reports and Publications .....	259
Branch Publications .....	288

## 1.0 INTRODUCTION

This report reviews subcontracted research and development activities under SERI's Photovoltaic Advanced Research and Development (PV AR&D) Project from October 1, 1987, to September 30, 1988.

### Background

The PV AR&D Project, under the U.S. Department of Energy's (DOE's) National Photovoltaics Program, sponsors high-risk, potentially high-payoff research and development in photovoltaic energy technology. The aim is to provide a technology base from which the private sector can choose options for further development and competitive application in U.S. electrical markets. The SERI project is responsible for most of the materials research and some of the module research performed under the National PV Program. Implementation of this program is based on cooperative research partnerships among the federal government, private industries, universities, and electric utilities, as outlined in the program's Five-Year Research Plan.\*

SERI's specific PV activities include the management of subcontracted R&D projects as well as internal research. The primary research activities are conducted in advanced photovoltaic material technologies, including amorphous silicon thin-film materials; polycrystalline thin films, such as copper indium diselenide, cadmium telluride, and their alloys; and high-efficiency crystalline cells, including silicon and gallium arsenide and their alloys. Transferring the R&D results to private industry in a timely and effective manner is a major objective of SERI's PV AR&D Project.

Subcontracted R&D is a significant part of the PV AR&D Project; more than 50% of the project's budget is allocated yearly to subcontracts. In FY 1988, this included more than 55 subcontracts with a total annualized funding of approximately \$13.5 million. Approximately two-thirds of the subcontracts were with universities, with a total funding of nearly \$4.7 million. In addition to the materials research activities listed above, subcontracted research is conducted under both the New Ideas and the University Participation Programs. Table 1-1 shows how the subcontract budget is distributed among the various task areas for FY 1988 and prior years. Figure 1-1 shows the distribution of subcontract funds by business category. Management of the subcontracted PV program is the responsibility of the Photovoltaic Program Branch. Table 1-2 identifies branch personnel according to their respective task areas.

This report summarizes the R&D activities of the subcontracted PV program. The research is described under the following headings: Amorphous Silicon Research Project (Section 2.0), Polycrystalline Thin Films (Section 3.0), Crystalline Silicon Materials Research (Section 4.0), High-Efficiency Concepts (Section 5.0), New Ideas Program (Section 6.0), and University Participation Program (Section 7.0). Each section is preceded by a brief overview of the task objectives and approaches and some of the key developments of FY 1988. The overviews are followed by technical summaries of each of the subcontracted efforts in FY 1988. These sections were provided by the subcontractors themselves or were derived from various project reports submitted by the subcontractors. Section 8.0 provides a list of active subcontracts in FY 1988, and a list of major subcontractor reports is given in Section 9.0.

---

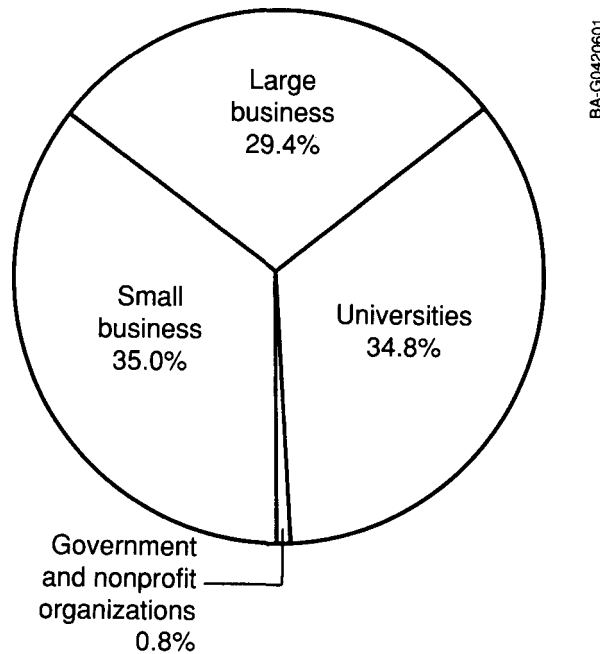
\*National Photovoltaics Program Five Year Research Plan, 1987-1991, Photovoltaics: USA's Energy Opportunity (DOE/CH10093-7), available from the National Technical Information Service, U.S. Department of Commerce, Springfield, VA 22161.

**Table 1-1. SERI Photovoltaic Program Branch Subcontract Budget History<sup>a</sup>**

Task Area	FY 1978-FY 1986 (\$M)	FY 1987 (\$M)	FY 1988 (\$M)
Amorphous Silicon Thin Films	43.3	9.2	6.7
Polycrystalline Thin Films	32.0	2.9	2.2
High-Efficiency Concepts (III-V)	24.6	3.0	1.3
Crystalline Silicon	20.7	0.4	0.6
New Ideas	17.0 <sup>b</sup>	0.5	0.1
University Program	<u>2.2</u>	<u>1.3</u>	<u>1.3</u>
<b>Total</b>	<b>140.2</b>	<b>17.3</b>	<b>12.2</b>

<sup>a</sup>Includes approximately 15% for program management, fees, etc.

<sup>b</sup>Includes \$9.0 million for photoelectrochemical cell research.

**Figure 1-1. Distribution of FY 1988 Subcontract Funds by Business Category**

**Table 1-2. SERI PV Program Branch Personnel**

Task Area	Contact Name	Telephone <sup>a</sup>
PV Program Branch	Thomas Surek, Manager Kathy Summers, Admin. Assist.	231-1371 231-1395
Amorphous Silicon Research Project	William Wallace, Manager Werner Luft James Ohi Byron Stafford	231-1380 231-1823 231-7681 231-7126
High-Efficiency Concepts, Crystalline Silicon Materials, and University Program	John Benner, Manager Cecile Leboeuf Bhushan Sopori	231-1396 231-1066 231-1383
Polycrystalline Thin Films	Kenneth Zweibel, Manager Richard Mitchell Harin Ullal	231-7141 231-1379 231-1841
New Ideas Program	Richard Mitchell, Manager	231-1379

<sup>a</sup> Area code (303); FTS number 327-xxxx.

### Key Accomplishments

Significant technical advances were made in all areas of the subcontracted PV program during FY 1988. In the following, some of the key accomplishments in each of the task areas are highlighted.

#### **Amorphous Silicon Research Project**

Four companies were awarded contracts in 1987 under the second government/industry cost-shared partnership for amorphous silicon research: ARCO Solar, Chronar Corporation, Energy Conversion Devices, Inc., and Solarex Corporation. The primary goal of this three-year, nearly \$40 million program—cost-shared 50% by the industrial partners—is to achieve 10% efficiency for single-junction submodules and 13% for multi-junction submodules having an area of about 900 cm<sup>2</sup>. The key accomplishments of the second year of that joint program follow.

- ARCO Solar achieved SERI-measured aperture-area efficiencies of 8.2% for a single-junction amorphous silicon 844-cm<sup>2</sup> submodule and 11.3% for an amorphous silicon/copper-indium-diselenide stacked, four-terminal, 900-cm<sup>2</sup> submodule. Chronar Corporation's large-area (2790 cm<sup>2</sup>), single-junction submodules were further improved in aperture-area efficiency to 6.7%; Chronar also fabricated same-band-gap, tandem-junction a-Si/a-Si large-area submodules with efficiencies up to 6.0% and improved stability against light-induced degradation. A triple-junction solar cell with an a-Si/a-Si/a-SiGe structure, fabricated by Energy Conversion Devices, Inc. (ECD), was measured at SERI to be 13.3% (active-area) efficient, and the corresponding 818-cm<sup>2</sup> submodule was 8.4% (aperture-area) efficient.
- In addition to the government/industry program, progress was made in fundamental research on amorphous silicon. Glasstech Solar, Inc., produced single-junction cells of

9% efficiency ( $0.121\text{ cm}^2$ ) in which the intrinsic layer was deposited at a rate of  $1.0\text{ nm/s}$  and 8% efficiency ( $0.58\text{ cm}^2$ ) at a rate of  $1.7\text{ nm/s}$ .

- A. Gallagher of the National Institute of Standards and Technology developed new methods for surface reaction probability measurements and for measuring the spatial distribution of depositing radicals for plasma-assisted chemical vapor deposition (CVD) of amorphous silicon. The measurements verified the dominance of deposition by  $\text{SiH}_3$  at low power densities from silane and demonstrated the difference in reaction probabilities for glow discharge from those for photo-CVD.
- Washington University researchers discovered a remarkable and novel phase-coherence phenomenon in their deuteron magnetic resonance studies. For high-quality a-Si:D,H, a unique multiple-spin echo reflects the presence of solitary HD molecules confined in mini-microvoids. This signal has not been observed for a-Si:D,H, a-Ge:D,H, or a-SiGe:D,H samples of lower quality, in which most microvoids are larger than a few angstroms.
- A Photovoltaics Safety Conference was held in Denver, Colo., in January 1988. The conference was attended by 79 persons from private industry, universities, research laboratories, U.S. national laboratories, and foreign organizations from 5 countries.
- The Jet Propulsion Laboratory (JPL) developed an electron cyclotron resonance microwave plasma CVD system and was able to fabricate a-SiC:H, a-C:H, and a-Si:H films. Deposition rates of  $2.5\text{ nm/s}$  and a photosensitivity of  $10^5$  were achieved for a-Si:H.
- The group under R. A. Street at Xerox PARC confirmed that boron and phosphorus are predominantly threefold coordinated in singly doped a-Si:H, but that compensated a-Si:H has more fourfold sites. They have started to promulgate a detailed theory of hydrogen bonding.
- The Institute of Energy Conversion (IEC) at the University of Delaware has prepared a-SiGe:H films with an optical band gap of  $1.3\text{ eV}$  (70% Ge) having an Urbach energy of  $46\text{ meV}$ , among the lowest recorded for that band gap, and indicative of negligible valence band-tail broadening relative to a-Si:H. Researchers found that the photoconductivity of a-SiGe:H films prepared from disilane and germane does not improve with hydrogen dilution, contrary to films from silane and germane.

### Polycrystalline Thin Films

Significant progress was made in FY 1988 in subcontracted research in polycrystalline thin films. The key accomplishments in both CdTe and CuInSe<sub>2</sub> solar cells and modules follow.

- ARCO Solar fabricated a large-area, 4-ft<sup>2</sup>, CuInSe<sub>2</sub> module with a power output of  $33.75\text{ W}$ . The aperture-area efficiency for this module is 8.7%, and it has a short-circuit current ( $I_{sc}$ ) =  $2.46\text{ A}$ , an open-circuit voltage ( $V_{oc}$ ) =  $23.035\text{ V}$ , and a fill factor (FF) = 0.6. ARCO Solar also produced a 938-cm<sup>2</sup> (aperture area) CuInSe<sub>2</sub> module with 11.1% efficiency and a power output of  $10.4\text{ W}$  measured at SERI. ARCO Solar's CuInSe<sub>2</sub> modules were also tested outdoors at SERI under open-circuit and load conditions. After two months of testing, no change in module output was observed. This is the first such test conducted on CuInSe<sub>2</sub> by an independent research group. ARCO Solar also reports achieving an active-area efficiency of 13.05% on a laboratory cell, which was verified by SERI.
- Boeing Electronics Company (BECO) demonstrated a SERI-verified total-area, single-junction efficiency of 12.5% using CuGaInSe<sub>2</sub>-based solar cells. The Ga content in the

film was 27%. Thin CdZnS (~300 Å) was grown by dip-coating, and ZnO:Al was deposited by radio frequency (RF) magnetron sputtering. In the past, BECO has demonstrated the stability of CuInSe<sub>2</sub> cells during 9000 hours of testing under one-sun illumination.

- Photon Energy fabricated large-area CdS/CdTe modules by a potentially low-cost spraying method. SERI verified a module output of 6.1 W and an efficiency of 7.3% (aperture area) on a near 1-ft<sup>2</sup>, monolithically interconnected submodule consisting of 27 cells in series. A "live" 4-ft<sup>2</sup> prototype module has also been delivered to SERI. Outdoor testing of CdTe submodules at SERI indicated no change in performance after two months of exposure to natural sunlight.
- Continued progress was made at Ametek to improve the single-junction, total-area efficiency of its devices to 11% for thin-film n-i-p CdTe solar cells. The thin-film CdTe is deposited by a potentially low-cost electrodeposition method. Ametek's n-i-p cells were tested for more than 3000 hours under one-sun illumination and load at 70°C with no degradation.
- International Solar Electric Technology (ISET) researchers developed a proprietary process to solve an adhesion problem they encountered at the Mo/CuInSe<sub>2</sub> interface. Peeling of the CuInSe<sub>2</sub> films was identified as a technological barrier in selenized CuInSe<sub>2</sub> devices.
- Several collaborative efforts between various groups resulted in rapid progress in many areas of polycrystalline thin-film research. Georgia Tech, in collaboration with Ametek, and JPL, in collaboration with Ametek, have both fabricated 9%-10% efficient n-i-p CdTe devices grown by metal-organic chemical vapor deposition (MOCVD). IEC collaborated with Ametek to develop four-terminal CdTe/CuInSe<sub>2</sub> solar cells. An efficiency of 9.4% was achieved. The University of South Florida interacted with Photon Energy to investigate the potential of HgTe contacts for CdTe modules.

### Crystalline Silicon

SERI joined with Sandia National Laboratories in a competitive procurement to select university research teams to contribute to the fundamental understanding of crystalline silicon materials properties. SERI awarded multiyear subcontracts to North Carolina State, Duke University, and the State University of New York at Albany. These will form the nucleus of a collaborative program to elucidate the chemical, structural, and electronic interactions of carbon, oxygen, and hydrogen with other defects in silicon.

- SERI established an in-house capability within the PV Program Branch for active participation with the subcontractors: hydrogenation applying Fourier transform infrared spectroscopy (FTIR) to characterize carbon-oxygen interactions and investigate optical processing for preservation of minority-carrier lifetime.
- In order to ensure that research addresses problems of major interest to industry, a meeting between subcontractors and PV industry representatives was organized to initiate direct interactions between the two groups.

### High-Efficiency Concepts

The efficiency of single-junction GaAs cells was further increased to establish wider margins of performance advantage under both one-sun and concentrated illumination. Spire increased the peak one-sun performance from 23.7% to 24.3% in cells delivered to SERI for verification. The previous record efficiency of single-junction concentrator

cells of approximately 28% (achieved in both GaAs and silicon) was bettered by researchers at Varian Associates, who achieved more than 29% for GaAs cells using a prismatic cover to reduce grid shadow losses. The performance of Varian's GaAs cells was also a key component of the demonstration of a mechanically stacked GaAs/Si concentrator cell of more than 31% efficiency at Sandia.

- Researchers at the Kopin Corporation achieved 20.7% efficiency with 4-cm<sup>2</sup>, thin-film GaAs cells. Such a high efficiency flat-plate technology, if continuing efforts are successful in establishing lower-cost processing, could enhance the viability of photovoltaic power generation in regions other than the southwestern United States. In a move towards higher efficiency, multiple-junction solar cells, Kopin delivered 19% efficient AlGaAs devices with a 1.65-eV band gap.
- Spire researchers continued to advance the performance of GaAs cells grown on silicon substrates, which are far lower in cost than GaAs substrates and would be directly applicable for use in concentrator systems. The technology also holds the promise of using active cells in the silicon with III-V top cells for multijunction flat-plate modules of more than 25% efficiency.

### New Ideas Program

A competitive solicitation for letters of interest (LOI) was issued in FY 1988 to more than 800 interested research facilities. These included universities, industry, and non-profit organizations. There were 92 responding LOIs for the Phase I evaluation under this solicitation. The evaluation of these 7-page proposals identified 24 that were in the competitive range. Those organizations were issued a request for proposal (RFP) at the end of FY 1988. The proposals received in response to this RFP will be evaluated during FY 1989, and multiple subcontracts will be awarded, with research starting in FY 1990.

- Researchers at ISET achieved Cu-doping of ZnTe deposited by the two-step electro-deposition process with repeatable resistivities of 0.1 to 1.0 ohm-cm. These Cu-doped films have a high optical transmission, which is required for their use as transparent back contacts in the top cells of four-terminal devices.
- Stanford University fabricated a device with a record efficiency of 22.3% (8.252-cm<sup>2</sup> aperture area, AM 1.5, one-sun illumination, SERI-measured). This cell had a high resistivity base, and a textured front with a lightly doped phosphorus diffused emitter.

### University Participation

The University Participation Program Solicitation for selection of programs to be awarded in June 1989 was mailed to more than 300 professors in July. Current participants in the program must be successful under this competitive procurement in order to continue their PV support. The program extended subcontracts from the FY 1985 solicitation to June 1989 to permit continuous support in cases in which the subcontractor wins a new award and to provide adequate notification for the others.

- The University Photovoltaic Symposia Series for the current subcontractors was completed in FY 1988. These were attended by more than 250 students, professors, invited speakers, and professionals in photovoltaics.

## Technology Transfer

The prompt and effective transfer of research results is a key element in the PV Program Branch's overall strategy. In addition to close working relationships with industrial and academic communities through subcontracts, such as the unique government/industry partnership in amorphous silicon, the primary means of information transfer are through subcontractor reports and review meetings. These reports are made available to the entire PV community, and the review meetings are open to all individuals and groups with an interest in this technology as well as to subcontractors. Frequent discussions with university and industry researchers and utility planners assist task managers in assessing future research needs and directions. The following is a list of some key FY 1988 accomplishments in the area of technology transfer.

- The PV Program Branch continued funding of subcontracts awarded under six competitive solicitations (issued in FY 1986) during this fiscal year. Such competitions permit research activities to be redirected and refocused on the most current and relevant areas; in addition, the competitions ensure that the best talents are selected to perform the research. The large number of responses received to all the solicitations indicates that the PV community views such competitions favorably. It is also significant that the subcontracts have resulted in approximately \$5.8 million in cost-sharing by industry.
- Approximately 500 researchers participated in various review meetings, conferences, and workshops organized by the PV Program Branch. The participants included subcontractors, SERI in-house researchers, individuals invited from outside the program (including the international PV community), and PV Program Branch personnel. The University Participation Program sponsored five symposia held at the participating universities. These served to introduce many students to the field of photovoltaic technology and were attended by professors, invited lecturers, and professionals from the PV industry. The Second Conference on PV Safety was held in January 1988 to enhance an awareness of the issues and introduce new technologies to improve safety in PV research and manufacturing. SERI also sponsored a topical workshop on a-Si CVD technology.
- During FY 1988, branch personnel and subcontractors contributed to two major photovoltaic conferences: the 8th Photovoltaic Advanced Research and Development Conference (November 1987), sponsored by SERI, as well as the 20th IEEE PV Specialists Conference (September 1988). In addition, the program sponsored seven workshops and university photovoltaic symposia focusing on topics such as safety, details of amorphous silicon CVD, and ion/photon-assisted deposition and doping. Collectively, these were attended by more than 200 students and professionals. Subcontractors' research results were widely disseminated to the PV community in more than 25 technical subcontractor reports and in numerous conference papers.
- Subcontractor review meetings were also organized for FY 1989. They will be held in the Amorphous Silicon, Polycrystalline Thin Films, and High Efficiency areas. A workshop on point defects in crystalline silicon is planned for July 1989.

## Conclusions

More than 50% of SERI's PV AR&D Project involves subcontracted research with industry, universities, and nonprofit laboratories. Significant technical advances were made in all areas of the subcontracted PV program during FY 1988. The major part of the subcontracted research in FY 1988 resulted from awards under six competitive solicitations initiated in FY 1986. Research progress was assessed through site visits, task review

meetings, and topical workshops. That progress is expected to continue during FY 1989, to help achieve the long-term goals of the DOE National Photovoltaics Program.

## 2.0 AMORPHOUS SILICON RESEARCH PROJECT

W. Wallace (Manager), W. Luft, J. Ohi, and B. Stafford

The objectives of this research in amorphous silicon are to improve and understand the optoelectronic properties of amorphous-silicon-based alloy materials and to improve the conversion efficiency and stability of single-junction and multijunction solar cells and submodules. The research is directed toward achieving the FY 1990 program goals, which are 10% efficiency for single-junction and 13% for multijunction submodules 900 cm<sup>2</sup> in area.

The technical plan of the Amorphous Silicon Research Project (ASRP) is divided into two principal activities: (1) multidisciplinary research and (2) fundamental research. The multidisciplinary research activities comprise the government/industry cost-shared programs with broad-based research teams located at the facilities of the individual companies. These teams perform directed research that covers aspects from starting materials to demonstration of proof-of-concept cells and submodules. Fundamental research activities involve basic, higher-risk, and supporting research at universities and research laboratories that aids industry by advancing the technology base. Cost-shared multidisciplinary programs address issues concerning single-junction and multijunction devices. Research is also performed to advance the conversion efficiency and the stability of both small-area cells and large (900 cm<sup>2</sup> and up) submodules fabricated by plasma-enhanced chemical vapor deposition. The stability encompasses both intrinsic aspects, such as the light-induced effect, and extrinsic aspects, such as diffusion or corrosion as a result of the environment. The efficiency improvement involves work on better light trapping, higher conductivity of interconnectors, and minimizing area losses due to interconnections.

After the successful completion of the first government/industry program, conducted from FY 1984 through FY 1987, the best single-junction a-Si cells had efficiencies as high as 11.7% and single-junction a-Si submodules had efficiencies up to 7.9%.

A second three-year government/industry program was started in FY 1987; the industry participants are ARCO Solar, Inc., Chronar Corporation, Energy Conversion Devices, Inc., and Solarex Corporation. The emphasis of this second program is on amorphous silicon multijunction technology. The major goals are to achieve by 1990 efficiencies of (1) 18% for multijunction cells (1 cm<sup>2</sup>), (2) 13% for multijunction submodules (900 cm<sup>2</sup>), and (3) 10% for single-junction submodules (900 cm<sup>2</sup>). Stability criteria (e.g., less than 5% degradation after exposure to the equivalent of two months of insolation) are associated with these efficiency goals. The status of this program, now in its second year, follows.

ARCO Solar achieved SERI-measured aperture-area efficiencies of 8.2% for a single-junction amorphous silicon 844-cm<sup>2</sup> submodule and 11.3% for an amorphous silicon/copper-indium-diselenide (CIS) stacked, four-terminal, 900-cm<sup>2</sup>, 55-cell submodule. The best a-Si/CIS 4-cm<sup>2</sup> tandem cell measured by ARCO Solar is 15.6% efficient, whereas the best value measured by SERI on a different tandem cell is 14.5%. The highest efficiency for a CIS cell measured by ARCO is 14.1%. Chronar Corporation's large-area (2790 cm<sup>2</sup>), single-junction submodules were further improved in aperture-area efficiency to 6.7%; in addition, Chronar fabricated same-band-gap, tandem-junction a-Si/a-Si large-area submodules with efficiencies up to 6.0% and improved stability against light-induced degradation. A triple-junction solar cell with an a-Si/a-Si/a-SiGe structure, fabricated by Energy Conversion Devices (ECD), was measured by SERI to be 13.3%

(active-area) efficient, and the corresponding 818-cm<sup>2</sup> submodule was 8.4% (aperture-area) efficient. The best low-band-gap (1.45 eV) a-SiGe:H:F cell had a 9.7% efficiency (ECD measurement). Solarex achieved 10.3% total-area efficiency for small-area, high-low-band-gap, two-cell stacks and 8.3% for three-cell stacks. For 1000-cm<sup>2</sup>, two-cell stack, high-low-bandgap submodules, Solarex obtained 6.3% total-area efficiency (SERI-verified).

In addition to the government/industry programs, fundamental research involves work on the light-induced effect, material deposition rates, alternative deposition methods, amorphous-silicon-based alloy materials, material and plasma characterization, and modeling. Summaries of these studies are contained in the pages that follow.

Title: Research on High-Efficiency, Multiple-Gap, Multi-Junction Amorphous Silicon-Based Alloy Thin Film Solar Cells

Organization: Energy Conversion Devices, Inc., Troy, Michigan

Contributors: S. Guha, principal investigator, A. Bannerjee, C. Bernotaitis, J. Burdick, E. Chen, T. Glatfelter, G. Hammond, M. Hopson, T. Laarman, M. Lyrette, R. Mohr, P. Nath, A. Pawlikiewicz, I. Rosenstein, R. Ross, D. Wolf, J. Yang, and K. Younan.

The research program is directed toward advancing the understanding of amorphous silicon-based alloys and their use in small area, multi-junction, multi-band gap solar cells. The principal objectives are (1) to develop a broad scientific base for the chemical, structural, optical, and electronic properties of amorphous silicon-based alloys; (2) to determine the optimum properties of alloy materials as they relate to high-efficiency cells; (3) to determine the optimum device configuration for multi-junction cells; and (4) to demonstrate by February 1990 the proof-of-concept, multi-junction amorphous silicon alloy-based solar cells having an efficiency of 18% under standard AM1.5 global insolation conditions and having an area of at least 1 cm<sup>2</sup>.

#### Approach/Present Tasks

ECD has been using rf glow-discharge decomposition approach to deposit amorphous silicon alloy materials (a-Si:H:F, a-SiGe:H:F). In order to obtain high efficiency with good stability, a multi-junction triple cell configuration has been used in which different band gap materials are used to capture the wide spectrum of solar photons. The different band gap materials are being optimized for incorporation in the cells. Novel cell designs are also being investigated to obtain higher efficiency with good stability. The tasks of the sub-contract relate to materials, single-junction cell and multi-junction cell research.

#### Status/FY 1988 Accomplishments

- High quality a-SiGe:H:F alloys have been developed with optical band gap down to 1.4 eV by glow-discharge decomposition of disilane, germane, silicon tetrafluoride and hydrogen. The films are characterized by low mid-gap density of states, sharp Urbach edge and uniform composition over large area deposition.
- High conductivity microcrystalline p<sup>+</sup> and n<sup>+</sup> doped alloys have been developed with optical band gap greater than 2 eV.
- A novel solar cell structure has been developed which utilizes band gap profiling in the intrinsic layer to obtain high efficiency.
- Single-junction solar cells with a-SiGe:H:F alloys (optical gap of 1.45 eV) in the intrinsic layer have been fabricated with an efficiency of 9.7%.

- A microscopic theoretical device model has been developed to explain the performance of single-junction p-i-n solar cells with a-Si or a-SiGe alloys in the intrinsic layer.
- Several important diagnostic techniques, including the DICE measurement and the quantum efficiency measurement of the component cells of a multi-junction device, have been developed and used to characterize and analyze single, tandem and triple devices.
- Dual-gap tandem cells have been fabricated with an efficiency of 13% as measured under global AM1.5 illumination.
- Triple-junction cells have been fabricated with a conversion efficiency of 13.7% as measured under AM1.5 global illumination, 25°C. This is the highest efficiency reported to date for any thin-film amorphous solar cell.
- A triple-junction module with an area of 840 cm<sup>2</sup> has been measured at SERI to give a world record performance of 8.4% conversion efficiency.

## References

1. Fluorinated Amorphous Silicon-Germanium Alloys Deposited From Disilane-Germane Mixture. S. Guha, J. S. Payson, S. C. Agarwal and S. R. Ovshinsky, J. Non-Cryst. Solids 97&98 (1987) 1455-1458.
2. Crucial Parameters and Device Physics of Amorphous Silicon Alloy Tandem Solar Cells. J. Yang, T. Glatfelter, R. Ross, R. Mohr, J. P. Fournier and S. Guha, J. Non-Cryst. Solids 97&98 (1987) 1303-1306.
3. A Novel Design for Amorphous Silicon Alloy Solar Cells. S. Guha, J. Yang, A. Pawlikiewicz, T. Glatfelter, R. Ross and S. R. Ovshinsky, Proceedings of the 20th IEEE Photovoltaic Specialists Conference (May 1988).
4. Numerical Modeling of Amorphous Silicon Based Multijunction Solar Cells. A. H. Pawlikiewicz, S. Guha, J. Yang, T. Glatfelter and R. Ross, Proceedings of the 20th IEEE Photovoltaic Specialists Conference (May 1988).
5. High Efficiency Multijunction Solar Cells Using Amorphous Silicon and Amorphous Silicon-Germanium Alloys. J. Yang, R. Ross, T. Glatfelter, R. Mohr, G. Hammond, C. Bernotaitis, E. Chen, J. Burdick, M. Hopson, and S. Guha, Proceedings of the 20th IEEE Photovoltaic Specialists Conference (May 1988).
6. The Effect of Dominant Junction on the Open Circuit Voltage of Amorphous Silicon Alloy Solar Cells. A. H. Pawlikiewicz and S. Guha, MRS Meeting, Reno, Nevada (Spring 1988).

**Title:** Research on Stable, High Efficiency, Large Area, Amorphous Silicon Based Submodules

**Organization:** Solarex Thin Film Division, Newtown, Pennsylvania

**Contributors:** A.W. Catalano, principal investigator, R.R. Arya, M.S. Bennett, B. Fieselmann, B. Goldstein, J. Morris, J. Newton, R.S. Oswald, R. Podlesny, S. Wiedeman, and L. Yang

The major objective of the present program is to demonstrate a conversion efficiency of at least 13% for a large area ( $900\text{ cm}^2$ ) multijunction submodule. Research highlights from Fiscal Year 1988 are presented.

### Semiconductor Material Research

- A wide range of feedstock gases have been selected, synthesized in-house if necessary, and used to deposit both undoped, doped, and trace-doped alloy films of SiC and SiGe. Gases used include  $\text{BF}_3$ ,  $\text{NF}_3$ ,  $\text{H}_2\text{SiGeH}_3$  (synthesized in-house),  $\text{GeF}_4$ ,  $\text{B}(\text{CH}_3)_3$  (synthesized in-house),  $\text{Si}_2\text{H}_6$ , and  $\text{SiH}_2(\text{CH}_3)_2$  along with the standard gases  $\text{SiH}_4$ ,  $\text{GeH}_4$ ,  $\text{CH}_4$ ,  $\text{H}_2$ ,  $\text{B}_2\text{H}_6$ , and  $\text{PH}_3$ .
- $\text{B}(\text{CH}_3)_3$  gas demonstrated improved compositional stability in the cylinder over the standard  $\text{B}_2\text{H}_6$  gas which decomposed over time, requiring increased monitoring and process adjustments in a manufacturing environment.
- No significant improvement in the deposition of SiGe alloys was observed using  $\text{Si}_2\text{H}_6$  instead of  $\text{SiH}_4$ . Solarex has optimized the SiGe deposition process using the lower cost  $\text{SiH}_4$ .
- A steady-state photocarrier grating (SSPG) technique is now operational at Solarex to measure the ambipolar diffusion lengths in alloy films. This technique has been used to study the effect of trace doping in SiGe alloys and to optimize the deposition conditions for SiGe and Si films.
- Trace doping of SiGe alloys with boron improves both the electron (observed by conductivity measurements) and hole (observed by SSPG) transport properties. The ambipolar diffusion length of SiGe alloys (1.6 eV) improved from approximately 1100 Å to 1500 Å using less than 0.2 ppm boron doping. Devices are being prepared to determine whether this material improvement translates into device efficiency improvements.
- A major effort was devoted to the development of microcrystalline doped layers and subsequent incorporation into devices for an expected increase in open circuit voltage as reported by two other research groups. Microcrystalline p-layers and n-layers were incorporated in devices and for the first time directly observed using TEM facilities at Amoco. No increase in open circuit voltage was observed.
- Raman spectroscopy has directly indicated a preferential favoring of Ge-Ge bonding over what is expected from a random mixing of atoms in SiGe alloys. Raman spectroscopy will be used to optimize the SiGe deposition process.
- Solarex's best small-area ( $0.75\text{ cm}^2$ ) multijunction device is a tandem SiC/SiGe (1.85/1.57 eV) device with an efficiency of 10.3% measured at SERI under an AM1.5 Xenon simulator at  $100\text{ mW/cm}^2$ .

- The high quality of Solarex's SiGe films is demonstrated by the achievement of 10.1% efficient small-area single-junction cell with a bandgap of 1.55 eV.
- The stability of multijunction cells has been measured and the results demonstrate that tandem cells are significantly more stable than single-junction cells. The stability of multijunction cells, based on measurements, is modeled as the average of the degradation rates of the individual cells in a multijunction structure.
- Stability studies of a Si/Si tandem cell resulted in only a 13% efficiency loss, from an initial 9% efficiency, over the equivalence of one year. This is a significant improvement over single junction cells with similar initial efficiencies. Based on Solarex's model and measurements, triple junction cells are expected to exhibit a slight gain in stability over tandem cells.

#### **Non-Semiconductor Material Research**

- More than 30 different encapsulants have been evaluated, and a general class of spray-on "paints" has been selected for further evaluation and development. A spray coating system has been tested and ordered. The "paints" are lower cost than EVA/Tedlar and can be easily automated. Initial submodules have passed environmental tests which included water immersion, thermal cycling, and humidity/freeze cycling. (JPL Block V tests)
- The rear metalization scheme being developed for submodules consists of ITO/ZnO/Ag. This is the same metalization scheme used in Solarex's 12% efficient small area single-junction cell.

#### **Submodule Research**

- Fill factors of approximately 75% have been achieved in submodules by decreasing the cell widths at the expense of increasing the inactive area. A 9.4% (active area) 400 cm<sup>2</sup> submodule was prepared with a fill factor of almost 75%. This indicates that the conductivity of the SnO<sub>2</sub> can limit the fill factor of production submodules.
- A SiC/SiGe submodule (1000 cm<sup>2</sup>) was measured at SERI under a simulator with a total area efficiency of 7.0%.
- A Si/Si tandem submodule was reported by Solarex which degraded less than 18% in efficiency over the equivalence of one year. This is a significant improvement of single junction submodules.
- The 2-step laser patterning method has been developed such that submodules have passed thermal cycling tests. The 2-step method eliminates a laser scribing step between the a-Si and metalization process steps. This results in a cost savings and an increase in reliability of the interconnect.

Title: Research on Stable, High-Efficiency, Large Area, Amorphous Silicon Based Submodules

Organization: Chronar Corporation, Princeton, NJ 08542

Contributors: A.E. Delahoy, Program Manager and Principal Investigator; F.J. Kampas, Principal Investigator; F.B. Ellis, Jr., E. Eser, S.C. Gau, H. Schade, T. Tonon, and H.A. Weakliem

### Objectives

This research program is designed to advance the state-of-the-art in a-Si:H submodule performance. The research encompasses both single and tandem junction submodules in 1 sq.ft. or 1x3 sq.ft. sizes, with specific goals for efficiency and stability. From Phase II (roughly FY88) onwards, the emphasis has been, and will continue to be, placed on tandem devices because of indications of their superior stability.

The research is divided into three fields (subtasks B1, B2, and B3), as follows:

B1. Semiconductor Materials. The objectives here include the deposition of amorphous silicon materials over large areas, the optimization of these materials as guided by physical, chemical, electrical and optical characterization, and the optimization of the efficiency and stability of small area p-i-n and p-i-n/p-i-n cells.

B2. Non-Semiconductor Materials. Here the objectives are the deposition of front and back contact materials ( $\text{SnO}_2$  and metallization) over large areas, the development of advanced back reflectors, and study of the thermal stability of the materials associated and interfaces.

B3. Submodules. The objectives here are the fabrication and optimization of large area interconnected devices on a monolithic substrate. This includes investigation of submodule configurations and patterning approaches, increase of active area, defect analysis, and a comparison of the light soak behavior of single and tandem junction submodules.

### Results

Subtask B1. We have applied the method of Ritter et al. for the determination of the ambipolar diffusion length  $L$  in photoconductive insulators [1] to obtain the following new results for a-Si:H: a) the light intensity dependence of  $L$  follows a power law  $L \propto F^{-s}$ , where  $F$  is the light flux, with  $s$  ranging from 0.14 to 0.20 [2], b) for the first time,  $L$  has been measured for the  $i$  layer within a p-i-n structure [3], and (c)  $L$  is almost constant for  $i$  layer thicknesses ranging from 0.1 to 1.0  $\mu\text{m}$  (unpublished). We had shown earlier that the method is self consistent, and that accurate values of  $L$  can be obtained, typically from 0.13 to 0.22  $\mu\text{m}$  for a-Si:H [4].

Direct measurements of the electron and hole mobility-lifetime ( $\mu t$ ) products were performed using a p-i-n structure having a thick (10  $\mu\text{m}$ ) i layer [5,6]. The  $\mu t$  products, determined from charge collection using strongly absorbed light, were  $\mu_{te} = 3.6 \times 10^{-7} \text{ cm}^2\text{V}^{-1}\text{s}^{-1}$  and  $\mu_{th} = 3.0 \times 10^{-8} \text{ cm}^2\text{V}^{-1}\text{s}^{-1}$ .

We have also pioneered the application of thermally stimulated currents (TSC) and current deep level transient spectroscopy (DLTS) to completed p-i-n solar cell structures [7]. Two categories of defect levels are observed (at 0.25 and 0.6 eV), with their concentration and energy distribution being changed by light soaking and annealing. From fill factor measurements, the collection length/i layer thickness ratio was determined, and was found to be inversely proportional to the high energy defect concentration [7,8].

Closed form expressions for the light intensity and temperature dependence of the IV curve and photocapacitance of p-i-n cells were verified experimentally, including the case of space charge distortion of the i layer field which occurs at low temperatures, or for thick or light soaked cells [9].

With regard to p-i-n cell optimization, we have worked primarily with the cell configuration: sodalime glass/SnO<sub>2</sub>/p a-SiC:H-it a-SiC:H - i a-Si:H - n a-Si:H/Al where it denotes a (thin) transitional i layer. The development of a new silicon carbide p layer having a graded carbon content has enabled us to achieve higher current densities as a result of outstanding blue response. The new p layer results in an external quantum efficiency of about 80% at 400  $\mu\text{m}$ , only slightly lower in fact than the peak QE (see Fig. 1). With standard Al metallization a 1  $\text{cm}^2$  single junction cell efficiency of 9.5% was attained.

Substantial progress was made during FY88 in the area of a-Si:H/a-Si:H tandem cells. A very reliable set of a-Si deposition conditions was achieved, and the conversion efficiency of 1  $\text{cm}^2$  cells was increased from 7.8% to 8.6% (see Fig. 2). Part of this improvement is attributable to the novel use of a TiO<sub>x</sub> (a conductive sub-oxide of Ti) layer interposed between the top and bottom stacks of the device (i.e. between n<sub>1</sub> and p<sub>2</sub>). We have shown the TiO<sub>x</sub> to be capable of improving voltage and fill factor with only an insignificant reduction in current through absorption. The cell in Fig. 2 has a  $V_{oc}$  of 1.72 volts (an average of 0.86V per stack) and a fill factor of 0.69. With optical enhancement, this tandem cell could reach 10% efficiency.

We continue to work assiduously at minimizing light-induced degradation in a-Si:H. Many conclusions from our work on light soaking were presented at the 8th European PV Solar Energy Conference in Florence [10]. These include: a) the demonstration of a stabilized state, b) the observation that cells in such a state cannot be annealed at or below the soaking temperature, c) that intermittent recovery in the dark does not result in superior operational stability (i.e. the appropriate parameter is simply accumulated light soak time), the corollary being that continuous illumination is fully justified to properly assess long-term behavior, and

d) that tandem cells are more stable than single junction cells. As a result of accelerated light soaking of cells prepared under standard and nonstandard conditions, five types of soaking behavior were observed and classified [5]. It is clear that, for commercial applications, the a-Si itself should be optimized with regard to stabilized efficiency and not initial efficiency.

In order to attain a higher throughput, and improved repeatability, two new a-Si:H deposition systems are being brought into service. One has been built (2 deposition chambers, manual operation), and the design for another has been completed and construction is underway (1 deposition chamber, 2 load locks, box carrier, computer controlled). Both are for 1 sq.ft. substrates.

**Subtask B2.** An extensive study of the deposition of SiO<sub>2</sub> barrier layers between sodalime glass and F-doped SnO<sub>2</sub> was carried out. The depositions were performed in a belt-driven muffle furnace by atmospheric CVD from SiH<sub>4</sub> and O<sub>2</sub> diluted in N<sub>2</sub>. The following properties were investigated: the dependence of SiO<sub>2</sub> growth rate on temperature and on SiH<sub>4</sub> and O<sub>2</sub> concentration; uniformity; powder production; and effect on SnO<sub>2</sub>. Details are given in [11]. Figure 3 shows the conductivity of 500-600 nm F-doped SnO<sub>2</sub> deposited on 200-300 nm SiO<sub>2</sub> on sodalime glass as a function of fluorocarbon flow rate with temperature as a parameter. The maximum conductivity is five times higher than without the SiO<sub>2</sub>.

Two approaches to optical enhancement of cell performance are being pursued. The first involves the experimental use of a borosilicate glass substrate and the formation of a graded index surface layer to serve as an AR coating. Less than 1% reflection at the air/glass interface has been demonstrated.

The second approach lies in superior light trapping resulting from the use of highly reflective back contact layers. Various types of multilayer metallizations were prepared by magnetron sputtering and were evaluated by IV and SR measurements. Using ITO/Ag, device quantum efficiencies at 700 nm were increased from 28% (with Al) to 50% (see Fig. 1). However, an unavoidable drop in FF was encountered. Preliminary results indicate that this can be avoided through the use of doped ZnO.

Studies of the thermal stability of Al-SnO<sub>2</sub> interfaces were completed, with the finding that humid air can lead to catastrophic failure of the contact [12]. A 100 Å Ti layer was found to be an effective diffusion barrier for Al.

**Subtask B3.** In preparing improved submodules, attention was paid to material uniformity, interconnect quality, increased active area, and removal of shunt-type defects. Laser scribing was consistently employed for all 3 layers (SnO<sub>2</sub>, a-Si:H, Al) and conditions were established

yielding good isolation of cells at the Al lasering step. Active area losses were reduced to 5-7% through real-time scribe tracking using a line scan camera. Best submodule performance data obtained during this period are summarized in Table I below. In achieving 1 ft.sq. panels producing 6 Watts of power, post-fabrication defect removal, by electrical and chemical means, proved particularly important. The IV curve of a 6 W tandem panel is shown in Fig. 4. Although new efficiency records have not yet been obtained through the use of back reflectors, it is encouraging that a 5.5W 1 ft. sq. panel was recently obtained employing sputtered ZnO/Al.

Research was also performed on a new submodule geometry termed the "dot contact interconnect scheme" utilizing 2 layers of back metallization separated by an insulator. The main features are an area utilization in excess of 98%, reduced  $I^2R$  losses in the transparent conductor, and greater flexibility in choosing combinations of output current and voltage.

Regarding stability, further promising results have been obtained using tandem panels. In 4 1/2 months continuous outdoor exposure, a glass-glass encapsulated 1 ft. sq. tandem submodule was found to decline in output power by only 14%.

Table I. Performance data for single junction and tandem junction submodules.

Panel size (sq.ft.)	1 x 1		1 x 3	
	Single	Tandem	Single	Tandem
Power (W)	5.9	6.0	17.7	15.0
Efficiency (%), active area	7.4	7.7	7.5	6.3
Efficiency (%), aperture area	7.0	7.2	6.9	5.9
$I_{sc}$ (A)	0.38	0.19	1.18	1.19
$V_{oc}$ (V)	23.9	48.3	23.6	24.3
FF	0.66	0.66	0.64	0.52

### Conclusions

Good progress has been made with regards to efficiency of a-Si/a-Si tandem cells, and the use of  $TiO_x$  to improve voltage and fill factor was discovered. As a result of careful processing and defect removal, 6 Watts per square foot has been demonstrated for tandem panels. Significant work remains to be done in the following areas: a) Optical enhancement. We estimate that currents can be increased by 18% through optical engineering involving the glass,  $SnO_2$ , and back contact. A high priority is the successful implementation of doped ZnO. b) Increase in active area. A further 5% can be obtained, e.g. through use of the dot contact scheme. c) A-Si:H quality control and uniformity. We anticipate that at least one of the new deposition systems will yield a 5% efficiency increase on these grounds. d) Increase in  $V_{oc}$ . Further research on the p-it-i-n

structure should lead to a 5% improvement of  $V_{oc}$ . These four improvements are multiplicative, and can yield a 36% increase in aperture area efficiency. Additional work on stability is also necessary.

### References

1. D. Ritter, E. Zeldov, and K. Weiser, *Appl. Phys. Lett.* 49, 791 (1986).
2. I. Balberg, A.E. Delahoy, and H.A. Weakliem, Light Intensity Dependence of the Ambipolar Diffusion Length in Hydrogenated Amorphous Silicon, 20th IEEE Photovoltaic Specialists Conference, Las Vegas, Nevada, Sept. 26-30, 1988.
3. I. Balberg, A.E. Delahoy, and H.A. Weakliem, Ambipolar Diffusion Length Measurements on Hydrogenated Amorphous Silicon p-i-n Structures, *Appl. Phys. Lett.* 53, 1949 (1988).
4. I. Balberg, A.E. Delahoy, and H.A. Weakliem, Self-Consistency and Self-Sufficiency of the Photocarrier Grating Technique, *Appl. Phys. Lett.* 53, 992 (1988).
5. A.E. Delahoy et al., Phase II Semi-Annual Technical Progress Report, March 16 - September 15, 1988, Subcontract No. ZB-7-06003-1.
6. R.S. Crandall, J. Kalina, and A.E. Delahoy, Direct Measurement of the Mobility - Lifetime Product of Holes and Electrons in an Amorphous Silicon p-i-n Cell, submitted for presentation at the 1989 Spring MRS Meeting.
7. A.E. Delahoy et al., Phase I Annual Technical Progress Report, March 15, 1987 - March 15, 1988, Subcontract No. ZB-7-06003-1.
8. H. Schade and A.E. Delahoy, Thermally Stimulated Currents and Fill Factors in p-i-n Amorphous Silicon Solar Cells, Proc. 8th E.C. Photovoltaic Solar Energy Conference (I. Solomon, B. Equer, P. Helm, Eds.) Kluwer Academic Publishers, Dordrecht 1988, p. 756.
9. R.S. Crandall, J. Kalina, and A.E. Delahoy, A Simplified Approach to Solar Cell Modeling, Materials Research Society Symposium Proceedings Volume 118, MRS 1988, p. 593.
10. A.E. Delahoy, T. Tonon, J.A. Cambridge, M. Johnson, L. Michalski, and F.J. Kampas, Light Soaking Studies on Amorphous Silicon Photovoltaic Devices and Modules, Proc. 8th E.C. Photovoltaic Solar Energy Conference (I. Solomon, B. Equer, P. Helm, Eds.) Kluwer Academic Publishers, Dordrecht 1988, p. 646.
11. F.B. Ellis, Jr., and J. Houghton, submitted for publication in Solar Energy Materials.
12. E. Eser, F. Ramos, and J. Grez, *J. Appl. Phys.* 64, 1238 (1988).

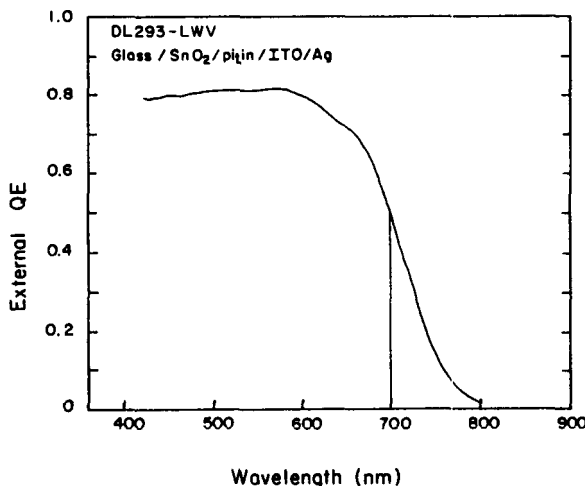


Fig. 1 External quantum efficiency for a single junction cell incorporating a graded carbon p layer and ITO/Ag back reflector. Note excellent response in blue and red portions of the spectrum.

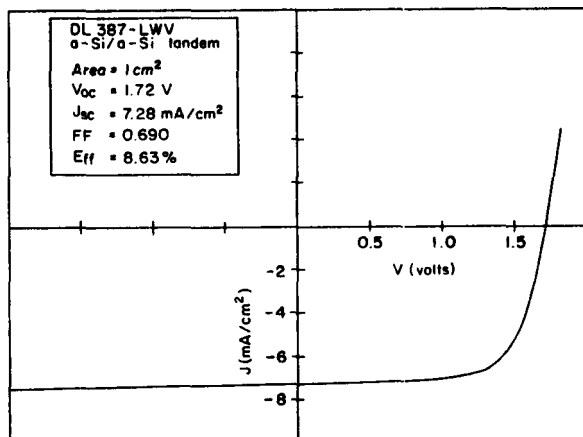


Fig. 2 IV curve under 100mW/cm<sup>2</sup> global AM1.5 irradiation for a 1cm<sup>2</sup> a-Si:H/a-Si:H tandem cell incorporating a  $\text{TiO}_x$  recombination layer. Conversion efficiency is 8.6%.

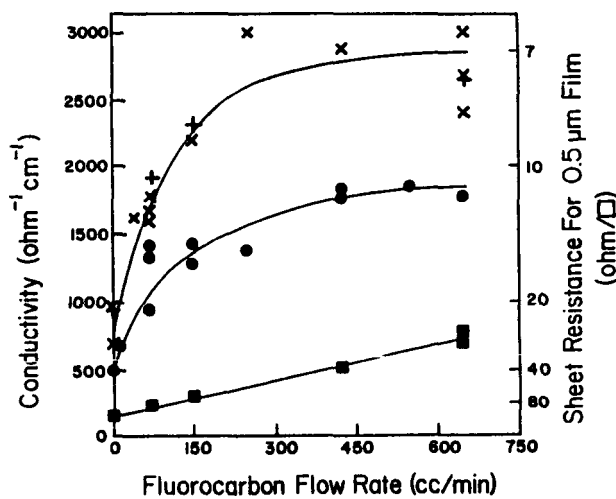


Fig. 3 Conductivity of F-doped  $\text{SnO}_2$  on  $\text{SiO}_2$ -coated sodalime glass as a function of deposition temperature and fluorocarbon flow rate. 608C (+), 584C (x), 537C (●), and 490C (■).

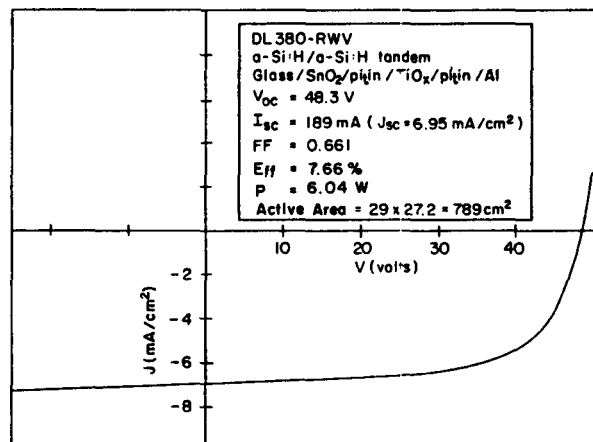


Fig. 4 IV curve under 100mW/cm<sup>2</sup> global AM1.5 irradiation for a 1 sq. ft. a-Si:H/a-Si:H tandem submodule consisting of 29 serially interconnected cells. The submodule has an active area efficiency of 7.7% and generates 6.0 Watts.

Title: Research on Amorphous Silicon-Based Thin Film Photovoltaic Devices

Organization: ARCO Solar, Inc., Camarillo, California

Contributors: D. L. Morel, principal investigator,  
W. Bottemberg, and K. W. Mitchell

The primary goal of this contract, which began July 1987, is to develop stable, 13% efficient tandem thin film modules. To achieve this goal, ARCO Solar has pursued the development of four-terminal tandem devices, as shown in Fig. 1, that use thin film silicon:hydrogen alloy (TFS), also known as amorphous silicon, as the top component and copper indium diselenide (CIS) as the bottom component. The primary advantage of this approach is the physical decoupling of the two circuits. Each is fabricated independently of the other, allowing discrete optimization of each device technology. The tandem module can be designed for either current or voltage matching of the component circuits.

ARCO Solar has chosen TFS and CIS as the semiconductors because they are the leading thin-film materials at present and because they have a near-ideal bandgap match of 1.7 eV and 1.0 eV, respectively. Long wavelength light that is not absorbed by TFS is coupled into the underlying CIS. Figure 2, the measured spectral response curves for TFS, CIS, and TFS-filtered CIS, demonstrate effective, but not optimized, optical coupling of the devices to achieve high photocurrents. Modeling calculations have been conducted that indicate practical, achievable efficiencies in the range of 20% for this combination [1].

### Progress

During Phase I (July 1987 - August 1988) of this contract, all Phase I goals and objectives were met or exceeded. Test structure device efficiencies for TFS/CIS tandem cells are summarized in Table 1 below. An efficiency of 15.6% for the tandem is in excess of the Phase I goal of 14%. SERI measured a value of 14.5% in its laboratories on a different set of samples. Due to a significant amount of cooperative effort in the measurements area over the past year, agreement between our measurements is now excellent.

We have also made substantial progress in scaling-up film and device properties to large areas. This has resulted in significant advancements in performance at the module level as shown in Table 2. The tandem module efficiency of 12.3% is in excess of the Phase I goal of 9.5% and rapidly approaching the primary project goal of 13%.

Demonstration of improved tandem cell and module performance presently depends on the development, modeling, and analysis of the component TFS and CIS technologies. As shown in Tables 3 and 4, progress has been made in these areas. The aperture efficiencies for 50-cell metal and ZnO-backed TFS modules have advanced to 9.4% and 9.1% respectively.

While the achievement of tandem efficiency goals is due to progress with both the TFS and CIS components, dramatic progress has been made with CIS in Phase I. Test device efficiency has been advanced to 14.1% with large-area compatible processing, and application of these advancements has resulted in an 11.2% aperture efficiency for a 55-cell, 30 x 33 cm module. These rapid advancements with CIS require concomitant progress with TFS and optical coupling efficiency to track the guidelines for tandems. While some progress has been made with

optical coupling, due to the texturing of the transparent conductors, much of the optical performance falls under the regime of non-specular optics, which adds considerably to the complexity.

Stability continues to be a significant performance factor for TFS. Long-term outdoor losses of 15-20% are not uncommon for prototype single-junction devices. Long-term assessment of CIS stability is hindered by the rapid advancements in performance. While we have data that show stable performance for a year outdoors for several devices, the ongoing changes that are being made in device fabrication require constant updating of the data base, which requires real-time data gathering. None of the data generated to date suggests a fundamental stability problem for CIS itself. In a tandem module we have observed a loss of 16% after several months of outdoor exposure. All of this loss is attributable to the TFS circuit.

### Summary

Significant progress has been made in device performance for TFS and CIS thin film technologies. This device level progress has been successfully transferred to large areas culminating in a tandem module efficiency of 12.3%.

Progress with CIS in particular has been rapid. The achievement of a module efficiency of 11.2% has exceeded expectations and requires further advances in TFS and optical coupling to track guidelines for optimum tandem performance.

TFS stability remains as an important performance issue. A real-world loss of 15-20% is often observed. Early CIS stability results look promising, and ongoing studies are continuing to verify stability for the latest devices.

Several papers have been presented highlighting the results of this work [2-11].

### References

1. K. W. Mitchell, "Detailed Modeling of Thin Film Polycrystalline and Thin Film Silicon:Hydrogen Alloy Multiple Junction Solar Cells," Technical Digest of the First International Photovoltaic Science and Engineering Conference, Kobe, Japan, pp. 691-694 (1984).
2. K. Mitchell, C. Eberspacher, R. Wieting, J. Ermer, D. Willett, K. Knapp, D. Morel, R. Gay, "Status of Thin Film Tandem PV Module Development," Technical Digest of the Third International Photovoltaic Science and Engineering Conference, Tokyo, Japan, pp. 443-448 (1987).
3. D. L. Morel, "Progress on High Efficiency Thin Film Solar Cells," Solar Cells 24, pp. 157-164 (1988).
4. W. Chesarek, K. Mitchell, A. Mason, L. Fabick, "EBIC Analysis of CuInSe<sub>2</sub> Devices," Solar Cells 24, pp. 263-270 (1988).
5. K. W. Mitchell, C. Eberspacher, J. Ermer, D. Pier, P. Milla, "Copper Indium Diselenide Photovoltaic Technology," Proc. 8th European Photovoltaic Solar Energy Conference, pp. 1578-1582 (1988).
6. D. L. Morel, K. Blaker, W. Bottemberg, L. Fabick, B. Felder, M. Gardenier, D. Kumamoto, D. Reinker, R. Rifai, "Development and Performance of 4-Terminal Thin Film Modules", see Ref. 5, pp. 661-665 (1988).

7. K. Mitchell, C. Eberspacher, J. Ermer, D. Pier, "Single and Tandem Junction CuInSe<sub>2</sub> Cell and Module Technology", Proc. 20th IEEE Photovoltaic Specialists Conference, Las Vegas, Sept. 1988 (to be published).
8. K. W. Mitchell, H. I. Liu, "Device Analysis of CuInSe<sub>2</sub> Solar Cells", see Ref. 7 (to be published).
9. W. R. Bottenberg, K. Blaker, D. Reinker, "Optical Considerations in the Performance of Hybrid, Four-Terminal Tandem Photovoltaic Modules", see Ref. 7 (to be published).
10. G. B. Turner, "Band Discontinuity and Bulk vs. Interface Recombination in CdS/CuInSe<sub>2</sub> Solar Cells", see Ref. 7 (to be published).
11. J. W. Park, R. J. Schwartz, J. L. Gray, G. B. Turner, "A Self-Consistent Numerical Model of Thin Film Silicon Hydrogen Alloy Solar Cells", see Ref. 7 (to be published).

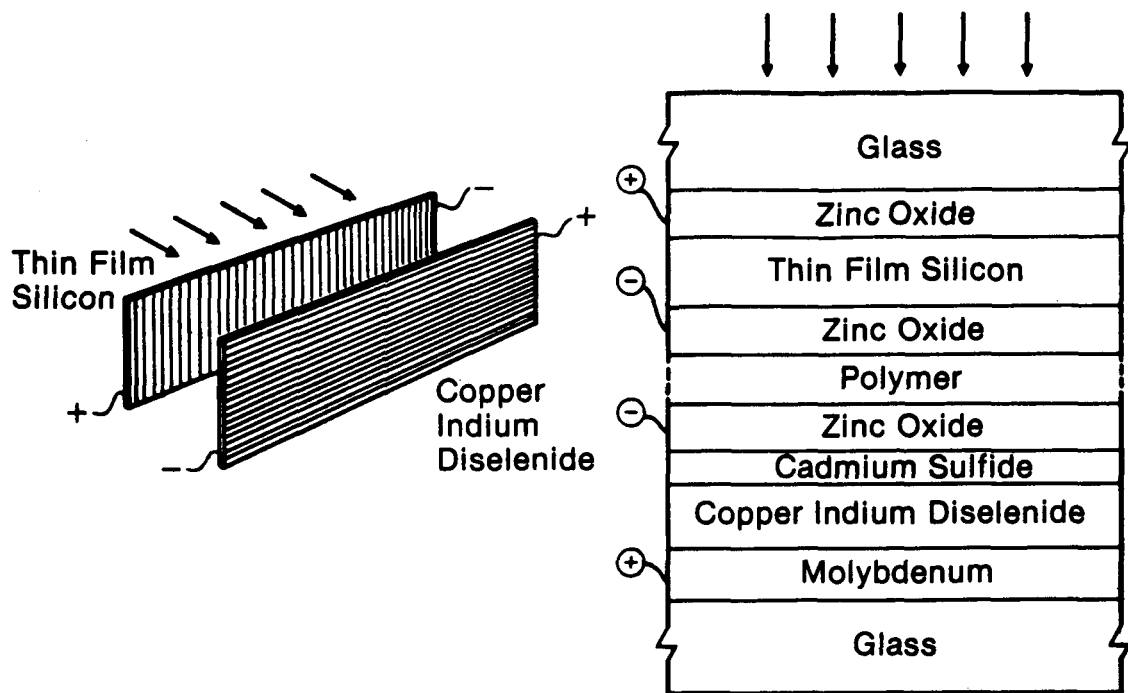


Fig. 1. Cross section of TFS/CIS tandem module.

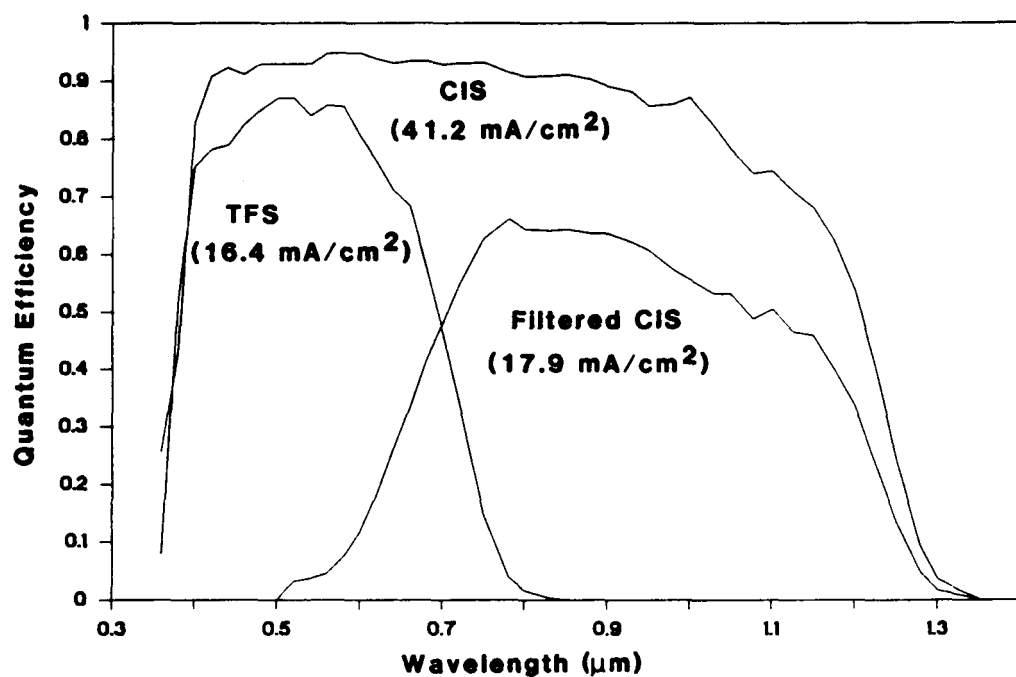


Fig. 2. Measured spectral response of TFS, CIS, and TFS-filtered CIS solar cells.

Table 1. 4-terminal tandem cell performance<sup>a</sup>.

4 cm <sup>2</sup> Cell	Eff. (%)	J <sub>sc</sub> (mA/cm <sup>2</sup> )	V <sub>oc</sub> (mV)	FF
Semitransparent TFS	10.3	16.4	871	0.72
Filtered CIS	5.3	17.9	432	0.68
Tandem	15.6			
Stand-Alone CIS	12.4	41.2	455	0.66

<sup>a</sup>Measured at ASTM air mass 1.5, global 100 mW/cm<sup>2</sup>, 25°C.

Table 2. 4-terminal tandem module performance<sup>a</sup>.

30x30 cm Module	Power (W)	Area <sup>b</sup> (cm <sup>2</sup> )	Eff. (%)	I <sub>sc</sub> (mA)	V <sub>oc</sub> (V)	FF
Semitransparent TFS	7.69	843	9.1	262	43.5	0.68
Filtered CIS	2.66	843	3.2	228	19.2	0.61
Tandem	10.35		12.3			
Stand-Alone CIS	7.62	844	9.0	611	21.2	0.59

<sup>a</sup>Measured at ASTM air mass 1.5, global 100 mW/cm<sup>2</sup>, 25°C.

<sup>b</sup>Aperture area.

Table 3. TFS and CIS cell performance<sup>a</sup>.

	Eff. (%)	J <sub>sc</sub> (mA/cm <sup>2</sup> )	V <sub>oc</sub> (mV)	FF
Semitransparent TFS	10.3	16.4	871	0.72
Stand-Alone CIS	14.1	41.0	508	0.68

<sup>a</sup>Measured at ASTM air mass 1.5, global 100 mW/cm<sup>2</sup>, 25°C.

Table 4. TFS and CIS module performance<sup>a</sup>.

	Power (W)	Area <sup>b</sup> (cm <sup>2</sup> )	Eff. (%)	I <sub>sc</sub> (mA)	V <sub>oc</sub> (V)	FF
Back Reflector TFS	7.9	844	9.4	277	42.8	0.67
Semitransparent TFS	7.7	843	9.1	262	43.5	0.68
Stand-Alone CIS	10.5	938	11.2	641	25.5	0.64

<sup>a</sup>Measured at ASTM air mass 1.5, global 100 mW/cm<sup>2</sup>, 25°C.

<sup>b</sup>Aperture area.

Title: Structural and Electronic Properties of Defects in Amorphous Silicon

Organization: Xerox Palo Alto Research center, Palo Alto, CA 94304

Contributors: J. B. Boyce, M. Hack, W. B. Jackson, J. Kakalios, S. E. Ready, R. A. Street (Principal Investigator), R. Thompson, C. C. Tsai, K. Winer

The objective of this research program is to obtain a comprehensive understanding of the structure and electronic properties of a-Si:H. The main emphasis is on the phenomena of metastability and thermal equilibrium, in which the density of electronic states depend on the electronic and thermal history of the material. Metastability effects are a significant problem with solar cells and other electronic devices. Our studies conclude that all the metastable phenomena have a common origin, and we have begun to unravel the complex interaction between the electronic states and the atomic structure that cause these effects.

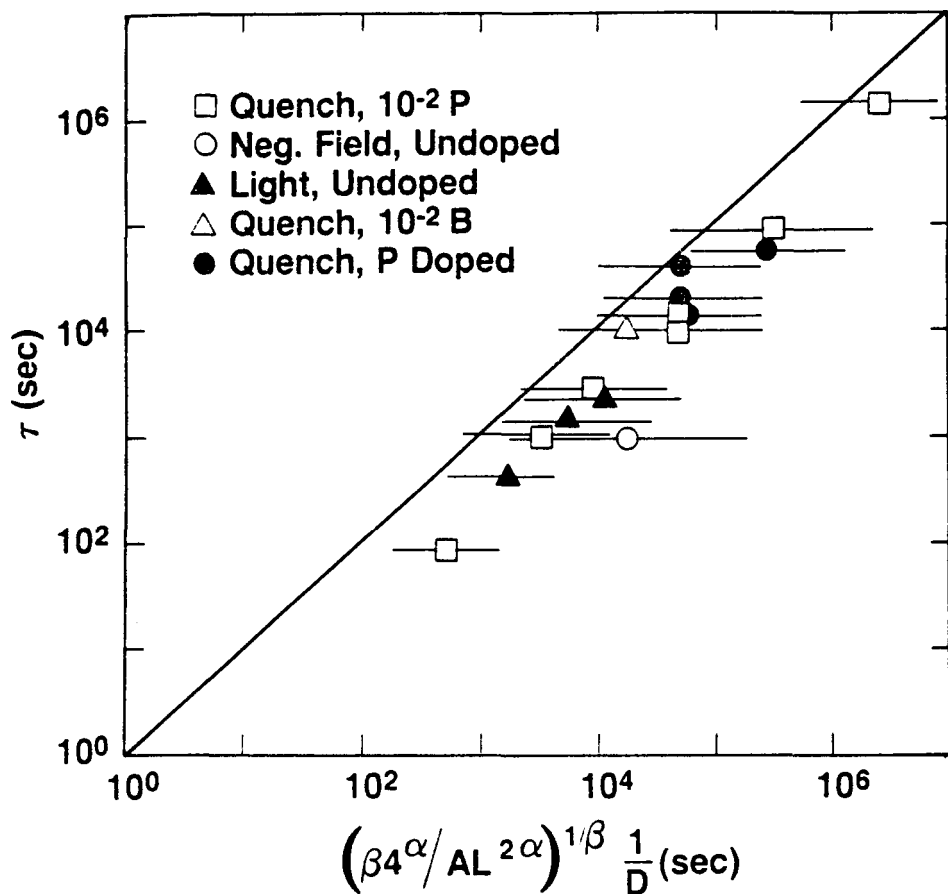


Fig. 1 A test of the prediction of an inverse relation between the hydrogen diffusion coefficient and the relaxation time. The diffusion coefficient was extrapolated to the various temperatures at which  $\tau$  was measured for a variety of different metastable effects.

The metastable defects created by prolonged light illumination are related to the thermal equilibration of the localized states. Both phenomena exhibit an annealing behavior which is characterized by a stretched exponential relaxation rate with similar time constants. Our research finds that the structural relaxation is enabled by the motion of bonded hydrogen in the a-Si:H network, and that the stretched exponential decay is caused by a dispersive hydrogen diffusion mechanism. A detailed theoretical analysis has been developed which predicts a quantitative relation between the hydrogen diffusion rate and the relaxation times. The comparison of these quantities in Figure 1 shows excellent agreement with the data. The solid line is the prediction of the model and the data points are from various metastability measurements. Both the time and temperature dependence are accounted for in this model. Furthermore, the theory also explains a diverse set of other experimental observations including the Meyer-Neldel rule for defect annealing, and the creation of light induced defects.

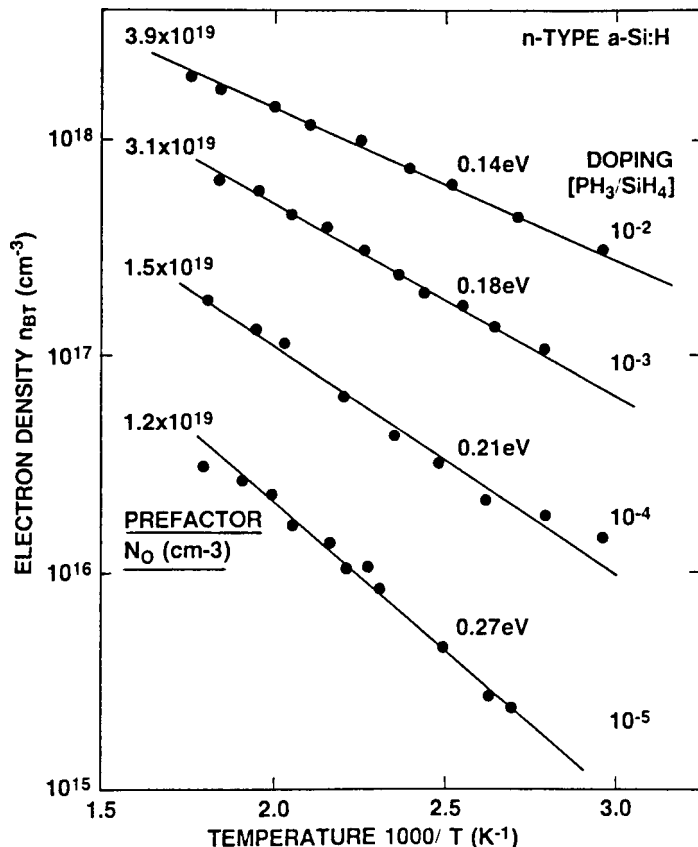


Fig. 2 The temperature dependence of the thermal equilibrium density of shallow states,  $n_{BT}$ , for different phosphorus doping levels. The activation energies and extrapolated prefactors are indicated.

In these annealing effects, the localized state distribution relaxes towards its equilibrium state. We have advanced our previous thermodynamic calculations of the equilibrium by showing that when the distribution of formation energies is included, the theory can account quantitatively for the doping and temperature dependence of the conductivity, defect density, and electron density. Experiments

demonstrate that the dopant states do indeed equilibrate and have a temperature dependent concentration.

The phenomenon of metastability links the structure and electronic properties of a-Si:H, and both aspects have been studied this year. We use the sweep out experiment to measure the density,  $n_{BT}$ , of shallow electrons and holes in the band tail, and the results are shown in Figure 2. The thermal equilibrium value of  $n_{BT}$  is thermally activated in both n-type and p-type material with doping dependent activation energies of up to 0.25 eV. These carriers dominate the electrical transport of a-Si:H and so are important to study. The magnitude of  $n_{BT}$  is related to the density of states distribution near the conduction or valence band edges, and to the dc conductivity. Numerical calculations of the thermodynamic models finds that our best estimate of the density of states readily accounts for the  $n_{BT}$  data.

We have also developed a method of measuring the effective carrier drift mobility in doped samples using sweep out experiments. The mobility is thermally activated and at low doping levels is similar to the mobility in undoped samples, but decreases with doping as shown in Figure 3. Our analysis indicates that the reduction is due to

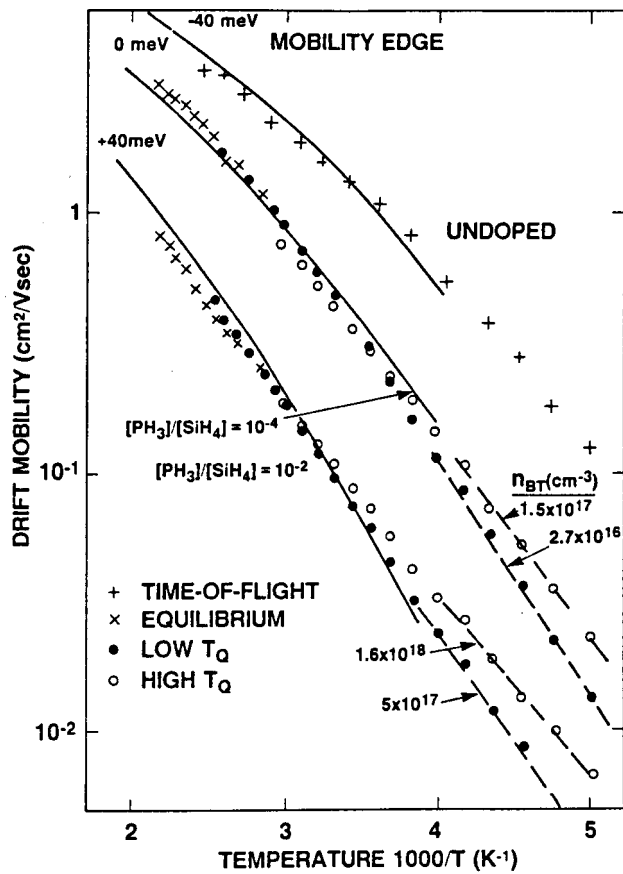


Fig. 3. Temperature dependence of the drift mobility extracted from the conductivity data of doped a-Si:H samples, and measured by time-of-flight on undoped material. Solid lines are calculated fits to the data assuming that the mobility edge is moved by the indicated amounts.

an effective shift of the mobility edge up into the conduction band, which we attribute to potential fluctuations induced by the charged defect and dopant states. We have also studied lithium doping as an alternative to the more conventional substitutional doping. However the lithium, introduced by diffusion, is nonuniformly distributed, and precipitates near the top and bottom surfaces. SIMS, PDS conductivity and ESR data show that the lithium introduces defects as with substitutional dopants, but find considerable differences in the details of the results.

Structural studies have focussed on the bonding of dopants and hydrogen. NMR experiments confirm that boron and phosphorus are predominately 3-fold coordinated in singly doped a-Si:H, but compensated a-Si:H has more 4-fold sites. NMR results showing the different response of boron in doped and compensated a-Si:H are shown in Figure 4. A detailed theory of hydrogen bonding has begun, particularly of the interstitial state and of the bonding near dopants. The initial calculations are made for the crystalline silicon structure, for reasons of computational tractability, and are

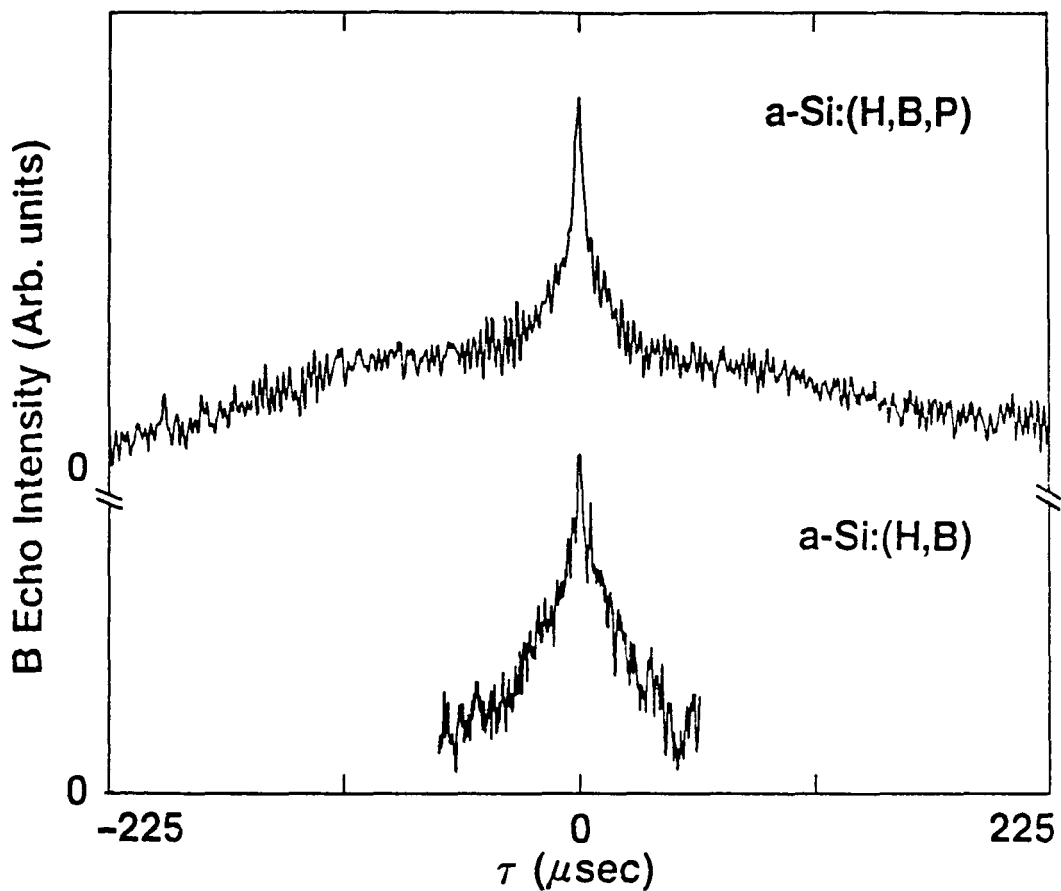


Fig. 4. Boron NMR echo intensity versus time in compensated (upper curve) and p-type (lower curve) a-Si:H. In both cases a fast and a slow component in time space are seen, corresponding to a broad and narrow line, respectively, in frequency space. But, in addition, a third, very slow component (very narrow frequency space line) is observed only for the compensated sample.

presently being extended to a-Si:H. We have also used SIMS, IR and Raman spectroscopy to study hydrogen bonding in microcrystalline silicon made by hydrogen dilution in an rf plasma. The hydrogen content decreases with dilution until the transition after which it increases. The hydrogen bonding configurations also change.

Over the past year we have constructed a remote microwave deposition system. The reactor is working and producing samples. Our initial investigations have been with hydrogen and deuterium plasmas and the characterization of the films. We have demonstrated doping with the same efficiency as for conventional rf plasma, and have begun to study the mechanisms of hydrogen incorporation into the films.

## Conclusions

The phenomena of metastability are very general in nature and are related to the thermal equilibration of the localized states of a-Si:H. Thermal equilibration of defects and dopants couples the structural and electronic states of the material, and leads to many of the characteristic electrical properties. Thermodynamic models are able to predict the observed properties quite accurately. For example, the contrasting properties of doped and compensated a-Si:H, the change in conductivity activation energy of doped a-Si:H, and the temperature dependence of the defect density in undoped material are all explained. The kinetic effects are due to hydrogen motion and again there is a good understanding of the relation between the relaxation of the electronic and defect properties, and the hydrogen diffusion. It is most important to understand better how the disorder in the silicon network bonding structure determines the equilibrium states and kinetics, in order to find ways of minimizing the device degradation effects.

## Bibliography

The electron drift mobility in doped amorphous silicon, R. A. Street, J. Kakalios and M. Hack, Phys. Rev., B38, 5603, 1988.

Realistic modeling of the electronic properties of doped amorphous silicon, M. Hack and R.A. Street, Appl. Phys Lett., 53, 1083, 1988.

Sweep out measurements of band tail carriers in a-si:H, R. A. Street, Philos. Mag., in press.

Theory of hydrogen passivation of shallow-level dopants in crystalline silicon, K. J. Chang and D. J. Chadi, Phys Rev. Lett., 60, 1422, 1988.

Connection between the Meyer-Neldel relation and multiple trapping transport, W. B. Jackson, Phys. Rev. B38, 3595, 1988.

Evidence for hydrogen motion in annealing of light induced metastable defects in hydrogenated amorphous silicon, W. B. Jackson and J. Kakalios, Phys. Rev. B37, 1020, 1988.

Kinetics of carrier-induced metastable defect formation in hydrogenated amorphous silicon, W. B. Jackson and M. D. Moyer, MRS Symp Proc, 118, 231, 1988.

Mechanisms of thermal equilibration in doped amorphous silicon, R. A. Street, M. Hack and J. Kakalios, Phys. Rev., B37, 4209, 1988.

Local structure of dopants in hydrogenated amorphous silicon, J. B. Boyce and S. E. Ready, in "Advances in Amorphous Semiconductors", H. Fritzsche, Ed. (World Scientific) in press.

Title: **Investigations of the Origins of Light-Induced Changes in Hydrogenated Amorphous Silicon**

Organization: University of Oregon, Eugene, Oregon

Contributor: J. David Cohen, Principal Investigator

A key objective of our research program is to evaluate in detail the changes in the electronic properties in a-Si:H which occur as a result of metastable changes in this material in order to help determine the microscopic mechanisms for such effects. During this year we concentrated on the photoinduced changes in a series of *n-type doped* a-Si:H samples of different doping levels using the techniques of drive level capacitance profiling and voltage pulse transient photocapacitance [1,2]. Such techniques had been applied in previous years to the study of *undoped* samples under this project [3,4] and found to be quite valuable in assessing the detailed metastable changes to the gap state distribution,  $g(E)$ , induced by light exposure and partial annealing.

A common result in many of such studies is the observed photoinduced increase in the midgap region of the density of states usually assumed to be dangling bond defects. In the case of undoped a-Si:H, the most widely accepted explanation is that these are created when the recombination of photoinduced carriers breaks weak Si-Si bonds [5,6]. In the case of doped films, however, the situation may be more complicated. Together with a mechanism similar to that in undoped films



we can also have activation or deactivation of dopant atoms. Reactions which have been suggested are



both of which require either the annihilation or creation of a dangling bond defect [7]. A systematic study of the correlation between the occupied bandtail (BT) states and dangling bond defects (D) should disclose which of these three reaction is dominant in n-type doped films.

All of our samples were grown on  $p^+$  crystalline silicon substrates by the glow discharge decomposition of silane. Sample 1 was doped with 30 vppm phosphine, sample 2 with 100 vppm and sample 3 with 300 vppm. Semitransparent Cr or Pd metal contacts were evaporated on the top surface of each sample. All samples were prepared in a light saturated state (state B) by exposure to 1.9 eV light from a cw Kr ion laser at 400 mW/cm<sup>2</sup>. Samples were then annealed for 15 minutes at a series of 30K temperature intervals starting at 350K (state B1) and ending at 470K (state A).

To determine the conduction bandtail occupation of states ( $N_{BT}$ ) we used drive-level profiling measurements as described previously [8,9]. That is, for a 10 kHz measurement frequency and a 250K temperature this method gives explicitly the value of the integral of the occupied states from the bulk Fermi level down to an energy of roughly 0.4 eV below  $E_C$ . The change in the number of deep gap states,  $N_D$ , was studied by the voltage pulse transient photocapacitance technique [10,11]. Such spectra appear qualitatively similar to and are interpreted in our study like sub-band-gap optical absorption spectra [12]; however, this method provides a substantially higher sensitivity than is possible in optical absorption measurements.

A set of such photocapacitance spectra are shown in Fig. 1 for sample 1 at three partially annealed states. Assuming that the valence bandtail state distribution does not show any significant light-induced changes [12] we have matched the spectra at energies greater than 1.7 eV and attribute the spectra below 1.5 eV as due to optical transitions from negatively charged dangling bonds ( $D^-$ ) to the conduction band. The signal level at 1.5 eV is, therefore, directly proportional to the number of negatively charged dangling bonds.

We display the changes observed in the number of  $D^-$  states,  $\Delta N_D$ , and the bandtail occupation,  $\Delta N_{BT}$ , for different partial annealed states in Figure 2. On the x-axis we plot the Fermi level ( $E_F$ ) position for each state as determined from the activation energy of electrical conductivity. We observe that as we approach state A the general trend for all three samples is, indeed, the decrease of the photoinduced  $D^-$  states and the increase of the occupied BT states. Note that we can move  $E_F$  to energies deeper than 0.8 eV in the lightly doped film, but this  $E_F$  shift decreases with doping. We also note that the number of photoinduced  $D^-$  states appears to scale with doping level as previously observed [13].

Most importantly, we see that in the lowest doped sample the light induced changes of the  $D^-$  states are annealed at significantly lower temperatures than the change in the bandtail occupation. This effect is less pronounced for sample 2 and non-existent for sample 3. Such behavior cannot be explained by any of the three reactions listed above. Although reaction 1 could explain the large shift in  $E_F$ , it also requires a correlation between changes in  $\Delta N_{BT}$  and  $\Delta N_D$  which is *not* observed in this case. Reaction 2 cannot explain the  $E_F$  motion and the increase in  $N_{BT}$ , while reaction 3 predicts photoinduced changes completely opposite from the ones observed. Even a combination of reactions 1 and 2 could not account for the observed changes.

We thus infer the existence of a defect reaction in the lower doped sample which can change the doping configuration of phosphorous independent of the changes in the  $D^-$  density. Such a conclusion was suggested some time ago by DLTS studies of metastable changes in lightly doped n-type a-Si:H films [14]. As the doping level is increased, however, we might expect reaction 2 to become dominant. In this case we should observe a small shift in  $E_F$ , a  $N_D$  signal decreasing significantly with increasing anneal temperature, and a very small change in  $N_{BT}$ . Sample 3 does appear to behave in this manner. Therefore our results strongly suggest that different reactions are dominant for the photoinduced changes at different doping levels. Our work also points out the importance of simultaneously monitoring changes in both  $D^-$  and bandtail states to test models of proposed defect reaction in a-Si:H.

## References

1. For a recent review see J.D. Cohen and A.V. Gelatos in Advances in Amorphous Semiconductors: I. Amorphous Silicon and Related Materials, ed. by H. Fritzsche (World Scientific, Singapore, 1988), pp. 475-512.
2. A.V. Gelatos and J. D. Cohen, Mat. Res. Soc. Symp. 118, 141 (1988).
3. SERI Annual Subcontract Report CY 1986. (October 1987). SERI/STR-211-3256. 30 pp.
4. J.D. Cohen, A.V. Gelatos, K.K. Mahavadi, and K. Zellama, Solar Cells 24, 287 (1988).
5. P.G. Caplan, E.H. Poindexter, B.E. Deal, and R.R. Razouk, J. Appl. Phys. 50, 5847 (1979).
6. H. Dersch, J. Stuke, and J. Beichler, Appl. Phys. Lett. 38, 456 (1981).
7. M. Stutzmann, W.B. Jackson, and C.C. Tsai, Phys Rev. B32, 23 (1985).

8. C.E. Michelson, A.V. Gelatos, and J.D. Cohen, *Appl. Phys. Lett.* **47**, 412 (1985).
9. K.K. Mahavadi, K. Zellama, J.D. Cohen, and J.P. Harbison, *Phys. Rev. B* **35**, 7776 (1987).
10. A.V. Gelatos, J.D. Cohen, and J.P. Harbison, *Appl. Phys. Lett.* **49**, 722 (1986).
11. A.V. Gelatos, K.K. Mahavadi, and J.D. Cohen, *Appl. Phys. Lett.* **53**, 403 (1988).
12. N.M. Amer and W.B. Jackson in *Semiconductors and Semimetals*, ed. by J. Pankove (Academic Press, New York, 1984), Vol. 21B, p. 83.
13. A. Skumanich, N.M. Amer, and W.B. Jackson, *Phys. Rev. B* **31**, 2263 (1985).
14. J.D. Cohen, D.V. Lang, J.P. Harbison, and A.M. Sergent, *Solar Cells* **2**, 119 (1983).

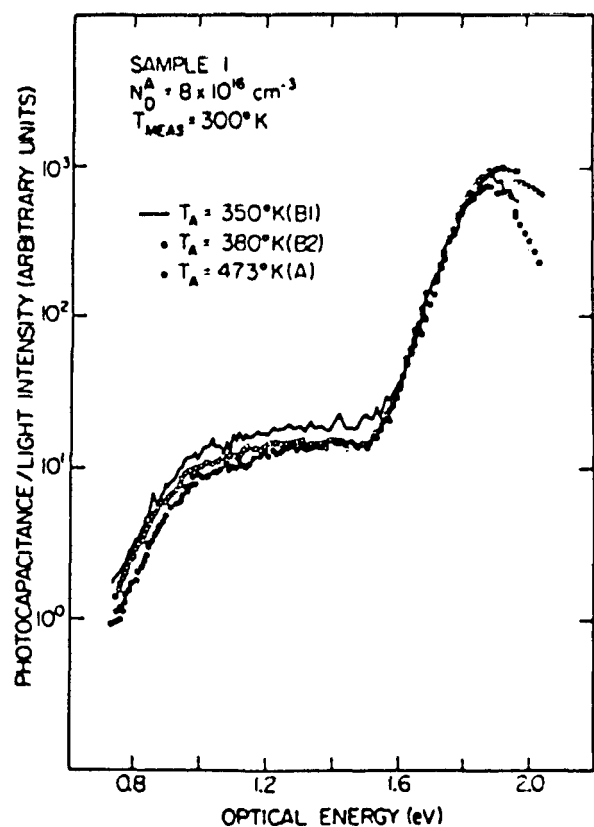


Fig. 1. Voltage pulse transient photocapacitance spectra for sample 1 at three partially annealed states. The signal level at 1.5 eV is proportional to the total dangling bond defect density.

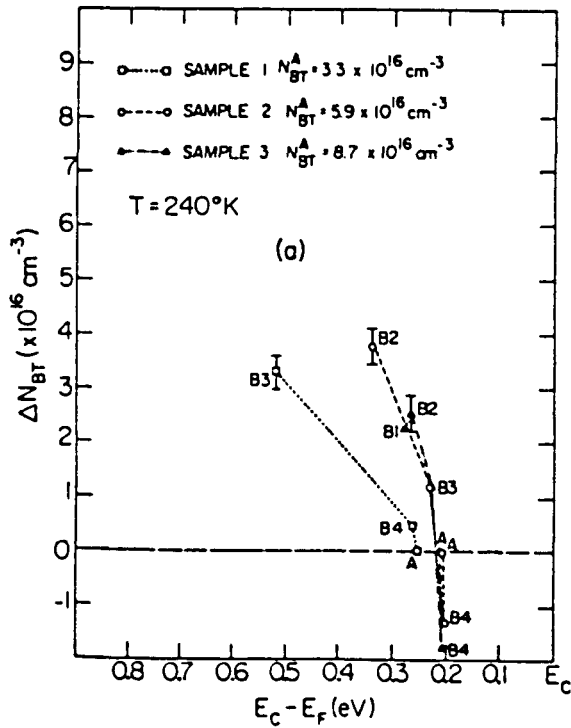


Fig. 2(a). Change in the occupied bandtail population as a function of Fermi level position for 3 n-type doped samples for a series of partial anneal metastable states between State B and State A.

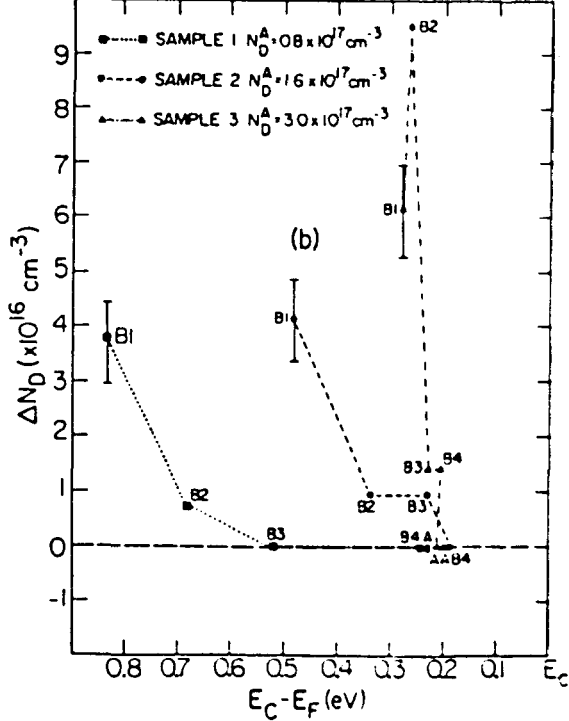


Fig. 2(b) Change in the dangling bond population as a function of Fermi level position for 3 n-type doped samples for a series of partial anneal metastable states between State B and State A.

**Effect of Charge Defects on Photoelectronic Properties  
of Hydrogenated Amorphous Silicon**

**Department of Physics and Astronomy  
University of North Carolina  
Chapel Hill, NC 27599-3255**

**M. Silver, Professor**

The objective of this research was to study the effects of charged defects on electronic transport, and recombination processes which are important in solar cell performance. To begin to attack this problem we have studied (1) forward bias time of flight (T.O.F.) in intrinsic and compensated<sup>1-3</sup> material (2) sweepout in i/ni structures both experimentally and theoretically<sup>4</sup> (3) low temperature hopping transport theoretically<sup>5</sup> and (4) a thermodynamic model for charged defects including potential fluctuations<sup>6,7</sup>.

The drift mobility in a-Si p+ - i - n+ junctions under forward bias has been studied by the voltage pulse technique as a function of d.c. bias. This technique shows a dependence of the drift mobility on d.c. voltage and forward bias current. These results do not agree with recent laser-induced time to flight measurements by Goldie, Le Comber and Spear (1988). The voltage pulse technique has been criticized by Goldie et al. 1988) as giving incorrect results due to an increase in capacitance under forward bias. In this paper we consider more carefully the question of the RC time constant under forward bias conditions and find that C does not change.

Electron drift-mobility measurements in hydrogenated amorphous silicon (a-Si:H) specimens far from thermal equilibrium are reviewed.<sup>2</sup> An introduction to experimental techniques is given, and results obtained with negative space-charge, under optical bias, and with single and double-injection are described. Quasi-Fermi level motion, charged defect limitation of transport, and defect meta-stability models are summarized.

The drift mobility in compensated a-Si:H as measured by standard T.O.F. is much less than in intrinsic material; presumably due to charge defects. In order to determine other differences in behavior between compensated and intrinsic material, we have studied the transient forward bias current of each in double injecting devices. We have found that: a) a much higher voltage is required in compensated material to obtain the same current as in the intrinsic; b) intrinsic and compensated samples show similar transient current responses but the compensated devices are much slower; c) the steady state current degrades in the compensated current but not in the intrinsic; and d) mobilities obtained by the voltage pulse technique in compensated material are at least three times larger than by the standard T.O.F. technique.

We compare results of simulated sweep-out currents in hydrogenated amorphous silicon i/n/i structures with earlier approximate analytic treatments and experimental data. Analysis in terms of space-charge-limited currents and emission-limited currents agrees qualitatively with the experimental results. The calculated results show that the Fermi energy,  $E_F$ , and the potential barrier at the forward biased n/i interface primarily determine the early sweep-out current vs time. In contrast to the approximate analytic results, our simulations show that a sharp decay of the current vs time as observed at higher sweep-out voltages does not necessarily require a peak in the density of localized states. This decay may also result from the conflict between the potentially large initial emission current from the n layer and the space-charge limitation imposed by the i layer. Some new experimental results at long times are also reported.

Recent experimental results on the low temperature drift mobility in amorphous silicon are examined on the basis of the approach to hopping transport developed by Silver and Bässler (1987). It is shown on general grounds that the main features of the experimental results, a sharply rising drift mobility below a critical temperature  $T_c$ , cannot be explained by a purely exponential tail state distribution, but are consistent with the distribution used by Spear and Cloude (1988) in model calculations in which there is a sharp decay of  $g(E)$  below approximately 0.12 e.v. followed by an exponential.

We consider the thermodynamics of the "dangling bond" defect in hydrogenated amorphous silicon (a-Si:h) assuming there are medium-range electrostatic potential fluctuations whose peak-to-peak magnitude is greater than the (positive) effective correlation energy. It is shown that significant concentrations of charged dangling bonds will result--negative defects with transition energies below the Fermi energy ( $E_F$ ) in regions of high potential and positive defects with transitions above  $E_F$  in regions of low potential. There are some grave consequences of these charged dangling bonds for transport and photostability in a-Si:H.

## Conclusions

All of our experiments and calculations are consistent with the premise that a copious supply of charge defects can co-exist with neutral  $T_3^0$  dangling bonds. Our thermodynamic model including the potential fluctuations predicts that  $10^{17} T_3^{\pm}$  bonds can be present even in intrinsic material. These charge defects can have dramatic effects upon the kinetics of recombination and on the Staebler-Wronski effect. Further, when neutralized as in optical bias experiments or double injection can lead to a substantial increase in the drift mobility. As a consequence, our standard models need to be re-examined.

## References

1. "Experiments and Discussion on the Electron Mobility in Amorphous Silicon," G. Winborne, Le Xu and M. Silver, to be published *Phil. Mag. Lett.*
2. "Drift Mobilities Far from Thermal Equilibrium in Hydrogenated Amorphous Silicon," E. A. Schiff and M. Silver, *Advances in Amorphous Semiconductors* edited by H. Fritzsche (World Scientific, in press).
3. "Comparison Between Forward Bias Currents in P/I/N and P/C(B/P)/N Hydrogenated Amorphous Silicon Diodes," G. Winborne, Le Xu and M. Silver, *Mat. Res. Soc. Proc.*, 118, 501-506 (1988).
4. "Computer Simulations of I/N/I Sweep-out Experiments in a-Si:H. Le Xu, G. Winborne, M. Silver and H. Branz, submitted for publication.
5. "Comments on Electron Transport in the Bank Tail States of Amorphous Silicon at Low Temperatures," M. Silver and W. E. Spear, to be published *Phil. Mag. Lett.*
6. "Potential Fluctuations and Charged Defects in Hydrogenated Amorphous Silicon," M. Silver and H. Branz, IBM Conference on Physics and Applications of Amorphous Semiconductors, Nov. 1988.
7. "Thermodynamic Model for Charged Defects Including Potential Fluctuations," H. Branz and M. Silver, in preparation.

Title: Photo-CVD of Amorphous Silicon Alloy Materials and Services

Organization: Institute of Energy Conversion, University of Delaware, Newark, Delaware

Contributors: Bill N. Baron (project manager), Steven S. Hegedus (principal investigator), Richard E. Rocheleau (principal investigator), Wayne A. Buchanan, David E. Albright, Neeraj Saxena

## Objectives

The objectives of this research are to develop Hg-sensitized photochemical deposition (photo-CVD) of amorphous silicon-germanium alloy materials and devices with properties and performance suitable for multijunction solar cells. Emphasis is placed on understanding the fundamental relations between material processing and device performance of amorphous silicon germanium alloy cells with optical bandgaps of 1.3 eV.

## Technical Approach

The photo-CVD reactors used in this work have been described elsewhere(1). The critical element in their operation is the presence of the flexible UV transparent curtain which separates the reactor into two chambers, eliminating deposition on the quartz window.

A systematic study of a-Si<sub>1-x</sub>Ge<sub>x</sub>:H deposited from SiH<sub>4</sub> or Si<sub>2</sub>H<sub>6</sub>, GeH<sub>4</sub> and He or H<sub>2</sub> yielding films with 0.1 < x < 0.95 and 1.1 < E<sub>g</sub> < 1.6 eV is being carried out. The a-SiGe:H films are deposited at pressures from 0.1 to 20 torr and temperatures from 25 to 350°C. Solar cells having the configuration glass/ITO/p-i-n with a-Si<sub>1-x</sub>Ge<sub>x</sub>:H (0 < x < 0.7) i-layers are fabricated and analyzed to determine optimum material processing and limits to solar cell efficiency.

## Significant Results

### a-SiGe:H Alloy Materials

#### Effect of Deposition Conditions on Band Gap

Figure 1 shows the E<sub>g</sub> as a function of Ge content and deposition temperature(2). For films deposited at a given temperature from mixtures of SiH<sub>4</sub> and GeH<sub>4</sub>, and Si<sub>2</sub>H<sub>6</sub> and GeH<sub>4</sub>, the band gap decreases with increasing Ge content. However, at a fixed Ge content, the band gap depends strongly on deposition temperature. For example, at 60% Ge, the band gap increases from 1.33 eV to 1.47 eV as the deposition temperature decreases from 250°C to 180°C. This is due to an increase in H content (from 630 cm<sup>-1</sup> IR absorption) as the deposition temperature is lowered.

### Hydrogen Bonding

The manner in which H is bonded in the a-SiGe:H films shows a strong dependence on substrate temperature and Ge content. The amount of Si dihydride bonding increases rapidly as the deposition temperature is decreased(2). Preferential attachment of H to Si increased with increasing Ge content. Similar trends were observed using  $\text{Si}_2\text{H}_6$ - $\text{GeH}_4$ .

### Photoconductivity ( $\sigma_p$ ) and Urbach Energy

Figure 2 shows  $\sigma_p$  (AM1.5, 25°C) vs. band gap for films deposited from  $\text{SiH}_4$  and  $\text{GeH}_4$  with  $\text{H}_2$  or He dilution. He is used as an inert gas to maintain constant total gas flow, and partial pressures of hydrides. The He and  $\text{H}_2$  data both show an increase in  $\sigma_p$  with temperature, with highest values at substrate temperatures above 205°C.  $\text{H}_2$  dilution increased  $\sigma_p$  by a factor of 4 at 1.35 eV from  $1 \times 10^{-6}$  to  $4 \times 10^{-6}$  S/cm. In contrast to films deposited from  $\text{SiH}_4$  and  $\text{GeH}_4$ ,  $\sigma_p$  of films deposited from  $\text{Si}_2\text{H}_6$  and  $\text{GeH}_4$  did not improve with  $\text{H}_2$  dilution.

We have measured the absorption edge on p-i-n devices using primary photocurrents (3) to determine the Urbach energy ( $E_u$ ). We found  $E_u$  from 43 to 46 meV for i-layers with bandgaps of approximately 1.74 (0% Ge) to 1.3 eV (70% Ge). These  $E_u$  values are among the lowest reported for those band gaps. Values less than 50 meV, as reported here, for  $E_g=1.5$  eV or lower indicate that negligible valence band-tail broadening occurs in high quality a-SiGe:H relative to a-Si:H.

### a-Si:H p-i-n Device Characterization and Analysis

#### Analysis of Diode Recombination and $V_{oc}$

A study(4) of  $V_{oc}$  in a-Si:H p-i-n solar cells deposited by photo-CVD and plasma-CVD with varying p-layer and carbon graded layer (GCL) thicknesses, and impurity levels was carried out by analyzing  $J(V)$  data measured on a-Si:H p-i-n devices under illumination. We found a 50-60 mV increase in  $V_{oc}$  for a GCL of about 100 Å. We have investigated variations in the gradient and the carbon content but found the total thickness to have the most dominant effect. We also found no improvement in  $V_{oc}$  with the GCL until impurities such as C and O were reduced below  $10^{20} \text{ cm}^{-3}$ . The GCL did not change the built-in voltage, but instead reduced recombination. We speculate that the GCL reduces recombination by either separating the photogenerated carriers in the i-layer from the defects at the p/GCL interface, or that the GCL modifies the band structure and increases the field, due to the graded electron affinity.

We investigated the behavior of devices having p-layer depositions from 45 to 120 seconds, corresponding approximately to thicknesses from 30 to 100 Å. Quantum efficiency (QE) values at 400 nm as high as 0.75 were obtained with the thinnest (45 second) p-layer, but  $V_{oc}$  and FF decreased significantly. It was noted that the blue QE (400 nm) tracked inversely with  $V_{oc}$ . We concluded(4) that the Schottky barrier at the TCO/p interface was affecting the current transport in cells with p-layers less than 100 Å.

by controlling the built-in potential and significantly increasing the recombination current  $J_{0L}$ . The reduction in  $A_L$  towards unity is also consistent with a Schottky barrier.

The recombination current density( $J_{0L}$ ) and  $A_L$  factor, for 14 a-Si:H solar cells having  $V_{OC}$  from 0.67 to 0.90 Volts were determined. Efficiencies ranged from 5 to 9.5%. Three of the devices were deposited by plasma-CVD, while the others were deposited by photo-CVD. The  $V_b$  for these cells was  $1.05 \pm 0.05$  V and  $A_L$  was  $1.5 \pm 0.1$ . If the diode mechanism under illumination was limited by diffusion and recombination, as proposed by others, we would expect to find  $A_L$  increasing with  $V_{OC}$  to  $A_L=2.0$ . Instead, we found that improvements in  $V_{OC}$  resulted from reductions in  $J_{00}$  arising from either p/i interface recombination or bulk recombination at localized i-layer defects, very near to the p/i interface.

#### Characterization of Defects in a-Si:H Solar Cells Using Sub-band Gap Photocurrent Spectroscopy

We have also used sub-band gap primary photocurrent (PPC) spectroscopy measured on p-i-n solar cells to examine the effects of light exposure on midgap defect state densities and on device performance(3). Figure 3 shows PPC spectra of a photo-CVD p-i-n cell deposited at  $205^{\circ}\text{C}$  and measured at selected intervals during light soaking at  $100 \text{ mW/cm}^2$ . Defect absorption increased by about a factor of 3 over 100 hours and was greatest between 1.2 and 1.3 eV, or 0.55 to 0.45 eV below the conduction band edge. We found a nearly logarithmic decrease in FF and an increase in  $\alpha(1.2 \text{ eV})$  with light soaking time, which strongly suggests that the two effects are related. This is the first time that the inverse relation between FF and photo-created i-layer defects has been directly demonstrated on the same device.

#### Conclusions

- ▶ State-of-the-art optoelectronic properties have been found for low band gap a-SiGe:H films deposited by photo-CVD, such as  $\sigma_p=4 \times 10^{-6} \text{ S/cm}$  and  $E_u = 46 \text{ meV}$ .
- ▶ Dependence of  $E_g$  and  $\sigma_p$  on deposition temperature at constant %Ge is related to hydrogen bonding.
- ▶  $V_{OC}$  in p-i-n a-Si:H devices is dominated by recombination at or near the p/i junction.
- ▶ Increase in light-induced defects between 1.0 and 1.4 eV above the valence band has been measured directly on a-Si:H p-i-n devices by sub-band gap photocurrents and correlated with the decrease in FF.

#### Future Directions

- ▶ Fabricate, optimize and characterize p-i-n and n-i-p devices having 1.3-1.4 eV a-SiGe:H i-layers.

- Develop improved amorphous and microcrystalline doped layers for low bandgap a-SiGe devices.
- Continue study of the origin of light-induced defects and their influence on solar cell performance.

1. Rocheleau, R.E.; Hegedus, S.S.; Buchanan, W.; Jackson, S.C. (1987), *Appl. Phys. Lett.* **51**(2) 13 July 1987, p. 133.
2. Hegedus, S.S.; Rocheleau, R.E.; Tullman, R.T.; Albright, D.E.; Saxena, N.; Buchanan, W.A.; Schubert, K.; Dozier, R. (1988) "Photo-assisted CVD of a-Si:H Solar Cells and a-SiGe:H Films", *Proc. 20th IEEE PVSC*, Las Vegas, NV, September 1988.
3. Hegedus, S.S. and Cebulka, J.M. (1988) "Characterization of Defects in a-Si:H Solar Cells Using Sub-band Gap Photocurrent Spectroscopy" *20th IEEE PVSC*, Las Vegas, NV, September 1988.
4. Hegedus, S.S. (1988) "The Open Circuit Voltage of Amorphous Silicon p-i-n Solar Cells", *Proc. 20th IEEE PVSC*, Las Vegas, NV, September 1988.

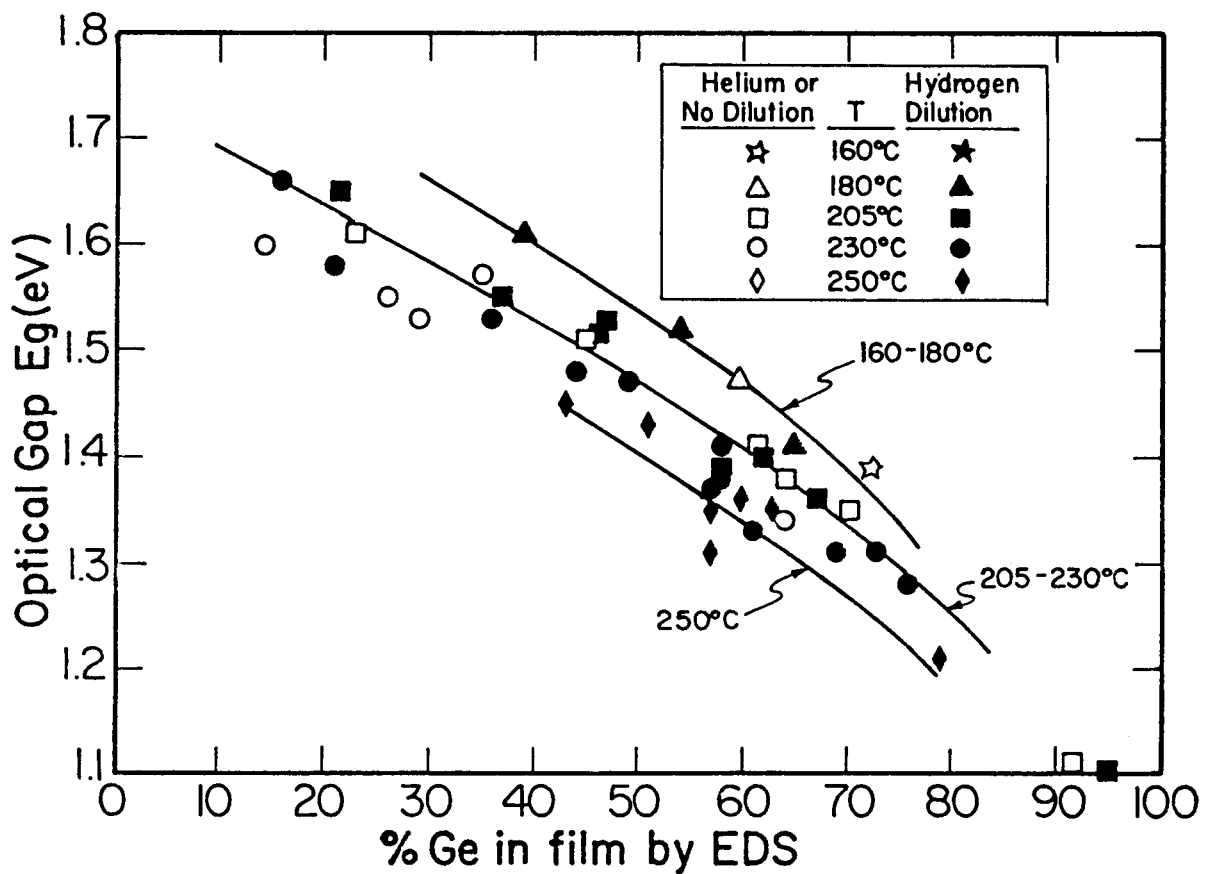


Figure 1. Optical gap vs. Ge content. Films deposited from  $\text{SiH}_4$  or  $\text{Si}_2\text{H}_6$ .

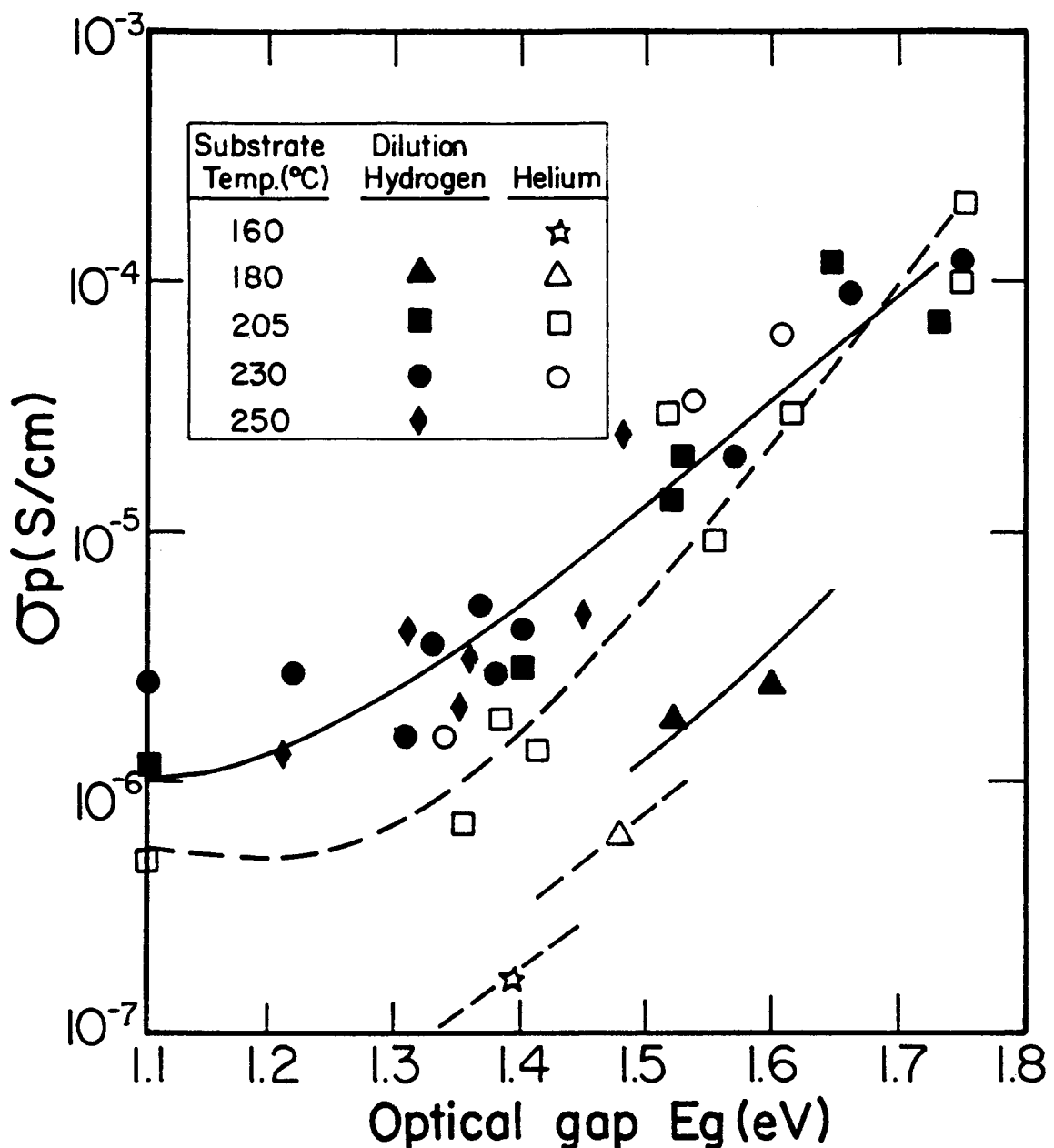


Figure 2. Photoconductivity vs optical gap for films deposited by photo-CVD from  $\text{SiH}_4$  and  $\text{GeH}_4$ .

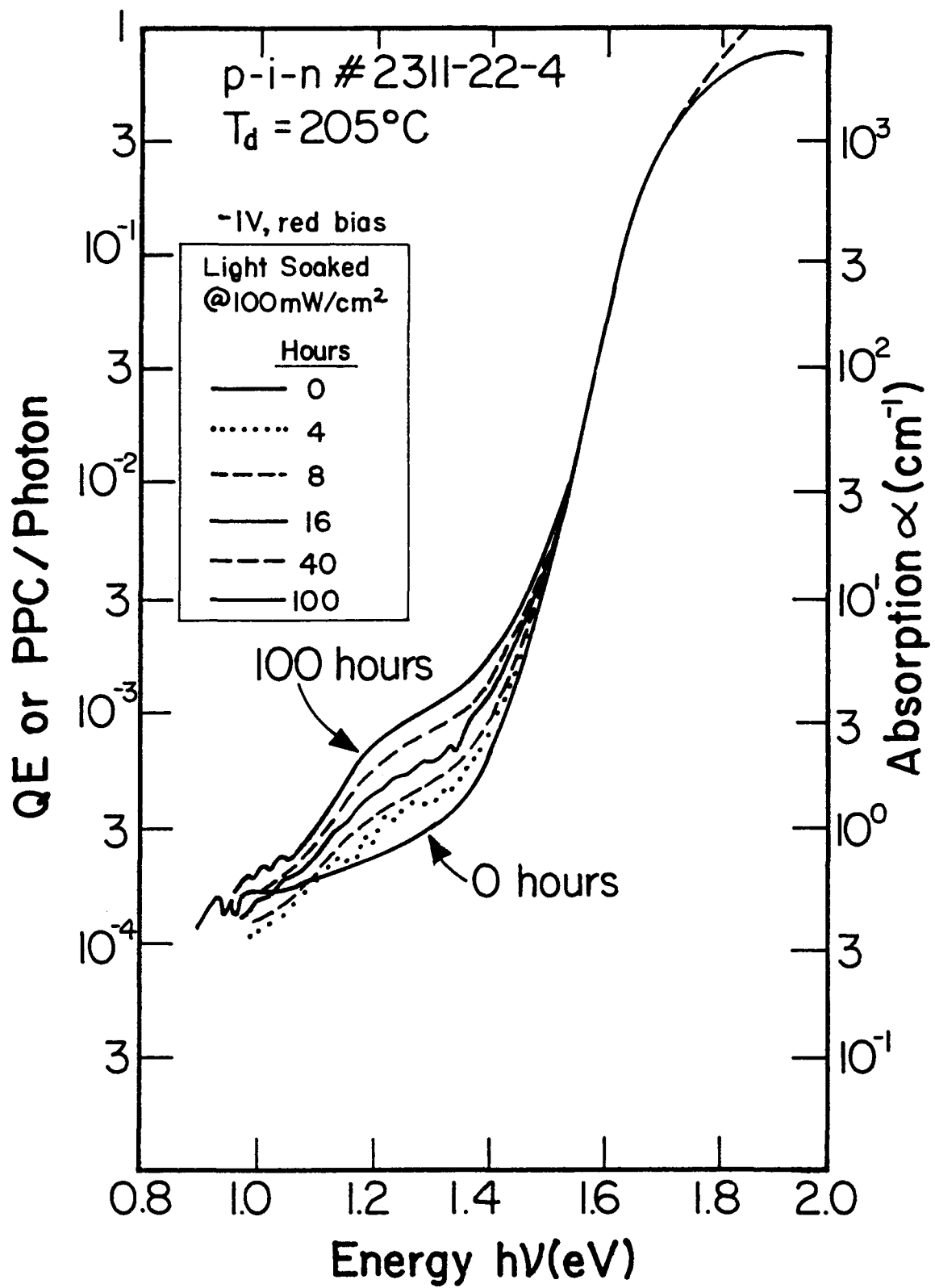


Figure 3. Sub-band gap  $\alpha(E)$  spectra for p-i-n cell  
 at various intervals during 100 hour  
 light soak.

**Title: Research on Amorphous Silicon-Germanium Alloys for Tandem Solar Cells**

**Organization:** Division of Applied Sciences, Harvard University, Cambridge, MA

**Contributions:** William Paul, principal investigator

## **Objectives**

The objectives of the work performed during fiscal year 1988 were (1) to carry out additional measurements on the structure of a-Si:H, a-Ge:H, a-Si<sub>1-x</sub>Ge<sub>x</sub>:H and a-Si<sub>1-x</sub>Ge<sub>x</sub>:H:F by differential scanning calorimetry, transmission electron microscopy and gas evolution, to complete measurements on the mobility-lifetime product and to write up and publish a full archival account of this research, (2) to continue an in-depth study of a-Ge:H prepared by r.f. glow discharge so as to discover the parameter values optimizing this end component of the a-Si<sub>1-x</sub>Ge<sub>x</sub>:H alloy series, (3) to collaborate with Professor Richard Norberg of Washington University in the preparation of films of a-Si and a-Ge containing deuterium, so that the Norberg laboratory can study deuteron magnetic resonances, which may be interpreted to give information on the microstructure of films on a 100 Å scale, (4) to continue a collaboration with Dr. K. L. Narasimhan of the Tata Institute, Bombay, India, on the properties of Schottky barriers to a-Si and like material, and (5) to continue a collaboration with Dr. M. L. Theye of the Laboratoire d' Optique, Paris, France, designed to explore low photon energy absorption spectra determined either by photothermal deflection spectroscopy or by steady state photoconductivity.

## **Approach**

The films required were made by r.f. glow discharge (1). The measurements made included conductivity versus temperature, optical absorption in the band-gap and sub-band-gap region of the spectrum, optical vibrational absorption in the infrared region, photoconductivity spectra, photoluminescence spectra, Raman spectra, transient photoconductivity (time-of-flight), gas evolution, transmission electron microscopy, differential scanning calorimetric spectra and deuteron magnetic resonance.

## **Discussion**

We have extended our investigation of a comparison of the properties of Si-Ge alloys produced alternatively from hydrides or fluorides, and published the results (2). We concluded, *inter alia*, that improvement in the photoelectronic properties of alloys of a-Si<sub>1-x</sub>Ge<sub>x</sub>:H would be helped by a better understanding of the properties of a-Ge:H, particularly the structural properties. Our research on a-Ge:H has involved measurement of the range of properties listed above on samples prepared with substrate temperature, r.f. power, H<sub>2</sub> dilution of the plasma and D.C. bias as preparation parameters subjected to systematic variation (3). Our collaborations with Professor Norberg and Dr. Narasimhan have produced new information on different microstructures of a-Si:H and a-Ge:H and their alloys (4) and on the current transport in a-SiGe alloy Schottky barriers (5). The collaborative work with Dr. M. L. Theye's group has proceeded to the development of a method to establish the location in amorphous samples of sub-band-gap optical absorption, specifically whether it occurs at the air-sample interface, in the bulk of the sample, or at the

sample-substrate interface. Such studies have obvious importance for the discovery of poor surfaces and poor interfaces in device structures.

## Future Research

The focus of our research in the immediate future (apart from our continuing collaborative programs) will be our attempts to discover why a-Ge:H has poorer photoelectronic properties than a-Si:H. The work to date has established that relatively high temperatures are required to produce films of high mass density which do not pick up contaminants from atmospheric gases after deposition, but that unfortunately the defect compensation in such films is not adequate. We shall therefore proceed on two fronts (1) to examine the consequences of preparation from plasmas strongly diluted with an inert gas, such as He, or containing an etchant such as  $\text{GeF}_4$ , and (2) the construction of a new apparatus capable of permitting studies of the plasma and plasma-surface interactions in processes not only of r.f. glow discharge, but also of photo-CVD. During this research examination of the films produced by electron microscopy, gas evolution and differential scanning calorimetry will be emphasized.

## References

1. Mackenzie, K. D., J. R. Eggert, D. J. Leopold, Y-M. Li, S. Lin and W. Paul, *Phys. Rev. B* **31**, 2198 (1985).
2. Mackenzie, K. D., J. H. Burnett, J. R. Eggert, Y-M. Li and W. Paul, *Phys. Rev. B* **38**, 6120 (1988).
3. Annual Report on Subcontract No. XB-7-06071-1, SERI/STR-211-3351 (May 1988).  
Annual Report on Subcontract No. XB-7-06071-2, period 1987-1988. Submitted December, 1988.
4. Annual Report on Subcontract No. XB-7-06055-1, period 1987, (December 1987).
5. Submitted to *J. Appl. Phys.* by D. K. Sharma, K. L. Narasimhan, S. Kumar, B. M. Arora, W. Paul, and W. A. Turner.

Title: Structure of Amorphous Silicon Alloy Films

Organization: Department of Physics, Washington University, St. Louis, Missouri

Contributors: R. E. Norberg and P. A. Fedders, principal investigators

The principal objective of this work has been to improve our understanding of the structure of amorphous silicon-germanium alloy films by means of joint theoretical and experimental approaches to the correlation of results of nuclear magnetic resonance, electron spin resonance, transmission electron microscopy, and other measurements. A major focus of the work is the examination of significant rearrangements of hydrogen that take place under various deposition and postdeposition conditions.

### Approach

Deuteron magnetic resonance (DMR) has been used to examine the structure of plasma-deposited film samples of a-Si:D,H; a-Si:D; a-Ge:D,H; and a-SiGe:D,F prepared [1] at Harvard by W. Paul and W. Turner. The results have been compared with DMR data obtained in samples provided by other laboratories including Xerox PARC (J. B. Boyce, et al.) and Xerox Webster (S. Kaplan, F. Jansen, and M. Machonkin). Table 1 lists plasma deposition parameters and DMR spin counts for some of the samples. DMR resolves and quantifies spectral components for tightly bound deuterium (TBD), weakly bound deuterium (WBD), rotating silyl groups, molecular D<sub>2</sub> and HD in microvoids, and molecular D<sub>2</sub> and HD isolated in reconstructed monovacancies. Calculations concerning strain effects on defect states are compared with electron spin resonance results.

### Silyl Rotors

Figure 1a shows 9K DMR spectra in a-Si:D,H (XPI) at five different pulse recovery times ranging from 0.005 to 1000 sec. At long recovery times the spectra show the 66 kHz doublet associated with tightly bound SiD (TBD) configurations and also a narrow central (NC) line arising from molecular D<sub>2</sub> and HD in microvoids. As the recovery time is decreased the SiD doublet saturates down and a fast-relaxing 22 kHz inner doublet becomes visible. This new signal arises from deuterated silyl groups [2] rotating rapidly compared to 22 kHz. The silyl signal finally vanishes at 0.01 sec, where a small molecular deuterium signal still remains. We conclude that the rotating groups must extend into spaces between microcrystalline inclusions. The 22 kHz silyl signal also is observed in a-SiD sample XW895 but is not observed in high quality a-Si films where TEM studies fail to show a microcrystalline component.

### Microvoids

A novel probe of microvoids is provided (Fig. 1b) by a 75.7 kHz DMR doublet characteristic of para-D<sub>2</sub> molecules whose molecular  $\Delta M_J$  rate has slowed to less than the 26 kHz intramolecular coupling frequency. The doublet is particularly clear in a-Ge where the 58 kHz TBD GeD doublet is well-resolved from the 75.7 kHz doublet for pD<sub>2</sub> contained in microvoids and vacancies. In bulk normal deuterium the 75.7 kHz doublet does not appear above 0.3 K. It is visible in a-Si and a-Ge up to about 50 K in unannealed samples and arises from the presence of large static electric field gradients (EFG) originating from the nearby Si or Ge matrix.

Figure 2 shows 30 K DMR spectra at two pulse recovery times in a high quality a-Si:D,H sample (H541). In the 0.6 sec spectrum the 66 kHz TBD SiD doublet has been saturated out leaving behind a two component central signal. There is a broad 40 kHz FWHM gaussian line and on top of that a narrow central line associated with molecular HD and D<sub>2</sub> contained in microvoids. It is to be noted that in this high quality film no more than about 6% of the 0.1 at% (or 60 ppm) molecular deuterium is located in microvoids with a characteristic dimension larger than 4 Å.

The line width of the narrow central line varies with temperature. However the width of the larger 40 kHz line is independent of temperature at least up to 100K. This broad line corresponds to 94% of the molecular deuterium present and reflects HD and D<sub>2</sub> molecules isolated and weakly bound in reconstructed monovacancies.

### Reconstructed Monovacancies

We have detected novel DMR solid echo signals arising from single HD and ortho-D<sub>2</sub> molecules, which we believe are weakly bound in reconstructed monovacancies in a-Si. Figure 2a shows three echoes which occur in high quality a-Si:D,H (H541) between 4.2 and 200 K. The echoes occur at times 1.210 $\tau$ , 2 $\tau$ , and 2.790 $\tau$ ; where  $\tau$  is the separation of the two rf pulses. The intensities of the outer satellite echoes indicate the amount of isolated HD molecules whose translational and rotational motions are restricted on a time scale of several milliseconds. The intramolecular HD parameters determined from molecular beam studies predict the occurrence of the satellite echoes at times (indicated by the inner vertical lines) some 4% different than observed. The difference arises from, and is a measure of, the electric field gradients associated with the surrounding a-Si matrix. We know that the containing monovacancies are reconstructed because the presence of a nearby dangling bond would prevent the observation of the echoes by shifting and smearing the phase recovery times.

Figure 2b shows ortho-D<sub>2</sub> solid echoes observed in perdeuterated a-Si:D (XW895). The auxilliary echoes occur at times 1.86 $\tau$  and 2.16  $\tau$  and arise from ortho-D<sub>2</sub> isolated in reconstructed monovacancies. The beats on the central 2 $\tau$  echo arise from the 75.7 kHz doublet (Fig. 1b) for frozen out para-D<sub>2</sub> molecules.

The amplitudes of the various solid echoes provide quantitative measures (Table I) of the HD and D<sub>2</sub> populations constrained in vacancies.

### Dangling Bonds and Floating Bonds

We have continued to investigate various aspects of the defect levels observed in the gap of a-Si. This is the primary charged defect in a-Si and there presently is a controversy [3-9] over whether the state is a 3-fold coordinated dangling bond state or a 5-fold coordinated floating bond state. Besides resolution of this controversy, it is important to obtain the fullest possible knowledge of this important defect state which can limit the electrical mobility of samples.

Our earlier calculations dealt with defect states in rather ideal configurations. However, in a-Si even 4-fold coordinated sites are not all identical, let alone defect sites. Typical bond angle distortions in a-Si are 5 to 10 degrees and one should expect distortions of at least this much (and possibly much more) about any defect. Our major result is that the energy level (in the gap) is quite strain dependent for the dangling bond but not for the floating bond. A strain broadened line is consistent with experimental results. Our calculations also show that the wave function of the dangling bond defect is relatively independent of strain but that the wave function of the floating bond defect is quite strain dependent. This should lead to a considerable strain broadening of the ESR hyperfine line for the floating bond which is not observed [10]. We conclude that the experimental data heavily favor the dangling bond.

### Conclusions

DMR provides quantitative measures of at least seven different D components in amorphous semiconducting films (tightly bonded D, weakly bonded D, silyl rotors, microvoid-contained D<sub>2</sub> and HD, frozen out p-D<sub>2</sub>, vacancy-isolated HD and o-D<sub>2</sub>. These components are being examined as a function of sample preparation conditions, post-deposition anneals, and illumination sequences. We seek to correlate structural changes with photo conversion efficiency and with light-induced metastabilities.

We have determined that:

- high quality a-Si:D,H has no more than 60 ppm molecular deuterium in microvoids larger than 4 $\text{\AA}$ .
- some less than highest quality a-Si:D,H samples have microcrystalline inclusions indicated by the presence of silyl rotors.
- in high quality a-Si:D,H most of the molecular deuterium is present as single molecules trapped in reconstructed monovacancies. This fraction appears to be mobile near room temperature.
- dangling bonds are a much more likely defect in a-Si than are floating bonds.

## References

1. K. D. Mackenzie, J. R. Eggert, D. J. Leopold, Y. M. Li, S. Lin, and W. Paul, Phys. Rev. B **31**, 1985, p. 2198.
2. P. Santos-Filho, M. P. Volz, and R. E. Norberg, Bull. Am. Phys. Soc. **33**, 663 (1988).
3. S. T. Pantelides, Phys. Rev. Lett. **57**, 2979 (1986).
4. S. T. Pantelides, Phys. Rev. Lett. **58**, 2825 (1987).
5. J. H. Stathis and S. T. Pantelides, Phys. Rev. B **37**, 6579 (1988).
6. P. A. Fedders and A. E. Carlsson, Phys. Rev. Lett. **58**, 1156 (1987), and Bull. Am. Phys. Soc. **33**, 228 (1988).
7. M. Stutzmann, Z. Phys. Chem. Neue Folge **151**, 211 (1987).
8. J. C. Phillips, Phys. Rev. Lett. **58**, 2824 (1987).
9. S. T. Pantelides, Phys. Rev. Lett. **60**, 1683 (1988).
10. M. Stutzmann and D. Biegelsen, Phys. Rev. Lett. **60**, 1082 (1988).

Table I. DMR Spin Counts (at.%) in Semiconductor Films

ID	Type	Power	T(C)	Flow (sccm)	P (torr)	N(D)	TBD	WBD	Doublet pD <sub>2</sub>	Echo oD <sub>2</sub>	Echo HD
H480	Si:D,H	10 W	230	SiH <sub>4</sub> 4 D <sub>2</sub> 75	0.7	4	2.9	0.9	<0.2		
H511	Ge:D,H	8W	260	GeH <sub>4</sub> 1 D <sub>2</sub> 40	0.95	1.3	0.5		← 0.8 →		
H541	Si:D,H	10 W	230	SiH <sub>4</sub> 4 D <sub>2</sub> 76	0.7	4.0	3.8	0.1	0.02		0.1
H579	Si:D	2.5W	230	SiD <sub>4</sub> 20	0.2						
XW895	Si:D	375 W	230	SiD <sub>4</sub> 200	0.25	23	19	1	3		
XP29	Si:D	15 W	230	SiD <sub>4</sub> Ar		10.3	8.2	2.1	0.05		

Figures 1a and 1b. DMR line shape components in a-Si and a-Ge.

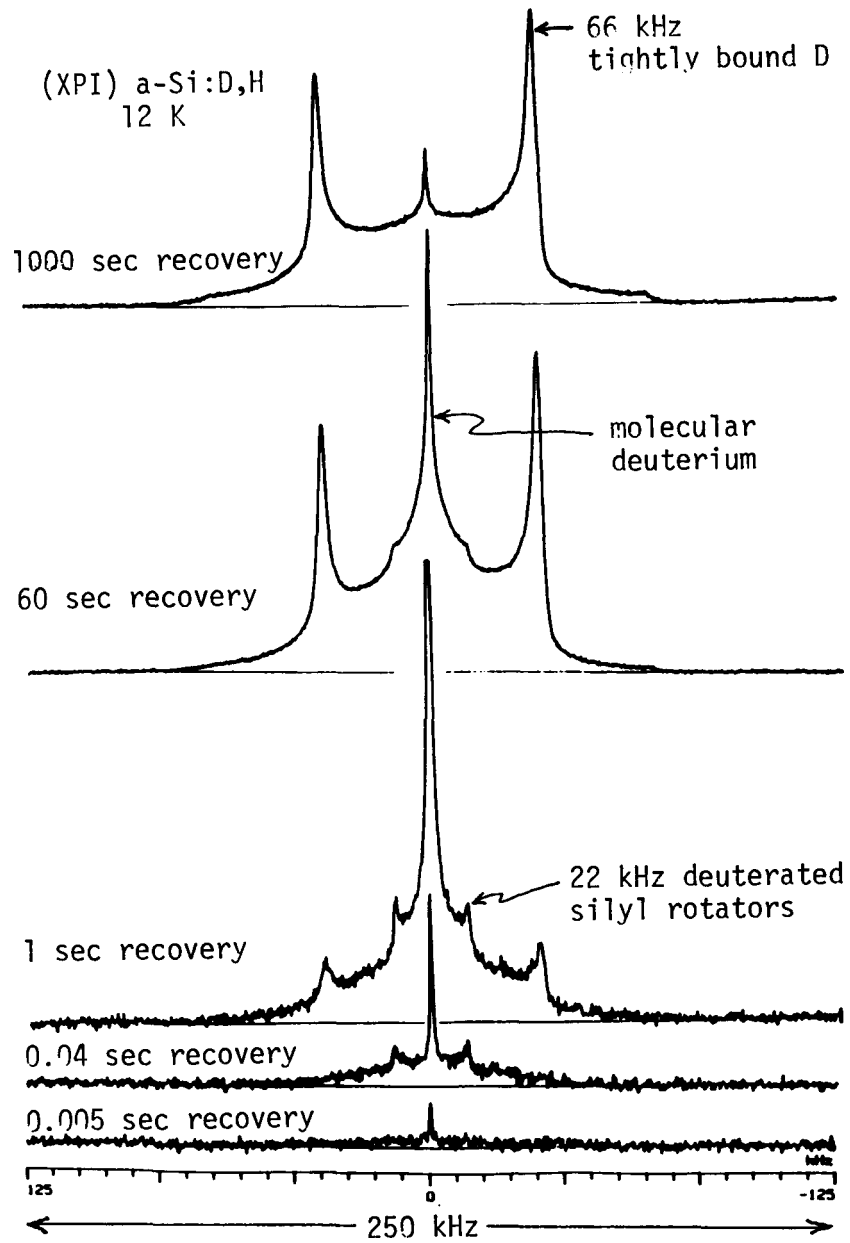


Figure 1a.

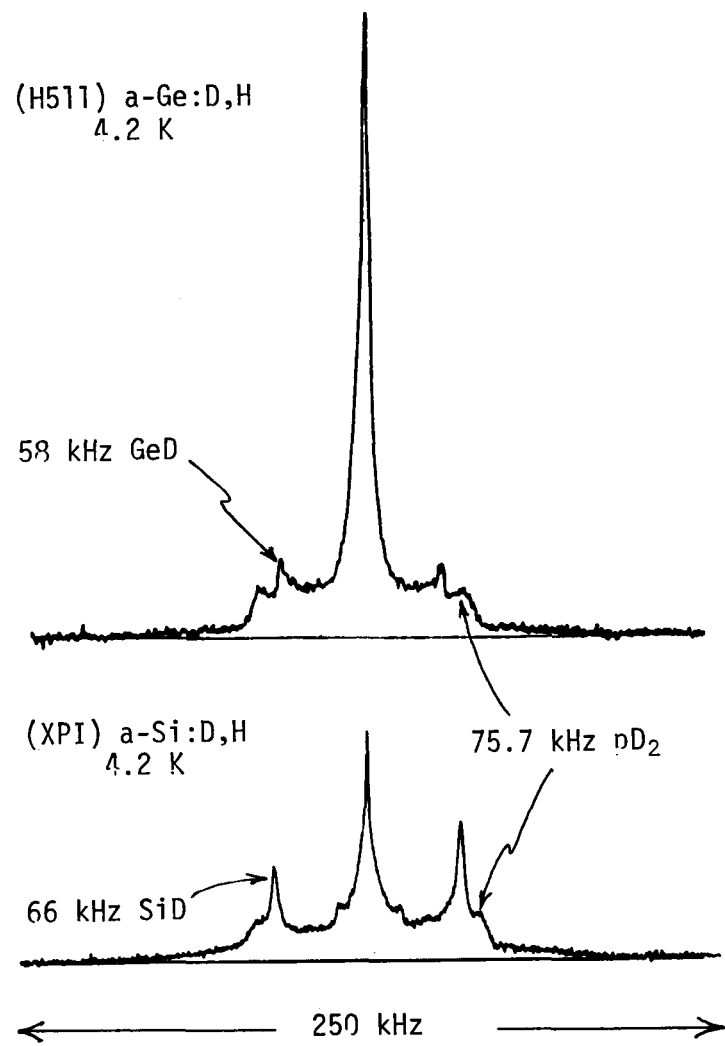


Figure 1b.

(H541) a-Si:D,H  
30 K

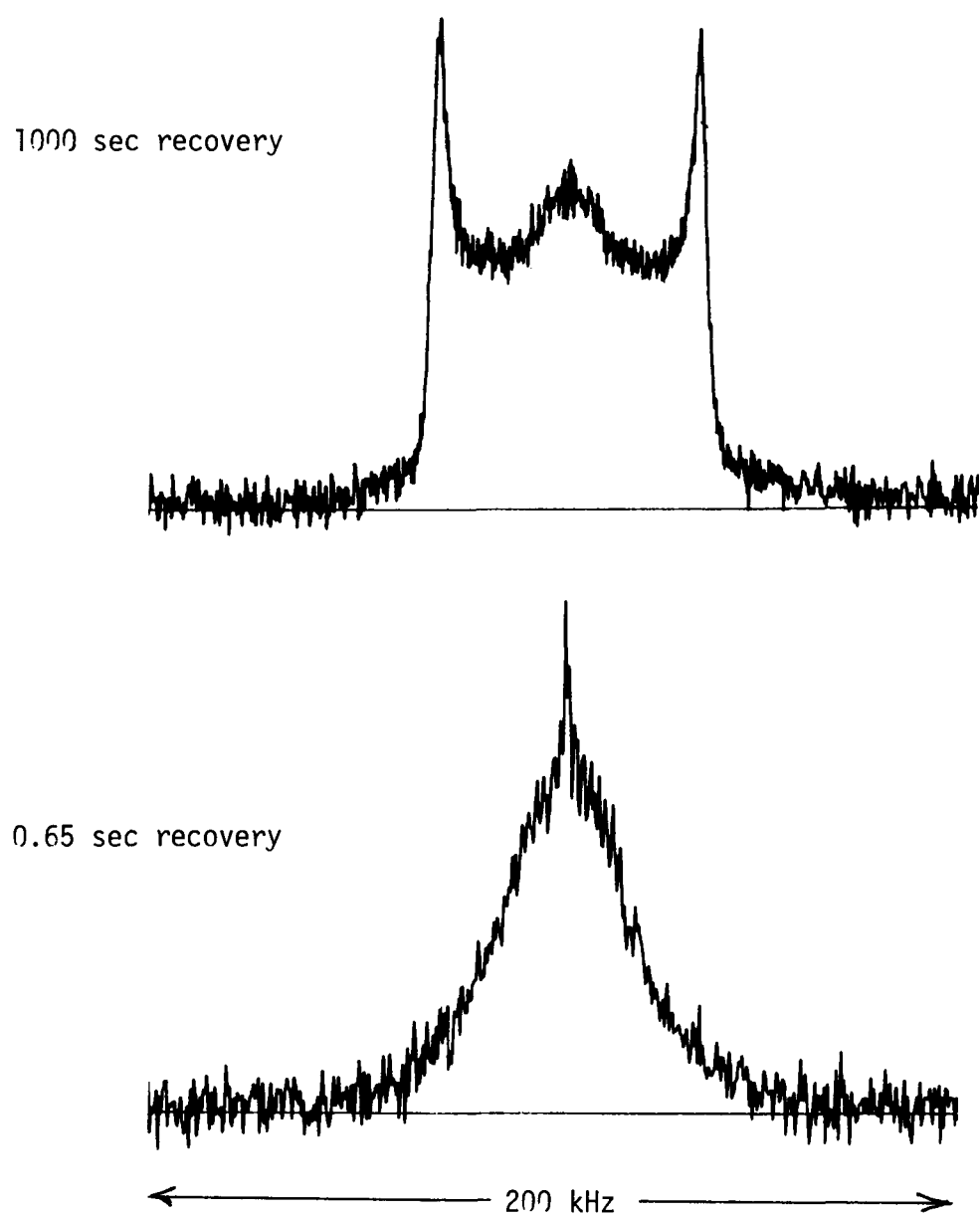


Figure 2.

Nearly recovered and partially-saturated DMR line shapes at 30 K in a-Si:D,H (H541). The broad central 40 kHz FWHM feature arises from single molecules of D<sub>2</sub> and HD weakly bound in reconstructed monovacancies. At the center the small narrow spike arises from a much smaller population of D<sub>2</sub> and HD in microvoids.

(H541) a-Si:D,H  
20 K

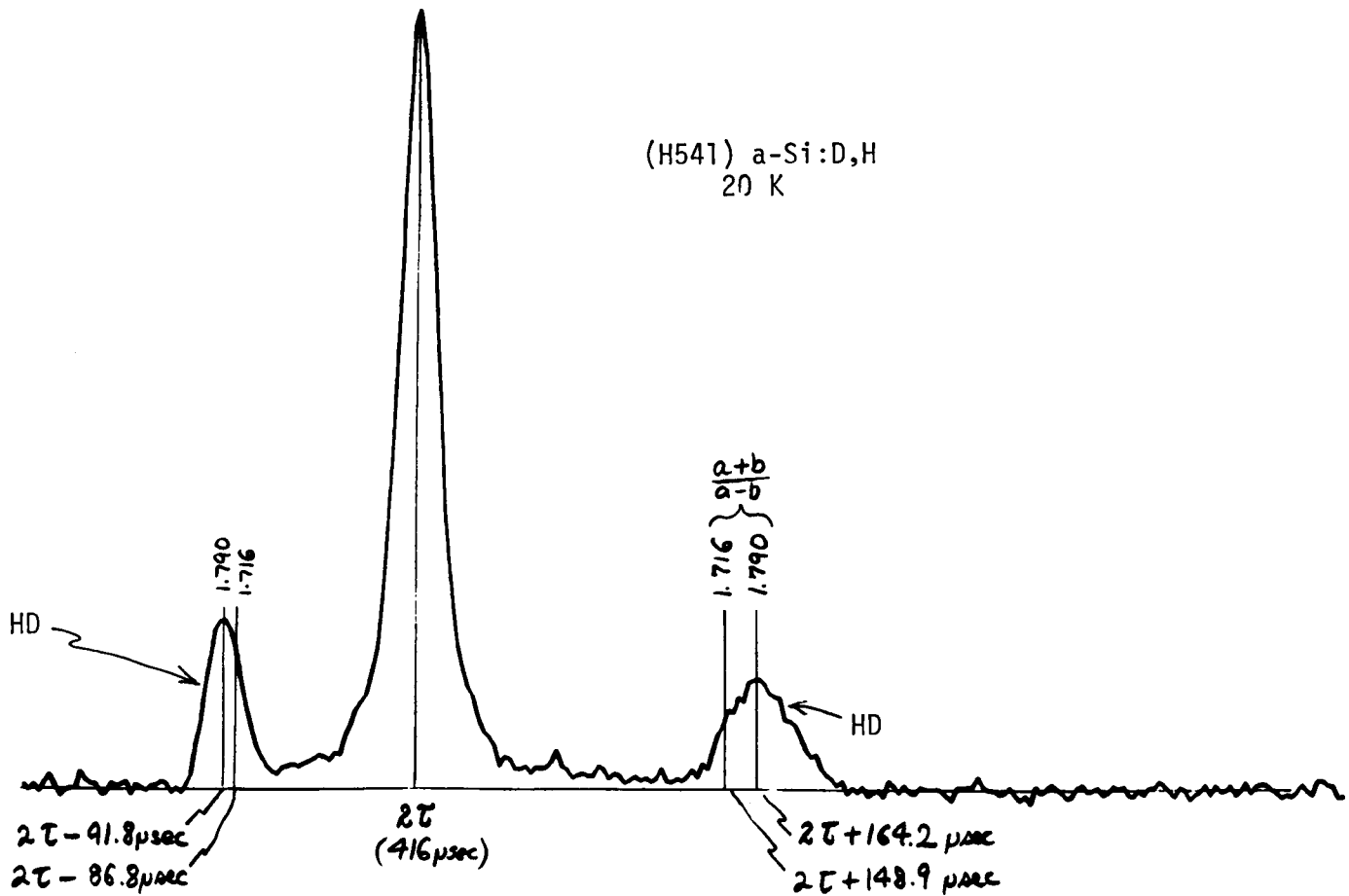


Figure 3a. Solid echoes from HD singles isolated in reconstructed monovacancies in a-Si.

(XP895) a-Si:D  
4.2 K

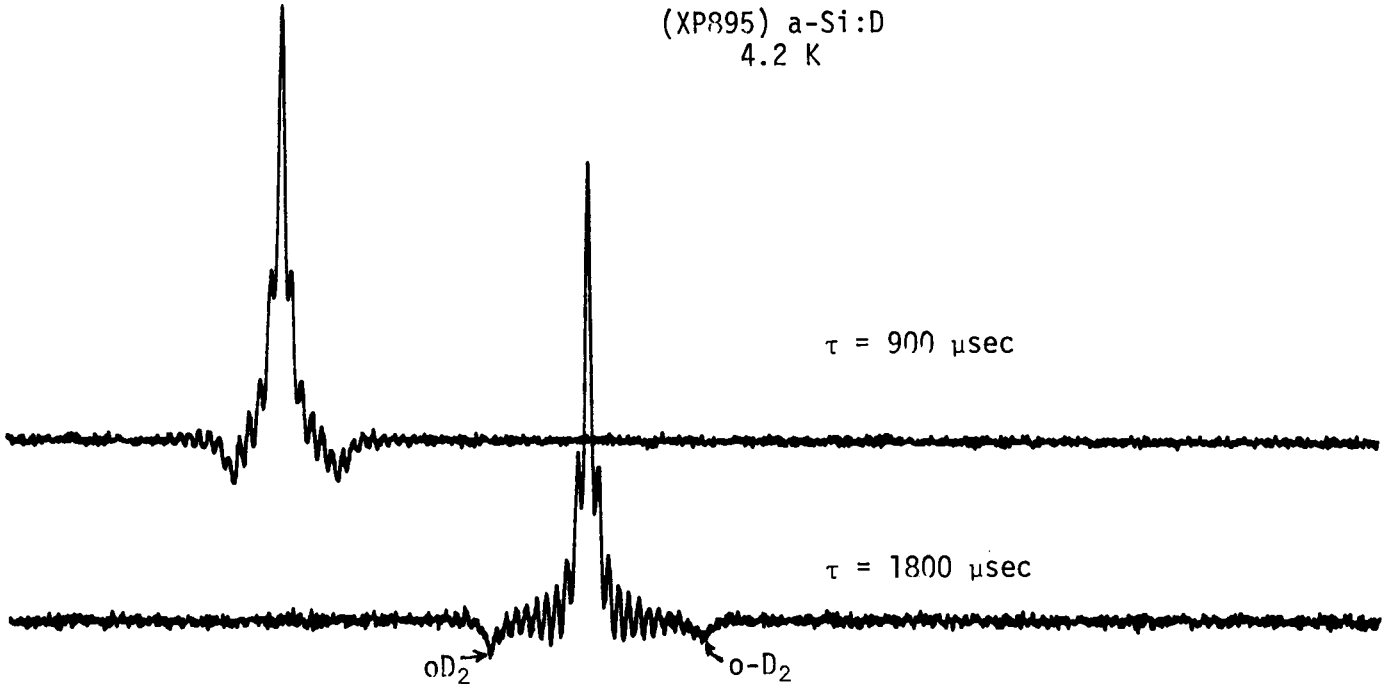


Figure 3b. Solid echoes from o-D<sub>2</sub> singles isolated in reconstructed monovacancies in a-Si.

**Title:** Deposition, Characterization and Optimization of Optically Transparent Films

**Organization:** Department of Chemistry, Harvard University, Cambridge, Massachusetts

**Contributors:** R. G. Gordon, principal investigator; J. Proscia, K. Gustin, J. Chapple-Sokol, D. Strickler, R. McCurdy and J. Hu

Transparent conducting materials are essential components of thin-film solar cells, in which they serve as front-surface electrodes. In tandem cells, back surface electrodes also need to be transparent. Finally, some designs for highly reflective back contacts also call for a transparent conducting layer. The compositions of these transparent conducting layers are usually based on oxides of tin, indium and/or zinc, and are hence referred to as transparent conducting oxides (TCO). In addition to having low electrical resistance and low optical absorption, the structure of a TCO must minimize reflection losses. The TCO must also resist degradation during cell fabrication and use. Finally, the method for making the TCO must be inexpensive and safe.

## Objectives

The general objectives are to improve the performance of TCO materials and the methods for their production. We aim to reduce their electrical resistance, optical absorption and reflection losses, and to avoid degradation of the materials. For the production method, the prime consideration is to deposit the TCO layers at a high rate with relatively simple apparatus.

## Approaches Taken

We have concentrated our attention primarily on tin oxide and zinc oxide, since indium oxide is too expensive for large-scale use in solar cells. Alternative materials, such as amorphous silicon-carbon and silicon-nitrogen alloys, and titanium oxide, were considered, but rejected because their performance is considerably inferior to tin oxide and zinc oxide.

As a preparation method, we used primarily chemical vapor deposition (CVD), since we have shown that high deposition rates are obtainable by CVD. When operated at atmospheric pressure, CVD requires only simple equipment which is commercially available and capable of large-area coating.

## Results for Electrical Conductivity of Tin Oxide

The electrical resistance of fluorine-doped tin oxide has been found to decrease as the deposition temperature increases. This improvement appears to result from two different effects: (1) At higher deposition temperatures, larger crystallites are formed, presumably because of greater mobility of the adsorbing species on the surfaces of the growing crystallites. Since there are fewer grain boundaries when the crystallites are larger, there is less scattering of the electrons by the grain boundaries, and hence lower electrical resistance. (2) At higher deposition temperatures, a larger fraction of the fluorine atoms were found to contribute a free electron to the conduction band, and a smaller proportion of the fluorine atoms are electrically inactive. The inactive fluorine atoms are deleterious to the electrical and optical properties, since they scatter electrons and thus reduce the electrical conductivity and increase the optical absorption. Apparently at higher deposition temperatures the greater mobility of the adsorbed fluorine atoms allows more of them to reach proper sites in the lattice where they substitute for oxygen atoms and become electrically active.

Higher deposition temperatures are not an unmitigated blessing, however, since they promote diffusion of sodium from the usual low-cost sodium-containing glass substrates into the TCO. The resulting sodium in the film increases the resistance by increasing the electron scattering. Sodium in the TCO is also thought to contribute to long-term instability to thin-film solar cells. Therefore, we have investigated sodium barriers which would reduce the diffusion of sodium from glass substrates into the TCO.

Films of silica<sup>1</sup> and of alumina<sup>2</sup> were deposited by CVD on glass substrates, and examined for their effectiveness as barriers to diffusion of sodium from the glass into tin oxide layers on top of the SiO<sub>2</sub> or Al<sub>2</sub>O<sub>3</sub>. Silica, the most commonly used barrier layer, proved to be a somewhat leaky barrier, transporting about 20% to 50% as much as sodium as no barrier, with the amount of leakage depending on the thickness of the barrier and time allowed for diffusion. The CVD alumina barriers were ideal, with no measurable sodium permeation.<sup>3</sup>

### Reflection Losses and Rough TCO Layers

A textured TCO surface reduces the loss of light by reflection from a solar cell, and thus improves the efficiency. We produced by CVD tin oxide layers with various amounts of roughness, and then deposited conventional amorphous silicon cells on these TCO layers. Variations in the CVD conditions gave different types of surface structures. The highest efficiencies were found for TCO layers which showed about 5 to 10% diffuse light scattering.<sup>4</sup> One mechanism that contributes to the growth of rough films by CVD, is a natural instability of the diffusion of the material through the vapor phase up to the surface of the growing film. A theory of this growth instability was developed, which shows how the length scale of the roughness is related to fundamental (but usually unknown) properties.<sup>5</sup>

### Degradation of TCO

Tin oxide films can be partly reduced by the hydrogen plasma conventionally used to deposit amorphous silicon cells. The tin thus released can diffuse into the amorphous silicon, causing degradation of cell performance. Several groups have shown that zinc oxide is more resistant to such reduction and degradation. Therefore we made some composite TCO layers by depositing a thin layer (~100 nm) of zinc oxide on top of a thicker layer (~600 nm) of tin oxide. Solar cells grown on this composite TCO showed improved performance compared to control ones without the zinc oxide. This improvement was observed despite the fact that this zinc oxide was nominally undoped, and thus had a fairly high bulk resistivity.

### Conclusions

Efficient transparent electrodes for solar cells can be formed from CVD tin oxide. Its performance has been optimized by choice of deposition conditions, protection from sodium diffusion by an alumina barrier, and protection from degradation during silicon deposition by a zinc oxide protective layer. Current work is directed to producing an entire TCO layer of zinc oxide by atmospheric pressure CVD. Since zinc is a less expensive and more abundant metal than tin, such a substitution has the potential to reduce the cost of solar cells.

## References

1. Chapple-Sokol, J.D. and R. G. Gordon, Thin Solid Films (to be published)
2. Gustin, K. M. and R. G. Gordon, J. Electronic Materials **17**(6), 1988, p. 509
3. Chapple-Sokol, J.D. and R. G. Gordon, submitted for publication.
4. Gordon, R. G., J. Proscia, F. B. Ellis, Jr., and A. E. Delahoy, Solar Energy Materials (to be published)
5. Palmer, B. J. and R. G. Gordon, Thin Solid Films **158**, 1988, p. 313

Title: Research on Material Properties of Device Quality Amorphous Silicon Deposited at High Deposition Rates Using Higher Order Silanes

Organization: Glassstech Solar, Inc., Wheat Ridge, Colorado, USA

Principal Investigator: Arun Madan

Research  
Contributors: H. Chatham, P.K. Bhat, C. Marshall, C.E. Matovich, A. Benson, J. Sandwisch

The major objectives of this program are to obtain improvements in the material properties of intrinsic amorphous silicon films deposited from higher order silanes at high deposition rates (up to 2.0 nm/s) and to achieve in FY 1989 an AM1.5 conversion efficiency of at least 9% over an area of 1 cm<sup>2</sup> with an amorphous silicon p-i-n solar cell fabricated at 2.0 nm/s using disilane. We have increased the deposition rate in disilane by increasing the rf power at 13.56 MHz (2.0 nm/s is achieved at ~60 mW/cm<sup>3</sup>) and by utilizing higher excitation frequencies (13.56 - 110 MHz). The general approach to achieving the objectives is to optimize intrinsic layer material properties with respect to discharge conditions with the assistance of plasma diagnostic measurements using optical emission spectroscopy and mass spectrometry. Devices are fabricated using the optimized intrinsic layers and then the p and n layer deposition conditions are altered to obtain optimum device performance.

### 1. Amorphous Silicon Materials Research

We have studied the influence of electrode separation on materials at three separations over a 40% range in disilane for a constant pressure-electrode separation product of 0.4 Torr-cm and deposition rates between 0.4 and 2.0 nm/s. Under these conditions, it appears that there is a small but significant advantage to using smaller separations. While the electrode separation has no apparent influence on the power density dependence of the light conductivity and the fraction of SiH<sub>2</sub> groups, the diffusion length for holes under light bias as measured by the surface photovoltage technique is ~30% larger at the smaller separation than at the larger separations. Furthermore, both the hydrogen content as determined from infrared absorption measurements in the 1900 - 2200 cm<sup>-1</sup> range and the band gap are reduced by decreasing the electrode separation.

We have also studied the influence of discharge excitation frequency on the properties of materials deposited from silane and disilane. The results show that the deposition rate increased monotonically with increasing frequency for constant power density in both silane and disilane

over the range 13.56 to 110 MHz (Fig. 1), in contrast to the results of Curtins et al<sup>1</sup> who observed a maximum in deposition rate at 70 MHz in silane. Comparison of films deposited at various deposition rates by changing the rf power density with those prepared by increasing the excitation frequency indicates that the dependence of material properties such as the light and dark conductivities and the dark conductivity activation energy is roughly independent of the method of increasing the deposition rate.

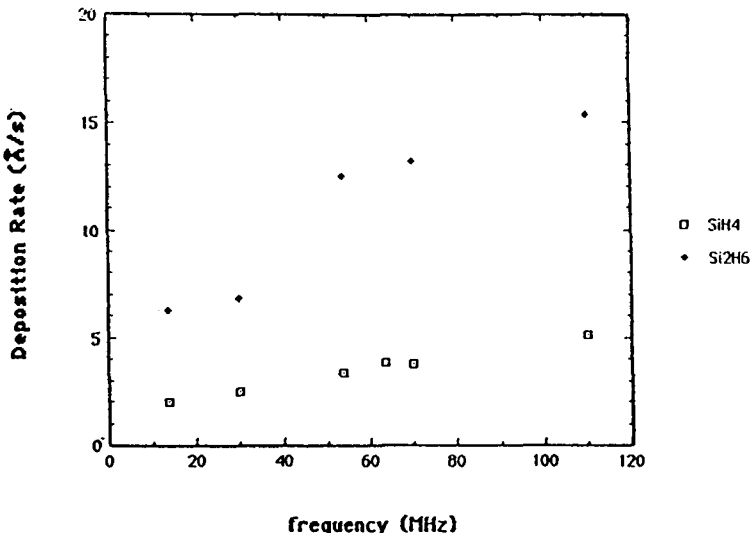


Figure 1 The dependence of the deposition rate on the excitation frequency in silane and disilane rf discharges.

## 2. Solar Cell Research

Device research during Phase II has focused on achieving a p-i-n device deposited at 2.0 nm/s with an AM1.5 efficiency of 9%. The best efficiencies achieved to date using 13.56 MHz rf discharges are 9% at 1.0 nm/s (Fig. 2) and an 8% device at 1.7 nm/s (Fig. 3). The first device fulfilled contract requirements for Phase I of this project.

Recent work has focused on the fabrication of devices using 110 MHz rf discharges to deposit the intrinsic layer. In accordance with materials results, the performance of devices fabricated at 2.0 nm/s and 110 MHz is comparable to the performance of devices fabricated at 2.0 nm/s using 13.56 MHz. At present, the best device result using 110 MHz is a device with 7.7% efficiency at 2.7 nm/s.

The major difficulties encountered in fabricating devices at high deposition rates from disilane are: 1) the necessity of working at high deposition temperatures (240-300°C) in order to obtain adequate optoelectronic properties for intrinsic layers deposited from disilane results in increased recombination at the p/i interface and, 2) transport properties are typically not as good in disilane films deposited at high deposition rates as in silane films deposited at low deposition rates. We are continuing to work toward reducing the influence of these effects on device performance.

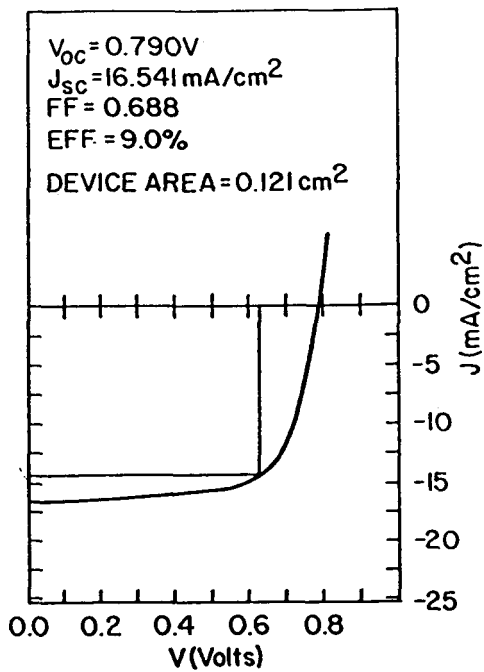


Figure 2 I-V characteristic of a device fabricated at 13.56 MHz using a disilane intrinsic layer deposited at  $\sim 1.0 \text{ nm/s}$ .

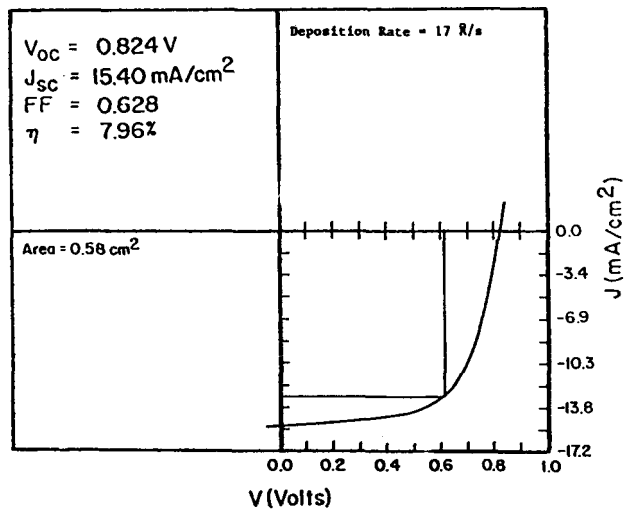


Figure 3 I-V characteristic of a device fabricated at 13.56 using a disilane intrinsic layer deposited at  $1.7 \text{ nm/s}$ .

### 3. Stability

We have completed some measurements of the effect of light soaking on devices fabricated from disilane at 0.7 nm/s and 1.9 nm/s. These results are shown in Figure 4. Stability appears to be slightly better than for silane devices fabricated at similar rates.

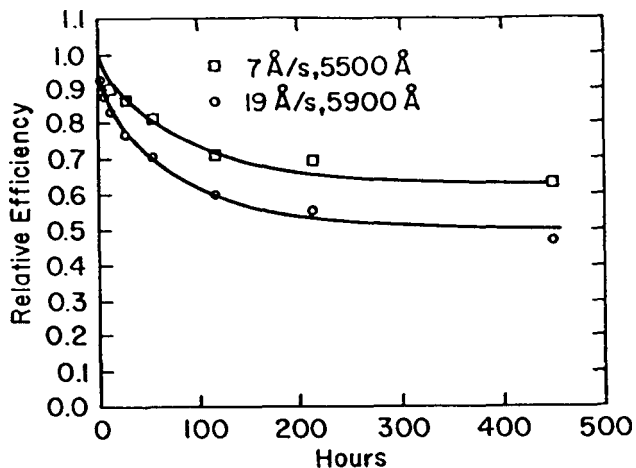


Figure 4 The dependence of efficiency on light soak time for device fabricated at 13.56 MHz using disilane intrinsic layers deposited at two deposition rates.

### Conclusions

Material properties show slight improvements as the electrode spacing is decreased. Furthermore, different methods of increasing the amount of dissociation in disilane discharges (frequency or power) have similar influences on the material properties. The efficiency of devices fabricated at high intrinsic layer deposition rates is limited by low absorption in the intrinsic films deposited at 2.0 nm/s and recombination at the p/i interface. However, it is possible to overcome these difficulties by careful optimization of device fabrication conditions.

### References

1. H. Curtins, N. Wyrtsch, and A.V. Shah, Electronics Letters 23, 228 (1987).

Title: Amorphous Silicon Photovoltaic Devices Prepared by Chemical and Photo-Chemical Vapor Deposition of Higher Order Silanes

Subtitle (Phase IV): Study of Microcrystalline Silicon-Carbon p-Layers Prepared by Photo-CVD and Glow Discharge

Organization: Chronar Corporation, Princeton, NJ 08542

Contributors: H. Schade, Principal Investigator; H. Chao, J. Kalina

Microcrystalline silicon (uc-Si:H) layers of both n and p-type exhibit high electrical conductivities, and are thus desirable as contact layers in p-i-n solar cell structures. Also, microcrystallinity has resulted in lower optical absorption and higher energy gaps, which makes p-type uc-Si:H a promising "window" layer material. Both rf glow discharge and photo-CVD methods have been applied to prepare uc-Si:H p and n-type materials. While there are a number of reports on using uc-Si:H n-layers in p-i-n cells, p-layers have been reported only recently [1,2]. The advantages of uc-Si:H have also been demonstrated in tandem-junction amorphous silicon-alloy cells [2,3], in which the use of highly conductive n and p-type uc-Si:H for the n/p junction resulted in lower resistances.

### Objectives

The objectives for phase IV of this subcontract were modified according to the subtitle: "Study of Microcrystalline Silicon-Carbon p-Layers Prepared by Photo-CVD and Glow Discharge". Specifically, the research goals during this year were

- \* to establish the preparation conditions for  $uc-Si_{1-x}C_x:H$  p-layers for both photo-CVD and rf glow discharge deposition methods,
- \* to apply these conditions to the incorporation of such layers into p-i-n solar cells, and
- \* to compare their performance.

### Properties of uc-Si:H

The preparation of uc-Si:H requires the following typical conditions that similarly apply to both photo-CVD [4] and rf glow discharge [5] deposition methods:

- \* high dilution ratio for silane or disilane in hydrogen, typically  $H_2/SiH_4 = 100$  for glow discharge, and  $H_2/Si_2H_6 = 60$  to 300 for photo-CVD,
- \* low deposition temperature, typically 100 to 200 °C,
- \* high rf power or UV intensity, typically 200 to 300 mW/cm<sup>2</sup> for glow discharge, 30 mW/cm<sup>2</sup> for UV intensity at a 3-cm lamp/substrate spacing.

A large flux of hydrogen atoms is believed to be the key to microcrystalline growth. The atomic hydrogen causes etching, which selectively removes

weak or strained Si-Si bonds, and thus results in the growth of microcrystalline material [6]. The high power densities, both rf power and UV intensity, obviously give rise to an increase in the atomic hydrogen that causes the etching.

The existence of microcrystallinity can be deduced from the following properties:

- \* electrical conductivity, 0.1 to  $>1$  S/cm,
- \* optical band gap,  $>2.0$  eV,
- \* Raman spectrum, a sharp crystalline TO mode at  $520\text{ cm}^{-1}$ .

The incorporation of uc-Si:H p-layers into p-i-n cell structures may require a protective layer [1] on the  $\text{SnO}_2$  substrate to avoid chemical reduction of the  $\text{SnO}_2$  during the initial phases of the deposition. This reduction [7] is considerably more severe under the high hydrogen dilution and high rf power or UV intensity required for microcrystalline growth. Furthermore, the initiation of microcrystalline growth may depend on the substrate material, and possibly is enhanced by some sort of a "seed" interlayer, like a-Si:H. Thus the optical and interface properties of the interlayer enter as additional parameters that need to be weighed against the microcrystalline p-layer properties to assess the ultimate solar cell performance.

### Deposition

Photo-CVD of both individual p-layers and whole p-i-n structures was performed in the previously described photo-CVD system [8]. For rf glow discharge deposition, this system was modified, by incorporating an electrode plate plane-parallel to the substrate surface. The main efforts were concentrated on the establishment of the deposition conditions for individual uc-Si:H p-layers. These conditions were then applied to the incorporation of such layers into p-i-n structures.

### Individual p-Layers

For the evaluation of microcrystallinity the depositions were made to a film thickness of about 100 nm on glass substrates. The dark conductivity in gap cell geometry was used to evaluate the microcrystallinity in the deposited films. While a-Si:H p-layers typically exhibit dark conductivities in the order of  $10^{-5}$  S/cm, microcrystallinity is indicated by dark conductivities larger than  $10^{-3}$  S/cm.

The optimization of the dark conductivity was conducted mainly for photo-CVD conditions. The dark conductivity was measured as a function of the main deposition parameters, namely temperature, pressure, flow rates and ratios, and film thickness. The deposition temperature has a major effect on the degree of microcrystallinity, and hence the dark conductivity. The highest conductivities (0.4 S/cm) were found for deposition temperatures between 190 and 200 °C (note that the actual substrate temperatures are estimated to be about 20 °C lower). The corresponding photo-CVD conditions are given below in Table I.

Also shown in this table are the deposition conditions for a uc-Si:H p-layer with a dark conductivity of 0.5 S/cm, obtained by rf glow discharge.

Table I: Deposition conditions for uc-Si:H p-layers, prepared by photo-CVD and rf glow discharge

Deposition conditions		Photo-CVD	Glow Discharge
Substrate heater	[°C]	200	190
Chamber pressure	[Torr]	1.76	1.00
H <sub>2</sub>	[sccm]	100	95
Si <sub>2</sub> H <sub>6</sub>	[sccm]	0.35	—
SiH <sub>4</sub>	[sccm]	—	0.32
He+2% B <sub>2</sub> H <sub>6</sub>	[sccm]	0.10	0.10
UV power	[mW/cm <sup>2</sup> ]	10	—
rf power	[mW/cm <sup>2</sup> ]	—	200

The films were also characterized by their optical band gaps determined from Tauc plots. Even without the incorporation of carbon, the optical gaps of uc-Si:H p-layers are found to range from 2.0 to 2.5 eV. As to be expected, the absorption coefficients at a chosen photon energy (2.48 eV) decrease with increasing gaps, typically from  $1.3 \times 10^5 \text{ cm}^{-1}$  at  $E_g=2.00 \text{ eV}$  to  $4.0 \times 10^4 \text{ cm}^{-1}$  at  $E_g=2.50 \text{ eV}$ . These data are summarized in Fig. 1. The scatter in the data is ascribed to the uncertainty in the film thickness. Furthermore, the measured relationship between the energy gaps and the slopes of the Tauc plots contains significant uncertainties, similar to those found by Cody et al. [9] in the range of lower gap values, which leads to additional uncertainties.

In preparation for the incorporation of microcrystalline p-layers into p-i-n cells, a comparison was made between the optical absorption of films deposited side-by-side onto glass and glass/SnO<sub>2</sub> substrates in three different deposition runs:

- \* under conditions for amorphous material,
- \* under conditions for microcrystalline material, with a-Si:H seed layer,
- \* under the same conditions, but without a-Si:H seed layer.

The results of this comparison are summarized in Table II.

The dark conductivity was studied as a function of the absorption coefficient (at 2.48 eV). Based on such a correlation, microcrystalline p-layers deposited onto SnO<sub>2</sub> substrates might be evaluated solely by optical measurements, without the need for conductivity measurements that are more difficult in the presence of the conducting SnO<sub>2</sub> substrate, compared to the gap cell arrangement on glass. As shown in Fig. 2, the dark conductivity of p-type uc-Si:H, in fact, increases with decreasing absorption coefficient, and according to Fig. 1, with increasing optical gap. However, the correlation found so far still contains large uncertainties that are caused by non-uniform film deposition (optical and electrical measurements were usually performed on different samples of the same deposition run). Such non-uniformities particularly affect the dark conductivity, which in a few cases was observed to differ by over an order of magnitude for samples of the same run.

Table II: Optical gaps and slopes, deduced from Tauc plots, and absorption coefficients (500 nm) for uc-Si:H p-layers deposited on glass and  $\text{SnO}_2$

Material	Energy Gap (eV)		Slope $(\text{cm}/\text{eV})^{-0.5}$		Absorption Coefficient $(10^5 \text{ cm}^{-1})$	
	glass	$\text{SnO}_2$	glass	$\text{SnO}_2$	glass	$\text{SnO}_2$
a-SiC:H	1.84	1.63	955	831	1.9	2.1
a-SiC:H/uc-Si:H	2.43	2.34	1288	1137	0.7	0.6
uc-Si:H	2.14	1.87	1074	760	1.1	0.9

In view of the incorporation of microcrystalline p-layers into p-i-n cells, we have investigated the conductivity as a function of the film thickness, using the optimum conditions established for 1-fringe films. Figure 3 shows that for thicknesses below about 50 nm (<0.5 fringe), the conductivity is considerably reduced. These results which apply to both photo-CVD and glow discharge films suggest that a certain film thickness is required, before microcrystalline regions are sufficiently large to support percolation for conduction. Even though the conductivity is about one order of magnitude lower for 0.5-fringe films, compared to 1 fringe, it is still a few orders of magnitude above typical values for p-type a-Si:H [10]. Note that we have no information yet, whether the conductivities measured in "horizontal" gap cell geometry also apply to "vertical" sandwich geometry, encountered in p-i-n structures.

### p-i-n Structures

A small number of p-i-n cells containing 40-nm thick uc-Si:H p-layers deposited on 2-nm thick a- $\text{Si}_{1-x}\text{C}_x\text{:H}$  seed layers was prepared by both photo-CVD and rf glow discharge by using the established growth conditions. So far, however, the I(V) data of these cells remained about equal to those of control cells with standard a- $\text{Si}_{1-x}\text{C}_x\text{:H}$  p-layers. Based on the absorption results shown in Table I, still thinner uc-Si:H p-layers are required for lower absorption; however, for the corresponding thickness the conductivity (Fig. 3) may hardly exceed that of a-Si:H p-layers. It thus appears that further optimization of uc-Si:H p-layer properties, or a- $\text{Si}_{1-x}\text{C}_x\text{:H}$  are required to find improved performance of p-i-n cell structures.

### References

1. Y. Hattori, D. Kruangam, K. Katoh, Y. Nitta, H. Okamoto, Y. Hamakawa, IEEE Photovoltaics Specialists Conference, New Orleans, 1987
2. S. Guha, J. Yang, P. Nath, M. Hack, Appl. Phys. Lett. 49, 218 (1986)

3. H. Sasaki, M. Aiga, M. Usui, K. Kawabata, T. Ishihara, S. Terazono, K. Sato, K. Okaniwa, T. Itagaki, G. Nakamura, Y. Yukimoto, K. Fujikawa, Photovoltaic Science and Engineering Conference, Beijing, 1986
4. S. Nishida, H. Tasaki, M. Konagai, K. Takahashi, J. Appl. Phys. 58, 1427 (1985)
5. G. Rajeswaran, P. E. Vanier, F. J. Kampas, R. R. Corderman, Mat. Res. Soc. Symp. Proc. Vol. 25 (1984), p.563
6. F. J. Kampas, J. Appl. Phys. 53, 6408 (1982)
7. H. Schade, Z E. Smith, J. H. Thomas III, A. Catalano, Thin Solid Films 117, 149 (1984)
8. see, e.g., A. E. Delahoy, Solar Cells 21, 153 (1987)
9. G. D. Cody, C. R. Wronski, B. Abeles, R. P. Stephens, B. Brooks, Solar Cells 2, 227 (1980)
10. H. Schade, Z E. Smith, A. Catalano, Solar Energy Materials 10, 317 (1984)

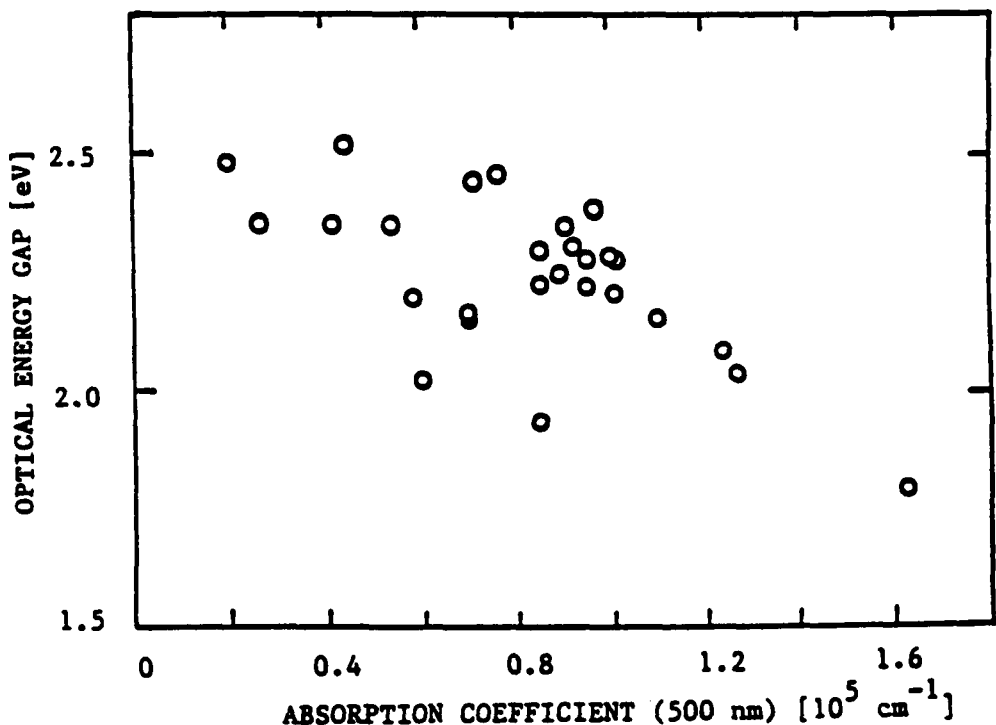


Fig. 1: Optical energy gaps as a function of the absorption coefficients at 500 nm (2.48 eV) for uc-SiH p-layers deposited on glass

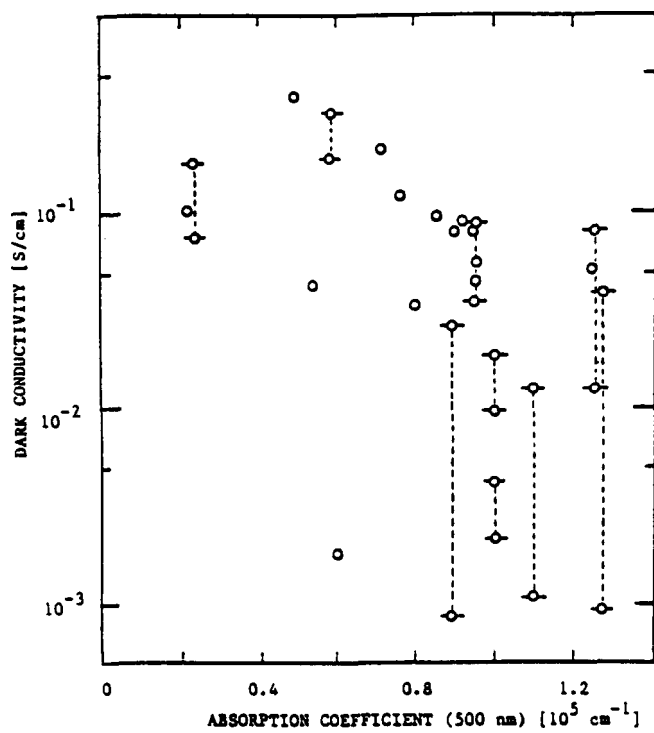


Fig. 2: Dark conductivity of uc-Si:H p-layers as a function of their optical absorption coefficient at 500 nm. The data points connected by dashed lines refer to different samples of the same deposition run.

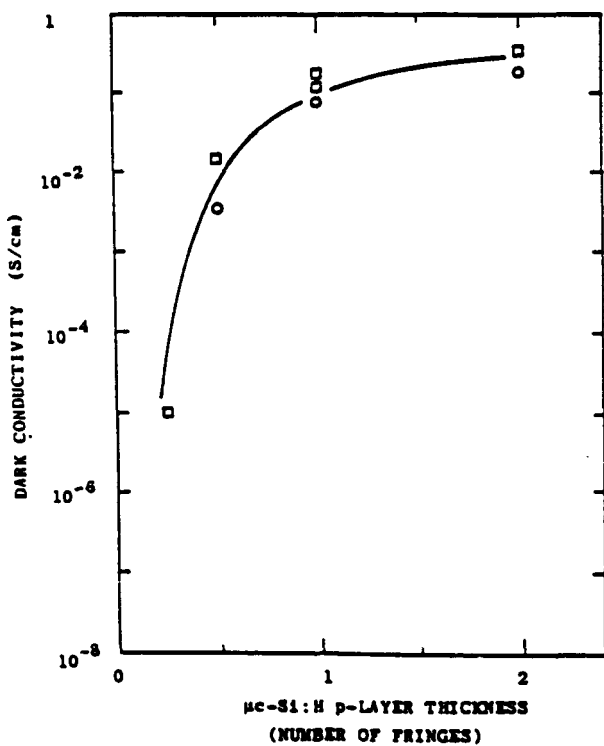


Fig. 3: Dark conductivity of uc-Si:H p-layers as a function of the film thickness

Title: Diagnostics of Glow Discharges Used To Produce Hydrogenated Amorphous Silicon Films

Organization: National Institute of Standards and Technology, Boulder, Colorado

Contributors: A. Gallagher, D. A. Doughty, J. Doyle, M. He, G. H. Lin

The overall objective of this work is to explain causes of glow-discharge produced a-Si:H and a-Si:Ge:H film quality, and its dependence on deposition discharge conditions. During this contract period this involved: (1) developing and verifying a method for measuring substrate reaction probabilities,  $\beta$ , of depositing species in silane and silane-germane discharges, (2) measuring  $\beta$  in silane discharges as a function of conditions, (3) developing and verifying a method for measuring the spatial distribution of deposition  $D(x)$  throughout silane and silane-germane discharges, (4) using this to measure  $D(x)$  for silane discharges under a variety of conditions relevant to a-Si:H film production, (5) interpreting these measurements to test and improve current deposition models, and explain causes of film-quality variations.

#### SURFACE REACTION PROBABILITY MEASUREMENT

The method developed and employed here to measure  $\beta$  is based on analogy to an optical "black-body," in which almost all photons entering a small hole (area  $A_H$ ) in the side of a large box (surface area  $A_B$ ) scatter many times inside and are absorbed before reescape, independent of the exact internal-surface absorption-coefficient  $k$  as long as  $k A_B/A_H \gg 1$ . In the present context this translates into all reactive molecules that pass in through a hole being absorbed inside a "box", independent of  $\beta$  as long as  $\beta A_B/A_H \gg 1$ . The "box" is a gap behind an electrode and the "hole" is a 0.010" x 0.100" slit in the electrode surface. After typically depositing about 1  $\mu\text{m}$  of intrinsic a-Si:H film on the substrate, film thickness is measured on the substrate and on the (disassembled) stainless-steel surfaces of the "box", using reflection interference fringes of a He-Ne (633 nm) laser beam. Here we translate the foil surfaces of the "box" across the focused laser spot and detect reflected-light fringes versus position.

We have measured  $\beta$  at  $T_s = 300$  K and 510 K, from low-power rf silane discharges, operated between stainless-steel plates with a 3.8 cm gap. The silane pressure was 0.17 Torr at 510 K, and 0.10 Torr at 300 K for equal gas density. The discharge power/flow is kept low enough to decompose less than 10% of the silane and the deposition rates studied were 0.5-2  $\text{\AA/s}$ . In essence, these are appropriate conditions for high-quality intrinsic a-Si:H film production. Our result is that  $\beta = 0.42 \pm 0.07$  at 510 K and  $0.39 \pm 0.08$  at 300 K.

This  $\beta \approx 0.4$  result is consistent with the discharge-surface  $\beta$  inferred for  $T_s = 300$  K in ref. 1, but not with the  $\beta \approx 0.10-0.15$  reported for a photo-CVD surface by Perrin and Broekhuizen<sup>2</sup>. Nonetheless, our calculations<sup>3</sup>, radical-density measurements<sup>1</sup>, and fiber-probe measurements reported in another section of this report are all consistent with predominately  $\text{SiH}_3$  deposition in rf discharges. Thus, both experiments are measuring  $\beta$  for  $\text{SiH}_3$ . This

apparent discrepancy is not unexpected or inconsistent with our surface-deposition model. As originally noted by B. Scott et.al.,<sup>4</sup> SiH<sub>3</sub> does not insert exothermically into Si-Si or Si-H bonds, hence SiH<sub>3</sub> should not insert into a fully H-passivated a-Si:H surface. The only reason SiH<sub>3</sub> does produce film growth is because the surface is not fully passivated, and this lack of passivation (hence  $\beta > 0$ ) can depend strongly on deposition conditions. In our current surface model a small fraction ( $< 10^{-3}$ ) of the surface Si bonds are empty of H atoms, and these empty bonds are reactive with SiH<sub>3</sub>.  $\beta$  thus includes the probability of SiH<sub>3</sub> surface diffusion to one of these reactive sites before reevaporation. The photo-CVD conditions studied by Perrin involved higher SiH<sub>4</sub> densities and lower deposition rates, both of which decrease the density of reactive surface sites relative to typical discharge film-production conditions. Our current model suggests that discharge-produced H atoms reaching the surface produce some of the Si dangling bonds(Si-) by a highly-exothermic H-abstraction reaction (H+Si-H → H<sub>2</sub>+Si-). In contrast, under Perrin's conditions almost all of the H atoms will react in the gas phase and not reach the surface. Discharge-produced ions and photons as well as abstraction by SiH<sub>3</sub> also play significant roles in producing reactive surface sites in discharges.

#### SPATIAL DISTRIBUTION OF DEPOSITING RADICALS

We are using small diameter (40  $\mu\text{m}$  and 5  $\mu\text{m}$ ) dielectric fibers strung between parallel-plate electrodes to spatially probe the distribution of depositing radical species in silane discharges. By measuring the a-Si:H or a-Si:Ge:H film thickness on the fiber versus position a map of the radical density is obtained. Typical discharge conditions are 100-200 mT of silane flowing at 10-30 sccm and a power level that results in a deposition rate of 0.5-2  $\text{\AA/s}$ . (High quality a-Si:H films are made under similar conditions.) The film thickness on the fiber is determined by scattering a focused HeNe (633 nm) laser beam off of the fiber and measuring diffraction fringes as the fiber is moved past the laser spot.

Figure 1(a) is an example of the results. This is a plot of the film thickness versus distance x from the powered electrode, following deposition from a 220 mT, low-power rf silane discharge at 520 K. This D(x), which we assume is proportional to the density of depositing species, can be analyzed in terms of the diffusion-reaction equation,<sup>3</sup>

$$-Dd^2n/dx^2 + R_n = S(x), \quad (1)$$

where D is the diffusion coefficient, R is the reaction rate for the species n with the background gas, and S(x) is the source function for the species n. Current understanding and measurements for silane discharges indicate that film deposition is dominated by neutral dissociation fragments, of which SiH<sub>2</sub> and SiH<sub>3</sub> dominate.<sup>3</sup> If SiH<sub>3</sub> is primarily responsible for deposition then R in eqn. (1) is effectively zero since SiH<sub>3</sub> does not react with silane. In this case the second derivative of D(x), shown in figure 1(b), would be proportional to the source function. If the depositing species reacts rapidly with silane, as is known to occur for SiH<sub>2</sub>,<sup>5,6</sup> then the R<sub>n</sub> term on the left side of eqn. (1) dominates, making n proportional to S(x). In this case the

distribution of material on the fiber would come close to mapping the source function  $S(x)$ .

Figure 1(c) shows the spatial distribution of 413 nm ( $\text{SiH}^*$ ) emission from the discharge while the fiber was being coated. Kampas and Griffith showed<sup>10</sup> that this emission, which has an electron-collision-energy threshold of 10.5eV, is due to a single electron impact on  $\text{SiH}_4$ , yielding  $\text{SiH}^*$ . The depositing species are expected to be produced via similarly "high-energy" electron-impact dissociation, and this light curve should be very similar to the source function  $S(x)$  for the depositing species. Clearly, the light curve in figure 1(c) does not resemble  $D(x)$  shown in figure 1(a), indicating that  $\text{SiH}_2$  and other reactive radicals are not responsible for the deposition. The light emission does closely match the second derivative of the film thickness in figure 1(b). This close match is consistent with the diffusion term on the left side of Eq. 1, indicating that deposition is dominated by a species that diffuses without gas reactions, i.e.,  $\text{SiH}_3$ .

#### CONCLUSIONS AND FUTURE WORK

During this contract year we have developed, verified and utilized two powerful new diagnostic techniques that yield very important characteristics of discharge thin-film deposition. From this, we have verified the dominance of  $\text{SiH}_3$  deposition at low powers and the validity of our model predictions of the cause of film-quality loss at high power. We are now in an excellent position to utilize these techniques to establish important film-quality determining characteristics of alloy-deposition discharges. We plan to now apply these to high and low deposition rate discharges in mixtures of silane, disilane, germane, and  $\text{H}_2$  gases, to establish deposition-rate and film-quality determining factors in these more complex systems.

#### REFERENCES

1. R. Robertson, D. Hils, H. Chatham and A. Gallagher, *Appl. Phys. Lett.* **43**, 544 (1983). R. Robertson and A. Gallagher, *J. Appl. Phys.* **59**, 3402 (1986).
2. J. Perrin and T. Broekhuizen, *Appl. Phys. Lett.* **50**, 433 (1987).
3. A. Gallagher, *J. Appl. Phys.* **63**, 2406 (1988).
4. B. A. Scott, R. M. Plecenik, and E. E. Simonyi, *Appl. Phys. Lett.* **39**, 73 (1981).
5. G. Inoue and M. Suzuki, *Chem. Phys. Lett.* **122**, 361 (1985).
6. J. M. Jasinski and J. O. Chu, *J. Chem. Phys.* **88**, 1678 (1988).

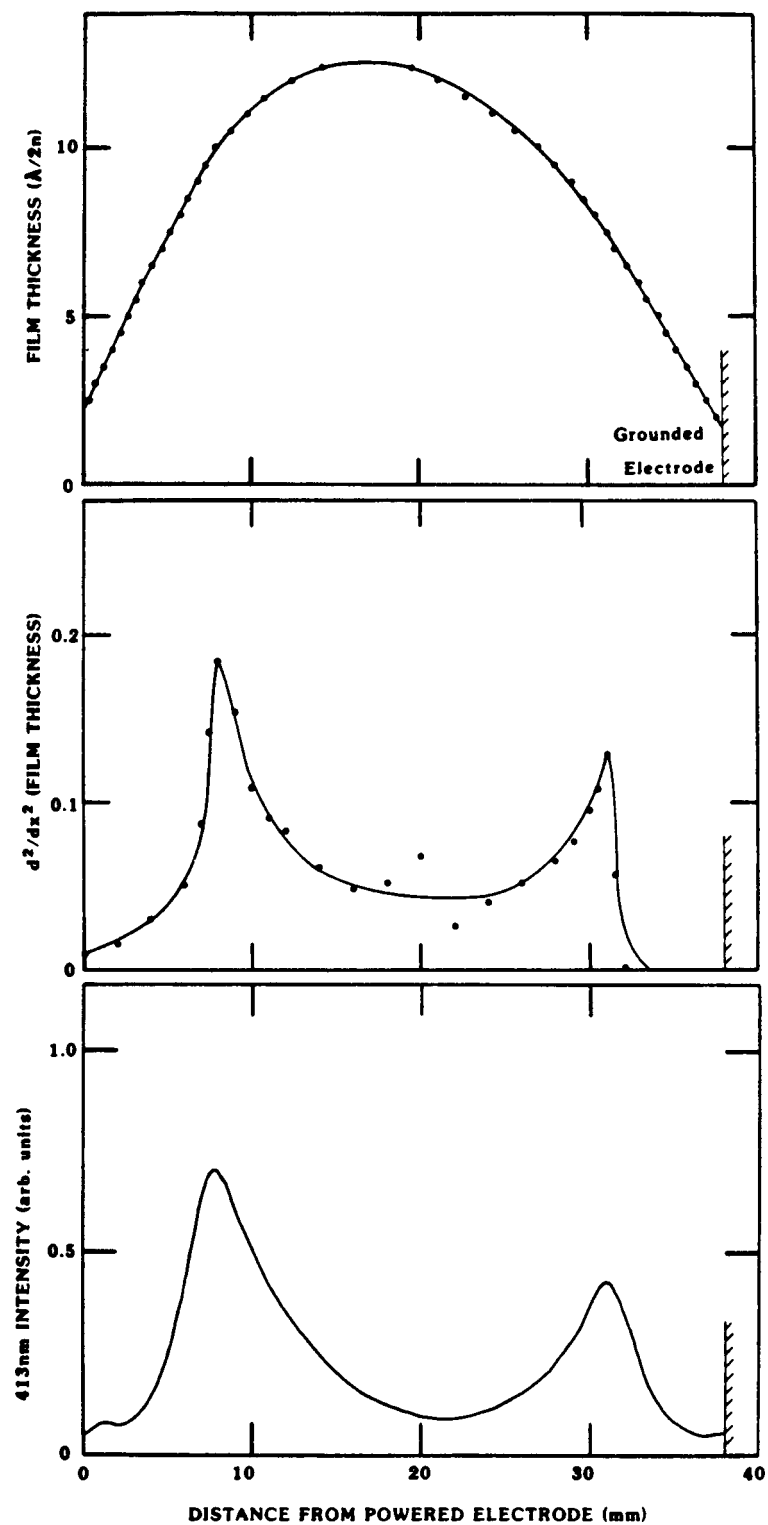


Figure 1 (a) Film thickness measured on the fiber, (b) second derivative of the film thickness variation, and (c) 413 nm optical emission from the discharge, all versus distance from the powered electrode. Discharge conditions: pressure = 220 mTorr, gas and electrode temperature = 520 K, flow rate = 30 sccm, fraction  $\text{SiH}_4$  depletion = 10% (low power).

Title: Study of Thermal and Light Induced Changes in Amorphous Silicon Alloy Materials

Organization: Department of Electrical Engineering, North Carolina A&T State University, Greensboro, North Carolina

Contributors: W. J. Collis, principal investigator; A. Shah, S. Bhamidipati.

The objective of this research program is to develop measurement techniques to aid in the study of the light-induced reversible changes which are observed to occur in hydrogenated amorphous silicon and related alloys. This effect, studied in some detail by Staebler and Wronski [1], appears to be the basis for the degradation of the characteristics of solar cells fabricated from these amorphous materials. A controlled environment system was set up for the measurement of the electrical characteristics (dark and photoconductance) of thin film amorphous samples supplied by SERI.

The system which maintains the sample environment during the measurement of the electrical characteristics has been described schematically in previous SERI quarterly and annual reports for this Subcontract. Briefly, a high vacuum chamber contains the sample on a temperature-controlled stage during in-situ electrical measurements of conductivity and exposure to light to induce the degradation. The a-Si:H/glass samples are prepared by evaporating aluminum coplanar gap electrodes. The gap is approximately 1x8 mm.

Optical exposure is achieved with a 1 kW xenon lamp. Interference filters are used to determine the spectral photoconductivity behavior. The spectral intensity is determined with a silicon photodiode which is mounted to slide directly over the sample. Typically, a full lamp spectrum is used during degradation exposure. The sample stage is maintained at room temperature with a circulating liquid cooling system. A pressure of  $10^{-5}$  -  $10^{-6}$  Torr is achieved in the sputter ion vacuum pump. Annealing of the samples is performed by heating the stage to 180-200 °C for several hours in vacuum.

An alternative exposure technique using a high intensity photoflash lamp was investigated. In those samples which exhibited a large sensitivity to light exposure, this flash source would quickly alter the conductivity after several flashes. Thus, this technique can be used as a means of quickly screening samples with regard to their optical stability.

Three samples of rf glow-discharge-deposited intrinsic a-Si:H were received from SERI for evaluation of the ion beam posthydrogenation and rehydrogenation processes. These samples had been subjected to a hydrogen ion implantation using a Kaufman ion source. In the posthydrogenation material the deposition took place at a high substrate temperature such that the hydrogen content was negligible. The rehydrogenated samples were deposited at 250 °C, then annealed at higher temperature for 24 hours to outdiffuse the hydrogen. Details of the hydrogenation process are described in Ref. [2].

Prior to the light degradation experiments, the samples were annealed at 190 °C for two hours. Optical exposures were performed with the xenon lamp source at full spectrum without optical filtering. The photocurrent at 700nm was recorded as a function of light exposure time. The photocurrent data were

fitted to the relationship  $I_{ph} = Kt^n$ . Dark currents were measured prior to the exposure period. The data indicated that the rehydrogenated sample and the standard a-Si:H sample have similar degradation exponents ( $n = -0.35$ ), but the rehydrogenated sample had a smaller light to dark current ratio. In contrast, the partially rehydrogenated sample had the largest photocurrent to dark current ratio and a lower sensitivity to optical exposure ( $n = -0.20$ ).

Continued characterization of available intrinsic amorphous Si:H alloys was performed. The measurement chamber system provides a reliable means of reproducibly testing the samples without causing physical degradation of the thin film layers. Data obtained from hydrogen ion beam implanted samples demonstrated that this technique can introduce hydrogen into the amorphous Si material to achieve an alloy which is similar to the original glow-discharge-deposited alloy in its electrical properties.

---

1. Staebler, D. L., and C. R. Wronski, "Optically induced conductivity changes in discharge-produced hydrogenated amorphous silicon," J. Appl. Phys., 51, 1980, p. 3262.
2. Tsuo, Y. S., E. B. Smith, and S. K. Deb, "Ion beam hydrogenation of amorphous silicon," Appl. Phys. Lett., 51, 2 November 1987, p. 1436.

Title: Study of Large Area Amorphous Silicon Films by Photo-CVD

Organization: Hughes Aircraft Company, Electro-Optical and Data Systems Group,  
El Segundo, CA

Contributors: Jacques Linder, Principal Investigator

Photochemical vapor deposition (photo-CVD) of a-Si:H films for photovoltaic applications is an alternative method to plasma deposition processes. Several research groups have reported efficient small area solar cells with either all layers or just the p-layer deposited by photo-CVD. The lack of energetic ions and electrons in the photo-CVD process may be beneficial during the p-layer deposition where energetic species can introduce interfacial defects which lower the conversion efficiency. At present, photo-CVD research has concentrated on small area deposition which is usually limited by the physical dimensions of the deposition chamber.

Hughes Aircraft has been investigating the photo-CVD process since 1976 and has pioneered the development of low-temperature silicon dioxide and silicon nitride films using photo-CVD. All depositions under this subcontract are done using an existing photo-CVD system which has a usable deposition area of 10 x 10 inches. Deposition of amorphous silicon on the quartz window is retarded by a film of Krytox, a perfluorinated polyether, on the window. All depositions are performed using 100% silane which has been mercury sensitized.

Deposition rates were determined at two silane pressures, 1.0 torr and 0.5 torr. The lower pressure is by far the more favorable with a deposition rate of approximately 1 A/s. Deposition rates at 1.0 torr are less by factors of two to three.

At present uniformity from the center to 4 inches on either side (across the gas flow) varies from 11 to 19%. The greatest thickness deviations occur from the center to the rear corners which are near the exhaust ports. These deviations are attributed to 1) greater distance from the center and 2) silane depletion near the exhaust ports. The deposition process is being changed in ways calculated to enhance thickness uniformity, e.g., variations in pressure or ultraviolet light intensity.

Title: Improvement of Small Area Amorphous Silicon Thin Film Photovoltaics on Polymer Substrate

Organization: 3M

Contributors: M.F. Weber, principal investigator; J.R. Gilbert, F.R. Jeffrey, and F.J. McFadden

### Objective

The goal of this research effort is to achieve a solar cell efficiency of 10% with amorphous silicon devices on polyimide substrate under AM1.5 insolation. To achieve this result, the program focuses on two components of the solar cell: 1) the optically transparent front conductor (TCO) in contact with the silicon and 2) the textured metal back contact.

The two respective tasks call for 1) reduced contact resistance between silicon and the TCO, and 2) increasing the short circuit current density via optimized texturing. The approaches taken towards improving efficiency, as they affect fill factor (ff), open circuit voltage ( $V_{o.c.}$ ) and short circuit current density ( $I_{s.c.}$ ), are discussed separately below.

### Results

#### Fill Factor

A critical step in obtaining good devices was to reduce or eliminate both the lighter gases ( $O_2$ ,  $N_2$ , and  $H_2O$ ), and the heavier aliphatic hydrocarbons from outgassing from the polyimide web during silicon deposition. With proper pretreatment of the web, devices with ff's greater than 0.70 are now routinely achieved with 5000 angstrom thick i-layers. Of course, a low contact resistance between the TCO and the silicon is a prerequisite for such a high fill factor. This was achieved with the use of a ZnO TCO. Previously, sputtered indium-tin oxide (ITO) was used as the TCO, but this material required a diffusion barrier such as  $SnO_2$  to be first deposited to prevent diffusion of indium into the top doped silicon layer. Fill factors were erratic and very rarely above 0.66. With the ZnO TCO, ff's in excess of 0.70 are routinely achieved.

#### Open Circuit Voltage

Given a low outgassing web, the approach to obtaining high  $V_{o.c.}$ 's is simply to increase the built-in voltage of the device. This was achieved with microcrystalline  $n^+$  and  $p^+$  doped layers. On a continuously moving web with the microcrystalline  $p^+$  layer deposited last, and light entering through this layer, voltages of 0.88 volt at 25°C are normally measured. In a single chamber system with  $p^+$  layer on top,  $V_{o.c.}$ 's of 0.94 volt can be obtained, but such cells have a low fill factor thus far. Voltages for p-i-n cells,  $n^+$  deposited last, are usually 0.90 to 0.91 volt, with ff's of 0.69 to 0.71.

### Short Circuit Current Density

With light entering the cell from the top, or last deposited layer, the bottom electrical contact layer must be properly textured to enhance the red light response of the cells. A variety of texture shapes and sizes has been found to enhance the current density. The best texture appears to be an undulating or pock-mark surface instead of discrete hillocks of aluminum metal grains. Over-coating the aluminum with silver again increases the red light response of the cells. The different texture features are controlled by the sputtering rate, gas pressure, and web temperature.

Given an optimum texture, the magnitude of  $I_{sc}$  depends on which TCO is chosen to complete the cell. Three cell designs have been tested in our labs, as well as theoretically modeled. Quarterwave optically thick coatings of ITO (~ 70 nm) produce the highest current density because of the excellent anti-reflecting properties of this coating. For large cells however, a metallic grid is required to counter the high sheet resistance (~ 100 ohms/square). Three quarterwave thick ITO (~ 225 nm) and very thick ZnO (~ 1.5 microns) yield about the same current density. On an optimally textured cell, under an ELH lamp with intensity determined with a SERI calibrated cell, the ZnO and three quarterwave ITO average about  $14.5 \text{ mA/cm}^2$ , whereas cells with the quarterwave thick ITO coating average  $16.3 \text{ mA/cm}^2$ .

### Conclusions

In spite of producing a lower current density, the ZnO coated cells produce the highest efficiencies for two reasons: a) lower sheet resistance of ZnO (~ 10 ohms/square) and b) lower contact resistance of the ZnO to the silicon (Less than  $1 \text{ ohm}\cdot\text{cm}^2$ ). The best cells have efficiencies of 8.9 to 9.0% with  $ff = 0.69$ ,  $V_{oc} = 0.90$ , and  $I_{sc} = 14.5 \text{ mA/cm}^2$ . The 10 ohm/square ZnO will also result in submodule active area efficiencies close to the reported small area efficiencies. Future work will focus on dielectric enhanced reflectors for the bottom textured contact to increase the short circuit current density.

Title: Hydrogenated Amorphous Silicon Device Modeling

Organization: University of Florida

Contributors: F. A. Lindholm, principal investigator, and K. Misiakos

### Objectives

The objectives of the research were to provide a computer simulation of the time of flight experiment to predict and interpret the terminal response following pulsed excitation. Numerical solutions and the associated physical interpretation illuminate the transport physics and assess the accuracy of the methods involved in the extraction of transport parameters. The interaction between free carriers and gap states were assessed on the basis of numerical results on the internal variable profiles. The influence on the transient photocurrent of band mobilities, transient trapping and transient emission was investigated, and certain analytical approximations were derived based on the interpretation of the computer solutions.

### Approach

The time of flight experiment has been extensively used to extract information about tail states in amorphous silicon [1]. The device under consideration is a  $0.62 \mu\text{m}$  thick a-Si:H cell under short circuit conditions. A 6 ps pulse of blue light having an absorption coefficient  $\alpha = 10^6 \text{ cm}^{-1}$  and a flux density of  $A = 10^{18} \text{ cm}^{-2}\text{s}^{-1}$  shines through the  $\text{P}^+$  layer. Each heavily doped layer is  $100 \text{ \AA}$  thick.

The computer simulation was based on the Poisson equation, the expression of current in terms of drift and diffusion of extended carriers and the continuity equation. The electron continuity equation was modeled as

$$n(x,t)/dt = (1/e)dJ_n/dx + G(x,t) - \int_{E_c}^{E_v} U_n(E,x,t)dE$$

$$U_n(E,x,t) = T_r[n(x,t)(1-F(E,x,t)-N_c \exp(-E/kT)F(E,x,t)]N_t(E)dE \quad (1)$$

In (1)  $G$  is the optical generation rate,  $F$  the occupation probability of a gap state,  $U_n$  is the net electron trapping rate,  $T_r$  the transition rates from free electrons to unoccupied traps,  $N_c$  the conduction band density of states and  $N_t(E)$  the gap state density. In (1) we used detailed balance to express the trap release rate as  $T_r N_c \exp(-E/kT)$ . The downward transition rates,  $T_r$ , were assumed energy independent. The energy is measured from the bottom of the conduction band. A similar equation was used for holes.

To accurately model the trapping and releasing process, the band gap, 1.7 eV, was divided into 400 segments and (1) was integrated over these segments. The kinetic rate equation for any trap level is

$$dF(E,x,t)/dt = U_n(E,x,t) - U_p(E,x,t) . \quad (2)$$

The cell was assumed shorted through out the transient. For the gap state density shown below, the electric field was uniform throughout the I layer having a variation of only 10%. For a tail state density 10 times higher the variation was 20%. The parameters used in the numerical simulation were:

Electron mobility in the I layer	(cm <sup>2</sup> /Vs)	20
Electron mobility in the heavily doped layers	(cm <sup>2</sup> /Vs)	10
Hole mobility in the I layer	(cm <sup>2</sup> /Vs)	2
Hole mobility in the heavily doped layers	(cm <sup>2</sup> /Vs)	1
Density of electron tail states in the I layer at the conduction band top	(cm <sup>-3</sup> /eV)	1E20
Density of hole tail states in the I layer at the valence band top	(cm <sup>-3</sup> /eV)	1E20
Density of electron tail states in the heavily doped layers at the conduction band bottom	(cm <sup>-3</sup> /eV)	1E21
Density of hole tail states in the heavily doped layers at the valence band top	(cm <sup>-3</sup> /eV)	1E21
Characteristic energy for electron tail states (eV)	(eV)	0.027
Characteristic energy for hole tail states	(eV)	0.045
Deep trap density in the I layer	(cm <sup>-3</sup> )	2E15
Deep trap density in the heavily doped layer	(cm <sup>-3</sup> )	4E16
Transition rates from free carriers to traps	(cm <sup>3</sup> /s)	10 <sup>-9</sup>
Mobility gap	(eV)	1.7

#### Numerical Results and Physical Interpretation

Figure 1 shows the magnitude of the terminal current as a function of time. We see that in the first 6 ps, during which the light still shines, the current increases almost linearly with time. This is the case because when the light is on, the generation rate is much higher than the capture rate. After the light is turned off, the current slowly declines slowly with time and then between 0.1-0.2 ns it starts dropping fast. The knee of the curve indicates a transit time,  $T_{tr}$ , of about 0.15 ns. The field in the I layer is quite uniform with an average value of  $E_{av}=20$  kV/cm. Therefore, we can infer a drift mobility of

$$\mu_{dr} = W / (T_{tr} * E_{av}) = .62 \times 10^{-4} / (1.5 \times 10^{-10} * 20 \times 10^3) \approx 20 \text{ cm}^2 / (\text{Vs}) .$$

This is the same as the extended carrier mobility ( $\mu_n=20$  cm<sup>2</sup>/(Vs)) used in the modeling. As discussed in the next section, this is a result of a transit time less than the lifetime against shallow trapping.

Figure 2 shows the electron density in excess of its thermal equilibrium value. The electron pocket drifts towards the  $N^+$  layer and at the same time spreads due to diffusion. In Figure 2 we can divide the plots into two groups. The first group, curves 1,2 and 3, corresponds to  $t < T_{tr}$  and shows the dynamics of the transport across the I layer. The peak of the pocket moves at a speed equal to the product of the drift mobility times the electric field. The second group, curves 4,5 and 6, shows the electron density after the electron pocket has already crossed the I layer. During this period the electron density is predominantly determined by the re-emission rate of electrons from the traps. That explains why the electron density at the I-heavily doped layer interface results from a analogous discontinuity in the electron mobility.

Figure 3 shows the gap state re-emission rate for electrons. Curves 4 and 5 show the same spatial dependence as curves 4 and 5 of Figure 2, which support the previous assumption that for  $t > T_{tr}$  the electron density is determined by the re-emission of trapped carriers. For  $t < T_{tr}$  the remission rate expands towards the  $N^+$  layer with the same speed as the electron pocket (Figure 2). However, the re-emission rate cannot follow the drop of the electron density with time near the  $P^+$  layer because of the time it takes for a carrier to be released, especially if it is trapped by a deep level. In the heavily doped layers the re-emission rate increases because the density of gap states there is higher than in the I layer.

Figure 4 shows the excess hole density. Most of the holes are confined in  $P^+$  layer and a very thin region adjacent to this layer. This is a result of the field action on the holes and of the excess holes being photogenerated in the vicinity of the  $P^+$  layer. Thus most of the action in the I layer is due to electrons which are the limiting carriers in this case.

Figure 5 shows the electron current density. The electron current in most of the device shows the same spatial dependence as the excess electron density in Figure 2. This is expected because the electron current is mainly drift current and the electric field is quite uniform in the I layer. Near the  $N^+$  ohmic contact the electron current reverses direction because electrons diffuse towards the ohmic contact. This direction reversal appears as a discontinuity in the logarithmic scale of Figure 5 and is better shown in Figure 6 which shows the same current in a linear scale. The electron current as electric current in the I layer is negative since electrons are moving towards the positive direction.

Figure 7 shows the displacement current. During the first 10 ps of the transient in most of the I layer the current is mainly displacement current since the photogenerated carriers did not have time to reach the bulk of the I layer. By comparing Figure 6 and 8 we see that the displacement current appears to be a reflection of the electron current with respect to the X axis. This is reasonable considering that the summation of the three currents is spatially independent and that the hole current is negligible away from the  $p^+$  contact.

In Figure 8 the current magnitude is shown for two different densities of tail states. For a tail state density of  $10^{21} \text{ cm}^{-3} \text{ eV}^{-1}$  at the edge of the bands, the current dependence on time has the characteristics of a dispersive transport. The current drops considerably before reaching the transit time and the

break point that defines the transit time is not as sharply defined as in the case of nondispersive transport that characterizes curve 1. So increasing the tail state density from  $10^{20} \text{ cm}^{-3} \text{ eV}^{-1}$  to  $10^{21} \text{ cm}^{-3} \text{ eV}^{-1}$  changes the transport from nondispersive to dispersive. The transit time for the high tail state density is 0.8 ns and corresponds to a drift mobility of  $4 \text{ cm}^2/(\text{Vs})$ .

### Conclusions

The drift mobility derived from Figure 1 is about the same as the free carrier mobility because the carrier transit time ( $\approx 0.15$  ns) is shorter than lifetime against tail state trapping,  $t_t = 1/(T_r N_t(0) k T_c) = 0.37$  ns. Here  $T_c$  is the characteristic energy of the conduction band tail states and  $N_t(0)$  is the tail state density just below the band edge. Therefore most of the carriers cross the I layer without being captured by the tail states. This explains the non-dispersive transport characteristics shown in Figure 1. The same figure shows at the break point a fast drop which shortly resolves and is followed by a power law dependence ( $\approx t^{-2}$ ) at longer times. The fast drop at the transit time can be explained considering the fact that in this model the pocket of electrons contains most of the injected charge and upon arrival at the back electrode, this charge is removed from the transport process. Then the current is determined by the rate at which the tail states release the charge. During this period, theoretical models predict that the current drops with time as  $t^{-1-\alpha}$ , where  $\alpha = T/T_c$  [2,3,4,5]. In our case  $\alpha = 26/27 \approx 1$ . Therefore, the power law dependence of  $t^{-2}$  shown in Figure 1 verifies these models.

Now we switch our attention to current decay that corresponds to  $N_t(0) = 10^{21} \text{ cm}^{-3} \text{ eV}^{-1}$ , as shown in Figure 8. Here, the carriers get trapped and released many times before they arrive at the back contact. Using the model developed by Tiedje and Rose [4] and Orenstein and Kastner [5] on the interaction between tail states and free carriers, for  $\alpha \approx 1$  we derive

$$\frac{n_{\text{free}}}{n_{\text{free}} + n_{\text{trap}}} = \frac{N_c / (k T N_t(0))}{\ln(\omega_0 t) + 1 + N_c / (k T N_t(0))} \quad (3)$$

In (3)  $n_{\text{free}}$  and  $n_{\text{trap}}$  are the free carrier and trapped carrier density, respectively,  $N_c = 210 \text{ cm}^{-3}$  is the conduction band effective density of states and  $\omega_0$  is the attempt to escape frequency which, through detailed balance, is  $\omega_0 = N_t T_r$ . Following Spear [6] we identify the ratio in (3) with the drift mobility  $\mu_{\text{dr}} = n_{\text{free}} / (n_{\text{free}} + n_{\text{trap}})$ . If  $W$  is the thickness of the sample layer, then the transit time can be calculated by solving the following equation [4]:

$$\int_0^{T_r} E \mu_{\text{dr}} dt = W \quad (4)$$

Numerical solution of (4) gives  $T_r = 0.85$  ns, a value that is in excellent agreement with Figure 8 and corresponds to a drift mobility of  $4 \text{ cm}^2/(\text{Vs})$ . For times greater than the transit time, the current decays as  $t^{-2}$ , which is the same time dependence as in the case of the low tail state density. This is demonstrated in Figure 8 by the parallel tails of the two plots for times greater than the transit times. Thus, the slope of the tail depends primarily on  $\alpha$  and can be used to calculate  $T_c$ . Finally, by integrating plots 1 and 2 in Figure 8 with respect to time, we find that the total collected charge is

almost the same to the charge injected by the light pulse. This is expected since the lifetime against deep trapping is of the order of 0.1  $\mu$ s, well below the transit time.

In conclusion, we verified predictions made by theoretical models [2,3,4,5] and found that increasing the tail state density from  $10^{20}$   $\text{cm}^{-3} \text{eV}^{-1}$  to  $10^{21}$   $\text{cm}^{-3} \text{eV}^{-1}$  changes the transport from nondispersive to dispersive and reduces the drift mobility by a factor of 5.

### References

1. T. Tiedje. The Physics of Hydrogenated Amorphous Silicon II. (1984). Ed. by J. D. Joannopoulos and G. Lucovsky. Topics Appl. Phys. Vol. 56 (Springer, Berlin, Heidelberg, New York). Chapt. 6.
2. G. Pfister and H. Scher. (1978). Adv. Phys. 27. 747.
3. H. Scher and E. W. Montroll. (1975). Phys. Rev. B12. 2455.
4. T. Tiedje and A. Rose. (1981). Solid State Communications 37. 49.
5. J. Orenstein and M. Kastner. (1981). Phys. Rev. Lett. 46. 1421.
6. W. E. Spear. (1969). J. Non-Cryst. Solids. 1. 197.

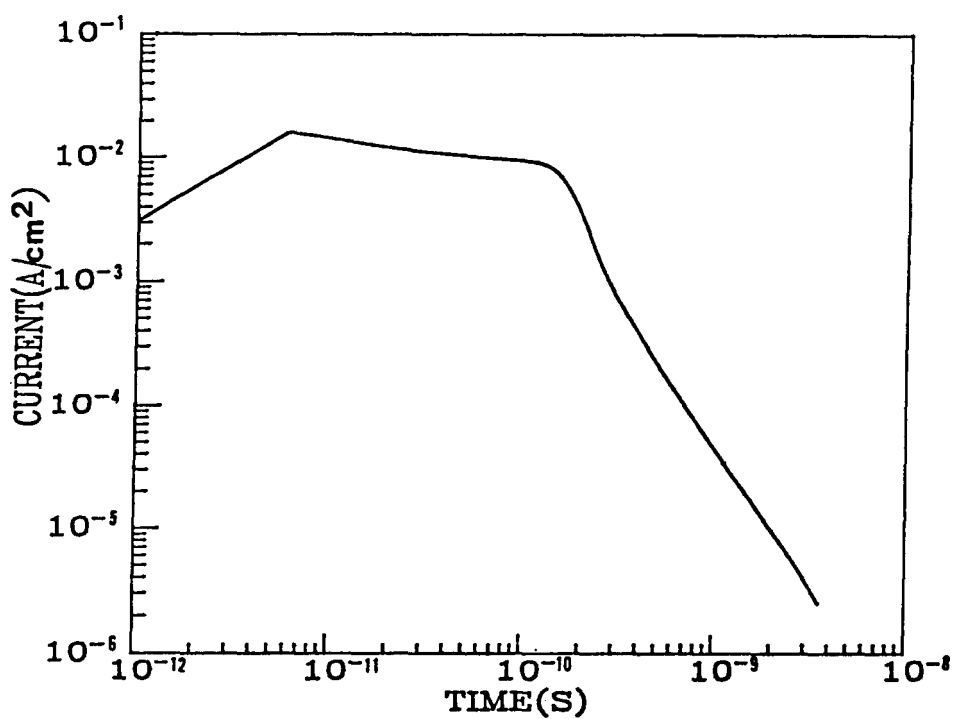


Figure 1. Terminal current magnitude vs time

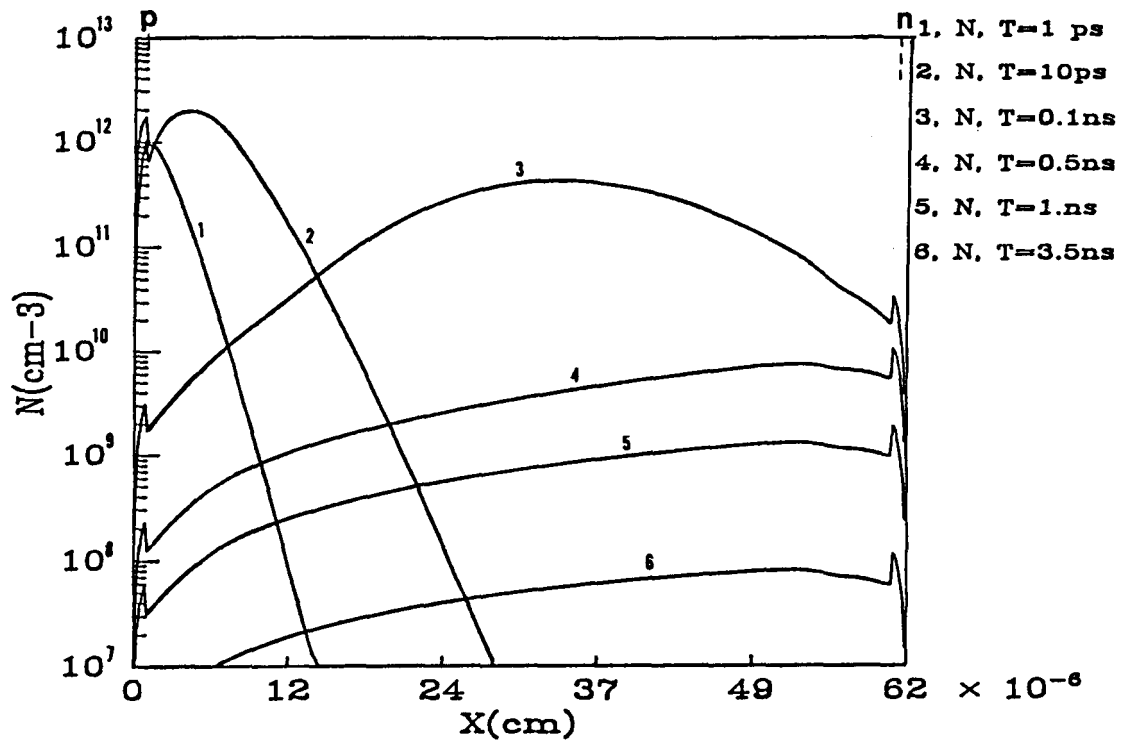


Figure 2. Excess electron density profiles as functions of time

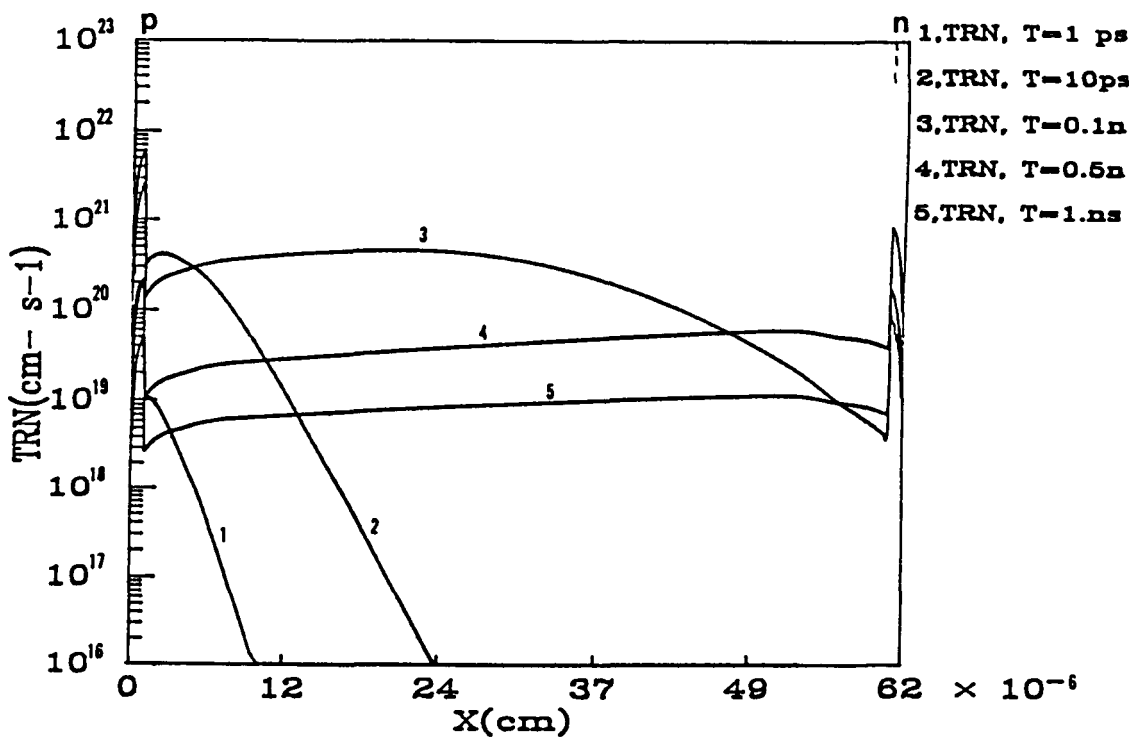


Figure 3. Release rate profiles of trapped electrons as functions of time

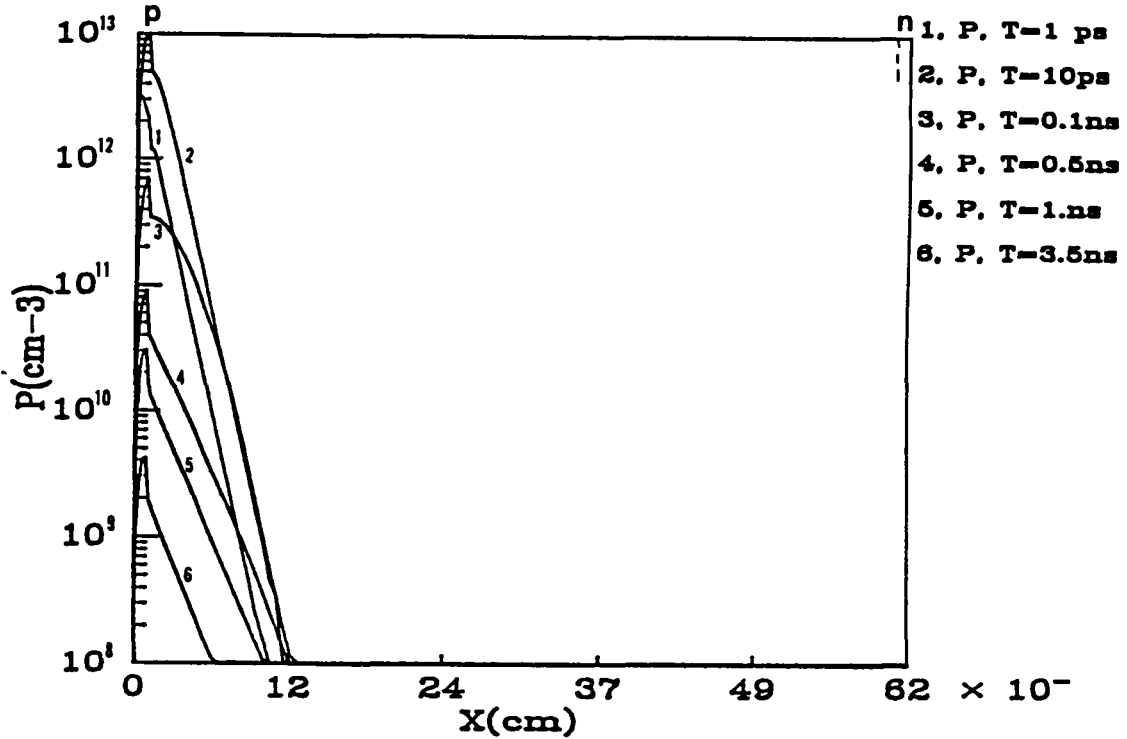


Figure 4. Excess hole density profiles as functions of time

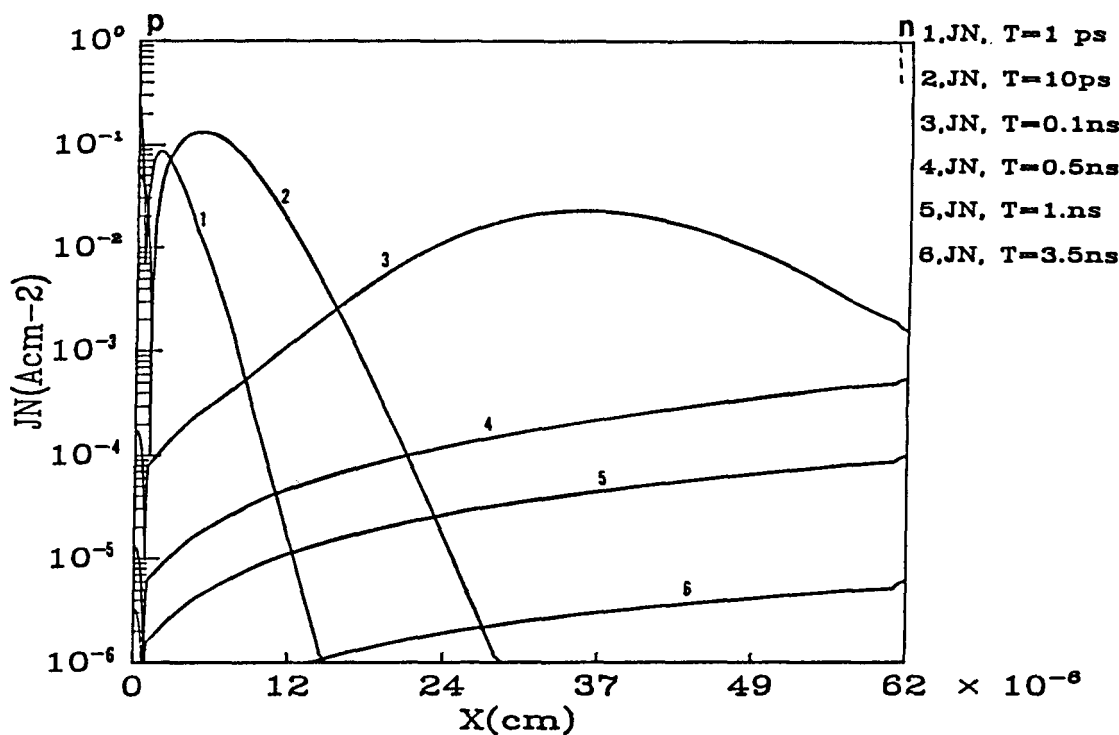


Figure 5. Electron current magnitude profiles as functions of time on a logarithmic scale

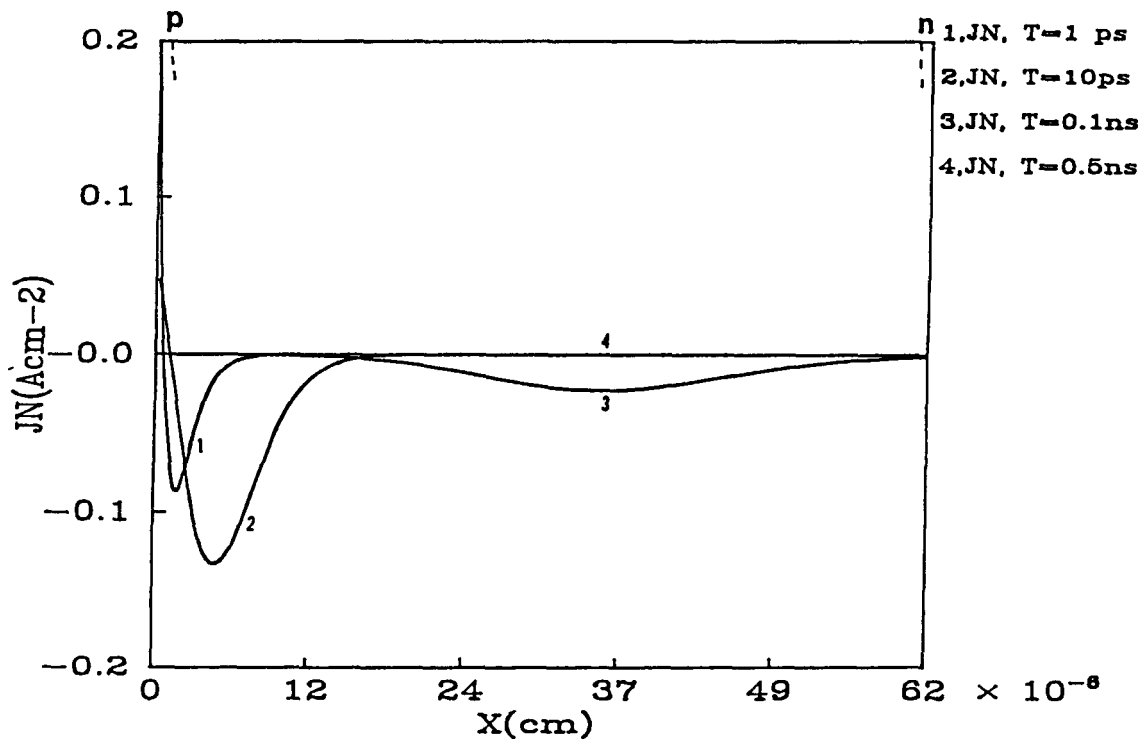


Figure 6. Electron current profiles as functions of time on a linear scale

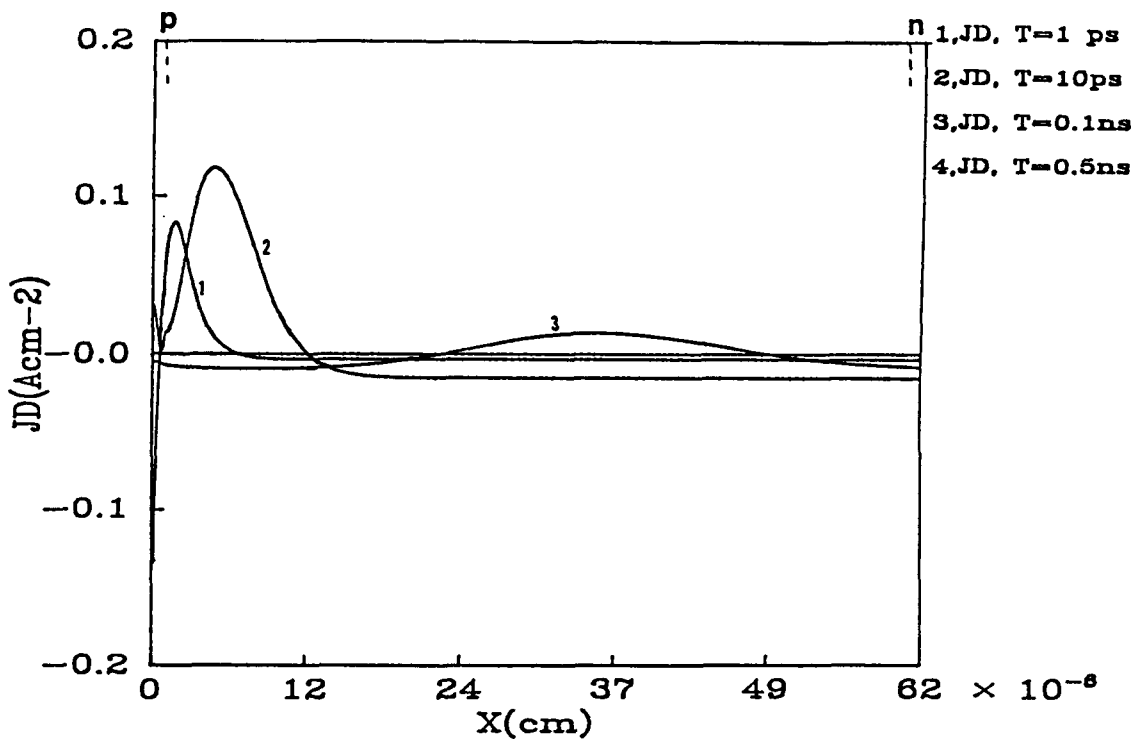


Figure 7. Displacement current profiles as functions of time

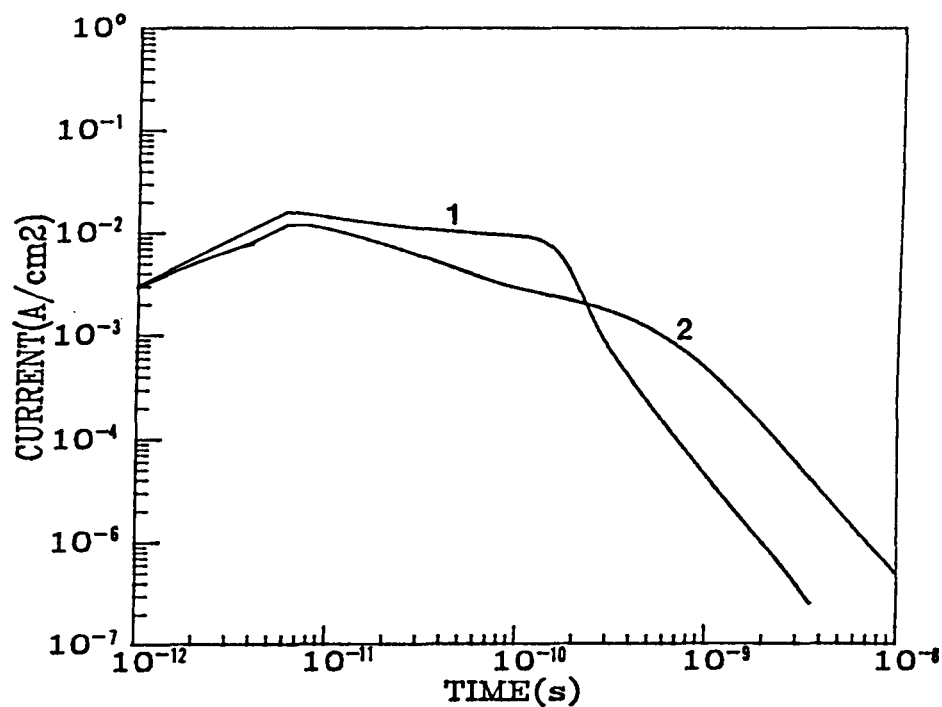


Figure 8. Terminal current magnitude profiles as functions of time

Title: Investigations of Stable Contact to Amorphous Silicon Thin Films

Organization: California Institute of Technology

Contributors: Marc-A. Nicolet, principal investigator  
Liem T. Tran, graduate student

Hydrogenated amorphous silicon (a-Si:H) photovoltaic cells with Ag contacts (used as high reflectance back-electrode) can experience losses in the electrical properties after a few hours at 150C. One possible mechanism that could account for the degradation is the potential instability of the Ag/a-Si:H interface. Metal induced crystallization of a-Si has been observed with Au at 150C and with Al at 230C (1). Effects of the same nature have also been observed in metal/poly-Si systems (400C for poly-Si/Al, 550C for poly-Si/Ag, and 200C for poly-Si/Au) (2). At a temperature well below the eutectic, Si atoms are first dissolved and then transported into the metal film, possibly preferentially by grain boundary paths. The Si then nucleates in the metal film. The size and form of the Si crystallites are determined by the initial thickness of the metal film and the annealing conditions. The objectives are to investigate the thermal stability of the metal/a-Si:H structure and to correlate structural changes with electrical performance changes at the junction.

All a-Si:H films used in these experiments were deposited by ARCO Solar using the same deposition process employed for high-efficiency solar cells. Substrates used were <111> 3-inch Si wafers. Films of Al (100 nm) and Ag (200 nm) were then rf sputter-deposited at Caltech onto the a-Si:H films. The samples were then annealed in an Ar-flushed furnace. X-ray diffractometry, Rutherford backscattering spectroscopy (RBS), SEM, & AES were employed to analyze the samples. To better reveal the crystallized Si grains, the Al or Ag films were etched away in some instances using aqua regia.

At 150C and after 120 hours of annealing, x-ray diffraction indicated the formation of Si crystallites in the Al/a-Si:H system. However, the crystallization process must be considerably slow at this temperature because (i) RBS spectra fail to reveal Si in Al, meaning the average bulk concentration of Si is less than 0.1% and, (ii) Si grains, if any, are below the 10 nm resolution limit of our SEM.

After 120 hours of 150C annealing the Ag/a-Si:H system, no polycrystalline Si is detected by x-ray diffractometry. Furthermore, RBS and AES are unable to detect any amount of Si in the Ag layer. After etching away the Ag film, we also do not observe any morphological change on the bare a-Si:H surface. Degradation of solar cells is reported after only a few hours at 150C, whereas our annealing time is 120 hours. The degradation of cells may be due to diffusion of dopants at the junctions (3); or it may be due to crystallization that is below the detection limit of our measurement techniques.

The crystallization process of a-Si:H in contact with Al are shown to occur in the range of 150C - 250C. This process is similar to the one observed in the temperature range of 400C to 560C with poly-Si. That this process is accelerated in a-Si:H is expected because of the higher free energy of a-Si:H compared to that of poly-Si. The structural and morphological change at the interface may have effects on the electronic properties of the solar cells. In the case of the Ag/a-Si:H system, the lowest temperature at which crystallization is observed is 250C. At 150C, no evidence of instability is obtained using our analytical techniques. Similar behavior is observed for i-, n-, and p-type a-Si:H films.

- (1) C.C. Tsai, M.J. Thompson, R.J. Nemanich, W.B. Jackson, and B.L. Stafford, "Summary Abstract: Metal-Amorphous Si Interface: Structural and Electrical Properties", *J. Vac. Sci. Technol. A1(2)*, Apr.-June 1983.
- (2) K. Nakamura, M.-A. Nicolet, J.W. Mayer, R.J. Blattner, and C.A. Evans, Jr., "Interaction of Al Layers with Polycrystalline Si", *J. Appl. Phys.*, 46(11), 1975.
- (3) H. Matsumura, M. Maeda, and S. Furukawa, "Study on Impurity Diffusion in Glow-Discharged Amorphous Si", *Jap. J. Appl. Phys.* 22(5), 771-774, 1983; H. Matsumura, K. Sakai, M. Maeda, and S. Furukawa, "Measurement of Boron Diffusivity in Hydrogenated Amorphous Si by Using Nuclear Reaction  $^{10}\text{B}(\text{n},\text{alpha})^7\text{Li}$ ", *J. Appl. Phys.* 54(6), 1983.

**Title:** **Hydrogenated Amorphous Silicon Films Prepared by  
Glow Discharge of Disilane**

**Organization:** UHT Corp., 145 Palisade St., Dobbs Ferry, New York,  
10522

**Contributors:** H. Wiesmann, principal investigator

The primary purpose of this program is to examine certain opto-electronic properties of amorphous silicon thin films deposited from disilane at high deposition rates. The results of the studies of these fundamental properties are being used to fabricate amorphous silicon glass/P-I-N/metal solar cells where the intrinsic layer is deposited at high deposition rates. The materials research consists of two foremost tasks. The first is to study the dependence of the RF power, gas composition and substrate temperature on the dihydride/monohydride ratio in undoped amorphous silicon films. The deposition rate is to be 15 angstroms/sec. or greater. The second task is to measure the dark and photoconductivity of intrinsic amorphous silicon films at AM1.5 insolation. These conductivities are to be examined as a function of RF power, gas composition and substrate temperature as in the previous task. The deposition rate is also 15 angstroms/sec. or greater. The device fabrication task is to demonstrate solar cells of  $0.25 \text{ cm}^2$  area. The intrinsic layer is to be deposited at no less than 15 angstroms/sec. and the solar cells should have an AM1.5 efficiency of at least 9%. A number of the major materials property studies has been completed. Some of the more interesting results are discussed below.

### **Infrared Absorption**

The infrared absorption was studied as a function of three deposition parameters, feedgas composition, substrate temperature and RF power. Analysis of the data requires assignment of the various peaks in the absorption spectra. The assignment of the various absorption bands was taken from the work of Cardona [1] and references cited therein. The observed bands are assigned as described below.

<u>Band</u>	<u>Assignment</u>
640 $\text{cm}^{-1}$	SiH wag (roll)
840,890 $\text{cm}^{-1}$ (doublet)	$(\text{SiH}_2)_2$ bend
875 $\text{cm}^{-1}$	$\text{SiH}_2$ bend (scissors)
2000 $\text{cm}^{-1}$	SiH stretch
2090 $\text{cm}^{-1}$	$\text{SiH}_2$ stretch

The amorphous silicon films were deposited onto 8 mil thick silicon wafers. The wafers were polished on one side and were p type with resistivities of 13 ohm-cm or greater. The deposited films were approximately 0.5 micrometers thick and the deposition rate was 15 angstrom/sec. or greater for all samples. The data was acquired on a Fourier transform infrared spectrometer. Each sample was mounted on a shuttle alongside a reference silicon substrate. The sample and the reference were each measured 200 times. This eliminated atmospheric absorption bands due to carbon dioxide and water vapor. A band at 1125  $\text{cm}^{-1}$  was observed in almost all the samples and is believed to be an  $\text{SiO}_2$  absorption band. The following procedure was used to calculate the dihydride/monohydride ratio. The  $\text{SiH}_2$  stretch band at  $\sim 2100 \text{ cm}^{-1}$  was deconvoluted from the SiH stretch band at  $\sim 2000 \text{ cm}^{-1}$ . The area of each band was measured and the area of the dihydride ( $2100 \text{ cm}^{-1}$ ) band was divided by the sum of the dihydride and monohydride bands. This procedure has no special significance but was plotted in this way in order to compare the data with data derived in previous work [2].

Five samples were deposited for each of the three data sets. The pressure was held constant in all cases at  $\sim 0.300$  Torr. The data for the infrared absorption versus substrate temperature is shown in Figure 1. The deposition parameters were as follows:

Gas Mixture;  $\text{Si}_2\text{H}_6$   
 Flow Rate; 12 sccm  
 RF Power; 5 Watts

The substrate temperature during deposition is plotted against the dihydride concentration as defined above. The dihydride concentration decreases smoothly as the temperature is increased. The substrate temperature is labeled onto the graph. The absorption bands at 840  $\text{cm}^{-1}$

and  $890\text{ cm}^{-1}$  is a doublet arising from the interaction of adjacent dihydride molecules. As the temperature is increased the doublet disappears leaving a single band at  $875\text{ cm}^{-1}$ , identified as the dihydride bending (scissors) mode. These observations are consistent with a decrease in the dihydride concentration as shown in figure 1. It should be noted that dihydride groups are still present at the highest substrate temperature investigated, 328 C.

The infrared absorption versus RF power is shown in Figure 2. The deposition parameters were as follows:

Gas Mixture;  $\text{Si}_2\text{H}_6$   
Flow Rate; 6 sccm  
Deposition Temperature; 260 C.

The decrease in the dihydride concentration is precipitous. While greatly reduced, the dihydrides are not, however, completely eliminated. The deposition rate for all the samples of Figure 2 were independent of RF power. This is called the supply limited regime. A calculation of the material deposited in the deposition chamber indicates a disilane utilization of greater than 75%. If high quality films could be deposited under these conditions, the economic benefits of almost complete gas utilization might be significant.

The infrared absorption versus feedgas composition is shown in Figure 3. The deposition parameters for the samples are;

Flow Rate; 6.8 sccm  $\text{Si}_2\text{H}_6$ , He variable  
Pressure; 0.300 Torr  
RF power; 10 Watts  
Substrate Temperature; 265 C.

Examination of the data shows that the dihydride concentration decreases steadily as the percentage helium in the gas mixture increases. This is the strongest correlation observed for affecting a decrease in the dihydride concentration. Unfortunately, the deposition rate decreased as the percentage of helium in the feedgas mixture increased. Our explanation for this is as follows. As helium is added to the gas mixture the total flow increases. The pressure was kept constant resulting in a decrease in the average residence time of the feedstock gasses. The disilane is inferred to be swept out of the

chamber before complete decomposition can occur.

The results obtained so far are consistent with previous work [2]. Those studies differed mainly in the gas flow rates and pressure at which the depositions were performed.

### **Light and Dark Conductivity**

Studies of the dark conductivity and AM1.5 photoconductivity have been completed as a function of two deposition variables. These are the RF power and the substrate temperature.

Variable	Temperature	RF Power
Pressure	0.305 Torr	0.305 Torr
Temperature	225,250,275,300,325 C	265 C.
Flow	6 sccm	6 sccm
Gas	disilane	disilane
RF Power	10 watts	10,20,30,40,50 Watts

The results are shown in Figures 4 and 5. In all cases very high conductivity ratios are observed exceeding  $10^5$  in almost all most cases. The films are assumed to be n-type with electrons as the majority carriers. The dark and light conductivity are observed to be independent of RF power as is illustrated in Figure 4. The mobility-lifetime product is constant and this would rule out damage due to ion bombardment as the variable limiting the attainable mobility-lifetime product for the majority carriers. These values are approximately one order of magnitude below those obtained for the best films deposited from monosilane at low deposition rates. The data in Figure 5 illustrates a somewhat more interesting behavior. Both the light and dark conductivity are observed to increase as the substrate temperature is increased even though the ratio remains relatively constant. This behavior is consistent with a decrease in the optical bandgap as the substrate temperature is raised.

### **Solar Cells**

Preliminary fabrication of glass/P-I-N/metal solar cells has been completed. The best efficiencies are in the range of 5%. The intrinsic layers are 4500 angstroms thick and are deposited at 15 angstroms/sec. or greater in all cases. The main factor limiting the efficiencies is the low values of the short circuit current, ~10

milliamperes/cm<sup>2</sup>. The greatest gains in efficiency to date have been obtained by optimizing the p-layer. A number of steps which should increase the efficiency included thicker intrinsic layers, graded buffer layers and reverse bias annealing. We hope to incorporate these improvements in the near future.

### **References**

- [1] Cardona, M., Vibrational Spectra of Hydrogen in Silicon and Germanium, *phys. stat. sol. (b)* 118, 463 (1983)
- [2] Wiesmann, H., et. al., Research on High Efficiency Single Junction Monolithic Thin Film Amorphous Silicon Solar Cells, Final Report, SERI contract IB-5-05004-1 (1986)

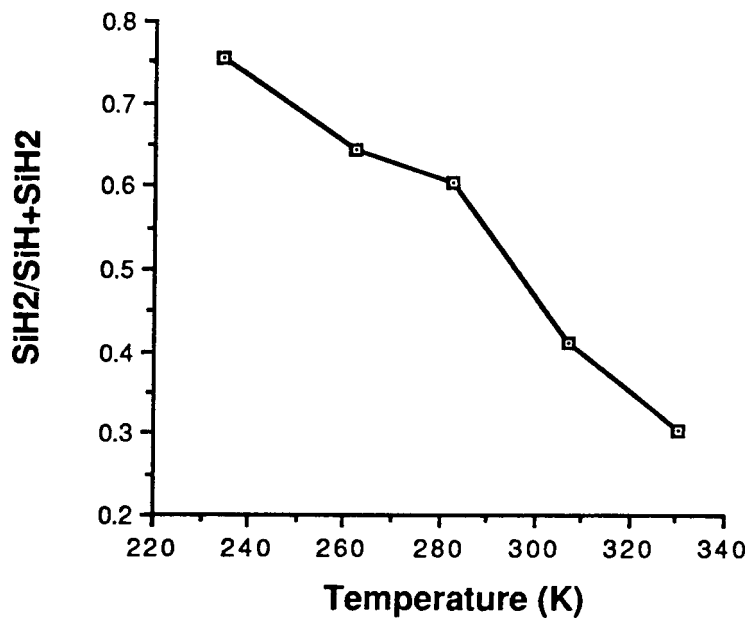


Figure 1. Dihydride concentration versus substrate temperature.

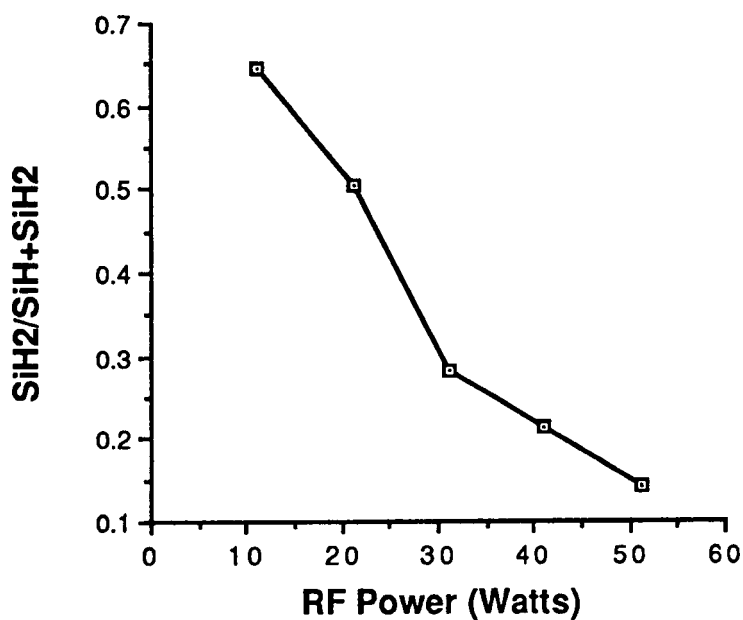


Figure 2. Dihydride concentration versus RF power.

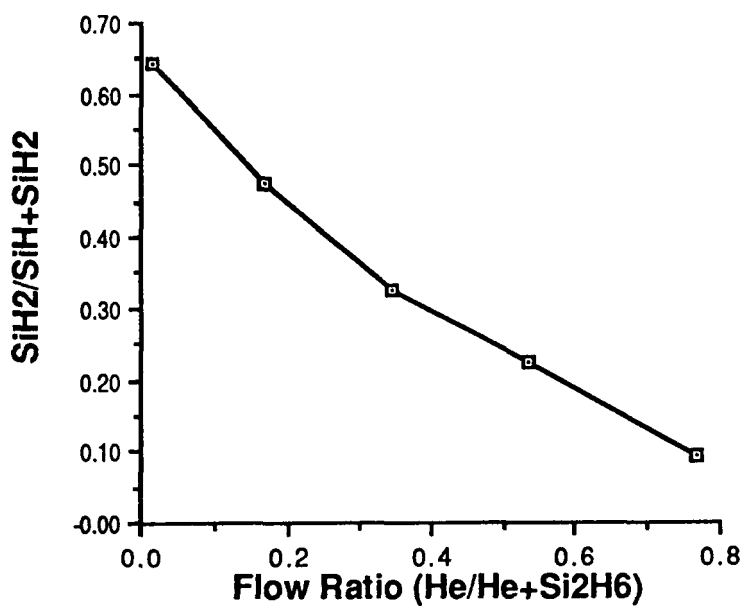


Figure 3. Dihydride concentration versus gas flow ratio.

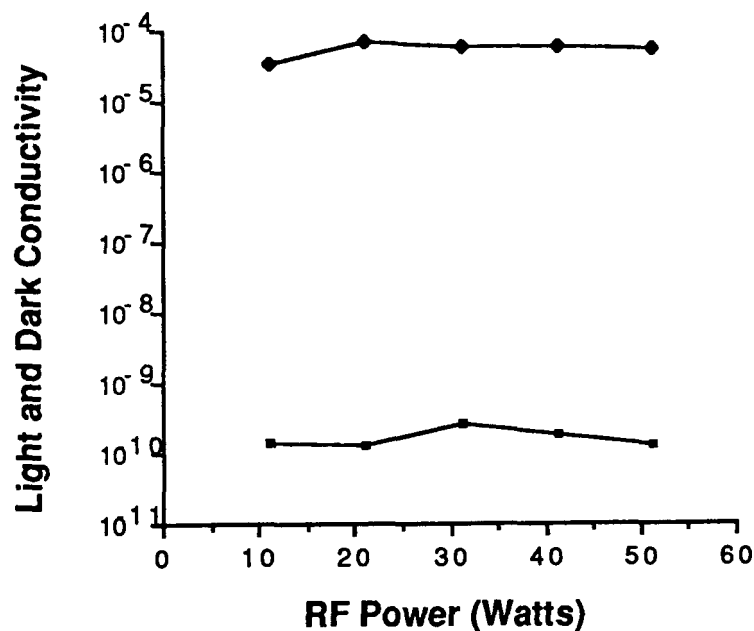


Figure 4. Dark and photoconductivity versus RF power.

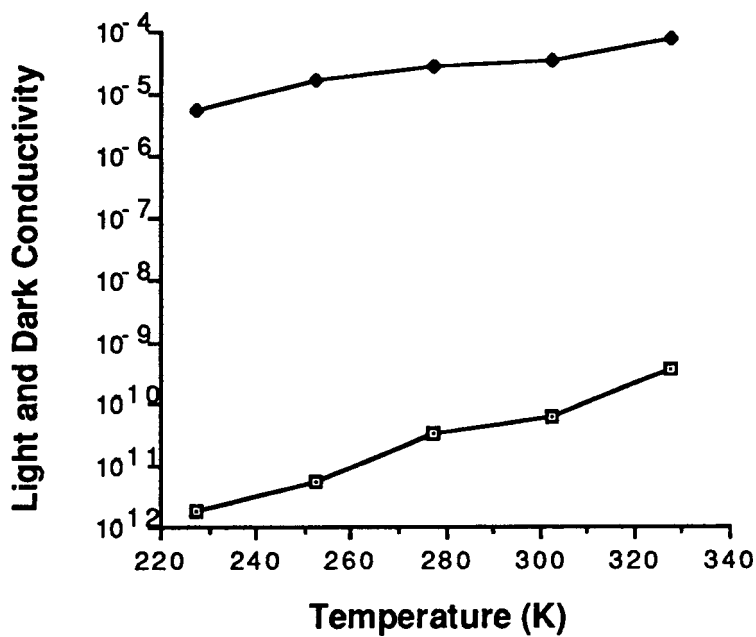


Figure 5. Dark and photoconductivity versus substrate temperature.

Title: Amorphous Silicon Deposition Research with In Situ Diagnostics

Organization: Jet Propulsion Laboratory, California Institute of Technology, Pasadena, California

Contributors: Y.H. Shing, principal investigator; J.W. Perry, C.L. Yang, C.E. Allevato and C.V. Matus

The objective of this research is to understand radio frequency (RF) glow discharge and electron cyclotron resonance (ECR) microwave plasma deposition of amorphous silicon (a-Si:H) and amorphous silicon carbon alloy (a-SiC:H) films through in situ plasma diagnostics.

JPL has established state-of-the-art a-Si:H and a-SiGe:H film deposition capabilities using the RF (13.56 MHz) glow discharge method and has implemented in situ plasma diagnostics using coherent anti-Stokes Raman spectroscopy (CARS), mass spectrometry (MS) and optical emission spectroscopy (OES) to investigate the kinetic behavior of various deposition conditions. Silane RF plasma diagnostics under device-quality a-Si:H film deposition conditions have been investigated using CARS and MS [1]. In order to elucidate some of the critical factors in the SiH<sub>4</sub>/GeH<sub>4</sub> plasma chemistry, we have performed in situ CARS measurements to determine closed-chamber disappearance kinetics and steady-state depletions on SiH<sub>4</sub> and GeH<sub>4</sub> mixed gas plasmas with or without hydrogen dilution [2]. Plasma diagnostics have revealed that the critical role of hydrogen dilution in GeH<sub>4</sub> containing plasma is to suppress the gas phase polymerization and to promote the incorporation of Ge into the film [3].

The development of ECR microwave plasma deposition technology has generated great interest in applying this technology for improving a-Si:H and a-SiC:H film depositions. For typical ECR depositions, a remote microwave plasma produced under the ECR condition is extracted through a divergent magnetic field and reacts with the source gas for film depositions. The separation of the plasma and the deposition chemistry introduces an additional degree of freedom in which the film properties can be optimized. In situ plasma diagnostics are employed to obtain the needed information to understand and to control the deposition processes.

#### ECR Microwave Plasma Deposition System

A state-of-the-art ECR plasma deposition system has been designed and setup at JPL for performing advanced deposition research on a-Si:H, a-C:H and a-SiC:H films. The JPL ECR deposition system (Figure 1) consists of an ECR ion source, a custom designed deposition chamber with in situ plasma diagnostic capabilities, a gas handling system and a high vacuum pumping system. The ECR plasma is generated by a 2.45 GHz microwave power source (300 - 1500 W) and a resonant magnetic field in a cylindrical plasma chamber. The microwave power is transmitted in a rectangular waveguide and coupled to the plasma chamber via a symmetrical mode coupler and a quartz window. The substrates are mounted on a sample stage which is located at a distance of 15 cm from the aperture of the ECR plasma chamber.

## Film Depositions and OES Plasma Diagnostics

ECR and RF glow discharge depositions of a-Si:H, a-C:H and a-SiC:H films and OES plasma diagnostics have been performed using  $\text{SiH}_4$ ,  $\text{CH}_4$ ,  $\text{H}_2$  and mixed gas plasmas [4]. Systematic investigations of the correlation between the a-Si:H film deposition rate and the OES studies have been carried out to establish a consistent data base needed for understanding the film growth mechanisms. In Figure 2(A), the deposition rate of a-Si:H films are plotted with different flow rates and RF power. The deposition rate of a-Si:H films using pure  $\text{SiH}_4$  as the source gas shows two ranges of linear dependence in the RF power with a clear change of slope. The OES spectra of steady-state  $\text{SiH}_4$  plasmas have also been measured with different RF power and flow rates. The  $\text{SiH}^*$  emission intensity shows similar dependence as a function of RF power and flow rates (Figure 2(B)). Both the deposition rate and the  $\text{SiH}^*$  emission intensity show the same value of RF power where the slope changes and this RF power value increases with the flow rate. The correlation between the film deposition rate and the  $\text{SiH}^*$  emission intensity suggests that  $\text{SiH}^*$  species are related to the neutral radicals which are responsible for the deposition of a-Si:H films.

Initial ECR deposition of a-Si:H films has been performed using  $\text{H}_2$  as the plasma gas and  $\text{SiH}_4$  as the source gas. It is found that the photosensitivity of ECR deposited a-Si:H films is improved by using only the  $\text{SiH}_4$  source gas. A light-to-dark conductivity ratio of  $1 \times 10^5$  and a deposition rate of  $25 \text{ \AA/s}$  have been obtained for ECR deposited a-Si:H films using a  $\text{SiH}_4$  flow rate of  $20 \text{ sccm}$ ,  $0.6 \text{ mTorr}$  chamber pressure, microwave power at  $300 \text{ W}$ , and a substrate temperature of  $240^\circ\text{C}$ . Figure 3 shows the ECR deposition rate of a-Si:H films and the  $\text{SiH}^*$  emission intensity of ECR plasma as a function of microwave power. The correlation between the deposition rate and the  $\text{SiH}^*$  emission intensity is also observed for the ECR deposition process. Because of the limited data available at present, whether the ECR depositions show two ranges of linear dependence on microwave power is not known. In addition, the ECR deposition process has a complex parameter space involving microwave coupling modes, resonant and extracting magnetic fields, chamber pressure, and microwave power. Systemmatic investigations are in progress for evaluating and optimizing the ECR deposition process.

Diamond-like and polymer-like a-C:H films have been deposited by RF glow discharge and ECR plasma techniques. The ECR deposition rate of a-C:H films is a factor of 2-4 higher than that of RF glow discharge. The ion energy impinging on the substrate plays an important role in modifying the structure of a-C:H films. It is apparent that a high ion energy is required for depositing hard, diamond-like a-C:H films.

## Transient OES and Film Characterizations

Systematic investigations of  $\text{SiH}_4$ ,  $\text{CH}_4$  and mixed gas plasma kinetics have been performed using transient optical emission spectroscopy. The transient emission intensities of  $\text{SiH}^*$ ,  $\text{CH}^*$ ,  $\text{H}^*$ , and  $\text{H}_2^*$  and  $\text{Si}^*$  were measured in closed-chamber glow discharge experiments using an OMA detection system. The transient OES spectra of a closed-chamber, pure  $\text{SiH}_4$  plasma with initial pressure of  $350 \text{ mTorr}$  and RF power density of  $40 \text{ mW/cm}^2$  (Figure 4) show that the  $\text{SiH}^*$  emission intensity has a complicated time dependence. The  $\text{SiH}^*$  emission shows two maxima occurring at different times. The first maximum may result from the response time needed for the  $\text{SiH}_4$  plasma to reach the

equilibrium state. The additional contributions to the second SiH\* emission maximum indicate that another mechanism for producing SiH\* may be activated due to the increase of the hydrogen content in the plasma. The kinetics for the similar CH<sub>4</sub> plasma do not show these complicated features, and only one simple decay is observed in the normal RF power range (Figure 5).

Optical properties of a-C:H films are characterized by infrared, Raman and optical transmission measurements. A typical IR spectrum of ECR deposited a-C:H films is shown in Figure 6. The characteristic IR absorption lines for CH stretching modes are identified as multi-peaks in the vicinity of 2950 cm<sup>-1</sup> and 1400 cm<sup>-1</sup>. The narrow line width resulting in partial resolution of several stretching modes at 2950 cm<sup>-1</sup> and the existence of H<sub>2</sub>O absorption modes (3500 cm<sup>-1</sup>, 1750 cm<sup>-1</sup>) indicate a polymer-like film structure which is susceptible to water molecule absorption. The Raman spectrum of a diamond like a-C:H film is shown in Figure 7, where a characteristic broad peak is found at 1580 cm<sup>-1</sup>. The optical bandgap of a-C:H films is determined by transmission measurements to be in the range of 1.0 - 1.5 eV for diamond-like films and in the range of 2.5 - 4.0 eV for polymer-like films.

### Conclusions and Future Plans

We have demonstrated that the steady-state and kinetic characteristics of ECR and RF glow discharge plasmas can be readily monitored by OES in real time during a-Si:H and a-SiC:H film depositions using an OMA detection system. The correlation between the deposition rate and the optical emission intensity of SiH\* suggests that SiH\* species are related to the neutral radicals which are responsible for the film depositions. The OES of the ECR plasma shows a strong emission at 434 nm from H\*, which is not detectable in the glow discharge plasma. This strong H\* emission indicates that the ECR plasma is more reactive than the RF glow discharge plasma. Transient OES spectra of SiH<sub>4</sub> and CH<sub>4</sub> plasmas in the RF glow discharge have shown different kinetics in SiH\* and CH\* emission intensities. Transient studies of the SiH\* emission intensity have indicated that additional mechanisms for producing SiH species become available in hydrogen diluted silane plasmas.

In our future research, ECR deposition of device-quality a-Si:H, a-C:H and a-SiC:H films will be continually developed by correlating in situ plasma diagnostics with film characterization experiments. The ECR deposition parameter space for a-Si:H, a-C:H and a-SiC:H films will be optimized as a function of partial pressure, substrate temperature, total pressure, microwave power and deposition mode by varying plasma and source gases. A high temperature sample stage will be build to extend the ECR deposition capabilities for crystalline SiC and diamond films. The ECR plasma diagnostics will be compared with glow discharge plasmas to determine the difference between ECR and glow discharge deposition processes.

### References

1. Y.H. Shing, J.W. Perry and A.M. Hermann, Proc. 19th IEEE Photovoltaic Specialists Conference (1987), 577.
2. Y.H. Shing, J.W. Perry and C.E. Allevato, Solar Cells, 24 (1988), 353.
3. J.W. Perry, Y.H. Shing and C.E. Allevato, Appl. Phys. Lett., 52 (1988), 2022.
4. C.L. Yang, Y.H. Shing and C.E. Allevato, Proc. 20th IEEE Photovoltaic Specialists Conference (1988), (in press).

Figure 1. Front view of the JPL ECR microwave plasma deposition system.

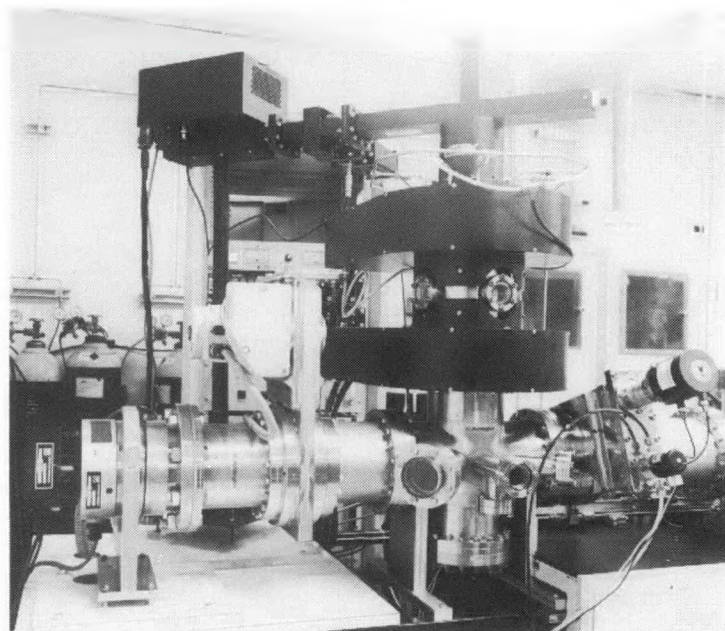


Figure 2(A). RF glow discharge deposition rate of a-Si:H films as a function of RF power.

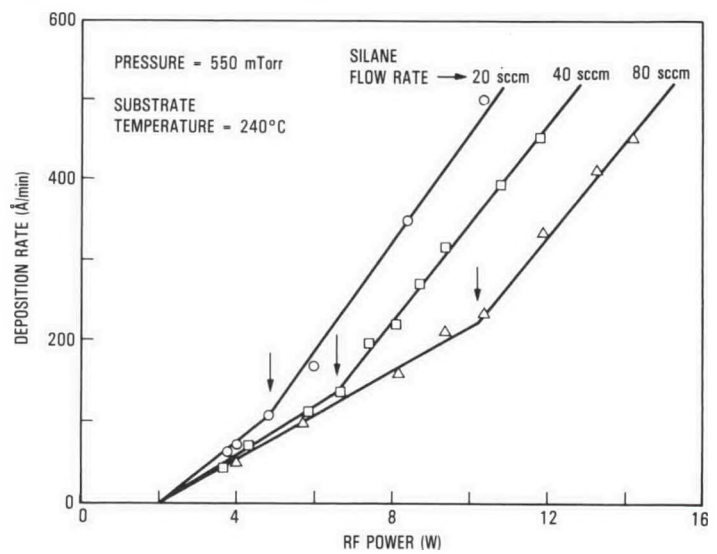


Figure 2(B). SiH\* emission intensity of SiH<sub>4</sub> RF plasmas as a function of RF power.

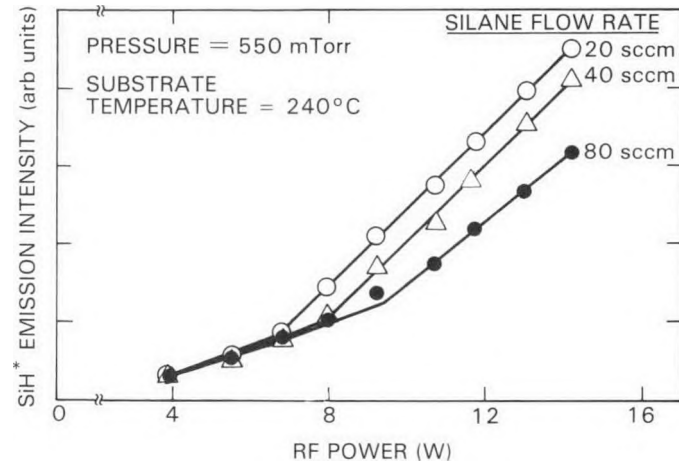


Figure 3(A). ECR microwave plasma deposition rate of a-Si:H films as a function of microwave power.

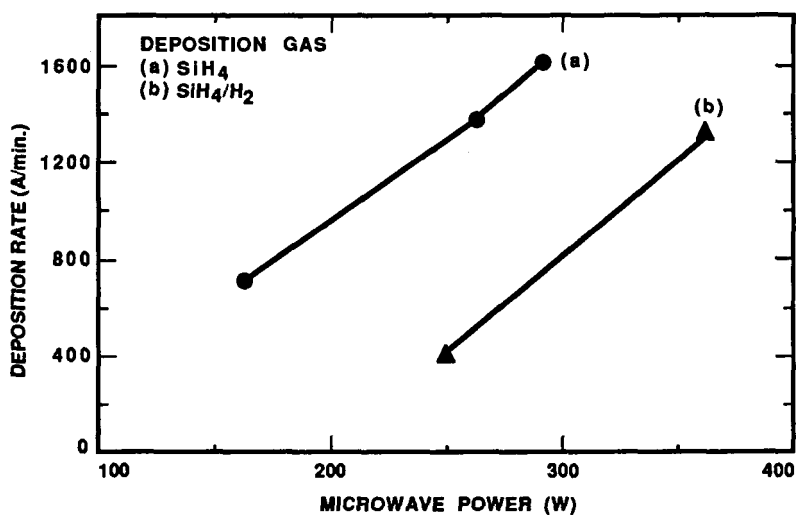


Figure 3(B). SiH\* emission intensity of SiH<sub>4</sub> and H<sub>2</sub> mixed gas ECR plasmas as a function of microwave power.

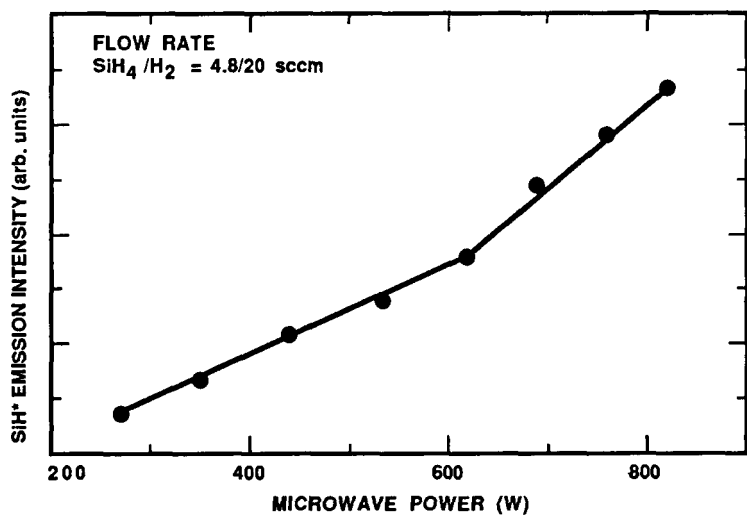


Figure 4. The emission intensity of SiH\* as a function of time for a closed-chamber SiH<sub>4</sub> plasma. Initial pressure = 530 mTorr; RF power density = 40 mW/cm<sup>2</sup>.

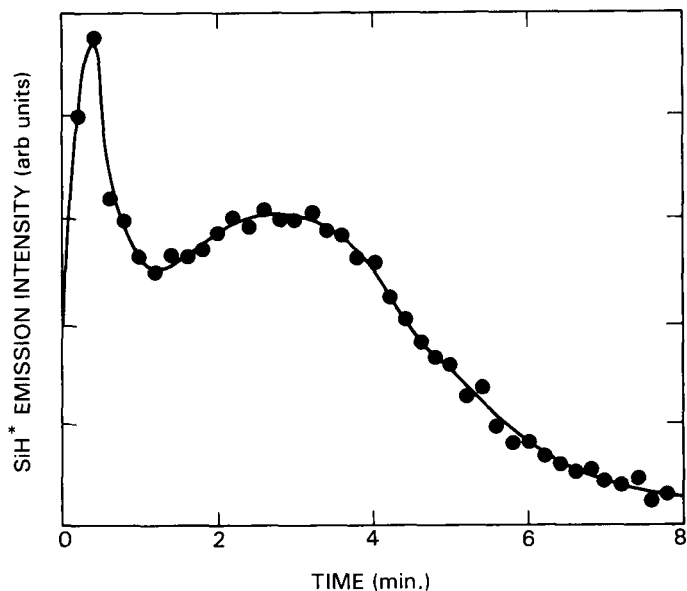


Figure 5. The emission intensity of  $\text{CH}^*$  as a function of time for a closed-chamber  $\text{CH}_4$  plasma. Initial pressure = 530 mTorr; RF power density = 40 mW/cm<sup>2</sup>.

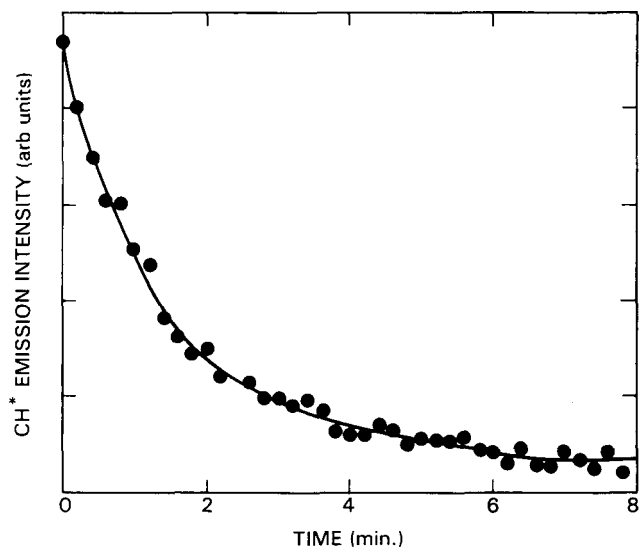


Figure 6. Typical infrared spectrum of ECR deposited a-C:H films.

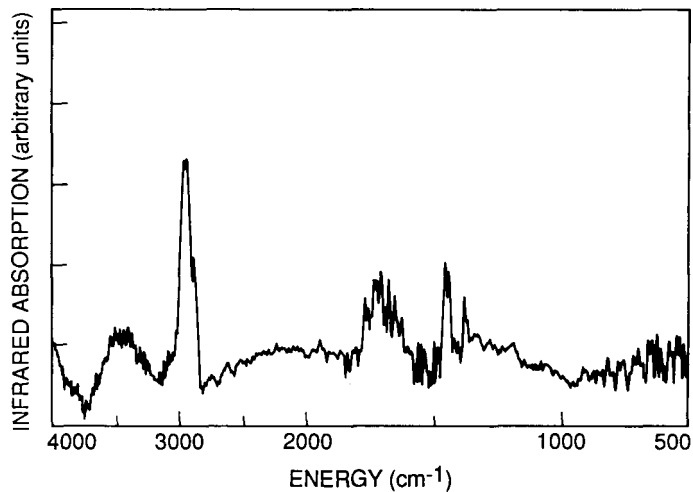
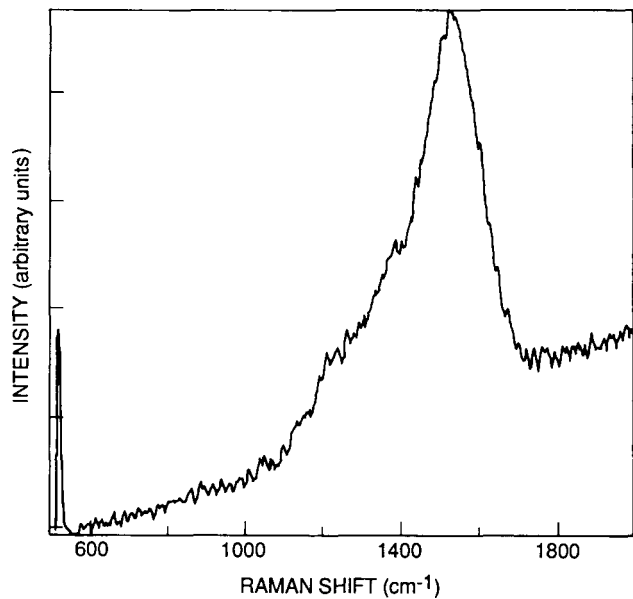


Figure 7. Raman spectrum of RF glow discharge deposited, diamond-like a-C:H films.



### 3.0 POLYCRYSTALLINE THIN FILMS

K. Zweibel (Manager), R. Mitchell, and H. S. Ullal

The objective of the Polycrystalline Thin Film Program is to develop thin-film, flat-plate modules that meet DOE's long-term goals of reasonable efficiencies (15%-20%), very low cost (near \$50/m<sup>2</sup>), and long-term reliability (30 years). The approach relies on developing solar cells based on highly light-absorbing compound semiconductors such as CuInSe<sub>2</sub> and CdTe and their alloys. These semiconductors are fabricated as thin-film cells (1-3  $\mu$ m thick) with minimal material and processing costs.

CuInSe<sub>2</sub> cells produced by ARCO Solar and by Boeing were measured at SERI at 12.9% efficiency (active area). ARCO Solar also reports the achievement of 14.1% efficiency, which has not yet been confirmed. Others surpassing 10% efficiency in CuInSe<sub>2</sub> are SERI and the Institute of Energy Conversion. Larger-area CuInSe<sub>2</sub> devices have also been fabricated with very high efficiencies. ARCO Solar has made a 938-cm<sup>2</sup> (aperture area) CuInSe<sub>2</sub> module with 11.1% efficiency (10.4 W) measured at SERI.

CuInSe<sub>2</sub> shows good proven stability under controlled conditions (9000 hours of illumination), and initial outdoor tests (ARCO) are also promising. We have conducted two-months of outdoor testing on ARCO Solar CuInSe<sub>2</sub> panels with no change in their efficiencies. These are the first such tests on CuInSe<sub>2</sub> by an independent agency.

Three U.S. laboratories (University of South Florida, Ametek, and Photon Energy) report CdTe cell efficiencies between 10.5% and 12%. Photon Energy has fabricated near-square-foot CdTe submodules measured outdoors at SERI at 7.3% efficiency (aperture area). Innovative designs are now addressing past difficulties in contacting CdTe. We have recently begun testing an encapsulated CdTe submodule provided by Photon Energy. After one month, it showed no degradation. As with the CuInSe<sub>2</sub>, this is the first independent testing of encapsulated devices made from this material.

The improved efficiencies and larger areas of CuInSe<sub>2</sub> and CdTe devices, and their apparent stability, are the major recent advances in these technologies. Polycrystalline cells require continued development to achieve 15%-20% conversion efficiencies. Two strategies are being used: development of single-junction cells and an innovative effort on two-junction cascade cells. Improvement of the single-junction technologies has been steady and reliable. This strategy remains the major focus of the task. Potentially achievable efficiencies approach 20%, and projections indicate the likelihood of fabricating modules of more than 15% efficiency. Developing two-junction, CuInSe<sub>2</sub>-based cascade cells permits even more ambitious long-term efficiency goals. Combining two well-matched single-junction modules into a cascade cell design could lead to module efficiencies of better than 20% at costs under \$60/m<sup>2</sup>. The materials being investigated for the top cells include CdTe and ZnTe alloyed with Mn, Mg, Zn, and Hg (Jet Propulsion Laboratory, Georgia Tech, and the University of South Florida).

Developing scalable, low-cost fabrication methods is important in providing industry with a foundation for future large-area, high-throughput commercial processes. Research methods for fabricating polycrystalline cells include, for CuInSe<sub>2</sub>, an electrochemical/selenization method (International Solar Electric Technology), a reactive-sputtering and hybrid sputtering/evaporation method (University of Illinois), and evaporation (Boeing); for CdTe, close-spaced sublimation (University of South Florida), evaporation (Institute of Energy Conversion), electrodeposition (Ametek), metal-organic chemical vapor deposition (MOCVD) (Georgia Tech and JPL), and proprietary methods (Photon Energy).

A recompetition of the Polycrystalline Thin Film Program was initiated with the release of a request for proposals (RFP) in FY 1986. The objective of the solicitation was to refocus the successful research of the past to the long-term goals of the DOE program. The research community responded favorably, as reflected in the many excellent technical proposals received in response to the solicitation. The contracts resulting from that RFP began in FY 1987, and the second year of excellent work that resulted from them is reported here.

Title: High-Efficiency Copper Ternary Thin-Film Solar Cells

Organization: International Solar Electric Technology (ISET)  
Inglewood, California

Contributors: V. K. Kapur and B. M. Basol, principal  
investigators; and R. C. Kullberg

The objective of this program is to develop a thin film CuInSe<sub>2</sub> (CIS) solar cell with a conversion efficiency approaching 12%. The technique used in preparing the CIS films is the two-stage process. The two-stage process involves, (1) sequential deposition of Cu and In layers onto a substrate, (2) selenization of this Cu/In stack in a H<sub>2</sub>Se atmosphere to form the compound.

Most of the work at ISET was carried out using glass/Mo substrates. Mo layers were E-Beam evaporated in our laboratory and they had a nominal sheet resistance of 0.08 ohms per square. Cu and In layers were electrodeposited onto the Mo coated glass substrates using specialized substrate preparation techniques and electrolytes. Selenization was carried out at around 400 C for about an hour. Solar cells were fabricated by evaporating CdS window layers and Al finger patterns on the CIS films. Details of the electrodeposition, selenization and device fabrication processes have been published in our previous reports and papers [1,2,3,4] and they will not be repeated here. The best solar cell we fabricated on an electrodeposited/selenized CIS film had an efficiency of 10.4% [4].

Our efforts during much of the present contract period were concentrated on large area deposition and the adhesion problem for the electrodeposited/selenized CIS films. During this period, we have started to work with 50 cm<sup>2</sup> area films and devices and built electrodeposition fixtures to plate uniform layers of Cu and In over these large areas. Although, large area CIS films with acceptable stoichiometric uniformity were successfully obtained, the adhesion of these films to the Mo substrates was not good. Two-stage process involves selenization of elemental Cu and In layers. Consequently, there is a volume expansion of the deposited Cu/In stack upon selenization. This volume expansion is a source of stress and it causes film detachment from the Mo coated substrate especially when the film is subjected to any wet chemical processing such as photolithography during device fabrication. It is clear that the bonding between Mo, which is a relatively inert material, and the CIS film is not strong enough to compensate for the forces exerted onto the CIS/Mo interface by the stresses resulting from the volume expansion. In studying the reasons and possible cures for the adhesion problem we have noticed that the adhesion was a function of the stoichiometry of the CIS film. Cu-rich films adhered well to the Mo coated substrates, possibly due to the presence of a second phase (copper selenide) at the CIS/Mo interface. Adhesion was found to be poor for near stoichiometric films, whereas, highly In-rich stoichiometries again promoted adhesion.

As part of our efforts to seek a solution to the adhesion problem we have started some work on CIS films prepared by an evaporation/selenization technique. In this method, Cu and In films were thermally evaporated on Mo coated glass substrates at pressures around  $5 \times 10^{-5}$  torrs. Resulting elemental stacked layers were selenized in the usual manner and devices were made by evaporating CdS or CdZnS window layers. Early results were very encouraging. Cells with efficiencies around 7% were obtained without any peeling problems. An illuminated I-V characteristics of a device prepared by this method is shown in Fig. 1. The spectral response of a similar cell is given in Fig. 2. [5]. We intend to pursue this evaporation/selenization technique for fabricating high efficiency solar cells. We will employ E-Beam evaporation method to obtain large area depositions of Cu and In layers. We also intend to pursue means and methods to improve adhesion of the electrodeposited/selenized films to large area substrates.

#### References

1. Kapur, V. K., B. M. Basol, and E. S. Tseng, Proc. 18th IEEE Photovoltaic Specialists Conf., IEEE, New York, 1985, p. 1429.
2. Kapur, V. K., B. M. Basol, and E. S. Tseng, Proc. 7th International Conf. on Ternary and Multinary Compounds, Snowmass, CO, 1986, p. 219.
3. Kapur, V. K., B. M. Basol, and E. S. Tseng, Solar Cells, 21, 1987, p. 65.
4. Photovoltaic Program Branch: Annual Report, FY1987. (March 1988). SERI/PR-211-3299. 84 pp. Available NTIS: Order No. DE88001155.
5. We are grateful to Dr. Robert Birkmire and the IEC group for CdZnS evaporation and device measurements.

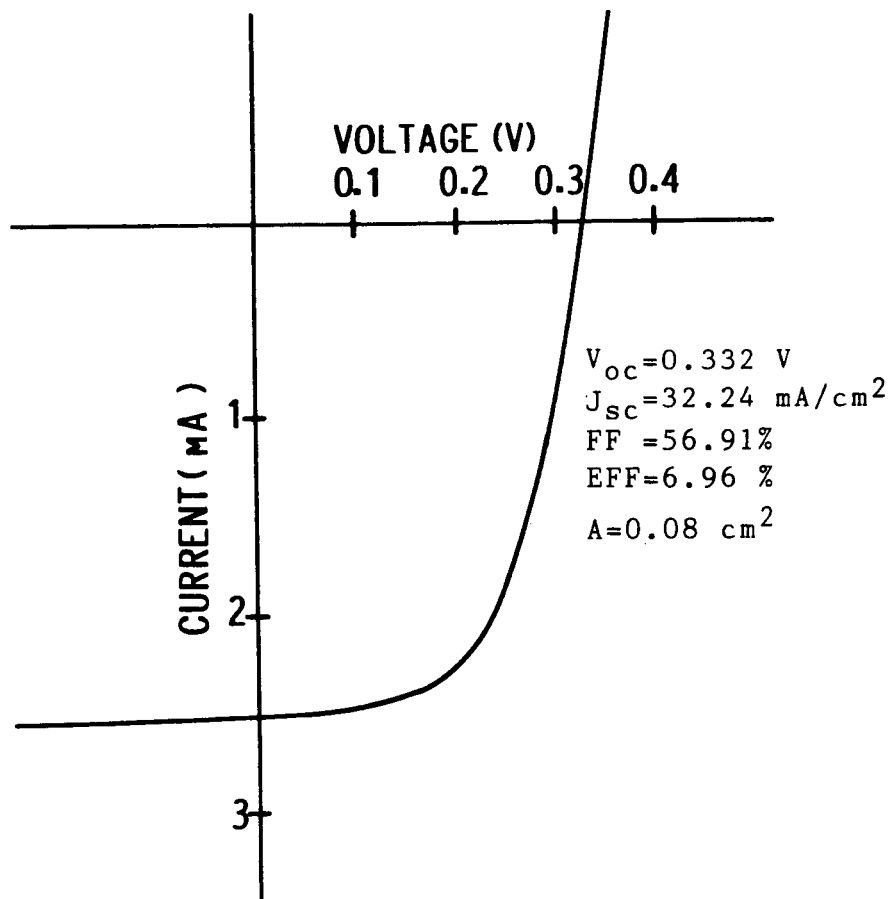


Fig. 1. Illuminated I-V characteristics of a preliminary device made on evaporated/selenized film.  $87.5 \text{ mW/cm}^2$  ELH simulation.

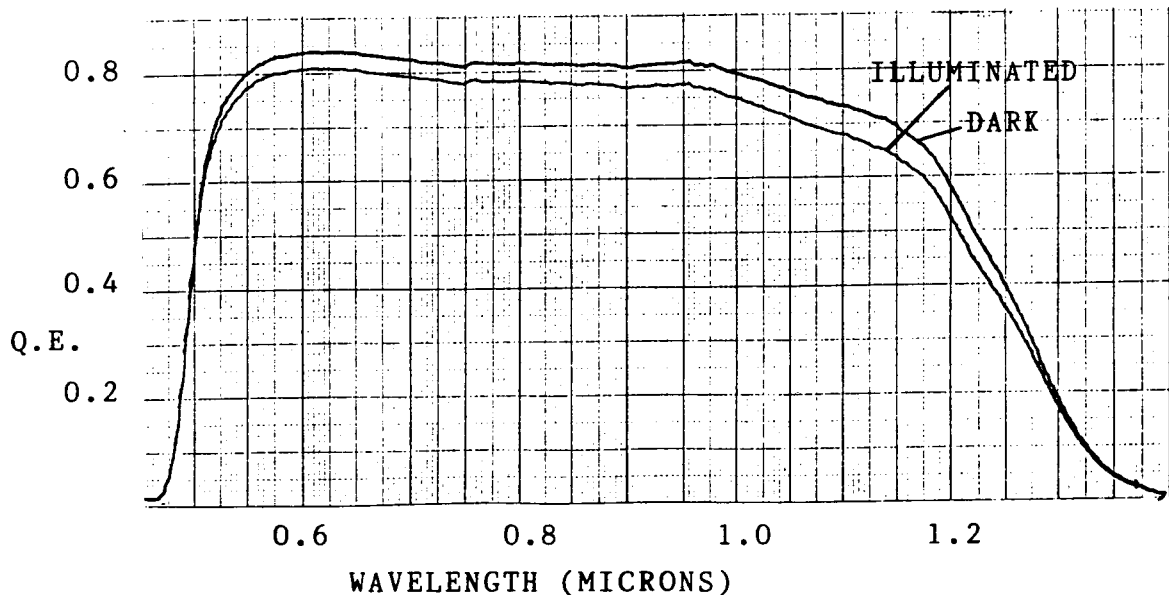


Fig. 2. Spectral response of a CdZnS/CIS solar cell.

**Title: High Efficiency CuInSe<sub>2</sub> and CuInGaSe<sub>2</sub> Based Cells and Materials Research**

**Organization: Boeing Electronics, P.O.Box 24969, M.S.9Z-80  
Seattle, WA. 98124-6269**

**Contributors: Walter E. Devaney, Wen S. Chen  
Reid A. Mickelsen, John M. Stewart;  
R. B. Gillette, Program Manager.**

**The present research program has as its general goal the continued improvement of photovoltaic devices based on the ternary compound CuInSe<sub>2</sub> and the related quaternary CuInGaSe<sub>2</sub>.**

**The approaches being pursued during the present research program are:**

- Improve performance of the CuInSe<sub>2</sub> and CuInGaSe<sub>2</sub> films.
- Develop new high bandgap window layers.
- Develop multilayer antireflection coatings for both the present CdZnS window layer and for new window layers.
- Fabricate high efficiency cells of 100 cm<sup>2</sup> area using a monolithic interconnect technology.

**During the first year of this program the major accomplishments have been:**

- A 12.5% efficient ZnO/thin CdZnS/CuInGaSe<sub>2</sub> cell of 1 cm<sup>2</sup> area has been fabricated. This is the highest total area efficiency yet confirmed for a polycrystalline thin film solar cell. Active Area Efficiency is 12.9%.
- Device Quantum Efficiencies of over 0.7 at 400nm have been achieved using the ZnO/thin CdZnS window layer system.
- Ta<sub>2</sub>O<sub>5</sub>/Al<sub>2</sub>O<sub>3</sub>/MgF<sub>2</sub> and Ta<sub>2</sub>O<sub>5</sub>/MgO/MgF<sub>2</sub> three layer Antireflection Coatings have been developed for CdZnS/CuInSe<sub>2</sub> and CdZnS/CuInGaSe<sub>2</sub> Solar Cells. The low reflection losses intrinsic to the ZnO/thin CdZnS/CuInGaSe<sub>2</sub> structure has been demonstrated.
- The interconnect technology needed for large area cells has been demonstrated for the ZnO/thin CdZnS/CuInGaSe<sub>2</sub> system.

- The fill factor problem encountered in devices using high ( $[Ga]/[Ga]+[In] > 0.3$ ) Gallium content  $\text{CuInGaSe}_2$  has been localized to the junction-near region using Voltage Biased Spectral Response.

The structure of the  $\text{CuInGaSe}_2/\text{CdZnS}/\text{ZnO}$  device is shown in Figure 1.

The AM1.5 I-V characteristics of the best  $\text{CuInGaSe}_2/\text{CdZnS}/\text{ZnO}$  cell fabricated to date as measured at SERI are shown in Figure 2. The use of  $\text{CuInGaSe}_2$  with gallium content of 0.27 has resulted in higher open circuit voltage. Figure 3. shows a comparison of the spectral response for this  $\text{CuInGaSe}_2/\text{CdZnS}/\text{ZnO}$  cell with a high efficiency  $\text{CuInSe}_2/\text{CdZnS}$  cell. The bandgap shift of the  $\text{CuInGaSe}_2$  relative to the  $\text{CuInSe}_2$  is clearly seen. The improved quantum efficiency at energies above the absorption edge of the  $\text{CdZnS}$  is also clear and is due to the combination of a very thin (less than 20 nm), high Zn content ( $[Zn]/[Zn]+[Cd]=0.2$ )  $\text{CdZnS}$  layer with the high bandgap  $\text{ZnO}$  layer.

The  $\text{CdZnS}$  layer used in these cells may be much thinner than previously reported  $\text{CuInGaSe}_2/\text{CdZnS}/\text{ZnO}$  devices. Analysis of the reflection and transmission characteristics of the thin  $\text{CdZnS}$  layer gives a thickness of 10 - 18 nm, with a most probable value of 16 nm. Such thicknesses are also required to model the quantum efficiency results, e.g. those of Figure 3.

The new  $\text{CuInGaSe}_2/\text{CdZnS}/\text{ZnO}$  cells also incorporate several other novel features. The interconnect technology developed for the large area  $\text{CuInSe}_2/\text{CdZnS}$  devices has been modified for the  $\text{ZnO}/\text{thin CdZnS}$  and used both to minimize shorting through the thin  $\text{ZnO}$  layer under the tab area and to minimize the tab area. A bilayer  $\text{ZnO}$  process has been utilized to minimize shunt leakage through defects in the  $\text{CdZnS}$  layer.

The present devices show several clear paths for further efficiency improvement. Optical absorption in the high conductivity  $\text{ZnO}$  layers in the near infrared indicates significant losses due both to free carrier absorption and to other, unidentified causes. Elimination or reduction of this absorption will result in higher currents. Shunt leakage identified with defects in the thin sulfide layer is significantly reducing the fill factor. A high lumped series resistance term is present in even the highest efficiency devices. For both these reasons fill factors are significantly lower than those seen in the best  $\text{CuInSe}_2/\text{CdZnS}$  cells. Elimination of these losses will result in significantly higher device efficiencies.

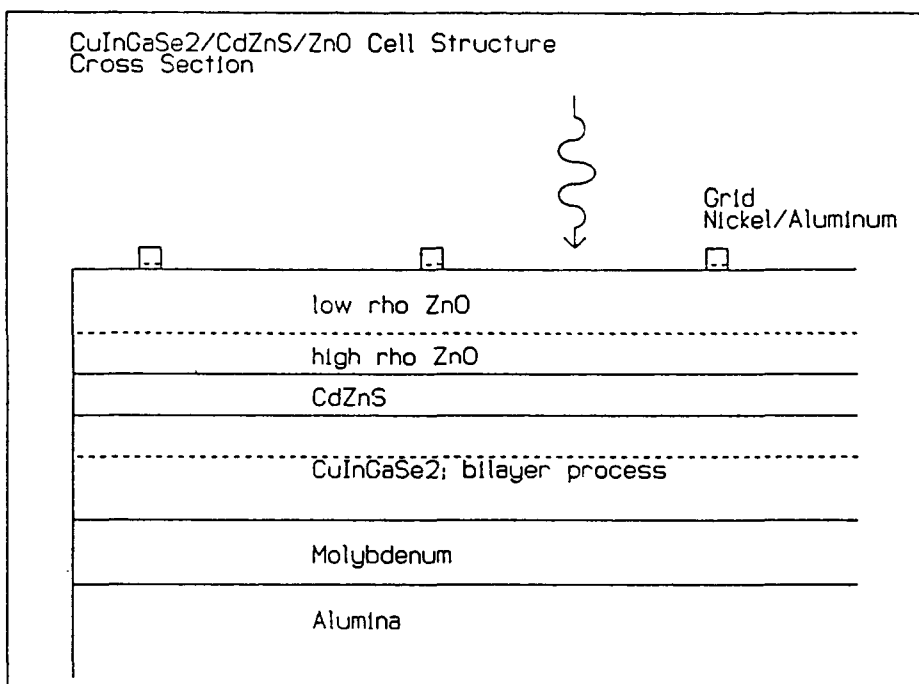


FIGURE 1: Structure of ZnO/thin CdZnS/CuInGaSe<sub>2</sub> Cell

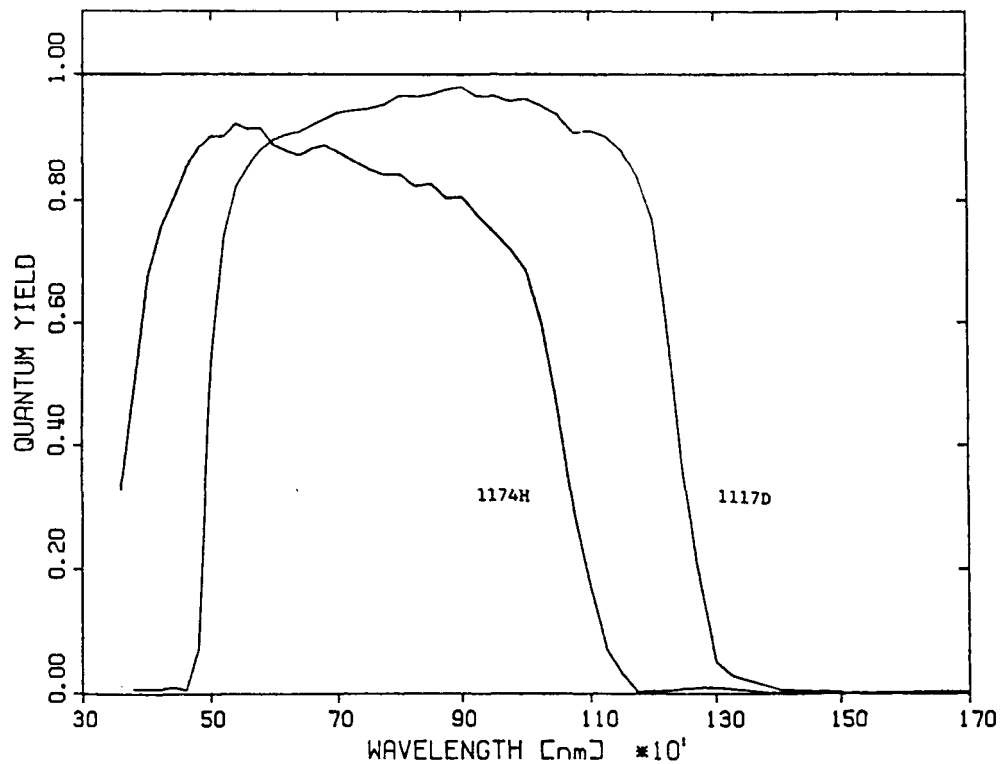


Figure 3: Comparison of Spectral Response of  
ZnO/thin CdZnS/CuInGaSe<sub>2</sub> Cell #1174H  
With CdZnS/CuInSe<sub>2</sub> Cell #1117D.

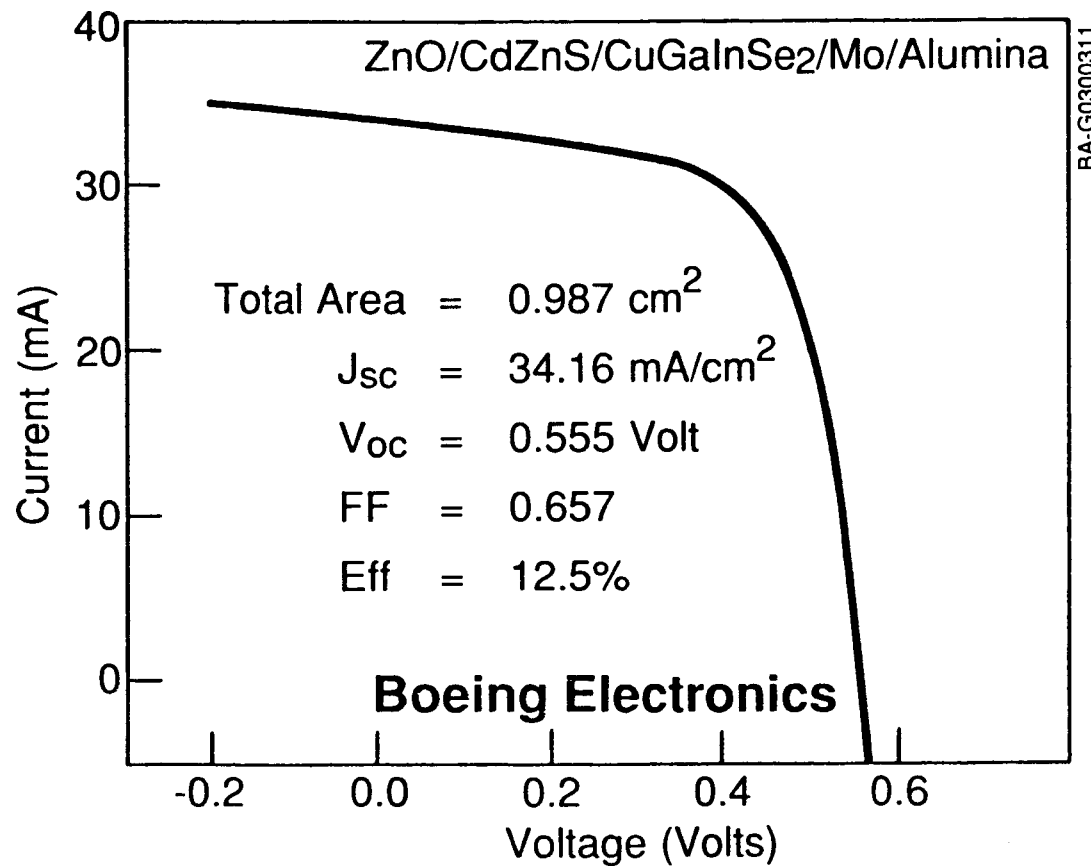


Figure 2: Current-Voltage Characteristics of the Best  
ZnO/Thin CdZnS/CuInGaSe<sub>2</sub> Cell

**Title:** Material Analysis and Device Optimization of  
**CuInSe<sub>2</sub>** Solar Cells

**Organization:** Institute of Energy Conversion,  
University of Delaware, Newark, Delaware

**Contributors:** B. N. Baron, Project Director; R. W. Birkmire and J. E. Phillips, Principal Investigators; W. N. Shafarman; B. E. McCandless; and M. Roy.

**Objectives**

The objectives of this research program are to develop a fundamental base of knowledge of the relationships between materials processing, materials properties and performance of stable, high efficiency thin-film CuInSe<sub>2</sub> solar cells. In order to achieve these objectives, the Institute of Energy Conversion is carrying out a two-year program of integrated research on materials and devices.

**Technical Approach**

**Materials Preparation and Analysis**

CuInSe<sub>2</sub> films are deposited by physical vapor deposition from molecular beams of elemental Cu, In, and Se that are generated by Knudsen-type effusion cells. Studies of the relationships linking the process variables (incident flux and substrate temperature) with film properties (composition, morphology, and resistivity) are being carried out.

Wide-band-gap (CdZn)S doped with indium window layers are deposited by physical vapor deposition from the co-evaporation of CdS, ZnS, and In from separate effusion cells. The relationships between Zn content, In doping level, resistivity and optical absorption are studied in order to determine the optimum window layer process conditions and properties. Transparent conductor layers of ITO and ZnO are sputter deposited and optimized for improve short circuit current and fill factor.

CuInSe<sub>2</sub> thin-films are deposited onto glass/window layer structures to evaluate "superstrate" device configurations.

**High-Efficiency Cell Fabrication and Analysis**

Single-junction CuInSe<sub>2</sub>/(CdZn)S cells with well-defined areas are fabricated and analyzed. Such devices are used to determine the optimum CuInSe<sub>2</sub> and window layer deposition conditions on the basis of material and device analysis.

Modeling and analysis of CuInSe<sub>2</sub>/(CdZn)S devices are carried out in order to guide optimization of efficiency, to provide understanding of the fundamental limits on efficiency of single-junction CuInSe<sub>2</sub> cells, and to establish directions for further research.

$\text{CuInSe}_2$  devices are fabricated on semitransparent glass/thin Mo substrates which allow measurement of bi-facial spectral response in order to determine the optical absorption coefficient and collection width of  $\text{CuInSe}_2$  in operational  $\text{CuInSe}_2/(\text{CdZn})\text{S}$  devices.

### Significant Results in FY 1988

The  $\text{CuInSe}_2$  films were grown in two distinct steps by physical vapor deposition from three elemental sources. Figure 1 shows the substrate temperature-time profile and metal flux ratios for the two steps during a representative deposition. First, a Cu-rich ( $\text{Cu}>26\%$ ) layer was deposited at a substrate temperature of  $300^\circ\text{C}$  with a ratio of  $\text{Cu:In}$  molar effusion rates of 1:1. After deposition of the first layer, the substrates were shuttered and the substrate temperature increased to  $450^\circ\text{C}$ . The In source temperature is also increased to give a  $\text{Cu:In}$  molar effusion rate ratio of 0.4:1. The molar effusion rate for the Se was constant throughout the entire deposition.

A dramatic change in morphology occurred when the Cu composition of the films exceeded 25%. The films changed from a specular surface at Cu content  $<25\%$  to a textured surface. In composite  $\text{CuInSe}_2$  films used for high efficiency solar cells, the Cu content in the first layer exceeds 26% which produces textured surfaces. The texture of the first layer is maintained during the growth of the second layer and thus controls the overall morphology of the composite film. Further, XRD measurements of single layer  $\text{CuInSe}_2$  films with  $\text{Cu}>27\%$ , indicate the presence of a  $\text{Cu}_2\text{Se}$  phase.

Diagnostic devices fabricated on films with the changed morphology do not respond to optimization heat treatments and have extremely poor diode characteristics. Thus, an upper limit on Cu content for fabricating devices is identified by a change in morphology which may be associated with the onset of a second ( $\text{Cu}_2\text{Se}$ ) phase.

Measured optical and electrical properties of  $(\text{CdZn})\text{S:In}$  films and window layers in  $\text{CuInSe}_2$  cells were used to determine the dopant level, Zn content, and window structure for high efficiency cells. As the In-doping level in the  $(\text{CdZn})\text{S}$  was raised, the resistivity reached a minimum and the absorption edge a maximum. The Burstein-Moss shift in the optical absorption edge, due to the degenerate In doping, decreased as the Zn content and resistivity increase. Heat treatments of  $\text{CuInSe}_2/(\text{CdZn})\text{S:In}$  cells, which are used to increase  $V_{\text{OC}}$ , were also found to increase sheet resistance of the window layer and reduce the  $J_{\text{SC}}$  of the cells. This reduction in  $J_{\text{SC}}$  was due to a shift in the  $(\text{CdZn})\text{S:In}$  optical absorption edge caused by compensation of the Burstein-Moss effect when the  $\text{CuInSe}_2/(\text{CdZn})\text{S:In}$  device was heat treated. Design of high efficiency large area cells therefore should be based on properties of the window layer in the optimized cell. However, knowing the relationship between properties of the window deposited on glass and those in an optimized device allows the properties of the window layer on glass to be used for device design. High efficiency,  $>10\%$ , cells have been achieved with several window layers as shown in Table 1. The highest  $J_{\text{SC}}$  was achieved

with  $\text{CuInSe}_2/\text{ZnO}$  but a device exhibited low  $V_{OC}$  ~0.2 volt. On the other hand,  $\text{ITO}/\text{CuInSe}_2$  structures were shorted. These results suggest that  $\text{ZnO}/\text{CdS}/\text{CuInSe}_2$  devices may be more tolerant of processing defects such as pin-holes in thin CdS layers.

A CIS cell having a superstrate structure was fabricated using a 7059/ITO transparent substrate with nominally 0.1 microns of CdS followed by a 2.0 CIS single layer film. The best device had a  $V_{OC}$  of 0.325 V, a  $J_{SC}$  of 30.3  $\text{mA}/\text{cm}^2$  and an efficiency of 5.9%.

The forward diode current in optimized  $\text{CuInSe}_2/(\text{CdZn})\text{S}$  devices with increasing Zn concentration (up to 26%) was investigated. Measurements included spectral response and current-voltage as a function of temperature. An activation energy equal to the bandgap of the  $\text{CuInSe}_2$  (1 eV) and independent of the Zn concentration of the  $(\text{CdZn})\text{S}$  was found. Analysis of the illuminated devices consistently yielded a diode ideality factor of 2. The above results support diode current dominated by SRH recombination in the  $\text{CuInSe}_2$ . Low temperature ( $T < 273^\circ\text{K}$ ) J-V behavior is due to the presence of a back diode in series with the main heterojunction solar cell (Figure 2).

Spectral response measurements done as a function of applied voltage can include non-negligible effects from the series resistance. These effects can cause changes in both the magnitude and shape of the spectral response curve as a function of the applied voltage. The changes in the spectral response curves of  $\text{CuInSe}_2/(\text{CdZn})\text{S}$  devices as a function of applied voltage can be quantitatively explained by series-resistance effects (Figure 3). Spectral response measurements as a function of voltage and light bias generally exhibit a wavelength independent decrease in response with increasing forward voltage bias. In addition, some devices show wavelength dependent changes as a function of applied voltage near the bandgap of the  $(\text{CdZn})\text{S}$  window layer. Previous attempts to model this behavior which focussed on voltage dependence of interface recombination, did not achieve satisfactory agreement with experimental data. By considering the series resistance and photoconductivity of the device, the effects of voltage and light bias on spectral response have been explained quantitatively.

By depositing  $\text{CuInSe}_2$  on semitransparent (400Å Mo) contact, high efficiency  $\text{CuInSe}_2/(\text{CdZn})\text{S}$  devices (>9%), which can be analyzed with light incident through both the Mo and  $(\text{CdZn})\text{S}$ , have been fabricated. Measurement of bi-facial spectral response have been analyzed to determine the diffusion length and space charge width of high efficiency devices without making assumptions about the optical absorption coefficients of polycrystalline  $\text{CuInSe}_2$ . Present results indicate a diffusion length of 1.0  $\mu\text{m}$  with a space charge width of 0.1  $\mu\text{m}$ . Anomalies in the shape of the spectral response curves suggest that field aided collection from both the Mo contact and the main junction may also play a role in the  $J_{SC}$  of the devices.

### **Conclusions and Areas for Future Activity**

As a result of these studies, the following conclusions were reached:

- ▶ The morphology of CuInSe<sub>2</sub> thin-films deposited by physical vapor deposition from elemental Cu, In and Se is determined by the Cu content of the first step in the two step process that is used to deposit device quality CuInSe<sub>2</sub>.
- ▶ High short circuit current can be achieved from a ZnO/CuInSe<sub>2</sub> heterojunction. Furthermore, ZnO/(CdZn)S window layers may be more tolerant to processing defects, such as discontinuities in thin, (CdZn)S, than ITO-based window layers.
- ▶ Open circuit voltage in CuInSe<sub>2</sub>/(CdZn)S heterojunction solar cells is determined by Shockley-Read-Hall space charge recombination in the space charge region of CuInSe<sub>2</sub> and is limited in current state-of-art CuInSe<sub>2</sub> thin-film material to 0.5 volt.
- ▶ Bi-facial spectral response measurements of CuInSe<sub>2</sub>/(CdZn)S devices fabricated on semi-transparent substrates is a useful technique for determining optical absorption coefficients, diffusion length and space charge width of CuInSe<sub>2</sub> in functioning high efficiency CuInSe<sub>2</sub> devices.
- ▶ A glass/ITO/CdS/CuInSe<sub>2</sub>/Pt superstrate device with an open circuit voltage of 0.32 volt and 5.9% efficiency has been fabricated.

Accordingly, future activities should include:

- ▶ Alternate methods for depositing CuInSe<sub>2</sub>, such as selenization of Cu and In metal layers.
- ▶ Bandgap modification of CuInSe<sub>2</sub> by alloying with optimal amounts of Ga and/or S to achieve open circuit voltage approaching 0.6 volt.
- ▶ Optimized window layers to achieve short circuit current approaching 50 mA/cm<sup>2</sup>.
- ▶ Continued analysis of bi-facial spectral response.
- ▶ Continued development and assessment of superstrate device.

Table 1  
CuInSe<sub>2</sub> Cell Results with Different Windows

Window	Thickness ( $\mu\text{m}$ )	$V_{\text{OC}}$ (V)	$J_{\text{SC}}^*$ (mA/cm <sup>2</sup> )	FF (%)	$\eta$ (%)
(CdZn)S:In/ITO	1.9	0.418	36.6	68.9	10.5
(CdZn)S:In/ITO	1.0	0.400	38.4	66.0	10.1
(CdZn)S/(CdZn)S:In/ITO	2.2	0.425	35.9	68.5	10.4
(CdZn)S:In	2.1	0.419	36.6	63.4	9.7
ZnO	1.5	0.22	39.8	47	4.0

\* EIH simulation at 32°C, 87.5 mW/cm<sup>2</sup>.  $J_{\text{SC}}$  normalized to 100 mW/cm<sup>2</sup>.

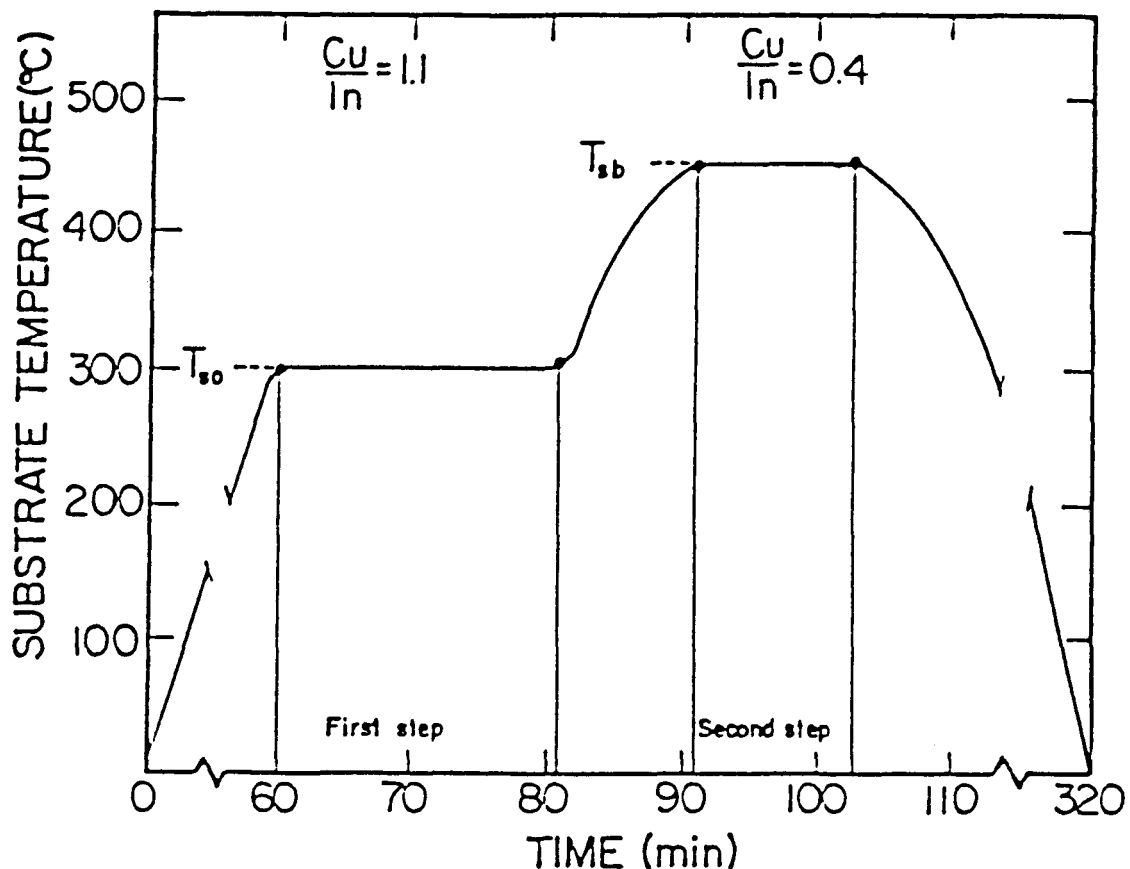


Figure 1. Substrate temperature - time profile and Cu/In incident flux ratio for first and second deposition steps.

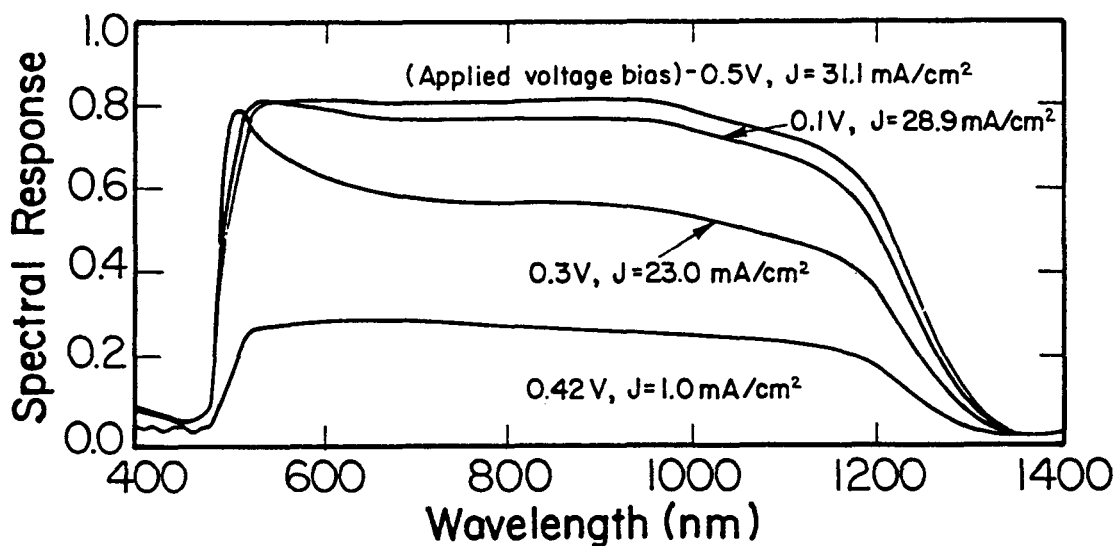


Figure 2. Current-voltage (J-V) characteristics of  $\text{CuInSe}_2/(\text{CdZn})\text{S}$  device as a function of temperature.

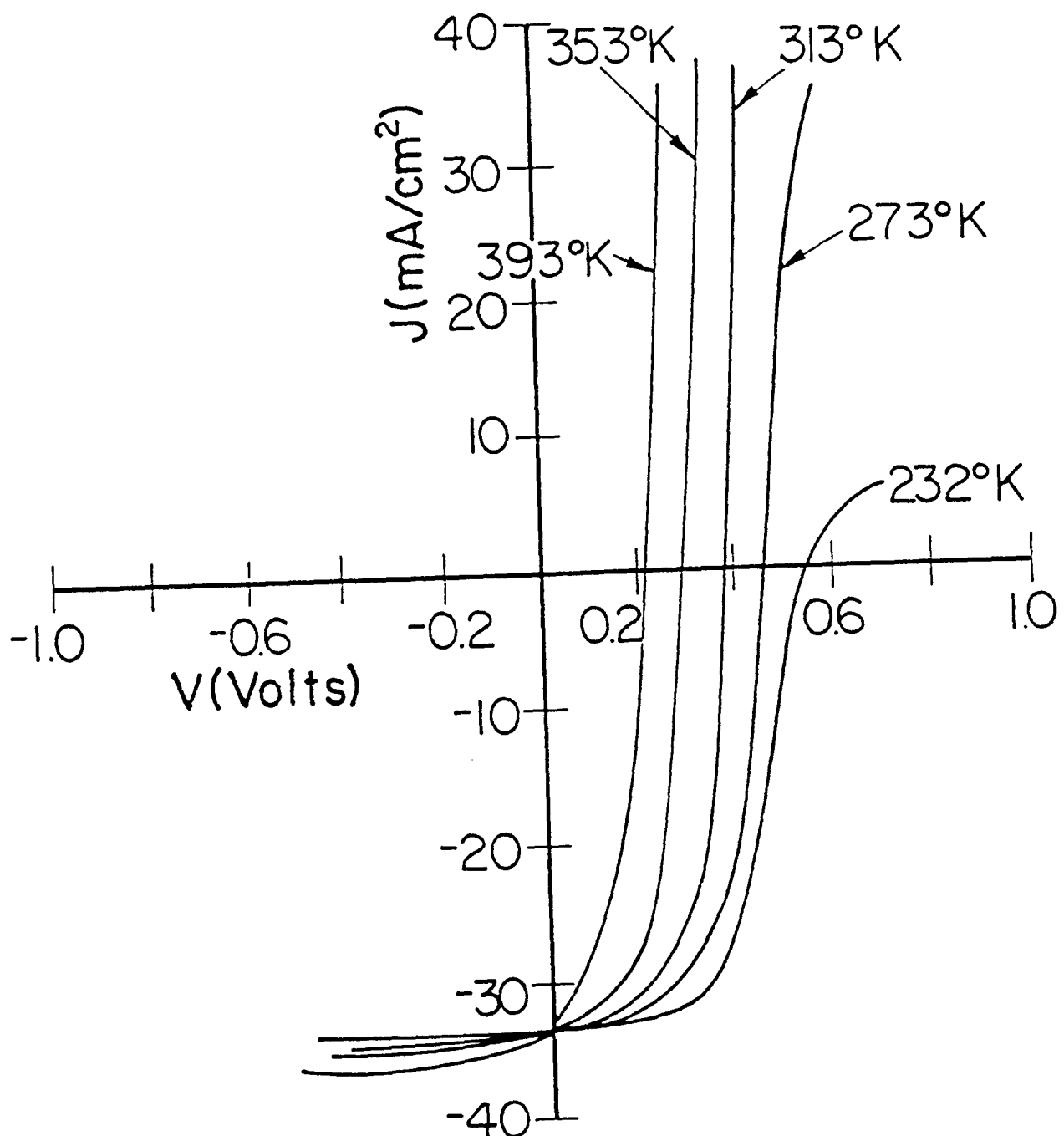


Figure 3. Spectral Response of Optimized CuInSe<sub>2</sub>/(CdZn)S Device.

**Title: Analysis of Loss Mechanisms in Polycrystalline Thin Film Solar Cells**

**Organization:** Physics Department, Colorado State University,  
Fort Collins, Colorado

**Contributors:** J. R. Sites, principal investigator, P. H. Mauk, and  
H. Tavakolian

The objective of this program is to design and demonstrate a system for routine, unambiguous, and quantitative analysis of loss mechanisms in individual polycrystalline solar cells. To be effective these procedures must be practical with equipment commonly available in solar cell laboratories and must be compatible with straightforward mathematical analysis. Reports from this work are listed in Refs. [1-4].

#### **Loss Mechanisms**

The values of current density and voltage at the maximum power point are shown graphically in Fig. 1 for CuInSe<sub>2</sub> and CdTe solar cells. The largest rectangles are the theoretically optimal values and are based only on bandgap, temperature, and an assumed 100 mW/cm<sup>2</sup> global spectrum. The smallest rectangles represent good quality polycrystalline cells by today's standards, and the area between extremes is divided by the estimated magnitudes of current and voltage losses. The effect of reducing any individual loss can be easily visualized. Note that, especially for CdTe, substantial efficiency improvement is possible through reductions in series resistance, reflection, and window absorption, completely independent to the junction part of the cell.

#### **Determination of Losses**

Each of the mechanisms shown in Fig. 1 can be determined from (a) current-voltage (I-V), (b) spectral response (SR), and (c) high frequency capacitance-voltage (C-V) measurements. Additional insight and accuracy, however, can be gained with (d) capacitance-frequency (C-f), (e) temperature variation in I-V, and (f) independent reflectivity measurements. The losses are determined as follows.

- (1) Reflection. Measured directly with a total reflection integrating sphere or estimated from the maximum spectral response. Note that the reflection is primarily diffuse in general with a significant fraction scattered at angles  $> 45^\circ$ .
- (2) Window Layer Absorption (CdS ABS). Calculated from the blue side of the SR curve after correction for reflection.
- (3) Collection Loss. Calculated from SR curve after correction for reflection and window layer absorption.
- (4) Series Resistance ( $R_S$ ). Deduced from I-V curve in forward bias. Primary effect is to reduce voltage at maximum power.

- (5) Built-In Potential ( $V_{bi}$ ). High frequency, reverse bias C-V curve is used to calculate hole density, which determines Fermi level on absorber side. Fermi level on electron side is near band edge and can be estimated. With assumption that conduction band edge is nearly continuous at interface,  $V_{bi}$  follows.
- (6) Junction Recombination (JTN. RCB.). Deduced from I-V curve, generally expressed by the slope and intercept of  $\ln (J + J_{SC})$  vs.  $V$  after series resistance correction. The slope is inverse to the diode quality factor. Additional information results from analysis of C-f data, which is related to extraneous state densities, and from temperature dependent I-V.

Figure 2 shows the quantitative effects of series resistance and of increased diode quality factor  $n$  on current and voltage at maximum power. The effect of other values can be found by interpolation or extrapolation.

#### Physical Model

The primary effect of polycrystallinity is large numbers of extraneous electronic states associated with crystallite boundaries. These states (1) supply many additional recombination paths, significantly increasing the unwanted forward current, and (2) compensate and hence greatly reduce the majority carrier density. In the case of evaporated  $\text{CuInSe}_2$ , the optimal condition appears to be excess indium on the crystallite surface, passivated with oxygen or similar material. However, the need for post-deposition oxidation, and the density of extraneous states, can apparently be substantially reduced with deposition processes more nearly approaching thermodynamic equilibrium.

#### References

1. Sites, J. R., "Device Physics Related to the Granular Nature of  $\text{CuInSe}_2$  Solar Cells," SERI/STR-211-3395 (September 1988).
2. Sites, J. R., "Calculation of Impact Ionization Enhanced Photovoltaic Efficiency," Solar Cells 25 (1988).
3. Sites, J. R., "Separation of Loss Mechanisms in Polycrystalline Solar Cells," Conf. Record of the 20th IEEE Photovoltaics Specialists Conference, Las Vegas, 1988.
4. Tavakolian, H., and J. R. Sites, "Effect of Interfacial States on Open Circuit Voltage," Conf. Record of the 20th IEEE Photovoltaics Specialists Conference, Las Vegas, 1988.

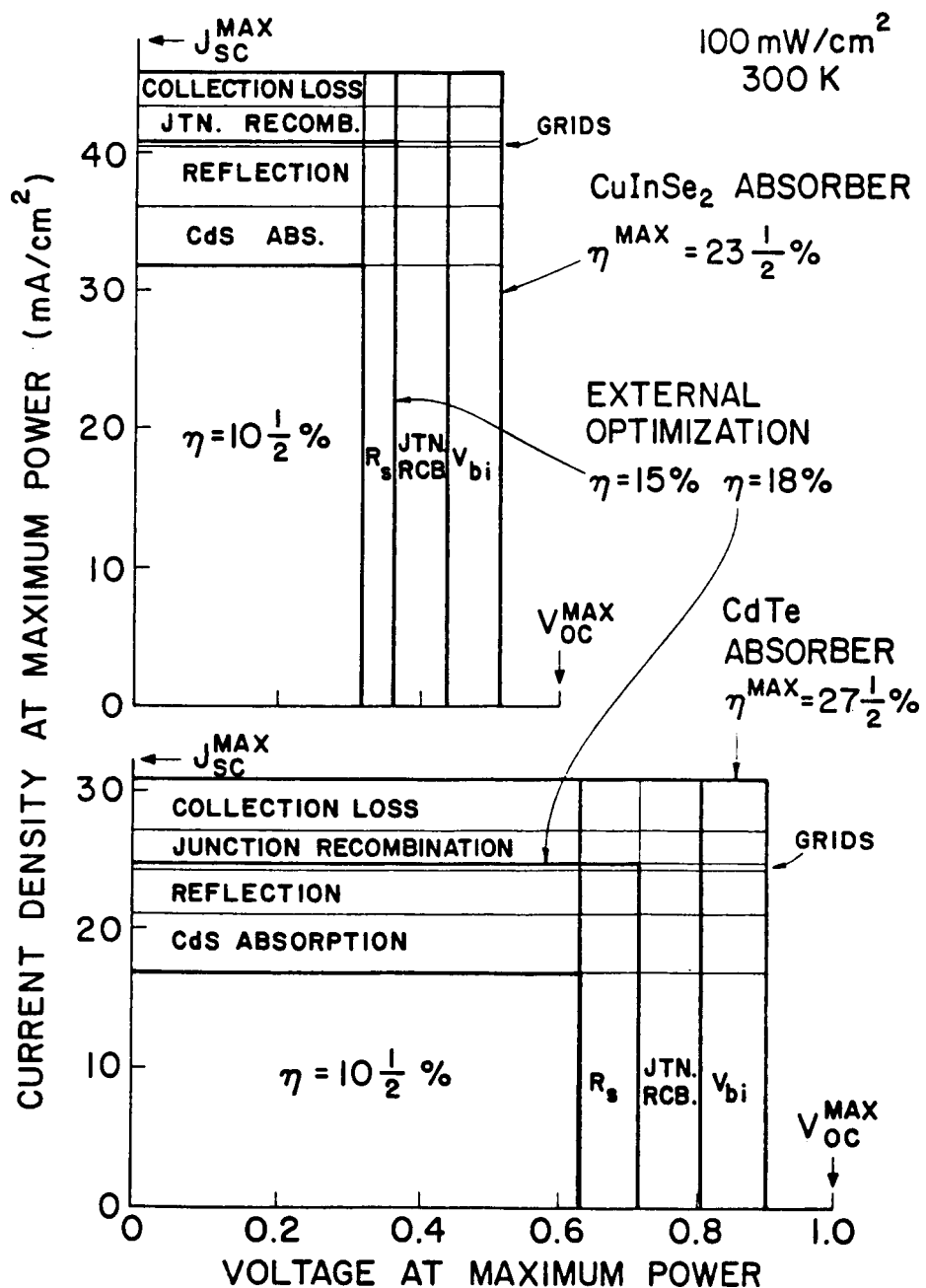


Fig. 1. Maximum power current density and voltage for  $\text{CuInSe}_2$  and  $\text{CdTe}$  cells. Estimated magnitudes of the primary loss mechanisms are shown.

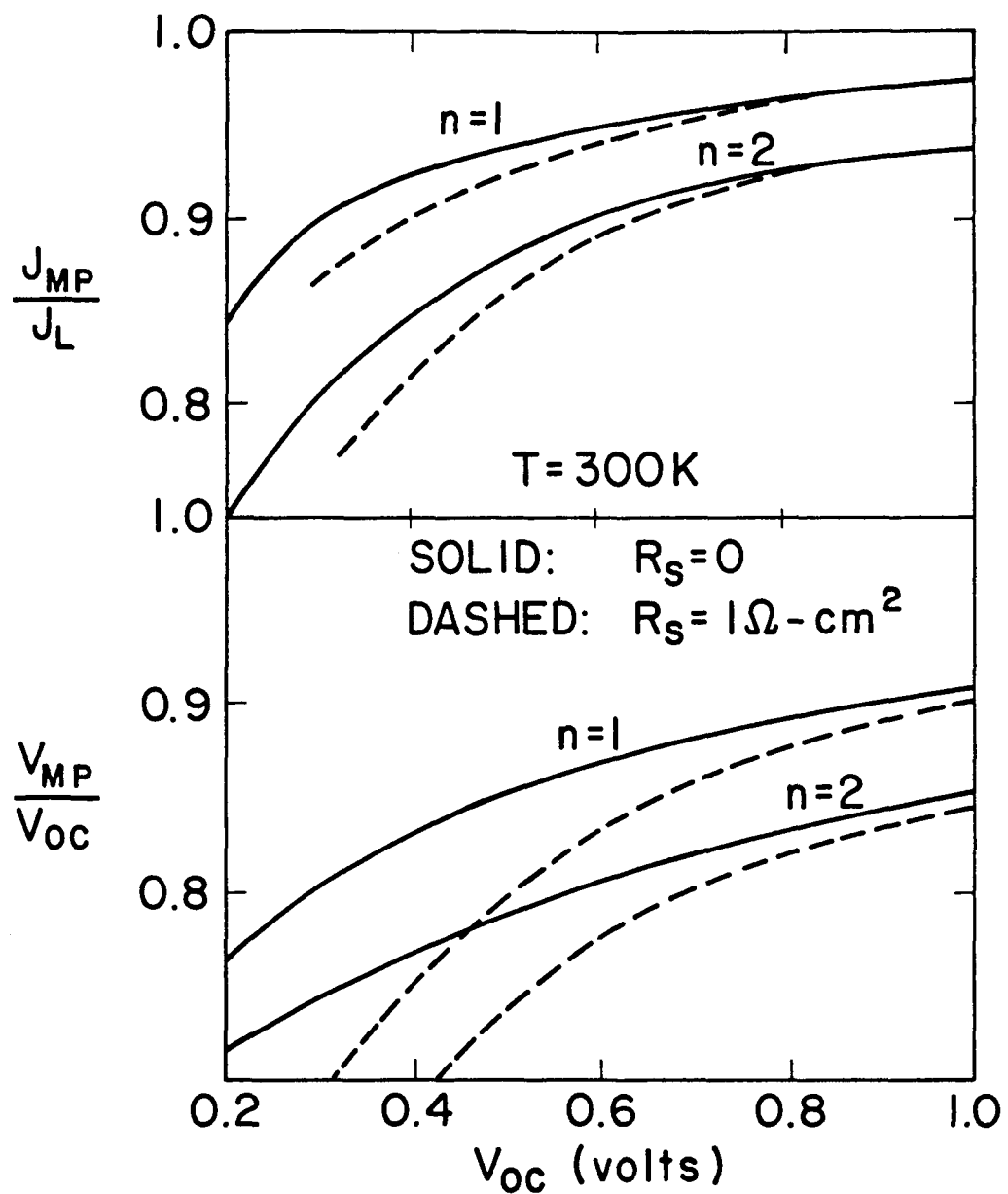


Fig. 2. Ratios of current density at maximum power  $J_{MP}$  to photocurrent  $J_L$  (assumed here to be  $J_{SC}$ ) and voltage at maximum power  $V_{MP}$  to the open circuit voltage  $V_{OC}$ . Two values of illuminated diode quality factor  $n$  and two of illuminated series resistance  $R_s$  are shown.

Title: Alternative Fabrication Techniques for High-efficiency  
**CuInSe<sub>2</sub> and CuInSe<sub>2</sub>-alloy Films and Cells**

Organization: University of Illinois

Contributors: A. Rockett, principal investigator; T.C. Lomasson, project engineer; H. Talieh, graduate research assistant.

The objective of this project is to investigate techniques which are clearly scalable to large areas and which are capable of producing CuInSe<sub>2</sub> for solar cell applications. The approach is to understand the chemical and kinetic mechanisms contributing to film growth. This understanding will serve to improve the processes under development, optimize deposition conditions, and ultimately to accelerate the return to service of large deposition facilities after periods of maintenance.

### Technical Approach

Only magnetron sputtering is in common use for coating very large area substrates with thin films. This coating technology is well established for architectural glass applications, although evaporation has also been used to coat smaller-area surfaces. Both of the CuInSe<sub>2</sub> deposition methods considered by this project are based on sputtering techniques. The two processes are reactive magnetron sputtering of Cu and In with ions from an Ar + H<sub>2</sub>Se plasma [1] and a hybrid process combining Ar magnetron sputtering of Cu and In with evaporation of Se from a conventional effusion cell [2,3]. Reactive sputtering experiments are being conducted in a four-chamber, diffusion-pumped vacuum system designed specifically for production of solar cells and including the capability of depositing a metal base electrode, the active CuInSe<sub>2</sub> layer, and a CdS window layer which completes the cell heterojunction. The hybrid process is being developed in a single-chamber high-vacuum system designed for initial deposition experiments. A second, ultra-high vacuum system is currently being converted for hybrid deposition of CuInSe<sub>2</sub>.

The experiments underway focus on understanding the fundamental processes at work during the growth of CuInSe<sub>2</sub> with particular emphasis on the chemical and kinetic pathways which the growth reactions follow. The experiments are being conducted as parametric studies of growth conditions with subsequent analyses of the deposited film compositions and uniformities. Future experiments will extend these studies to smaller scales using transmission electron microscopy and other techniques capable of high spatial resolution.

### Results for FY 88

The reactive sputtering approach has been shown [5] to produce device-quality CuInSe<sub>2</sub>. Experiments during this contract period have focused on understanding the structural and compositional nature of films deposited by reactive sputtering. Transmission electron microscope (TEM) analysis of stoichiometric material deposited by reactive sputtering has shown the layers to be high-quality, single-phase, chalcopyrite-structure. Strongly Cu-rich films were found to include some second-phase grains which were determined to be stoichiometric Cu<sub>2</sub>Se. Films are preferentially (112)-oriented on all substrates examined. Annealing of the deposited layers in air at 200 °C was also shown to produce large changes in resistivities of both p- and n-type material, as observed for layers deposited by other techniques.

While investigation of the hybrid process is at a much earlier stage than reactive sputtering, the technique has been shown to be very well behaved. The hybrid process permits linear control of the metal fluxes with target current and the Se flux was found to depend exponentially on the temperature of the effusion cell, as expected. Furthermore, changes in film composition vary in direct proportion to the incident fluxes of both the metal and Se atoms.[4] For example, plots of

the metal atom ratio in the films, determined by energy-dispersive X-ray fluorescence spectroscopy (EDX), as a function of the incident metal-atom flux ratio are shown in Figure 1.[4] A similar behavior is observed for Se incorporation as a function of the incident flux with the exception that excess Se is not incorporated into  $\text{CuInSe}_2$  at elevated temperatures. The resulting films are chalcopyrite-structure with a (112) preferred orientation and  $\text{Cu}_2\text{Se}$  second-phase precipitates appearing in sufficiently Cu-rich material.

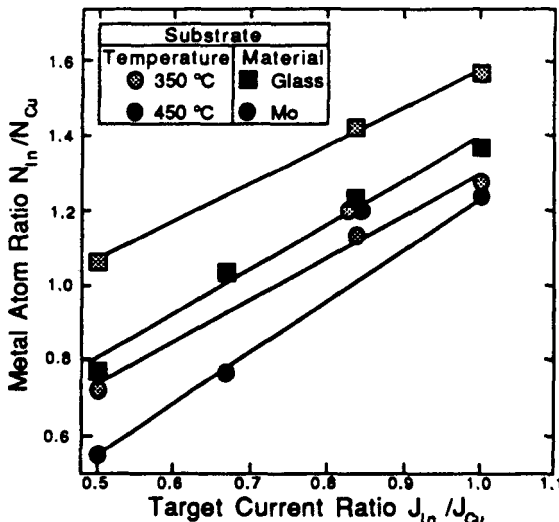


Figure 1. Shows the change in film composition as a function of target current ratio for both glass and Mo substrates at two substrate temperatures. The Se effusion cell temperature was fixed at 320 °C giving a flux equivalent to a Se deposition rate of 1.5 nm s<sup>-1</sup>. Note that the 350 °C films on glass contain the most In and that the trends are linear, independent of the In/Cu atom ratio.

Studies of the effect of the substrate on film composition have also been conducted. It has generally been assumed that there is no significant difference between  $\text{CuInSe}_2$  grown on glass and on Mo by physical vapor deposition techniques. The experiments on hybrid-deposited films have demonstrated qualitative and quantitative differences in film compositions for layers grown on the two substrates. (See Figure 2.) This effect is undergoing further study to determine the mechanism for establishing the different compositions. Preliminary results suggest that the difference is not due to changes in the substrate temperature nor does the variation result from the substrate chemistry affecting the film directly. One possible mechanism, now under study, is that some higher-energy photons emitted by the substrate heater pass through the glass substrate and the  $\text{CuInSe}_2$  film and modify the chemistry of the growing surface.

Secondary ion mass spectrometry (SIMS) analyses of the deposited layers show that some films exhibit a thin In-rich layer near the surface, consistent with previous reports for evaporated layers. The presence of such a layer may strongly influence the EDX composition analyses in the direction of higher In contents. While the analyses do not indicate any intermixing of the CIS and Mo layers, the composition analyses do show some evidence of diffusion of the Cu, In, and Se into intergranular regions of the Mo base contacts when films are deposited at elevated temperatures.

Finally, a Cu-In alloy film deposited in the hybrid sputtering system has been selenized at International Solar Energy Technology, Inc., and fabricated into a solar cell. The resulting device was found to be an active solar cell with an open circuit voltage of 0.31 V. Additional devices based on hybrid-deposited material will be produced in the near future at the University of Illinois and elsewhere.

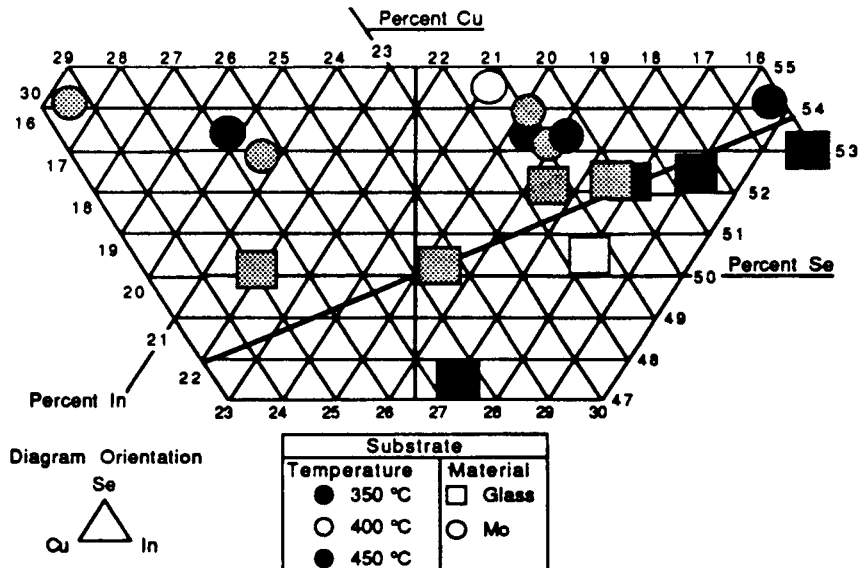


Figure 2. Compares the film compositions, plotted on a ternary phase diagram, for Mo and glass substrates. Films grown on glass follow a line (the bold line rising diagonally to the right) connecting  $\text{Cu}_2\text{Se}$  with  $\text{In}_2\text{Se}_3$  while films on Mo follow a line of constant Se content as the Cu-to-In flux ratio was changed.

### Conclusions and Future Research

The reactive sputtering process is both simple to implement and scalable to large-area coatings. Reactive sputtering has been shown to produce high-quality, chalcopyrite material but no high-efficiency devices have been produced from reactive-sputtered films. The hybrid process has shown no limitations in terms of film compositions achieved or microstructures produced. This technique has also not provided high-efficiency devices to-date but a major effort has not been made in this area. Future efforts will center on fabrication of high-efficiency devices using both techniques. This goal will be achieved by extending the current fundamental understanding of the two deposition processes and by applying this understanding to correcting the problems encountered in device production.

- [1] See John A. Thornton, T.C. Lomasson, H. Talieh, and B.-H. Tseng, *Solar Cells* 24, 1 (1988), and references therein.
- [2] John A. Thornton, *Solar Cells* 21, 41 (1987).
- [3] A. Rockett, T.C. Lomasson, L.C. Yang, H. Talieh, P. Campos, and John A. Thornton, "Deposition of  $\text{CuInSe}_2$  by the Hybrid Sputtering and Evaporation Method", *Proceedings, 20th IEEE Photovoltaic Specialists Conference*, Las Vegas, Sept. 26-30, 1988, IEEE, New York, in press.
- [4] A. Rockett, T.C. Lomasson, P. Campos, L.C. Yang, and H. Talieh, "Growth of  $\text{CuInSe}_2$  by Two Magnetron-Sputtering Techniques", to be published in *Thin Solid Films*, in press.

**Title:** Novel Thin-Film CuInSe<sub>2</sub> Fabrication

**Organization:** Department of Physics, J. William Fulbright College of Arts and Sciences,  
University of Arkansas, Fayetteville, Arkansas

**Contributors:** G. D. Mooney and A. M. Hermann

The objective of this program is to produce device quality, CuInSe<sub>2</sub> thin films by laser annealing elemental sandwiched Cu:In:Se layers.

This method of fabrication of CuInSe<sub>2</sub> is desirable because it eliminates the use of the highly toxic HSe<sub>2</sub> gas presently used in the thermal anneal method of fabrication. Our initial work involved deposition of the elemental layers by means of electrodeposition. We have successfully deposited Cu, In, and Se by this method in the atomic proportion 1:1:2. Our original efforts in the laser anneal phase of the experiment involved mechanically scanning the prepared sandwiched structure in front of a stationary CW Argon laser beam. We have just completed the construction of a four-source thermal evaporation system so fabrication of the sandwiched structures will now include films deposited by vacuum methods.

### **Elemental Layer Deposition**

The films that have been laser annealed to date were prepared by electrodeposition. The layering was carried out by fixing the target layer thickness of the Cu to be 1000 Å. In order to achieve the proper atomic proportion of 1:1:2 (Cu:In:Se) this Cu starting thickness required the In layer to be 2210 Å and the Se layer to be 4610 Å.

The copper was deposited using a bath of .5M CuSO<sub>4</sub> and .8M H<sub>2</sub>SO<sub>4</sub> mixed with a volume ratio of 1:1 [1]. This bath was maintained at room temperature. The In was deposited using a bath of In(SO<sub>3</sub>NH<sub>2</sub>)<sub>3</sub> (Indium sulfamate) [1] which was also held to room temperature. The selenium was plated [2] using a bath of .001M SeO<sub>2</sub>, .25M citric acid and .15M sodium citrate mixed in a volume ratio of 2.5:1:1. This bath had to be maintained at 90 °C in order to obtain the black/gray crystalline phase of Se. Because the In layers were unstable in the Se bath, the best ordering for the layers was found to be Cu:In:Cu:Se as shown in figure 1. In this ordering scheme, 500 Å was deposited in each Cu layer to achieve the proper atomic proportion.

### **Laser Annealing**

The prepared, layered films were annealed using a CW Argon laser. The films were scanned in front of a 2mm, stationary beam by a mechanical scanner that has two-dimensional motion controlled by a variable speed dc motor and a series of gears. To date, we have annealed our films with a horizontal scan sped of 2mm/s using a beam power of four watts.

## X-Ray Analysis

Using the experimental and theoretical results obtained by Kazmerski et. al. [3], we have determined the existence of the chalcopyrite phase of  $\text{CuInSe}_2$  by observing a peak at  $2\theta = 26.6$  in our x-ray diffraction measurements (figure 2). This is the primary peak for the chalcopyrite phase. Also present are undesirable binary compounds. In figure 2 the other peaks present correspond to copper oxide and the molybdenum of the substrate.

## Recommendations

To increase the quality of the films, we plan to increase the percentage of the chalcopyrite phase in the films and eliminate the binary compounds so the films will be single phase. To achieve these goals we plan to more accurately control the pre-annealed layer thickness by using vacuum techniques as our primary deposition methods. Also, to help eliminate the binary oxides, a chamber has been designed with a quartz window so the films can be annealed in a vacuum. We also have planned, a systematic varying of the annealing parameters so the optimum annealing conditions can be determined.

---

1. Vijay K. Kapur, Bulent M. Basol, and Eric S. Tseng, Proc. 18<sup>th</sup> Photovoltaic Specialist Conf., 1985, IEEE, New York, p. 1429.
2. J. Herrero and J. Ortega, Solar Energy Materials, **16** (1987) 477-485.
3. L. L. Kazmerski, M. S. Ayyagari, G. A. Sanborn, F. R. White, and A. J. Merrill, Thin Solid Films, **37** (1976) 323-334.

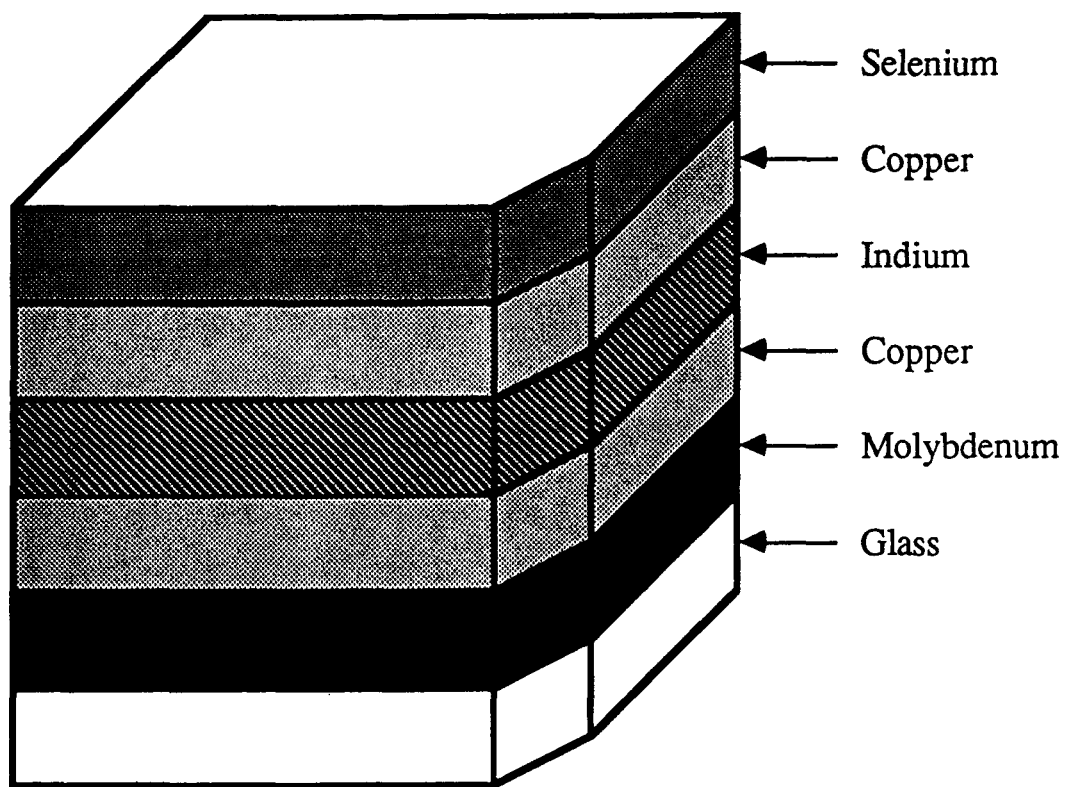


Figure 1. Pre-Annealed Sandwich Structure on Mo coated Glass

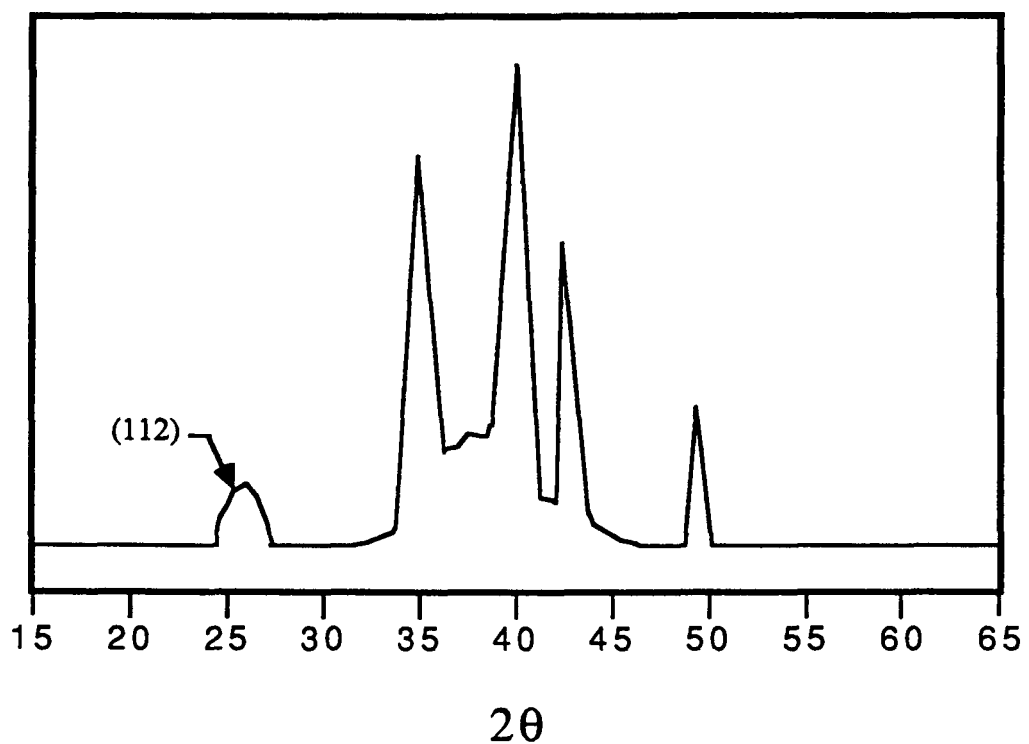


Figure 2. X-Ray Diffraction Pattern of Post-Annealed Film

**Title:**

**Polycrystalline Thin-Film Cadmium Telluride  
Solar Cells**

**Organization:**

Ametek Applied Materials Laboratory,  
Harleysville, Pennsylvania

**Contributors:**

P. Meyers, Principal Investigator,  
R. Liu, K. Ramanathan

The overall objective of this subcontract is to develop thin-film solar cells that are improvements on the present state of the art. The work is centered around the polycrystalline n-i-p configuration utilizing CdS/CdTe/ZnTe. Already, devices of this structure have been produced with confirmed efficiency of 11% - (Figure 1) this is the highest confirmed efficiency of any thin film CdTe solar cell.

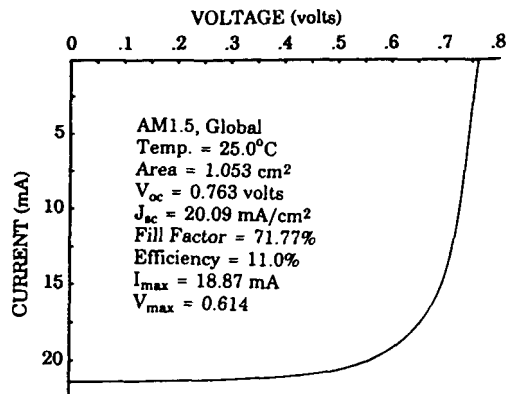


Figure 1 I-V curve of CdS/CdTe/ZnTe cell

**Polycrystalline n-i-p Solar Cells**

The structure CdS/CdTe/ZnTe, shown in Figures 2 and 3, is well suited to the n-i-p design for the following reasons [1,2]:

1. Each semiconductor material is utilized in its preferred type. CdS is always n-type, ZnTe is generally p-type, and AML's process produces good-quality, high-resistivity (intrinsic) CdTe.
2. Reviews of the published literature corroborate the prediction that there is no spike either in the conduction-band edge at the n-i interface or in the valence band at the i-p interface. Such spikes would inhibit the collection of photogenerated carriers.
3. At each interface there is a step that prevents collection of unwanted charge carriers, i.e., holes are reflected from the n-i interface and electrons are reflected from the i-p interface.

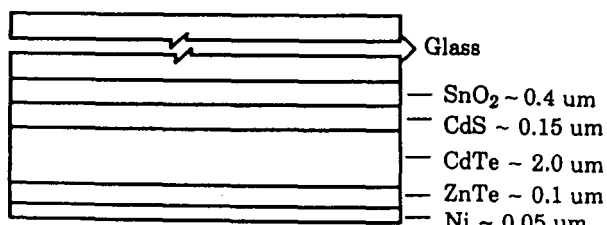


Figure 2 Structure of the CdS/CdTe/ZnTe cell

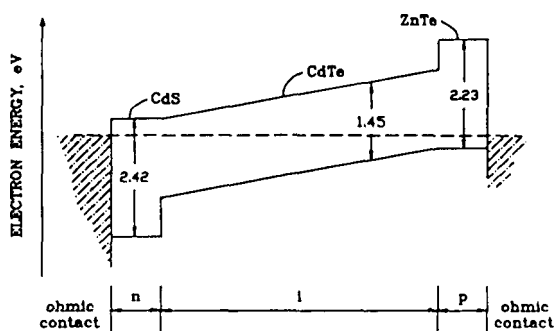


Figure 3 Energy band diagram of CdS/CdTe/ZnTe

During the course of this subcontract AML has produced, by intentional variations of the fabrication procedure, devices with the CdS/CdTe/ZnTe configuration in which the location of the maximum field strength within the CdTe layer varied from device to device. This effect was observed with spectral response, and with EBIC measurements performed at SERI [2]. In the most efficient devices, most of the CdTe layer is active in carrier collection, but the maximum field strength occurs at a depth of approximately 0.5 um from the CdS/CdTe interface. These experiments demonstrate that material engineering is possible with this design.

Not the least of the advantages of the n-i-p design is its suitability for use as the top cell in a cascade configuration. A transparent n-i-p solar cell has been produced with a SERI confirmed efficiency of 9.4% and IR transmission of 35%. AML personnel are collaborating with other SERI subcontractors to exploit this potential:

The optimum cascade partner to CIS has a band gap in the range of 1.6-1.7 eV, slightly larger than the 1.44-eV band gap of CdTe. Because both  $\text{Cd}_{1-x}\text{Mn}_x\text{Te}$  and  $\text{Cd}_{1-x}\text{Zn}_x\text{Te}$  can be produced with band gaps in this range, it may be possible to substitute one of them for CdTe in the n-i-p design.

1. R. Stirn of JPL has developed procedures for the low-temperature deposition of CdTe and  $\text{Cd}_{1-x}\text{Mn}_x\text{Te}$  by MOCVD. Several devices have been produced in which CdS-coated  $\text{SnO}_2$ /glass is shipped to JPL for deposition of the CdTe alloy and then returned to AML for completion. This collaboration has produced 9+% n-i-p solar cells with CdTe as the i-layer.
2. In a similar collaboration with Georgia Tech., A. Rohatgi, S. Ringel, E. Meeks, and J. Walsh are producing  $\text{Cd}_{1-x}\text{Zn}_x\text{Te}$  films by MBE and  $\text{Cd}_{1-x}\text{Mn}_x\text{Te}$  films by MOCVD. At this point we have produced CdS/CdTe/ZnTe n-i-p solar cells with an efficiency of 9.7% using MOCVD CdTe.
3. R. Birkmire and J. Phillips at IEC have developed procedures to routinely produce 10+% efficient CIS solar cells. AML has supplied these researchers with a large-area, 3-in. x 6-in., transparent n-i-p solar cell that can be patterned and incorporated into a four-terminal cascade device. In a preliminary effort, these have been cascaded to produce 9.9% devices. Work continues on methods of improving the optical transmission of the CdTe n-i-p cell. In addition, jointly produced n-i-p solar cells, utilizing CdTe vacuum evaporated at IEC, have reached 7+%.

Another aspect of the research is to substitute  $\text{Cd}_{1-x}\text{Zn}_x\text{S}$  for CdS. A new inverted pyrolytic reactor has been used to produce CdZnS films with a band gap of 2.8 eV. Devices with 8+% efficiency have been produced using 2.6 eV material.

In addition, we are optimizing methods for ZnTe deposition. Experiments to determine the effects of substrate temperature, deposition rate, and Cu doping level on ZnTe properties are being performed. Results of these will provide input for the design of an improved ZnTe deposition system, which is to be constructed later in the program.

### Stability

Stability testing continues [3]. Solar cells, loaded at their maximum power point, were tested under simulated AM1 light. The cells were kept in a slight positive pressure of nitrogen inside an aluminum cylinder with a quartz lid. The illumination cycle was six hours on and two hours off. There was no reduction in power output after more than 3000 hours of illumination.

### Conclusions

Results to date indicate that the polycrystalline n-i-p structure has the potential to make significant advances to the state of the art of thin-film solar cells. In order to realize that potential, additional work needs to be done: control over deposition parameters must be improved so that film quality can be reliably optimized; the effects of interface states and interdiffusion at the heterojunction interfaces must be understood and controlled; and we must utilize new materials whose properties are better suited to high-efficiency devices. All of these avenues are addressed by the current subcontract plan.

---

1. Meyers, P.V., 7th E.C. PV Solar Energy Conf., 1986, pp. 1211-1213.
2. Meyers, P.V., "Design of a Thin Film CdTe Solar Cell," Solar Cells, 23 (1987) pp. 59-67.
3. Meyers, P.V., "Ametek's CdTe Solar Module Development Program," Solar Cells, 24 (1988) pp. 35-42. (Presented at SERI 8th PV Advanced R&D Proj. Rev. Mtg., Denver, Co., Nov. 1987.)

### Related Articles

Meyers, P.V. and Liu, C.H., "Progress Toward Development of a Production Process for Thin Film CdTe Solar Modules," 8th European PV Conference, Florence, May 1988.

Rohatgi, A., Ringel, S.A., Welch, J., Meeks, E., Pollard, K., Erbil, A., Summers, C.J., Meyers, P.V., and Liu, C.H., "Growth and Characterization of CdMnTe and CdZnTe Polycrystalline Thin Films for Solar Cells," Solar Cells, 24 (1988) pp. 185-194. (Presented at SERI 8th PV Advanced R&D Proj. Rev. Mtg., Denver, Co., Nov. 1987.)

Doty, M. and Meyers, P.V., "Safety Advantages of CdTe Based PV Module Plant," SERI PV Safety Conf., Denver, Co., Jan. 1988.

Title: High-Efficiency Large-Area CdTe Panels

Organization: Photon Energy, Inc., El Paso, Texas

Contributors: S. P. Albright, principal investigator;  
B. Ackerman, R. Chamberlin, J. F. Jordan, and V. P. Singh

The major objectives of this program during 1988 are:

- \* Development of materials technology and fabrication processes to support the establishment of limited-volume production of 1 ft<sup>2</sup> cadmium sulfide/cadmium telluride photovoltaic panels with 7% efficiency using processes that are scalable to larger area panels.
- \* Development of encapsulation techniques and life-testing methods that provide for less than 10% degradation over a 5-year panel life.
- \* Demonstration of feasibility for larger area panels by delivery of a 4 ft<sup>2</sup> "live" panel to SERI.

The following areas of research have been pursued as a means of accomplishing these objectives:

- \* Encapsulation issues and panel design
- \* Contact chemistry and stability improvement
- \* Improvements in uniformity and reproducibility
- \* Characterization and Doping of CdTe

#### Panel Efficiency Improvement

Table 1 shows the progress up through FY1988 in terms of actual deliverables to SERI. The panel output measurements were done at the SERI PV Module Testing and Performance Facility. Progress has been achieved through characterization of CdTe material and devices and through improvement of both the understanding of and the control of deposition and processing steps. Figure 1 shows the current-voltage performance curve for the 6.1 watt 1 ft<sup>2</sup> panel measured at SERI on the Spire simulator.[1]

Table 1. Progress of Panel Output Improvement

Date	Output	Active Area	Active Area Eff	Aperture Area Eff
June '87	4.0W	660cm <sup>2</sup>	6.1%	5.4%
Nov '87	4.4W	660cm <sup>2</sup>	6.6%	5.8%
March '88	4.7W	686cm <sup>2</sup>	6.8%	6.1%
Oct '88	6.1W	752cm <sup>2</sup>	8.1%	7.3%

## Larger Area Panels

In addition to the rapid progress made in panel efficiency, PEI has also delivered to SERI the world's largest known, single-substrate, CdS/CdTe panel. Due to equipment limitations, the delivered 4 ft<sup>2</sup> panel was manufactured by a continuous belt process, not the batch process typically utilized at PEI. This large-area deliverable therefore shows feasibility for continuous flow processing of panels up to at least 4 ft<sup>2</sup>. It also indicates the commitment at PEI to produce large area terrestrial photovoltaics and to meet stringent economic objectives by continued interest in the lowest cost processing methods available. Continuous processing of large area, low cost CdS/CdTe panels has been proposed by Jordan *et al.*[2]

## Small Cell Efficiency Improvement

Cells measuring .302 cm<sup>2</sup>, processed after cutting from 1 ft<sup>2</sup> panels, have achieved as high as 10.6% efficiency, measured on the PEI solar simulator. The IV curve under 100 mW/cm<sup>2</sup> insolation is shown in Figure 2. The feasibility of achieving 70% fill factor has been exhibited at PEI. Further efficiency improvements should be attainable by reducing the absorption losses in the 6  $\mu$ m thick CdS layer. Approximately 12-13% active area efficiency should be achievable after a complete optimization of both electronic losses and window material losses on small cells.

## Material Characterization

Art Nelson and Amy Swartzlander at the SERI Measurement and Analysis Laboratory have continued throughout the year to provide surface analysis on CdTe for PEI. Such analyses have greatly improved our insight into the actual chemistry involved after the use of various surface etches to prepare ohmic contacts to CdTe. The results of a five sample analysis by XPS are shown in Table 2.[3] The initial oxide formed on the CdTe surface is cadmium rich (Cd/Te = 1.3 - 1.7) compared to the oxide formed after further oxidation (Cd/Te = .95). The high initial Cd/Te ratio has been claimed to be due to Cd out-diffusion by Danaher *et al.*[4] and Bryant *et al.*[5]. Work will be done to further elucidate the details.

Table 2. ESCA Data at various stages of a Typical Etch

	Cd/Te	Te <sup>0</sup> /Te <sup>+</sup>	Cd/Te after sputter
#1: 200°C, air	1.7	~1.9	1.1(10min.)
#2: 200°C, air+Br <sub>2</sub>	.04	<.02	.03(5min.)
#3: 200°C, air+Br <sub>2</sub> , +NaOH	2.6	>100	1.3(5min.)
#4: 200°C, air+NaOH only	1.9	>100	1.0(5min.)
#5: 530°C, air	.95	~.02	1.3(5min.)

## Device Characterization

Device characterization has included IV curve analysis, capacitance, spectral response, and EBIC. Dr. V. P. Singh (of the University of Texas at El Paso)

and several graduate students are continuing to develop a model based on these characterizations. These characterization and modeling efforts have indicated that, (1) Interface states and/or deep levels can, and often do, dominate the electronic characteristics of CdS/CdTe devices, and (2) Improvement of the reverse saturation current by better passivation (through better processing) of these interface states results in a dramatically improved open circuit voltage and overall device efficiency.[6] In addition, EBIC analysis indicates significant non-uniform doping across a shallow homojunction on PEI devices.[7] Improvements in passivation techniques for reducing recombination losses, and improvements in doping uniformity are indicated, by the device characterization program, as the major means by which the device electronic characteristics may be improved.

#### **Panel Life Testing Results**

The encapsulation and life testing program has indicated that a properly encapsulated panel is stable after continuous outdoor exposure for at least 2+ months (the length of the test so far). The term of the test up to the present is somewhat short, so extrapolation of the stability of these panels to a five or ten year period is premature. However, no inherent material degradation mode has been found with the present PEI structure, and life testing to the present on that structure shows stable, reliable performance on PEI panels. A 4" x 6" subpanel was delivered to SERI for their own life testing in December 1988.

#### **Conclusions**

The considerable progress achieved during FY1988 at PEI can be succinctly summarized:

- \* The 7% efficiency milestone for 1 ft<sup>2</sup> panels has been achieved and exceeded
- \* The world's largest single-substrate CdS/CdTe panel (measuring 4 ft<sup>2</sup>) has been delivered to SERI
- \* Stable outdoor life testing results are being observed

#### **Future Activity**

The objectives for FY1989 are similar to those for FY1988 with different efficiency and stability milestones. The FY1989 milestones include:

- \* Delivery of a 1 ft<sup>2</sup> panel to SERI measuring 9% efficiency
- \* Delivery of a 4 ft<sup>2</sup> panel to SERI measuring 7% efficiency
- \* Show by life-testing less than 10% degradation for a 10 year period

The tasks implemented in order to achieve these objectives include:

- \* Performance optimization of small area CdTe cells
- \* Panel Efficiency Optimization
- \* Encapsulation and Stability testing

## References

1. Rummel,S., D.Waddington, K.Zweibel, and L.Kazmerski, unpublished, from SERI PV Module Testing and Performance Facility, October, 1988.
2. Jordan,J.F., S.P.Albright, "Large-Area CdS/CdTe Photovoltaic Cells", Solar Cells, Elsevier Sequoia, The Netherlands. Vol 23, pp 107-113, 1988.
3. Nelson,A., A.Swartzlander, SERI, Private Communication, 1988.
4. Danaher,W.J., L.E.Lyons, G.C.Morris, "Thin Film CdS/CdTe Solar Cells", *Applic. Surf. Sci.*, 22/23 (1985) pp 1083-1090.
5. Bryant,F.J., A.K.Harris, S.Salkalchen and C.G.Scott, *Thin Solid Films* 105 (1983) 343.
6. Albright,S.P., V.P.Singh, J.F.Jordan, "Junction Characteristics of CdS/CdTe Solar Cells", Solar Cells, Elsevier Sequoia, The Netherlands. Vol 24, pp 43-56, 1988.
7. Kenney,R.H., J.C.McClure and V.P.Singh, "Electron Beam Induced Currents in Thin Film CdS-CdTe Heterojunction Cells", *Proc. of 8th European Photovoltaic Solar Energy Conf.*, May 9-13, 1988, Florence, Italy.

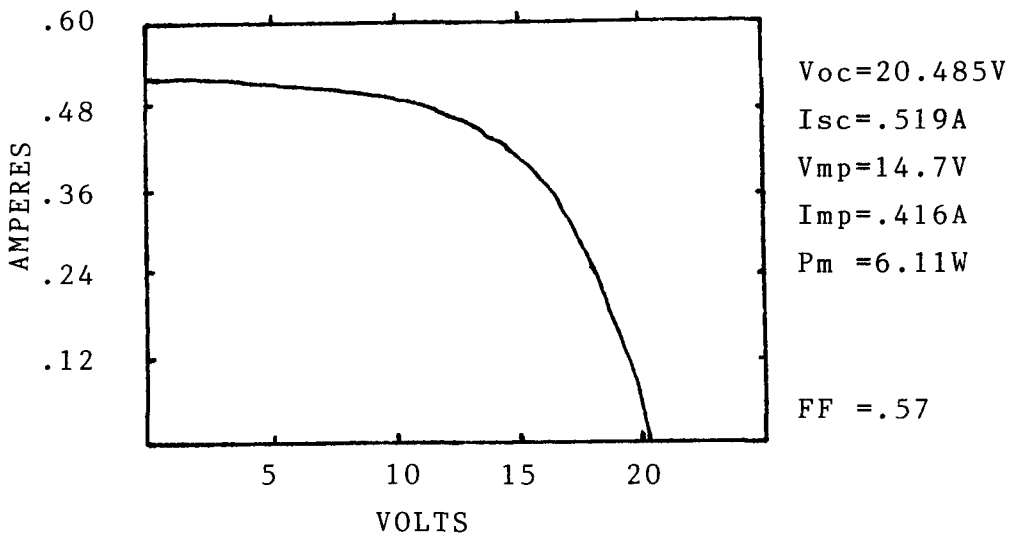


Figure 1 Current\_Voltage response for a 1 ft<sup>2</sup> panel delivered to SERI as measured on the Spire simulator at SERI

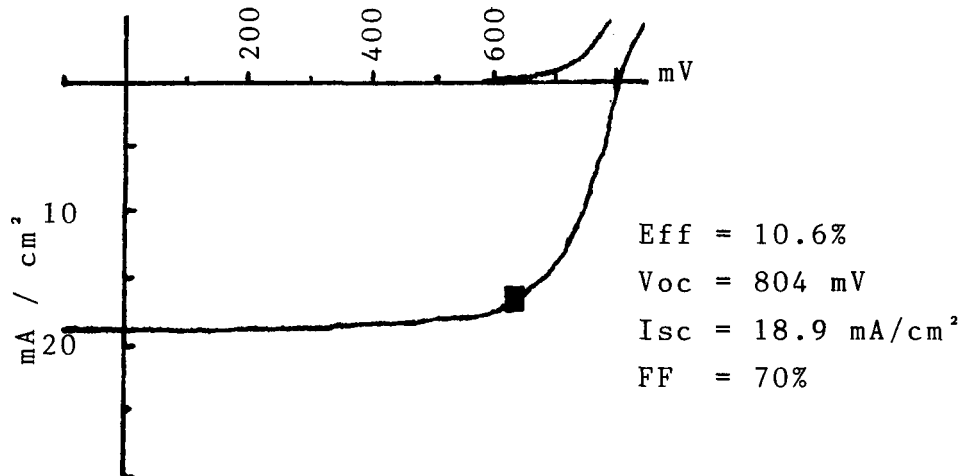


Figure 2 Current-Voltage response for the best cell to date (Area=.302cm<sup>2</sup>)

**Title:** **Thin Film Cadmium Telluride Solar Cells**

**Organization:** Southern Methodist University, Dallas, Texas  
(until May, 31, 1988)  
University of South Florida, Tampa, Florida  
(from July 1, 1988)

**Contributions:** T. L. Chu, S. S. Chu, Principal Investigators  
C. Ferekides, K. D. Han, Y. X. Han, Y. H. Liu,  
M. K. Mantravadi, and M. Song

The major objective of this program is to investigate the preparation, characterization, and optimization of thin-film cadmium telluride heterojunction solar cells in order to demonstrate a quantum efficiency of 75% at  $0.44\text{ }\mu\text{m}$  and a photovoltaic conversion efficiency of 11.5% or greater. In addition, transparent thin film mercury zinc telluride solar cells with a photovoltaic conversion efficiency of 8% will be developed as the top member in two-cell cascade structures. The cadmium telluride solar cell has the configuration: ohmic contact/p-CdTe/TCS/glass substrate. The technical approach to the fabrication of CdTe solar cells consists of (1) the deposition of a transparent conducting semiconductor (TCS) on a glass substrate, (2) the deposition of p-CdTe films on TCS/glass substrates by close-spaced sublimation (CCS), (3) the formation of ohmic contacts to p-CdTe films, and (4) the characterization and optimization of solar cells. The mercury zinc telluride solar cell has a similar configuration as CdTe cells, and mercury zinc telluride films is deposited by metalorganic chemical vapor deposition (MOCVD).

**Transparent Conducting Semiconductor (TCS)**

The photovoltaic characteristics of thin-film CdTe solar cells depend strongly on, among other factors, the properties of TCS or heterojunction partner. Cadmium sulfide is the most commonly used TCS for CdTe solar cells; however, CdS has a bandgap of 2.42 eV and shows limited transparency to radiation with energy greater than the bandgap energy. Among the commonly known larger bandgap non-stoichiometric oxides, only  $\text{SnO}_2$  ( $E_g = 3.8\text{ eV}$ ) and  $\text{ZnO}$  ( $E_g = 3.3\text{ eV}$ ) appear to be feasible on the basis of chemical reactivities.

$\text{ZnO}$  films have been deposited by MOCVD and by precipitation from solution. The MOCVD technique utilizes the oxidation of dimethylzinc by nitrous oxide at  $200^{\circ}$  -  $250^{\circ}\text{C}$  in a helium flow using trimethylaluminum as a dopant. In the solution technique,  $\text{ZnO}$  is precipitated slowly onto the substrate surface by the reaction of sodium hydroxide and a zinc salt. Both techniques have produced adherent films with resistivity lower than  $0.005\text{ ohm-cm}$  and transmission greater than 80% in the visible region.

In addition, thin CdS films ( $0.02\text{-}0.03\text{ }\mu\text{m}$ ) have been deposited by vacuum evaporation and by precipitation from solution. Such films can transmit a significant fraction of radiation with energy greater than the bandgap energy, e.g., approximately 60% at 450 nm.

**Ohmic Contact to p-CdTe Films**

The formation of low resistance contact to p-CdTe films is difficult due to the large work function of p-CdTe. Mercury telluride, one of the few materials with higher work function than p-CdTe, has been shown to be a promising contact material. Since the vapor deposition of HgTe films is tedious, the use of a p-HgTe-graphite paste as a contact to p-CdTe has been developed. P-HgTe was

synthesized from a mercury-deficient mixture of the elements in a sealed tube and mixed with colloidal graphite. This mixture was directly applied to the surface of p-CdTe films followed by heat treatment in an inert atmosphere. The contact resistance, estimated from the electrical characteristics of p-HgTe/p-CdTe/SnO<sub>2</sub>/glass structures, is 1-1.5 ohm-cm<sup>2</sup>. This relatively high contact resistance is due presumably to the fact that the lowest resistivity of intrinsically doped p-HgTe obtainable is 0.02-0.05 ohm-cm. Recent results indicated that extrinsically doped p-HgTe had lower resistivity, about 10<sup>-3</sup> ohm-cm. The use of low resistivity p-HgTe could reduce the contact resistance.

### Photovoltaic Characteristics

Thin films CdTe solar cells of the configuration p-CdTe/TCS/glass have been prepared using SnO<sub>2</sub> and CdS (about 0.03  $\mu$ m thickness) as the TCS, and CdTe films of 200-300 ohm-cm resistivity were deposited by CSS. Solar cells with SnO<sub>2</sub> as the TCS always showed open-circuit voltages below 0.7 V, as compared with 0.75 V or higher for solar cells using CdS. This is due presumably to the chemical interaction between SnO<sub>2</sub> and CdTe during the CSS process.

The majority of solar cells were of the configuration p-CdTe/CdS/SnO<sub>2</sub>/glass, and HgTe paste was used as contacts. The open-circuit voltage and the short-circuit current density are in the range of 0.73 - 0.76 V and 21-23 mA/cm<sup>2</sup>, respectively. Figure 1 shows an example of the illuminated current-voltage characteristics of a thin film CdTe solar cell of 1.2 cm<sup>2</sup> area under global AM 1.5 conditions. The open-circuit voltage, short-circuit current density, and fill-factor are 0.745 V, 21.62 mA/cm<sup>2</sup>, and 65.75%, respectively, corresponding to a conversion efficiency of 10.67. The relatively low fill factor is due presumably to the HgTe/CdTe contact resistance which could be reduced by optimizing the contacting technique. The use of thin CdS films has improved the response of the solar cell in the blue region, as shown by its quantum efficiency, Fig. 2.

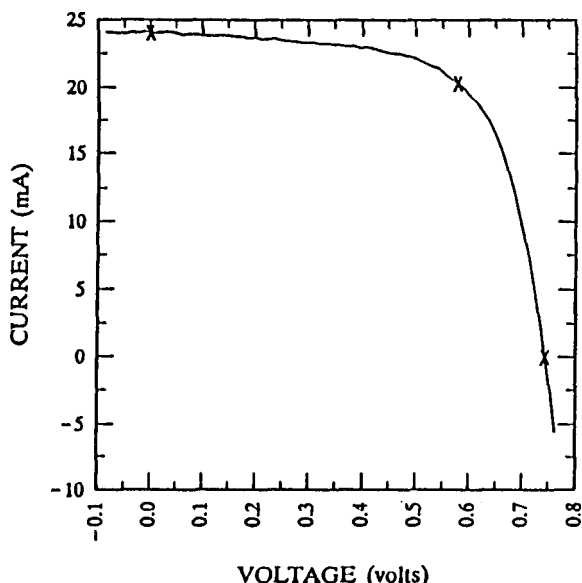


Figure 1. Current-voltage characteristics of a solar cell of the configuration p-HgTe/p-CdTe/CdS/SnO<sub>2</sub>/glass under global AM1.5 conditions.

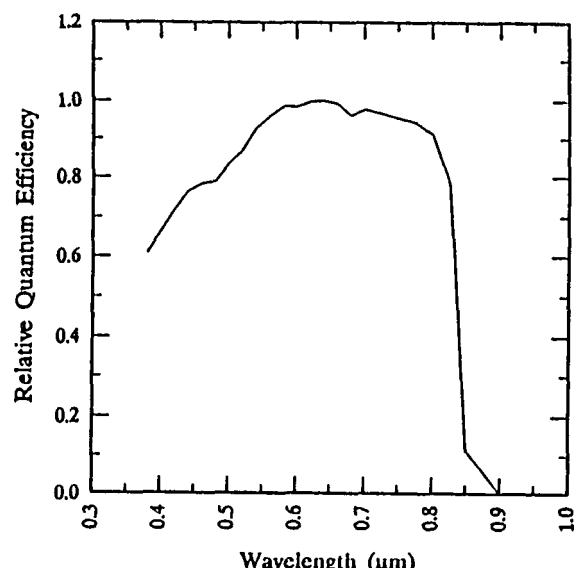


Figure 2. The relative quantum efficiency of a CdS/CdTe solar cell with about 300 $\text{\AA}$  of CdS.

Title: High Efficiency Cadmium and Zinc Telluride Based Thin Film Solar Cells

Organization: Georgia Institute of Technology  
Atlanta, Georgia 30332

Contributors: A. Rohatgi, C. J. Summers, A. Erbil, R. Sudharsanan, S. A. Ringel, J. Welch, and K. T. Pollard

Objective:

The objective of this program is to develop wide bandgap (1.6 - 1.8 eV) polycrystalline thin films to be used as absorber material in the top-cell of the cascade cell structure. Target-cell efficiency is 10% with 80% subgap transmission. CdMnTe films are being grown by MOCVD while CdZnTe films are being deposited by MBE.

Thin-Film Growth:

CdTe and CdMnTe films were grown by metalorganic chemical vapor deposition (MOCVD) on glass/SnO<sub>2</sub>/CdS substrates. CdMnTe films were grown using dimethylcadmium, diethyltellurium, and tricarbonyl methylcyclopentadienyl manganese as source materials for Cd, Te, and Mn respectively. The CdMnTe films were grown at substrate temperature of 420°C, while CdTe films were grown at substrate temperature in the range of 300°C to 400°C with diallyltellurium as a source for Te.

CdZnTe and CdTe films were grown by MBE. Elemental sources were used instead of CdTe and ZnTe sources, for all constituents having a purity of at least 5N. The substrates were baked out at 250°C for 3-4 hours before film growth. The substrate temperature was kept at 275°C for 30 minutes to commence film growth and increased to 300°C for the remainder of the run. Growth rates were typically ~1 um/hr for both CdTe and CdZnTe. In selected instances CdTe and CdZnTe films were doped with Sb using conventional and laser-assisted technique.

Film Characterization:

X-ray diffraction (XRD), surface photovoltage (SPV), Auger electron spectroscopy, Infrared spectroscopy, Raman scattering, and photoluminescence (PL) measurements were done to characterize films for composition, bandgap, film thickness, compositional uniformity, and film quality.

XRD, SPV, and PL measurements showed that we were successful in growing CdMnTe and CdZnTe films with the bandgap of 1.7 eV. Figure 1 shows the SPV spectra of MBE-grown CdTe and CdZnTe films along with MOCVD-grown CdTe and CdMnTe polycrystalline films. Figure 2 shows the Auger depth profile plots of MBE-CdTe and MOCVD-CdMnTe polycrystalline films on glass/SnO<sub>2</sub>/CdS substrates. Auger measurements on MBE-grown CdTe and CdZnTe, MOCVD-grown CdTe films indicated uniform composition. In the case of MOCVD-grown CdMnTe films Auger depth profile measurements indicated a non-uniform composition and accumulation of Mn at the interface. In-situ Auger measurements on CdZnTe films confirmed the presence of Sb in doped films. From IR measurements, thicknesses of CdTe, CdZnTe, and CdMnTe films were estimated and these measurements were useful in optimizing the growth temperature. IR measurements suggested that the optimum substrate temperature for growing CdMnTe films is ~420°C.

### Cell Fabrication and Analysis:

Front wall solar cells were fabricated with glass/SnO<sub>2</sub>/CdS/CdZnTe or CdMnTe/ZnTe/Au structure. This was done in collaboration with AMETEK. The films were annealed at 400°C for 30 minutes in air followed by a mild etch of Br:Methaonal. Both n-i-p and n-p solar cells were fabricated. n-i-p structure was fabricated by depositing Cu doped ZnTe layer. Ni contacts were deposited through a shadow mask.

Figure 3 shows the spectral response of n-p and n-i-p CdTe and CdZnTe solar cells. The n-i-p spectral response is higher over most of the spectral range in both cases. This is consistent with higher values of  $J_{sc}$ ,  $V_{oc}$ , fill factor and efficiency of n-i-p cells. Table 1 gives the solar cell parameters of CdTe, CdZnTe, and CdMnTe solar cells. The cell data and spectral response measurements indicate that we were successful in making 7.5-9.7% polycrystalline CdTe solar cells by MBE and MOCVD and 3.6% efficient CdZnTe solar cells.

One of the problems at present in obtaining high efficiency CdZnTe and CdMnTe cells is the reduction of bandgap after annealing in air at 400°C. Figure 4 shows the transmission spectra of CdZnTe films before and after processing. The bandgap of CdZnTe films is reduced from 1.7 to 1.55 eV after processing. The transmission spectrum of annealed CdZnTe film (Figure 5) not only shows reduction in bandgap but also indicates an increased sub-bandgap absorption with increasing annealing time. This suggested that the optimum annealing condition is different for CdZnTe films. In order to confirm this, CdZnTe films were annealed in air at different temperatures. Figure 5 shows the SPV response of CdZnTe samples. The SPV response increases without any change in the bandgap or Zn content up to an annealing temperature of 385°C. This indicates that annealing improves the film quality. However, SPV response of the film annealed at 410°C decreased drastically. This quality degradation was associated with a shift in the absorption edge towards low bandgap, identical to what was observed in the transmission measurements. These results indicate that the optimum annealing condition for MBE-grown CdZnTe film is 385°C. The 3.7% CdZnTe solar cell went through the 410°C/30 min. anneal, which may be the reason for the low efficiency. Cells are now being fabricated with optimum annealing condition with the goal of achieving CdZnTe efficiencies approaching 10%.

**Table 1. Solar Cell Parameters of Our Best CdTe, CdZnTe, and CdMnTe n-i-p Cells. The Zn Concentration is 40% in CdZnTe and Mn Concentration is 10% in CdMnTe Films.**

Samples	Efficiency %	$V_{oc}$ mV	$J_{sc}$ mA/cm <sup>2</sup>	Fill Factor
MBE-CdTe	7.1	740	17.1	55.7
MBE-CdTe	7.6	666	17.5	65.3
MOCVD-CdTe	9.3	713	22.6	57.7
MBE-CdZnTe	3.6	511	14.4	48.4
MOCVD-CdMnTe	6.0	680	20.6	44.2

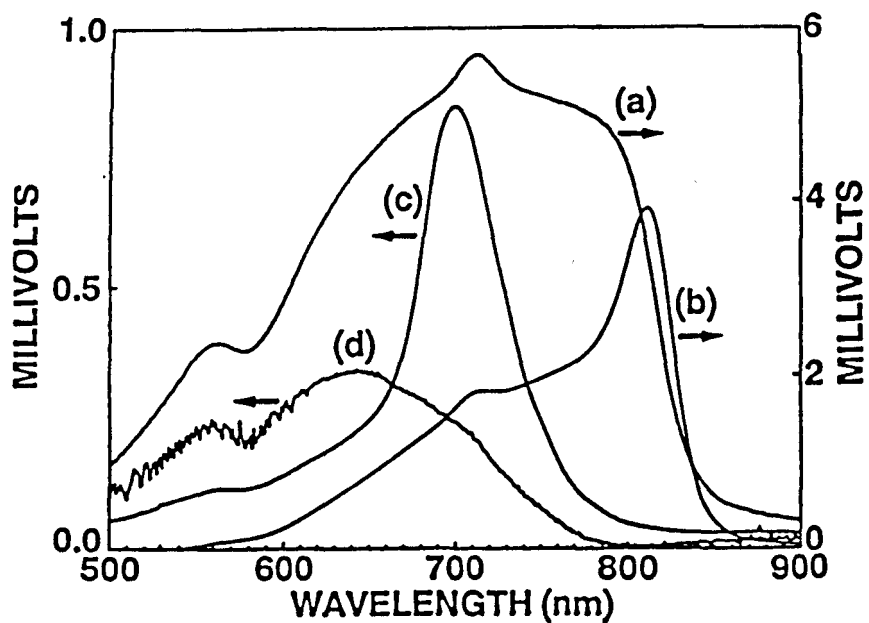


Figure 1. SPV spectra of (a) MBE-CdTe, (b) MOCVD-CdTe, (c) CdZnTe, and (d) CdMnTe.

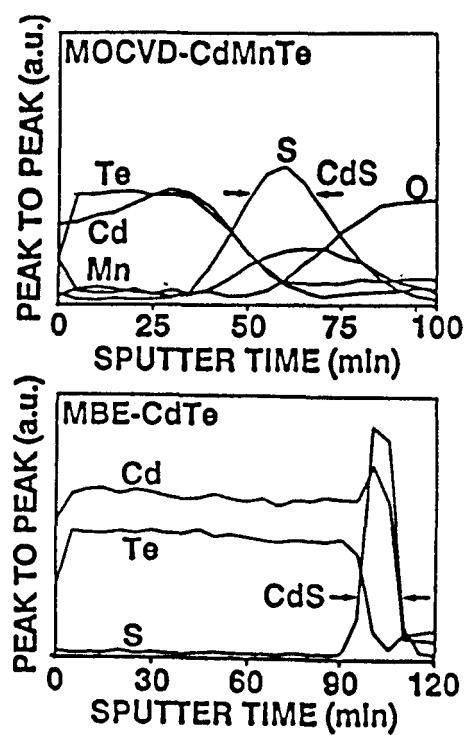


Figure 2. Auger Depth Profile Plots of (a) MBE-CdTe and (b) MOCVD-CdMnTe.

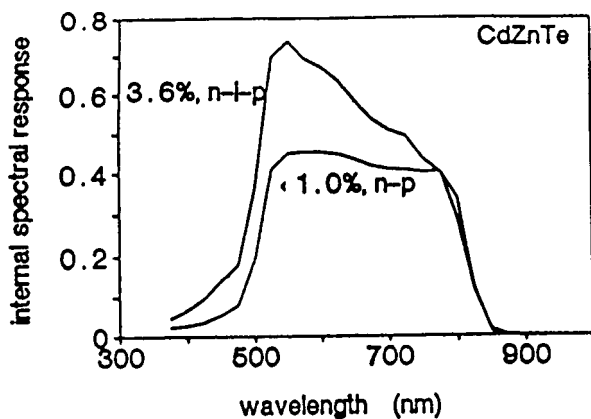


Figure 3. Spectral Response of n-p and n-i-p (a) CdTe and (b) CdZnTe Cells.

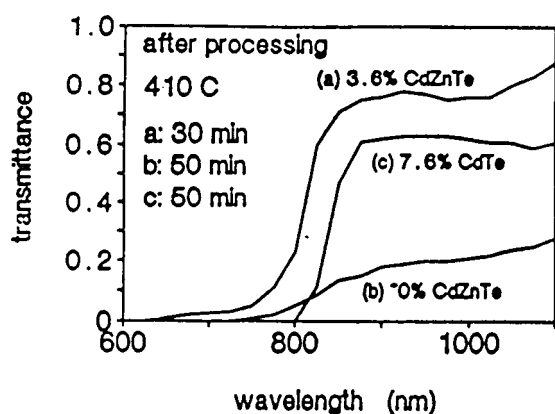
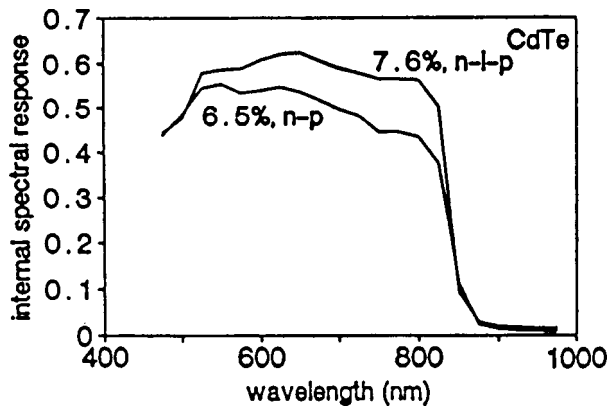
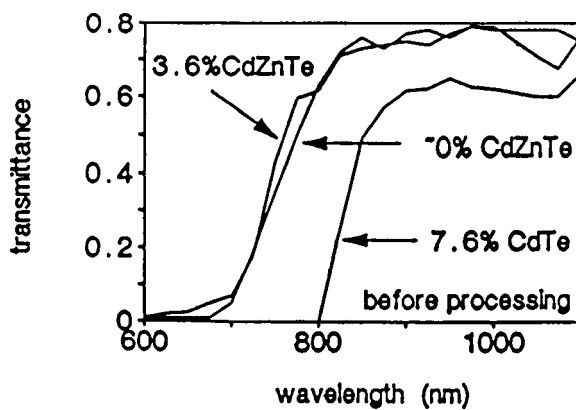


Figure 4. Transmission Spectra of CdTe and CdZnTe Films.



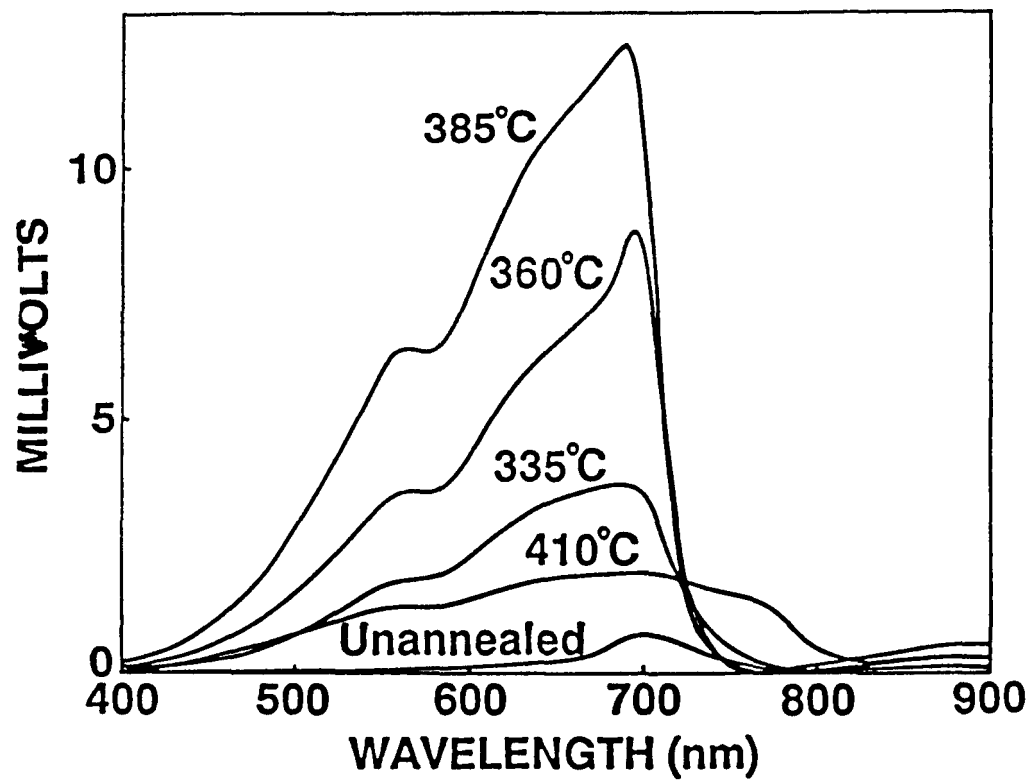


Figure 5. SPV Spectra of CdZnTe Film Annealed at Different Temperatures.

Title: Wide Bandgap II-VI Window and Photon Absorber Materials for Cascaded Cells

Organization: Jet Propulsion Laboratory, California Institute of Technology, Pasadena, California

Contributors: R.J. Stirm and A. Nouhi

The objective of this task is to collaborate with industry on the use of films of medium bandgap Cd(Mn)Te deposited by metalorganic chemical vapor deposition (MOCVD) for application as top-cell absorbers in cascaded solar cells.

#### Cell Structure

A concept for further increasing solar cell efficiencies is that of optically stacking in tandem two or more junction devices having different values of bandgap ( $E_g$ ). For potential use with a CuInSe<sub>2</sub>/CdS lower bandgap cell (1.0 eV), we have chosen the photon absorbing material in the upper cell to be Cd<sub>1-x</sub>Mn<sub>x</sub>Te with x ~ 0.15 ( $E_g$  = 1.7 eV). Further, the structure of the upper cell, a CdS/CdMnTe/ZnTe n-i-p device, has been patterned after the successful n-i-p cell developed by Ametek Applied Materials Laboratory utilizing electrodeposited CdTe (Ref. 1). The choice of CdMnTe for the upper cell was made because of numerous reported difficulties working with CdZnTe for various purposes, and because of recent success in growing CdMnTe by MOCVD (Ref. 2), a process amenable to production of large-area devices.

The n-i-p structure would seem to be even more appropriate for a higher bandgap pseudo-binary compound of CdTe because of the expected difficulty in strongly doping p-type and in contacting that material. Figures 1 and 2 show a proposed II-VI cascaded solar cell and suggested energy band line-up at zero bias for CdS/CdMnTe/ZnTe, respectively. It can be seen that the band offsets for photo-generated carriers are quite low at both interfaces, which with the full depletion of the i-layer, promises high short-circuit currents that have, indeed, been observed. Contacting to p-ZnTe is also considerably easier than it is to high resistivity CdTe or CdMnTe.

#### Results

In collaboration with Ametek Applied Materials laboratory, n-i-p solar cells have been made with CdTe and CdMnTe, both grown by MOCVD at temperatures between 400 and 450°C. In the Annual Report for FY1987 (Ref. 3), small-area cells using MOCVD-grown CdTe were reported to have obtained a best efficiency of 7.5% for global AM1.5 simulation. The values for  $V_{OC}$  (675 mV),  $J_{SC}$  (20.6 mA/cm<sup>2</sup>), and fill factor (54%) were not much less than typical values reported for CdTe/CdS solar cells fabricated by other processes, except for the fill factor value, which may have been suppressed by high series resistance.

More recent devices have been improved by optimizing the growth and post heat treatment procedures. The best value of efficiency obtained to date is 9.4% (Ref. 4), with further improvements in  $V_{OC}$  (697 mV) and  $J_{SC}$  (22.1 mA/cm<sup>2</sup>). The fill factor, however, has not been much improved. A further improvement in that to only 71% would project a cell efficiency of 11%. Figures 3 and 4 show the dark current-voltage characteristic and spectral response for this cell, respectively.

Similar structures using  $\text{Cd}_{0.85}\text{Mn}_{0.15}\text{Te}$  grown by MOCVD have not been nearly as successful. Although  $\text{CdMnTe}$  films have been grown on glass with  $x$  values (Mn composition) as high as 60%,  $\text{CdMnTe}$  films grown on  $\text{CdS}$  and heat treated at  $410^\circ\text{C}$  in  $\text{N}_2$ , which was found to be optimum for  $\text{CdTe}/\text{CdS}$ , showed a marked degradation. In addition to the observation that there was little photovoltaic activity in these structures, transmitted light measurements indicated an apparent shift in the optical bandgap of the  $\text{CdMnTe}$  from the original 1.7 eV towards the value for  $\text{CdTe}$  (1.5 eV). Increasing the heat treatment time increased the shift in absorption edge toward lower energies. A phase separation of the pseudo-binary compound into two separate binary compounds of  $\text{CdTe}$  and  $\text{MnTe}$  could explain these observations. Indeed, depth profiling with Auger Electron Spectroscopy at the Georgia Institute of Technology has shown a tendency for the Mn to move towards the interface with  $\text{CdS}$ , while the Cd moves towards the outer surfaces (Ref. 5).

A possible explanation for phase separation is the effect of misfit strain arising from the substrate,  $\text{CdS}$ , in this case, although  $\text{CdMnTe}$  films grown on  $\text{GaAs}$  without trace  $\text{O}_2$  do not show this phenomenon. Misfit strain has recently been shown to affect the miscibility gap in heteroepitaxial layers of  $\text{InGaP}$  and to be orientation dependent, as expected (Ref. 6). Experiments to verify this conjecture and to hopefully modify the heat treatment procedure for the case of  $\text{CdMnTe}$  films are planned, as well to explore the potential for  $\text{CdMgTe}$  films as the photon absorber which may not undergo phase separation.

### Conclusions

The deposition of II-VI thin films by MOCVD procedures has been proven viable for n-i-p  $\text{CdS}/\text{CdTe}/\text{ZnTe}$  solar cell structures, with photovoltaic parameters the near-equal of alternate  $\text{CdTe}$  cells fabricated by other means (except for fill factor). However, similar to reported problems by others on the use of ternary II-VI compounds for various purposes in photovoltaics, substitution of  $\text{CdMnTe}$  for  $\text{CdTe}$  showed unexpected difficulties. The problems were manifested by an apparent phase separation as a consequence of  $400^\circ\text{C}$  heat treatments in  $\text{N}_2$ .

Further investigation should explore the potential role of trace amounts of  $\text{O}_2$  in the post heat treatment process and possible alternate heat treatments that are required for improved junction properties.

## References

1. P.V. Meyers, *Solar Cells* 23, 59 (1988).
2. A. Nouhi and R.J. Stirm, *Appl. Phys. Letters* 51, 2251 (1987).
3. Photovoltaic Program Branch: Annual Report, FY1987. (March 1988). SERI/PR-211-3299. 309 pp. Available NTIS: Order No. DE88001155.
4. A. Nouhi, R.J. Stirm, P.V. Meyers and C.H. Liu, *J. Vac. Sci. Technol.*, May/June, 1989.
5. R. Sudharsanan, Z.C. Feng, S. Perkowitz, A. Rohatgi, K.J. Pollard, and A. Erbil, *J. Vac. Sci. Technol.*, May/June, 1989.
6. F.C. Larche' W.C. Johnson, C.S. Chiang and G. Martin, *J. Appl. Phys.* 64, 5251 (1988).

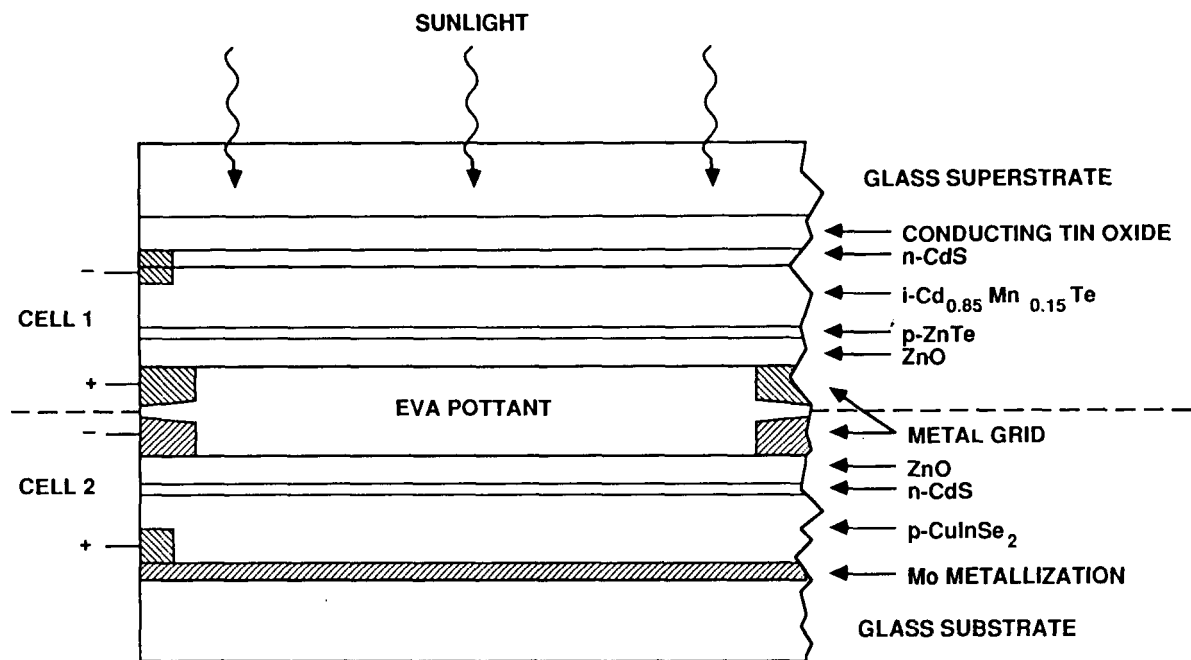


Figure 1. Proposed structure for a II-VI thin-film cascaded solar cell utilizing  $\text{CuInSe}_2$  and  $\text{CdMnTe}$  in the lower and upper cells, respectively.

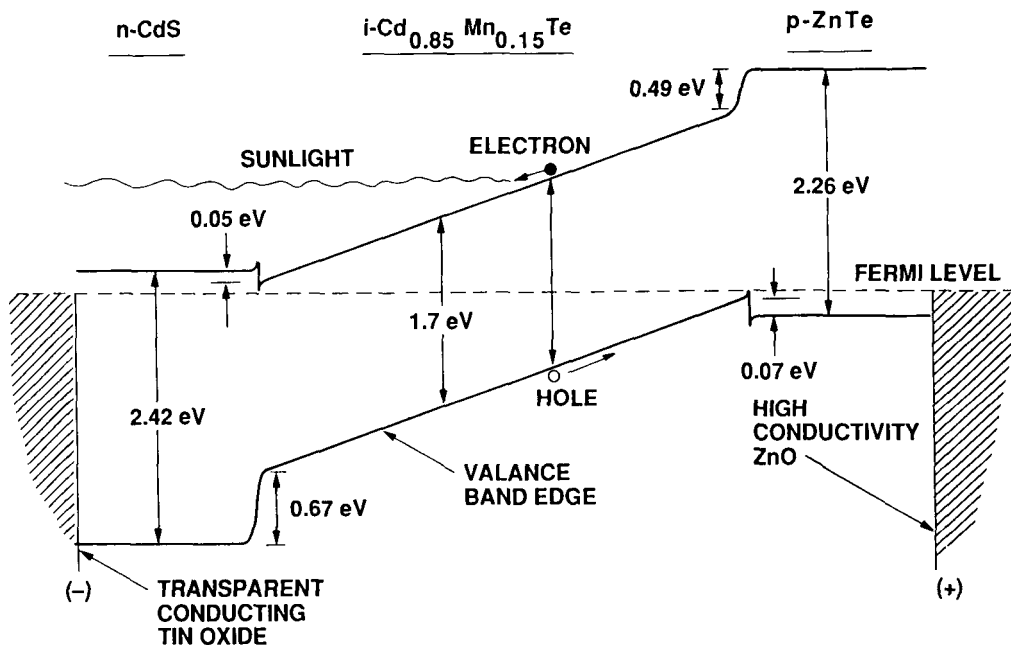


Figure 2. Energy band diagram for the n-i-p structure of the upper solar cell shown in Figure 1.

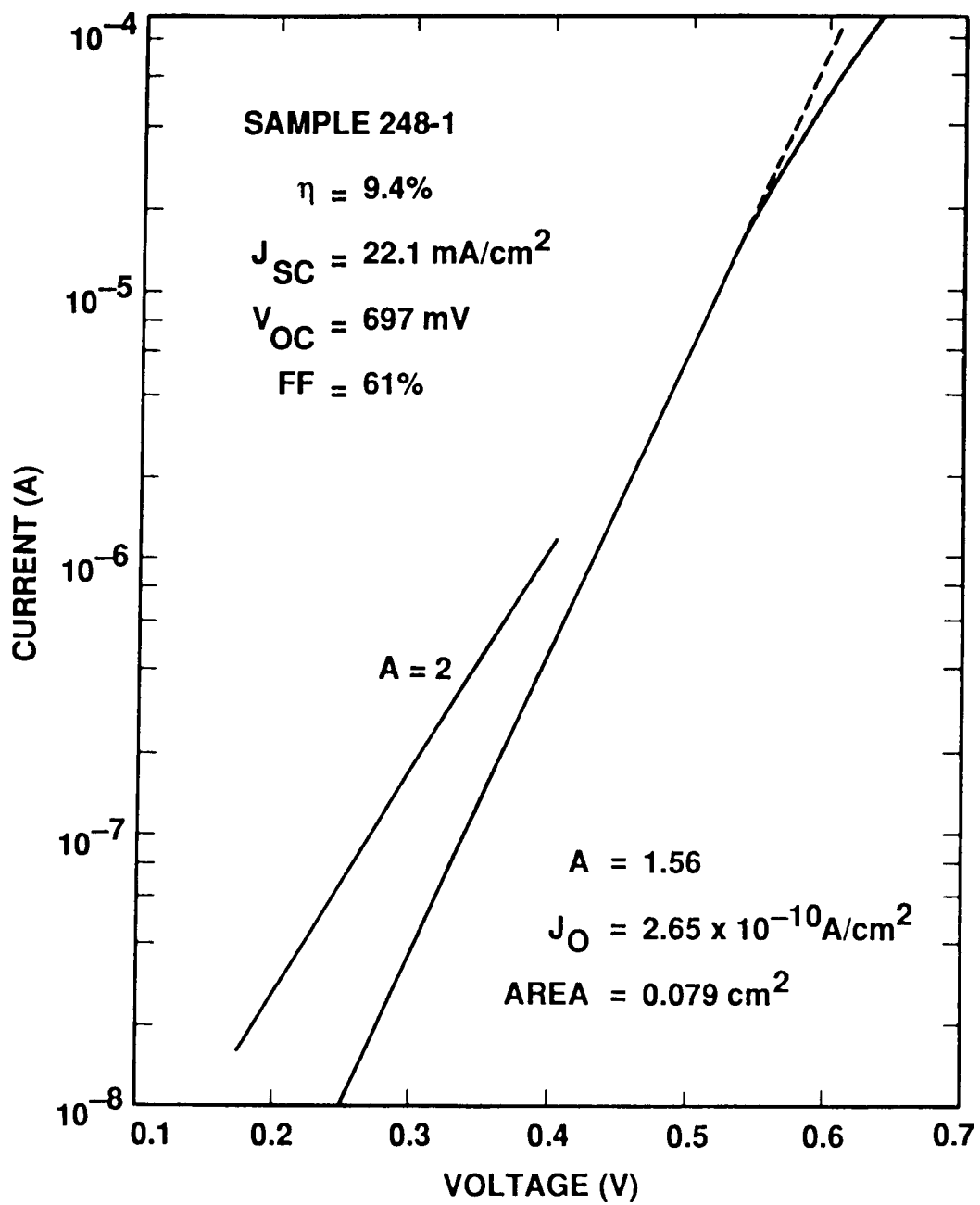


Figure 3. Dark current-voltage characteristic and photovoltaic parameters for cell No. 248-1.

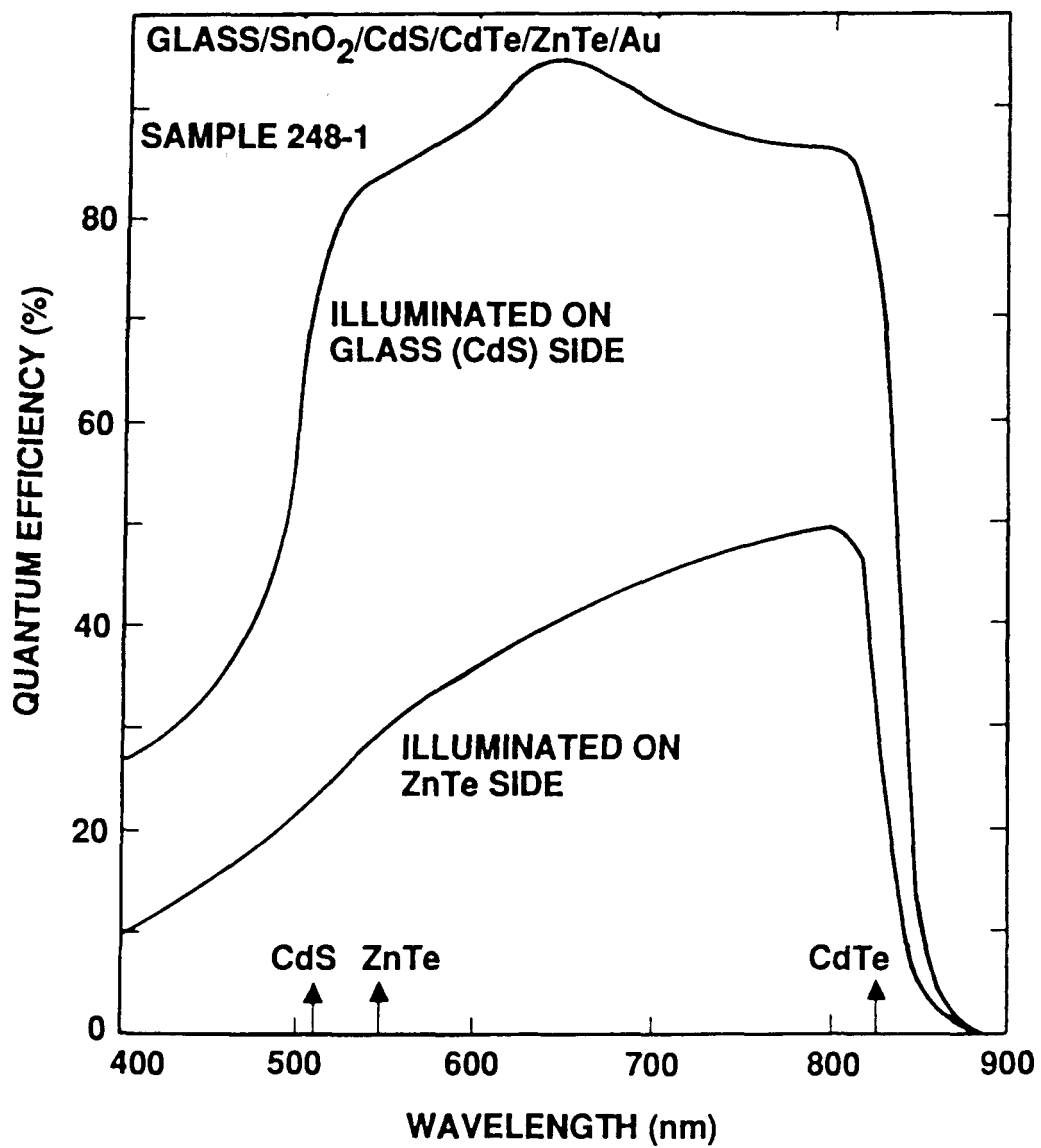


Figure 4. Spectral response for cell No. 248-1 for light entering the CdS side (upper curve) and ZnTe side (lower curve).

Title: CuInSe<sub>2</sub> Based Cascade Solar Cells

Organization: Institute of Energy Conversion, University of Delaware, Newark, Delaware

Contributors: B.N. Baron, Project Director; J.E. Phillips and R.W. Birkmire, Principal Investigators; W.A. Buchanan, B.E. McCandless; and R.E. Rocheleau

The objective of this research is to demonstrate a proof-of-concept cascade solar cell using CuInSe<sub>2</sub> for the low band gap bottom cell and either CdTe or a-Si as the top cell.

### Technical Approach

Among the various cascade structures proposed for achieving high efficiency, the monolithic two-terminal cascade structure employing a thin-film CuInSe<sub>2</sub> cell for the low-band-gap bottom component is a natural extension of efforts to develop low-cost, high-efficiency, thin-film photovoltaic cells(1). The capability to fabricate single-junction, CuInSe<sub>2</sub> thin-film devices that have a 10% efficiency has been established at the Institute of Energy Conversion(IEC) under a SERI subcontract. Therefore, the primary emphasis of this research is on the high-band-gap component cells and on the fabrication and analysis of cascade cells.

A two-cell stack structure with (CdZn)S/CuInSe<sub>2</sub> for the bottom cell with either CdS/CdTe or a-Si for the top cell and a suitable transparent interconnect has been selected for development.

Conventional high-efficiency CdTe cells require processing at temperatures greater than 400°C. In contrast to techniques that have been proven for fabricating single-junction CdTe devices, the CuInSe<sub>2</sub>-based monolithic two-terminal approach further requires first depositing CdTe on the ohmic contact and then forming the CdS layer. Since CuInSe<sub>2</sub> devices degrade with exposure to temperatures above 300°C, low-temperature physical vapor deposition of p-type CdTe, with a goal of 10<sup>3</sup> ohm-cm, was studied. Candidate transparent interconnect systems included thin layers (less than 50Å) of Cu or Ag in combination with conductive oxides such as ITO, SnO<sub>2</sub>, and ZnO.

Photochemical vapor deposition (photo-CVD) was used to fabricate a-Si:H top cells on CuInSe<sub>2</sub>-based substrates. Under a SERI subcontract, IEC has used photo-CVD to fabricate 10%-efficient a-Si p-i-n cells on textured tin oxide substrates. Primary concern in the development of the a-Si top cell for a monolithic tandem cell with a CuInSe<sub>2</sub>-based bottom cell was process compatibility. For example, a-Si device fabrication is known to be extremely sensitive to residual gas impurities, while CuInSe<sub>2</sub> devices can be severely degraded by chemical reducing agents.

The fabrication and analysis of two-terminal cascade cells was aimed at the practical realization of monolithic structures, with CuInSe<sub>2</sub> devices serving as both the substrate and the low-band-gap component. This also included fabricating diagnostic three-terminal devices that allow the

individual component cells to be tested. Such devices also were used to determine contributions to electrical and optical losses from the transparent interconnect layers.

### Significant Results in FY 1988

#### CdTe/CuInSe<sub>2</sub> Cascade Cells

In order to remove the high temperature heat treatment step from the fabrication of CdTe solar cells, the CdTe resistivity must be controllable over the range 1 to 1000 ohm-cm by extrinsic doping during deposition at low temperature (T<300°C). Bicknell et al. (2) reported low resistivity epitaxial CdTe:Sb films deposited using laser assisted MBE techniques. Polycrystalline CdTe films were deposited over the substrate temperature range 175 to 300°C by co-evaporation of CdTe and Sb under continuous argon/krypton laser irradiation at 647 nm. Cross-grain resistivities at room temperature were typically 10<sup>8</sup> ohm-cm in the dark and 10<sup>6</sup> ohm-cm in the light. Similar results were obtained for films grown without laser irradiation during growth.

Evaporation of CdTe on to substrates coated with thin (10 to 50Å) layers of group Ib dopant, Cu or Ag, was also investigated. Substrate temperatures were 180 and 250°C. Room temperature cross-grain resistivities ranged from 10<sup>3</sup> to 10<sup>6</sup> ohm-cm under white light illumination (100 mW/cm<sup>2</sup>). Diagnostic n/p heterojunction CdS:In/CdTe:Ag/TCO/glass and CdS:In/CdTe:Cu/TCO/glass devices were fabricated. The range of open circuit voltage was from 0.1 to 0.37 volt, short circuit currents were 1 to 7 mA/cm<sup>2</sup> and fill factors were less than 45%. Heat treatments in air at 200°C did not improve device performance.

Alternate approaches for utilizing CdTe-based cells as the top cell component in a CuInSe<sub>2</sub>-based cascade cell should be explored. For monolithic two-terminal cascade cells, these alternatives should include: low temperature n-i-p devices in which intrinsic CdTe is formed over p<sup>+</sup> ZnTe; and superstrate CuInSe<sub>2</sub> configurations in which a CdS/CuInSe<sub>2</sub> cell is formed on a completed glass/TCO/CdTe cell, thereby eliminating the need for low temperature CdTe processing. Non-monolithic approaches to cascade cells employing CdTe and CuInSe<sub>2</sub> should focus on improvements in transparent CdTe cells with emphasis on reducing optical losses.

#### a-Si/CuInSe<sub>2</sub> Cascade Cells

Monolithic two-terminal a-Si:H - CuInSe<sub>2</sub>/CdS solar cells were prepared and characterized. The key issues were: 1) smoothing the CuInSe<sub>2</sub> surface for deposition of unshorted a-Si:H cells, 2) transparent interconnect between cells, and 3) fabrication procedures to provide a third terminal for diagnostic analysis of each component cell(3).

The structure used in this work for the fabrication of monolithic tandem solar cells is shown in Figure 1. The as-deposited 3 micron thick CuInSe<sub>2</sub> film has a granular surface with defects and protrusions which may extend as high as 5 microns above the film surface. In early devices, replication

of this morphology by the CdS, ZnO, and a-Si:H layers resulted in shorting of the a-Si:H top cell. This was overcome by etching the CuInSe<sub>2</sub> in an aqueous-bromine solution (4) prior to deposition of the subsequent layers. Removal of approximately 1 micron from the CuInSe<sub>2</sub> film resulted in a specular CuInSe<sub>2</sub> surface with no detectable defects or protrusions greater than 2000Å. ZnO was used as a transparent interconnect between the CdS and a-Si:H. ZnO may also act as a diffusion barrier between the CdS and the a-Si:H although this role has not been confirmed. The n-i-p a-Si:H solar cell was deposited by photochemical vapor deposition using procedures that have produced a 10% efficient p-i-n cell on textured tin-oxide coated glass(5). The cell area was 0.08 cm<sup>2</sup>.

Table 1 summarizes the current-voltage data for the highest efficiency tandem cell and the corresponding individual a-Si:H and CuInSe<sub>2</sub> cells before and after air heat treatment at 150°C. The heat treatment improved both the a-Si:H and CuInSe<sub>2</sub> cells yielding a 5.8% efficient tandem cell. Figure 2 shows the current-voltage characteristics for the tandem cell and its component cells. The open circuit voltage is 1.06 V consistent with the component cell voltages. The behavior of the component cells is uncharacterized by high series resistance which may be due to a Ni/ZnO contact resistance and/or to the sheet resistance of the ZnO interconnect layer.

The short circuit current of the tandem cell is 10 mA/cm<sup>2</sup> and is limited by the current of the n-i-p a-Si:H cell. Figure 3 shows spectral response curves for the component cells measured under white light (ELH) bias at 87 mW/cm<sup>2</sup>. Optical interference from the top cell and interconnect accounts for the structure in the CuInSe<sub>2</sub> cell spectral response curve. The short circuit current of the CuInSe<sub>2</sub> cell agrees with calculated values based on optical transmission data of the a-Si:H cell. The low current of the a-Si:H cell is attributed to the n-i-p configuration.

Further efficiency improvements will require optimizing the a-Si:H cell for illumination through the n-layer and current matching between the top and bottom cells. The latter may be accomplished by narrowing the a-Si:H bandgap by alloying the silicon with germanium. Such devices have the potential of achieving efficiency over 16%.

### Conclusions and Areas for Future Work

Major conclusions reached as a result of this research are:

- A monolithic two-terminal cascade solar cell with 6% efficiency which utilizes a CuInSe<sub>2</sub> heterojunction bottom cell in tandem with an a-Si n-i-p top cell and ZnO inter-layer was fabricated.
- The performance of two-terminal CuInSe<sub>2</sub> cascade cells is presently limited by the a-Si n-i-p top cell.
- Further work is required to develop a low temperature process for fabricating CdTe-based solar cells that is compatible with a CuInSe<sub>2</sub>-based monolithic cascade cell.

Future research on CuInSe<sub>2</sub>-based cascade solar cells should focus on:

- ▶ Optimization of a-Si n-i-p top cell in monolithic two-terminal device.
- ▶ Development of transparent CdTe-based cells for mechanically stacked cascade cells.

---

1. Meakin, J. D.; Birkmire, R.W.; DiNetta, L.C.; Lasswell, P.G.; Phillips, J.E. (1986) Solar Cells 16, pp447-456.
2. Bicknell, R.W.; Giles, N.C.; Schetzina, J.F. (1986) Appl. Phys. Lett. 49, pp 1735-1737.
3. Phillips, J.E.; Birkmire, R.W.; DiNetta, L.C.; Meakin, J.D. (1985) Proceedings of the Symposium on Materials and New Processing Technologies for Photovoltaics, New Orleans, LA, 1985 (Electrochemical Society, New Jersey, 1985), 163-172.
4. Birkmire, R.W. and McCandless, B.E. (1988) Appl. Phys. Lett. 53(2), 140-141.
5. SERI Science and Technology Brief, "Photochemical Vapor Deposition" Photovoltaics/11, (1988) SERI/SP-320-2734.

---

Table 1. Current-voltage data for the highest efficiency tandem cell and the corresponding component cells before and after a 4.5 hour air heat treatment at 150°C.

Cell	Condition	V <sub>OC</sub> (V)	J <sub>SC</sub> <sup>a</sup> (mA/cm <sup>2</sup> )	FF (%)	Eff (%)
Tandem	Initial	0.78	10.1	32.2	2.9
Tandem	Heat Treated	1.06	10.8	44.1	5.8
a-Si:H	Initial	0.59	9.2	31.5	2.0
a-Si:H	Heat Treated	0.74	9.8	37.2	3.1
CuInSe <sub>2</sub>	Initial	0.11	10.5	27.5	0.4
CuInSe <sub>2</sub>	Heat Treated	0.31	15.2	37.3	2.0

<sup>a</sup> ELH 87.5 mW/cm<sup>2</sup> simulation at 32°C.

---

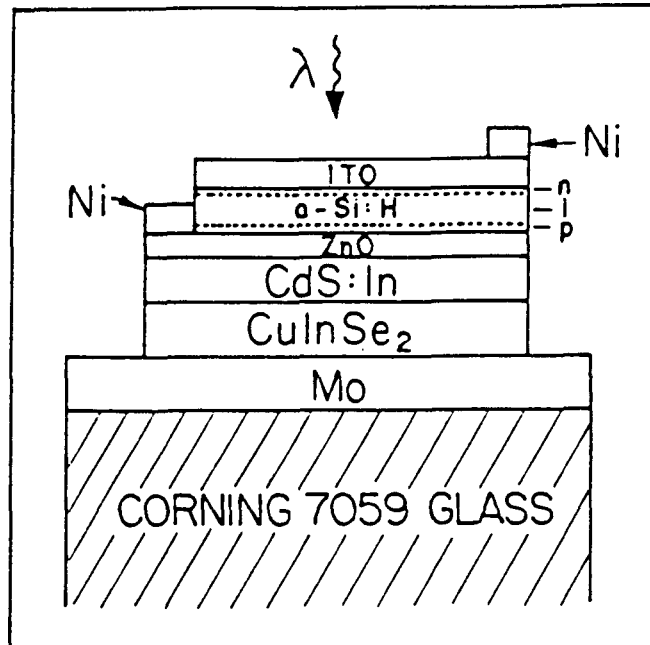


Figure 1. Cross-section of the a-Si:H - CuInSe<sub>2</sub>/CdS monolithic tandem solar cell.

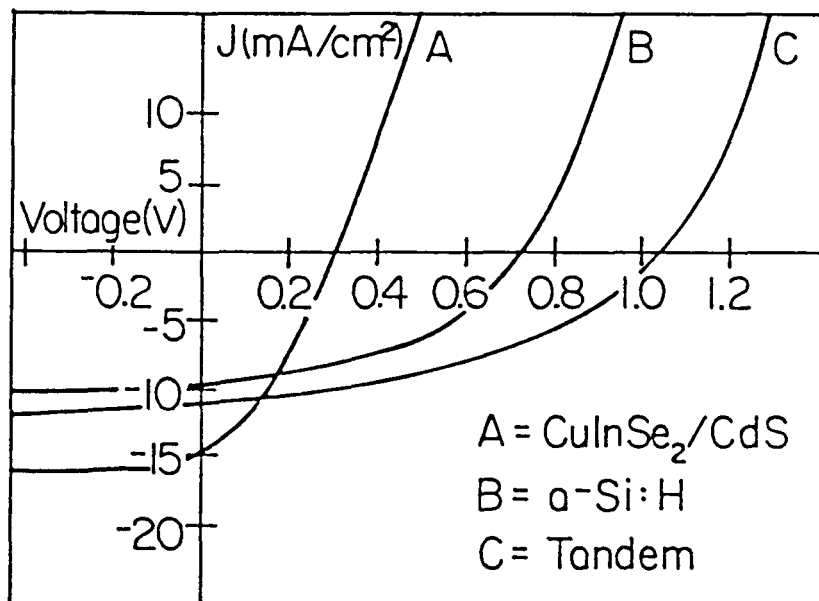


Figure 2. Current-voltage characteristics of the tandem cell and the component a-Si:H and CuInSe<sub>2</sub>/CdS cells. ELH simulation at 87.5 mW/cm<sup>2</sup> at 32°C.

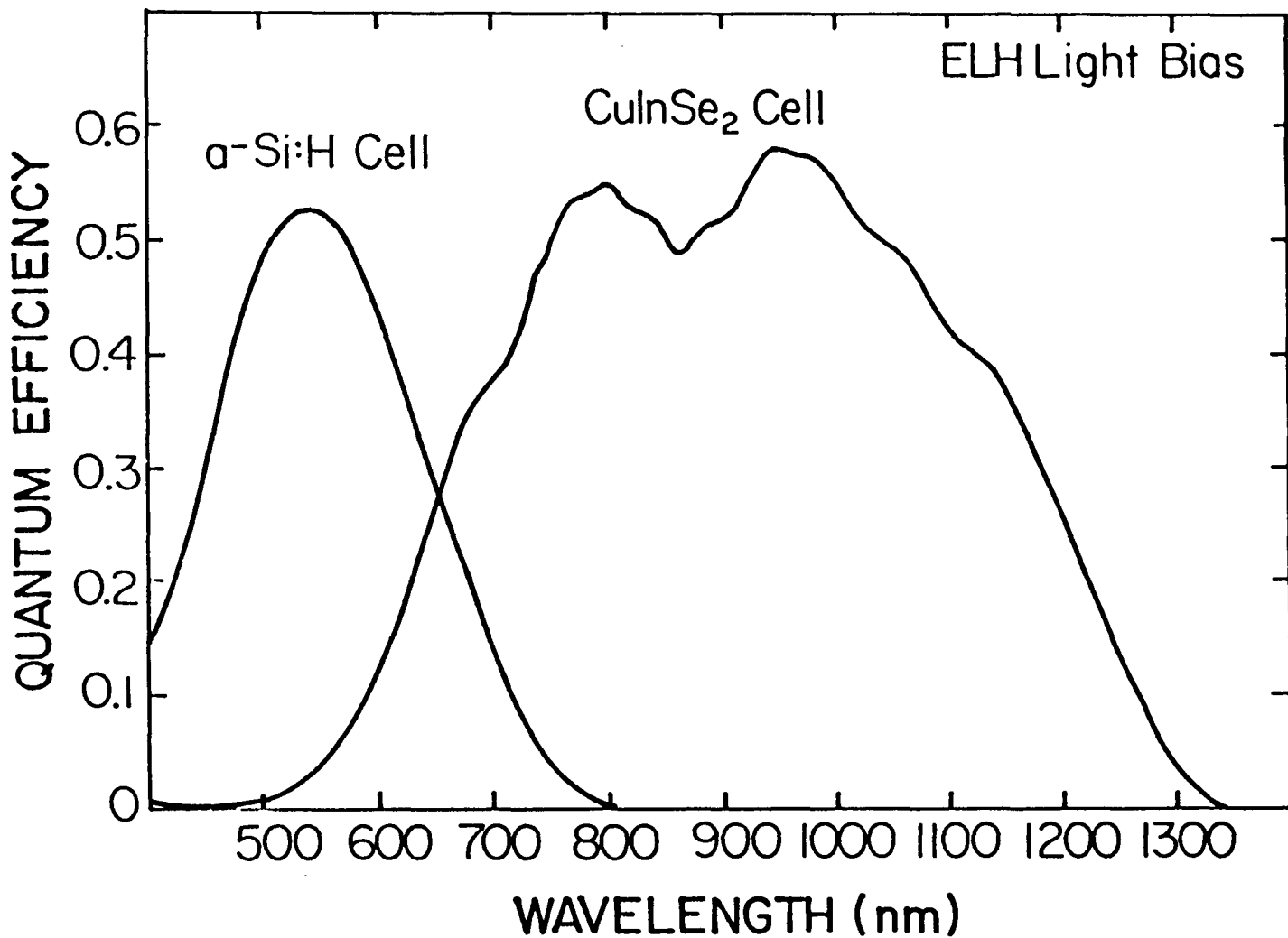


Figure 3. Spectral response of the component a-Si:H and CuInSe<sub>2</sub>/CdS cells under ELH bias at 87.5 mW/cm<sup>2</sup> at 32°C.

#### 4.0 CRYSTALLINE SILICON MATERIALS RESEARCH

J. Benner (Manager) and B. Sopori

At present, crystalline silicon photovoltaic technology has not been surpassed by the newer thin-film approaches in module-level efficiency, long-term stability, or produced energy cost. Yet, in spite of the technology's relative maturity, continued research is expected to yield improvements in performance and production cost. This program supports research in universities and coordinates the transfer of sample materials and information among universities, industry research groups, and SERI. The objective of this project is to improve our fundamental understanding of electrically active defects in various forms of crystalline and polycrystalline silicon.

During FY 1988, three university teams were selected from a public competition to perform three-year research activities investigating the structural and chemical defects in silicon. In particular, they will investigate the interactions of carbon and oxygen at local defects and along dislocations. The mechanisms under which atomic hydrogen treatments passivate certain defects will also be identified. The investigations will utilize samples provided by the photovoltaic industry as well as materials with specific carbon or oxygen concentrations, or both, provided by SERI. In the coming year, these efforts will be complemented by additional unique characterization capabilities to be provided through two smaller subcontracts with the Georgia Institute of Technology (impurity and structural characterization) and the University of Southern California (electrical characterization).

Title: The Effectiveness and Stability of Impurity/Defect Interactions and Their Impact on Minority Carrier Lifetime

Organization: Department of Materials Science and Engineering, North Carolina State University, Raleigh, North Carolina

Contributors: G. A. Rozgonyi, F. Shimura, and Z. Radzimski

The objective of this research is to establish the effectiveness of gettering as a viable technique to improve the material quality of low-cost silicon substrates. The research is directed at the chemical and electrical behavior of defect interfaces in crystalline silicon wafers, dendritic web and EFG ribbons.

The scope of this research extends to the following areas:

1. Use of specially designed model epitaxial silicon structures to study basic properties such: a) the characteristics of impurity (metallic) diffusions in the presence of defects and impurity trapping at the defects, b) the region of influence of defects for impurity capture, c) the deactivation of defects by impurities such as hydrogen.
2. Investigations on magnetic CZ (MCZ) material to evaluate its potential as a high efficiency solar cell substrate; comparison of minority carrier lifetime in FZ, CZ and MCZ wafers subject to thermal annealing and simulated internal gettering treatments.

## I. Minority carrier lifetime of MCZ wafers

Silicon materials with an increasingly higher quality have been produced for the fabrication of electronic devices in very large scale integration (VLSI) and ultra large scale integration (ULSI). These advanced materials have also provided the best material for the highest efficiency solar cells. Because of its potential higher crystal quality for producing, magnetic-field applied Czochralski (MCZ) silicon is now receiving more interest as a substrate [1]. The application of a magnetic field to molten silicon during crystal growth reduces the thermal melt convection, thermal gradient and temperature fluctuations at the solid-liquid interface. This results in a reduced incorporation of point defects into the growing crystal and smaller radial fluctuations of impurity concentrations.

The samples used in this study were 5 inch diam MCZ, 4 inch diam CZ and FZ silicon crystals ( $p<100>$ , B-doped, 5~7 ohm-cm). Metal-oxide-semiconductor (MOS) capacitors were fabricated on these samples for subsequent C-t measurements. The generation lifetime was measured at room temperature, while the recombination lifetime was measured at an elevated temperature (i.e., 90°C) by monitoring the relaxation of an MOS capacitor to a pulsed voltage. Fig. 1 plots the generation and recombination lifetimes as a function of initial oxygen concentration. This figure shows: (i) the recombination lifetime of FZ silicon is higher than that of CZ silicon, as is well known, (ii) most MCZ silicon has a higher minority carrier lifetimes than CZ and FZ silicon; particularly, MCZ silicon with a high initial oxygen concentration achieves extremely high generation lifetimes of greater than a milli-second, and (iii) among MCZ silicon, the generation lifetime increases with initial oxygen concentration; however, the recombination lifetime decreases with the initial oxygen concentration.

A generation lifetime ( $\tau_g$ ) is derived from the carrier generation in the surface depletion region in an MOS capacitor. Therefore, it represents the material quality near the surface of the wafer. A recombination lifetime ( $\tau_r$ ), on the other hand, reflects the bulk wafer properties within a diffusion length, since minority carriers generated near the surface recombine too rapidly at the elevated temperature to contribute to the signal. From this perspective, the dependence of minority carrier lifetime on starting materials grown with different techniques can be explained as follows. MCZ silicon has fewer grown-in point defects than CZ silicon, as described above. Assuming the

same initial oxygen concentration in CZ silicon as in MCZ silicon, one can expect that more grown-in  $\text{SiO}_2$  can be formed in CZ silicon than in MCZ silicon because of more point defects as heterogeneous nucleation centers for oxygen precipitation. Accordingly, MCZ silicon shows a higher minority carrier lifetime than that of CZ silicon because of fewer recombination centers such as oxygen precipitates. For FZ silicon, oxygen-related defects are negligible; however, the high temperature fluctuations and thermal gradient at the solid-liquid interface in growing FZ silicon introduce a high density of point defects. These induced point defects are known to form clusters (e.g., A- or B-swirl defects). Because of the higher density of point defect clusters, FZ silicon may show a lower minority carrier lifetime than MCZ silicon. Comparing the minority carrier lifetime data for CZ and FZ silicon shown in Fig. 1, one may conclude that  $\text{SiO}_2$  precipitates degrade the lifetime more than point defect clusters do.

In summary, minority carrier lifetime measurements have shown the superiority of MCZ silicon to both conventional CZ and FZ silicon. This superiority is attributed to the magnetically stabilized crystal growth environment which reduces grown-in point defects. MCZ silicon, engineered to have high  $\tau_g$  and low  $\tau_r$  is desired for application to surface devices such as ICs; while MCZ silicon with both a high  $\tau_g$  and a high  $\tau_r$  is desired for devices such as solar cells in which the diffusion length is a critical factor. Further details can be found in reference [2].

## II. Impurity /defect interactions

In addition to the defects and impurities inherent in as-grown Czochralski crystals, others are introduced during silicon device processing. In particular, metallic impurities such as Cu, Au, Ni, Fe, etc. are known to degrade the performance of electronic devices. For example, metallic impurities with deep energy levels near the middle of the band gap act as recombination centers, resulting in shorter minority carrier life time and excessive leakage currents in p-n junctions. A new extrinsic gettering scheme utilizing epitaxial misfit dislocations generated by Ge-doping has been proposed to improve electrical parameters such as leakage current and minority-carrier lifetime [3]. These interfacial misfit dislocations offer favorable sinks for metallic impurity gettering below active device regions subsequently fabricated in a pure, capping Si layer. A schematic and representative TEM micrograph of the model gettering study sample are illustrated in Figs. 2(a) and (b), respectively. The alternating open diffusion windows and blocking oxide masks were defined on the surface of the Si capping epitaxy. Nickel was deliberately introduced by thermal evaporation under vacuum ( $\sim 10^{-6}$  torr) to approximately 30 nm thickness and then diffused by subsequent annealing at 600 to 1000°C under vacuum. Cross-section TEM revealed the microstructure associated with nickel gettering by the epitaxial misfit dislocation network.

Fig. 3 is a series of weak-beam, dark field cross-sectional TEM images of the misfit dislocations from wafers which were annealed at 600, 850, 940, and 1000°C. For all annealing conditions, gettering activity and precipitate nucleation was observed only in the vicinity of the misfit dislocations. No evidence of precipitation was observed in the Si capping layer and the defect-free condition of the capping Si epitaxial layer has been preserved. After 1000°C annealing, see Fig. 3a, precipitates are observed both as individual particles on misfit dislocations, and also in a periodic array of colonies immediately adjacent to the misfit dislocations within the Si(Ge) buried epitaxial layer. The colonies are distributed along the misfit dislocation with an average spacing of approximately 1000 Å. The size of each precipitate inside the colony ranges from 50 to 100 Å. As the annealing temperature is lowered, the density of precipitates along the misfit dislocations decreases significantly in a consistent manner. After 940°C annealing, precipitates are found to nucleate in a similar manner to those observed after 1000°C annealing; however, the density has decreased, see Fig. 3b. After 850°C annealing, see Fig. 3c, colonies are no longer present and the  $\sim 50$  Å diameter isolated individual precipitates are confined to the misfit dislocation line

itself. After 600°C annealing, see Fig. 3d, some fine precipitate decoration along the dislocations is observed. The systematic progression of precipitate morphology as a function of temperature indicates that the sample that has undergone the 600°C anneal has the most uniform decoration along the misfit dislocations.

These results lead to an opportunity to discuss the gettering activity by the misfit dislocations. Nickel is known to diffuse extremely fast via an interstitial diffusion mechanism. The calculated diffusion length based on the diffusivity data is of the order of  $10^3$   $\mu\text{m}$  at the temperatures employed in this study. This is two orders of magnitude longer than the distance from the source to the sink, i.e., capping epitaxial layer thickness. It is clear that diffusion is not a limiting factor in gettering of nickel at the temperatures employed in this experiment. The large temperature dependence of solid solubility of Ni in Si favors a short incubation time. The Ni solubility at 1000°C is three orders of magnitude higher than that at 600°C. As the solubility decreases upon cooling, the supersaturation of Ni leads to precipitation – presumably in the form of a silicide. The higher solubility at higher temperature (e.g., 1000°C) results in a greater supersaturation level which yields a higher precipitation rate upon cooling. There is no evidence of homogeneous precipitation in the Si matrix. The misfit dislocations clearly provide a preferred nucleation site for precipitation.

In conclusion, it was found that the amount of nickel gettered by misfit dislocations is dominated by the strong temperature dependent solubility of Ni in Si, whereas the diffusivity of Ni in the temperature range studied is so high that it has only a negligible influence. Precipitation occurs either on or in the immediate vicinity of the misfit dislocations. The probable gettering mechanisms for Ni by the misfit dislocations are: (1) The large temperature dependence of solubility which favors short incubation time for nucleation, and (2) the nucleation enhancement by the localized strain effects in the vicinity of misfit dislocation. Further details have been published in reference [4]. These studies will be extended to web and EFG samples in later stages of this program.

---

1. T. Suzuki, N. Isawa, K. Hoshi, Y. Kato, and Y. Okubo, in Semiconductor Silicon / 1986, edited by H. R. Huff, T. Abe and B. Kolbesen, (Electrochemical Society, Pennington, NJ, 1986), p.142.
2. T. Higuchi, E. Gaylord, G. A. Rozgonyi, and F. Shimura, *Appl. Phys. Lett.* **53**, 1850 (1988).
3. A. S. M. Salih, Z. Radzimski, J. Honeycutt, G. A. Rozgonyi, K. E. Bean and K. Lindberg, *Appl. Phys. Lett.* **50**, 1678 (1987).
4. D. M. Lee, J. B. Posthill, F. Shimura, and G. A. Rozgonyi, *Appl. Phys. Lett.* **53**, 370 (1988).

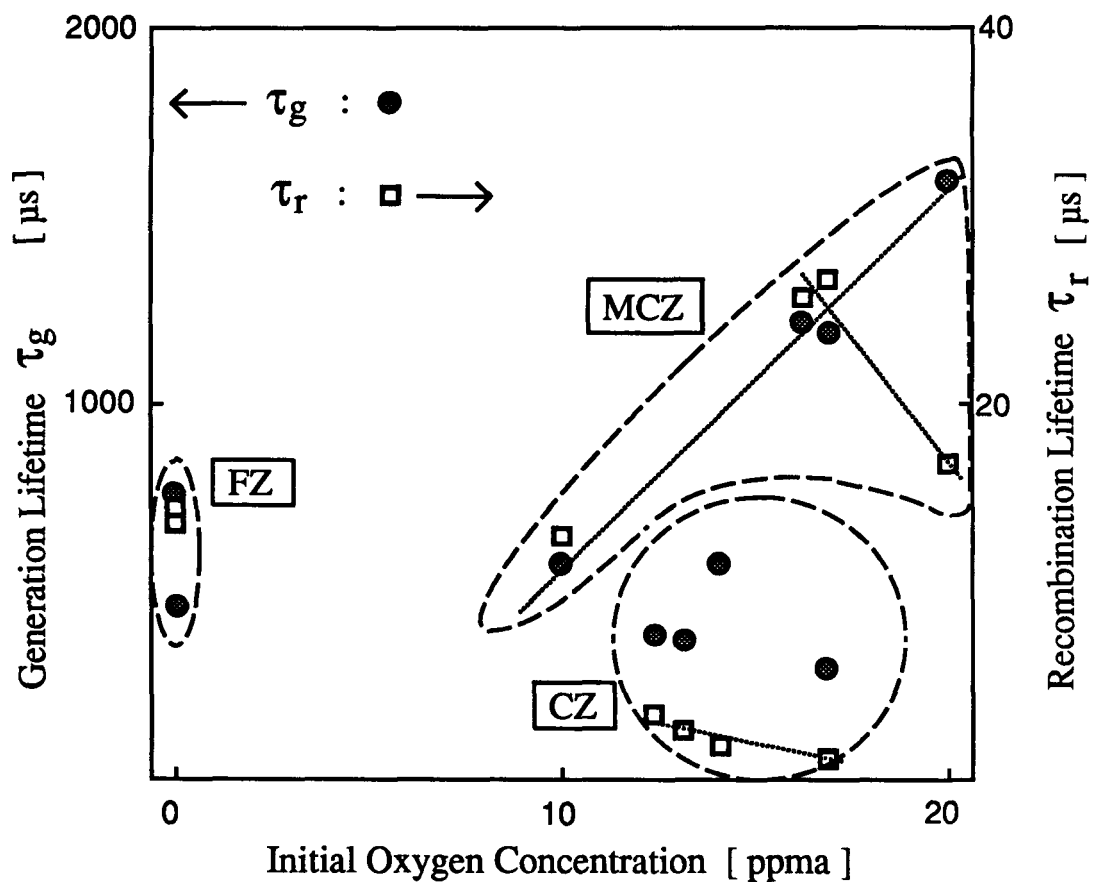


Fig. 1. Generation ( $\tau_g$ ) and recombination ( $\tau_r$ ) lifetimes of MCZ, CZ, and FZ silicon samples as a function of initial oxygen concentration.

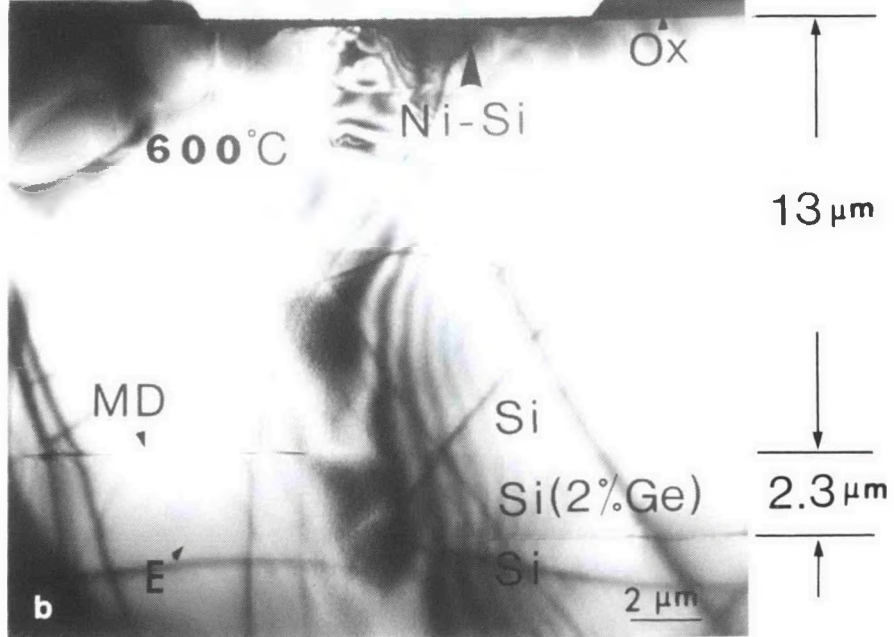
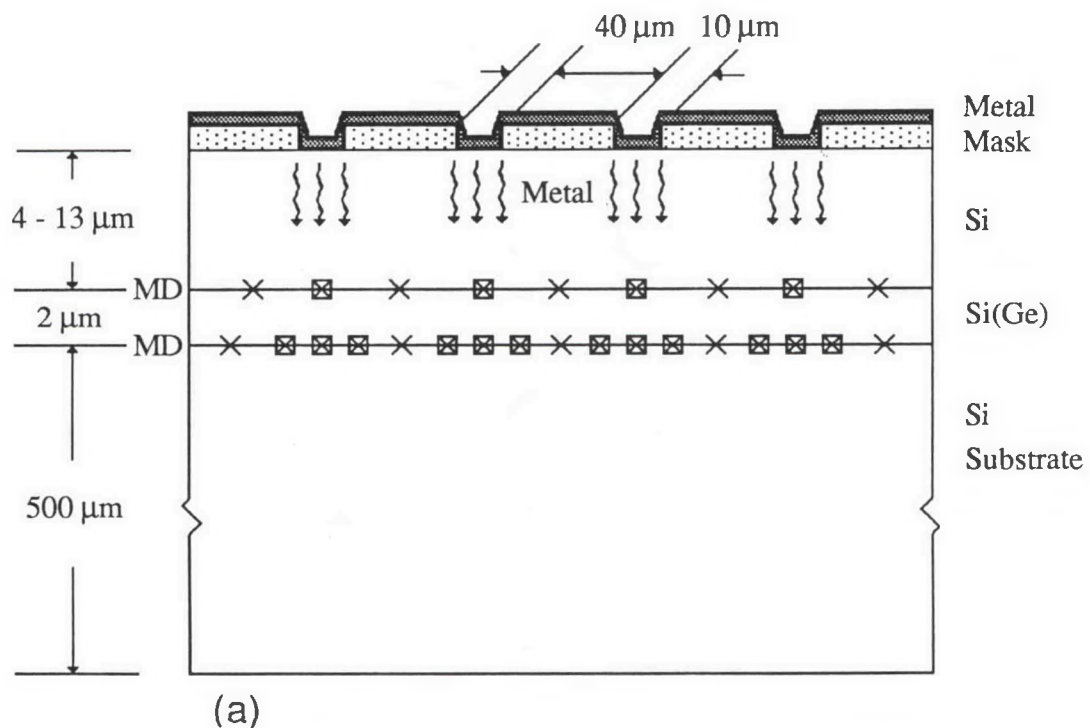


Fig. 2 (a) Schematic diagram of sample structure used to investigate the impurity/defect interactions and (b) cross-sectional TEM micrograph showing a misfit dislocation line (MD) at upper Si(Ge) interface and an-end-on dislocation (E) at lower interface, as well as diffusion window configuration over 13  $\mu\text{m}$  of defect-free capping epitaxy layer following 600°C anneal of 30 nm Ni deposit.

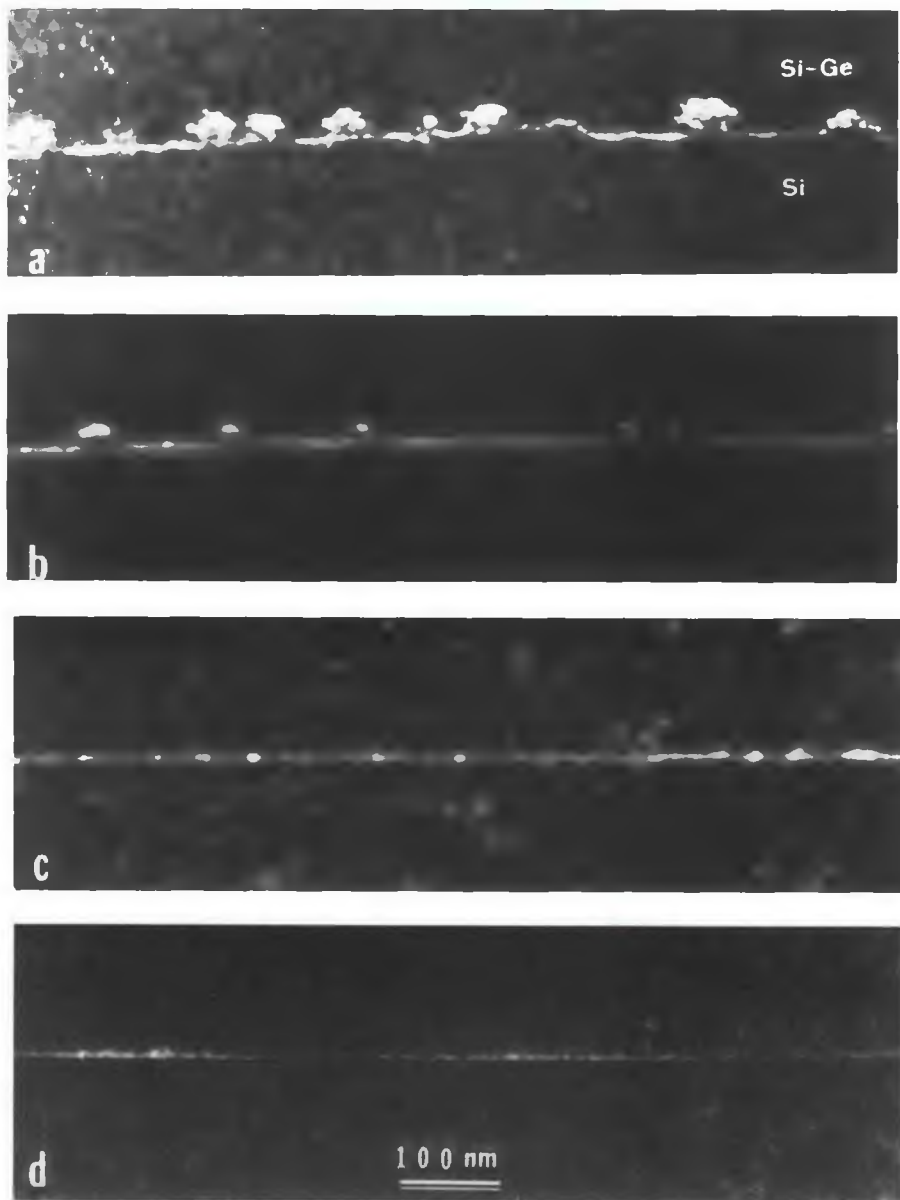


Fig. 3. Series of weak-beam DF images of misfit dislocations after Ni diffusion at various temperature anneals; (a) 1000°C, (b) 940°C, (c) 850°C, and (d) 600°C, respectively. Diffusion was from the front side surface. Reduced precipitation is clearly associated with decreasing annealing temperature. Diffraction conditions for weak-beam images are (a)  $g/3g$  (2̄20), (b)  $g/2g$  (2̄20), (c)  $g/2g$  (̄220), and (d)  $g/3g$  (2̄20). The background speckle contrast has been found to be enhanced when observing thinner regions of the specimen, which is characteristic of weak-beam imaging, and is not a result of bulk precipitation.

**Title: Basic Studies of Point Defects and Their Influence on Solar Cell Related Electronic Properties of Crystalline Silicon**

**Organization:** School of Engineering, Duke University, Durham, North Carolina

**Contributors:** U.M. Goesele, principal investigator; B. Marioton, W. Suck, and W. Taylor

Agglomerates of oxygen, carbon, and intrinsic point defects together with dislocations are suspected to limit the minority carrier diffusion length in solar-grade crystalline silicon. The agglomeration of oxygen and carbon is associated with volume changes which may partly be accommodated by intrinsic point defects. In order to formulate a quantitative model of precipitation and agglomeration during crystal growth the thermal equilibrium concentration and the diffusivity of self-interstitials as well as the source/sink efficiency of dislocations for point defects have to be measured. The present report concentrates on preliminary gold diffusion experiments designed to investigate the sink efficiency of dislocations for silicon self-interstitials.

#### Background Information on the Diffusion of Gold in Silicon

Gold in silicon is mainly dissolved on substitutional sites ( $Au_s$ ) but diffuses almost exclusively in its interstitial form,  $Au_i$ . The change-over from interstitial to substitutional site is accomplished by the kick-out mechanism [1]



which involves silicon self-interstitials denoted by  $I$ . The incorporation of substitutional gold requires the generation of self-interstitials and their subsequent annihilation at appropriate sinks such as surfaces or dislocations. Measurements of the concentration profiles of  $Au_s$ , diffusing from a gold layer on the surface into dislocated silicon, can therefore be conveniently be used to determine the sink efficiency of dislocations.

For the high dislocation density, typical for solar-grade crystalline silicon, we expect that the dislocations keep the self-interstitial concentration always close to its equilibrium value  $C_i^{eq}$ . Under these circumstances the concentration profile of in-diffusing  $Au_s$  should reflect a constant effective diffusivity

$$D_{eff}^{(i)} = D_i C_i^{eq} / C_s^{eq} \quad (2)$$

which is well-known from measurements in deformed single-crystalline silicon [2]. In (2)  $D_i$  denotes the  $Au_i$  diffusivity,  $C_i^{eq}$  the solubility of  $Au_i$ , and  $C_s^{eq}$  the solubility of  $Au_s$ .

On the other hand, if dislocations would not act as sinks, typical U-shaped profiles should be observed which are characterized by a strongly concentration dependent effective diffusivity [12]

$$D_{\text{eff}}^{(I)} = \frac{D_I C_1^{\text{eq}}}{C_s^{\text{eq}}} \left( \frac{C_s^{\text{eq}}}{C_s} \right)^2 , \quad (3)$$

where  $D_I$  is the diffusivity of self-interstitials. Such profiles are typical for gold diffusion into dislocation-free silicon [1]. The limiting cases (2) and (3) can easily be distinguished experimentally. As it turns out, the experimental gold profiles into solar-grade crystalline silicon indicate a behavior just in between (2) and (3) in spite of the high dislocation density.

### Experimental Approach and Preliminary Results

A thin layer of gold is evaporated on one side of solar-grade p-type crystalline silicon (EFG ribbons from Mobil Solar Energy Corporation). The samples are then encapsulated in quartz and annealed for various times and temperatures typically between 900 and 1100°C. After the samples have been bevelled, spreading resistance profiles, indicative of the  $\text{Au}_s$  concentration, are measured across the samples. Because of some resistivity fluctuations in the starting silicon and because of large fluctuations in the dislocation density in different grains of the material, a fairly large variation in the profiles can be found even for the same annealing conditions.

Representative spreading resistance profiles for gold diffusion at 950°C for 300 seconds, 30 minutes and 3 hours are shown in Figure 1 and compared to the starting profile without gold diffusion. It is clearly seen that the spreading resistance (and therefore also the gold concentration) increases with diffusion time. Even before any quantitative analysis we may draw the following conclusions.

- i) Contrary to expectation, the high dislocation density in solar-grade is not efficient enough to prevent a supersaturation of self-interstitials. Otherwise the profiles in Fig. 1 would fairly smoothly develop from the left-hand side (where the gold is deposited on the surface) and move over to the right as expected for the constant diffusivity of eq. (2).
- ii) Dislocations in solar-grade crystalline silicon nevertheless act as sinks for self-interstitials, although to much less a degree than expected. The sink behavior of the dislocations causes the local spreading resistance fluctuations throughout the samples.

A quantitative analysis, which requires a transformation to actual gold concentration values, measuring of the local dislocation density by etching, and an appropriate computer simulation program taking into account variable point-defect dislocation interactions is in progress.

### References

1. W. Frank, U. Gösele, A. Mehrer, and A. Seeger, in: Diffusion in Crystalline Solids, G.E. Murch and A.S. Nowick, eds. (Academic Press, New York, 1984) p. 64.
2. N.A. Stolwijk, M. Perret, and H. Mehrer, in: Diffusion in High Technology Materials 1988, D. Gupta, A.D. Romig, and M.A. Dayananda, eds. (Trans. Tech. Publ. Brookfield, VT, 1988) p. 79.

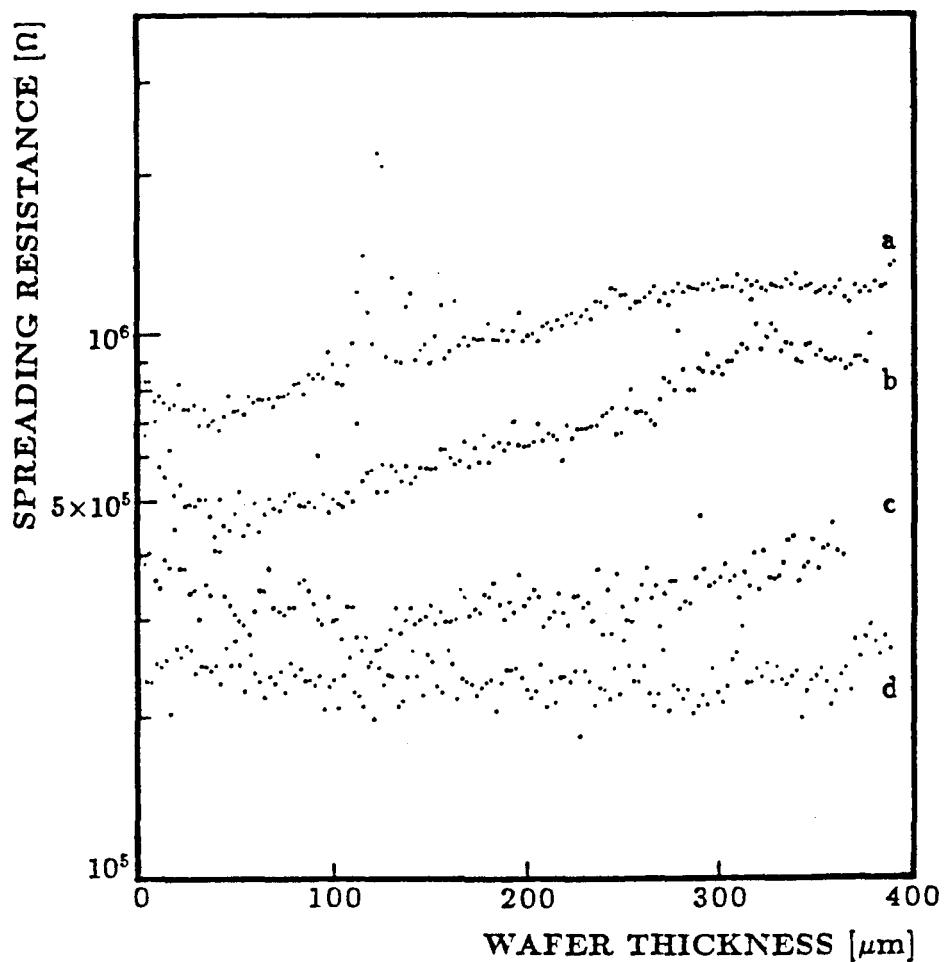


Figure 1. Spreading resistance profiles of solar-grade crystalline silicon after gold diffusion from the left-hand side at 950°C for 3 hours (a), 30 minutes (b), 300 seconds (c), and without gold diffusion (d).

Title: **Passivation and Gettering Studies in Solar Cell Silicon**

Organization: Institute for the Study of Defects in Solids,  
Physics Department, The University at Albany,  
Albany, N. Y. 12222

Contributors: J. W. Corbett, principal investigator; D. Angell,  
T. D. Bestwick, P. Deák, P. Jones, J. L. Lindström, F. Lu, T.-M. Lu,  
G. S. Oehrlein, C. Ortiz-Rodriguez, S. J. Pearton, A. Sályom, G. J.  
Scilla, R. K. Singh, L. C. Snyder, A. J. Tavendale, R.-Zh. Wu, A.  
Yapsir, J.- Zh. Yuan, and Y. Zhang.

This research program has two major aspects: 1) The study of hydrogen in crystalline silicon; and 2) the study of gettering in crystalline silicon. In the hydrogen studies are concerned with how hydrogen is introduced into silicon (by wet-etching, boiling, plasma treatment, injection from a Kaufman source, etc.), its configurations and diffusion mechanisms, and the nature of its interactions with defects. The gettering studies are concerned with "internal gettering" (i.e., gettering at oxygen-related defects) of iron-group transition metals, and radio-tracer studies on these elements as well.

### **Hydrogen-Related Studies.**

Implantation of hydrogen into silicon is well understood, although the resultant damage is not<sup>1,2</sup>. The other means of introducing hydrogen into silicon are even less understood; some of our work is directed at improving this understanding. We have carried out, and are continuing, studies of the interactions of hydrogen with a silicon surface<sup>3</sup>, of etching of silicon by hydrogen<sup>4</sup> (such as may occur in a gas or in a liquid), and plasma- and reactive-ion-etching<sup>5,6</sup>; we will extend these studies to other introduction means as we make progress.

We have studied the configuration of the hydrogen once it is introduced into silicon, and its diffusion mechanisms, the latter studies necessarily including the study of the interactions of hydrogen with defects<sup>7-11</sup>. Our theoretical work<sup>7-9</sup> and that of others<sup>12-16</sup> have argued that the bond-centered (BC) site is the lowest energy configuration for isolated hydrogen in silicon, and that the anti-bonding (AB) site is a higher energy local minimum. The BC-site is clearly indicated in the EPR results of Gorelkinskii *et al.*<sup>17</sup> for the AA-9 center, and by the correlative results for the anomalous muon<sup>18</sup>; channeling studies<sup>19,20</sup> also support this ordering of sites.

Infra-red<sup>21-23</sup>, channeling<sup>24, 25</sup> and theoretical<sup>26, 27</sup> studies supported by perturbed angular correlation studies<sup>28-30</sup> have established that the hydrogen de-activating a shallow acceptor is

essentially at the BC-site as proposed by Pankove *et al.*<sup>31</sup> as that for the shallow donor is at an AB-site as proposed by Johnson *et al.*<sup>26</sup>. We have found that there remain some complexities<sup>32</sup> which we are studying using Rutherford Back-scattering, channeling, and standing-wave x-ray measurements. In the normal boron-deactivation experiment the hydrogen is introduced at ca. 125°C and the boron activity is restored by annealing at ca. 200°C; we have found<sup>5</sup> that introducing hydrogen at ca. 50°C results in hydrogen that remains relatively free so that it can move deeper into the material upon annealing at ca. 125°C; this is distinct from the field-induced migration found by Tavendale *et al.*<sup>33</sup> and the deactivation observed following mechanical-polishing<sup>34</sup> in which the boron recovers upon annealing to ca. 100°C. The process which anneals at ca. 170°C we attribute to the hydrogen at the BC-site; that at ca. 70°C to the AB-site, with a small energy barrier between the two sites; and we argue that *both* sites deactivate the hydrogen. Even so this does not explain the relative mobile hydrogen which can migrate deeper into the crystal without an applied field; since the boron is *not reactivated* as Tavendale found, we must assume that this hydrogen is an extra hydrogen, such as might occur if a boron could trap two (or more) hydrogens at AB-sites, the first one being most strongly bound; we are exploring this model further.

Much of the information about interactions which hydrogen may have we are finding from studies of the diffusion profiles. Figures 1 and 2 show the profiles obtained for deuterium (to permit SIMS measurements) for various resistivities of n- and p-type silicon<sup>10</sup>. It

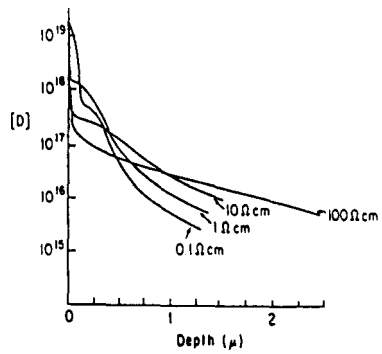


Fig. 1. Deuterium profiles for various resistivities of n-Si.

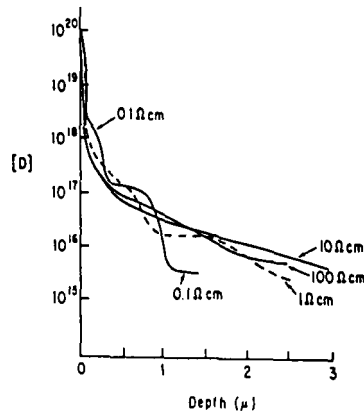


Fig. 2. Deuterium profiles for various resistivities of p-Si.

will be noted that the nature of the profiles in p-type material for 0.1 and 1  $\Omega\text{-cm}$  is different from that for the 10 and 100  $\Omega\text{-cm}$  material; it is from this difference that we argued<sup>11</sup> that the donor energy level for the hydrogen is at ca.  $E_V + 0.30 (\pm 0.10)$  eV. The profiles in the 10 and 100  $\Omega\text{-cm}$  p-type material and the tails of the profiles in the n-type material all have the shape expected when the diffusion is dominated by molecule formation; Fig. 3 shows a fit to the 100  $\Omega\text{-cm}$  p-type data with these parameters: diffusion coefficient  $D = 2 \times 10^{-11}$   $\text{cm}^2/\text{s}$ ; capture radius for molecule formation  $R_m = 0.1 \text{ \AA}$ . The capture radius is smaller than atomic size, but is consistent with a steric reaction hindrance due to the distortions of the lattice expected for the hydrogen configurations. The diffusion coefficient is comparable to that observed in other measurements, i.e., less than expected from the extrapolation of the van Wieringen-Warmholz data<sup>35</sup>. Clearly in the n-type data there is a dependence on the impurity concentration which causes a "bump" in the shallow region of the profile and a diminished slope to the molecule formation profile; our working model for this process involves the reactions:



These reactions would account for the apparent reactivation of the donor, shown here as X, [or as referred to in the literature the incom

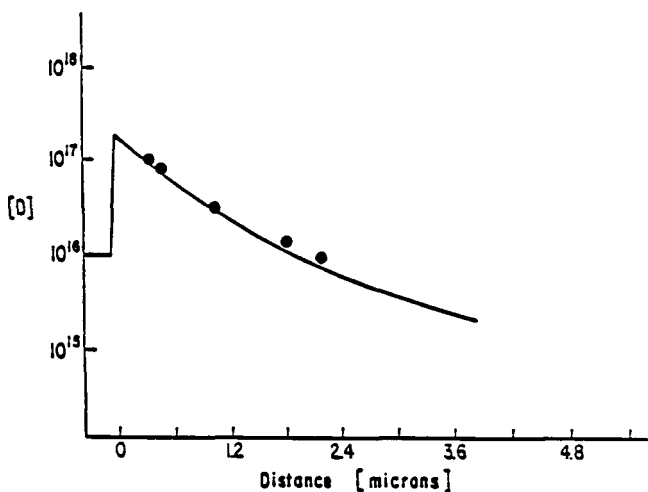


Fig. 3. Fit to the 100  $\Omega\text{-cm}$  p-type data with molecule-formation.

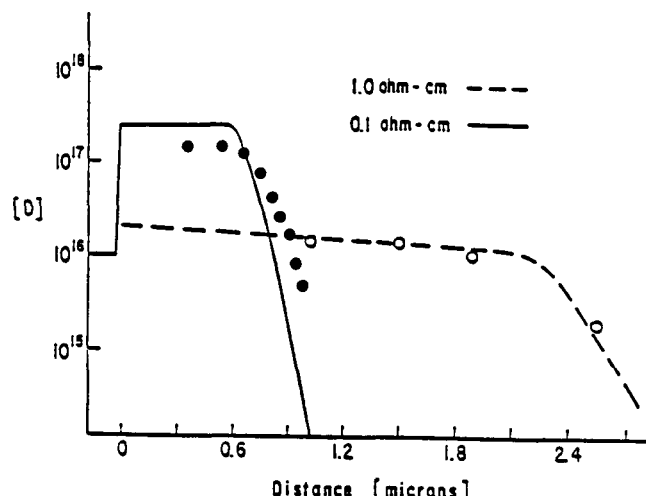


Fig. 4. Fit of the low-resistivity p-type data with impurity trapping.

*plete deactivation of the donor], and the qualitative features of the diffusion profiles; we are seeking a quantitative description. The low-resistivity p-type material has three clear stages to the profiles: 1) The shallow, high concentration regime; 2) The intermediate regime; and 3) The low-concentration deepest regime. Regime 3 has the clear hall-marks of impurity trapping, i.e., a plateau equal to the impurity concentration and an exponential fall-off of the slope of which depends on the impurity concentration. Figure 4 shows one of our attempts to achieve a quantitative description of this regime; the quantitative treatment of all of the profiles is sensitive to the surface hydrogen concentration--we have data now in which the hydrogen surface concentration is varied, as well as temperature dependent data, so that we expect to obtain unambiguous values of the fitting parameters. The parameters used in Fig., 3 were  $D = 4 \times 10^{-11} \text{ cm}^2/\text{s}$  and the boron-hydrogen capture radius  $R_B = 2.6 \text{ \AA}$ . In the spirit of Occam's razor, we have not incorporated an electric field in the description of these profiles, although that is on the agenda after achieving the best parameters without the field. It will be noted that  $R_B$  is atomic in size, and not the much larger size that could occur if, as we expect, the interaction between the boron and the hydrogen is Coulombic at long range. Regime 2 is clearly hydrogen and impurity dependent, which argues against it being due to an intrinsic defect (e.g., a vacancy or an interstitial) whether hydrogen-decorated or not; our working model for regime 2 is that described by reactions 1) and 2) above, although we still have to obtain a satisfactory quantitative fit. Regime 1 is clearly associated with the damage observed in TEM measurements<sup>36,37</sup>, and the evidence from the profile is that the damage nucleates after considerable diffusion has taken place with the deuterium constituting regime 2 back-diffusing into the depth associated with regime 1. Although the {111} planar defects observed in regime 1 could be due to the partially dissociated multivacancy defects that we have discussed earlier, we are inclined to the view proposed by Johnson et al.<sup>36</sup> that a number of hydrogens in BC-sites interact through their associated distortions to form an extended planar defect. We have performed calculations<sup>38</sup> on such a defect, and find that the strain interaction will stabilize a planar defect; we further find that subsequent hydrogens will bond in the same bond axis, i.e., one on each silicon, without forming a molecule, and thereby form an incipient crack, a prototype of a defect causing the brittleness of silicon grown in hydrogen gas.*

### **Gettering-Related Studies**

It is well known that oxygen precipitates act as gettering sites for the iron-group transition elements, i.e., for the major "fast diffusers." We have completed several studies<sup>39-41</sup> related to these problems, including identifying<sup>41</sup> the defect created when a vacancy interacts with an iron atom. A major problem in gettering studies is the indirect nature of the measurement studying the transition

element, e.g., EPR can identify the transition element if it is in the proper charge state, DLTS can identify an electrical level which may be associated with a transition element. We have begun studies using radio-active tracers to better follow the introduction and history of the transition elements. Another aspect of gettering at oxygen defects is identifying the oxygen defects of which there are a plethora of varieties<sup>42</sup>. We have carried out a number of studies<sup>43-51</sup> helping to clarify the nature of the electrical properties of the 450°C thermal donors, the new shallow donors, the anomalous oxygen diffusion mechanism, and the nature and structure of the core of the thermal donors, and of the thermal donors, and oxygen-related recombination centers. We anticipate exploiting this knowledge in our gettering studies.

## References

1. S. J. Pearton, J. W. Corbett, and T.-S. Shi, *Appl. Phys. A* **43** (1987) 153.
2. S. J. Pearton, M. Stavola, and J. W. Corbett in Proc. ICDS-15, in press.
3. J. W. Corbett, D. Peak, S. J. Pearton, and A. Sganga in *Hydrogen in Disordered and Amorphous Solids*, eds. G. Bambakidis and R. C. Bowman (Plenum, N.Y. 1986) p. 61.
4. F. Lu, J. W. Corbett, and L. C. Snyder, *Phys. Lett.* in press.
5. J. L. Lindström, G. S. Oehrlein, G. J. Scilla, A. S. Yapsir, and J. W. Corbett, *J. Appl. Phys.*, in press.
6. T. Bestwick, G. S. Oehrlein, D. Angell, P. Jones, and J. W. Corbett, to be published.
7. P. Deák, J. L. Lindström, J. W. Corbett, S. J. Pearton, and A. J. Tavendale, *Phys. Lett. A* **126** (1988) 427.
8. P. Deák, L. C. Snyder, and J. W. Corbett, *Phys. Rev. B* (1988) in press.
9. P. Deák, L. C. Snyder, and J. W. Corbett in *New Developments in Semiconductor Physics*, eds. G. Ferenczi and F. Beleznay (Springer Verlag, Berlin, 1988) 163.
10. J. W. Corbett, J. L. Lindström, S. J. Pearton, and A. J. Tavendale, *Solar Cells* **24** (1988) 127-133.
11. J. T. Borenstein, D. Angell, and J. W. Corbett, Fall MRS meeting, 1988, in press.
12. C. G. DeLeo, M. Doragi, and W. B. Fowler, *Phys. Rev. B* (1988), in press.
13. A. A. Bonapasta, A. Lapicciarella, N. Tomassini, and M. Capizzi, to be published.
14. C. G. Van der Walle, Y. Bar-Yam, and S. T. Pantelides, *Phys. Rev. Lett.* **60** (1988) 2761.
15. C. G. DeLeo and W. B. Fowler, *Phys. Rev. B* **31** (1985) 6861.
16. C. G. DeLeo and W. B. Fowler, *Phys. Rev. Lett.* **56** (1986) 402.
17. Yu. V. Gorelkinskii and N. N. Nevinnyi, *Pis'ma Zh. Tekh. Fiz.* **13** (1987) 105.

18. R. Kiefl, M. Celio, T. L. Estle, G. M. Luke, S. R. Kreitzman, J. H. Brewer, D. R. Noakes, E. J. Ensaldo, and K. Nishiyama, *Phys. Rev. Lett.* **58** (1987) 1780.
19. S. T. Picraux and F. Vook, *Phys. Rev. B* **18** (1978) 2066.
20. B. Bech Nielsen, *Phys. Rev. B* **37** (1988) 6353.
21. M. Stavola, S.J. Pearton, J. Lopata, and W.C. Dautremont-Smith, *Appl. Phys. Lett.* **50** (1987) 1086-1088.
22. K. Bergman, M. Stavola, S.J. Pearton, and T. Hayes, *Phys. Rev. B* (1988) in press.
23. B. Pajot, A. Chari, M. Aucouturier, M. Astier, and M. Chantre, *Solid State Comm.* (1988) in press.
24. A.D. Marwick, G.S. Oehrlein, and N.M. Johnson, *Phys. Rev. B* **36** (1987-1) 4539-4542.
25. A.D. Warwick, G.S. Oehrlein, J.H. Barrett, and N.M. Johnson, *Phys. Rev. B* **36** (1987) in press.
26. N. M. Johnson, C. Herring, and D. J. Chadi, *Phys. Rev. Lett.* **56** (1986) 769.
27. K.J. Chang and D.J. Chadi, *Phys. Rev. Lett.* **60** (1988) 1422-1425.
28. M. Deicher, G. Grübel, E. Recknagel, and T. Wiechert, in *Defects in Semiconductors*, ed. H.J. von Bardeleben (Trans Tech Publ., Zürich, 1986) 1141-1146.
29. T. Wiechert, H. Skudlik, M. Deicher, G. Grübel, R. Keller, E. Recknagel, and L. Song, *Phys. Rev. Lett.* **59** (1987) 2087.
30. T. Wiechert, M. Deicher, G. Grübel, R. Keller, N. Schulz and H. Skudlik, *Appl. Phys. A* (1988) in press.
31. J. J. Pankove, P. J. Zanucchi, C. W. Magee, and G. Lukovsky, *Appl. Phys. Lett.* **46** (1985) 421.
32. Y. Zhang and J. W. Corbett, to be published.
33. A.J. Tavendale, A.A. Williams, D. Alexiev, and S.J. Pearton, in *Oxygen, Carbon, Hydrogen, and Nitrogen in Crystalline Silicon*, eds., J. C. Mikkelsen, S. J. Pearton, J. W. Corbett, and S. J. Pennycook, (Materials Res. Soc. Pittsburgh, 1986) p. 469.
34. A. Schnegg, H. Prigge, M. Grundner, P.O. Hahn, and H. Jacob in *Defects in Electronic Materials*, eds. M. Stavola, S. J. Pearton, and G. Davies, (MRS, Pittsburgh, 1988) p. 291.
35. A. Van Wieringen and N. Warmoltz, *Physica* **22** (1956) 849.
36. N.M. Johnson, F.A. Ponce, R.A. Street, and R.J. Nemanich, *Phys. Rev. B* **35** (1987-1) 4166.
37. S.-J. Jeng, G.S. Oehrlein, and G.J. Scilla, 1988 to be published,
38. C. Ortiz-Rodriguez, D. Deák, L. C. Snyder, and J. W. Corbett, to be published.
39. P. W. Wang, H. S. Cheng, W. M. Gibson, and J. W. Corbett, *J. Appl. Phys.* **60** (1986) 1336.
40. P.W. Wang, Y. P. Feng, W. L. Roth, and J. W. Corbett, *J. Non-Cryst. Solids* **104** (1988) 81.
41. Zh. P. You, M. Gong, J.-Y. Chen, and J. W. Corbett, *J. Appl. Phys.* **63** (1988) 324.
42. See the several pertinent review articles in *Oxygen, Carbon, Hydrogen and Nitrogen in Crystalline Silicon*, eds. J. C.

Mikkelsen, Jr., S. J. Pearton, J. W. Corbett, and S. J. Pennycook (MRS, Pittsburgh, 1986) and in *Defects in Electronic Materials*, eds. M. Stavola, S. J. Pearton, and G. Davies, (MRS, Pittsburgh, 1988).

- 43. J. T. Borenstein, J. W. Corbett, M. Herder, S. N. Sahu, and L. C. Snyder, *J. Phys. C: Solid State Phys.*, **19** (1986) 2893.
- 44. J. T. Borenstein, D. Peak, and J. W. Corbett, in *Oxygen, Carbon, Hydrogen and Nitrogen in Crystalline Silicon*, eds. J. C. Mikkelsen, Jr., S. J. Pearton, J. W. Corbett, and S. J. Pennycook (MRS, Pittsburgh, 1986)
- 45. J. A. Griffin, H. Navarro, J. Weber, L. Genzel, J. T. Borenstein, J. W. Corbett, and L. C. Snyder, *J. Phys. C: Solid State Phys.* **19** (1986) L579.
- 46. L. C. Snyder, J. W. Corbett, P. Deák, and R.-Zh. Wu in *Defects in Electronic Materials*, eds. M. Stavola, S. J. Pearton, and G. Davies (MRS, Pittsburgh, 1988) p. 179.
- 47. K. Banerjee, V. A. Singh, and J. W. Corbett, *Semicond. Sci. & Tech.* **3** (1988) 542.
- 48. L. C. Snyder, J. W. Corbett, P. Deák, and R.-Zh. Wu in *New Developments in Semiconductor Physics*, eds. G. Ferenczi and F. Beleznay (Springer Verlag, Berlin 1988) 147-156.
- 49. P. Deák, L. C. Snyder, J. W. Corbett, R.-Zh. Wu and A. Sályom in *Proc. ICDS-15, Budapest, 1988*, in press.
- 50. L.C. Snyder, P. Deák, R.-Zh. Wu, and J. W. Corbett in *Proc. ICDS-15, Budapest, 1988*, in press.
- 51. L. C. Snyder, P. Deák, R.-Zh. Wu, and J. W. Corbett in *Proc. Shallow Donor Conf., Linköping, Sweden, 1988*, in press.

## 5.0 HIGH-EFFICIENCY CONCEPTS

J. Benner (Manager) and C. Leboeuf

The objective of the High-Efficiency Concepts Task is to evaluate and develop advanced photovoltaic technologies capable of energy conversion efficiencies in excess of 20% for flat-plate configurations and 30% in concentrator systems. These goals are discussed in DOE's Five-Year Research Plan as technology targets for the late 1990s. Even on this longer term horizon, it is difficult to envision a technology capable of achieving such high efficiencies without incorporating the demonstrated performance of crystalline III-V semiconductors. Thus, the High-Efficiency Concepts Task has become synonymous with III-V compound semiconductor research.

Research in gallium arsenide (GaAs) and related compounds emphasizes the control of heteroepitaxial growth. This work supports the eventual development of two photovoltaic technologies. First, heteroepitaxy will be essential in any low-cost, single-crystal, thin-film photovoltaic technology. As with any thin-film approach, these high-efficiency cells would have very low materials costs. The challenge is to develop the technologies to yield the single-crystal films needed for high efficiency. This area emphasizes research in growth of the binary compound GaAs in the novel regimes required to meet flat-plate module cost goals. Specifically, this requires heteroepitaxial growth on significantly dissimilar substrates, such as silicon or various crystalline interfacial layers, or lateral epitaxial growth over amorphous or polycrystalline substrates. The binary compound is selected for this research to avoid the additional chemical and kinetic complexity associated with the growth of ternary and quaternary alloys. Second, multijunction cells by their very design will require heteroepitaxy. In many of the proposed tandem structures, the component semiconductors do not share the same lattice constant. The key topic in this area is the heteroepitaxial growth of ternary and quaternary alloys of III-V compounds. The alloys of study include AlGaAs, GaInAs, AlGaInAs, GaAsP, GaAsSb and AlGaAsSb. Each of these alloys is quite different from GaAs in that the properties of a given alloy change significantly even with relatively small changes in composition. In the growth process, the composition and quality of the growing crystal are affected by the concentration of sources in the gas stream, the growth temperature, and the total and local gas flow rates, as well as the dopant, dopant source material, substrate, source impurities, and reactor history. The emphasis of this research is to identify and control the key mechanisms affecting film quality.

Progress during the past year continued at an encouraging pace. University subcontractors' extensive publications in the technical literature contributed to our understanding of gas flow and chemical reaction effects in MOCVD and elucidated the crystallographic characteristics of several important heterostructures. In cells, the multidisciplinary industrial teams pushed the technology to increased cell areas and efficiencies in several technologies for both one-sun and concentrator applications. The efficiencies of GaAs cells grown on silicon substrates were greatly improved, rising from 11.6% to 17.6%, as confirmed by SERI. The CLEFT (cleavage of lateral epitaxial films for transfer) thin-film technology also reached an important goal by exceeding 20% efficiencies for cell areas greater than  $4 \text{ cm}^2$ . Progress in improving concentrator cells also yielded increases of more than 10% in efficiency; single-junction GaAs cell performance rose from 26% to more than 28% under approximately 400x concentration.

**Title: Basic Studies of III-V High-Efficiency Cell Components**

Organization: Purdue University, School of Electrical Engineering, W. Lafayette, IN 47907

Contributors: M.S. Lundstrom and M.R. Melloch, principal investigators, R.F. Pierret, faculty associate, M.S. Carpenter, H.L. Chuang, A. Keshavarzi, M.E. Klausmeier-Brown, J.M. Morgan, and T.B. Stellwag, research assistants

The objective of this research is to explore dark current mechanisms in GaAs-related solar cells. Our group is now engaged in basic studies which are directed at providing information and understanding essential for attaining cell efficiencies near the thermodynamic limit. The work is motivated by three questions: 1) what are the values of the key physical parameters which control cell performance? 2) what are the dominant recombination loss mechanisms in present-day, high-performance cells? and 3) how should cells be designed to minimize recombination losses? These basic studies, complemented by the sophisticated numerical device simulation capability at Purdue, should provide an understanding of how to maximize cell performance. Although the work is specifically directed at GaAs-based solar cells, the methodology being developed for diagnosing cell performance and for the design of new cells should be broadly applicable.

A broad investigation of minority carrier transport and recombination in GaAs is underway. Work to explore heavy doping effects in  $p^+$ -GaAs and their influence on solar cell performance was a major emphasis of the past year's efforts as was work to characterize and suppress perimeter recombination. The significant results of this work are summarized below and described in detail in our annual report [1].

So-called bandgap narrowing effects have proven to be of fundamental importance to silicon solar cells. In last year's report we described a sequential etch technique developed to characterize heavy doping effects in  $p^+$  GaAs [4]. During the past year, we have, in collaboration with researchers at Spire Corporation, applied this technique to a variety of solar cells and have mapped out heavy doping effects from  $N_A \approx 10^{17}$  to  $10^{19} \text{ cm}^{-3}$  [4]. The results, displayed in Fig. 1, show that for the heaviest doping densities, the equilibrium  $np$  product is at least one order of magnitude higher than it is in lightly doped GaAs. Such heavily doped regions often serve as back-surface fields in solar cells, and these results suggest that the interface recombination velocity of such homojunction barriers will be significantly degraded by bandgap narrowing effects. Bandgap narrowing will also increase the dark current associated with the emitter of a  $p^+$ /n heteroface solar cell.

In last year's annual report, we described experiments on  $p-p^+$  homojunction back-surface fields which showed that such barriers were ineffective in confining minority carrier electrons. The high barrier recombination velocities could be explained by bandgap narrowing effects, which would lower the barrier height, or by defects located at the junction. An experiment to identify the cause of the high barrier recombination velocity was designed and conducted [8]. A special test diode was fabricated on a film grown by molecular beam epitaxy in our laboratory. The dark I-V characteristics were then monitored as the film was successively etched. The results showed a clear dependence of the barrier recombination velocity on the width of the  $p^+$  barrier, as displayed in Fig. 2. We conclude that the high recombination velocity is due to a bulk effect and not to defects at the interface. By analyzing the results, we deduced the  $n_{ie}^2 D_n$  product in the  $p^+$  barrier and found that the result was in close agreement with our previous experiments on bandgap narrowing [3].

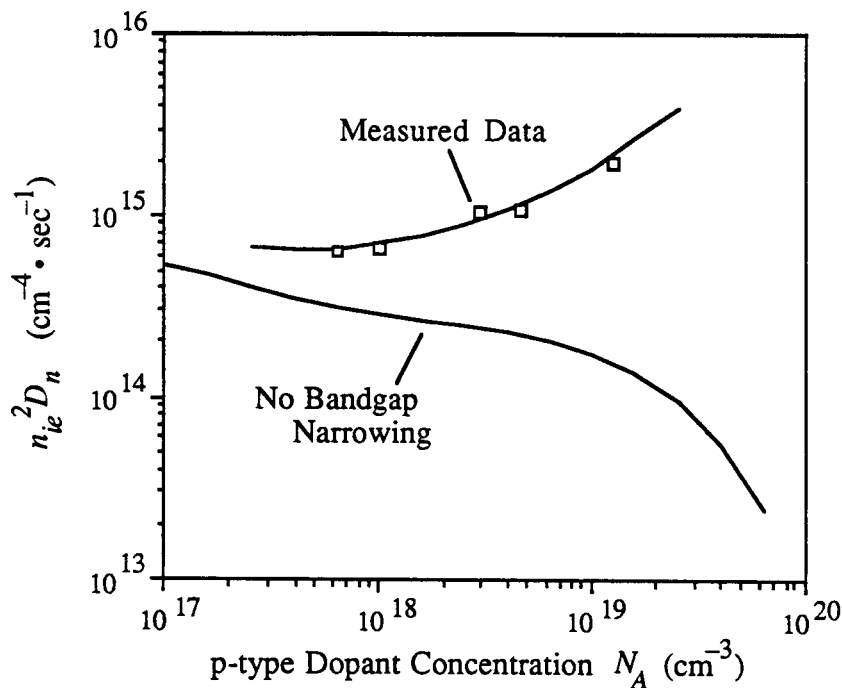


Fig. 1 Product of intrinsic concentration squared times the minority carrier diffusion coefficient versus majority hole concentration for  $p^+$ -GaAs. (After [4])

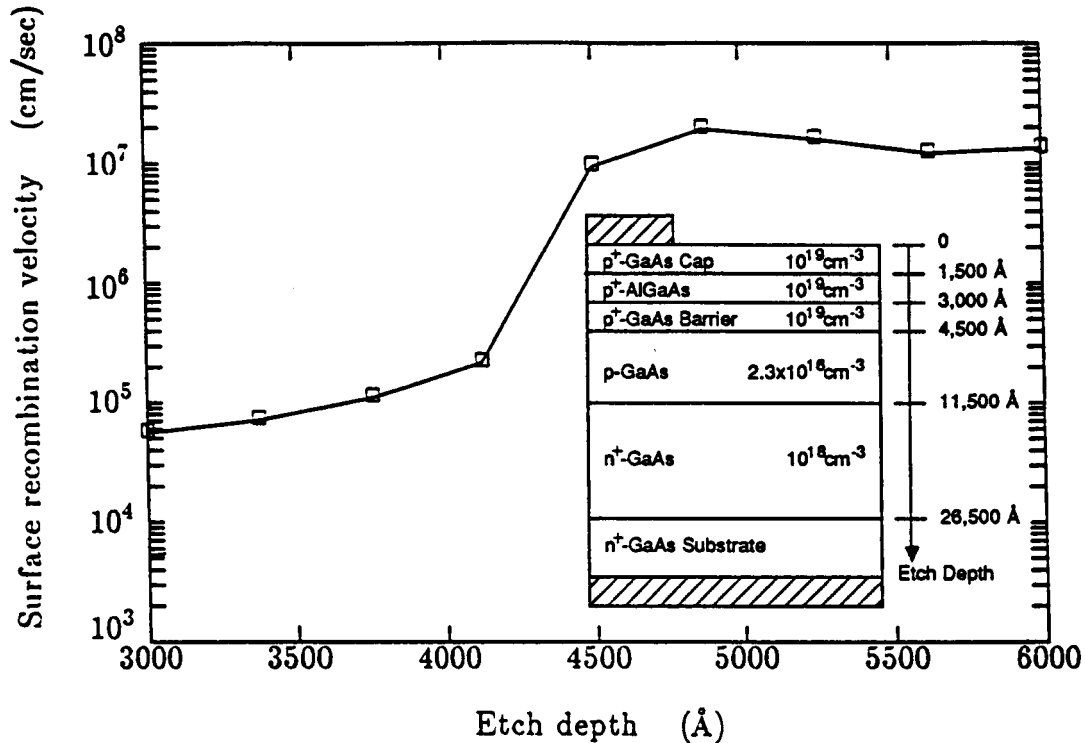


Fig. 2 Effective front surface recombination velocity versus etch time deduced by successively etching the structure displayed in the inset. (After [8])

Our conclusion is that  $p-p^+$  back-surface fields are ineffective minority carrier mirrors because of bandgap narrowing effects. Heterojunction back-surface fields must be used for effective confinement of minority carriers [7].

Much of our research has been directed at relating measured current versus voltage characteristics to the material properties of cells. One concern is the influence of recombination of carriers at the exposed perimeter of the cell. Typical cells are quite large - often much larger than  $0.5\text{ cm} \times 0.5\text{ cm}$ , so that perimeter effects might be assumed to be small. We undertook experiments to quantify perimeter effects and found them to be surprisingly important [6]. Two effects were observed. The first was a shunt leakage thought to be associated with conductive oxides at the cell's perimeter. Proper treatment of the edge, such as dipping the cells in hydrochloric acid, often completely removes this shunt leakage. The second effect is on the cell's  $n=2$  current component. By examining how the  $n=2$  current scales with cell perimeter and with cell area, we established that for  $0.5$  by  $0.5$  cm cells, the perimeter completely dominates the  $n=2$  current. Even for the much large  $2$  by  $2$  cm and  $4$  by  $4$  cm cells, the perimeter can have a surprisingly large effect. This fact is a simple consequence of the extremely high bulk lifetimes being obtained in present-day cells and the high surface recombination velocity associated with bare GaAs surfaces.

The  $n=2$  current component can lower the one-sun fill factor of GaAs cells, so careful treatment of the perimeter is essential. But under concentration, only the  $n=1$  current, which scales with cell area and not with perimeter, is important. Perhaps the most important implications of this work are for the diagnostic evaluations of cells, which frequently employ the  $n=2$  current. For example, we have found it to be extremely difficult to correlate deep level transient spectroscopy (DLTS) measurements to the  $n=2$  current. The probable reason is that DLTS probes bulk defects, but the  $n=2$  current is sensitive to surface defects.

According to recent reports, the treatment of GaAs surfaces with  $\text{Na}_2\text{S}$  is effective in lowering the surface state density. Such treatments could be useful for GaAs-related solar cells; the  $n=2$  current associated with perimeter recombination might be eliminated, and the need for AlGaAs window layers might be removed. We have examined this chemical treatment and found that it lowered the  $n=2$  edge current by a factor of three. Unfortunately, a sizeable shunt leakage was also introduced. We also found that  $(\text{NH}_4)_2\text{S}$  lowers the  $n=2$  edge current by a factor of three, but it has the advantage of introducing virtually no shunt leakage. If such treatments prove effective and robust, they could be very important for solar cells.

During the past year we advanced our understanding of GaAs-based cells in a number of ways. First, we completed the first study of bandgap narrowing effects in  $p$ -type GaAs and showed that such effects have important implications for GaAs-based solar cells. Secondly, we provided a clear understanding of  $p-p^+$  GaAs homojunction barriers, demonstrated their ineffectiveness, and explained the result as a consequence of bandgap narrowing. Thirdly, we clearly established the important influence of the mesa perimeter on solar cell performance. And finally, we developed a new chemical treatment for passivating GaAs surfaces and demonstrated one application to solar cells.

Future work on heavy doping effects will be directed at assessing the significance of heavy doping effects in  $n^+$ -GaAs and at extracting the minority carrier mobility from time-of-flight measurements. Also planned is additional work on surface passivation of III-V semiconductors and an examination of recombination mechanisms in AlGaAs cells.

## References

- [1] M.S. Lundstrom, M.R. Melloch, R.F. Pierret, M.S. Carpenter, H.L. Chuang, P.D. DeMoulin, M.E. Klausmeier-Brown, G.B. Lush, D.P. Rancour, "Basic Studies of III-V High-Efficiency Cell Components," School of Electrical Engineering Technical Report, TR-EE-88-XX, December, 1988.
- [2] M.S. Lundstrom, "Device Physics of Crystalline Solar Cells," *Solar Cells*, Vol. 24, pp. 91-102, 1988.
- [3] M.E. Klausmeier-Brown, C.S. Kyono, P.D. DeMoulin, S.P. Tobin, M.S. Lundstrom, and M.R. Melloch, "Sequential Etch Analysis of Electron Injection in  $p^+$  GaAs," *IEEE Trans. Electron Dev.*, Vol. ED-35, pp. 1159-1161, 1988.
- [4] M.E. Klausmeier-Brown, M.S. Lundstrom, M.R. Melloch, and S.P. Tobin, "Effects of Heavy Impurity Doping on Electron Injection in  $p^+$ -n GaAs Diodes," *Applied Phys. Lett.*, Vol. 52, pp. 2255-2257, 1988.
- [5] M.S. Carpenter, M.R. Melloch, M.S. Lundstrom, and S.P. Tobin, "Effects of  $Na_2S$  and  $(NH_4)_2S$  Edge Passivation Treatments on the Dark Current-Voltage Characteristic of GaAs pn Diodes," *Applied Phys. Lett.*, Vol. 52, pp. 2157-2159, 1988.
- [6] P.D. DeMoulin, S.P. Tobin, M.S. Lundstrom, M.S. Carpenter, and M.R. Melloch, "Influence of Perimeter Recombination on High-Efficiency GaAs P/N Heteroface Solar Cells," *IEEE Electron Dev. Lett.*, Vol. EDL-9, pp. 368-370, August 1988.
- [7] M.E. Klausmeier-Brown, H.L. Chuang, P.D. DeMoulin, M.S. Lundstrom, M.R. Melloch, and S.P. Tobin, "Influence of Band Gap Narrowing Effects on Solar Cell Performance," presented at the 20th IEEE Photovoltaic Specialists Conf., Las Vegas, NV, Sept., 1988.
- [8] H.L. Chuang, P.D. DeMoulin, M.E. Klausmeier-Brown, M.R. Melloch, and M.S. Lundstrom, "Evidence for Bandgap Narrowing Effects on Be-Doped,  $p-p^+$  homojunction barriers," *J. Appl. Physics*, Vol. 64, pp. 6361-6364, 1988.

**Title:** Research on Semiconductors for High Efficiency Solar Cells

**Organization:** Rensselaer Polytechnic Institute, Troy, New York

**Contributors:** J. M. Borrego and S. K. Ghandhi, principal investigators

The aim of this program is to explore problems associated with the fabrication of large area, high efficiency solar cells. Emphasis is placed on understanding the growth process and the evaluation of stress in the growing layers, and in the interaction of fabrication processes with the structural mechanics of the growing layer. Additional topics include materials studies of interest in improving the efficiency of solar cells. Finally, advances, non-invasive diagnostic techniques are being developed for studying the characteristics of substrates and layers at the wafer level. The work performed during this program has been subdivided into five tasks, which are now detailed.

### **Computer Models for OMVPE Growth**

This task is aimed at the development of computer programs which are specifically directed to OMVPE in practical growth situations, and which are capable of experimental verification. During the past year, a completely new and more powerful program, involving the direct solution of the Navier Stokes equations in two-dimensional form, was written. The program allowed the explanation of unexpected effects of susceptor slope and system pressure on the growth rate. Streamline profiles representing the reactor velocity fields for a variety of susceptor tilts and pressures predicted by the model are shown in Fig. 1. A paper on this subject has been accepted for publication [1].

### **Reaction Mechanisms for OMVPE Growth**

A major problem in the growth of compound semiconductors by OMVPE is the presence of gas phase depletion reactions, especially for indium-containing materials such as GaInAs. A study of these reactions was undertaken to determine appropriate reaction rates required as inputs to the computer model described above. Investigation of additional aspects of the gas phase chemistry that occurs during the OMCVD growth process has been pursued during the past year. Mass spectroscopy was employed due to its high sensitivity and ability to yield a more direct identification of gaseous species than other techniques for gas phase analysis. Strong evidence has been observed for alkyl exchange effects in this study. These effects are of critical importance in understanding the growth process because they delay the pre-reaction of alkyls in the growth of indium-based alloys. A paper on this subject has been submitted for publication.

### **Mismatched Epitaxial Systems**

Many solar cell structures call for the heteroepitaxial growth of materials to obtain an increased photovoltaic conversion efficiency. An understanding of the problems of mismatched systems to improve electrical quality should allow greater flexibility in the design of solar cells with lattice-mismatched epitaxial layers. The GaAs-on-Si system is the vehicle for this study. Layers of GaAs grown on silicon have shown evidence of tilt, an important characteristic of mismatched epitaxy, since it provides a mechanism for strain relief. The magnitude of this tilt, relative to substrate misorientation and to process

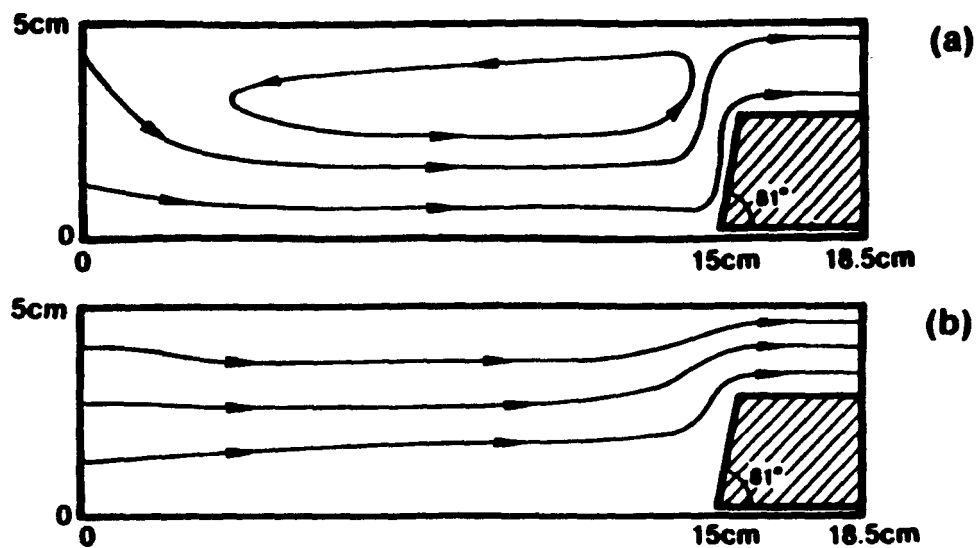


FIG. 1: Streamline plots of the velocity fields in the reactor for an  $81^\circ$  sloped susceptor and (a)  $P = 760$  torr, and (b)  $P = 76$  torr

parameters such as cleaning procedures, growth time, and temperature, have been studied. A paper reporting on these findings has been accepted for publication [2].

### Material Studies

Photoluminescence (PL) is an important technique for the study of many materials aspects of solar cells, especially in conjunction with x-ray, Hall effect, and electrical measurements such as DLTS. One such study has aimed at the development of a simple technique to obtain bulk minority carrier lifetime, based on the temperature-dependence at approximately 300K of the band-edge PL intensity. This work is ongoing. In another study in this task, the effects of heavy doping in solar cell layers have been explored. Work with Si:GaAs and SIMS results indicate significant advantages for silicon as a dopant for solar cell applications. A paper on this topic has been submitted to the Journal of Crystal Growth.

### Microwave Diagnostics

Non-invasive techniques for measurement of material parameters of importance to solar cells are under investigation in this task. A microwave system has been assembled for this purpose which incorporates a magnetic field arrangement. Transient microwave photoconductivity measurements can be made with this system, which yields minority carrier lifetime without the necessity of forming ohmic contacts on the sample. Comparisons between the measurements by conventional photoconductivity transient decay and microwave decay have been excellent. This work is described in a paper presented at a conference earlier this year [3].

### References

1. Chinoy, P.B.; et al. "An Experimental and Theoretical Study of Growth in Horizontal Epitaxial Reactors", (accepted for publication), Journal of Electronic Materials.
2. Ghandhi, S.K.; Ayers, J.E.. "Strain and Misorientation in GaAs Grown on Si (001) by Organometallic Epitaxy", (accepted for publication), Applied Physics Letters.
3. Borrego, J.M.; et al. "Interface Recombination Velocity and Diffusion Constant in Hi-Lo and p<sup>+</sup>-n GaAs Junctions, Measured by a Microwave Technique", Proceedings of the 20th IEEE PV Specialists Conference, September, 1988, Las Vegas, NV.

Title: High Efficiency Thin-Film GaAs and Ternary III-V Solar Cells

Organization: Kopin Corporation, Taunton, Massachusetts

Contributors: R.P. Gale and John C.C. Fan, principal investigators; R.W. McClelland, B.D. King, and J.V. Gormley

The objectives of this research program are to demonstrate large-areas and high-efficiencies in thin-film III-V solar cells. Kopin's approach is to use high-efficiency GaAs/AlGaAs structures in a single-crystal thin film. The thin film was obtained using the CLEFT separable film technology. The CLEFT process allows for substrate reuse, an extremely important feature in order to lower the cost of cell manufacture.

Kopin has made significant progress in FY88. Thin-film cell areas were increased to 4 cm<sup>2</sup>, and one-sun efficiencies over 20% were obtained [1]. The cell fabrication process was simplified, while a substrate reuse program was implemented. Bulk AlGaAs cells were made from 1.65 eV bandgap material, and exhibited over 19% one-sun efficiency.

#### Thin-Film GaAs Cell Results

Thin-film cell areas were increased from 1 cm<sup>2</sup> to 4 cm<sup>2</sup> with the design and introduction of a new mask set, and simplification of the fabrication process. Cells were obtained with one-sun AM1.5 global efficiencies over 20%. The illuminated I-V of one such cell measured at SERI is shown in Fig. 1. This was the highest 4 cm<sup>2</sup> thin-film cell efficiency measured at SERI.

#### Substrate Reuse

As one of the advantages of our approach is the reuse of substrates, during FY88 we implemented a program of substrate reuse. The flow chart for the fabrication and reuse process is shown in Fig. 2. After substrates are masked, grown on, and separated from the thin-film cell layer, they are ready for recycling. The substrates are first cleaned and then sent to a commercial vendor for a light repolish which removes less than 12 microns of material from the substrate. After receipt at Kopin, the substrates are reintroduced into the masking process. At the end of FY88, substrates had successfully gone through the reuse cycle once. It is estimated that each substrate can be reused about 10 times with this procedure.

#### AlGaAs Cell Results

The quality of AlGaAs material grown by OMCVD was improved to the point where high-efficiency AlGaAs high-bandgap cells were fabricated. These AlGaAs bulk cells with bandgap of 1.65 eV had efficiencies up to 19.1% (AM1.5 global), measured at SERI.

A double-heterostructure AlGaAs cell with 1.65 eV absorbing layers was fabricated on a bulk substrate. The cell layers were grown by OMCVD at conditions determined in part by work carried out with the assistance of Dr. R. Ahrankiel of SERI. The aluminum arsenide content of the absorbing layers was 20%, with a higher composition AlAs back-surface field layer, and an

indirect AlGaAs window layer on the front of the cell. The best cell, shown in Fig. 3, had an open-circuit voltage of 1.21 V, a short-circuit current of  $18.4 \text{ mA/cm}^2$ , and a fill factor of 0.86 for an AM1.5 global efficiency of 19.1%. These cells had improved voltage and fill factor from previously fabricated high-bandgap cells, due largely to the high-quality AlGaAs material grown. The AlGaAs quality is demonstrated by the external quantum efficiency for our best cell as measured at SERI and shown in the figure 4. The response is equivalent to our high-efficiency GaAs cells in the blue, or short-wavelength region of the spectrum, and is excellent in the red region. Material quality is critically dependent on the presence of water vapor, which was minimized by stringent leak-testing and tightening of the deposition system.

### Summary

High efficiencies in larger-area thin-film solar cells have been demonstrated. Work is ongoing to further increase the cell areas, to lower the cost of the processing, and to apply this approach to high-efficiency tandem cells.

### References

1. R.P. Gale, R.W. McClelland, B.D. King, and J.V. Gormley, Conf. Record of the 20th IEEE Photovoltaic Specialists Conference (New York: IEEE, 1988).

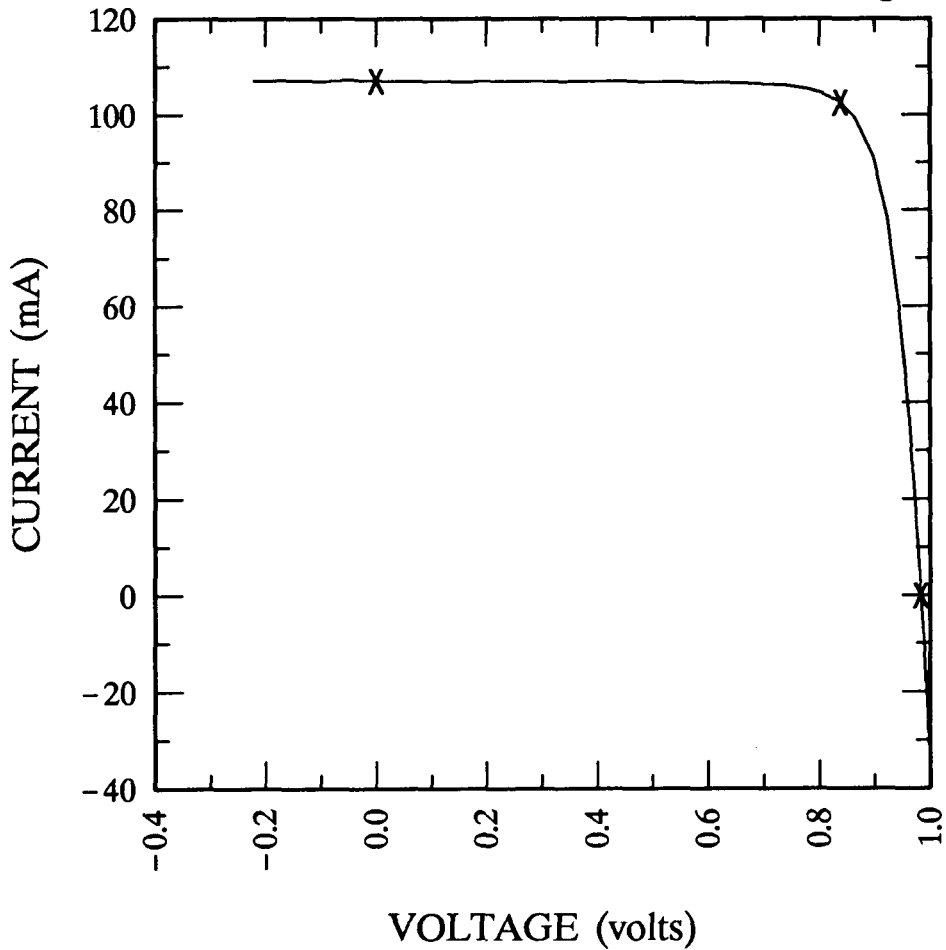
Sample: 5097R

Temperature = 25.0°C

Jan. 9, 1989 4:07 pm

Area = 4.000 cm<sup>2</sup>

**SERI** \*



$$V_{OC} = 0.9841 \text{ volts}$$

$$I_{SC} = 107.0 \text{ mA}$$

$$J_{SC} = 26.76 \text{ mA/cm}^2$$

$$\text{Fill factor} = 81.63 \text{ \%}$$

$$I_{max} = 102.5 \text{ mA}$$

$$\text{Efficiency} = 21.5 \text{ \%}$$

$$V_{max} = 0.8387 \text{ V}$$

Figure 1: I-V Curve of a 4-cm<sup>2</sup> Thin-Film GaAs Solar Cell (AM1.5 global).

### CLEFT SUBSTRATE REUSE

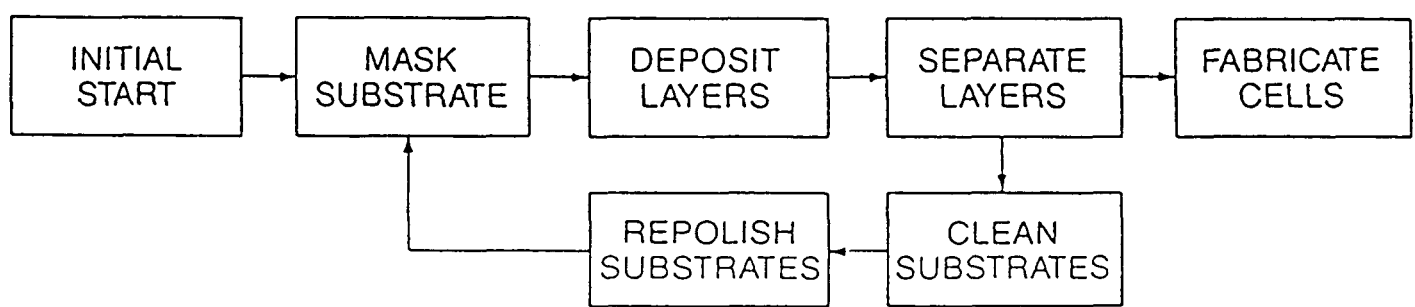


Figure 2: Substrate Reuse Process Sequence.

AlGa(0.6)As/GaAs, global, 1000W/m<sup>2</sup>

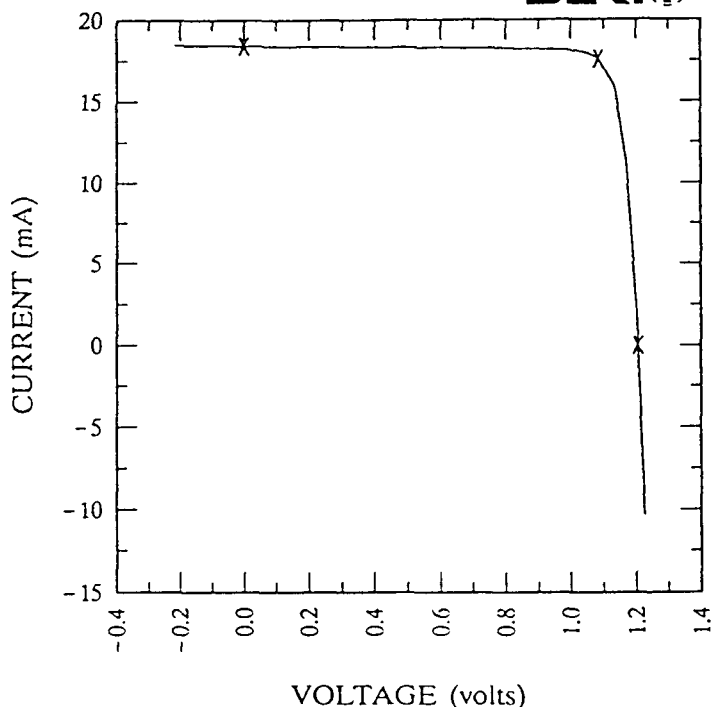
Sample: 5876F-2

Temperature = 25.0°C

Jun. 3, 1988 3:49 pm

Area = 1.000 cm<sup>2</sup>

**SERI**



$$V_{OC} = 1.206 \text{ volts}$$

$$I_{SC} = 18.42 \text{ mA}$$

$$J_{SC} = 18.42 \text{ mA/cm}^2$$

$$\text{Fill factor} = 85.79 \text{ \%} \quad I_{max} = 17.58 \text{ mA}$$

$$\text{Efficiency} = 19.1 \text{ \%} \quad V_{max} = 1.084 \text{ V}$$

Figure 3: I-V Curve of a 1-cm<sup>2</sup> Bulk AlGaAs High-Bandgap Solar Cell (AM1.5 global).

## AlGa(0.6)As

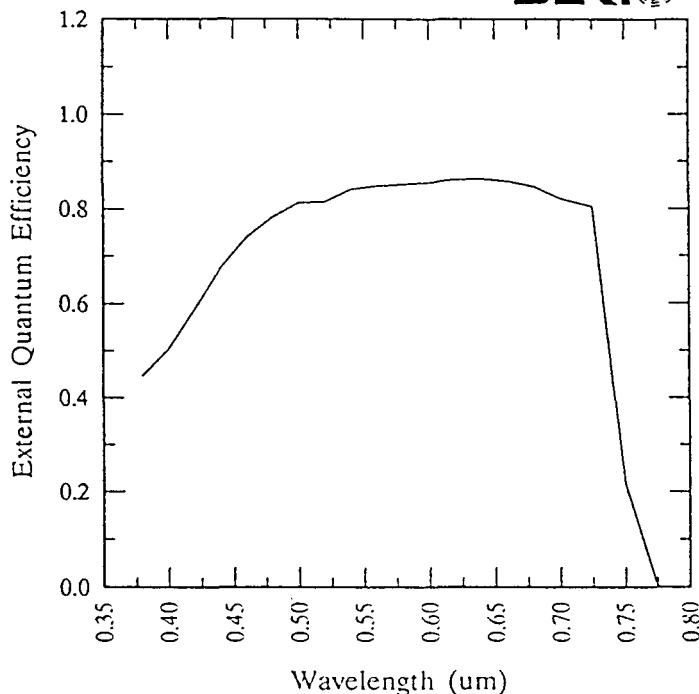
Sample: 5876F-4

Temperature = 25.0°C

Jun. 3, 1988 3:18 pm

Area used = 1.000 cm<sup>2</sup>

**SERI**



Light bias = 18.2 mA

Zero voltage bias

Figure 4: External Quantum Efficiency Curve of a 1-cm<sup>2</sup> Bulk AlGaAs High-Bandgap Solar Cell (AM1.5 global).

Title: Gallium Arsenide Based Ternary Compounds and Multibandgap Solar Cell Research

Organization: Spire Corporation, Patriots Park, Bedford, MA 01730

Contributors: S.M. Vernon and S.P. Tobin, Co-principal Investigators

### Introduction

The overall goal of this research is to establish a technology for producing very high efficiency solar cells for terrestrial photovoltaic applications using either multijunction or single-junction cell concepts. The approach taken involves the growth of GaAs or GaAs-based ternary materials onto GaAs or Si substrates by the metalorganic chemical vapor deposition (MOCVD) technique. The specific objectives of this past year's research were to improve the performance and understanding of GaAs homoepitaxial cells and of GaAs-on-Si heteroepitaxial cells; successes in both of these areas are described below.

### High Efficiency Cell Studies

Our GaAs-on-GaAs cell research has led to the production of the highest one-sun solar cell ever reported. The efficiency of this  $0.25 \text{ cm}^2$  GaAs cell has been measured at SERI to be 24.3% (AM1.5 Global, 25°C) with the following detailed parameters:  $V_{oc} = 1.02\text{V}$ ,  $J_{sc} = 27.5 \text{ mA/cm}^2$ , and  $FF = 86.5\%$ . The illuminated I-V curve of this cell is shown in Figure 1. The factors that have led to achieving this increased efficiency include improvements in the areas of both cell design and MOCVD growth.

The cell-design improvements have involved such tasks as optimization of the emitter doping and AlGaAs window layer thickness and composition, and a detailed loss analysis of the cell performance; progress in these areas has benefited greatly from our collaboration with Prof. Mark Lundstrom and his students at Purdue University. The MOCVD-growth optimization has centered mostly on the formation of the GaAs-GaAlAs interface in order to achieve consistently low values of surface-recombination velocity and reproducible composition profiles. The development of a technique for accurately determining the thickness and compositional profile of the GaAlAs window layer has been a major factor here; this new technique involves the computer modelling of optical reflectance data using a Spire-developed code known as REFIT. The reproducibility of our present solar cell technology is demonstrated by the fact that many cells with efficiencies over 24% AM1.5 have been produced from four consecutive device-processing batches using material from several MOCVD runs spanning a time frame of several months.

### GaAs-on-Si Studies

During this past year we have greatly improved the performance of our GaAs-on-Si cells, from an efficiency of 11.6% to 17.6% (AM1.5 Global, 25°C, measured at SERI). In addition to cell-design optimization studies and the advances in our baseline GaAs cell technology discussed above, the GaAs-on-Si cell

improvements have been due mostly to a significant reduction in defect density in the GaAs-on-Si epilayers. This increase in material quality has resulted from the adoption and optimization of a new deposition process for GaAs-on-Si known as thermal cycle growth (TCG). This technique, first reported by Yamaguchi [1], consists of building up the GaAs-on-Si buffer layer by a repetitive series of deposition and high-temperature annealing steps. Using the TCG process, we have succeeded in reducing the defect density in our GaAs-on-Si by approximately two orders of magnitude, resulting in a significant increase in minority-carrier lifetime. Our research efforts in this area have been significantly augmented by the participation of Drs. Al-Jassim, Ahrenkiel, and Matson of SERI.

The use of hydrogen passivation was explored as a means of passivating electrically active defects in GaAs-on-Si solar cells. The hydrogenation process was accomplished by means of a Kaufmann ion source through the collaboration of Ms. Cecile Leboeuf at SERI. Although initial results appeared promising in that increases in  $V_{oc}$  were obtained, this line of research is no longer being pursued due to the finding that the resultant damage from the hydrogenation process leads to an overall decrease in cell performance.

#### Concentrator Cells

For GaAs-on-Si cells, operation at high solar concentrations provides a means of improving performance by minimizing the importance of the space-charge-recombination current due to the dislocations. We have fabricated GaAs-on-Si concentrator cells and achieved efficiencies as high as 18.5% at 370 suns. As these particular cells were fabricated before our recent improvement in material quality due to the TCG optimization effort, even higher efficiencies, possibly over 20%, may be expected in the near future. For GaAs-on-GaAs baseline cells, efficiencies as high as 25.4% have been achieved at a concentration ratio of 207 suns.

#### On-going Studies and Future Directions

A number of GaAs-on-Si improvement studies are presently in progress. One interesting experiment is the study of the effects of dislocation density on cell performance. The approach taken here is the introduction of intentional dislocations in a well-controlled manner into GaAs-on-GaAs cells by the use of a lattice-mismatched GaAsP intermediate layer. Solar cells have been fabricated in GaAs layers containing between  $10^4$  and  $10^8$  dislocations/cm $^2$ ; similar structures are also being characterized by EBIC, TEM, low-temperature photoluminescence, double-crystal X-ray rocking curves, and minority-carrier lifetime measurements. The results of this research should further our understanding of the relationship between solar cell performance and material properties.

In the upcoming months we plan to continue the study and optimization of high-quality GaAs homoepitaxial cells; an efficiency goal of over 25% at one-sun AM1.5 seems reasonable. The GaAs-on-Si cell studies will also continue; material improvement by the use of strained-layer and thermal-annealing techniques is the avenue to be pursued.

## Publications

The research conducted in this program has resulted in a number of articles being published in the scientific literature over the course of this past year. These are listed below:

"Heterointerface Stability in GaAs-on-Si Grown by Metalorganic Chemical Vapor Deposition," S.J. Pearton, D.L. Malm, L.A. Heimbrook, C.R. Abernathy, R. Caruso, S.M. Vernon, and V.E. Haven, *Appl. Phys. Lett.* 51, 682, (1987).

"Minority-Carrier Properties of GaAs Grown on Silicon," R.K. Ahrenkiel, M.M. Al-Jassim, D.J. Dunlavy, K.M. Jones, S.M. Vernon, S.P. Tobin, and V.E. Haven, *Appl. Phys. Lett.* 53, 222 (1988).

"Device Processing and Analysis of High Efficiency GaAs Cells," S.P. Tobin, S.M. Vernon, C. Bajgar, L.M. Geoffroy, C.J. Keavney, M.M. Sanfacon, and V.E. Haven, *Solar Cells* 24, 103, 1988.

"Photoluminescence Studies of Heteroepitaxial GaAs-on-Si," B.A. Wilson, C.E. Bonner, R.C. Miller, S.K. Sputz, T.D. Harris, M.A. Lamont, R.D. Dupuis, S.M. Vernon, V.E. Haven, R.M. Lum, and J.K. Klingert, *J. Electronic Materials*, 17, 115 (1988).

"Thickness Dependence of Material Quality in GaAs on Si Grown by Metalorganic Chemical Vapor Deposition," S.J. Pearton, C.R. Abernathy, R. Caruso, S.M. Vernon, K.T. Short, J.M. Brown, S.N.G. Chu, M. Stavola, and V.E. Haven, *J. Appl. Phys.* 63, 775 (1988).

"Minority Carrier Lifetime of GaAs on Silicon," R.K. Ahrenkiel, M.M. Al-Jassim, D.J. Dunlavy, K.M. Jones, S.M. Vernon, S.P. Tobin, and V.E. Haven, *Proc. of the 20th IEEE PVSC*, Las Vegas, September 1988, to be published.

"Efficiency Improvements in GaAs-on-Si Solar Cells," S.M. Vernon, S.P. Tobin, V.E. Haven, C. Bajgar, T.M. Dixon, M.M. Al-Jassim, R.K. Ahrenkiel, K.A. Emery, *Proc. of the 20th IEEE PVSC*, Las Vegas, September 1988, to be published.

"Influence of bandgap narrowing effects in p<sup>+</sup>-GaAs on Solar Cell Performance," M.E. Klausmeier-Brown, P.D. DeMoulin, H.L. Chuang, M.S. Lundstrom, M.R. Melloch and S.P. Tobin, *Conf. Rec. 20th IEEE Photovoltaic Specialists Conf.*, 1988, to be published.

"Influence of Perimeter Recombination on High-efficiency GaAs p/n Heteroface Solar Cells," P.D. DeMoulin, S.P. Tobin, M.S. Lundstrom, M.S. Carpenter and M.R. Melloch, *IEEE Electron Dev. Lett.* 9, 368-370 (1988).

"Effects of Na<sub>2</sub>S and (NH<sub>4</sub>)<sub>2</sub>S Edge Passivation Treatments on the Dark Current-voltage Characteristics of GaAs pn Diodes," M.S. Carpenter, M.R. Melloch, M.S. Lundstrom, and S.P. Tobin, *Appl. Phys. Lett.* 52, 2157-2159 (1988).

"Effects of Heavy Impurity Doping on Electron Injection in p<sup>+</sup>-n GaAs Diodes," M.E. Klausmeier-Brown, M.S. Lundstrom, M.R. Melloch, and S.P. Tobin, *Appl. Phys. Lett.* 52, 2255-2257 (27 June 1988).

"Sequential Etch Analysis of Electron Injection in p<sup>+</sup>-GaAs," M.E. Klausmeier-Brown, C.S. Kyono, P.D. DeMoulin, S.P. Tobin, M.S. Lundstrom and M.R. Melloch, IEEE Trans. Elect. Dev. 35, 1159-1161 (1988).

#### References

1. Y. Itoh, T. Nishioka, A. Yamamoto, and M. Yamaguchi, Techn. Dig. of Intl. PVSEC-3, Tokyo, Japan, paper C-IVa-4, 1987.

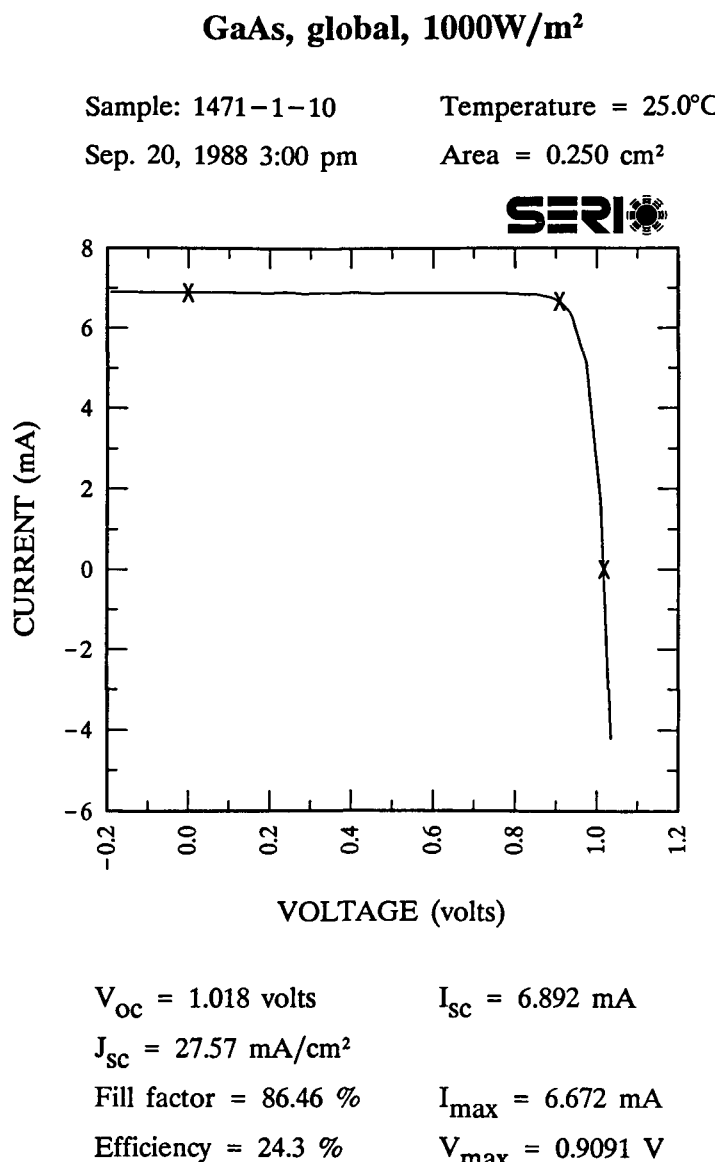


Figure 1. Efficiency measurement of world-record GaAs solar cell (data courtesy of K. Emery, SERI).

Title: Advanced High-Efficiency Concentrator Cells  
Organization: Varian Research Center, Palo Alto, California  
Contributors: H. F. MacMillan, principal investigator, B-C. Chung, J. C. Schultz, D. D. Liu, L. D. Partain, G. F. Virshup and J. G. Werthen

The goal of this research program is the development of a multijunction, monolithic, two-terminal cascade solar cell with a power conversion efficiency of at least 30% at solar concentrations of 400 to 1000 AM1.5D and at an operating temperature of 50°C. The cell materials are grown by organometallic vapor phase epitaxy on GaAs substrates.

Device modeling studies of cascade solar cells have identified the 1.75-eV/1.15-eV bandgap combination for optimum utilization of the AM1.5 spectrum [1]. Varian has focused efforts on this bandgap combination, and specifically on 1.75-eV  $\text{Al}_{0.2}\text{Ga}_{0.8}\text{As}$  and 1.15-eV  $\text{In}_{0.2}\text{Ga}_{0.8}\text{As}$  component cells grown on GaAs with appropriate intervening lattice grading layers. Component cells have been fabricated that demonstrate near-theoretical efficiencies during the preceding year of this contract. However, attempts to grow and fabricate the monolithic cascade have generally yielded discouraging results, primarily because of the difference in lattice constant between the two component cells. This difficulty in growing high-quality junctions in lattice-mismatched structures has been exacerbated by the necessity for two grading layers. The first grading layer is grown with compressive stress between the GaAs substrate and the lower  $\text{In}_{0.2}\text{Ga}_{0.8}\text{As}$  cell. The second grading layer is grown with tensile stress between the lower cell and the upper  $\text{Al}_{0.2}\text{Ga}_{0.8}\text{As}$  cell. The greatest difficulties arise in achieving excellent materials quality in the grading layer which is subjected to tensile stress, and in the overlying  $\text{AlGaAs}$  cell.

Early in the current year of this contract period, we succeeded in fabricating 1.93-eV  $\text{Al}_{0.38}\text{Ga}_{0.62}\text{As}$  cells with outstanding efficiency; 14.9% AM1.5G. Device modeling predicts that there is a relatively small efficiency penalty (2 percentage points) incurred by using the lattice-matched combination, 1.93-eV  $\text{AlGaAs}/1.42\text{-eV GaAs}$ , compared to the lattice-mismatched combination 1.75-eV  $\text{AlGaAs}/1.15\text{-eV InGaAs}$ . Consequently, early in this contract year we shifted our research efforts from the 1.75-eV/1.15-eV combination to the 1.93-eV/1.42-eV combination.

An additional consideration is that because of the larger bandgap of the lower cell in the 1.93-eV/1.42-eV combination, a third component cell is now possible. The third cell can be grown on the reversed side of the substrate in a second growth step [2]. With a bandgap of 1.05-eV, the third component cell can generate the same photocurrent as each of the upper component cells. Furthermore, the lattice mismatch results in the lower junction being under compressive stress only, which our previous results have shown to be tractable. Consequently we have undertaken to demonstrate the feasibility of this new structure with component cells grown on both sides of the substrate.

During the past year we have concentrated on the following areas of development: (1) growth and fabrication of high-efficiency component cells 1.93-eV  $\text{AlGaAs}$ ,  $\text{GaAs}$ , and 1.05-eV  $\text{InGaA}$  (2) growth and fabrication of 1.93-eV  $\text{AlGaAs}/\text{GaAs}$  metal-interconnected cascade cells, and (3) two-sided growth and fabrication of  $\text{GaAs}$  and 1.05-eV  $\text{InGaAs}$  three-terminal cascade cells.

Summaries of the most significant research results of the past year follow.

1. 1.93-eV AlGaAs cells have been fabricated that demonstrate efficiencies as high as 14.9% AM1.5G and 14.1% AM1.5D [3]. GaAs cells with overlying 1.93-eV AlGaAs simulated cells have been fabricated with efficiencies as high as 12.3% AM1.5D. These results imply that a cascade of these components should demonstrate a 1-sun efficiency of 26.4% AM1.5D, without current matching or approximately 25% AM1.5D with current-matched, two-terminal operation.
2. A 1.93-eV AlGaAs/1.42-eV GaAs metal-interconnected cascade cell (MICC) has been fabricated with a 1-sun efficiency of 23.9% AM1.5G. This is the highest efficiency for a multijunction cell reported to date, and at the time of measurement, the highest AM1.5G efficiency ever reported [4].
3. A 1.42-eV GaAs/1.05-eV InGaAs MICC has been fabricated that demonstrates a 1-sun efficiency of 23.0%, AM1.5D. The upper GaAs cell has an efficiency of 21.2%, and the InGaAs cell on the opposite side of the GaAs substrate has an efficiency of 1.8%. This result is a proof-of-concept for a three-junction cascade grown in part on both substrate surfaces.
4. Efficiencies as high as 28.1% at 400 AM1.5 suns concentration for n/p cells and 27.5% at 1000 AM1.5 suns concentration for p/n cells have been demonstrated. The high performance is due to improved optimization of the MOCVD process, particularly regarding emitter doping, and improved cell fabrication procedures (gridline definition and edge passivation) developed during this contract [5].
5. GaAs concentrator cells have been fabricated with these same processes on low-doped substrates and with a low-obscuration backside grid metallization. When assembled and tested at Sandia with an underlying Si cell in a four-terminal, mechanically-stacked cascade, a total efficiency of 31% at 350 AM1.5 suns concentration was demonstrated. This is the first time a photovoltaic efficiency over 30% has been achieved [6].

In the work to date, the focus has been on developing component and cascade cells designed for one-sun operation. Portions of this work were supported in part by the Defense Advanced Research Projects Agency. In future work, the focus will shift to concentrator designs for each of the component and cascade cells. In particular, emphasis will be placed on reducing the series resistances of metal interconnects and grown-in interconnects for concentrator application.

## References

1. K. W. Mitchell, Proceedings 15th IEEE Photovoltaic Specialists Conf., (1981), p. 142.
2. S. Kamath and R. Loo at Hughes Research Laboratories first proposed this structure.
3. B-C. Chung et al., "High-Efficiency AlGaAs Solar Cells Grown by Metalorganic Vapor Phase Epitaxy", presented at 20th IEEE PVSC, Las Vegas (Sept. 1988).

4 G. F. Virshup, B-C. Chung and J. G. Werthen, "23.9% Monolithic Multijunction Solar cell", presented at 20th IEEE PVSC, Las Vegas (Sept. 1988).

5. H. F. MacMillan et al., "28% Efficient GaAs Concentrator Solar Cells" presented at 20th IEEE PVSC, Las Vegas (Sept. 1988).

6. J. M. Gee and G. F. Virshup, "A 31%-Efficient GaAs/Silicon Mechanically-Stacked, Multijunction Solar Cell" presented at 20th IEEE PVSC, Las Vegas (Sept. 1988).

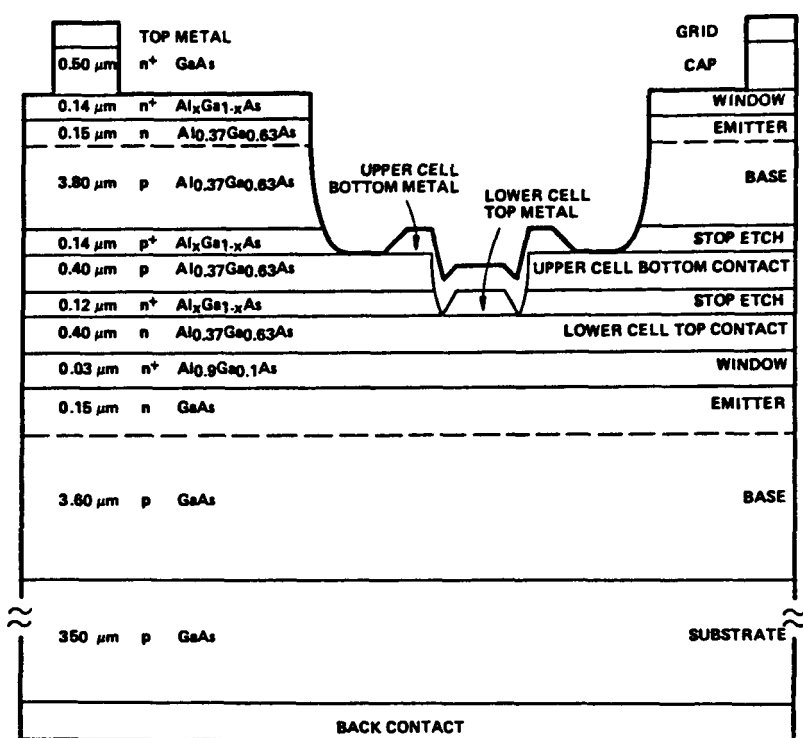


Fig. 1 Cross-section structure of 1.93-eV AlGaAs/1.42-eV GaAs metal-interconnected cascade cell (MICC) with exaggerated detail of metal interconnect features.

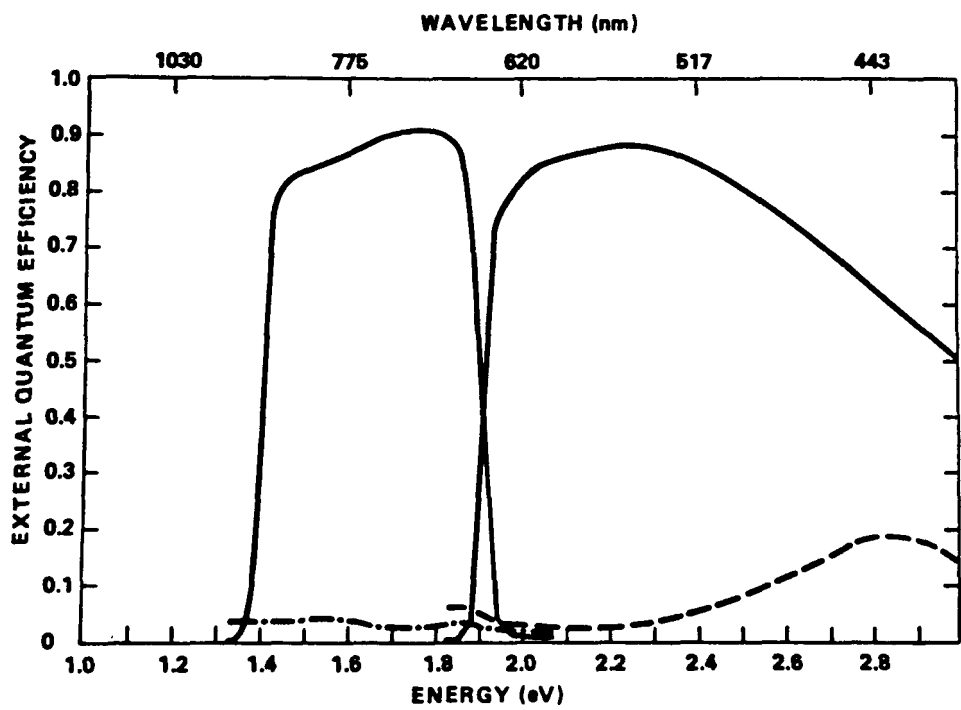


Fig. 2 External spectral responses of 1.93-eV AlGaAs and GaAs component cells in MICC.

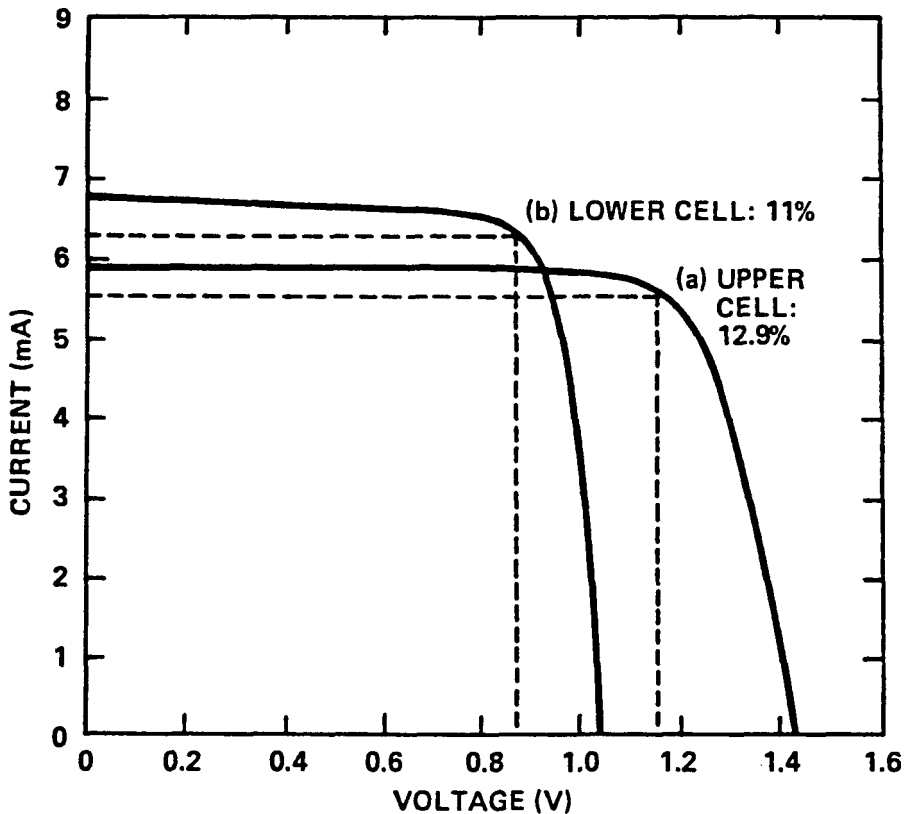


Fig. 3 Current-voltage characteristics of the MICC component cells at AM1.5G with the unmeasured cell at its maximum power point.

Title: Research on Large Scale MOCVD Deposition

Organization: Spire Corporation, Patriots Park, Bedford, MA 01730

Contributors: J. Daly, Principal Investigator  
C. Roberts

### Introduction

The full realization of DOE's goal of producing low cost, flat panel modules with at least 20% conversion efficiency requires the development of large-area ( $>1000 \text{ cm}^2$ ) deposition systems which maintain the high epilayer quality, uniform doping, and efficient source utilization of smaller, conventional systems. The significant cost involved in the development of such large reactors makes it imperative that accurate theoretical models of the MOCVD process be developed to aid in the design of such systems. However, the models must be verified against a comprehensive body of experimental data acquired from actual production reactors.

The goal of the current research is to advance state-of-the-art theoretical models of the MOCVD process so that the models may become accurate tools for the design of future large-scale production reactors. This is being accomplished by:

- Collaboration with Julian Szekely & Associates, who are performing numerical simulations of growth conditions for Spire's standard 4.5-inch diameter reactor and Spire's new, 10-inch diameter ( $1000^+ \text{ cm}^2$  deposition area) reactor.
- Extensive experimental testing of both reactors under conditions which are designed to identify the discrepancies between theory and experiment.
- Feedback of the experimental results to the modellers for appropriate adjustment of the model.

### Modelling Results for Existing MOCVD Reactors

Spire's standard geometry MOCVD reaction chamber is a barrel-type graphite susceptor surrounded by a quartz bell jar as depicted in Figure 1. The new, large area ( $\sim 1000 \text{ cm}^2$ ) reactor is of similar shape.

Computer simulations of flow dynamics, temperature profiles, and mass transport were performed using the actual geometry and dimensions of each reactor. Further, a range of operating conditions were modelled, including reactor pressure, susceptor temperature, hydrogen flow rate, and cold wall vs. warm wall container.

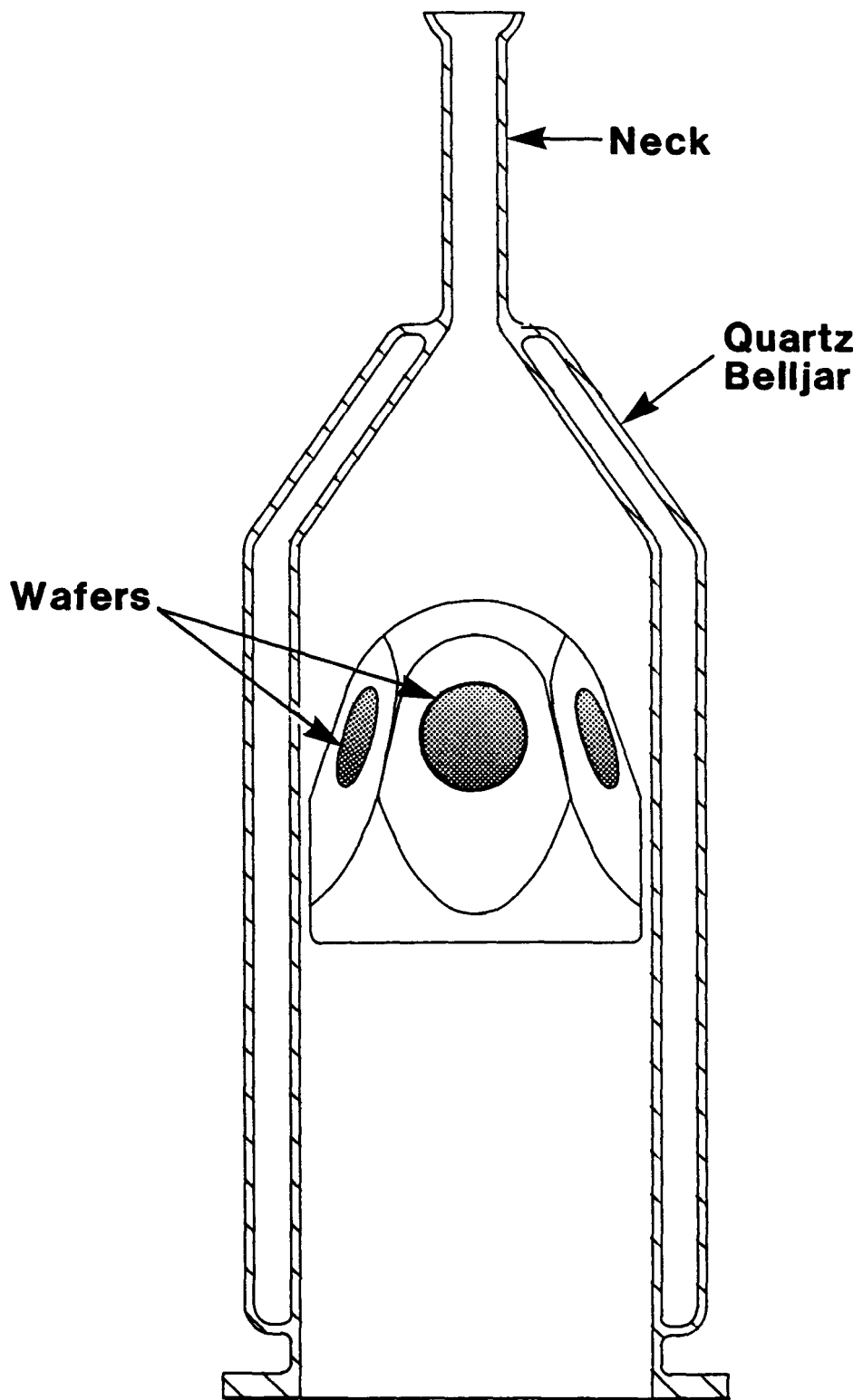
The predicted growth rates obtained for Spire's standard 450 reactor under various operating conditions are presented in Figure 2. In case (a), the reactor is operated under atmospheric pressure with hydrogen flow rate chosen to yield near-optimum thickness uniformity over the wafer deposition region. In case (b), reactor pressure is reduced to several tens of millitorr while other conditions remain the same as in case (a). The change in shape of the curve from a slightly "humped" shape to one which decreases monotonically as some fractional power law indicates a transition from free (natural) convection dominated flow to forced laminar flow. In case (c) the pressure remains as in (b) but flow rate is increased to achieve optimum uniformity. In both cases, the epilayer thickness uniformity over a 2-inch wafer is predicted to be better than +5%.

#### Experimental Results

Experimental follow-up of these predictions has resulted in substantial qualitative agreement with the theoretical model. These experiments include flow visualization by seeding the carrier gas with titanium dioxide dust particles and looking at the scattered light from incident laser radiation, as well as actual thickness uniformity measurements from epilayers grown under exactly the same operating conditions as the ones in the computer simulations. As in cases (a) and (c), it is possible, experimentally, to obtain uniform thickness epilayers under both free convection-dominated and forced convection (laminar) flow conditions. The differences between theory and experiment are in the predicted values of flow, pressure, etc., at which transitions in flow properties are expected and in the actual value of growth rates, though the trend in top-to-bottom uniformity may agree. This indicates that some of the constants used in the model (viscosity, diffusivity, specific heat, . . .) may require adjustment in order to obtain quantitative as well as qualitative agreement.

#### On-going Efforts and Future Directions

Experimental efforts regarding the large scale ( $\sim 1000 \text{ cm}^2$ ) reactor continue. Flow visualization experiments have just concluded after indicating the need for low pressure operation in order to achieve good uniformity. An experimental matrix of epilayer growth experiments, based on orthogonal design principles, is now underway and is expected to continue for up to three months. During that time, thickness and doping uniformity measurements will be made and the results used to adjust the theoretical model in order to achieve better quantitative agreement with experiment.



88744

FIGURE 1. SCHEMATIC ILLUSTRATION OF SPIRE'S STANDARD SPI-MO CVD™ 450 REACTION CHAMBER.

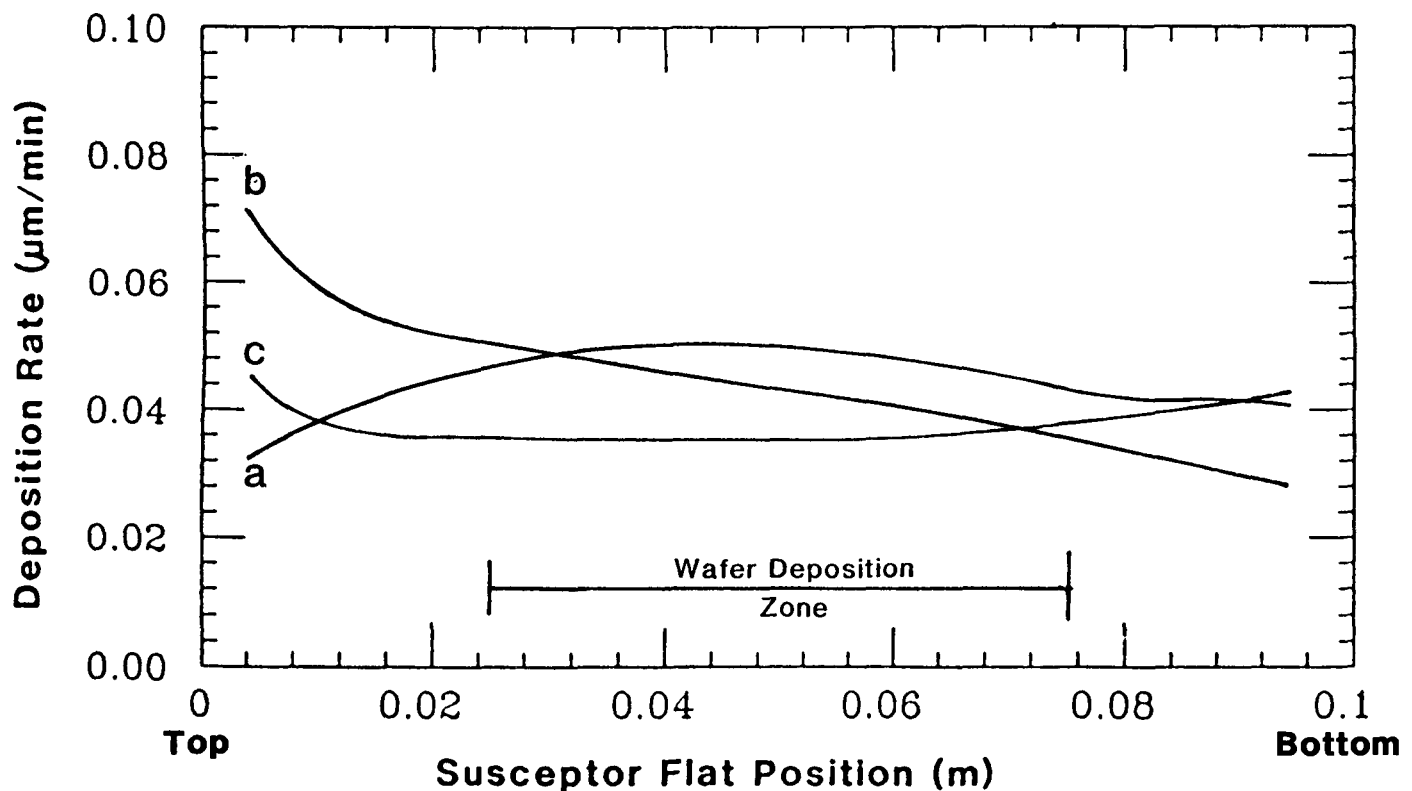


FIGURE 2. CALCULATED GROWTH RATE CURVES FOR THE SPI-MO CVD<sup>TM</sup> 450.  
 (a) Atmospheric pressure and total gas flow rate chosen to yield optimum uniformity. (b) Same as (a), but low pressure. (c) Same as (b) but flow rate increased to obtain optimum uniformity.

## 6.0 NEW IDEAS PROGRAM

R. Mitchell (Manager)

The objective of the New Ideas Task is to identify new photovoltaic materials, device configurations, and concepts and to conduct preliminary research and development in the areas that show the most promise. Subcontracted research in this task that shows significant potential is transferred into the appropriate major task area within the DOE Photovoltaic Program for continued support.

The New Ideas Task provides public solicitations for new and innovative research ideas that are relevant under the Photovoltaic Advanced Research and Development Project's guidelines to perform high-risk, long-term, and potentially high-payoff research and development. These solicitations for new and innovative research ideas are submitted by universities, businesses, and nonprofit organizations. Subcontracts are awarded to study the most promising concepts associated with these solicitations. These subcontracts are reviewed, and successful concepts are selected for renewal with a second year of funding. In FY 1988, the program did not have sufficient funding to carry out a renewal of those research efforts funded in FY 1987. However, the remaining research under these programs was continued on the funding originally allotted for this effort. These concepts included the avalanche heterostructure and superlattice solar cell developed by Georgia Tech Research Institute; the low-cost techniques for producing CdZnTe devices for cascade-cell applications researched by International Solar Electric Technology; the hydrogen radical enhanced growth of InP solar cells investigated by Rensselaer Polytechnic Institute; and the high-efficiency flat-plate silicon solar cells investigated by Stanford University.

During FY 1988, the New Ideas Task issued a competitive solicitation for New Ideas for Photovoltaic Conversion. The solicitation received almost 100 letters of interest (LOI). Preliminary evaluation and selection of these LOI responses identified several promising concepts for further evaluation. During FY 1989, expanded proposals from these finalists will be evaluated and several concepts will be chosen for support. Successful subcontracted research activities under this solicitation will begin in the fall of 1989.

Three concepts funded during the FY 1987 solicitation have been selected to receive a delayed second year of funding. During FY 1989, these concepts will be funded for an additional year and monitored. This monitoring and an evaluation will allow successful subcontracts to be selected for possible funding by the appropriate major program area.

Title: New Concepts for High Efficiency Energy Conversion:  
The Avalanche Heterostructure and Superlattice Solar Cells

Organization: Georgia Tech Research Institute  
Atlanta, GA 30332

Contributors: C.J. Summers, A. Rohatgi, K.F. Brennan, A. Torabi and  
H. M. Harris

Objective:

The objective of this program is to perform modeling, material growth and device fabrication of the variable spaced superlattice photodiode concept in order to establish its feasibility and potential as a photovoltaic device.

Approach:

The specific structures investigated this year were heterojunction or superlattice, single junction solar cells, in which the energy gap of the p-side of the junction is more than twice the bandgap of the n-side. In these devices, photon-generated electrons on the p<sup>+</sup>-side are injected by the internal electric field over the interface into the low bandgap layer. Because they experience the full difference in bandgap energies efficient impact ionization occurs and a maximum current gain of two can be realized. Thus, the energy of the electrons in the wide bandgap region is conserved by adding it to the current generated by the low bandgap side of the junction. The efficiency of the injection process is determined by the abruptness of the heterojunction which must be shorter than the phonon scattering mean free path ~100Å. To relieve this constraint, it is also proposed to develop variably spaced superlattice energy filter devices for the junction region, which afford high-energy injection by providing a tunneling channel in a biased superlattice.

To determine the utility of this approach, we have therefore addressed the following issues: 1) the formulation of a realistic theory to predict the enhancement possible with an Avalanche Solar Cell, 2) the development of MBE growth techniques to achieve atomically abrupt interfaces in the AlGaAs/GaAs system, 3) an investigation of dipole-interface-doping (DID) techniques to achieve larger conduction band-offsets, 4) an investigation into variably spaced superlattice structures, and finally, 5) the development of a CBE system for HgCdTe-CdMnTe alloy growth to grow structures with large conduction band-offsets.

Modeling:

A calculation has been made of the efficiency of a heterojunction avalanche solar cell using Henry's model.(1) This data shows that for a AM0 spectrum and ideal cell properties, the cell efficiency is increased from 28.8% for a one bandgap cell to 35.3% for a two-bandgap heterojunction avalanche cell. For 1000 suns concentration the efficiency increases to ~34.9% and 45.4%, respectively. A more exact model which takes into account the junction properties is in development and results will soon be presented. A model for resonant tunneling in multiple quantum well structures was also developed for designing variable spaced superlattice structures.

### Material Growth:

A reflection high energy electron diffraction (RHEED) system was developed for monitoring intensity oscillations to perform insitu measurements of growth rate and alloy composition and to develop growth techniques for obtaining atomically smooth surfaces. These measurements and photoluminescence studies showed that the smoothness of the GaAs/AlGaAs and AlGaAs/GaAs interfaces could be improved by interrupting growth for 60s at the interface and by growing at 600 and 700°C, respectively, for GaAs and  $Al_{0.35}Ga_{0.65}As$ . Using the above theory and these growth techniques, new variably spaced superlattice structures were investigated. For the first time, resonant tunneling through 2- and 3-quantum well AlGaAs/GaAs structures was observed using the higher  $n=2$  quantum states, in the first, second, or the third quantum well. These devices exhibit excellent room temperature, as well as low temperature NDR effect.(2) This effect should allow more flexible electron injection schemes to be developed. Special measuring circuitry was also developed to unambiguously analyze these devices under constant current or constant voltage conditions to determine whether the resonant tunneling structures are, in fact, intrinsically bistable.

Delta-doping has also been investigated for use in the dipole-interface-doping technique to adjust bandgap offsets. As shown by Figure 1, doping concentration of  $3 \times 10^{13} \text{ cm}^{-2}$  ( $\sim 1 \times 10^{20} \text{ cm}^{-3}$ ) have been measured in a 30Å wide profile and are believed possible in a 8Å thick layer.(3) It appears that the width of the delta doped layer is narrower than the resolution of SIMS and the electrochemical C-V profiler measurements. X-ray results indicate that the crystalline quality of the GaAs epitaxial layer is not compromised by delta doping even at high concentrations. Work is currently being performed for Be p-type delta doping of GaAs and AlGaAs.

### Chemical Beam Epitaxy of II-VI Materials:

Also during this report period, a chemical beam epitaxy system was constructed and low x-valued  $Hg_{1-x}Cd_xTe$  alloys were grown with near state-of-the-art properties. This worked entailed the modification of a Varian GEN II system for CBE growth by fitting a Balzers turbomolecular pump, a cooled Hg-vapor trap, and an EMCORE toxic gas handling system. For the source ensemble a Varian gas injector was installed and a gas handling system for metalorganic Te has been designed and delivered from EMCORE. A new fast response Hg-vapor source was also developed for this system under a related program.(4)

### References:

1. C.H. Henry, J. Appl. Phys. 51, 4194 (1980)
2. A. Torabi, C.J. Summers, H.M. Harris and K.F. Brennan Am. Phys. Soc. 33, 701 (1988).
3. A. Torabi, R.B. Haugen, H.M. Harris and C.J. Summers, J. Vac. Sci. & Tech., April 1989.
4. B.K. Wagner, R.G. Benz II and C.J. Summers, J. Vac. Sci. & Tech., May 1989.

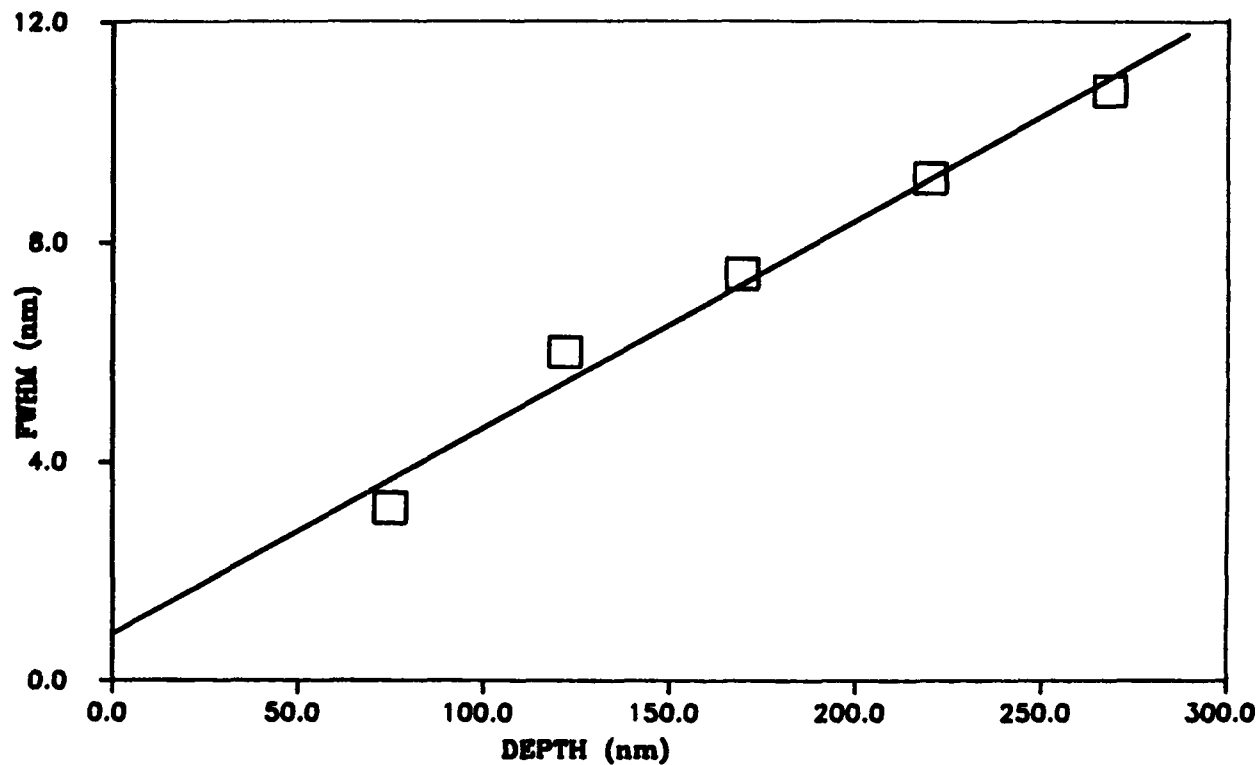


Fig. 1. Full width at half maximum (FWHM) of planar doped layers as obtained from C-V profile v.s. the depth of the layer.

Title: Low Cost Technique for Producing CdZnTe Devices for Cascade Cell Application

Organization: International Solar Electric Technology (ISET), Inglewood, California

Contributors: Bulent M. Basol, Vijay K. Kapur, principal investigators; and Richard C. Kullberg

The objective of this project is to develop  $Cd_{1-x}Zn_xTe$  devices with low resistivity ZnTe contacts to be used as top cells in tandem structures. During the first year of the program, the two-stage process has been used to prepare ZnTe, CdTe and  $Cd_{1-x}Zn_xTe$  ( $0 < x < 1$ ) thin films of various compositions [1,2]. Extrinsic doping of these films has been demonstrated. Preliminary devices with around 4% efficiency have been fabricated.

The two-stage technique involves depositing thin films of the elemental components of a compound, and reacting these components to form the desired compound. Our efforts in this project mostly concentrated on the electroplating technique as the method of deposition for the Cd, Zn and Te layers. We, however, also used vacuum evaporation especially for depositing films on insulating substrates.

#### Elemental Layer Deposition

The first important step of the present process is to deposit uniform films of Te, Cd and Zn. The morphology of these elemental layers greatly affects the morphology of the films obtained after reaction. For evaporated Te, Cd and Zn layers, morphology control does not present a problem. But, for electroplated films, it is essential to use electrolytes and electrodeposition parameters that yield smooth, continuous and uniform films.

Glass substrates coated with ITO or ITO/CdS were employed in this work. The plated area of each sample was 2.56cmx2.56cm. During deposition, electrical contact to the samples was made along the four edges of the plated area, using contacts which were isolated from the plating solution. Depositions were carried out galvanostatically at room temperature and various different current densities were employed to optimize the morphology and the uniformity of the deposited films.

The Te plating bath consisted of an acidic  $TeO_2$  solution. The tellurium concentration in a typical electrolyte was 3000-3500 ppm. For Te layers, film morphology is a strong function of the plating current density. Te plating is diffusion limited.

Therefore, very high current densities tend to give black deposits with powdery morphologies, especially for films thicker than approximately 2000 Å. In a static plating system, current density values of around 3 mA/cm<sup>2</sup> give shiny Te deposits with

good morphology. Much higher current densities can be used in a plating system with flowing electrolyte.

Morphology control for the Cd and Zn layers is also very important. These elements, especially Zn, are known to grow in dendrites when electrodeposited. To break the dendritic growth and to obtain small grained smooth deposits, brightener additives have to be used in the Cd and Zn deposition baths. SEM pictures of plated surfaces shown in Fig.1a and Fig.1b demonstrate this point. Fig.1a is a SEM picture of a Cd deposit on a glass/ITO/Te substrate obtained from a simple CdSO<sub>4</sub> solution with no additives. The Cd film is discontinuous and it is in the form of islands of large crystallites. Fig. 1b, on the other hand, shows the morphology of a Cd film deposited using a CdSO<sub>4</sub> bath containing additives. Here, the substrate coverage is good and small long grains of Cd are visible. Cd plating current densities in the order of 20 mA/cm<sup>2</sup> were found to be adequate for coating over Te films. Zn plating current densities over Te were as high as 500 mA/cm<sup>2</sup>, whereas, Zn coating over Cd could be carried out satisfactorily at lower current densities of 20-50 mA/cm<sup>2</sup>.

### Reaction

Reaction of the stacked layers to form the compounds was carried out in a tube furnace in flowing Ar, or N<sub>2</sub>. Reaction times ranged from 30 minutes to 2 hours. Reaction temperatures varied from 350° C to 580° C. At the end of the reaction period the tube was cooled down to room temperature and the samples were removed for analysis.

### Film Measurements

Films were examined by SEM, X-Ray diffraction and optical transmission measurements. Since, in-plane resistivity measurements were not possible for films on conducting substrates, a set of samples were also prepared by vacuum evaporating Cd, Zn and Te layers onto glass substrates. Cu doping experiments were carried out on these samples. The resistivities of the films with and without doping were then measured and compared as a function of film stoichiometry.

X-ray diffraction data taken from a series of films with varying compositions is given in Fig.2. The substrate for these films was ITO coated glass and the reacted film thicknesses were in the 1 micron range. The reaction temperature and time were 550° C and 1 hour respectively. The data in Fig.2 clearly demonstrates the composition change for the Cd<sub>1-x</sub>Zn<sub>x</sub>Te alloy. The position and intensity of the diffraction peaks at 2θ= 21.45, 30.5, 35.4, 37.7, 51 and 60.6 degrees are similar for all the samples. These peaks are associated with the ITO substrate. The remaining major peaks are associated with cubic Cd<sub>1-x</sub>Zn<sub>x</sub>Te. As expected, these peak positions shift in the direction of smaller diffraction angles as the film stoichiometry becomes Cd-rich. Also, the 200

peak ( $2\theta=29.3$ ), which is prominent in the ZnTe film, gets diffused as the stoichiometry approaches CdTe. The 400 peak which can be observed in the CdTe sample overlaps with the ITO diffraction peak in the Zn-rich compositions. The "a" values for the measured films were graphically determined and the film compositions were estimated as shown in Fig. 2. The "a" values for the ZnTe and CdTe films agree very well with the values given in the ASTM cards (6.1026 Å and 6.481 Å respectively).

Table 1 gives the measured resistivity values for a set of films that were prepared on glass substrates by sequentially evaporating the elemental components and reacting them in nitrogen atmosphere. Halves of these samples were doped with Cu. The reaction temperature and the reaction time were 500°C and 30 minutes respectively. Film thicknesses were in the range of 0.4-0.8 microns. It is clearly observed from Table 1 that the resistivities of Zn-rich films are generally lower than the Cd-rich ones and the effectiveness of Cu doping is much higher for these Zn-rich samples. This result is in accordance with the general experience that it is more difficult to deposit low-resistivity p-type CdTe polycrystalline thin films than to deposit low resistivity p-type ZnTe films.

Figure 3 shows the optical transmission of Sample 18 which was 0.4 microns thick. The reaction temperature and time for this ZnTe film were 500°C and 30 minutes respectively. After reaction, this sample was specular and its average transmission was higher than 65%. The transmission value was not affected much by doping. The band edge observed in Fig.3 is sharp and it yields a bandgap value of about 2.25 eV. These are the first low resistivity ZnTe films prepared by the two-stage process and they can be effectively used in tandem solar cell structures.

#### Devices

Preliminary devices were made using some of the films prepared by the two-stage process. Since the aim was to evaluate the performance of the absorber layers only, ZnTe contacts were not employed in these initial devices. Instead, Ni or Mo metal contacts were used. Although cells with the structure of glass/metal/ $\text{Cd}_{1-x}\text{Zn}_x\text{Te}/\text{CdS}$  were fabricated, they were not very successful. Best results were obtained using the glass/CdS/ $\text{Cd}_{1-x}\text{Zn}_x\text{Te}/\text{metal}$  structures. The best cell parameters obtained for CdTe and  $\text{Cd}_{0.9}\text{Zn}_{0.1}\text{Te}$  devices were  $J_{sc}=15 \text{ mA/cm}^2$ ,  $V_{oc}=0.55 \text{ V}$  and  $FF=0.45$ .

#### Conclusions

In conclusion, we have demonstrated the use of the two-stage process for the preparation of  $\text{Cd}_{1-x}\text{Zn}_x\text{Te}$  alloy films. We have also demonstrated that cost effective electrodeposition steps can be used in the two-stage process. We have made solar cells on films prepared by this technique. These devices need further

improvement but the preliminary results are promising. The next phase of the program will focus on the efficiency improvement of the devices.

#### References

1. B.M. Basol and V.K. Kapur, Thin Solid Films, 1988 (in press).
2. B. M. Basol, V. K. Kapur, R. C. Kullberg and R. L. Mitchell, Proc. 20th IEEE Photovoltaic Specialists Conf., IEEE, New York, 1988, (in press).

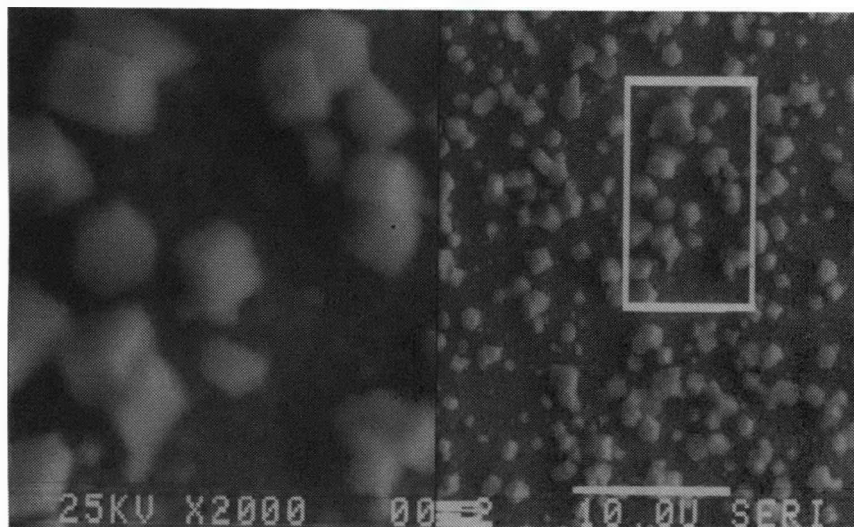


Fig. 1a. SEM picture of a Cd deposit on a glass/ITO/Te substrate demonstrating spotty plating. Electrolyte used to deposit this film did not contain any additives.

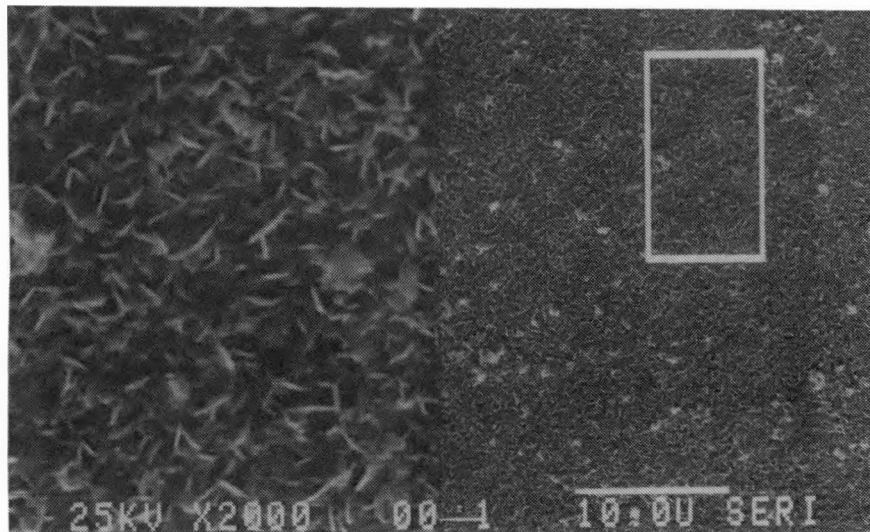


Fig. 1b. SEM picture of a Cd deposit obtained from an electrolyte containing brightener additives. Coverage is much better than Fig.1a.

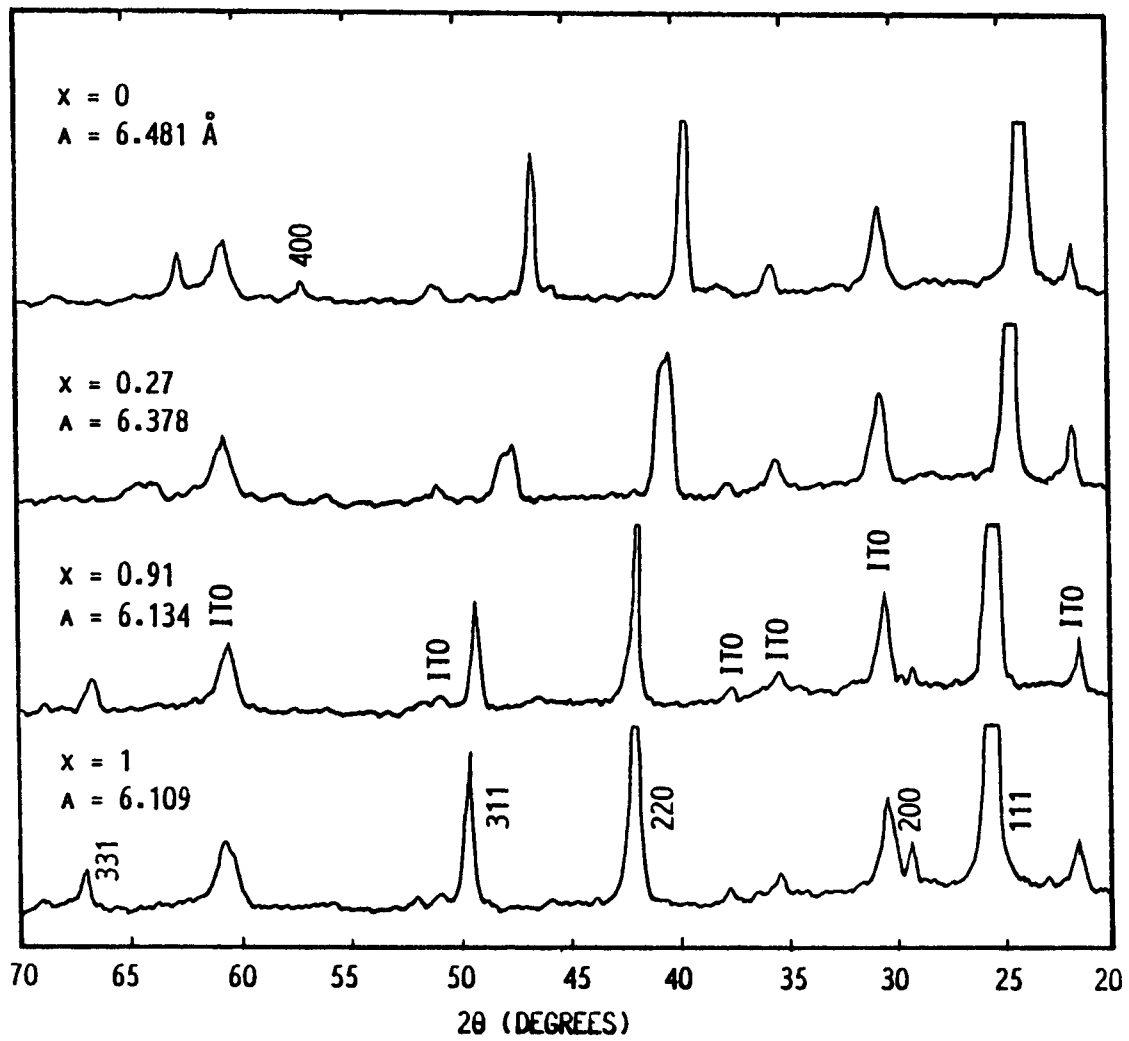


Fig. 2. X-Ray diffraction data taken for  $Cd_{1-x}Zn_xTe$  films prepared by the two-stage process. "A" is the determined unit cell dimension.

Sample #	x	Resistivity (ohm-cm)			
		Undoped		Doped	
		Dark	Illuminated	Dark	Illuminated
18	1	$3 \times 10^3$		$6 \times 10^{-1}$	
26	0.8	$5 \times 10^3$		25	
22	0.4	$> 10^5$	$10^5$	$7 \times 10^3$	$4 \times 10^3$
21	0.2	$> 10^5$	$> 10^5$	$> 10^5$	$4 \times 10^4$

Table 1. Resistivity values for  $\text{Cd}_{1-x}\text{Zn}_x\text{Te}$  films deposited by the two-stage process. Illumination intensity was 100 mW/cm<sup>2</sup>.

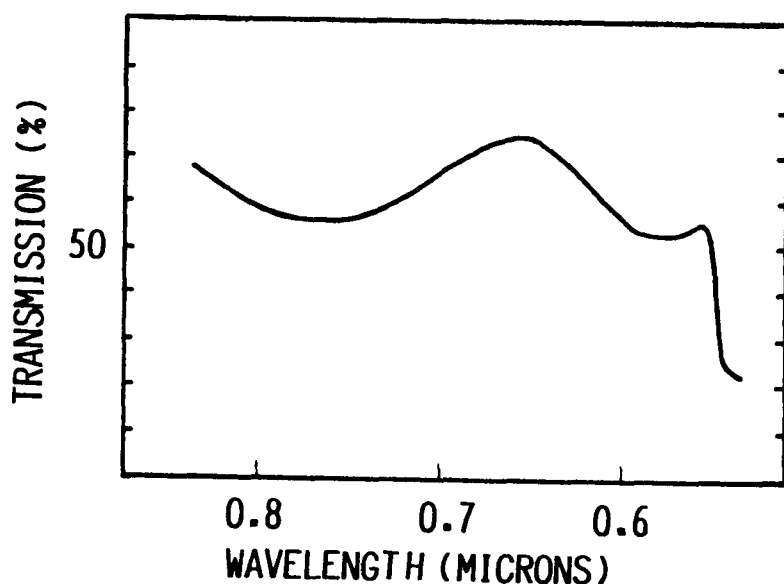


Fig. 3. Optical transmission of Sample 18 (see Table 1). Bandgap value is 2.25 eV.

**Title:** Hydrogen Radical Enhanced Growth of Solar Cells

**Organization:** Electrical Computer and Systems Engineering Department, Rensselaer Polytechnic Institute, Troy, New York

**Contributors:** S. K. Ghandhi, J. M. Borrego, J. Iacoponi, S. Nellenback and M. S. Wang

The objective of this program is to explore the use of free radicals for the OMVPE growth of solar cell materials and structures. Indium phosphide was chosen as the growth material since it has many photovoltaic applications and because it is very sensitive to deterioration if grown at high temperatures. The free radicals can help OMVPE epitaxial growth in two distinct ways. First, they can help the substrate cleaning process before growth by removing any free oxides which may have been left from the wet chemical etching before epitaxy. Second, the free radicals can be used for enhancing the breakdown of the metal-organic bond to allow the growth reactions to occur at lower temperatures.

**Epitaxial Growth Reactor**

A microwave system was designed and constructed for the generation of  $H\cdot$  and  $He\cdot$  in the 1-2 Torr range. An S-band magnetron operating at 2.45 GHz can supply up to 100 W of microwave power to a critically coupled coaxial microwave cavity for the generation of a microwave plasma. A low pressure OMVPE reactor has been designed and constructed to be used with the microwave generated radical species. It operates on the 1-10 Torr range and has a glove box to prevent exposing the reaction chamber to ambient during the load/unload cycle. A schematic diagram of the reactor is shown in Fig. 1. The reactor is a vertical type reactor with a resistance heated susceptor. The microwave cavity which generates the  $H\cdot/He\cdot$  radicals is placed just before the reaction chamber and the generated radicals enter the chamber by one of its sides. The phosphorus source is pure  $PH_3$  and the indium source is TMI through which  $H_2$  carrier gas is passed. The exhaust gases are trapped in a liquid nitrogen cold trap and then passed through a series of wash bottles to remove harmful species before discharging to the atmosphere.

A quantitative and qualitative analysis of the plasma generated was performed in order to characterize the system. A Langmuir probe was used to measure electron temperature and density at the susceptor. The density but not the temperature of the electrons in the plasma increases with increased RF power and with decreased pressure.

**Growth Results**

Growth runs have been performed and the system is performing satisfactorily. All growth has been on SI InP and the epitaxial layers grown have been in the 1-2  $\mu m$  thickness range. Experiments were performed to determine the effect of  $H\cdot$  and  $He\cdot$  on substrate cleaning. Growth at low temperature, without the free radicals, is very sensitive to surface contamination resulting in a nucleation period of

uncontrolled duration and a growth rate varying from run to run. We have found that a cleaning step with either plasma prior to conventional growth, eliminates this problem. The duration of the cleaning step is more critical with  $H\bullet$  than with  $He\bullet$ . The reason being that too long a cleaning step with  $H\bullet$  tends to selectively remove the P from the InP causing indium droplet formation on the InP surface.

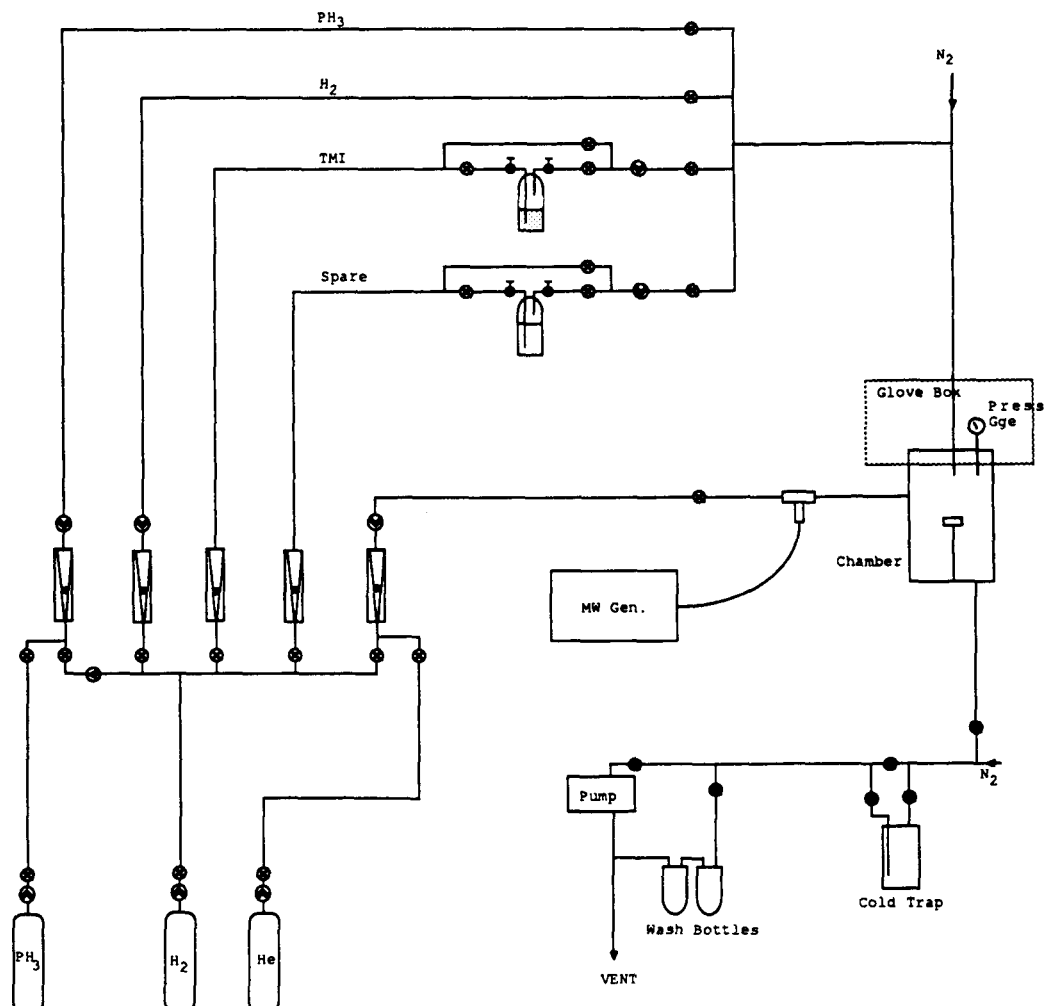
A series of runs with and without  $He\bullet$  were made in order to determine the growth rate vs  $1/T$  curve and it is shown in Fig. 2. The above curve shows that the  $He\bullet$  does not change the growth rate above  $500^\circ C$ . At low temperatures, the growth seems to be very dependent on the initiation process and tends to be highly variable when no plasma is used. The activation energy for no plasma growth is 4-6 kcal/mole while for plasma growth it drops to 2-3 kcal/mole.

#### **Layer Evaluation**

The grown layers have been characterized by both optical and scanning electron microscopy. The morphology of the layers was generally good with the layers grown at lower temperatures appearing better as well as those grown with the  $He$  plasma. All the layers grown were n-type and n-p conversion with decreased V/III ratio is not seen as is the case for GaAs.

#### **Conclusions and Recommendations**

The results obtained thus far indicate that the use of  $He$  plasma stabilizes the OMVPE growth of InP at low temperatures. It is believed that it is caused by a more effective removal of contamination prior to growth. We have found that  $He\bullet$  is to be preferred over  $H\bullet$  during the clean step because it avoids the selective etching of P on the InP. The main thrust in any follow-up work should be directed toward evaluating the quality of the layers for high efficiency solar cell fabrication. In particular measurement of excess minority carrier lifetime and fabrication of solar cells should be carried out in order to assess the usefulness of the technique for achieving high efficiency solar cells.



- Bellows Valve
- Needle Valve
- Check Valve
- Regulator
- Ball/Plug Valve

Fig. 1 - Schematic Diagram of InP OMVPE Microwave Generated Plasma Reactor.

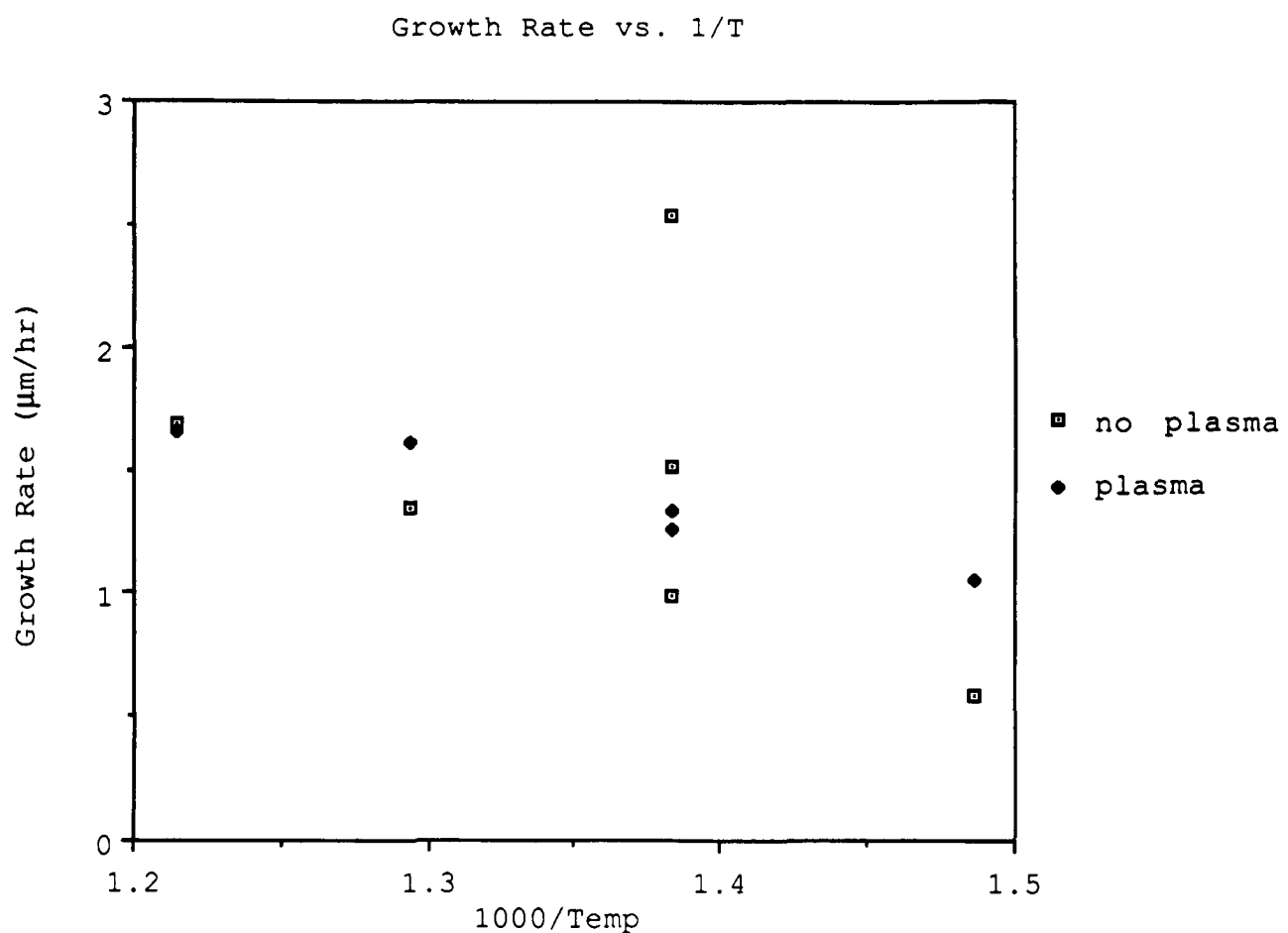


Fig. 2 - Indium Phosphide Growth rate vs  $1/T$  with and without He plasma.

Title: High Efficiency Flat-Plate Silicon Solar Cells

Organization: Stanford Electronics Laboratories, McCullough 204,  
Stanford, CA 94305 (U.S.A) (415) 723-0503

Contributors: R. M. Swanson, R. R. King

This report describes two new types of large-area ( $> 8.5 \text{ cm}^2$ ), backside, point-contact solar cells with doped surfaces, designed for use in unconcentrated sunlight. One type was fabricated on an intrinsic substrate with an optimized phosphorus diffusion on the sunward surface. The apertured-area efficiency was independently measured to be 22.3% at one sun (0.100 W/cm<sup>2</sup>), 25°C, the highest reported for a silicon solar cell. The other type is constructed on a doped substrate, and has an apertured-area efficiency of 20.9%, the highest reported for a point-contact solar cell with a base in low-level injection. Both cells have record open-circuit voltages above 700 mV.

## Introduction

The goal of this research program is to investigate the ways in which the point-contact solar cell may be optimized for one-sun operation. Point-contact solar cells were originally designed as concentrator cells, and have achieved 28% efficiency at 150 suns (15 W/cm<sup>2</sup>), 25°C[1]. Efficiencies of 22.2% at one sun (0.1 W/cm<sup>2</sup>) have been reported for concentrator cells of the point-contact type with a 0.15 cm<sup>2</sup> area [2] [3] [4], even though the design was optimized for an incident intensity more than 2 orders of magnitude greater than one sun. The most important physical phenomena that must be considered when reoptimizing the point-contact cell for one-sun operation are: the rapid drop in voltage with decreasing incident intensity observed in standard point contact cells; the optimum surface and bulk doping concentrations to achieve the longest possible lifetime of carriers in the cell; and the parasitic perimeter recombination. These points are addressed in references[5] and [6].

## Background

By introducing a planar dopant diffusion at the surface of a solar cell, thereby creating a built-in electric field that repels one type of carrier from the surface, it is possible to reduce surface recombination in the cell [7] [8]. The architecture of a point-contact solar cell that incorporates this concept is shown in Figure 1, where the shaded regions at the front (sunward) and back surfaces indicate planar dopant diffusions. To construct the best possible cell of the type with planar diffusions on a highly-injected substrate, the  $J_o$  of the diffusions must be minimized. A matrix of test structures has been fabricated to measure the  $J_o$  of phosphorus diffusions at an oxidized silicon surface, for both textured and untextured surfaces, for a range of surface doping concentrations, and for two different drive-in and oxidation schedules [5]. It was observed that  $J_o$  tends to decrease with decreasing phosphorus concentration in the doped glass, for a given furnace schedule. This

indicates that for the range of doping levels covered in this study, lower surface phosphorus concentration,  $N_{D,surf}$ , yields lower values of  $J_o$ .

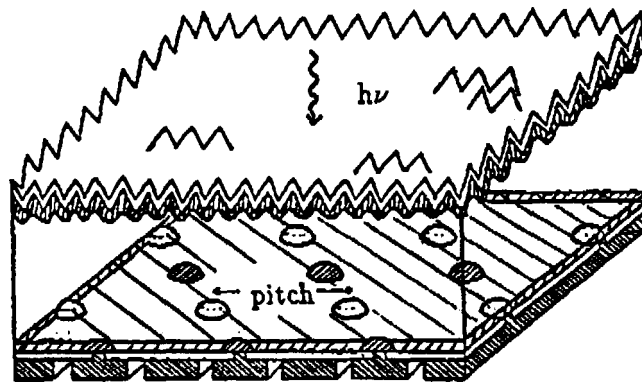


**Figure 1.** A cross-section of a textured, point-contact solar cell, with front and back surface diffusions.

Standard point-contact cells have a substrate which is in high-level injection (HLI), and the rate of the dominant recombination mechanism (Shockley-Read-Hall recombination at the undoped surface) is proportional to  $n$ , the carrier concentration in the cell. Under these conditions, the diode ideality factor of the cell is approximately equal to 2. So the cell will have a lower maximum-power voltage than a cell with the same open-circuit voltage,  $V_{oc}$ , but with an ideality factor of 1. To lower the ideality factor, and thereby increase the fill factor, the cell substrate can be doped so that the cell is in low-level injection (LLI) at one sun. For this more conventional structure, the ideality factor is close to unity. An alternative method is to use a high-resistivity, highly-injected substrate with planar dopant diffusions on one or both sides. The surface recombination rate at a planar diffusion on an HLI substrate is proportional to  $n^2$ , rather than  $n$  [8], bringing the ideality factor of the cell closer to unity for this case as well. A further advantage of surfaces with planar diffusions is that the recombination rate at carrier concentrations that are typical of one-sun operation can be made lower than for an undoped surface, allowing higher values of  $V_{oc}$ . Open-circuit voltages greater than 700 mV have been measured for point-contact cells both with a substrate in LLI, and with HLI substrates that have a planar diffusion on the front surface.

## Cell Results

Large-area ( $> 8.5 \text{ cm}^2$ ), backside, point-contact solar cells were fabricated on high-resistivity ( $100 \Omega \cdot \text{cm}$ ,  $N_D \approx 4 \times 10^{13} \text{ cm}^{-3}$ ) substrates, with a textured front surface, and a planar phosphorus diffusion on the front surface only [5] [6]. The substrate of this type of cell is in high-level injection (HLI) at one sun. The open-circuit voltage of one such cell, called OS7-G, is 706 mV at  $0.100 \text{ W/cm}^2$ ,  $25^\circ\text{C}$ , as measured at the Solar Energy Research Institute (SERI). Figure 2 shows the illuminated I-V characteristics of this  $197 \mu\text{m}$  thick cell. A standard  $0.15 \text{ cm}^2$  point-contact cell designed for concentrated sunlight, with undoped surfaces, has achieved a  $V_{oc}$  of 681 mV at  $0.100 \text{ W/cm}^2$ ,  $24^\circ\text{C}$  [3], indicating that the sunward planar diffusion in cell OS7-G reduces recombination significantly. The sheet resistance of the planar diffusion on the front surface of cell OS7-G is  $760 \pm 160 \Omega/\square$ , and the  $J_o$  of the planar diffusion is  $\sim 4 \times 10^{-14} \text{ A/cm}^2$  as measured on a test structure. At the carrier concentration corresponding to the cell's maximum-power voltage, this is equivalent to an effective surface recombination velocity of  $1.6 \text{ cm/s}$ , much lower than the typical values of 5 to  $15 \text{ cm/s}$  observed on undoped, textured surfaces. A planar diffusion on the back side should increase  $V_{oc}$  even further, but more work is needed to solve the difficulties in fabricating a point-contact cell with a planar diffusion of the correct dose on the back side.

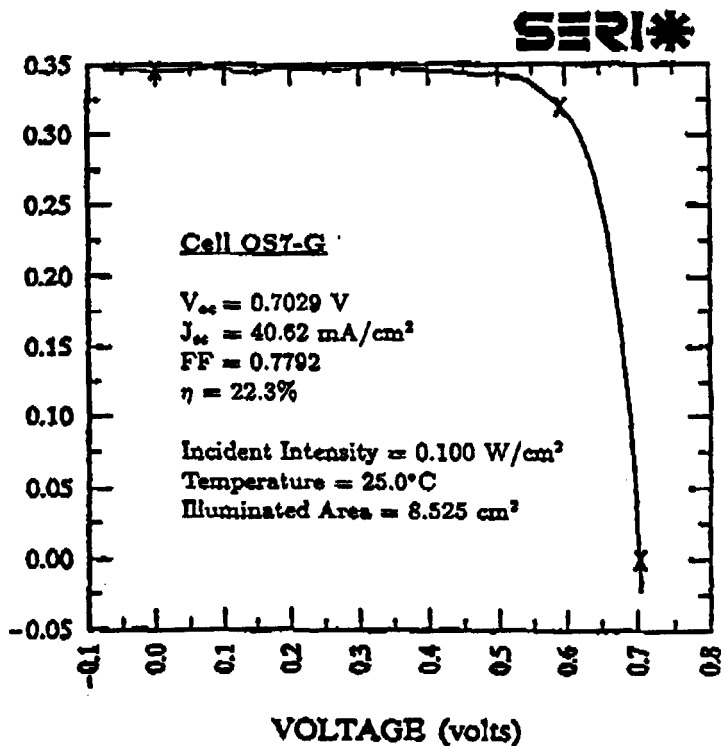


**Figure 2.** Illuminated I-V curve of cell OS7-G at  $0.100 \text{ W/cm}^2$ ,  $25^\circ\text{C}$ , as measured at SERI. Cell OS7-G is a cell with a high resistivity substrate, a textured front surface, and a lightly doped, planar, phosphorus diffusion on the front surface only. This diffusion is used only as a passivation.

An apertured-area efficiency of 22.3% at one sun ( $0.100 \text{ cm}^2$ ),  $25^\circ\text{C}$  was measured at SERI for cell OS7-G, referenced to the illuminated area of  $8.525 \text{ cm}^2$ . Of course, the cell has no metal grid in this region since it is a backside-contact cell. The fill factor was measured to be 0.779, and the responsivity (the short-circuit current density,  $J_{sc}$ , divided by incident intensity) was  $0.406 \text{ A/W}$ . To the best of our knowledge, the highest previously reported apertured-area efficiency for a silicon solar cell at one sun is 22.2% at  $0.100 \text{ W/cm}^2$ ,  $24^\circ\text{C}$  [2][3][4], measured on cells designed for concentrated sunlight, with apertured areas smaller than  $0.2 \text{ cm}^2$ . For comparison, the highest total-area efficiency that has been reported for a silicon solar cell at one sun is 21.4% [9].

The efficiency measured for cell OS7-G is all the more remarkable since this cell is far from optimized. The mask set used to fabricate the cell was designed for a cell with an n-type substrate in low-level injection, and has 7 times more p-type contacts than n-type contacts. Unfortunately, this geometry is inappropriate for use on a highly-injected substrate, because it makes the current crowding voltage drop around the n-type emitters much larger than it needs to be. Were it not for this effect, the fill factor would be significantly higher than the measured value of 0.7792 for cell OS7-G.

Point-contact cells with an n-type substrate ( $0.2\text{-}0.3 \Omega\text{-cm}$ ,  $N_D \approx 2.4 \times 10^{16} \text{ cm}^{-3}$ ) in low-level injection (LLI) were also fabricated [6]. The bulk lifetime of this material is  $\sim 900\mu\text{s}$ , compared to  $\sim 5000\mu\text{s}$  in  $100 \Omega\text{-cm}$  silicon. This case is similar to a highly-injected substrate with planar dopant diffusions on both sides, since the hole and electron quasi-fermi levels are approximately constant across the substrate, and the all-important surfaces are in low-level injection for both of these cases. The I-V curve of one such cell, called OS5-3, is shown in Figure 3. It has a textured front surface, an apertured area of  $8.506 \text{ cm}^2$ , and a thickness of  $186 \mu\text{m}$ . This cell was measured to have an open-circuit voltage of  $0.703 \text{ V}$ , a fill-factor equal to 0.841, a responsivity of  $0.353 \text{ A/W}$ , and an apertured-area efficiency of 20.9%, at  $0.101 \text{ W/cm}^2$ ,  $25^\circ\text{C}$ , at Stanford University under natural sunlight. The responsivity of cell OS5-3 was referenced to the value of responsivity measured at SERI for cell OS7-G. The main advantage of this type of cell over one with a base in HLI is the increase in fill factor that results from the low diode ideality factor of a cell with an LLI substrate.

Another point-contact cell with a substrate in LLI, an untextured front surface, and an area of  $8.900 \text{ cm}^2$ , has a  $V_{oc}$  of  $0.709 \text{ V}$  at  $0.100 \text{ W/cm}^2$ ,  $25^\circ\text{C}$ , as measured at SERI [5]. Unfortunately, its efficiency was limited by series resistance. To the best of our knowledge, this cell, along with cells OS7-G and OS5-3, have higher open-circuit voltages than any previously reported silicon solar cells, as opposed to a test structure [10].

The authors would like to thank B. L. Sopori and Keith Emery of the Solar Energy Research Institute for measuring the cells discussed in this paper. This work was supported by SERI and Sandia National Laboratories.

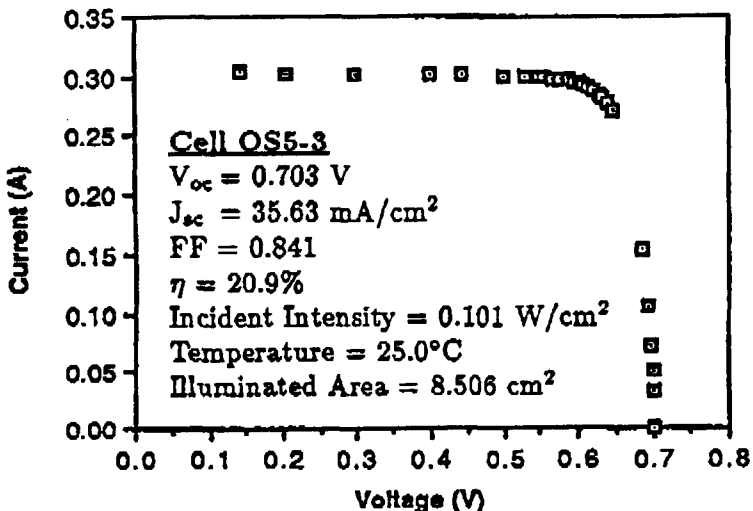


**Figure 3.** Illuminated I-V curve of cell OS5-3 at  $0.101 \text{ W/cm}^2$ ,  $25^\circ\text{C}$ , as measured at Stanford University under natural sunlight. Cell OS5-3 is a point-contact cell built on a uniformly phosphorus-doped substrate with  $N_D \approx 2.4 \times 10^{16} \text{ cm}^{-3}$ . The front surface is textured.

## References

- [1] R. A. Sinton and R. M. Swanson, *IEEE Trans. Electron Devices*, **ED-34**, 2116 (1987).
- [2] M. A. Green, Z. Jianhua, A. W. Blakers, M. Taouk, and S. Narayanan, *IEEE Electron Devices Lett.*, **EDL-7**, 583, (1986).
- [3] R. A. Sinton, Y. Kwark, J. Y. Gan, and R. M. Swanson, *IEEE Electron Devices Lett.*, **EDL-7**, 567, (1986).
- [4] The efficiency reported in [3], measured at Sandia National Labs, was later graded down to 21.7% after publication. The same cell was measured to be 21.9% efficient at SERI.
- [5] R. R. King, R. A. Sinton, R. M. Swanson, in *Conference Record, IEEE 20th Photovoltaic Specialists Conference, Las Vegas, NV, September 1988*, (IEEE, New York, 1988).
- [6] R. R. King, R. A. Sinton, R. M. Swanson, submitted for publication to *Appl. Phys. Lett.* (1989).
- [7] S.-Y. Chiang, B. G. Carbajal, and G. F. Wakefield, in *Conference Record, IEEE 19th Photovoltaic Specialists Conference, Washington, D. C., June 1978*, (IEEE, New York, 1978), p.1290.
- [8] D. E. Kane and R. M. Swanson, in *Conference Record, IEEE 18th Photovoltaic Specialists Conference, Las Vegas, NV, October 1985*, (IEEE, New York, 1985), p.578.
- [9] M. A. Green, J. Zhao, A. Wang, X. Dai, A. Milne, C. M. Chong, F. Zhang, A. Sproul, and A. W. Blakers, in *Joint Crystalline Cell Research and Concentrating Collector Projects Review, Sandia Report SAND88-0522, UC-270, Albuquerque, NM, July 1988*, (NTIS, Springfield, VA, 1988), p.215.
- [10] E. Yablonovitch, T. Gmitter, R. M. Swanson and Y. H. Kwark, *Appl. Phys. Lett.*, **47**, 1211 (1985).

**Title:** Performance of MBE Solar Cells

**Organization:** Department of Electrical Engineering, Howard University,  
Washington, DC 20059

**Contributors:** M. G. Spencer, principal investigator, L. Meyers, and R. Morrell

Molecular beam epitaxy (MBE) has proven to be an excellent system for obtaining epitaxial layers with precise thickness and compositional control. Using this growth technique, it is possible to investigate innovative concepts utilizing "tailored" potential barriers to increase solar cell efficiency. However, in order to obtain the maximum efficiency from MBE material, it is necessary to find the conditions for crystal growth that will optimize solar cell performance. Howard University has continued the growth and fabrication of MBE solar cells, and has found that using p<sup>+</sup> layers with excessive doping concentrations or low substrate temperatures, or both, produce solar cell wafers with low efficiency or low yield, or both. Researchers believe that the reason for this result is the mechanism of Be incorporation. Photoluminescence of Be-doped MBE layers has indicated that poor-quality layers result from high doping levels or low substrate temperatures, or a combination of these [1]. This work suggests that Be may be incorporated on interstitial sites under these growth conditions [1,2]. Such incorporation is controlled by growth temperatures and Fermi-level position. Howard University has found that its best results occurred for a growth temperature of 700°C, a p<sup>-</sup> layer concentration of  $2 \times 10^{16} \text{ cm}^{-3}$  and a p<sup>+</sup> concentration of  $1 \times 10^{18} \text{ cm}^{-3}$ . High doping in the p<sup>+</sup> layer seems to affect the p<sup>-</sup> layer by out-diffusion of defects. With these growth conditions, we have obtained solar cell efficiencies in excess of 11% (without AR coating).

### Characterization of MBE Solar Cells

Previously, we had characterized our solar cells by time resolved, photoluminescence and efficiency measurements. It was found that the efficiency of the cells was dependent on the concentration of the p<sup>+</sup> layer and the growth conditions of that layer. In order to pursue this result, we have done extensive characterization of the p-type MBE layers by DLTS.

### DLTS Measurements [3]

Metastable defects have been studied by deep-level transient spectroscopy (DLTS) in a variety of semiconductors, including Si[4], InP, and Al<sub>x</sub>Ga<sub>1-x</sub>As. We have studied the metastable defect in p-type Al<sub>x</sub>Ga<sub>1-x</sub>As which was grown by molecular-beam-epitaxy (MBE). The metastability was observed during a study of the defects in p- and n-type Al<sub>x</sub>Ga<sub>1-x</sub>As as a function of the MBE growth parameters. Optically detected magnetic resonance (ODMR) measurements were also carried out in search of spectra which could be correlated with the DLTS. Other results from this growth study have already been reported.

The defects studied here are hole traps in Be-doped Al<sub>x</sub>Ga<sub>1-x</sub>As, with activation energies between 0.2 eV and 0.5 eV above the valence band. Different DLTS spectra are observed depending upon whether the sample is cooled to 90° K from a high temperature with zero bias or a reverse bias applied to it. The effect has been observed to be completely reversible, which is an important characteristic of a metastable defect. The properties of the defects described here are similar to those reported by Chantre for iron-aluminum centers in Si[4]. In the Si work, the system is modeled as n interstitial iron which can reside at either of two locations relative to an aluminum acceptor. In thermal equilibrium, the iron will reside at the lattice site with the lowest total electronic plus lattice coordinate energy. For one charge state this energy will be a minimum at one site, and for another charge state it may have a minimum at another lattice location. The model also

requires an energy barrier between the two states, which controls the rate at which the defect will move between the sites.

DLTS experiments are able to study metastable defects because the technique probes defects in the depletion region of a diode. By setting the voltage across the diode it is possible to move the edge of the depletion region and change the charge state of defects there. Since it is expected that the metastable defect's motion from one lattice site to another is an activated process, annealing experiments can be used to study the kinetics of the motion. The first step in these experiments is to set the defect at a specific lattice site by putting it in one of the charge states. This is done by applying either a small forward bias or a reverse bias to the diode at a high temperature. After cooling to an intermediate temperature, the bias is changed, causing the defect to either emit or capture a hole. Because of the energy barrier, there is a finite rate with which the defects will move from the high energy state to the lower one. In an isochronal annealing experiment, the sample is maintained at the intermediate temperature for a period of time and then it is quickly cooled to liquid nitrogen temperatures. The DLTS data are then recorded on warming the sample. The defects studied here appear to be multistable as several peaks are observed indicating that the interstitial may reside at more than two locations.

The interest in using MBE to grow heterostructure devices with abrupt profiles has led to studies of Be diffusion in GaAs and AlGaAs[5-7], and the effect of Be on disordering of superlattices[8,9]. These results are often discussed in terms of an interstitial-substitutional model for Be diffusion, particularly when doping to Be concentrations greater than  $10^{18} \text{ cm}^{-3}$ . These results suggest a connection between the metastable defect and interstitial Be.

## Current Experimentation

Samples have been grown with varying concentrations of p<sup>+</sup> material and secondary layers of p<sup>-</sup> material. DLTS studies have been conducted to see whether defects produced in the p<sup>+</sup> layers have diffused into the p<sup>-</sup> regions. In preliminary results, we have observed the presence of these defects. We believe that understanding the roles of these defects in reducing the efficiency of solar cells will allow for the production of higher quality ones in the future.

## References

1. Duhamel, N., P. Henoc, F. Alexandre, and E. K. Rao, *App. Phys. Lett.*, **39**(1), 1981, p. 49.
2. Woodall, J. private communication.
3. R. Magno, R. Shelby and T. A. Kennedy, M. G. Spencer, *Metastable Defects in Be Doped Al<sub>x</sub>Ga<sub>1-x</sub>As*, in press, 1989.
4. A. Chantre in Defects in Electronic Materials, edited by M. Stavola, S. J. Pearton, and G. Davies (Materials Research Society, Pittsburgh, 1988), p. 37.
5. D. C. Miller and P. M. Asbeck, *J. Appl. Phys.* **57**, 1816 (1985).
6. J. N. Miller, D. M. Collins, and N. J. Moll, *Appl. Phys. Lett.* **46**, 960 (1985).
7. P. Enquist, G. W. Wicks, L. F. Eastman, and C. Hitzman, *J. Appl. Phys.* **58**, 4130 (1985).
8. M. Kawabe, N. Shimizue, F. Hasegawa, and Y. Nannachi, *Appl. Phys. Lett.* **46**, 849 (1985).
9. N. Kamata, K. Kobayashi, K. Endo, T. Suzuki, and A. Misu, *Jpn. J. Appl. Phys.* **26**, 1092 (1987)

## 7.0 UNIVERSITY PARTICIPATION PROGRAM

J. Benner (Manager) and C. Leboeuf

The objective of this program is to maximize the contribution of universities to the future of photovoltaic technology by focusing on the traditional needs and strengths of that community. Thus, it provides a forum in which the university researchers identify research topics critical to the advancement of photovoltaic technology with minimal influence from current programmatic interests. The participants are then permitted to pursue proposed basic and applied research ideas in an environment designed to foster creativity by limiting requirements for delivery of reports and samples and achievement of specific goals. Reporting is limited to annual reports and journal publications. Research symposia, organized by the participants, are held periodically and are open to all students, program participants, and outside researchers. The intent of the initiative is to provide continuity of funding over a minimum three-year period to allow universities to build and support interdisciplinary teams with specialized expertise that can be applied to furthering the technology base of photovoltaics. Such a program is expected to attract the most highly qualified university research teams to the DOE National Photovoltaics Program. The University Participation Program also supports the photovoltaic industry through the technology transfer that occurs not only by the publication of research results in the technical literature, but also through enhanced student awareness of photovoltaic technology and the education of future professionals.

During FY 1988, SERI issued the third solicitation for letters of interest in order to initiate new subcontracts in FY 1989. Existing participants, whose subcontracts were awarded in 1986 and 1987, needed to respond to the competition in order to seek a continuation of their projects. The periods of performance of existing subcontracts were adjusted as necessary to permit continuity of funding if proposers were successful in the current competition. The technical review and selection process will be performed using review teams consisting predominantly of other university professors and industrial research scientists.

**Title:** Low Temperature MOCVD Processes for High Efficiency Solar Cells

**Organization:** University of Southern California, Los Angeles, CA 90089-0483

**Contributors:** P. Daniel Dapkus, Principal Investigator, S. P. DenBaars, B. Y. Maa, W. G. Jeong, Q. Chen

## Introduction

Metalorganic chemical vapor deposition (MOCVD) is widely used to fabricate high efficiency III-V solar cells. The process suffers the disadvantages of being carried out at relatively high temperatures and inefficiently utilizes highly toxic precursors. These characteristics frustrate attempts to fabricate multijunction solar cells and create extra hazard and cost, respectively. This program is directed to resolve these difficulties by providing a better understanding of the gas phase and surface kinetics of MOCVD, by exploring techniques for low temperature growth of III-V materials and device structures, and by exploring photoenhanced MOCVD processes.

## Gas Phase Chemistry of MOCVD Precursors

During the past year we have made operational a molecular beam mass spectrometer to examine *in situ* the gas phase decomposition of MOCVD precursors. The apparatus has been used to corroborate our earlier measurements and conclusions based upon *ex situ* IR measurements. (See Figure 1.)

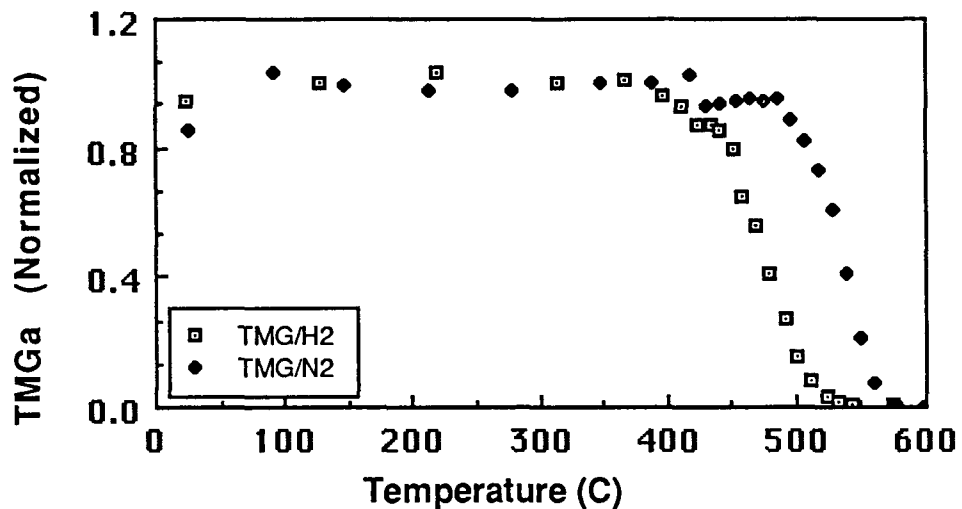


Fig. 1 - Temperature dependence of the TMGa concentration in H<sub>2</sub> and N<sub>2</sub>.

The sequence of reactions leading to the decomposition of trimethylgallium (TMGa) in various carrier gases has been examined in some detail. By comparing the reaction product concentrations from the decomposition of TMGa in H<sub>2</sub> and N<sub>2</sub>, we have been able to show that the decomposition in H<sub>2</sub> results from both homolytic fission of CH<sub>3</sub> radicals and from the attack of TMGa by H radicals. This has been demonstrated by observing that the activation energy for decomposition is a function of the TMGa/H<sub>2</sub> ratio as shown in Table I.

Table I Rate Constants (  $\ln K = A + \frac{E_a}{RT}$  )

[TMGa] [H <sub>2</sub> ]	0.00304	0.0171	0.0803	$\infty$
A	31.3	31.7	31.7	37.9
E <sub>a</sub> (kcal/mole)	50.9	51.5	54.8	64.6

### Surface Processes in Low Temperature MOCVD

The data obtained in this program and recent data on the decomposition of AsH<sub>3</sub> the presence of GaAs substrates<sup>1,2</sup> indicates that the the decomposition of the organometallic will limit the growth rate of III-V's at low temperatures. It is thus important to understand the heterogeneous decomposition of TMGa. To do so we have employed both direct and empirical approaches. Direct measurements of saturated monolayer Ga depositions on InAs has been observed by XPS using our deposition/surface analysis system. By measuring the magnitude of the Ga signal versus TMGa exposure time, we were able to determine the exposure necessary for monolayer coverage. In addition we were able to determine that these deposits contained no detectable C, indicating that the Ga species contained no CH<sub>3</sub> radicals. Since these results are contrary to our ALE results, we believe that this observation is a consequence of our inability to rapidly quench the substrate temperature between exposures. As a result we are setting up a real time surface analysis capability based on reflection difference measurements<sup>2</sup> to add to our current system.

### ALE Growth of GaAs

Atomic layer epitaxy (ALE) is a low temperature surface controlled regime of MOCVD in which the substrate is alternately exposed to the III and V precursors to effect growth. We have extended the work on the growth of III-V compounds by ALE reported last year to include InAs, GaAs, and InP. We have, in particular, extended the thermal ALE of GaAs to lower temperatures (370°C) and we have investigated the photoassisted growth of GaAs by ALE at similar temperatures. This allows us to compare the kinetics of growth in the two regimes. We have observed that the kinetics of thermally driven ALE are limited at these temperatures by steric hindrance effects. At these low temperatures, the initial Ga adsorbate contains excess alkyl radicals that physically block adjacent

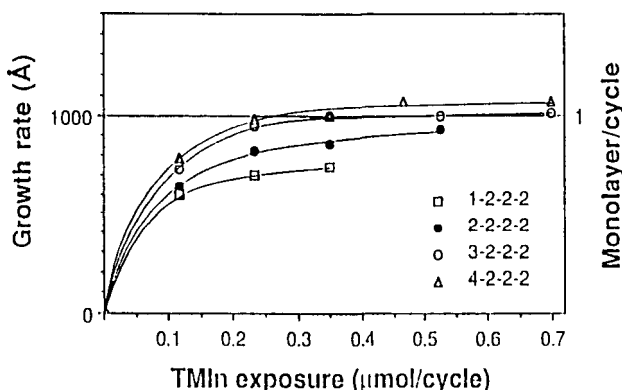


Fig. 2 - Dependence of growth rate of InAs upon TMIn exposure for various exposure times.

lattice sites and limit the coverage to less than a full monolayer. The decomposition or desorption of this adsorbate must occur before the sites so blocked are available for adsorption of further Ga adsorbates. The time for this to occur is several seconds at 370°C. A similar effect is observed in the ALE growth of InAs at 340°C. This is shown in Fig.2 where we show the growth rate as a function of the TMIn exposure for various exposure times. Note that as long as the alkyl exposure time is less than some threshold time, less than one monolayer is grown per exposure cycle.

The threshold time can be drastically reduced by exposing the substrate to visible light during the III exposure. In the case of GaAs at 370°C one monolayer can be formed in less than 10 msec with a light intensity of 200 W/cm<sup>2</sup>.<sup>3</sup> Under these conditions, the AsH<sub>3</sub> reaction becomes the rate limiting step. We are currently exploring the effects of UV irradiation during the arsine exposure as a means to enhance the growth rate.

### **Conclusions and Future Work**

Photoassisted ALE appears to be a practical means to grow GaAs at low temperatures. The inherent uniformity of the process and the potential for scale up are motivation to study further the limits to the achievable growth rate and the fundamental growth mechanisms.

**Title: Improvement of Bulk and Epitaxial III-V semiconductors for Solar Cells by Creation of Denuded Recombination Zones**

**Organisation:** Department of Electrical and Computer Engineering, Carnegie Mellon University, Pittsburgh, Pennsylvania

**Contributors:** A. G. Milnes and T. E. Schlesinger, principal investigators, A. Li, Z-Q Fang, D. Wong and H. K. Kim.

Short diffusion lengths are an important limiting factor in the performance of solar cells made from III-V semiconductor materials. CMU has conducted systematic studies of defect concentrations and diffusion lengths in bulk GaAs in order to identify the carrier-lifetime-limiting defects in n-type GaAs and determine means by which the concentration of these might be reduced. Information on defects was obtained primarily from deep level transient spectroscopy measurements (DLTS) and diffusion lengths were measured with the electron beam induced current (EBIC) technique.

### **Theoretical considerations**

CMU researchers have considered the simple models commonly used to express carrier trapping and recombination action by point defects in terms of capture cross section and capture kinetics. Applying these to the problem of identifying a recombination center in a semiconductor, it is apparent that the degree to which any given defect may act as a recombination center depends on whether the material is n- or p- type. In particular, important recombination centers will be characterized by a "large" minority carrier capture cross section, with a somewhat less stringent requirement on majority carrier capture cross section. This underscores the importance of including minority trap characterization in any comprehensive study aimed at identification of important lifetime controlling centers in any material. A study of majority carrier traps in both n- and p- type material is not equivalent to characterizing both in, for example, n-type material since CMU has found experimentally that the hole traps which can be observed by DLTS in n-type material do not appear in p-type Zn doped material.

The problem of minority carrier injection by electrical means to characterize minority carriers with DLTS was then considered. It was found that DLTS measurements may systematically underestimate the concentrations of minority carrier traps which act as recombination centers if these have majority carrier capture cross sections of magnitude comparable to their minority carrier capture cross sections. (This is true even for arbitrarily long "filling pulses".) Relative concentrations of any given trap as varying between specimens can nevertheless be accurately determined if current density during the carrier-injecting electrical pulse is kept constant. Such considerations also suggest that certain combinations of temperature-varying electron and hole capture cross sections may result in strong variations of DLTS peak height with rate window and this has been observed experimentally.

### **Identification and reduction of lifetime-limiting centers in bulk GaAs**

CMU researchers have investigated the effect of a variety of different treatments on the diffusion lengths in GaAs wafers. The treatments applied included sealed ampoule anneals in the temperature range 600 to 900 °C for times of between 10 minutes and 90 hours on specimens provided with a variety of capping layers -- aluminum and iron films; anodic and thermally grown oxides. Anneals with indium and gallium present in the ampoule were also done. Rapid thermal and sealed ampoule proximity anneals (with two specimens placed polished face to polished face, or one specimen face down on a polished silicon wafer) were carried out, with and without reverse surface damage in the temperature range 900 to 1050 °C for times ranging from 25 seconds to 80 minutes. The effect of exposure to a hydrogen plasma was also examined. The treatment selected for in depth study as the most promising was the proximity anneal, without reverse surface damage.

Figure 1 shows the effect of relatively mild rapid thermal and sealed ampoule proximity anneals on the electron trap structure. The short anneals of 25 to 50 seconds in the chosen temperature range (900 to 1050 °C) were found to result in large changes in the electron trap structure to a depth of at least 10  $\mu\text{m}$  from the wafer surface, with very little change in diffusion length. The 1000° C 16 minute anneal reduced all electron traps except EL2 by at least an order of magnitude to below the detection limits of the apparatus (about  $2 \times 10^{13} \text{ cm}^{-3}$  for the  $1 \times 10^{17} \text{ cm}^{-3}$  Si doped specimens) but resulted in only a 50% improvement in diffusion length. No obvious correlation between EL2 concentration and diffusion lengths was found by examining the data available from these anneals, and from some of the other treatments listed above. From these results, CMU researchers concluded that the defects which manifest themselves as electron traps are not those which limit diffusion lengths in n-material with diffusion lengths of the order of 1  $\mu\text{m}$ .

In order to study hole traps in n-type material, a simple low-temperature method of pn junction fabrication was developed. This involves a zinc evaporation followed by a 5 minute 550 °C diffusion in 10%  $\text{H}_2$  forming gas with the Zn coated polished face of the specimen placed against a silicon slice with an evaporated Zn layer. Indium ohmic contacts are made on the rear surface by an anneal at 330 °C for 1 minute. Diodes are defined by masking off areas with dots of melted apiezon wax, and then mesa etching with a potassium iodide/iodine aqueous solution followed by a bromine/methanol etch.

Hole trap spectra in Si and Te doped liquid encapsulated Czochralski (LEC) and Horizontal Bridgman (HB) wafers obtained from a number of different vendors were studied. Figure 2 shows a typical spectrum, with three traps appearing in the  $10^{15} \text{ cm}^{-3}$  range. The trap labelled HCX was found to be present in all the bulk, n-type specimens examined, whereas HCW only appeared in some specimens, and HCY only in the Si doped specimens, and in varying concentrations depending on the particular crystal. HCX was not found in an n-type Si doped molecular beam epitaxy (MBE) specimen with a pn junction fabricated by the same method as used for the bulk specimens, or in Be doped MBE material or Zn doped LEC material.

Initial data indicates that high temperature anneals change HCX and HCY concentrations by small amounts, roughly comparable to what might be expected from the observed changes in diffusion length. 950 °C anneals for 60 to 80 minutes on Te doped material containing no hole traps other than HCX in the  $10^{15} \text{ cm}^{-3}$  initial concentration range were found to increase diffusion length from an initial value of 0.8  $\mu\text{m}$  before anneal to between 1.7 and 1.9  $\mu\text{m}$  after anneal (Figure 3). Work is currently being done to establish explicitly the relationship between changes in HCX and HCY concentration and diffusion lengths in specimens which have been annealed.

Preliminary measurements of the activation energy and capture cross section of HCX show it to represent an energy level at about  $E_v + 0.3 \text{ eV}$  with a hole capture cross section in the  $10^{-14} - 10^{-15} \text{ cm}^2$  range. Its concentration in material of diffusion length of about 1  $\mu\text{m}$  is in the  $10^{15} \text{ cm}^{-3}$  range. These results strongly suggest that HCX plays an important role in controlling the minority carrier lifetimes in bulk material. The emission line for HCX lies in a position somewhat close to that reported for HL6 and HL11 in earlier studies. CMU researchers believe HCX to be a native defect complex and not a simple impurity defect level.

#### **Hole traps in MBE material**

CMU has described the reduction of electron traps in n-type MBE material by isoelectronic In and Sb doping, and also by increases in growth temperature [1]. This study has now been extended to the case of hole traps in p-type MBE material. The dominant hole trap (ie the hole trap of largest concentration -  $10^{15} \text{ cm}^{-3}$ ) in Be doped (mid  $10^{16} \text{ cm}^{-3}$ ) p-type MBE layers was found

to have an energy level at about  $E_v + 0.56$  eV (H4). This trap was also observed in n-type MBE layers on which p<sup>+</sup>n junctions had been fabricated for DLTS measurements by the method described above. The concentration of H4 was reduced by three orders of magnitude by increasing the growth temperature from 500 to 600 °C but additions of 0.2 to 2% In or Sb for growths at 500 or 550°C were found to have no affect on the concentration of this trap [2]. Another hole trap at  $E_v + 0.29$  (H2) was reduced by isoelectronic doping. The trap H4 is believed to be the antisite defect (As<sub>Ga</sub>) related whereas the other trap is believed to involve vacancies.

### Conclusion

The research has shown from simple models the importance of the study of minority carrier traps. A method of improving diffusion lengths in bulk n-GaAs by high temperature wafer anneals has been demonstrated. Electron and hole traps in n-type bulk GaAs have been studied and the results obtained strongly indicate that a hole trap, HCX, may be responsible for limiting the lifetime in this class of material [3]. Raising the growth temperature has been found to suppress the dominant hole trap in MBE material but isoelectronic doping does not affect the concentration of this trap.

Research is currently under way to determine the limits on improvement of diffusion lengths by high temperature wafer anneals of GaAs. The nature and origin of the traps HCX and HCY are under study, and attempts are being made to verify whether these are indeed the dominant recombination centers in bulk n-type GaAs.

### References

1. A. Z. Li, H. K. Kim, J. C. Jeong, D. Wong, T. E Schlesinger, and A. G. Milnes, Trap suppression by isoelectronic In or Sb doping in Si-doped n-GaAs grown by molecular-beam epitaxy", *J. Appl. Phys.* **64**, 3497 (1988).
2. Aizhen Li, H. K. Kim, J. C. Jeong, D. Wong, J. H. Zhao, Z.-Q. Fang, T. E Schlesinger, and A. G. Milnes, "Trap Gettering by Isoelectronic Doping of p-GaAs and n-GaAs Grown by Molecular Beam Epitaxy", presented at the Int. MBE Conference, Japan, August 1988 and accepted for publication in the Journal of Crystal Growth.
3. Details of the theoretical analysis and the results obtained from defect and lifetime studies on bulk GaAs are in preparation and will be published elsewhere.

Fig. 1. Electron trap reduction as a result of annealing

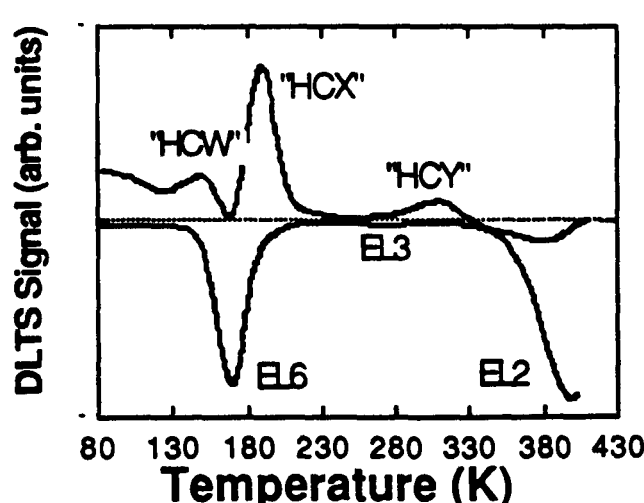
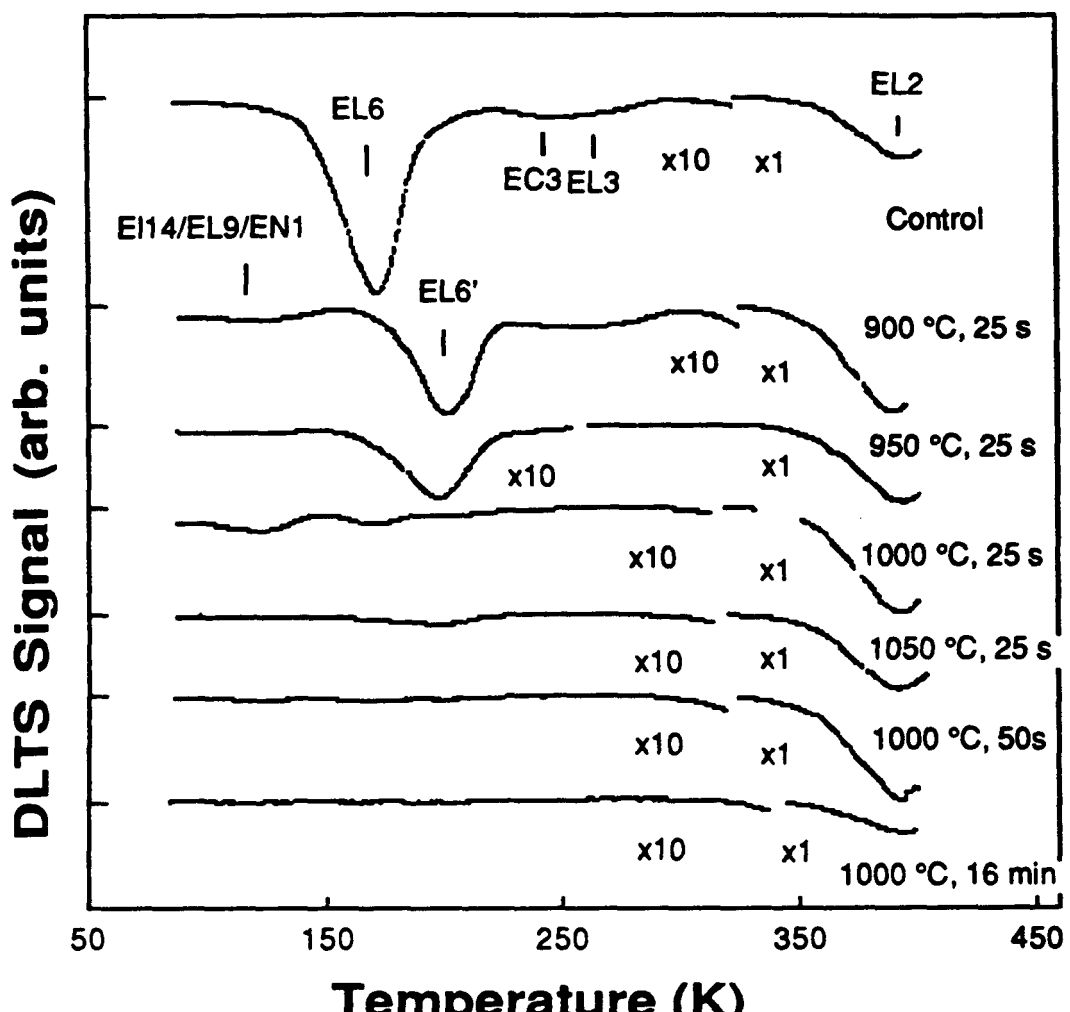


Fig. 2. Hole and electron traps in bulk n-type GaAs

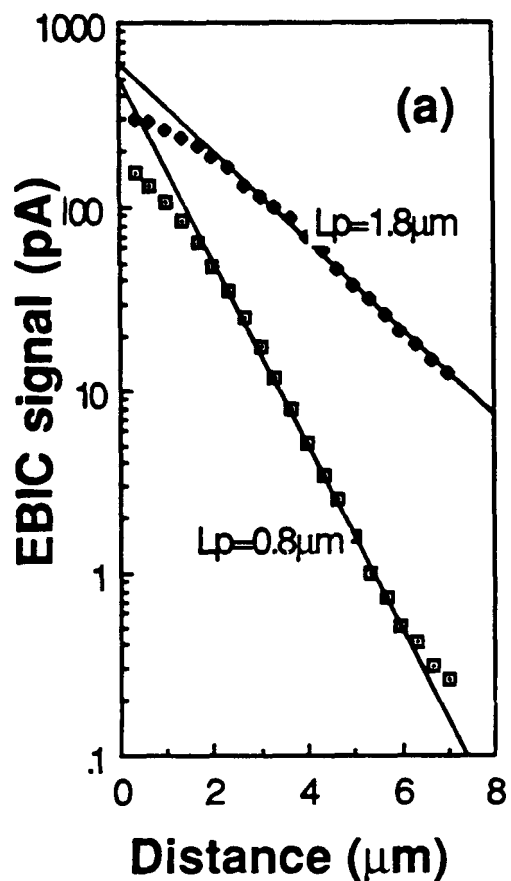
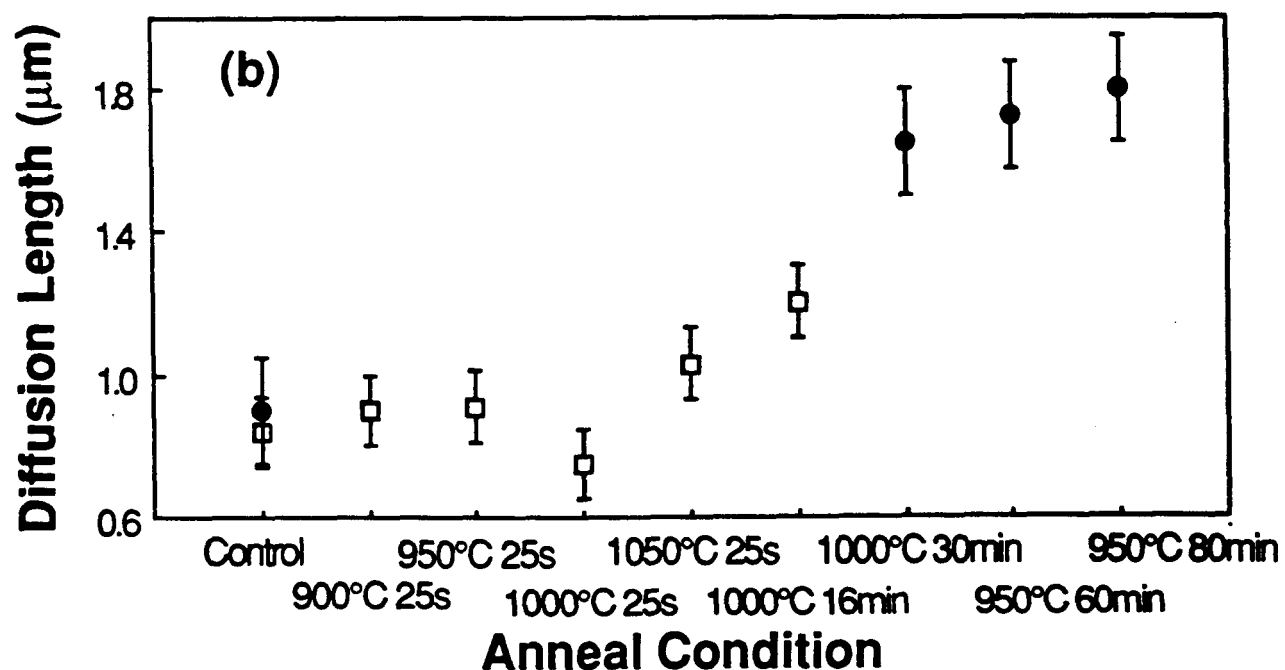


Fig. 3. (a) EBIC data showing an improvement in diffusion length resulting from an 80 minute 950°C anneal

(b) Diffusion lengths as a function of anneal condition. Solid circles represent data from one series of measurements and squares from another series on a different crystal.



Title: Electronic Processes in Thin Film PV Materials

Organization: Department of Physics, University of Utah, Salt Lake City, Utah

Contributors: P.C. Taylor, principal investigator, G.A. Williams, W.D. Ohlsen, C. Lee, S. Gu, I. Viohl

One important class of materials for PV conversion of solar energy is the group of thin film amorphous semiconductors based on hydrogenated amorphous silicon (a-Si:H). Important alloys include a-Si<sub>x</sub>Ge<sub>1-x</sub>:H and a-Si<sub>x</sub>C<sub>1-x</sub>:H which are used to produce narrower band gaps for tandem cells and larger bandgaps for top-surface p-layers, respectively. Currently little is known concerning the defects and impurities which create enhanced densities of electronic states in the gap in these films. In addition, both the alloys and a-Si:H itself currently exhibit electronically-, thermally- and optically-induced metastabilities (Staebler-Wronski effect). The metastabilities adversely affect device performance and make projections of useful device lifetimes difficult.

### Objectives

One major objective of the research is to characterize the roles of defects and impurities in amorphous, tetrahedrally-coordinated thin films. A second fundamental objective is to determine the quality of the interfaces and junctions which occur in PV devices by employing surface-sensitive optical and resonant techniques. A final important objective is to understand the electronic metastabilities in these amorphous thin films.

### Discussion

The approach used in the research is to employ experimental probes of local order, such as magnetic resonance or optical spectroscopy or a combination of the two techniques, to examine the electronic properties of semiconducting films and multiple layer structures. The materials studied are those of technological importance for photovoltaic solar energy conversion. No major changes in the research emphasis are anticipated during the extension of the final phase of the contract.

The contract is divided into six tasks. The first task involves the training of graduate students. Two graduate students have been trained directly under the support of this contract and three are currently being trained. Because the average time to obtain a Ph.D. degree in physics (after the bachelors degree) is six years, it is anticipated that it will take longer than the present contract to complete the training of two of these last three graduate students.

The second task concerns studies of the metastabilities in a-Si:H and related alloys [1,2]. We are currently investigating [3,4] with electron spin resonance (ESR) the occurrence of metastabilities after light soaking (Staebler-Wronski effect) and after rapid quenching from elevated temperatures (~ 475 K) in i-layers of a-Si:H and p-i-n structures based on a-Si:H. Also under current investigation are molecular hydrogen (H<sub>2</sub>) diffusion

processes in a-Si:H i-layers [2]. These studies employ nuclear magnetic resonance (NMR) measurements.

After quenching from ~ 480 K to 300 K the electron spin resonance (ESR) signal in hydrogenated amorphous silicon (a-Si:H) films and powders increases in the dark with time spent at room temperature. The increased ESR intensity can be removed by annealing at temperatures  $\geq$  370 K. For other a-Si:H films subjected to irradiation, the increase of the ESR spin intensity with time does not follow a unique power law. Although these results have been observed previously (see the September 1987 Annual Technical Status Report) [5], we have recently observed [3,4] the same features on samples from ARCO Solar, Solarex Corp., Plasma Technology and our own sample made in-house. A representative curve is shown in Fig. 1. The fact that these features occur in samples of low initial dark spin density ( $< 10^{16} \text{ cm}^{-3}$ ) from many different sources suggests that the phenomena we have observed are general.

Modulation spectroscopy was performed [6] on amorphous semiconducting films of a-Si:H, using a chopped  $\text{Ar}^+$  ion laser beam as the modulating source. The results show that oscillation fringes in the modulated reflection ( $\Delta R$ ) and transmission ( $\Delta T$ ) are due to the thermal modulation of the index of refraction through the thermal modulation of the band gap  $E_g$ . Therefore the signal amplitude  $\Delta R_{pp}$  in the  $\Delta R$  spectrum gives a measure of the quantity  $\partial E_g / \partial T$ . The temperature dependence of  $\Delta R_{pp}$  in a-Si:H between 1.8 K and 300 K is found to be consistent with the known behavior of  $\partial E_g / \partial T$  as shown in Fig 2. This effect may be useful for nonlinear optical devices.

The third task involves the characterization of defects in a-Si:H and related alloys. In the third year of the contract we have been looking primarily at metastable optical absorption and paramagnetism in a-Si:H i-layers [7,8,9]. After rapid cooling from 210°C a characteristic electron spin resonance (ESR) and a characteristic below-gap optical absorption (as measured by PDS) have been observed to grow with time at room temperature in hydrogenated amorphous silicon (a-Si:H). Typical growth curves are shown in Fig. 3. Both the increased ESR and the increased optical absorption anneal at temperatures above about 100°C. These unexpected results may have important consequences for our understanding of the electronic properties of a-Si:H.

The increase with time in the optical absorption and ESR at room temperature after rapid quenching from elevated temperature can be explained in several ways [8]. Possibilities include (1) the creation of additional defects, (2) the rearrangement of charge into dangling bond defect states from another set of paramagnetic states which is at similar energy as the neutral silicon dangling bond states but which is not detected by ESR, and (3) the conversion of positively and negatively charged silicon dangling bonds into neutral ones. The creation of additional defects might be associated with hydrogen diffusion, which has been proposed to affect thermal equilibration in doped a-Si:H. Because these samples are i-layers these changes may be due to changes in band bending which may be driven by changes in trapped charge at the film/air and film/substrate interfaces.

A study of gap states in a-Si:H and related alloys constitutes the fourth task of the contract [7,10,11]. Under this task we have been investigating photoluminescence absorption spectroscopy (PLAS) of i-layers of a-Si:H, and of B-doped a-Si:H and of a-SiGe:H alloys [8]. Measurements have been

performed on films of various thicknesses (about 3000 Å - 1.5  $\mu\text{m}$ ) as a function of temperature (4.2 - 250 K). At the higher temperatures the absorption spectra approach those which are observed by photothermal deflection spectroscopy at 300 K. At low temperatures ( $T \leq 200$  K) in films of a-Si:H, a peak is observed in the sub-gap absorption at about 1.15 eV. This peak, whose position is independent of temperature, is increased after irradiation at 300 K with band gap light. This peak in the absorption is difficult to detect at temperatures above about 250 K because of the increased importance of absorption in the Urbach tail near 1.15 eV as the band gap decreases with increasing temperature.

The fifth task concerns the characterization of interfacial effects in a-Si:H and related alloys. During the third year of the contract we have concentrated on the characterization of possible interface states in a-Si:H as measured by the PLAS technique [9]. We are currently testing different waveguide structures and different sample thicknesses to see if the absorption peak at 1.15 eV is related to an interface phenomenon. A detailed understanding of the mode structure is necessary before any definitive conclusions can be drawn. Typical electric field distributions for the first four TE modes are shown in Fig. 4.

The final task (number 6) is the construction and testing of an in-house glow-discharge deposition facility. During the past year we have developed our own growth capabilities with a glow discharge system purchased from Plasma Technology and modified by us. This system, which exists in the Microelectronics Laboratory run by the College of Engineering at the University of Utah, is currently making state-of-the-art i-layers of a-Si:H. We have characterized these films with ESR ( $< 10^{16}$  dark spins/cm<sup>3</sup>), PDS, photoconductivity ( $\sigma_{\text{pc}}/\sigma_{\text{dark}} > 10^4$ ) and several other techniques. We are now using our own samples for optically-induced ESR, ODMR, PLAS and several other on-going experiments. We currently have active collaborative efforts with ARCO Solar, Inc. Solarex Corp., Plasma Technology, North Carolina State University, the University of Chicago, Harvard University and the University of Marburg. All of these institutions have provided well characterized samples to us for various research purposes.

### Conclusions

The research is proceeding on schedule. In the extension of the third phase of the contract we will concentrate on (1) the continued training of graduate students, (2) the kinetics of the metastable paramagnetism (both thermally and optically induced) in a-Si:H, p-i-n structures based on a-Si:H, and alloys related to a-Si:H, (3) the temperature dependence of the below gap absorption in doped films of a-Si:H and in alloys related to a-Si:H, (4) characterization by PDS and ESR of interface states in a-Si:H and in rapidly quenched a-Si:H films, and (5) the use of our own growth facility for samples of a-Si:H, a-Si<sub>x</sub>Ge<sub>1-x</sub>:H and doped layers in these two systems.

### References

1. "Photoluminescence in Hydrogenated Silicon-Germanium Alloys" (with R. Ranganathan, M. Gal and J.M. Viner) in Amorphous Silicon Semiconductors - Pure and Hydrogenated, A. Madan, M. Thompson, D. Adler and Y. Hamakawa, eds. (Materials Research Society, Pittsburgh, 1987), p. 293.

2. "Possible Diffusion of Molecular Hydrogen Along Microvoids in Device-Quality a-Si:H" (with E.J. VanderHeiden and W.D. Ohlsen) in Amorphous Silicon Semiconductors--Pure and Hydrogenated, A. Madan, M. Thompson, D. Adler and Y. Hamakawa, eds. (Materials Research Society, Pittsburgh, 1987), p. 159.
3. "Metastable Optical Absorption and Paramagnetism in Hydrogenated Amorphous Silicon" (with J.M. Viner, C. Lee and W.D. Ohlsen), MRS Symposium Proceedings 118, 309 (1988).
4. "Electron Spin Resonance of Optically-Induced and Thermal Metastabilities in a-Si:H" (with C. Lee, W.D. Ohlsen and M.S. Bennett) in Proc. Int. Topical Conf. on Hydrogenated Amorphous Silicon Devices and Technology (1988), in press.
5. P.C. Taylor, in Photovoltaic Program Branch: Annual Report, FY1987, (March 1988). SERI/PR-211-3299, p. 230. Available NTIS: Order No. DE88001155.
6. "Thermal Modulation of the Refractive Index in Amorphous Semiconducting Thin Films" (with R. Ranganathan and M. Gal), Phys. Rev. B37, 10216 (1988).
7. "Subgap Absorption in a-Si:H Using Photoluminescence Absorption Spectroscopy (PLAS)" (with R. Ranganathan), J. Non-Cryst. Solids 97+98, 707 (1987).
8. "Below Gap Absorption in a-Si:H and Related Alloys" (with R. Ranganathan and M. Gal), Solar Cells 24, 257 (1988).
9. "Experimental Aspects of Photoluminescence Absorption Spectroscopy in a-Si:H and Related Alloys" (with R. Ranganathan and M. Gal) in Advances in Amorphous Semiconductors, H. Fritzsche, ed. (World Scientific, Singapore, 1988), in press.
10. "Laser Spectroscopy of Amorphous Semiconductors," in Laser Spectroscopy of Solids, Vol 2, W.M. Yen, ed. (Springer-Verlag, New York, 1988), in press.
11. "Absorption in Amorphous Silicon Doping-Modulated Multilayers" (with R. Durny, S. Ducharme and J.M. Viner), J. Non-Cryst. Solids 97+98, 927 (1987).

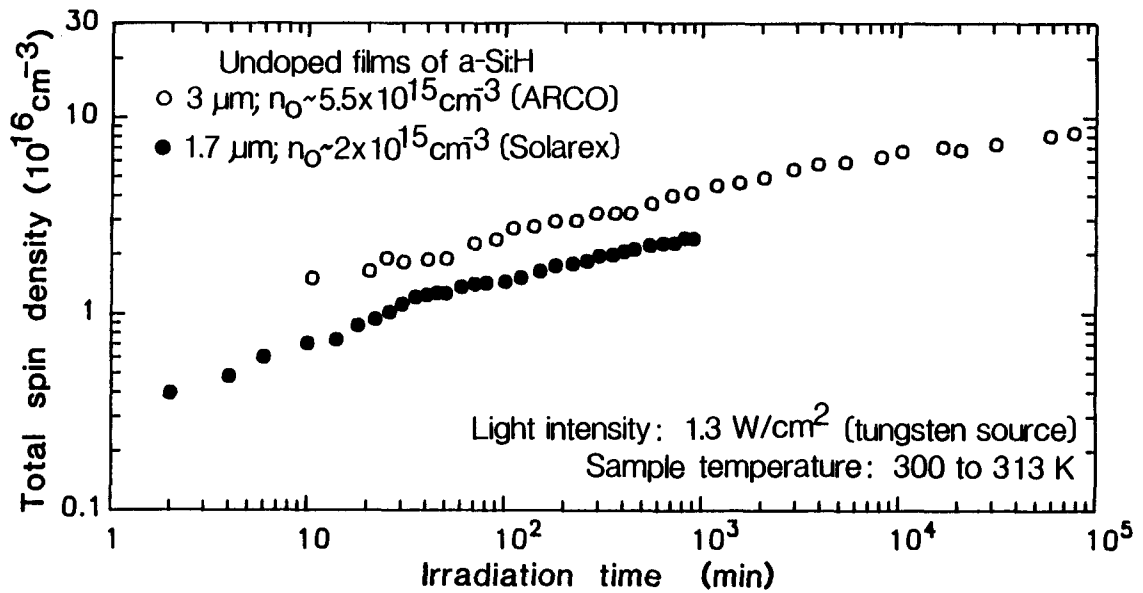


Figure 1. Total ESR spin density versus irradiation time.

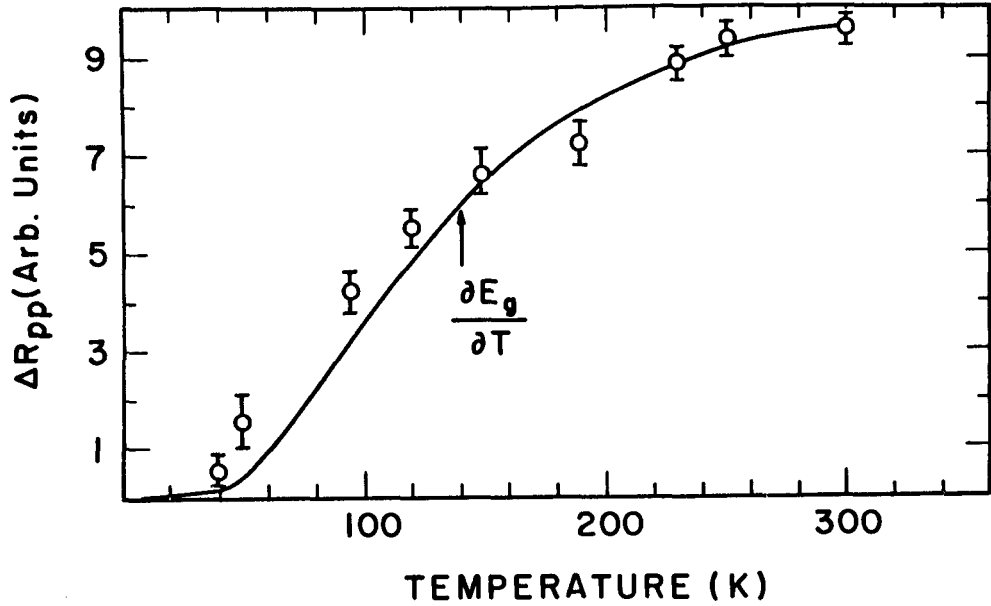


Figure 2. Temperature dependence of the peak-to-peak amplitude of  $\Delta R$ . The solid line is  $dE_g/dT$  calculated from existing data and the circles are data points for the average intensity of the biasing beam. These data were taken at 40 Hz modulation.

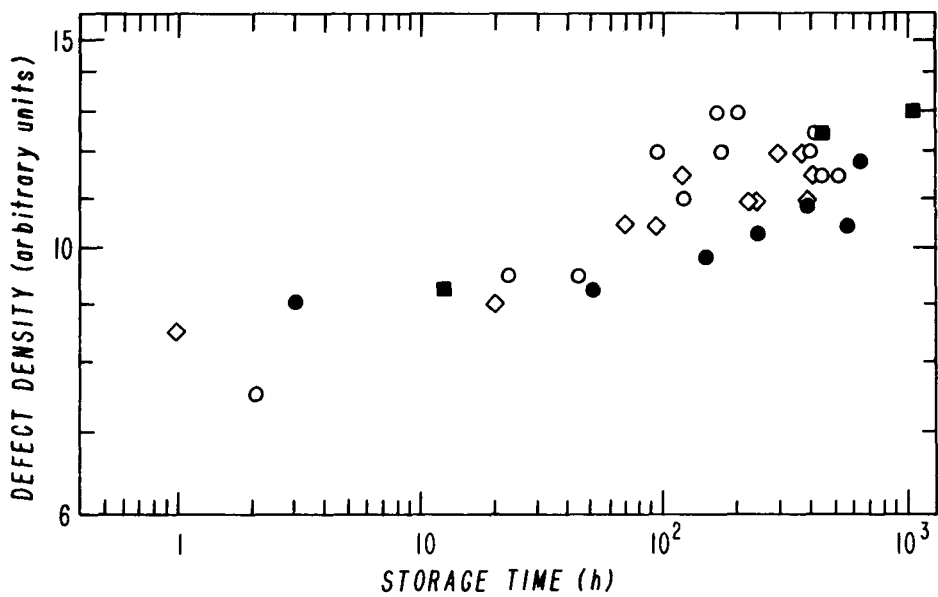


Figure 3. ESR spin density (open symbols) and integrated optical absorption (filled symbols) as a function of storage time in the dark at room temperature following rapid quenching from 210°C. The open diamonds and open circles are data for films quenched in deionized ice water and ethyl alcohol, respectively. The solid circles and squares are data from the first and second quenching experiments, respectively.

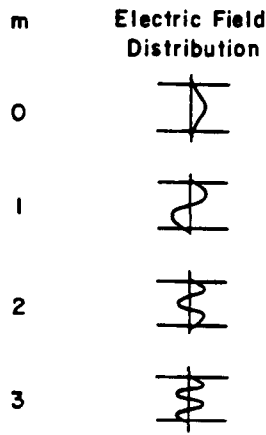


Figure 4. Schematic diagram of the TE waveguide mode indexed by  $m$  (left side) showing the corresponding electric field distribution  $E_x$  (right side).

Title: Defects and Photocarrier Processes in Hydrogenated Amorphous Silicon Germanium Alloys

Organization: Department of Physics, Syracuse University, Syracuse, New York

Contributors: E. A. Schiff, principal investigator; H. Antoniadis, S. Hotaling, J. K. Lee, and S. Zafar, research assistants.

This research project utilizes electron spin resonance and transient photocarrier spectroscopies to study bonding defects and excess carrier transport in hydrogenated amorphous silicon and silicon-germanium alloys (a-Si<sub>1-x</sub>Ge<sub>x</sub>:H). It is widely accepted that the defect observed in electron spin resonance (the D center) controls photocarrier recombination in these materials, but a fully satisfactory model for recombination has not yet been found. These defects also exhibit a metastability which causes their density to increase following photoexcitation, thus degrading materials performance in photovoltaic and other applications. The objective of our research is to obtain a detailed understanding in a-Si<sub>1-x</sub>Ge<sub>x</sub>:H of the interrelationship between photocarrier evolution and bonding defects including metastability effects.

In the remainder of this report we present some highlights of our research. In particular the following topics will be described:

*Defects in a-Si<sub>1-x</sub>Ge<sub>x</sub>:H:* A report on our progress in understanding (i) the electron spin resonance (ESR) lineshape of a-Si<sub>1-x</sub>Ge<sub>x</sub>:H in terms of Si and Ge related D centers, and (ii) the thermal defect metastability in a-Si:H originally reported by the University of Utah group.

*Electron drift-mobility in a-Si:H:* Progress includes (i) the first picosecond domain measurements (in collaboration with Brown University), (ii) studies of the anisotropy of the electron drift-mobility, and (iii) studies of the effects of illumination-induced defect metastabilities.

#### Defects in a-Si<sub>1-x</sub>Ge<sub>x</sub>:H

The widely accepted interpretation of the electron spin resonance lineshape near room-temperature in undoped a-Si:H is that it is due entirely to a single defect, the D-center; the microscopic identity of this defect is disputed, but it is generally considered to be a dangling bond on a threefold coordinated Si atom. In pure a-Ge:H a similar defect is found. In alloys (a-Si<sub>1-x</sub>Ge<sub>x</sub>:H) presumably both types of defects appear. However, the details of separating them and of identifying "matrix effects" (a Ge dangling bond should have a different signature in a Si matrix than in a Ge matrix) are still unclear [1]. We have addressed this problem using the integrated electron spin resonance lineshape and a *nonlinear* least squares analysis procedure based on cylindrically symmetric defects. Fig. 1 illustrates the deconvolution we obtain for very dilute a-Si<sub>1-x</sub>Ge<sub>x</sub>:H; in addition to the usual Si D center a broad and shifted alloy line is found. A cylindrically symmetric defect may be characterized by its two principal g-values, and in Fig. 2 we present preliminary estimates for the two values for the alloy line (circular points) as well as for the Si D center (squares). Remarkably the estimates for the two principal g-values are reversed for the two defects; we

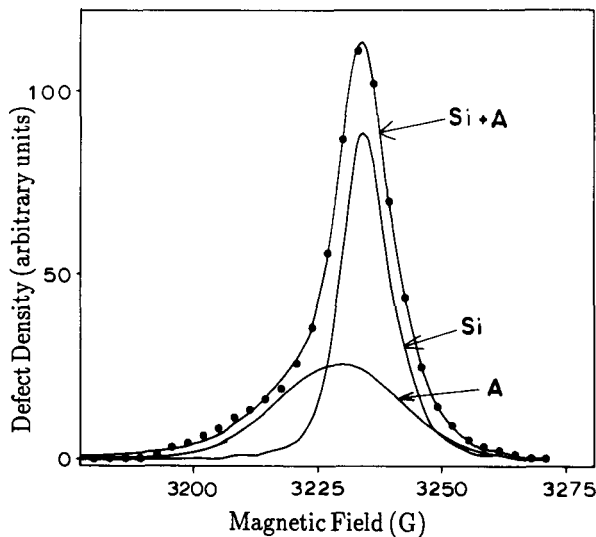


Figure 1: A deconvolution of the electron spin resonance lineshape in a-Si<sub>1-x</sub>Ge<sub>x</sub> ( $x = 0.03$ ) into two components representing the unmodified  $D^0$  center in a-Si:H (denoted Si) and the Ge-induced line (denoted A).

are still working to assess the statistical significance of these estimates. The simplest interpretation of the trend in Fig. 2 is that the lineshape in alloys can be analyzed in terms of a Ge-related defect (presumably a  $D$ -center) which exhibits a matrix shift as the Ge concentration in the alloy is increased. We have found no need to invoke a similar matrix shift of the Si line, which has negligible intensity for  $x > 0.2$ .

The most substantial progress in our ESR research on defect stability in a-Si:H has been upon the unusual effect first reported by the University of Utah group [2]. This effect, which is quite distinct from light-induced metastability, was initially reported simply as a slow increase in the

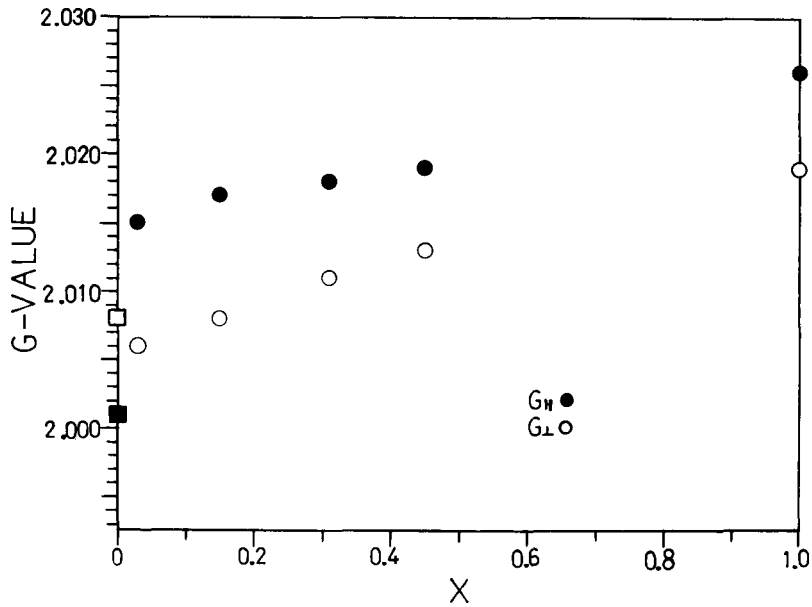
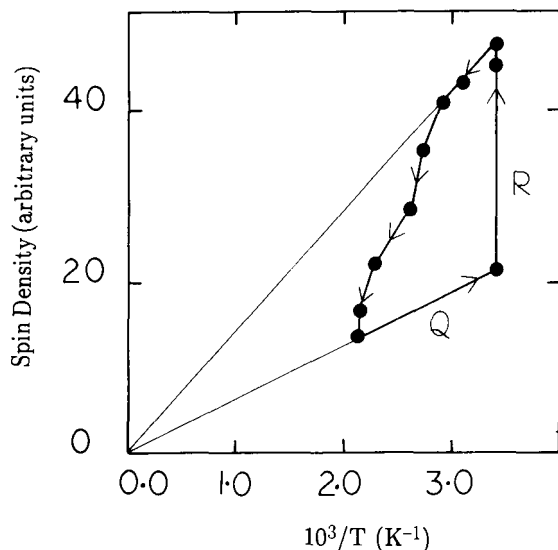


Figure 2: The nonlinear least squares fitting procedure yields estimates of both principal values of the g-tensor for the A-line of a-Si<sub>1-x</sub>Ge<sub>x</sub>:H; these are plotted as a function of alloy concentration  $x$ . The results suggest that a matrix shifted Ge-related defect is responsible for the A line; the significance of the reversal of the two components of the g-tensor between a-Si:H and a-Ge:H is under study.



**Figure 3:** The strength of the  $D$  center electron spin resonance signal is plotted for a thermal cycle in a freshly deposited a-Si:H specimen. Annealing reduces the defect density (ESR signal strength declines below the thin Curie-law lines of constant density). Quenching preserves the defect density, which then slowly increases at room-temperature. The metastability of this defect is distinct from that of light-induced effects, suggesting that two distinguishable classes of  $D$  center may be present.

$D$ -center signal in the dark at 300 K. In Fig. 3 we show one thermal cycle conducted on a newly-deposited specimen exhibiting this effect; the thin lines drawn through the origin indicate constant defect density (Curie-law behavior). The vertical line labeled R indicates the isothermal path taken by the spin-density as it rests at room-temperature for several days. Annealing of the specimen completely reverses the increase in the spin density found at room-temperature, and the observed defect density is constant during the quench to room-temperature.

Study of many cycles in several specimens indicates that this effect is not interfacial in origin, but that its magnitude declines with specimen aging. Since these stability effects are quite distinct from those associated with light, the possibility that a second class of  $D$  center has been revealed – presumably with electronic properties distinct from those of light-induced defects – needs to be assessed.

### Electron Drift Mobility in a-Si:H

Drift-mobilities are the ratio of a photocarrier's drift-velocity to the electric field. Since drift-mobilities are usually measured using transient response techniques following photogeneration, in most semiconductors the results depend upon the time-regime of the measurement. In a-Si:H two time-regimes may be distinguished. At short times transport is usually described entirely in terms electrons occupying conduction bandedge states; in this domain we have participated in an experiment extending the time regime into the picosecond domain. At longer times most electrons are trapped by deep levels (almost certainly in  $D$  states); however, the evolution of an electron following deep-trapping remains controversial [3], and as a consequence there is no widely accepted model for electron recombination in a-Si:H. Our research at Syracuse is essentially unique as a systematic effort to unravel this problem using transient photocurrent methods, and in particular we have been focusing on the possibility that the apparent discrepancies between various measurements of the electron drift-mobility may reflect anisotropic transport in a-Si:H.

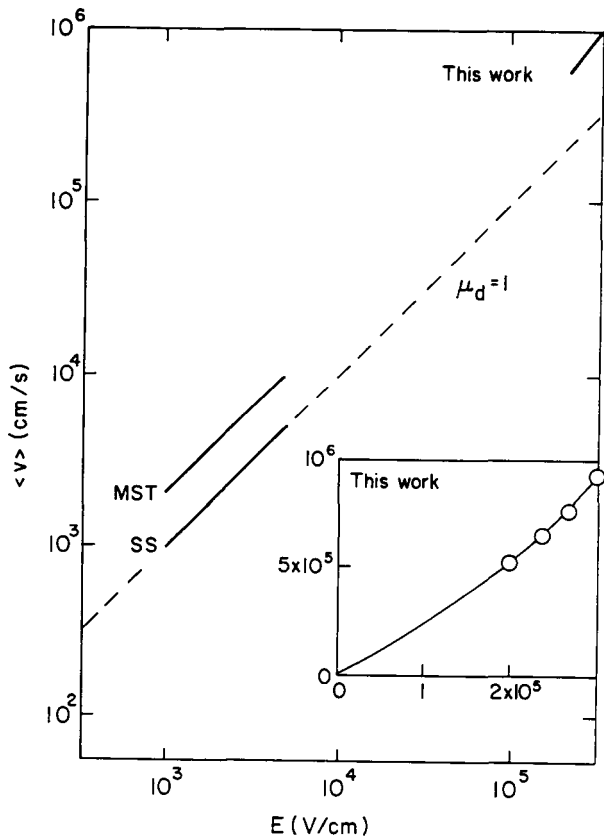


**Figure 4:** The relationship of the average electron drift-velocity versus electric field in undoped a-Si:H at room temperature. MST, SS refer to conventional photocurrent detected time-of-flight. This work refers to optically detected time-of-flight [4]. The dashed line indicates the function expected for a drift-mobility of  $1 \text{ cm}^2/\text{V}\cdot\text{s}$ .

The principal result of research in the short-time regime has been the first true, picosecond domain electron drift-velocity measurements in a-Si:H. The results were obtained by a collaboration of Brown University, Syracuse University, and Energy Conversion Devices, Inc. using optical detection techniques at Tauc' laboratory at Brown [4]. Figure 4 presents a summary of room-temperature drift-velocity vs. electric field results in a-Si:H in the short-time regime; the new data are at substantially higher electric-fields and correspond to much shorter times than earlier work using photocurrent detection. Since the drift-mobility is simply the ratio of the drift-velocity and the field, it is evident from these data that no substantial mobility change occurs in the new regime. This fact is an important constraint on models for electron transport in a-Si:H, and in addition it justifies the use of low-field drift-mobility measurements in modeling devices with high-field domains.

The long-time regime of the electron drift-mobility is experimentally controversial; it is also extremely important, since long-time experiments are attempts to probe the recombination of electrons. Essentially the controversy is the following. In convincing experiments Street and other workers have shown that electron transport terminates fairly abruptly with the "deep-trapping" of electrons by  $D^0$  defects (see the recent review [3]). In Fig. 5 (left) we illustrate our recent measurements of the deep-trapping effect for a single specimen of a-Si:H after several illumination intervals. As the  $D^0$  density is increased, the short-time phase for transport (associated

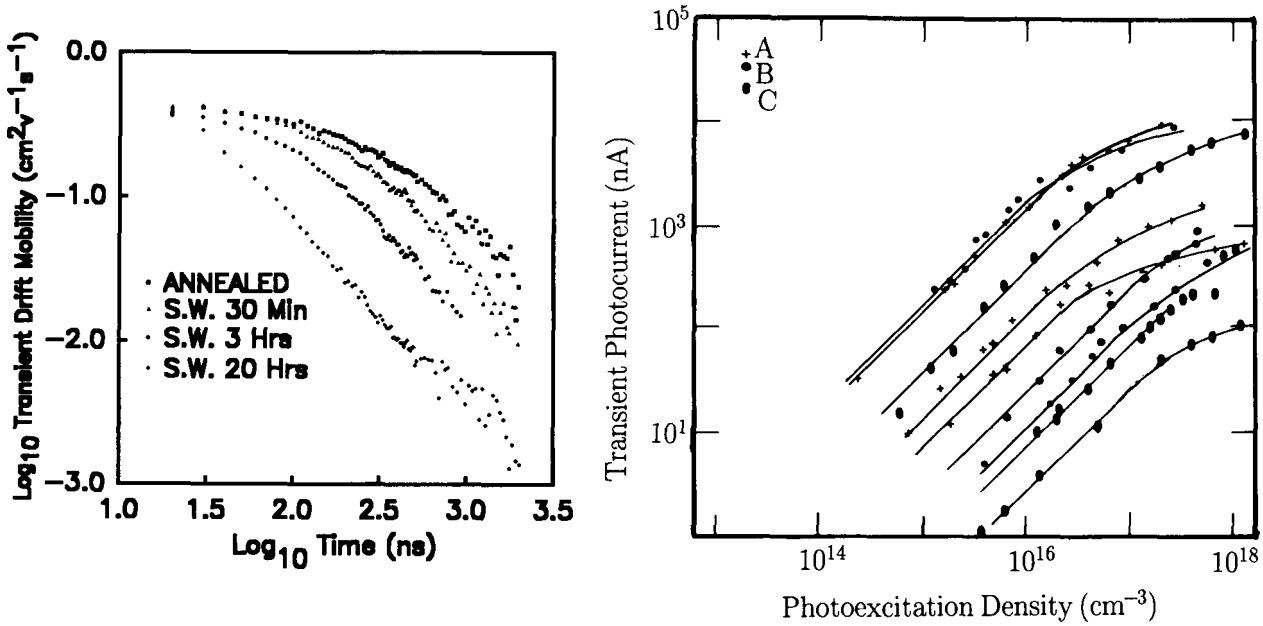


**Figure 5:** (left) The electron transient drift-mobility in undoped a-Si:H at room-temperature for a specimen in several states of light-exposure. The deep-trapping cutoff in the transient drift-mobility occurs at earlier times after light-exposure due to the increased density of deep-levels. (right) Dependence of the electron transient photocurrent in undoped a-Si:H one microsecond following photogeneration for three specimens (A-C) in three states of light-exposure. We associate these photocurrents with re-emission of electrons from  $D^-$  levels; the onset of sublinearity then corresponds to saturation of the occupancy of the  $D^-$ . The very rapid decline of the photocurrent with increasing defect density indicates that the effective binding energy of the photoinduced  $D^-$  becomes deeper as the density increases.

with a drift-mobility of order  $1.0 \text{ cm}^2/\text{V}\cdot\text{s}$ ) cuts off at earlier and earlier times.

The key question regarding these measurements is whether the deep-trapping cutoff is complete (and thus tantamount to recombination). The most extensive studies of the electron drift-mobility in a-Si:H have been for electric fields parallel to the growth axis of the film (the *axial* field direction). These measurements have not indicated any significant electron transport following deep-trapping. However, there are numerous reports of transport perpendicular to the growth axis (the *planar* direction) even after deep-trapping. Prior to deep-trapping the electron drift-mobilities reported for both types of experiment are comparable, and indeed Fig. 4 (left) was obtained for planar fields. We recently proposed that the apparent dichotomy between the two experimental geometries in fact reflects anisotropic electron transport in a-Si:H [5].

We have previously analyzed the long-time planar transient photocurrents in terms of electron re-emission from  $D^-$  [3,6]. Fig. 5 (right) shows some of our recent work along these lines. The measured photocurrent one microsecond

after photogeneration is plotted versus the photoexcited density of electrons for three specimens (A-C) in three states of light exposure. In previous work we have shown that similar saturation curves are obtained in the millisecond domain as well [6]. The onset of sublinearity at high photoexcitation densities coincides adequately with the  $D^0$  density measured by electron spin resonance, as would be anticipated from the re-emission model. The magnitude of the photocurrent at low excitation densities declines precipitously with light-exposure - far more rapidly than the defect density increases. The consequences of this observation within the  $D^-$  re-emission model are quite surprising, since they suggest that the  $D^-$  band in the electronic density of states both increases in strength and falls further away from the conduction band as a result of light exposure.

## SUMMARY

The principal results described above are:

- (i) The electron spin-resonance lineshape in a-Si<sub>1-x</sub>Ge<sub>x</sub>:H may be decomposed into a simple Si  $D$ -center and matrix shifted Ge-related defects; there appears to be no practical need for incorporating matrix effects for the Si  $D$ -center.
- (ii) The Si  $D$ -center metastability originally reported by the University of Utah group is a bulk property of a-Si:H exhibiting an irreversible aging effect in our specimens.
- (iii) The conventional estimate of the short-time domain electron drift-mobility in a-Si:H at 300 K of order 1 cm<sup>2</sup>/V-s is valid at fields as high as  $3 \times 10^5$  V/cm and at times as short as 10 ps.
- (iv) The long-time domain electron drift-mobility in a-Si:H is apparently anisotropic. Planar drift-mobilities are quite similar to axial drift-mobilities until deep-trapping occurs. At longer times the planar drift-mobility may be analyzed in terms of re-emission from  $D^-$  states, but the position of this level relative to the conduction bandedge is not constant for differing specimens or differing states of light-exposure.

## REFERENCES

1. F. Finger, W. Fuhs, G. Beck and R. Carius, *J. Non-Cryst. Solids* **97&98**, 1015 (1987).
2. C. Lee, W. D. Ohlsen, and P. C. Taylor, in *Stability of Amorphous Silicon Alloy Materials and Devices*, edited by B. L. Stafford and E. Sabisky (American Institute of Physics, New York, 1987), p. 93.
3. E. A. Schiff, M. A. Parker, and K. A. Conrad, in *Amorphous Silicon Technology*, edited by A. Madan, *et al* (Materials Research Society, Pittsburgh, 1988).
4. E. A. Schiff, R. I. Devlen, H. T. Grahn, J. Tauc, and S. Guha, *submitted*.
5. M. A. Parker and E. A. Schiff, *Phys. Rev. B* **37**, 10426 (1988).
6. K. A. Conrad and E. A. Schiff, *Solid State Comm.* **60**, 291 (1986).

**Title: Ion-Assisted Deposition Doping of p-CdTe**

**Organization:** Department of Materials Science and Engineering Stanford University  
Stanford, CA 94305

**Contributors:** R.H. Bube, Principal Investigator, A. L. Fahrenbruch, D. Kim,  
A. Lopez-Otero, and P. Sharps

The purpose of this work is to investigate ion-assisted physical vapor deposition of p-CdTe and to determine the influence of co-doposition of ionized dopant atoms on the growth, structural, and photoelectronic properties of the deposited films.

**Method of Approach**

The primary problems for the utilization of polycrystalline p-CdTe based solar cells are those of obtaining sufficiently low series resistance and high  $V_{oc}$ . Sufficiently increasing the p-type doping density in the CdTe would lower both bulk and contact resistivity. Control of  $V_{oc}$  has been obtained by variation of the relative doping levels in CdS and CdTe [2] for single-crystal based solar cells; thus control of p-type doping promises to be a tool for maximizing  $V_{oc}$  in polycrystalline cells as well.

Many of the dopants successfully used in bulk semiconductor growth present problems in the case of film growth from the vapor due to low incorporation probabilities and/or surface segregation. However, impingement of low-energy dopant ions on the growing film during deposition can be used to significantly increase the sticking probability and/or incorporation of the dopant species [1,3].

Our apparatus consists essentially of an ion source, a movable Faraday cup to monitor ion current, an effusion cell for CdTe, and a heated substrate holder, all situated in a vacuum system with a base pressure of  $\approx 6 \times 10^{-8}$  Torr. The ion source uses a boron nitride Knudsen cell to supply the dopant atoms and an ionizer section with a tungsten filament and a graphite anode and grid. Elemental As and P have been used as dopants. Epitaxial CdTe films were grown on single-crystal n- and p-CdTe and BaF<sub>2</sub> substrates at typical rates of 0.1-0.3  $\mu\text{m}/\text{min}$  and substrate temperatures  $T_{\text{sub}} = 300\text{-}500^\circ\text{C}$ . Polycrystalline films on graphite and 7059 glass were simultaneously grown.

**Significant Results**

Results on junction transport mechanisms for diodes prepared using the epitaxial films, elucidation of the deep states using DLTS, and properties of n-CdS/p-CdTe solar cells were used to characterize the films. Carrier densities were measured by Mott-Schottky, thermo-electric power, and Hall effect methods and results for all three methods are in good agreement. In general, for the homoepitaxial layers, using ion energies of 30-80 eV, the carrier density increased smoothly with increasing ion current up to a maximum  $\approx 10^{17} \text{ cm}^{-3}$  at an ion current of  $\approx 1 \mu\text{A}/\text{cm}^2$  [4] (e.g., Fig. 1). For ion currents larger than that the carrier density decreased sharply and deep level density increased. Deep level density decreased for increasing  $T_{\text{sub}}$  and Schottky diode characteristics for the films grown at  $T_{\text{sub}} = 500^\circ\text{C}$  were better than those for the Bridgman grown single-crystal substrates, showing lower reverse current densities.

Solar cell results [5,6] showed that ion damage appears to compromise the quantum efficiency, even at the relatively low ion energies used. The best solar cells were grown on an ion-doped homoepitaxial layer plus a thin, undoped CdTe layer adjacent to the CdS, showing an unoptimized solar efficiency of  $\approx 6.2\%$ .

Graded doping structures have been fabricated by changing the ion flux during growth, as shown in Fig. 2.

In related work, the near-surface reduction of carrier density in p-CdTe:P on heat treatment at temperatures above  $\approx 400^\circ\text{C}$  is shown to be explained by compensation by formation of  $\text{P}_{\text{Cd}}$  anti-site donors, and not by out-diffusion of P [7].

## Conclusions

Results show that controlled doping in p-CdTe epitaxial films up to  $\approx 6 \times 10^{16} \text{ cm}^{-3}$  for ion-assisted deposition with As ions and to  $\approx 10^{17} \text{ cm}^{-3}$  for P has been achieved using ion energies of 30-80 eV. For P, using a growth rate of  $\approx 0.15 \mu\text{m}/\text{min}$ , a substrate temperature of  $450^\circ\text{C}$ , and an ion energy of 80 eV, a maximum in carrier density of  $2 \times 10^{17} \text{ cm}^{-3}$  appears for an ion current of  $0.7 \mu\text{A}/\text{cm}^2$ , corresponding to  $\approx 1.5\%$  of the impinging P ions being electrically active in the deposited film [5,6]. At  $T_{\text{sub}} = 500^\circ\text{C}$ , epitaxial film carrier densities of  $\approx 10^{17} \text{ cm}^{-3}$  can also be achieved and the film quality, as measured by Schottky diode performance, appears to be superior to Bridgman grown single-crystal material.

---

1. J.E. Greene and S.A. Barnett, *J. Vac. Sci. Technol.* **21**, 285 (1982).
2. C.M. Fortmann, A.L. Fahrenbruch, and R.H. Bube, *J. Appl. Phys.* **61**, 2038 (1987).
3. N. Matsunaga, T. Suzuki, and K. Takahashi, *J. Appl. Phys.* **49**, 5710 (1978).
4. A. Fahrenbruch, A. Lopez-Otero, P. Sharps, and R.H. Bube, *Proc. 19th IEEE Photovoltaic Spec. Conf.* (1987) p. 1309.
5. P. Sharps, A.L. Fahrenbruch, A. Lopez-Otero, and R.H. Bube, presented at Materials Research Society Meeting, Boston, 11/29-12/2/88. To be published, Vol. 28A, *MRS Symposium Proceedings*.
6. P. Sharps, A.L. Fahrenbruch, A. Lopez-Otero, and R.H. Bube, *Proc. 20th IEEE Photovoltaic Spec. Conf.* (1988).
7. D. Kim, A.L. Fahrenbruch, and R.H. Bube, *Proc. 20th IEEE Photovoltaic Spec. Conf.* (1988).

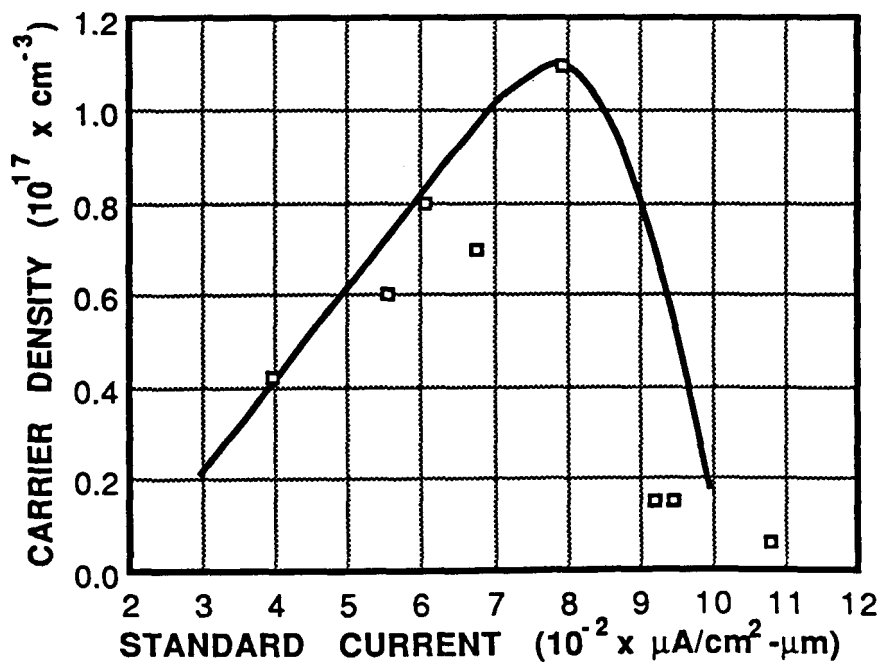


Figure 1. Carrier density as a function of "standard" ion current for an ion energy of 60 eV and a growth temperature of 400°C. [Because of variability of film thickness, the ion current was divided by the film thickness ( $\approx 10 \mu\text{m}$ ) to standardize it.]

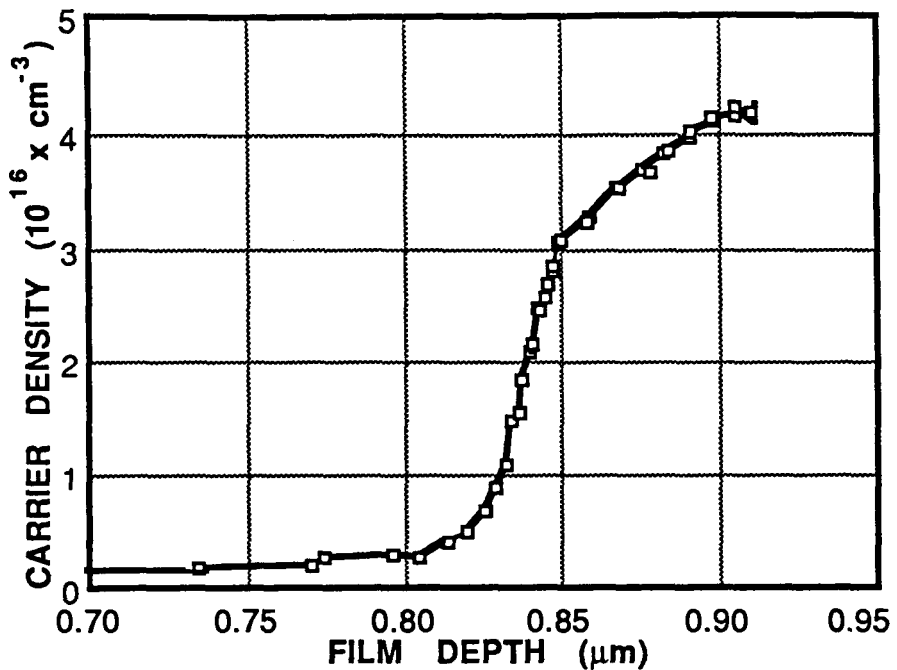


Figure 2. Carrier density as a function of film depth, where the ion flux was changed abruptly from  $\approx 0.5 \mu\text{A}/\text{cm}^2$  to zero at a film depth of  $\approx 0.85 \mu\text{m}$ .

**Title : Rapid Liquid Phase Epitaxy of Gallium Arsenide Photovoltaic Devices**

**Organization : Department of Physics, Brown University, Providence, Rhode Island.**

**Contributors : E.E. Crisman and H.J. Gerritsen, principal investigators; S.K.F Karlsson, C.B. Roberts, and D.T. Schaafsma.**

The research underway is an effort to establish the technique of liquid phase epitaxy from a flowing solution (herein called RLPE for rapid LPE) as an efficient means of producing high quality, thick layers of III-V compounds for photovoltaic, optoelectronic, microwave, and very large scale integrated (VLSI) devices. In this process, growth is achieved by placing a single crystal seed wafer in a laminar flow stream of a group III metal such as Ga (alloys with In or Al are also suitable) saturated with GaAs, or whatever material is to be grown, and undercooling the seed wafer with nitrogen to produce a temperature gradient across the solid/liquid interface. The temperature of the alloy material is maintained at the liquidus temperature for that particular combination. The constant temperature maintained in the melt and the steady flow of melt across the substrate ensure saturation throughout the growth cycle, which leads to large, time-independent growth rates (up to  $14\mu\text{m}/\text{min}$  observed), compared to conventional LPE techniques (typically  $10\mu\text{m}/\text{hour}$ ). The RLPE process also has advantages over other epitaxy methods like metalorganic chemical vapor deposition (MOCVD) and molecular beam epitaxy (MBE) aside from the faster growth rates. RLPE does not involve any of the hazardous reactants used in MOCVD (such as arsine and phosphine) and does not require the high vacuum apparatus or associated large capital outlay of MBE systems.

The GaAs seed wafers used in last year's experiments were of two orientations:  $<111>\text{B}$ , and  $<100>$  tilted  $2^\circ$  to  $<110>$ . The  $<100>$  substrates were Cr doped, semi-insulating ( $10^8 \Omega\text{-cm}$ ), while the  $<111>\text{B}$  substrates were either Cr doped semi-insulating (similar to the above) or Cd doped p-type ( $1.3 \times 10^{-3} \Omega\text{-cm}$  resistivity,  $2 \times 10^{16}$  carrier concentration, mobility  $212 \text{ cm}^2/\text{V}\cdot\text{s}$  at 300K). In addition, some n-type Ge substrates were tried, as well as several VPE GaAs on Ge substrates. The Ge substrates have not fared well in this process; in fact, all those attempted to date have evidenced significant (often complete) meltback in Ga, due to the high solubility of most metals in Ga. One solution to this problem is to try a different base, such as lead, which does not have an impurity level in GaAs and which has low solubility for Ge. The RLPE technique is well suited to such applications.

Two GaAs melts have been used to produce specimens this year; one a Si-doped solution calculated to yield p-type epilayers on  $<100>$  faces and n-type on  $<111>\text{B}$  faces grown at  $800^\circ\text{C}$  (due to the amphoteric nature of Si in GaAs), and the other a Te-doped n-type melt. The concentrations of the alloys are chosen such that the saturated liquidus temperature falls at approximately  $800^\circ\text{C}$ ; however, this temperature will be lowered once greater temperature gradients (more efficient cooling) can be achieved. The lower growth temperature should reduce the dislocation concentration, which is a consistent problem with bulk-grown material.

Aside from the choice of substrate and melt type, the most important parameter remaining is the flow rate of the melt across the substrate. In the laminar flow regime, this rate ranges from  $5\text{cm}^3/\text{min}$  to  $20\text{cm}^3/\text{min}$ . The theoretical growth rates and the results accumulated to date are shown in Fig. 1. One improvement in the apparatus was the introduction of a liquid nitrogen-cooled heat exchanger for pre-cooling the nitrogen gas used to create the thermal gradients across the substrates.

The thickness measurements have been accomplished by sectioning the wafers (either by cutting or cleaving), applying a stain to highlight the epilayers, and then viewing the sample on edge in either a traveling optical microscope or a scanning electron microscope. A table of thicknesses, along with type, hall mobility, and photoluminescence peaks for all the 1988 specimens is given in Fig. 2. The cutting technique suffers from difficulty in polishing the cut edges, which may be the reason why these specimens do not stain well. The cleaving technique, on the other hand, stains well, but yields epilayer and substrate edge faces which are nonparallel.

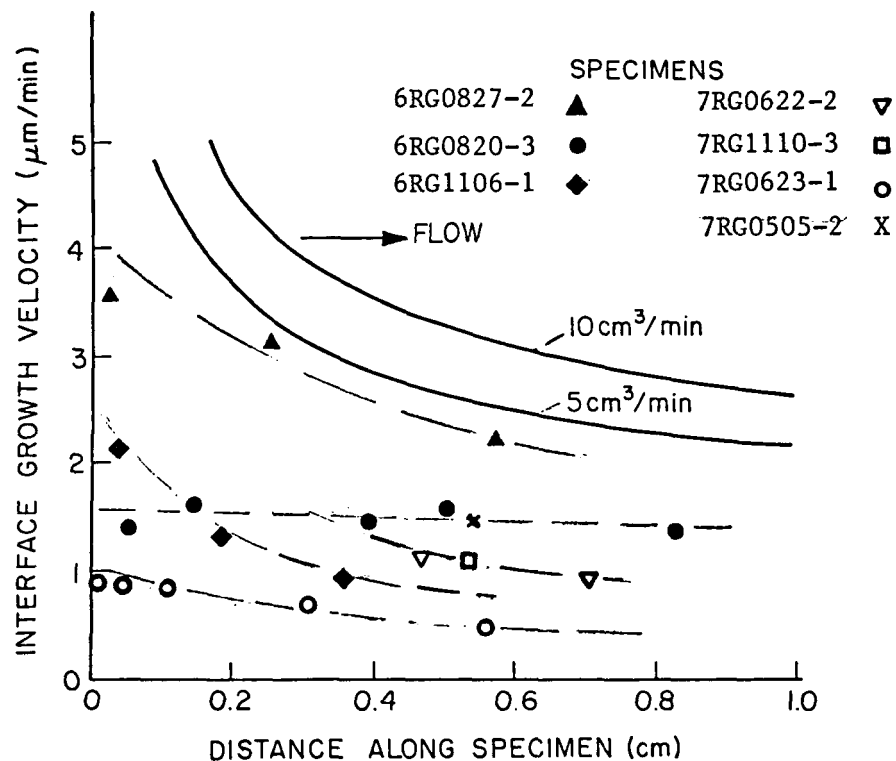


Fig. 1 Theoretical Curves (solid lines) and Experimental Data (plotted points) for Growth Rate vs. Flow Rate in RLPE Process

The specimen mobilities below represent an average of Van der Pauw measurements. Two mobilities are found from three probe configurations using the equation

$$\mu_i = \frac{4.412712 \times 10^7}{B} * \left( \frac{\Delta R_i}{f_i * (\bar{R}_{v_i} + \bar{R}_{v_{i+1}})} \right), \quad (i = 1, 2)$$

where  $\Delta R_i$  is the average Hall resistance in the two transverse directions minus the background Hall resistance and  $\bar{R}_{v_i}$  is the average Van der Pauw resistance for the  $i$ th contact permutation. The  $f$  value is approximated from

$$f_i = 1 - \delta R_i \frac{\ln 2}{2} - \delta R_i^2 \left( \frac{(\ln 2)^2}{4} - \frac{(\ln 2)^3}{12} \right),$$

where

$$\delta R_i = \left( \frac{R_{v_i} - R_{v_{i+1}}}{R_{v_i} + R_{v_{i+1}}} \right).$$

Fig. 2 Table of Measurements for 1988 RLPE Specimens

Sample Number	Substrate Identification	Thickness (μm)	Type	Mobility (cm <sup>2</sup> /V · s)	PL Peaks (eV)
0112-1 <sup>§</sup>	<111>B Cr				1.395, 1.277
0112-2 <sup>§</sup>	<111>B Cr		p		1.395
0112-3 <sup>§</sup>	n-type Ge	meltback			
0127-1 <sup>§</sup>	<111>B Cd	meltback			1.505, 1.481, 1.444
0127-2 <sup>§</sup>	<111>B Cd	5.08	p (weak)		
0127-3 <sup>§</sup>	<111>B Cd	15.24	p		1.506, 1.482, 1.4
0211-1	<111>B Cr	30.5			1.50 <sup>†</sup> , 1.41 <sup>†</sup> , 1.4
0211-2	<111>B Cd				1.48 <sup>†</sup> , 1.53 <sup>†</sup> , 1.52
0211-3	<111>B Cd	17.8	n (strong)		1.52, 1.46
0218-1	<111>B Cr	5.08	n	2700	
0218-2	<111>B Cr	10.2	n	213 <sup>‡</sup>	1.506
0218-3	<111>B Cr	114.3	n	909	
0308-1	<100> Cr		n		
0308-2	<100> Cr		n		
0308-3	<100> Cr		n		
0317-1	<111>B Cd				1.504
0317-2	<111>B Cd		n (weak)		
0317-3	<111>B Cd		n		
0623-1	<111>B Cr				
0707-1	Si on Al <sub>2</sub> O <sub>3</sub>	meltback			
0707-2	GaAs on Si	meltback			
0707-3	GaAs on Ge	meltback			
0708-1	Ge	meltback			
0708-2	Si on Al <sub>2</sub> O <sub>3</sub>	meltback			
0708-3	Ge	meltback			
1028-1 <sup>¶</sup>	<100> Cr	meltback			
1028-2 <sup>¶</sup>	<100> Cr	meltback			
1028-3 <sup>¶</sup>	<111>B Cd	meltback			1.34 (weak)
1104-1 <sup>¶</sup>	Al <sub>2</sub> O <sub>3</sub>	no growth			
1104-2 <sup>¶</sup>	Al <sub>2</sub> O <sub>3</sub>	no growth			
1104-3 <sup>¶</sup>	Al <sub>2</sub> O <sub>3</sub>	no growth			
1115-1 <sup>¶</sup>	<111>B Cd	no growth			
1115-2 <sup>¶</sup>	<111>B Cd	no growth			
1115-3 <sup>¶</sup>	<111>B Cd	no growth			

Unmarked samples indicate Te-doped melts; <sup>§</sup> indicates Si-doped, <sup>¶</sup> indicates InGaAs melts.

Data taken at 77K except: <sup>†</sup> 7.4K; <sup>‡</sup> 300K.

Photoluminescence data was obtained using a lock-in detection system (modulation frequency about 1kHz) with a 7102-type photomultiplier tube as the detector. Two lasers were used to excite the specimens: one a 500mW AlGaAs diode laser; the other a variable-power argon ion laser. The specimens can thus be measured at several different wavelengths and the data can then be used to compare surface vs. bulk recombination velocities. This technique was used to compare the PL efficiencies of MBE (SERI) specimens with an AlGaAs window layer and RLPE (Brown) without a window layer,

and the results are plotted in Fig. 3. The MBE sample is less wavelength-sensitive due to the AlGaAs capping layer, which enhances the short-wavelength PL efficiency of the sample. At the long wavelength end of the spectrum (791nm), the ratio of efficiencies (at equal excitation power) was about 6 to 1 in favor of the capped-MBE. After the AlGaAs layer was etched off (in ammonium hydroxide : hydrogen peroxide), this ratio decreased to approximately 2.5:1. In addition, the ratio between etched MBE and uncapped RLPE specimens decreased from 2.5:1 to 1.5:1 over a period of several weeks (or less), indicating a further degradation of the MBE surface due to reaction with the ambient atmosphere of the laboratory. The luminescence of this AlGaAs layer, measured prior to etching, was undetectable with the above apparatus, even at the shortest wavelength and at 4.5K.

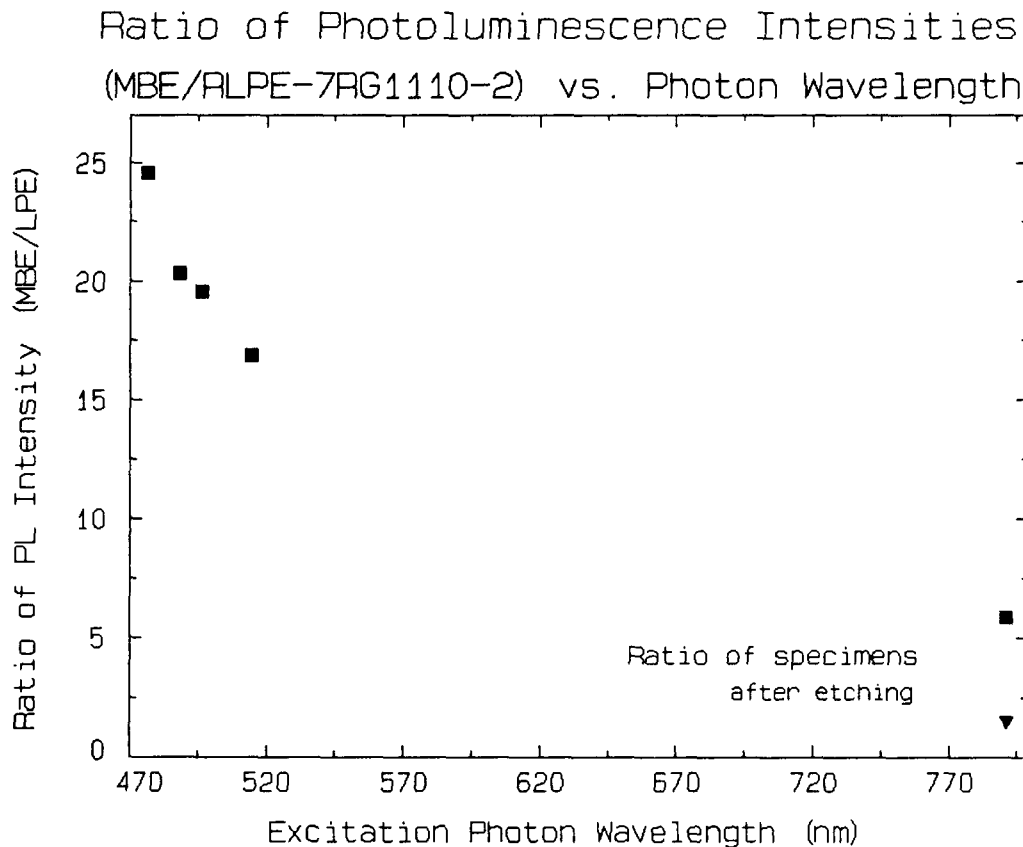


Fig. 3 MBE to RLPE PL Signal Ratio vs. Wavelength

We are presently engaged in attempting to grow  $\text{Ga}_{0.9}\text{InAs}_{0.1}$  layers on  $\langle 111 \rangle \text{B}$  Cd-doped and  $\langle 100 \rangle$  Cr-doped substrates to demonstrate the advantages of RLPE for growing 'tailored' compositions of III-V ternaries. The next phase of our research will be to repeat this experiment using an AlGaAs melt, and then to design and fabricate a double-well growth crucible to produce PN junctions. Also, we plan to study turbulent flow RLPE once the theoretical analysis and design of a new turbulent growth chamber are complete. Ternary growths will be demonstrated during the six month extension to the contract which begins January, 1989. The double well growth chamber will be designed during that period also.

**Title:** **New Approaches for High Efficiency Solar Cell:  
Role of Strained Layer Superlattices**

**Organization:** Electrical and Computer Engineering Department, North Carolina State University, Raleigh, North Carolina 27695-7911

**Contributors:** S. M. Bedair and N. A. El-Masry

### **Objective**

The objective of the research program is to address current problems that are hindering progress towards achieving high efficiency cascade solar cell structures. Problems include proper interconnect between the two cells and the lack of compatible material systems for the optimum bandgap combinations. During the last year we have concentrated our activities on addressing potential techniques that can be used to reduce defects generated when incompatible material systems or poor quality substrates are being used in solar cells.

In order to achieve such goals, we have carried out fundamental studies to understand the behavior of defects and dislocations in strained layer superlattices buffer films and the mechanisms involved in their reduction. Studies were carried out for the case of homoepitaxy of GaAs film on GaAs substrates and for heteroepitaxy of GaAs on Si substrates.

### **Experimental Approach**

Several superlattice structures such as GaAs-InGaAs and GaAs-GaAsP have been previously used as buffer layers to reduce defects originating from the substrate or from heterointerfaces. However, we have recently reported that selecting a superlattice of  $\text{GaAs}_{1-y}\text{P}_y - \text{In}_x\text{Ga}_{1-x}\text{As}$  ( $y = 2x$ ) that is grown lattice matched to GaAs has several advantages over other SLS composed of binary-ternary structures [1,2]. This ternary-ternary SLS has been adopted in this study since it allows wide variations, 0-2%, in the intrinsic elastic strain between the successive layers. Also, with this SLS there will be no limitations on the number of superlattice periods.

The SLS was grown by metalorganic chemical vapor deposition (MOCVD). The composition of the ternary alloys  $x$  and  $y$  were adjusted such that the SLS was lattice matched to GaAs. The values of  $x$  and the corresponding values of  $y$  were varied in the ranges of 8-25% and 16-40%, respectively. The individual layer thicknesses varied from 80-500 Å depending on the ternary composition and the critical layer thicknesses.

Several characterization techniques such as x-ray topography (XRT), Electron Beam Induced Current (EBIC) and TEM were used to study the dislocation interactions with SLS. Combinations of these techniques allows us to investigate dislocation density in the range  $10^2$  to  $10^8 \text{ cm}^{-2}$ . XRT is suitable in characterizing defect density less than  $10^6 \text{ cm}^{-2}$  and thus was used for structures grown on GaAs substrates. GaAs/Si substrate samples, with dislocations density higher than  $10^8 \text{ cm}^{-2}$  were studied by TEM. EBIC bridges the

two techniques and was used to characterize structures grown both on GaAs and on Si substrates. Sample for EBIC testing consists of a Se-doped 0.5  $\mu\text{m}$  thick GaAs ( $n = 10^{16}\text{cm}^3$ ) grown directly on the substrates with and without the SLS buffers. Schottky diodes rectifying junctions was then achieved by Al metalization.

## Results

### A. Defects in GaAs Homoepitaxy

Several types of dislocations have been observed and are schematically illustrated in Figure 1. In this figure curves 1 through 4 depict threading dislocations originating from the substrate bent due to the misfit strain, whereas curve 5 depicts a dislocation unperturbed by the SLS.

When there is sufficient stress at the substrate/SLS interface the threading substrate dislocation may glide at this interface creating a misfit dislocation segment. The length of this segment depends on the local stress or line tension on the dislocation. Once the stress decreases then the dislocation threads to the surface. The misfit stress can be reduced locally by variations in composition or film thickness. The substrate dislocation may also glide within one of the internal interfaces of the SLS if sufficiently high local stress is developed. An XRT obtained from a substrate Bragg reflection then only yields an image of the substrate component of this dislocation as shown in Figure 2. The EBIC image in Figure 3 shows threading dislocations which glide at the substrate/SLS interface and also those which glide at the SLS interfaces. Details of these studies have been previously published [3,4]. We have previously shown that this SLS buffer had resulted in reduction in defects density in epilayers by several order of magnitude from that of the substrate [5].

### B. GaAs Grown on Si Substrates

Our current efforts in utilizing GaAsP-InGaAs SLS to reduce threading dislocations indicated that in areas of low dislocation density almost all threading dislocations are blocked and bent along the SLS interfacial planes [6]. The bent dislocations in the low density regions can propagate along the SLS interface a distance of several microns without disturbance this occurs in the absence of a strain field generated by a neighboring dislocation. There is a critical separation distance between the threading dislocations below which the local relaxation offered by the dislocations will relax the SLS. The residual strain ( $\epsilon$ ) will be misfit strain. The critical separation distance can be estimated as:

$S_{\text{crit.}} = b/f$ , where  $b$  is Burger's vector edge component of the threading dislocation in the strained film plane. The calculated values of  $S_{\text{crit}}$  and  $f$  are as follows:

<i>f</i>	0.0075	0.0108	0.0144
S( $\text{\AA}$ )	267	185	139

From the table it becomes obvious that the higher the misfit strain in the SLS the shorter the distance allowed between the dislocations threading and interacting with the superlattice, i.e., the higher the dislocation density that the SLS can handle. Thus, the effectiveness of the superlattice in bending dislocations is improved by utilizing higher strain level, thicker layers (closer to  $h_{c,\max}$ ) and large number of periods of the SLS [7].

Annealing is a thermal process that mobilizes the dislocations and activates their slip mechanism. Annealing by itself has been demonstrated by us and others to reduce dislocation in the GaAs epilayer thus allowing lower defect density to impinge on SLS, leading to an improvement in its effectiveness. Thus, combining SLS's with annealing prior and during the SLS growth can activate the dislocation slip systems and force the unbent dislocations to glide and enhance their interactions with the strained interfaces of the SLS. We found that the interaction between SLS and threading dislocations is enhanced by intermittent annealing as shown in Figure 4. Also, it is clearly indicated that the threading dislocations are strongly confined within the annealed two series of SLS and that gliding along the SLS interfaces occurred. By this intermittent annealing process the grown-in threading dislocation density can be dramatically reduced [8]. This will allow the gradual reduction of the dislocation density and the subsequent SLS to powerfully bend the threading dislocations without the local relaxation of the SLS strain by the high threading dislocation density. A combination of annealing and SLS resulted in defect density in low  $10^6/\text{cm}^2$  range.

We have also observed that in order to keep dislocations that are already bent at the SLS interfaces from threading up to the GaAs epilayer, high values of strain and layer thickness close to  $h_{\max}$  are required. We are currently in the process of optimizing the SLS structure parameters (strain, layer thickness and number of periods) to grow GaAs/Si with low defect density Si.

We have also carried out comparative studies of heteroepitaxial GaAs films grown on Si substrates using EBIC and plan-view TEM techniques and have identified areas of high and low dislocation density [9]. Good agreement exists regarding the lateral extent and dimensions of these regions in both techniques. In particular, those areas of low dislocation density were observed to be free of electrically active defects. Indeed, the absence of recombination centers in these regions would imply that an overall improvement in minority carrier lifetime and diffusion length had been achieved.

Thus, GaAs on Si with high dislocation density may still have decent diffusion length and can be potentially good material for solar cells. We will continue our efforts in reducing defects in GaAs on Si substrates and investigate the impact on the performance of single junction and multijunction solar cells.

## References

1. T. Katsuyama, J. Schetzina and S.M. Bedair, *J. Appl. Phys.* **62**, 498 (1987).
2. T. Katsuyama, Y.J. Yang and S.M. Bedair, *IEEE Elect. Device Lett.*, **EDL-8**, 240 (1987).
3. Z.J. Radzimski, G. Rozgonyi and S.M. Bedair, *Appl. Phys. Lett.*, **52**, 1692 (1988).
4. Z.J. Radzimski, B.L. Jiang, G. Rozgonyi, N. Hamaguchi and S.M. Bedair, *J. Appl. Phys.* **64**, 2328 (1988).
5. M.A. Tischler, T. Katsuyama, N. El-Masry and S.M. Bedair, *Appl. Phys. Lett.* **46**, 294 (1985).
6. N. El-Masry, T.P. Humphrey, J. Tarn, N. Hamaguchi, N. Karam and S.M. Bedair, *Appl. Phys. Lett.* **51**, 1608 (1987).
7. N. El-Masry, N. Hamaguchi, J. Tarn and S.M. Bedair, *Mat. Res. Soc.* **91**, 99 (1987).
8. N. El-Masry, J. Tarn, N. Karam and S.M. Bedair, *Mat. Res. Soc. Proceeding*, Dec. 1988.
9. T.P. Humphrey, N. Hamaguchi, N. El-Masry and S.M. Bedair, *Appl. Phys. Lett.*, *J. Appl. Phys.* **64**,

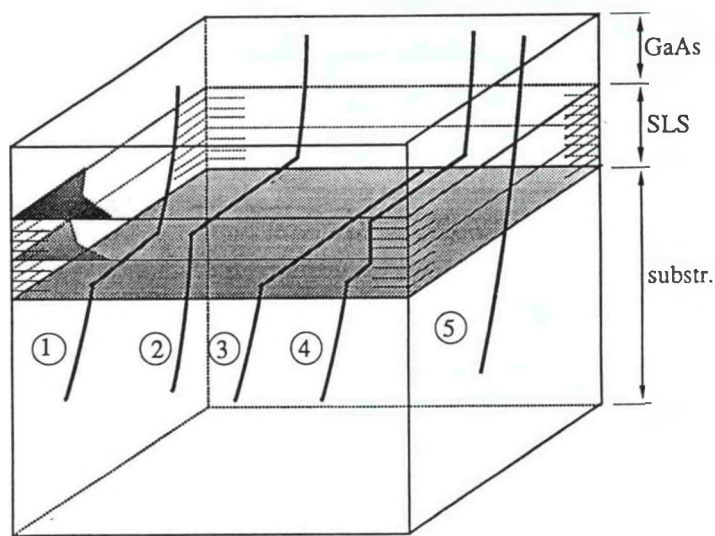


Figure 1 Schematic representation of dislocation configurations in SLS.



Figure 2 XRT showing dislocations that are bent at substrate/SLS interface.

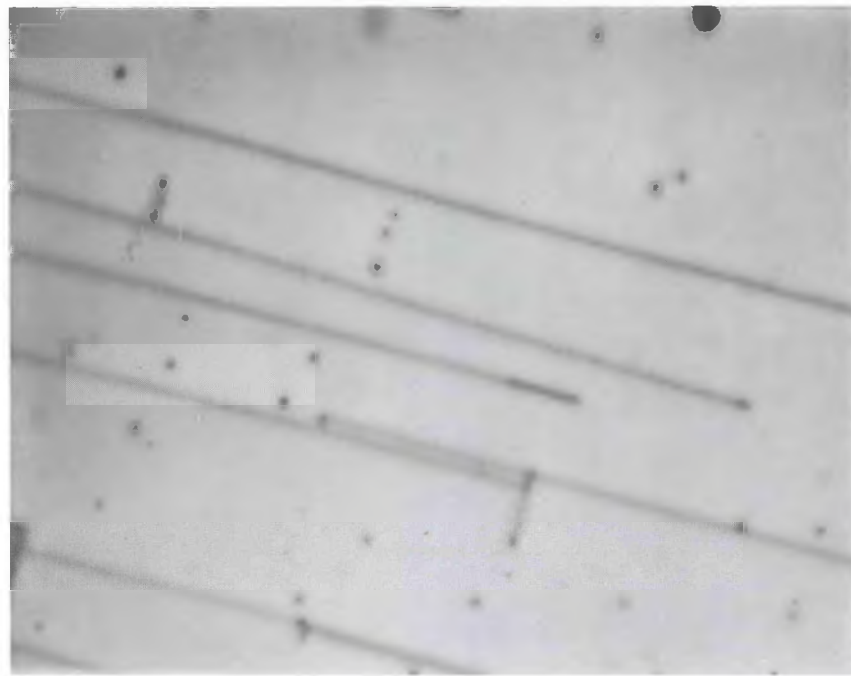


Figure 3 EBIC showing dislocations that are bent at SLS interfaces and substrate/SLS interface.

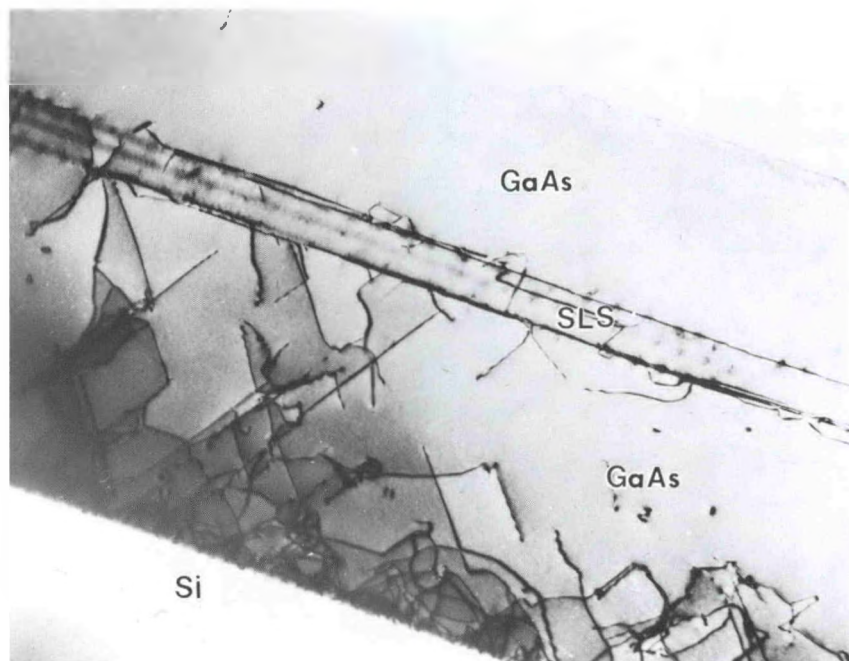


Figure 4 Combined effect of annealing and SLS in reducing defects in GaAs grown on Si substrate.

## 8.0 LIST OF ACTIVE SUBCONTRACTS

Active Contract List  
(FY 1988 Funding)

Contractor, Principal Investigator, Address	Work Title (Research Activity)	Contract Number	Total Funding (\$K)	FY 1988 Funding (\$K)	Start/End Dates
<b>AMORPHOUS SILICON, FY 1988</b>					
ARCO Solar Labs. D. Morel 20554 Plummer St. Chatsworth, CA 91311	Research on Stable High-Efficiency Large Area, a-Si Based Submodules	06003-3	2023.5	599.3	7/87 11/90
Chronar Corp. A. Delahoy P.O. Box 177 Princeton, NJ 08540	Research on Stable High-Efficiency Large Area a-Si Based Submodules	06003-1	2793.2	1297.8	3/87 6/90
Energy Conv. Dev. S. Guha 1675 W. Maple Rd. Troy, MI 48084	Research on High-Efficiency, Multiple-Gap, Multi-Junction a-Si Based Alloy Thin Film Solar Cells	06003-4	2699.3	1249.3	3/87 5/90
Glasstech Solar, A. Madan 12441 W. 49th Ave. Wheatridge, CO 80033	Research on Material Properties of Device Quality a-Si Deposited at High Deposition Rates Using Higher Order Silanes	06002-1	435	205	5/87 7/89
Harvard Univ. W. Paul 1350 Mass. Ave Cambridge, MA 02138	Structural & Electronic Studies of a-SiGe:H Alloys	18131	130	65	7/88 8/89
Harvard Univ. R. Gordon 1350 Mass.Ave Cambridge, MA 02138	Characterization & Comparison of Optically Transparent Conducting Film	18148	110	55	10/88 11/89
Minn. Mng. Mfg. (3M) F. Jeffrey/M. Weber 3M Center St. Paul, MN 55144	Improvement of a-Si Thin Film Photovoltaics on Polymer Substrate	07271	300	300	3/88 5/89

**Active Contract List (Continued)**  
**(FY 1988 Funding)**

Contractor, Principal Investigator, Address	Work Title (Research Activity)	Contract Number	Total Funding (\$K)	FY 1988 Funding (\$K)	Start/End Dates
<b>AMORPHOUS SILICON, FY 1988</b>					
Solarex Corp. D. Carlson 1335 Piccard Dr. Rockville, MD 20850	Research on High-Efficiency Single-Junction Monolithic Thin Film a-Si Solar Cells	06003-2	2861.2	1300	1/87 4/90
National Bureau Stnds. Quantum Physics Div. Boulder, CO 80303	Diagnostics of Glow Discharges Used to Produce a-Si:H Films	09078	431.8	105.8	4/84 11/30/88
Univ. Delaware R. Rocheleau/ S. Hegedus Newark, DE 19716	Photo-Chemical Vapor Deposition of a-Si Alloy Materials and Devices	18092	255	255	5/88 8/89
Univ. of Oregon J. Cohen Dept. Physics Eugene, OR 97403	Investigation of Origins of Metastable Light-Induced Changes in a-Si:H	18061	103.9	49.4	4/88 3/90
Xerox Corp. R. Street 3333 Coyote Hill Rd. Palo Alto, CA 93404	Research on Electronic & Structural Properties of a-Si Alloys	06056	1134.8	235	11/86 8/89
Chronar Corp. A. Delahoy P.O. Box 177 Princeton, NJ 08540	a-Si PV Devices Prepared by Chemical & Photochemical Vapor Deposition of Higher Order Silanes	04092	1105.7	0.0	9/84 11/88
Cal. Inst. Tech. M. Nicolet Pasadena, CA 91125	Investigations of Stable Contact to a-Si Thin Films	07133	60	30	9/87 10/88
Hughes Aircraft F. Gebhart Los Angeles, CA 90074	Study of Large Area a-Si Films by Photo-CVD	07193	39.9	0.0	11/87 1/89
U. North Carolina M. Silver Chapel Hill, NC 27599	Studies on Relative Effects of Charged & Neutral Defects in a-Si:H	07183	61.9	0.0	10/87 12/88

**Active Contract List (Continued)**  
**(FY 1988 Funding)**

Contractor, Principal Investigator, Address	Work Title (Research Activity)	Contract Number	Total Funding (\$K)	FY 1988 Funding (\$K)	Start/End Dates
<b>AMORPHOUS SILICON, FY 1988</b>					
U H T Corp. H. Wiesmann 145 Palisade St. Dobbs Ferry, NY 10522	Hydrogenated a-Si Films Prepared by Glow Discharge of Disilane	07209	69.6	0.0	12/87 12/88
Washington University R. Norberg/P. Fedders Lindell & Skinner Blvds. St. Louis, MO 63130	Research into the Structures of a-Si Alloy Films	06055	104.9	55.0	1/87 3/89
<b>POLYCRYSTALLINE THIN FILMS, FY 1988</b>					
Colo. State Univ. J. Sites Fort Collins, CO 80523	Analysis of Loss Mechanisms in Polycrystalline T.F. Solar Cells	18080	80	40	4/88 5/90
Georgia Tech. A. Rohatgi Atlanta, GA 30332	High-Efficiency CdZnTe Thin Film Cells	06031-1	373.8	150	6/87 11/89
Int'l Solar Elec. Tech. V. Kapur Englewood, CA 90301	High-Efficiency CuInSe <sub>2</sub> and CuInSe <sub>2</sub> Alloy Cells	06031-6	626.2	290	3/87 4/89
Photon Energy S. Albright El Paso, TX 79906	High-Efficiency Large Area CdTe & CdHgTe Panels	06031-3	485	226	7/87 7/89
Univ. of Delaware J. Phillips I.E.C. Newark, DE 19716	Two Terminal CuInSe <sub>2</sub> Based Cascade Cells	06031-7	425.7	213.9	1/87 3/89
Univ. of Delaware R. Birkmire I.E.C. Newark, DE 19716	Materials Analysis & Device Optimization of Solar Cells	06031-5	688.9	353	1/87 3/89
Univ. of S. Florida T. & S. Chu Tampa, FL 33620	Thin Film CdTe, ZnTe & Hg <sub>1-x</sub> Zn <sub>x</sub> Te Solar Cells	18091	299.9	199.9	7/88 8/90

**Active Contract List (Continued)**  
**(FY 1988 Funding)**

Contractor, Principal Investigator, Address	Work Title (Research Activity)	Contract Number	Total Funding (\$K)	FY 1988 Funding (\$K)	Start/End Dates
<b>POLYCRYSTALLINE THIN FILMS, FY 1988</b>					
Ametek P. Meyers 352 Godshall Dr. Harleysville, PA 19438	Polycrystalline Thin Film CdTe Solar Cells	06031-2	1109.2	227.1	6/87 9/89
Boeing Electric Co. W. Devaney P.O. Box 3999 Seattle, WA 98124	High-Efficiency CuInSe <sub>2</sub> & CuInGaSe <sub>2</sub> Based Cells	06031-8	756.6	297.9	11/87 12/89
Colo. State University J. Sites Ft. Collins, CO 80523	Device Physics Related to the Granular Nature of CuInSe <sub>2</sub> Solar Cells	06035	70	35	4/86 5/88
Louisiana State Univ. P. Ajmera Dept. Elec. & Computer Engineering Baton Rouge, LA 70803-5901	Fabrication & Characterization of Heterostructure PV Devices from Vacuum Grown Thin Films of ZnSnP <sub>2</sub>	18016	30	30	1/88 9/88
Univ. of Arkansas A. Hermann Fayetteville, AK 72701	Novel Thin-Film CuInSe <sub>2</sub> Fabrication	18017	15	15	1/88 2/89
Univ. of Illinois A. Rockett (acting) 809 S. Wright St. Champaign, IL 61820	Alternate Fabrication Techniques for High-Efficiency CuInSe <sub>2</sub> & CuInSe <sub>2</sub> Alloy Films & Cells	06031-9	155.1	155.1	8/87 11/89
<b>ADVANCED HIGH EFFICIENCY, FY 1988</b>					
Kopin Corp. J. Fan 695 Myles Standish Taunton, MA 02780	High-Efficiency, Thin Film GaAs and Ternary III-V Solar Cells	18083	335	335	4/88 6/89
Purdue Res. Found. Lundstrom/Mellock Hovde Hall West Lafayette, IN 47907	Basic Studies of III-V High-Efficiency Cell Components	05018-1	609.3	105	5/85 8/89

**Active Contract List (Continued)**  
**(FY 1988 Funding)**

Contractor, Principal Investigator, Address	Work Title (Research Activity)	Contract Number	Total Funding (\$K)	FY 1988 Funding (\$K)	Start/End Dates
<b>ADVANCED HIGH EFFICIENCY FY 88</b>					
Rensselaer Poly. Inst. S. Ghandhi/J. Borrego Troy, NY 12180	Res. on Semiconductors for High-Efficiency Solar Cells	05018-2	755	125	9/85 7/89
Spire Corp. S. Vernon Patriots Park Bedford, MA 01730	Gallium Arsenide Based Ternary Compounds & Multi-bandgap Solar Cell Research	18063	291.3	179.6	4/88 6/89
Kopin Corp. J. Fan 695 Myles Standish Taunton, MA 02780	High-Efficiency, Thin Film GaAs and Ternary III-V Solar Cells	07045	651.3	561.3	2/87 5/88
Spire Corp. J. Daly Patriots Park Bedford, MA 01730	Research on Large Scale MOCVD Deposition	18042	297.7	297.7	5/88 7/89
Univ. of CO R. Hayes Boulder, CO 80309	Device Modeling & Analysis of III-V Solar Cells	07198	41.1	41.1	8/87 11/88
Univ. of So. California S. Forrest University Park Los Angeles, CA	Nondestructive Electrical Analysis of Photovoltaic Materials	07132	56.9	56.9	6/87 7/88
Varian Associates C. Lewis 611 Hansen Way Palo Alto, CA 94303	Advanced High-Efficiency Concentrator Solar Cell Research	06004	827.2	306	3/86 5/88
<b>NEW IDEAS, FY 1988</b>					
Georgia Tech. C. Summers Atlanta, GA 30332	Avalanche Heterostructure & Superlattice Solar Cells	06074-1	103.4	103.4	6/87 7/88
I.S.E.T B. Basol 8635 Aviation Bl. Inglewood, CA 90301	Low-Cost Techniques for Producing CdZnTe Devices	06074-2	99.3	99.3	6/87 12/88

**Active Contract List (Continued)**  
**(FY 1988 Funding)**

Contractor, Principal Investigator, Address	Work Title (Research Activity)	Contract Number	Total Funding (\$K)	FY 1988 Funding (\$K)	Start/End Dates
<b>NEW IDEAS, FY 1988</b>					
Rensselaer Poly. Inst. S. Ghandhi/J. Borrego Troy, NY 12181	Hydrogen Radical Enhanced Growth of Solar Cells	06074-3	100.1	100.1	6/87 4/89
Stanford Univ. R. Swanson 660 Arguello Way Stanford, CA 94305	High-Efficiency Flat Plate Silicon Solar Cells	06074-4	101.1	101.1	6/87 7/88
Vactronic Lab. C. Wronski 160 Wilbur Place Bohemia, NY 11716	Novel Precursor Compound for High Rate Deposition	06074-5	94.3	94.3	2/88 3/89
<b>UNIVERSITY PROGRAM, FY 1988</b>					
No. Carolina State Univ. S. Bedair Box 7003 Raleigh, NC 27695	New Approaches to High-Efficiency Solar Cells by MOCVD	05009-1	502	86.7	9/85 12/88
University of Utah C. Taylor 302 Park Bldg. Salt Lake City, UT 84112	Electronic Process in Thin Film PV Materials	05009-2	686.8	113.2	9/85 12/88
Univ. of So. California D. Dapkus University Park Los Angeles, CA 90089	Low Temperature MOCVD Growth Process for High-Efficiency Solar Cells	05009-3	516	85	9/85 12/88
Stanford University R. Bube 660 Arguello Way Stanford, CA 94305	Ion Beam Doping of II-VI Compounds during Physical Vapor Deposition	05009-4	714.7	123.8	9/85 12/88
Brown University J. Garritsen Box 1929 Providence, RI 02912	Rapid Liquid Phase Epitaxy of Ternary III-V Semiconductors for Tandem Solar Cell Applications	05009-5	509.4	82.4	9/85 12/88

**Active Contract List (Continued)**  
**(FY 1988 Funding)**

Contractor, Principal Investigator, Address	Work Title (Research Activity)	Contract Number	Total Funding (\$K)	FY 1988 Funding (\$K)	Start/End Dates
<b>UNIVERSITY PROGRAM FY88</b>					
Syracuse Univiversity E. Schiff Skytop Rd. Syracuse, NY 13244	Research on Defects & Photocarrier Processes in a-Si:H Alloys	06005-2	352.9	116	9/86 11/89
Carnegie-Mellon Univ. Milnes/Schlesinger 5000 Forbes Ave. Pittsburgh, PA 15213	Improvement of Bulk Epitaxial III-V Semiconductors for Solar Cells by Creation of Denuded Recombination Zones	06005-3	312	130	9/86 11/89
Univ. of Illinois W. Jenkins 1101 W. Springfield Ave. Urbana, IL 61801	Surface Reactions during Growth of CuInSe <sub>2</sub> Films from CuInSe Vapors	06005-1	319.6	101	9/86 11/89
<b>CRYSTALLINE SILICON, FY 1988</b>					
No. Carolina State Univ. G. Rozgonyi Box 7003 Raleigh, NC	Effectiveness & Stability of Impurity Defect Interactions & their Impact on Minority Carrier Lifetime	18097-2	140	140	6/88 7/89
Duke University U. Goesele 001E Allen Build. Durham, NC 27706	Point Defects & their Influence on Solar Cell Related Electric Properties of Crys. Silicon	18097-1	99.3	99.3	7/88 8/89
Georgia Tech. A. Rohatgi Atlanta, GA 30332	Impurity Characterization Support for Silicon	18155	25	25	10/88 12/89
SUNY/Albany J. Corbett Albany NY 12201	Passivation & Gettering in Solar Cell Silicon	18097-3	126.7	126.7	7/88 8/89

**Active Contract List (Concluded)**  
**(FY 1988 Funding)**

Contractor, Principal Investigator, Address	Work Title (Research Activity)	Contract Number	Total Funding (\$K)	FY 1988 Funding (\$K)	Start/End Dates
<b>CRYSTALLINE SILICON, FY 1988</b>					
Univ. of So. California S. Forrest University Park Los Angeles, CA 90089	Electric Characterization Support for Crystalline Silicon	18154	25	25	10/88 12/89
Cornell University D. Ast 120 Day Hall Ithaca, NY	Role of Carbon, Oxygen, & Hydrogen in Solar Solar Silicon	06125	93.1	71.6	6/87 10/88

## BIBLIOGRAPHY

### Subcontractor Reports and Publications

Abid, B.; Gong, J. R.; Goslowsky, H. G.; Bachmann, K. J. (1987). "CuInS<sub>2-y</sub>Se<sub>2-2y</sub> and CuGa<sub>x</sub>In<sub>1-x</sub>Se<sub>2</sub>: Bulk Crystal Growth Conditions and Properties." Conference Record of the Nineteenth IEEE Photovoltaic Specialists Conference-1987; May 4-8, 1987; New Orleans, Louisiana. New York: The Institute of Electrical and Electronics Engineers, Inc.; pp. 1305-1308. Work performed by Department of Chemistry and Department of Materials Science and Engineering, North Carolina State University, Raleigh, North Carolina.

Adler, D. (1987). "Density of States of Amorphous Semiconductors." Physics of Amorphous Semiconductor Devices; 15-16 January 1987; Los Angeles, California, Proceedings of SPIE - The International Society for Optical Engineering, Volume 763, Adler, D., ed. Bellingham, WA: SPIE - The International Society for Optical Engineering; pp. 2-9. Work performed by Center for Materials Science and Engineering, Massachusetts Institute of Technology, Cambridge, Massachusetts.

Adler, D.; Haggerty, J. S. (February 1988). Laser-Heated CVD Process for Depositing Thin Films for Low-Cost Solar Cell Applications. SERI/STR-211-3235. 213 pp. Work performed by Massachusetts Institute of Technology, Cambridge, Massachusetts. Available NTIS: Order No. DE88001162.

Adomines, A.; Liu, R. (1987). "Thin Film Submodule Testing." Photovoltaic Thin Film Module Reliability Testing and Evaluation Workshop; August 13-14, 1987; Lakewood, Colorado, SERI/CP-275-3239, Mrig, L., ed. Golden, CO: Solar Energy Research Institute; pp. 117-133. Work performed by Ametek/Applied Materials Laboratory, Harleysville, Pennsylvania.

Agnello, P. D.; Ghandhi, S. K. (May/June 1988). "The Reactions of Triethylindium and Trimethylgallium with Arsine Gas." Solar Cells (24:1-2); pp. 117-126. Presented at the 8th Photovoltaic Research and Development Project Review Meeting, Denver, Colorado, November 15-18, 1987. Work performed by Electrical, Computer and Systems Engineering Department, Rensselaer Polytechnic Institute, Troy, New York.

Ajmera, P. K.; Shin, H. Y. (February 1988). Growth and Characterization of Thin Films of ZnSnP<sub>2</sub>, Final Subcontract Report, 15 October 1983-31 May 1987. SERI/STR-211-3216. 69 pp. Available NTIS: Order No. DE88001164.

Albright, S. P.; Jordan, J. F.; Singh, V. P.; Ackerman, B. (1987). "Research on Large Area CdS/CdTe Solar Panels." Proceedings of the Polycrystalline Thin Film Program Meeting; July 20-22, 1987; Lakewood, Colorado. SERI/CP-211-3171. pp. 13-18. Work performed by Photon Energy, Inc., Dallas, Texas, and The University of Texas at El Paso, El Paso, Texas.

Albright, S. P.; Singh, V. P.; Jordan, J. F. (May/June 1988). "Junction Characteristics of CdS/CdTe Solar Cells." Solar Cells (24:1-2); pp. 43-56. Presented at the 8th Photovoltaic Research and Development Project Review Meeting, Denver, Colorado, November 15-18, 1987. Work performed by Photon Energy, Inc., El Paso, Texas.

Arya, R. R. (1988). "High Efficiency Amorphous Silicon Based Solar Cells: A Review." Amorphous Silicon Technology, Materials Research Society Symposium Proceedings, Volume 118, Madan, A. et al., eds. Pittsburgh, PA: Materials Research Society;

pp. 569-580. Presented at the MRS Spring Meeting, Reno, Nevada, April 5-8, 1988. Work performed by Thin Film Division, Solarex Corporation, Newtown, Pennsylvania.

Amorphous Silicon Technology, Materials Research Society Symposium Proceedings, Volume 118, Madan, A. et al., eds. Pittsburgh, PA: Materials Research Society; pp. 569-580. Presented at the MRS Spring Meeting, Reno, Nevada, April 5-8, 1988. Work performed by Thin Film Division, Solarex Corporation, Newtown, Pennsylvania.

Arya, R. R.; Bennett, M. S.; Catalano, A.; Rajan, K. (November 1987). "Effect of a-Si:C:H Graded p/i Interface on the Performance and Stability of a-Si:H p-i-n Solar Cells." 3rd International Photovoltaic Science and Engineering Conference, November 3-6, 1987, Tokyo, Japan; Technical Digest. Tokyo: Secretariat of International PVSEC-3; pp. 457-460. Work performed by Solarex Thin Film Division, Newtown, Pennsylvania.

Arya, R. R.; Catalano, A.; Newton, J. L.; Morris, J. (November 1987). "High Efficiency a-Si:Ge:H Single and Stacked Junction Solar Cells." 3rd International Photovoltaic Science and Engineering Conference, November 3-6, 1987, Tokyo, Japan; Technical Digest. Tokyo: Secretariat of International PVSEC-3; pp. 725-729. Work performed by Solarex Thin Film Division, Newtown, Pennsylvania.

Aspen, F. E.; Grimmer, D. P.; Jacobson, R. L.; Jeffrey, F. R.; Tran, N. T. (June 1988). Research on High-Efficiency, Single-Junction, Monolithic, Thin-Film Amorphous Silicon Solar Cells, Semiannual Subcontract Report No. 3, 1 December 1985 - 31 May 1986. SERI/STR-211-3343. 64 pp. Work performed by Electronic and Information Sector Laboratories, 3M Company, St. Paul, Minnesota. Available NTIS: Order No. DE88001176.

Aspen, F. E.; Grimmer, D. P.; Jacobson, R. L.; Jeffrey, F. R.; Tran, N. T. (June 1988). Research on High-Efficiency, Single-Junction, Monolithic, Thin-Film Amorphous Silicon Solar Cells, Final Technical Report, February 1987. SERI/STR-211-3344. 127 pp. Work performed by Electronic and Information Sector Laboratories, 3M Company, St. Paul, Minnesota. Available NTIS: Order No. DE88001177.

Bachmann, K. J.; Goslowsky, H. G. (1987). "Growth of Bulk Single Crystals of Semiconducting Ternary Compounds and Alloys." Ternary and Multinary Compounds; Proceedings of the 7th International Conference; Snowmass, Colorado, September 10-12, 1986. Pittsburgh, PA: Materials Research Society; pp. 169-175. Work performed by Department of Chemistry, North Carolina State University, Raleigh, North Carolina.

Bar-Yam, Y.; Joannopoulos, J. D.; Adler, D. (1987). "Photo-Induced Degradation and Stability in Semiconductor Devices." International Conference on Stability of Amorphous Silicon Alloy Materials and Devices; January 28-30, 1987; Palo Alto, California, AIP Conference Proceedings 157, Stafford, B. L.; Sabisky, E., eds. New York: American Institute of Physics; pp. 185-192. Work performed by Center for Materials Science and Engineering, Massachusetts Institute of Technology, Cambridge, Massachusetts.

Baron, B. N.; Hegedus, S. S.; Jackson, S. C. (February 1988). Low-Band-Gap, Amorphous-Silicon-Based Alloys by Photochemical Vapor Deposition, Final Subcontract Report, 1 October 1985-30 November 1986. SERI/STR-211-3214. 29 pp. Work performed by Institute of Energy Conversion, University of Delaware, Newark, Delaware. Available NTIS: Order No. DE88001165.

Basol, B. M. (January/February 1988). "Electrodeposited CdTe and HgCdTe Solar Cells." Solar Cells (23:1-2); pp. 69-88. Work performed by International Solar Electric Technology, Inglewood, California.

Basol, B. M.; Kapur, V. K. (1987). "Electrodeposition Techniques for Cd(Zn)Te Thin Film Preparation." Proceedings of the Polycrystalline Thin Film Program Meeting; July 20-22, 1987; Lakewood, Colorado. SERI/CP-211-3171. p. 155. Work performed by International Solar Electric Technology (ISET), Inglewood, California.

Bedair, S. M. (1987). "New Approaches for High Efficiency Solar Cells." Proceedings of the 1987 High-Efficiency Photovoltaic Subcontractors' Review Meeting; May 19-20, 1987; Golden, Colorado. SERI/CP-211-3152. Golden, CO: Solar Energy Research Institute; pp. 15-19. Work performed by Department of Electrical and Computer Engineering, North Carolina State University, Raleigh, North Carolina.

Bennett, M. S.; Newton, J. L.; Rajan, K. (1987). "Annealing Kinetics of Photo-Degraded a-Si:H Solar Cells." International Conference on Stability of Amorphous Silicon Alloy Materials and Devices; January 28-30, 1987; Palo Alto, California, AIP Conference Proceedings 157, Stafford, B. L.; Sabisky, E., eds. New York: American Institute of Physics; pp. 207-214. Work performed by Solarex Thin Film Division, Newtown, Pennsylvania.

Bennett, M. S.; Newton, J. L.; Rajan, K. (1987). "Influence of Electric Field on Stability." Seventh E. C. Photovoltaic Solar Energy Conference; Proceedings of the International Conference; Sevilla, Spain; 27-31 October 1986. Dordrecht/Boston: D. Reidel Publishing Company; pp. 544-548. Work performed by Solarex Corporation, Newtown, Pennsylvania.

Bennett, M. S.; Wiedeman, S.; Newton, J. L.; Rajan, K. (1987). "Investigation of Photo-Induced Degradation by Means of Photothermal Deflection Spectroscopy." Amorphous Silicon Semiconductors - Pure and Hydrogenated, Materials Research Society Symposia Proceedings, Volume 95, Madan, A., et al., eds. Pittsburgh, PA: Materials Research Society; pp. 577-582. Presented at the MRS Spring Meeting, Anaheim, California, April 21-24, 1987. Work performed by Solarex Corporation, Newtown, Pennsylvania.

Bennett, M. S.; Wiedeman, S.; Rajan, K.; Smoot, M. (1987). "Light-Induced Degradation and Annealing Behaviour of Amorphous Silicon: A Comparison of Films and Devices." Amorphous Silicon Semiconductors - Pure and Hydrogenated, Materials Research Society Symposia Proceedings, Volume 95, Madan, A., et al., eds. Pittsburgh, PA: Materials Research Society; pp. 601-606. Presented at the MRS Spring Meeting, Anaheim, California, April 21-24, 1987. Work performed by Solarex Corporation, Newtown, Pennsylvania.

Bhat, P. K.; Chatham, H.; Del Cueto, J.; von Roedern, B.; Madan, A. (May/June 1988). "Optoelectronic Properties and Plasma Diagnostics of High Deposition Rate a-Si:H Films Using Disilane." Solar Cells (24:1-2); pp. 57-65. Presented at the 8th Photovoltaic Research and Development Project Review Meeting, Denver, Colorado, November 15-18, 1987. Work performed by Glasstech Solar, Inc., Wheat Ridge, Colorado.

Bhat, P. K.; Chatham, H.; Madan, A. (June 1988). Preparation and Properties of High-Deposition-Rate a-Si:H Films and Solar Cells Using Disilane, Annual Subcontract Report, 1 May 1987 - 30 April 1988. SERI/STR-211-3364. 38 pp. Work performed by Glasstech Solar, Inc., Wheatridge, Colorado. Available NTIS: Order No. DE88001191.

Bhat, P. K.; Chatham, H.; Shing, Y. H.; Perry, J. W. (December 1987). "Growth of Glow Discharge Hydrogenated Amorphous Silicon." Journal of Non-Crystalline Solids (97&98, Part II); pp. 1383-1386. Presented at the Twelfth International Conference on Amorphous and Liquid Semiconductors, Prague, Czechoslovakia, August 24-28, 1987.

Work performed by Glasstech Solar, Inc., Wheatridge, Colorado, and Jet Propulsion Laboratory, Pasadena, California.

Bhimnathwala, H. G.; Taskar, N. R.; Lee, W. I.; Bhat, I. B.; Ghandi, S. K.; Borrego, J. M. (1987). "Photovoltaic Properties of CdTe Layers Grown by OMVPE." Conference Record of the Nineteenth IEEE Photovoltaic Specialists Conference-1987; May 4-8, 1987; New Orleans, Louisiana. New York: The Institute of Electrical and Electronics Engineers, Inc.; pp. 1476-1481. Work performed by Electrical, Computer and Systems Engineering Department, Rensselaer Polytechnic Institute, Troy, New York.

Birkmire, R. W.; Hegedus, S. S.; McCandless, B. E.; Phillips, J. E.; Shafarman, W. N. (1987). "Analysis of a Transparent Cu/ITO Contact and Heat Treatments on CdTe/CdS Solar Cells." Conference Record of the Nineteenth IEEE Photovoltaic Specialists Conference-1987; May 4-8, 1987; New Orleans, Louisiana. New York: The Institute of Electrical and Electronics Engineers, Inc.; pp. 967-971. Work performed by Institute of Energy Conversion, University of Delaware, Newark, Delaware.

Birkmire, R. W.; McCandless, B. E. (11 July 1988). "Specular CuInSe<sub>2</sub> Films for Solar Cells." Applied Physics Letters (53:2); pp. 140-141. Work performed by Institute of Energy Conversion, University of Delaware, Newark, Delaware.

Birkmire, R. W.; McCandless, B. E.; Shafarman, W. N. (January/February 1988). "CdTe/CdS Solar Cells with Transparent Contacts." Solar Cells (23:1-2); pp. 115-126. Work performed by Institute of Energy Conversion, University of Delaware, Newark, Delaware.

Birkmire, R. W.; Meakin, J. D.; Phillips, J. E.; Rocheleau, R. E. (1987). "Analysis and Optimization of CuInSe<sub>2</sub> Solar Cells." Proceedings of the Polycrystalline Thin Film Program Meeting; July 20-22, 1987; Lakewood, Colorado. SERI/CP-211-3171. pp. 81-86. Work performed by Institute of Energy Conversion, University of Delaware, Newark, Delaware.

Birkmire, R. W.; Phillips, J. E. (October 1987). Stable, High-Efficiency, CuInSe<sub>2</sub>-Based, Polycrystalline Thin-Film Tandem Solar Cells, Final Subcontract Report, 16 March 1984 - 15 March 1987. SERI/STR-211-3249. 122 pp. Work performed by Institute of Energy Conversion, University of Delaware, Newark, Delaware. Available NTIS: Order No. DE88001116.

Birkmire, R. W.; Phillips, J. E.; Rocheleau, R. E. (1987). "Two-Terminal CuInSe<sub>2</sub>-Based Cascade Cells." Proceedings of the Polycrystalline Thin Film Program Meeting; July 20-22, 1987; Lakewood, Colorado. SERI/CP-211-3171. pp. 183-189. Work performed by Institute of Energy Conversion, University of Delaware, Newark, Delaware.

Borrego, J. M.; Ghandhi, S. K. (October 1987). Research on Single-Crystal CdTe Solar Cells, Final Subcontract Report, 1 February 1985 - 1 February 1987. SERI/STR-211-3224. 100 pp. Work performed by Electrical Computer and Systems Engineering Department, Rensselaer Polytechnic Institute, Troy, New York. Available NTIS: Order No. DE88001115.

Borrego, J. M.; Ghandhi, S. K. (1987). "Research on Semiconductors for High Efficiency Solar Cells." Proceedings of the 1987 High-Efficiency Photovoltaic Subcontractors' Review Meeting; May 19-20, 1987; Golden, Colorado. SERI/CP-211-3152. Golden, CO: Solar Energy Research Institute; pp. 67-73. Work performed by Electrical, Computer, and Systems Engineering Department, Rensselaer Polytechnic Institute, Troy, New York.

Bothra, S.; Bhimnathwala, H. G.; Parat, K. K.; Ghandi, S. K.; Borrego, J. M. (1987). "Characterization and Modelling of Open Tube Diffused N+P Bulk InP Solar Cells." Conference Record of the Nineteenth IEEE Photovoltaic Specialists Conference-1987; May 4-8, 1987; New Orleans, Louisiana. New York: The Institute of Electrical and Electronics Engineers, Inc.; pp. 261-266. Work performed by Electrical, Computer and Systems Engineering Department, Rensselaer Polytechnic Institute, Troy, New York.

Bottenberg, W.; Mitchell, K. W.; Wieting, R. (May 1988). Research on Amorphous-Silicon-Based Thin-Film Photovoltaic Devices, Semiannual Subcontract Report, 1 July 1987 - 31 December 1987. SERI/STR-211-3350. 106 pp. Work performed by ARCO Solar, Inc., Camarillo, California. Available NTIS: Order No. DE88001169.

Boyce, J. B.; Ready, S. E.; Tsai, C. C. (December 1987). "Local Structure of Dopants in Compensated and Singly-Doped Amorphous Silicon." Journal of Non-Crystalline Solids (97&98, Part I); pp. 345-348. Presented at the Twelfth International Conference on Amorphous and Liquid Semiconductors, Prague, Czechoslovakia, August 24-28, 1987. Work performed by Xerox Palo Alto Research Center, Palo Alto, California.

Bragagnolo, J. A. (October 1987). Research on High-Efficiency, Stacked, Multijunction, Amorphous Silicon Alloy Thin-Film Solar Cells, Final Subcontract Report, 11 October 1983-30 October 1986. SERI/STR-211-3231. 123 pp. Work performed by Spire Corporation, Bedford, Massachusetts. Available NTIS: Order No. DE88001108.

Bragagnolo, J. A.; Littlefield, P.; Mastrovito, A.; Storti, G. (1987). "Optimum Deposition Conditions for a-(Si,Ge):H Using a Triode-Configured RF Glow Discharge System." Conference Record of the Nineteenth IEEE Photovoltaic Specialists Conference-1987; May 4-8, 1987; New Orleans, Louisiana. New York: The Institute of Electrical and Electronics Engineers, Inc.; pp. 878-883. Work performed by Spire Corporation, Bedford, Massachusetts.

Branz, H. M.; Capuder, K.; Lyons, E. H.; Haggerty, J. S.; Adler, D. (15 November 1987-II). "Conductivity and Quenched-In Defects in Hydrogenated Amorphous Silicon." Physical Review. B, Condensed Matter (36:15); pp. 7934-7940. Work performed by Massachusetts Institute of Technology, Cambridge, Massachusetts.

Branz, H. M.; Lyons, E. H.; Capuder, K.; Haggerty, J. S.; Adler, D. (1987). "Metastable Effects in the DC Conductivity of Hydrogenated Amorphous Silicon." International Conference on Stability of Amorphous Silicon Alloy Materials and Devices; January 28-30, 1987; Palo Alto, California, AIP Conference Proceedings 157, Stafford, B. L.; Sabisky, E., eds. New York: American Institute of Physics; pp. 199-206. Work performed by Department of Physics, Massachusetts Institute of Technology, Cambridge, Massachusetts; Energy Laboratory, Massachusetts Institute of Technology, Cambridge, Massachusetts; and Department of Electrical Engineering and Computer Science, Massachusetts Institute of Technology, Cambridge, Massachusetts.

Bube, R. H. (January/February 1988). "CdTe Junction Phenomena." Solar Cells (23:1-2); pp. 1-17. Work performed by Department of Materials Science and Engineering, Stanford University, Stanford, California.

Bube, R. H.; Fahrenbruch, A. L.; Lopez-Otero, A.; Chien, K. F.; Sharps, P. (1987). "Vapor Phase and Ion-Assisted Doping of Thin Film p-CdTe." Proceedings of the Polycrystalline Thin Film Program Meeting; July 20-22, 1987; Lakewood, Colorado. SERI/CP-211-3171. pp. 43-49. Work performed by Department of Materials Science and Engineering, Stanford University.

Cahen, D. (1987). "Some Thoughts on Defect Chemistry of Ternaries." Ternary and Multinary Compounds; Proceedings of the 7th International Conference; Snowmass, Colorado, September 10-12, 1986. Pittsburgh, PA: Materials Research Society; pp. 433-442. Work performed by The Weizmann Institute of Science, Rehovot, Israel.

Cahen, D.; Hodes, G. (December 1987). Ternary Adamantine Materials for Low-Cost Solar Cells, Final Subcontract Report, 1 November 1984 - 31 December 1986. SERI/STR-211-3289. 44 pp. Work performed by Weizmann Institute of Science, Rehovot, Israel. Available NTIS.

Carlson, D. E. (1987). "Light-Induced Effects in Amorphous Silicon Solar Cells." Proceedings of the International Workshop on Amorphous Semiconductors; Beijing, China; 13-18 October 1986. Singapore: World Scientific Publishing Co.; pp. 193-198. Work performed by Solarex Thin Film Division, Newtown, Pennsylvania.

Carlson, D. E. (1987). "New Developments in Amorphous Silicon Solar Cells." Proceedings of the International Workshop on Amorphous Semiconductors; Beijing, China; 13-18 October 1986. Singapore: World Scientific Publishing Co.; pp. 321-326. Work performed by Solarex Thin Film Division, Newtown, Pennsylvania.

Carlson, D. E.; Arya, R. R.; Bennett, M. S.; Catalano, A.; D'Aiello, R. C.; Dickson, C. R.; Fortmann, C. M.; Goldstein, B.; Morris, J.; Newton, J. L.; Wiedeman, S. (May/June 1988). "Progress Toward High Efficiency Multijunction Cells and Submodules at Solarex." Solar Cells (24:1-2); pp. 165-169. Presented at the 8th Photovoltaic Research and Development Project Review Meeting, Denver, Colorado, November 15-18, 1987. Work performed by Solarex Thin Film Division, Newtown, Pennsylvania.

Carpenter, M. S.; Melloch, M. R.; Dungan, T. E. (4 July 1988). "Schottky Barrier Formation on  $(\text{NH}_4)_2\text{S}$ -treated n- and p-type (100) GaAs." Applied Physics Letters (53:1); pp. 66-68. Work performed by School of Electrical Engineering, Purdue University, West Lafayette, Indiana.

Carpenter, M. S.; Melloch, M. R.; Lundstrom, M. S.; Tobin, S. P. (20 June 1988). "Effects of  $\text{Na}_2\text{S}$  and  $(\text{NH}_4)_2\text{S}$  Edge Passivation Treatments on the Dark Current-Voltage Characteristics of GaAs pn Diodes." Applied Physics Letters (52:25); pp. 2157-2159. Work performed by School of Electrical Engineering, Purdue University, West Lafayette, Indiana, and Spire Corporation, Bedford, Massachusetts.

Catalano, A.; Arya, R. R.; Fortmann, C. M.; Morris, J.; Newton, J. L.; O'Dowd, J. G. (1987). "High Performance, Graded Bandgap a-Si:H Solar Cells." Conference Record of the Nineteenth IEEE Photovoltaic Specialists Conference-1987; May 4-8, 1987; New Orleans, Louisiana. New York: The Institute of Electrical and Electronics Engineers, Inc.; pp. 1506-1507. Work performed by Thin Film Division, Solarex Corporation, Newtown, Pennsylvania.

Catalano, A.; Fortmann, C. M.; Newton, J. L.; Arya, R. R.; Wood, G. (November 1987). "High Efficiency a-Si<sub>1-x</sub>C<sub>x</sub>:H Single and Stacked Junction Solar Cells." 3rd International Photovoltaic Science and Engineering Conference, November 3-6, 1987, Tokyo, Japan; Technical Digest. Tokyo: Secretariat of International PVSEC-3; pp. 705-708. Work performed by Solarex Thin Film Division, Newtown, Pennsylvania.

Catalano, A.; Newton, J. L.; Arya, R. R.; Wiedeman, S. (November 1987). "Opto-Electronic Properties of Amorphous Si<sub>1-x</sub>Ge<sub>x</sub>:H Films Prepared by DC Glow Discharge." 3rd International Photovoltaic Science and Engineering Conference,

November 3-6, 1987, Tokyo, Japan; Technical Digest. Tokyo: Secretariat of International PVSEC-3; pp. 61-64. Work performed by Solarex Thin Film Division, Newtown, Pennsylvania.

Catalano, A.; Wood, G. (15 February 1988). "Method for Improved Short-Wavelength Response in Hydrogenated Amorphous Silicon-Based Solar Cells." Journal of Applied Physics (63:4); pp. 1220-1222. Work performed by Thin Film Division, Solarex Corporation, Newtown, Pennsylvania.

Catalano, A.; Wood, G. (1988). "Short Wavelength Response in a-Si:H p-i-n Diodes: A Simple Method to Minimize Interface Recombination." Amorphous Silicon Technology, Materials Research Society Symposium Proceedings, Volume 118, Madan, A., et al., eds. Pittsburgh, PA: Materials Research Society; pp. 581-586. Presented at the MRS Spring Meeting, Reno, Nevada, April 5-8, 1988. Work performed by Thin Film Division, Solarex Corporation, Newtown, Pennsylvania.

Chahed, L.; Vuye, G.; Theye, M. L.; Li, Y. M.; Mackenzie, K. D.; Paul, W. (December 1987). "Comparative Study of the Optical Absorption Spectra of Amorphous Hydrogenated Silicon Derived from Photothermal Deflection Spectroscopy and Photoconductivity Measurements." Journal of Non-Crystalline Solids (97 & 98, Part I); pp. 727-730. Presented at the Twelfth International Conference on Amorphous and Liquid Semiconductors, Prague, Czechoslovakia, August 24-28, 1987. Work performed by Laboratoire des Solides, Universite Pierre et Marie Curie, Paris, France, and Division of Applied Sciences, Harvard University, Cambridge, Massachusetts.

Chatham, H.; Bhat, P. K. (1988). "Comparative Discharge Diagnostic Study of Silane, Disilane, and Germane RF Discharges Using Optical Emission Spectroscopy and Mass Spectrometry." Amorphous Silicon Technology, Materials Research Society Symposium Proceedings, Volume 118, Madan, A., et al., eds. Pittsburgh, PA: Materials Research Society; pp. 31-36. Presented at the MRS Spring Meeting, Reno, Nevada, April 5-8, 1988. Work performed by Glasstech Solar, Inc., Wheat Ridge, Colorado.

Chen, W. S.; Stewart, J. M.; Stanbery, B. J.; Devaney, W. E.; Mickelsen, R. A. (1987). "Development of Thin Film Polycrystalline  $\text{CuIn}_{1-x}\text{Ga}_x\text{Se}_2$  Solar Cells." Conference Record of the Nineteenth IEEE Photovoltaic Specialists Conference-1987; May 4-8, 1987; New Orleans, Louisiana. New York: The Institute of Electrical and Electronics Engineers, Inc.; pp. 1445-1447. Work performed by Boeing High Technology Center, Seattle, Washington.

Chesarek, W.; Mitchell, K.; Mason, A.; Fabick, L. (July/August 1988). "EBIC Analysis of  $\text{CuInSe}_2$  Devices." Solar Cells (24:3-4); pp. 263-270. Presented at the 8th Photovoltaic Research and Development Project Review Meeting, Denver, Colorado, November 15-18, 1987. Work performed by ARCO Solar, Inc., Chatsworth, California.

Chu, S. S.; Chu, T. L. (1987). "Thin Film Solar Cells from II-VI Solid Solutions." Proceedings of the Polycrystalline Thin Film Program Meeting; July 20-22, 1987; Lakewood, Colorado. SERI/CP-211-3171. pp. 167-171. Work performed by Southern Methodist University, Dallas, Texas.

Chu, S. S.; Chu, T. L.; Han, K. D.; Liu, Y. Z.; Mantravadi, M. K. (1987). "Chemical Vapor Deposition of Cadmium Tellurium Films for Photovoltaic Devices." Proceedings of the Tenth International Conference on Chemical Vapor Deposition 1987, Electrochemical Society Proceedings Volume 87-8, Cullen, G. W.; Blocher, J. M., Jr., eds. Pennington, NJ: The Electrochemical Society; pp. 982-989. Presented at the October 1987 Meeting

of The Electrochemical Society, Honolulu, Hawaii. Work performed by Southern Methodist University, Dallas, Texas.

Chu, T. L. (June 1988). Thin-Film Cadmium Telluride Solar Cells, Final Subcontract Report: 1 May 1985 - 31 May 1988. SERI/STR-211-3365. 44 pp. Work performed by Southern Methodist University, Dallas, Texas. Available NTIS: Order No. DE88001183.

Chu, T. L. (January/February 1988). "Thin Film Cadmium Telluride Solar Cells by Two Chemical Vapor Deposition Techniques." Solar Cells (23:1-2); pp. 31-48. Work performed by Electrical Engineering Department, Southern Methodist University, Dallas, Texas.

Chu, T. L. (October 1987). Thin-Film Cadmium Telluride Solar Cells, Annual Subcontract Report, 1 May 1986 - 31 May 1987. SERI/STR-211-3229. 33 pp. Work performed by Southern Methodist University, Dallas, Texas. Available NTIS: Order No. DE88001107.

Chu, T. L.; Chu, S. S. (1987). "Thin Film Cadmium Telluride Solar Cells." Proceedings of the Polycrystalline Thin Film Program Meeting; July 20-22, 1987; Lakewood, Colorado. SERI/CP-211-3171. pp. 1-7. Work performed by Southern Methodist University, Dallas, Texas.

Chu, T. L.; Chu, S. S.; Ang, S. S. T. (1 August 1988). "Electrical Properties of CdS/CdTe Heterojunctions." Journal of Applied Physics (64:3); pp. 1233-1237. Work performed by Southern Methodist University, Dallas, Texas.

Chu, T. L.; Chu, S. S.; Han, K. D.; Han, Y. X.; Liu, Y. H.; Mantravadi, M. K. (May/June 1988). "Efficient Thin Film Cadmium Telluride Heterojunction Solar Cells." Solar Cells (24:1-2); pp. 27-34. Presented at the 8th Photovoltaic Research and Development Project Review Meeting, Denver, Colorado, November 15-18, 1987. Work performed by Southern Methodist University, Dallas, Texas.

Cohen, J. D. (October 1987). Investigations of the Origins of Metastable, Light-Induced Changes in Hydrogenated Amorphous Silicon, Annual Subcontract Report, 1 February 1986 - 28 February 1987. SERI/STR-211-3256. 30 pp. Work performed by University of Oregon, Eugene, Oregon. Available NTIS: Order No. DE88001117.

Cohen, J. D.; Gelatos, A. V.; Mahavadi, K. K.; Zellama, K. (July/August 1988). "Junction Capacitance Studies of Deep Defects in Undoped Hydrogenated Amorphous Silicon." Solar Cells (24:3-4); pp. 287-297. Presented at the 8th Photovoltaic Research and Development Project Review Meeting, Denver, Colorado, November 15-18, 1987.

Crandall, R. S.; Kalina, J.; Delahoy, A. (1988). "Simplified Approach to Solar Cell Modeling." Amorphous Silicon Technology, Materials Research Society Symposium Proceedings, Volume 118, Madan, A., et al., eds. Pittsburgh, PA: Materials Research Society; pp. 593-598. Presented at the MRS Spring Meeting, Reno, Nevada, April 5-8, 1988. Work performed by Chronar Corporation, Princeton, New Jersey.

Dagan, G.; Tenne, R.; Endo, S.; Cahen, D. (1987). "Selective Electrochemical Etching of P-CuInSe<sub>2</sub>." Ternary and Multinary Compounds; Proceedings of the 7th International Conference; Snowmass, Colorado, September 10-12, 1986. Pittsburgh, PA: Materials Research Society; pp. 133-138. Work performed by Departments of Structural Chemistry and Material Research, the Weizmann Institute of Science, Rehovot, Israel, and Science University of Tokyo, Tokyo, Japan.

Dagan, G; Cahen, D. (1987). "Ternary Chalcogenide-Based Photoelectrochemical Cells, IX. Photovoltaic Activity of n-AgInSe<sub>2</sub>." Ternary and Multinary Compounds; Proceedings of the 7th International Conference; Snowmass, Colorado, September 10-12, 1986. Pittsburgh, PA: Materials Research Society; pp. 71-76. Work performed by Department of Structural Chemistry and Center for Energy Research, the Weizmann Institute of Science, Rehovot, Israel.

Daly, J. T.; Gerritsen, H. J.; Crisman, E. E.; Karlsson, S. K. F.; Alexiou, S.; Roberts, C. (1987). "Enhancing Liquid Phase Epitaxial Growth Rates." Proceedings of the 1987 High-Efficiency Photovoltaic Subcontractors' Review Meeting; May 19-20, 1987; Golden, Colorado. SERI/CP-211-3152. Golden, CO: Solar Energy Research Institute; pp. 61-64. Work performed by North Carolina State University, Raleigh, North Carolina.

Damaskinos, S.; Meakin, J. D.; Phillips, J. E. (1987). "Interpretation of an Oxidation/Reduction Experiment on High Efficiency CuInSe<sub>2</sub>/CdS Devices." Conference Record of the Nineteenth IEEE Photovoltaic Specialists Conference-1987; May 4-8, 1987; New Orleans, Louisiana. New York: The Institute of Electrical and Electronics Engineers, Inc.; pp. 1299-1304. Work performed by Institute of Energy Conversion, University of Delaware, Newark, Delaware.

Dapkus, P. D. (1987). "Low Temperature MOCVD Growth Processes for High Efficiency Solar Cells." Proceedings of the 1987 High-Efficiency Photovoltaic Subcontractors' Review Meeting; May 19-20, 1987; Golden, Colorado. SERI/CP-211-3152. Golden, CO: Solar Energy Research Institute; pp. 55-58. Work performed by University of Southern California, Los Angeles, California.

Delahoy, A. E.; Tonon, T. (1987). "Light-Induced Recovery in a-Si:H Solar Cells." International Conference on Stability of Amorphous Silicon Alloy Materials and Devices; January 28-30, 1987; Palo Alto, California, AIP Conference Proceedings 157, Stafford, B. L.; Sabisky, E., eds. New York: American Institute of Physics; pp. 263-270. Work performed by Chronar Corporation, Princeton, New Jersey.

Demetriou, E. C.; Rothwarf, A. (1987). "Admittance Study of the CuInSe<sub>2</sub>/CdS Solar Cell." Conference Record of the Nineteenth IEEE Photovoltaic Specialists Conference-1987; May 4-8, 1987; New Orleans, Louisiana. New York: The Institute of Electrical and Electronics Engineers, Inc.; pp. 764-769. Work performed by ECE Department, Drexel University, Philadelphia, Pennsylvania.

DeMoulin, P. D.; Kyono, C. S.; Lundstrom, M. S.; Melloch, M. R. (1987). "Dark IV Characterization of GaAs P/N Heteroface Cells." Conference Record of the Nineteenth IEEE Photovoltaic Specialists Conference-1987; May 4-8, 1987; New Orleans, Louisiana. New York: The Institute of Electrical and Electronics Engineers, Inc.; pp. 93-97. Work performed by School of Electrical Engineering, Purdue University, West Lafayette, Indiana.

Devaney, W. E.; Mickelsen, R. A. (May/June 1988). "Vacuum Deposition Processes for CuInSe<sub>2</sub> and CuInGaSe<sub>2</sub> Based Solar Cells." Solar Cells (24:1-2); pp. 19-26. Presented at the 8th Photovoltaic Research and Development Project Review Meeting, Denver, Colorado, November 15-18, 1987. Work performed by Boeing High Technology Center, Boeing Electronics Company, Seattle, Washington.

Devaney, W. E.; Mickelsen, R. A.; Chen, W. S.; Stanbery, B. J.; Stewart, J. M.; Lytle, F. W.; Burnett, A. F. (November 1987). Cadmium Sulfide/Copper Ternary Heterojunction Cell Research, Final Subcontract Report, 1 October 1984 - 31 May 1987. SERI/

STR-211-3230. 130 pp. Work performed by Boeing High Technology Center, Seattle, Washington. Available NTIS: Order No. DE88001122.

Doyle, J.; Robertson, R.; Lin, G. H.; He, M. Z.; Gallagher, A. (15 September 1988). "Production of High-Quality Amorphous Silicon Films by Evaporative Silane Decomposition." Journal of Applied Physics (64:6); pp. 3215-3223. Work performed by Joint Institute for Laboratory Astrophysics, University of Colorado, and National Bureau of Standards, Boulder, Colorado.

Durny, R.; Ducharme, S.; Viner, J. M.; Taylor, P. C.; Haneman, D. (December 1987). "Absorption in Amorphous Silicon Doping-Modulated Multilayers." Journal of Non-Crystalline Solids (97 & 98, Part II); pp. 927-930. Presented at the Twelfth International Conference on Amorphous and Liquid Semiconductors, Prague, Czechoslovakia, August 24-28, 1987. Work performed by Department of Physics, University of Utah, Salt Lake City, Utah, and Department of Condensed Matter Physics, University of New South Wales, Kensington, Australia.

Eggert, J. R.; Paul, W. (15 March 1988). "Recombination in Disordered Semiconductors: The Nearest-Available-Neighbor Distribution." Physical Review. B, Condensed Matter (37:8); pp. 4051-4059. Work performed by Department of Physics, Harvard University, Cambridge, Massachusetts.

El-Masry, N. A.; Hamaguchi, N.; Tarn, J. C. L.; Karam, N.; Humphreys, T. P.; Moore, D.; Bedair, S. M.; Lee, J. W.; Salerno, J. (1987). "Defect Reduction in GaAs Epilayers on Si Substrates Using Strained Layer Superlattices." Heteroepitaxy on Silicon II, Materials Research Society Symposia Proceedings, Volume 91, Fan, J. C. C.; Phillips, J. M.; Tsaur, B-Y., eds. Pittsburgh, PA: Materials Research Society; pp. 99-103. Presented at the MRS Spring Meeting, Anaheim, California, April 21-23, 1987. Work performed by Electrical and Computer Engineering Department, North Carolina State University, Raleigh, North Carolina, and Kopin Corporation, Taunton, Massachusetts.

Eser, E.; Ramos, F.; Grez, J. (1 August 1988). "Thermal Stability of Aluminum-Tin-Oxide Thin-Film Interface." Journal of Applied Physics (64:3); pp. 1238-1244. Work performed by Chronar Corporation, Princeton, New Jersey.

Eser, E.; Urbanski, E. (21 December 1987). "Photodegradation in Hydrogenated Amorphous Silicon Films at a High Level of Illumination." Applied Physics Letters (51:25); pp. 2124-2126. Work performed by Chronar Corporation, Princeton, New Jersey.

Fahrenbruch, A. L.; Lopez-Otero, A.; Chien, K. F.; Sharps, P.; Bube, R. H. (1987). "Vapor Phase and Ion-Assisted Doping of Thin Film p-CdTe." Conference Record of the Nineteenth IEEE Photovoltaic Specialists Conference-1987; May 4-8, 1987; New Orleans, Louisiana. New York: The Institute of Electrical and Electronics Engineers, Inc.; pp. 1309-1314. Work performed by Department of Materials Science and Engineering, Stanford University, Stanford, California.

Fedders, P. A.; Carlsson, A. E. (15 May 1988). "Defect States at Floating and Dangling Bonds in Amorphous Si." Physical Review. B, Condensed Matter (37:14); pp. 8506-8508. Work performed by Department of Physics, Washington University, St. Louis, Missouri.

Flint, J. H.; Branz, H. M.; Harris, C. J.; Haggerty, J. S.; Adler, D. (December 1987). "Boron Incorporation in Hydrogenated Amorphous Silicon Films Prepared by Chemical Vapor Deposition." Journal of Non-Crystalline Solids (97 & 98, Part II); pp. 1419-1422. Presented at the Twelfth International Conference on Amorphous and Liquid

Semiconductors, Prague, Czechoslovakia, August 24-28, 1987. Work performed by Massachusetts Institute of Technology, Cambridge, Massachusetts.

Floyd, B. H.; Borrego, J. M. (1987). "n-AlGaAs p-GaAs Graded Heterojunction for High Concentration Ratios." Conference Record of the Nineteenth IEEE Photovoltaic Specialists Conference-1987; May 4-8, 1987; New Orleans, Louisiana. New York: The Institute of Electrical and Electronics Engineers, Inc.; pp. 81-86. Work performed by Electrical, Computer and Systems Engineering Department, Rensselaer Polytechnic Institute, Troy, New York.

Fortmann, C. M. (1988). "Role of Structural Inhomogeneities on the Transport Properties of a-SiGe:H." Amorphous Silicon Technology, Materials Research Society Symposium Proceedings, Volume 118, Madan, A., et al., eds. Pittsburgh, PA: Materials Research Society; pp. 691-696. Presented at the MRS Spring Meeting, Reno, Nevada, April 5-8, 1988. Work performed by Thin Film Division, Solarex Corporation, Newtown, Pennsylvania.

Fortmann, C. M.; O'Dowd, J.; Newton, J. L.; Fischer, J. (1987). "Light Induced Degradation and Structure of High Efficiency a-Si:H, a-SiGe:H and a-SiC:H Solar Cells." International Conference on Stability of Amorphous Silicon Alloy Materials and Devices; January 28-30, 1987; Palo Alto, California, AIP Conference Proceedings 157, Stafford, B. L.; Sabisky, E., eds. New York: American Institute of Physics; pp. 103-110. Work performed by Solarex Thin Film Division, Newtown, Pennsylvania, and Dept. of Materials Science and Engineering, University of Pennsylvania, Philadelphia, Pennsylvania.

Gal, M.; Taylor, P. C.; Usher, B. F.; Orders, P. J. (1 November 1987). "Photoluminescence in Strained InGaAs-GaAs Heterostructures." Journal of Applied Physics (62:9); pp. 3898-3901. Work performed by School of Physics, University of New South Wales, Kensington, Australia; Department of Physics, University of Utah, Salt Lake City, Utah; and Telecom Australia Research Laboratories, Clayton, Victoria, Australia.

Gale, R. P.; King, B. D.; Fan, J. C. C. (1987). "Large-Area GaAs CLEFT Layers for Solar Cell Application." Conference Record of the Nineteenth IEEE Photovoltaic Specialists Conference-1987; May 4-8, 1987; New Orleans, Louisiana. New York: The Institute of Electrical and Electronics Engineers, Inc.; pp. 293-295. Work performed by Kopin Corporation, Taunton, Massachusetts.

Gale, R. P.; McClelland, R. W.; King, B. D.; Gormley, J. M.; Fan, J. C. C. (1987). "High Efficiency, Thin-Film GaAs Solar Cells." Proceedings of the 1987 High-Efficiency Photovoltaic Subcontractors' Review Meeting; May 19-20, 1987; Golden, Colorado. SERI/CP-211-3152. Golden, CO: Solar Energy Research Institute; pp. 29-31. Work performed by Kopin Corporation, Taunton, Massachusetts.

Gale, R. P.; Zavracky, P. M.; McClelland, R. W.; Fan, J. C. C. (1987). "GaAs/AlGaAs Heterostructure Point-Contact Concentrator Cells." Conference Record of the Nineteenth IEEE Photovoltaic Specialists Conference-1987; May 4-8, 1987; New Orleans, Louisiana. New York: The Institute of Electrical and Electronics Engineers, Inc.; pp. 63-66. Work performed by Kopin Corporation, Taunton, Massachusetts.

Gallagher, A. C. (1 April 1988). "Neutral Radical Deposition from Silane Discharges." Journal of Applied Physics (63:7); pp. 2406-2413. Work performed by Joint Institute for

Laboratory Astrophysics, National Bureau of Standards and University of Colorado, Boulder, Colorado.

Gallagher, A. C. (March 1988). "Apparatus Design for Glow-Discharge a-Si:H Film-Deposition." International Journal of Solar Energy (5:5-6); pp. 311-322. Work performed by Joint Institute for Laboratory Astrophysics, National Bureau of Standards and University of Colorado, Boulder, Colorado.

Gallagher, A. C.; Doyle, J.; He, M.; Lin, G. H.; Scott, J. (January 1988). Diagnostics of Glow Discharges Used to Produce Hydrogenated Amorphous Silicon Films, Annual Subcontract Report, 15 April 1986 - 14 June 1987. SERI/STR-211-3288. 52 pp. Work performed by National Bureau of Standards and University of Colorado, Boulder, Colorado. Available NTIS: Order No. DE88001151.

Gelatos, A. V.; Mahavadi, K. K.; Cohen, J. D.; Harbison, J. P. (1 August 1988). "Transient Photocapacitance and Photocurrent Studies of Undoped Hydrogenated Amorphous Silicon." Applied Physics Letters (53:5); pp. 403-405. Work performed by University of Oregon, Eugene, Oregon, and Bell Communications Research, Inc., Red Bank, New Jersey.

Glatfelter, T.; Burdick, J. (1987). "Method for Determining the Conversion Efficiency of Multiple-Cell Photovoltaic Devices." Conference Record of the Nineteenth IEEE Photovoltaic Specialists Conference-1987; May 4-8, 1987; New Orleans, Louisiana. New York: The Institute of Electrical and Electronics Engineers, Inc.; pp. 1187-1193. Work performed by Energy Conversion Devices, Inc., Troy, Michigan.

Glatfelter, T.; Burdick, J.; Fournier, J. P.; Boman, L. (1987). "Outdoor Performance Measurements Comparing Different Types of Multiple-Cell a-Si Alloy Photovoltaic Devices: Dependence on Spectral Content." Conference Record of the Nineteenth IEEE Photovoltaic Specialists Conference-1987; May 4-8, 1987; New Orleans, Louisiana. New York: The Institute of Electrical and Electronics Engineers, Inc.; pp. 194-199. Work performed by Energy Conversion Devices, Inc., Troy, Michigan.

Gordon, R. G. (June 1988). Optimization of Transparent and Reflecting Electrodes for Amorphous Silicon Solar Cells, Final Subcontract Report, 1 October 1986 - 31 November 1987. SERI/STR-211-3332. 70 pp. Work performed by Department of Chemistry, Harvard University, Cambridge, Massachusetts. Available NTIS: Order No. DE88001175.

Greenwald, A.; Bragagnolo, J. A.; Leonard, M. (1987). "Textured Tin-Oxide Films for High Efficiency Amorphous Silicon Solar Cells." Conference Record of the Nineteenth IEEE Photovoltaic Specialists Conference-1987; May 4-8, 1987; New Orleans, Louisiana. New York: The Institute of Electrical and Electronics Engineers, Inc.; pp. 621-625. Work performed by Spire Corporation, Bedford, Massachusetts.

Guha, S.; Payson, J. S.; Agarwal, S. C.; Ovshinsky, S. R. (December 1987). "Fluorinated Amorphous Silicon-Germanium Alloys Deposited from Disilane-Germane Mixture." Journal of Non-Crystalline Solids (97 & 98, Part II); pp. 1455-1458. Presented at the Twelfth International Conference on Amorphous and Liquid Semiconductors, Prague, Czechoslovakia, August 24-28, 1987. Work performed by Energy Conversion Devices, Inc., Troy, Michigan.

Haak, R. (1987). "Light-Induced Changes in Photocapacitance Characteristics of Hydrogenated Amorphous Silicon." International Conference on Stability of Amorphous Silicon Alloy Materials and Devices; January 28-30, 1987; Palo Alto, California, AIP

Conference Proceedings 157, Stafford, B. L.; Sabisky, E., eds. New York: American Institute of Physics; pp. 54-61. Work performed by Rockwell International Science Center, Thousand Oaks, California.

Haak, R.; Menezes, S.; Bachmann, K. J. (1987). "Characterization of Deep Levels and Interface States in CuInSe<sub>2</sub>." Conference Record of the Nineteenth IEEE Photovoltaic Specialists Conference-1987; May 4-8, 1987; New Orleans, Louisiana. New York: The Institute of Electrical and Electronics Engineers, Inc.; pp. 961-966. Work performed by Rockwell International Science Center, Thousand Oaks, California, and Chemistry Department, North Carolina State University, Raleigh, North Carolina.

Hack, M.; Shur, M. (December 1987). "Analysis of Amorphous Silicon Thin-Film Transistors." Journal of Non-Crystalline Solids (97&98, Part II); pp. 1291-1294. Presented at the Twelfth International Conference on Amorphous and Liquid Semiconductors, Prague, Czechoslovakia, August 24-28, 1987. Work performed by Xerox Palo Alto Research Center, Palo Alto, California.

Hack, M.; Street, R. A. (19 September 1988). "Realistic Modeling of the Electronic Properties of Doped Amorphous Silicon." Applied Physics Letters (53:12); pp. 1083-1085. Work performed by Xerox Palo Alto Research Center, Palo Alto, California.

Hack, M.; Street, R. A.; Shur, M. (December 1987). "Capacitance Studies of Thermal Equilibrium Changes in N-Type Amorphous Silicon." Journal of Non-Crystalline Solids (97 & 98, Part II); pp. 803-806. Presented at the Twelfth International Conference on Amorphous and Liquid Semiconductors, Prague, Czechoslovakia, August 24-28, 1987. Work performed by Xerox Palo Alto Research Center, Palo Alto, California.

He, Y.; Mackenzie, K. D.; Paul, W. D. (1987). "Staebler-Wronski Effects in a-Si<sub>1-x</sub>Ge<sub>x</sub>:H and a-Si<sub>1-x</sub>Ge<sub>x</sub>:H:F Alloys." Abstracts of Presentation, International Conference on Stability of Amorphous Silicon Alloy Materials and Devices; January 28-30, 1987; Palo Alto, California. SERI/CP-211-3090. Golden, CO: Solar Energy Research Institute; p. 99. Work performed by Division of Applied Sciences, Harvard University, Cambridge, Massachusetts.

Hegedus, S. S.; Lin, H-S.; Moore, A. R. (August 1, 1988). "Light-Induced Degradation in Undoped Hydrogenated Amorphous Silicon Films Studied by the Surface Photovoltage Technique: A Comparison of Lifetime Versus Space-Charge Effects." Journal of Applied Physics (64:3); pp. 1215-1219. Work performed by Institute of Energy Conversion, University of Delaware, Newark, Delaware.

Hegedus, S. S.; Salzman, N.; Fagen, E. (15 May 1988). "The Relation of Dark and Illuminated Diode Parameters to the Open-circuit Voltage of Amorphous Silicon p-i-n Solar Cells." Journal of Applied Physics (63:10); pp. 5126-5129. Work performed by Institute of Energy Conversion, University of Delaware, Newark, Delaware, and Department of Electrical Engineering, University of Delaware, Newark, Delaware.

Hegedus, S. S.; Schmidt, M.; Salzman, N. (1987). "Measurement of the Built-In Potential in Amorphous Silicon p-i-n Solar Cells." Conference Record of the Nineteenth IEEE Photovoltaic Specialists Conference-1987; May 4-8, 1987; New Orleans, Louisiana. New York: The Institute of Electrical and Electronics Engineers, Inc.; pp. 210-215. Work performed by Institute of Energy Conversion and Department of Electrical Engineering, University of Delaware, Newark, Delaware.

Hegedus, S. S.; Tullman, R. M.; Lin, H. S.; Cebulka, J. M.; Buchanan, W. A.; Dozier, R.; Rocheleau, R. E. (1987). "Low Bandgap Amorphous Silicon-Germanium Alloys for Thin Film Solar Cells Using a Novel Photo-CVD Reactor." Conference Record of the Nineteenth IEEE Photovoltaic Specialists Conference-1987; May 4-8, 1987; New Orleans, Louisiana. New York: The Institute of Electrical and Electronics Engineers, Inc.; pp. 867-871. Work performed by Institute of Energy Conversion, University of Delaware, Newark, Delaware.

Hollingsworth, R. E.; Bhat, P. K.; Madan, A. (December 1987). "Microcrystalline and Wide Band Gap p+ Window Layers for a-Si p-i-n Solar Cells." Journal of Non-Crystalline Solids (97&98, Part I); pp. 309-312. Presented at the Twelfth International Conference on Amorphous and Liquid Semiconductors, Prague, Czechoslovakia, August 24-28, 1987. Work performed by Glasstech Solar, Inc., Wheatridge, Colorado.

Jackson, W. B. (1987). "New Light-Induced Metastable Changes in Donor and Acceptor Levels: The Role of Hydrogen." International Conference on Stability of Amorphous Silicon Alloy Materials and Devices; January 28-30, 1987; Palo Alto, California, AIP Conference Proceedings 157, Stafford, B. L.; Sabisky, E., eds. New York: American Institute of Physics; pp. 17-23. Work performed by Xerox Palo Alto Research Center, Palo Alto, California.

Jackson, W. B.; Kakalios, J. (15 January 1988). "Evidence for Hydrogen Motion in Annealing of Light-Induced Metastable Defects in Hydrogenated Amorphous Silicon." Physical Review, B, Condensed Matter (37:2); pp. 1020-1023. Work performed by Xerox Palo Alto Research Center, Palo Alto, California.

Jacobson, R. L.; Jeffrey, F. R.; Westerberg, R. K.; Williams, R. C. (1987). "Amorphous Silicon p-i-n Layers Prepared by a Continuous Deposition Process on Polyimide Web." Conference Record of the Nineteenth IEEE Photovoltaic Specialists Conference-1987; May 4-8, 1987; New Orleans, Louisiana. New York: The Institute of Electrical and Electronics Engineers, Inc.; pp. 588-592. Work performed by 3M Company, St. Paul, Minnesota.

Jeffrey, F. R.; Vernstrom, G. D.; Weber, M. F.; Gilbert, J. R. (1987). "Effects of Silicon: Carbon P+ Layer Interfaces on Solar Cells." Amorphous Silicon Semiconductors - Pure and Hydrogenated, Materials Research Society Symposia Proceedings, Volume 95, Madan, A., et al., eds. Pittsburgh, PA: Materials Research Society; pp. 539-543. Presented at the MRS Spring Meeting, Anaheim, California, April 21-24, 1987. Work performed by Electronic and Information Laboratories, 3M Company, St. Paul, Minnesota.

Joardar, K.; Jung, C. O.; Wang, S.; Schroder, D. K.; Krause, S. J.; Schwuttke, G. H.; Meier, D. L. (1987). "Effect of the Twin Planes in Dendritic Web Silicon on Its Electrical Characteristics." Conference Record of the Nineteenth IEEE Photovoltaic Specialists Conference-1987; May 4-8, 1987; New Orleans, Louisiana. New York: The Institute of Electrical and Electronics Engineers, Inc.; pp. 799-803. Work performed by Arizona State University, Tempe, Arizona, and Westinghouse R&D Center, Pittsburgh, Pennsylvania.

Johnson, N. M.; Wolff, S. H.; Doland, C. D.; Walker, J. (1988). "Dependence of Hydrogen Incorporation in Undoped a-Si:H and uc-Si:H on Hydrogen Dilution during PECVD." Amorphous Silicon Technology, Materials Research Society Symposium Proceedings, Volume 118, Madan, A., et al., eds. Pittsburgh, PA: Materials Research Society; pp. 85-90. Presented at the MRS Spring Meeting, Reno, Nevada, April 5-8, 1988. Work performed by Xerox Palo Alto Research Center, Palo Alto, California.

Jordan, J. F.; Albright, S. P. (January/February 1988). "Large-Area CdS/CdTe Photovoltaic Cells." Solar Cells (23:1-2); pp. 107-113. Work performed by Photon Energy, Inc., El Paso, Texas.

Kakalios, J.; Street, R. A. (December 1987). "Thermal Equilibrium Processes in Doped Amorphous Silicon." Journal of Non-Crystalline Solids (97 & 98, Part II); pp. 767-774. Presented at the Twelfth International Conference on Amorphous and Liquid Semiconductors, Prague, Czechoslovakia, August 24-28, 1987. Work performed by Xerox Palo Alto Research Center, Palo Alto, California.

Kakalios, J.; Street, R. A. (1987). "Thermally-Induced Instabilities and the Staebler-Wronski Effect in Doped Amorphous Silicon." International Conference on Stability of Amorphous Silicon Alloy Materials and Devices; January 28-30, 1987; Palo Alto, California, AIP Conference Proceedings 157, Stafford, B. L.; Sabisky, E., eds. New York: American Institute of Physics; pp. 179-184. Work performed by Xerox Palo Alto Research Center, Palo Alto, California.

Kakalios, J.; Street, R. A.; Tsai, C. C.; Weisfield, R. L. (1987). "Thermal Equilibration and Growth of Doped Amorphous Silicon." Amorphous Silicon Semiconductors - Pure and Hydrogenated, Materials Research Society Symposia Proceedings, Volume 95, Madan, A., et al., eds. Pittsburgh, PA: Materials Research Society; pp. 243-248. Presented at the MRS Spring Meeting, Anaheim, California, April 21-24, 1987. Work performed by Xerox Palo Alto Research Center, Palo Alto, California.

Kapur, V. K.; Basol, B. M.; Nguyen, N. L.; Kullberg, R. C. (1987). "High Efficiency Copper Ternary Thin Film Solar Cells - An Update." Proceedings of the Polycrystalline Thin Film Program Meeting; July 20-22, 1987; Lakewood, Colorado. SERI/CP-211-3171. p. 97. Work performed by International Solar Electric Technology, Inglewood, California.

Kapur, V. K.; Basol, B. M.; Tseng, E. S. (1987). "Preparation of Thin Films of Chalcopyrites for Photovoltaics." Ternary and Multinary Compounds; Proceedings of the 7th International Conference; Snowmass, Colorado, September 10-12, 1986. Pittsburgh, PA: Materials Research Society; pp. 219-224. Work performed by International Solar Electric Technology, Inglewood, California.

Karam, N. H.; Liu, H.; Yoshida, I.; Bedair, S. M. (4 April 1988). "Direct Writing of GaAs Monolayers by Laser-Assisted Atomic Layer Epitaxy." Applied Physics Letters (52:14); pp. 1144-1146. Work performed by Electrical and Computer Engineering Department, North Carolina State University, Raleigh, North Carolina.

Kennedy, T. A.; Magno, R.; Spencer, M. G. (15 April 1988). "Optically Detected Magnetic Resonance of Native Defects in  $Al_xGa_{1-x}As$ ." Physical Review B, Condensed Matter (37:1); pp. 6325-6331. Work performed by Naval Research Laboratory, Washington, DC, and Department of Electrical Engineering, Howard University, Washington, DC.

Kim, H. K.; Schlesinger, T. E.; Milnes, A. G. (March 1988). "Digital Deep Level Transient Spectroscopy Considered for Discrimination of Traps Closely Spaced in Emission Coefficients in Semiconductors." Journal of Electronic Materials (17:2); pp. 187-191. Work performed by Department of Electrical and Computer Engineering, Carnegie Mellon University, Pittsburgh, Pennsylvania.

Klausmeier-Brown, M. E.; Kyono, C. S.; DeMoulin, P. D.; Tobin, S. P.; Lundstrom, M. S.; Melloch, M. R. (July 1988). "Sequential Etch Analysis of Electron Injection in

p+-GaAs." IEEE Transactions on Electron Devices (35:7); pp. 1159-1161. Work performed by Eastman Kodak Corporation; School of Electrical Engineering, Purdue University, West Lafayette, Indiana; Department of Electrical and Computer Engineering, University of Texas at Austin; and Spire Corporation, Bedford, Massachusetts.

Klausmeier-Brown, M. E.; Kyono, C. S.; Rancour, D. P.; Carpenter, M. S.; Melloch, M. R.; Lundstrom, M. S.; Pierret, R. F. (1987). "Experimental Characterization of Minority Carrier Mirrors for Gallium Arsenide-Based Solar Cells." Conference Record of the Nineteenth IEEE Photovoltaic Specialists Conference-1987; May 4-8, 1987; New Orleans, Louisiana. New York: The Institute of Electrical and Electronics Engineers, Inc.; pp. 1174-1179. Work performed by School of Electrical Engineering, Purdue University, West Lafayette, Indiana.

Klausmeier-Brown, M. E.; Lundstrom, M. S.; Melloch, M. R.; Tobin, S. P. (27 June 1988). "Effects of Heavy Impurity Doping on Electron Injection in p+-n GaAs Diodes." Applied Physics Letters (52:26); 2255-2257. Work performed by Eastman-Kodak Corporation; School of Electrical Engineering, Purdue University, West Lafayette, Indiana; and Spire Corporation, Bedford, Massachusetts.

Landis, G. A.; Pearsall, N. M. (1987). "Assessment of Critical R&D Issues for Thin-Film PV Technologies." Conference Record of the Nineteenth IEEE Photovoltaic Specialists Conference-1987; May 4-8, 1987; New Orleans, Louisiana. New York: The Institute of Electrical and Electronics Engineers, Inc.; 1435-1440. Work performed by Department of Physics, Brown University, Providence, Rhode Island, and Newcastle upon Tyne Polytechnic, Newcastle upon Tyne, United Kingdom.

Lee, C.; Ohlsen, W. D.; Taylor, P. C. (1987). "Time Dependence of the ESR of Localized Electronic States in a-Si:H at 300 K." International Conference on Stability of Amorphous Silicon Alloy Materials and Devices; January 28-30, 1987; Palo Alto, California, AIP Conference Proceedings 157, Stafford, B. L.; Sabisky, E., eds. New York: American Institute of Physics; pp. 193-198. Work performed by Department of Physics, University of Utah, Salt Lake City, Utah.

Lee, W. I.; Taskar, N. R.; Bhat, I. B.; Borrego, J. M.; Ghandi, S. K. (1987). "DLTS Studies of N-Type CdTe Grown by Organometallic Vapor Phase Epitaxy." Conference Record of the Nineteenth IEEE Photovoltaic Specialists Conference-1987; May 4-8, 1987; New Orleans, Louisiana. New York: The Institute of Electrical and Electronics Engineers, Inc.; pp. 785-790. Work performed by Electrical, Computer and Systems Engineering Department, Rensselaer Polytechnic Institute, Troy, New York.

Lewis, C. R.; Macmillan, H. F.; Chung, B.-C.; Virshup, G. F.; Liu, D. D.; Partain, L. D.; Werthen, J. G. (May/June 1988). "Recent Developments in Multijunction Solar Cell Research." Solar Cells (24:1-2); pp. 171-183. Presented at the 8th Photovoltaic Research and Development Project Review Meeting, Denver, Colorado, November 15-18, 1987. Work performed by Varian Research Center, Device Laboratory, Palo Alto, California.

Lin, G. H.; Doyle, J. R.; He, M.; Gallagher, A. (1 July 1988). "Argon Sputtering Analysis of the Growing Surface of a-Si:H Films." Journal of Applied Physics (64:1); pp. 188-194. Work performed by Joint Institute for Laboratory Astrophysics, University of Colorado, and National Bureau of Standards, Boulder, Colorado.

Lo, C. F.; Adler, D.; Johnson, K. H. (June 11, 1988). "Theoretical Calculation of the Effective Correlation Energy of the Hydrogenated Amorphous Germanium Dangling Bond by the Self-Consistent-Field X-Alpha Scattered-Wave Method and Comparison of Results between a-Si:H and a-Ge:H." Journal of Non-Crystalline Solids (103:1); pp. 3-8. Work performed by the Department of Physics, the Department of Electrical Engineering and Computer Science, and the Department of Materials Science and Engineering, Massachusetts Institute of Technology, Cambridge, Massachusetts.

Lo, C. F.; Johnson, K. H.; Adler, D. (January 1988). "Theoretical Investigation of the Dangling Bond Defects in Hydrogenated Amorphous Silicon (a-Si:H) by the Self-Consistent-Field X-Alpha Scattered-Wave Cluster Molecular-Orbital Method." Journal of Non-Crystalline Solids (99:1); pp. 97-103. Work performed by Department of Physics, Department of Materials Science and Engineering, and Department of Electrical Engineering and Computer Science, Massachusetts Institute of Technology, Cambridge, Massachusetts.

Lommasson, T. C.; Burnett, A. F.; Kim, M.; Chou, L. H.; Thornton, J. A. (1987). "Chalcopyrite CuInSe<sub>2</sub> Films Prepared by Reactive Sputtering." Ternary and Multinary Compounds; Proceedings of the 7th International Conference; Snowmass, Colorado; September 10-12, 1986. Pittsburgh, PA: Materials Research Society; pp. 207-212. Work performed by Department of Material Science and Coordinated Science Laboratory, and Department of Electrical and Computer Engineering, University of Illinois, Urbana, Illinois.

Lommasson, T. C.; Talieh, H.; Meakin, J. D.; Thornton, J. A. (1987). "CuInSe<sub>2</sub> Photovoltaic Devices Prepared by Reactive Sputtering." Conference Record of the Nineteenth IEEE Photovoltaic Specialists Conference-1987; May 4-8, 1987; New Orleans, Louisiana. New York: The Institute of Electrical and Electronics Engineers, Inc.; pp. 1285-1290. Work performed by Department of Materials Sciences and Coordinated Science Laboratory, University of Illinois, Urbana, Illinois, and Institute of Energy Conversion, University of Delaware, Newark, Delaware.

Lucovsky, G.; Lin, S. Y.; Wong, C. K. (1987). "Localized States in a-Si Associated with Non-Tetrahedral Bonding Environments." 18th International Conference on the Physics of Semiconductors; Stockholm, Sweden; August 11-15, 1986. Singapore: World Scientific Publishing Co Pte Ltd.; Volume 2, pp. 1073-1076. Work performed by Department of Physics, North Carolina State University, Raleigh, North Carolina.

Lucovsky, G.; Tsu, D. (December 1987). "Differences between Direct and Remote Plasma Enhanced CVD." Journal of Non-Crystalline Solids (97&98, Part I); pp. 265-268. Presented at the Twelfth International Conference on Amorphous and Liquid Semiconductors, Prague, Czechoslovakia, August 24-28, 1987. Work performed by Department of Physics, North Carolina State University, Raleigh, North Carolina.

Lundstrom, M. S.; Melloch, M. R. (1987). "Basic Studies of III-V High Efficiency Cell Components." Proceedings of the 1987 High-Efficiency Photovoltaic Subcontractors' Review Meeting; May 19-20, 1987; Golden, Colorado. SERI/CP-211-3152. Golden, CO: Solar Energy Research Institute; pp. 45-49. Work performed by School of Electrical Engineering, Purdue University, West Lafayette, Indiana.

Mackenzie, K. D.; Burnett, J. H.; Eggert, J. R.; Li, Y. M.; Paul, W. (15 September 1988). "Comparison of the Structural, Electrical and Optical Properties of Amorphous Silicon-Germanium Alloys Produced from Hydrides and Fluorides." Physical Review. B,

Condensed Matter (38:9); pp. 6120-6136. Work performed by Division of Applied Sciences and Department of Physics, Harvard University, Cambridge, Massachusetts.

Mackenzie, K. D.; Burnett, J. H.; Eggert, J. R.; Li, Y. M.; Paul, W. (December 1987). "Improvement of Photoconductive Response in Amorphous Silicon-Germanium Alloys Produced from Fluorides Instead of Hydrides." Journal of Non-Crystalline Solids (97 & 98, Part II); pp. 1019-1022. Presented at the Twelfth International Conference on Amorphous and Liquid Semiconductors, Prague, Czechoslovakia, August 24-28, 1987. Work performed by Division of Applied Sciences, Harvard University, Cambridge, Massachusetts.

Mackenzie, K. D.; Paul, W. (December 1987). "Transient and Steady-State in a-Si<sub>1-x</sub>Ge<sub>x</sub>:H,F Alloys." Journal of Non-Crystalline Solids (97 & 98, Part II); pp. 1055-1058. Presented at the Twelfth International Conference on Amorphous and Liquid Semiconductors, Prague, Czechoslovakia, August 24-28, 1987. Work performed by Division of Applied Sciences, Harvard University, Cambridge, Massachusetts.

Mackenzie, K. D.; Paul, W. (1987). "Comparison of Properties of a-Si<sub>1-x</sub>Ge<sub>x</sub>:H and a-Si<sub>1-x</sub>Ge<sub>x</sub>:H:F." Amorphous Silicon Semiconductors - Pure and Hydrogenated, Materials Research Society Symposia Proceedings, Volume 95, Madan, A., et al., eds. Pittsburgh, PA: Materials Research Society; pp. 281-292. Presented at the MRS Spring Meeting, Anaheim, California, April 21-24, 1987. Work performed by Division of Applied Sciences, Harvard University, Cambridge, Massachusetts.

MacMillan, H. F.; Arau, B. A.; Ford, C. W.; Hamaker, H. C.; Lewis, C. R.; Virshup, G. F.; Werthen, J. G. (1987). "Advanced High-Efficiency Concentrator Cells." Proceedings of the 1987 High-Efficiency Photovoltaic Subcontractors' Review Meeting; May 19-20, 1987; Golden, Colorado. SERI/CP-211-3152. Golden, CO: Solar Energy Research Institute; pp. 1-6. Work performed by Device Laboratory, Varian Research Center, Palo Alto, California.

Mahan, A. H.; Raboisson, P.; Menna, P.; Mascarenhas, A.; Tsu, R. (May/June 1988). "Why the Photoconductivity Decreases in a-SiC:H and a-SiGe:H when the Amount of Alloying Increases." Solar Cells (24:1-2); pp. 195-203. Presented at the 8th Photovoltaic Research and Development Project Review Meeting, Denver, Colorado, November 15-18, 1987. Work performed by Solar Energy Research Institute, Golden, Colorado; Centre National de la Recherche Scientifique, Valbonne, France; ENEA/FARE-FOTO, Portici, Italy, and Electrical Engineering Department, North Carolina A&T State University, Greensboro, North Carolina.

Marshall, J. M.; Street, R. A.; Thompson, M. J.; Jackson, W. B. (March 1988). "Hole Carrier Drift-Mobility Measurements in a-Si:H, and the Shape of the Valence-Band Tail." Philosophical Magazine B (57:3); pp. 387-397. Work performed by Department of Materials Engineering, University College of Swansea, Swansea, U.K., and Xerox Palo Alto Research Center, Palo Alto, California.

McCurdy, R. J.; Gordon, R. G. (1 May 1988). "Compensating Impurities as the Limiting Factor in Atmospheric Pressure Chemical Vapor Deposition of a-Si:H from Mg<sub>2</sub>Si Generated Higher Silanes." Journal of Applied Physics (63:9); pp. 4669-4676. Work performed by Department of Chemistry, Harvard University, Cambridge, Massachusetts.

McCurdy, R. J.; Gordon, R. G. (1988). "Effects of Substrate Temperature and Gas Phase Chemistry on the APCVD of a-Si:H Films from Disilane." Amorphous Silicon Technology, Materials Research Society Symposium Proceedings, Volume 118, Madan, A., et al., eds.

Pittsburgh, PA: Materials Research Society; pp. 97-102. Presented at the MRS Spring Meeting, Reno, Nevada, April 5-8, 1988. Work performed by Department of Chemistry, Harvard University, Cambridge, Massachusetts.

Meakin, J. D. (1987). "Polycrystalline Thin-Film Solar Cells." 1985 Workshop on the Physics of Non-Conventional Energy Sources and Materials Science for Energy; I.C.T.P., Trieste, 2nd-20th, September 1985. Singapore: World Scientific; pp. 122-142. Work performed by Institute of Energy Conversion, University of Delaware, Newark, Delaware.

Meissner, D.; Turner, J. A.; Nozik, A. J. (1987). "Use of Photocapacity for the Study of Superlattice Photoelectrodes (Abstract)." Abstracts of Papers; 193rd ACS National Meeting; American Chemical Society; Denver, Colorado; April 5-10, 1987. Washington, DC: American Chemical Society; COLL 28.

Menezes, S. (1987). "Electrosynthesis of Novel Materials in the  $\text{CuInSe}_2\text{I}-\text{I}-\text{Cu}+\text{HI}$  Solar Cell, (Abstract No. 831)." Electrochemical Society, Extended Abstracts, Volume 87-2. Pennington, NJ: The Electrochemical Society, Inc.; p. 1183. Presented at the Electrochemical Society Fall Meeting, Honolulu, Hawaii, October 18-23, 1987. Work performed by Rockwell International Science Center.

Meunier, M.; Flint, J. H.; Haggerty, J. S.; Adler, D. (1 October 1987). "Laser-Induced Chemical Vapor Deposition of Hydrogenated Amorphous Silicon. II. Film Properties." Journal of Applied Physics (62:7); pp. 2822-2829. Work performed by Massachusetts Institute of Technology, Cambridge, Massachusetts.

Meyers, P. V. (May/June 1988). "Ametek's CdTe Solar Module Development Program." Solar Cells (24:1-2); pp. 35-42. Presented at the 8th Photovoltaic Research and Development Project Review Meeting, Denver, Colorado, November 15-18, 1987. Work performed by Ametek Applied Materials Laboratory, Harleysville, Pennsylvania.

Meyers, P. V. (January/February 1988). "Design of a Thin Film CdTe Solar Cell." Solar Cells (23:1-2); pp. 59-67. Work performed by Ametek Applied Materials Laboratory, Harleysville, Pennsylvania.

Meyers, P. V. (1987). "Polycrystalline Cadmium Telluride n-i-p Solar Cell." Proceedings of the Polycrystalline Thin Film Program Meeting; July 20-22, 1987; Lakewood, Colorado. SERI/CP-211-3171. pp. 9-11. Work performed by Ametek Applied Materials Laboratory, Harleysville, Pennsylvania.

Mickelsen, R. A.; Avery, J. E.; Chen, W. S.; Devaney, W. E.; Murray, R.; Stanbery, B. J.; Stewart, J. M.; Olsen, L. C.; Rothwarf, A. (1987). "CuInSe<sub>2</sub> and CuInGaSe<sub>2</sub> Solar Cell Research." Proceedings of the Polycrystalline Thin Film Program Meeting; July 20-22, 1987; Lakewood, Colorado. SERI/CP-211-3171. pp. 61-69. Work performed by Boeing High Technology Center, Seattle, Washington; Joint Center for Graduate Study, University of Washington; and Drexel University, Philadelphia, Pennsylvania.

Mickelsen, R. A.; Chen, W. S. (1987). "Development of Thin-Film CuInSe<sub>2</sub> Solar Cells." Ternary and Multinary Compounds; Proceedings of the 7th International Conference; Snowmass, Colorado, September 10-12, 1986. Pittsburgh, PA: Materials Research Society; pp. 39-47. Work performed by High Technology Center, Boeing Electronics Company, Seattle, Washington.

Mickelsen, R. A.; Stanbery, B. J.; Avery, J. E.; Chen, W. S.; Devaney, W. E. (1987). "Large Area CuInSe<sub>2</sub> Thin-Film Solar Cells." Conference Record of the Nineteenth IEEE

Photovoltaic Specialists Conference-1987; May 4-8, 1987; New Orleans, Louisiana. New York: The Institute of Electrical and Electronics Engineers, Inc.; pp. 744-748. Work performed by Boeing High Technology Center, Seattle, Washington.

Misiakos, K.; Lindholm, F. A. (1 July 1988). "Analytical and Numerical Modeling of Amorphous Silicon p-i-n Solar Cells." Journal of Applied Physics (64:1); pp. 383-393. Work performed by Department of Electrical Engineering, University of Florida, Gainesville, Florida.

Mitchell, K. W. (1987). "Copper Indium Diselenide Research at ARCO Solar." Proceedings of the Polycrystalline Thin Film Program Meeting; July 20-22, 1987; Lakewood, Colorado. SERI/CP-211-3171. pp. 89-96. Work performed by ARCO Solar, Inc., Chatsworth, California.

Mitchell, K. W.; Eberspacher, C.; Cohen, F.; Avery, J.; Duran, G.; Bottenberg, W. (January/February 1988). "Progress Towards High Efficiency Thin Film CdTe Solar Cells." Solar Cells (23:1-2); pp. 49-57. Work performed by ARCO Solar, Inc., Chatsworth, California.

Norberg, R. E.; Fedders, P. A. (May 1988). Structure of Amorphous Silicon Alloy Films, Annual Subcontract Report, 15 January 1987 - 14 January 1988. SERI/STR-211-3352. 34 pp. Work performed by Department of Physics, Washington University, St. Louis, Missouri. Available NTIS: Order No. DE88001167.

Nouhi, A.; Stirn, R. J. (28 December 1987). "Heteroepitaxial Growth of  $Cd_{1-x}Mn_xTe$  on GaAs by Metalorganic Chemical Vapor Deposition." Applied Physics Letters (51:26); pp. 2251-2253. Work performed by Jet Propulsion Laboratory, California Institute of Technology, Pasadena, California.

Nouhi, A.; Stirn, R. J.; Hermann, A. M. (1987). "CuInSe<sub>2</sub>/ZnSe Solar Cells Using Reactively Sputter-Deposited ZnSe." Conference Record of the Nineteenth IEEE Photovoltaic Specialists Conference-1987; May 4-8, 1987; New Orleans, Louisiana. New York: The Institute of Electrical and Electronics Engineers, Inc.; pp. 1461-1465. Work performed by Jet Propulsion Laboratory, Pasadena, California.

O'Dowd, J. G. (November 1987). "Model for Light Scattering by Rough Tin Oxide." Solar Energy Materials (16:5); pp. 383-391. Work performed by Thin Film Division, Solarex Corporation, Newtown, Pennsylvania.

Panayotatos, P.; Whitlock, J.; Sauers, R. R.; Husain, S.; Sadrai, M.; Bird, G. R. (1987). "Recent Advances in Optimally Designed p-n Organic Semiconductor Solar Cells." Conference Record of the Nineteenth IEEE Photovoltaic Specialists Conference-1987; May 4-8, 1987; New Orleans, Louisiana. New York: The Institute of Electrical and Electronics Engineers, Inc.; pp. 889-894. Work performed by Department of Electrical Engineering and Department of Chemistry, Rutgers, The State University of New Jersey, Piscataway, New Jersey.

Parker, M. A.; Schiff, E. A. (December 1987). "Geometry Problem for Photocarrier Drift Mobilities in a-Si:H." Journal of Non-Crystalline Solids (97 & 98, Part I); pp. 627-630. Presented at the Twelfth International Conference on Amorphous and Liquid Semiconductors, Prague, Czechoslovakia, August 24-28, 1987. Work performed by Department of Physics, Syracuse University, Syracuse, New York.

Parsons, G. N.; Kusano, C.; Lucovsky, G. (1987). "Effects of Band Bending on the Optical, Electrical and Photo-Electronic Properties of a-Si:H Thin Films in Surface Cell Structures." Disordered Semiconductors. New York: Plenum Press; pp. 587-602. Work performed by Department of Physics, North Carolina State University, Raleigh, North Carolina, and Hitachi Central Research Laboratory, Tokyo, Japan.

Parsons, G. N.; Kusano, C.; Lucovsky, G. (1987). "Effects of Surface and Interface Depletion Regions on the Photoconductivity of a-Si:H in Surface Cell Structure." Interfaces, Superlattices, and Thin Films, Materials Research Society Symposia Proceedings, Volume 77, Dow, J. D.; Schuller, I. K., eds. Pittsburgh, PA: Materials Research Society; pp. 589-594. Presented at the MRS Fall Meeting, Boston, Massachusetts, December 1-6, 1986. Work performed by Department of Physics, North Carolina State University, Raleigh, North Carolina, and Hitachi Central Research Laboratory, Tokyo, Japan.

Parsons, G. N.; Lucovsky, G. (1987). "Estimation of Defect State Densities from Bulk Photoelectronic Properties of a-Si, Ge:H Alloys." Amorphous Silicon Semiconductors - Pure and Hydrogenated, Materials Research Society Symposia Proceedings, Volume 95, Madan, A., et al., eds. Pittsburgh, PA: Materials Research Society; pp. 341-346. Presented at the MRS Spring Meeting, Anaheim, California, April 21-24, 1987. Work performed by Department of Physics, North Carolina State University, Raleigh, North Carolina.

Parsons, G. N.; Tsu, D. V.; Lucovsky, G. (1988). "Growth of a-Si:H Films by Remote Plasma Enhanced CVD (RPECVD)." Amorphous Silicon Technology, Materials Research Society Symposium Proceedings, Volume 118, Madan, A., et al., eds. Pittsburgh, PA: Materials Research Society; pp. 37-42. Presented at the MRS Spring Meeting, Reno, Nevada, April 5-8, 1988. Work performed by Department of Physics, North Carolina State University, Raleigh, North Carolina.

Parsons, G. N.; Tsu, D. V.; Lucovsky, G. (December 1987). "Optical and Electrical Properties of a-Si:H Films Grown by Remote Plasma Enhanced Chemical Vapor Deposition (RPECVD)." Journal of Non-Crystalline Solids (97 & 98, Part II); pp. 1375-1378. Presented at the Twelfth International Conference on Amorphous and Liquid Semiconductors, Prague, Czechoslovakia, August 24-28, 1987. Work performed by Department of Physics, North Carolina State University, Raleigh, North Carolina.

Partain, L. D.; Kuryla, M. S.; Weiss, R. E.; Werthen, J. G.; Virshup, G. F.; MacMillan, H. F.; Hamaker, H. C.; King, D. L. (1987). "26.1% Solar Cell Efficiency for GaAs Mechanically Stacked on Ge." Conference Record of the Nineteenth IEEE Photovoltaic Specialists Conference-1987; May 4-8, 1987; New Orleans, Louisiana. New York: The Institute of Electrical and Electronics Engineers, Inc.; pp. 1504-1505. Work performed by Chevron Research Company, Richmond, California; Varian Research Center, Palo Alto, California; and Sandia National Laboratories, Albuquerque, New Mexico.

Paul, W. D.; Mackenzie, K. D. (May 1988). Research on Amorphous Silicon-Germanium Alloys for Tandem Solar Cells, Annual Subcontract Report, 1 July 1986 - 31 August 1987. SERI/STR-211-3351. 80 pp. Work performed by Division of Applied Sciences, Harvard University, Cambridge, Massachusetts. Available NTIS: Order No. DE88001168.

Pawlakiewicz, A. H.; Guha, S. (1988). "Effect of Dominant Junction on the Open Circuit Voltage of Amorphous Silicon Alloy Solar Cells." Amorphous Silicon Technology, Materials Research Society Symposium Proceedings, Volume 118, Madan, A., et al., eds. Pittsburgh, PA: Materials Research Society; pp. 599-604. Presented at the MRS Spring

Meeting, Reno, Nevada, April 5-8, 1988. Work performed by Energy Conversion Devices, Inc., Troy, Michigan.

Pernisz, U. C.; Tarhay, L.; D'Errico, J. J.; Sharp, K. G. (1987). "Fluorinated Silane Precursors to Amorphous Silicon." Conference Record of the Nineteenth IEEE Photovoltaic Specialists Conference-1987; May 4-8, 1987; New Orleans, Louisiana. New York: The Institute of Electrical and Electronics Engineers, Inc.; pp. 582-587. Work performed by Dow Corning Corporation, Midland, Michigan.

Perry, J. W.; Shing, Y. H.; Allevato, C. E. (13 June 1988). "Diagnostics of Silane and Germane Radio Frequency Plasmas by Coherent Anti-Stokes Raman Spectroscopy." Applied Physics Letters (52:24); pp. 2022-2024. Work performed by Jet Propulsion Laboratory, California Institute of Technology, Pasadena, California.

Ranganathan, R.; Gal, M.; Taylor, P. C. (July/August 1988). "Photoluminescence Absorption Spectroscopy in a-Si:H and Related Alloys." Solar Cells (24:3-4); pp. 257-262. Presented at the 8th Photovoltaic Research and Development Project Review Meeting, Denver, Colorado, November 15-18, 1987.

Ranganathan, R.; Gal, M.; Viner, J. M.; Taylor, P. C. (1987). "Photoluminescence in Hydrogenated Silicon-Germanium Alloys." Amorphous Silicon Semiconductors - Pure and Hydrogenated, Materials Research Society Symposia Proceedings, Volume 95, Madan, A., et al., eds. Pittsburgh, PA: Materials Research Society; pp. 293-298. Presented at the MRS Spring Meeting, Anaheim, California, April 21-24, 1987. Work performed by Department of Physics, University of Utah, Salt Lake City, Utah.

Ranganathan, R.; Taylor, P. C. (December 1987). "Subgap Absorption in a-Si:H Using Photoluminescence Absorption Spectroscopy (PLAS)." Journal of Non-Crystalline Solids (97 & 98, Part I); pp. 707-710. Presented at the Twelfth International Conference on Amorphous and Liquid Semiconductors, Prague, Czechoslovakia, August 24-28, 1987. Work performed by Department of Physics, University of Utah, Salt Lake City, Utah.

Ready, S. E.; Boyce, J. B.; Tsai, C. C. (1987). "NMR Study of the Spacial Relation of Hydrogen to Phosphorous and Boron in Amorphous Silicon." International Conference on Stability of Amorphous Silicon Alloy Materials and Devices; January 28-30, 1987; Palo Alto, California, AIP Conference Proceedings 157, Stafford, B. L.; Sabisky, E., eds. New York: American Institute of Physics; pp. 229-234. Work performed by Xerox Palo Alto Research Center, Palo Alto, California.

Rocheleau, R. E.; Hegedus, S. S.; Buchanan, W. A.; Tullman, R. M. (1987). "Effects of Impurities on Film Quality and Device Performance in a-Si:H Deposited by Photo-Assisted CVD." Conference Record of the Nineteenth IEEE Photovoltaic Specialists Conference-1987; May 4-8, 1987; New Orleans, Louisiana. New York: The Institute of Electrical and Electronics Engineers, Inc.; pp. 699-704. Work performed by Institute of Energy Conversion, University of Delaware, Newark, Delaware.

Rocheleau, R. E.; Meakin, J. D.; Birkmire, R. W. (1987). "Tolerance of CuInSe<sub>2</sub> Cell Performance to Variations in Film Composition and the Implications for Large Area Cell Manufacture." Conference Record of the Nineteenth IEEE Photovoltaic Specialists Conference-1987; May 4-8, 1987; New Orleans, Louisiana. New York: The Institute of Electrical and Electronics Engineers, Inc.; pp. 972-976. Work performed by Institute of Energy Conversion, University of Delaware, Newark, Delaware.

Rocheleau, R. E.; Tullman, R. M.; Albright, D. E.; Hegedus, S. S. (1988). "Amorphous Silicon-Germanium Deposited by Photo-CVD: Effect of Hydrogen Dilution and Substrate Temperature." Amorphous Silicon Technology, Materials Research Society Symposium Proceedings, Volume 118, Madan, A., et al., eds. Pittsburgh, PA: Materials Research Society; pp. 653-658. Presented at the MRS Spring Meeting, Reno, Nevada, April 5-8, 1988. Work performed by Institute of Energy Conversion, University of Delaware, Newark, Delaware.

Rohatgi, A.; Ringel, S. A.; Welch, J.; Meeks, E.; Pollard, K.; Erbil, A.; Summers, C. J. (May/June 1988). "Growth and Characterization of CdMnTe and CdZnTe Polycrystalline Thin Films for Solar Cells." Solar Cells (24:1-2); pp. 185-194. Presented at the 8th Photovoltaic Research and Development Project Review Meeting, Denver, Colorado, November 15-18, 1987. Work performed by Microelectronics Research Center, Georgia Institute of Technology, Atlanta, Georgia, and Ametek Applied Materials Laboratory, Harleysville, Pennsylvania.

Rohatgi, A.; Summers, C. J.; Erbil, A. (1987). "High Efficiency Cadmium and Zinc Telluride Based Thin Film Solar Cells." Proceedings of the Polycrystalline Thin Film Program Meeting; July 20-22, 1987; Lakewood, Colorado. SERI/CP-211-3171. pp. 161-164. Work performed by Georgia Institute of Technology, Atlanta, Georgia.

Ross, R. G., Jr.; Mon, G. R.; Wen, L.; Gonzalez, C. C.; Sugimura, R. S. (July/August 1988). "Measurement and Characterization of Thin Film Module Reliability." Solar Cells (24:3-4); pp. 271-278. Presented at the 8th Photovoltaic Research and Development Project Review Meeting, Denver, Colorado, November 15-18, 1987.

Ross, R.; Mohr, R.; Fournier, J. P.; Yang, J. (1987). "Status of Flourinated Amorphous Silicon-Germanium Alloys and Multijunction Devices." Conference Record of the Nineteenth IEEE Photovoltaic Specialists Conference-1987; May 4-8, 1987; New Orleans, Louisiana. New York: The Institute of Electrical and Electronics Engineers, Inc.; pp. 327-330. Work performed by Energy Conversion Devices, Inc., Troy, Michigan.

Ruberto, M. N.; Rothwarf, A. (1987). "Experimental and Theoretical Study of the Time Dependent Open Circuit Voltage in CuInSe<sub>2</sub>/CdS Solar Cells." Conference Record of the Nineteenth IEEE Photovoltaic Specialists Conference-1987; May 4-8, 1987; New Orleans, Louisiana. New York: The Institute of Electrical and Electronics Engineers, Inc.; pp. 1329-1334. Work performed by Electrical and Computer Engineering Department, Drexel University, Pittsburgh, Pennsylvania.

Schafer, D. E. (February 1988). MOCVD Techyniques for CdTe Solar Cells, Final Subcontract Report, 15 February 1985 - 1 April 1987. SERI/STR-211-3218. 49 pp. Work performed by Honeywell Physical Sciences Center, Bloomington, Minnesota. Available NTIS: Order No. DE88001163.

Schafer, D. E. (1987). "Low Temperature MOCVD of CdTe and HgTe for CdTe/ITO Solar Cells." Proceedings of the Polycrystalline Thin Film Program Meeting; July 20-22, 1987; Lakewood, Colorado. SERI/CP-211-3171. pp. 51-53. Work performed by Honeywell Physical Science Center, Bloomington, Minnesota.

Schiff, E. A. (1987). "Transient Photocurrent Characterization of Amorphous Semiconductors." Physics of Amorphous Semiconductor Devices; 15-16 January 1987; Los Angeles, California, Proceedings of SPIE - The International Society for Optical Engineering, Volume 763, Adler, D., ed. Bellingham, WA: SPIE - The International

Society for Optical Engineering; pp. 39-46. Work performed by Department of Physics, Syracuse University, Syracuse, New York.

Schiff, E. A.; Parker, M. A. (4 April 1988). "Optical and Electrical Detection of Photocarrier Time of Flight." Physical Review Letters (60:14); p. 1454. Work performed by Department of Physics, Syracuse University, Syracuse, New York.

Scott, C. G. (1987). Anisotropic Tribological Behavior of Single-Crystal Silicon. Chicago, IL: University of Illinois; 122 pp. B.A. Thesis, Bowdoin College, University of Illinois, Chicago, Illinois.

Shing, Y-H.; Perry, J. W.; Allevato, C. E. (July/August 1988). "Amorphous Silicon Germanium Alloy Film Deposition with In Situ Plasma Diagnostics." Solar Cells (24:3-4); pp. 353-362. Presented at the 8th Photovoltaic Research and Development Project Review Meeting, Denver, Colorado, November 15-18, 1987. Work performed by Jet Propulsion Laboratory, California Institute of Technology, Pasadena, California.

Shing, Y-H.; Perry, J. W.; Coulter, D. R.; Radhakrishnan, G. (1987). "Amorphous Silicon Deposition Diagnostics Using Coherent Anti-Stokes Raman Spectroscopy." Amorphous Silicon Semiconductors - Pure and Hydrogenated, Materials Research Society Symposia Proceedings, Volume 95, Madan, A., et al., eds. Pittsburgh, PA: Materials Research Society; pp. 237-242. Presented at the MRS Spring Meeting, Anaheim, California, April 21-24, 1987. Work performed by Jet Propulsion Laboratory, Pasadena, California.

Shing, Y-H.; Perry, J. W.; Hermann, A. M. (1987). "In situ Process Diagnostics of Silane Plasma for Device-Quality a-Si:H Deposition." Conference Record of the Nineteenth IEEE Photovoltaic Specialists Conference-1987; May 4-8, 1987; New Orleans, Louisiana. New York: The Institute of Electrical and Electronics Engineers, Inc.; pp. 577-581. Work performed by Jet Propulsion Laboratory, Pasadena, California.

Silver, M.; Cannella, V. (December 1987). "Simplified Analytic Model for Double Injection Applied to Amorphous Silicon Alloys." Journal of Non-Crystalline Solids (97&98, Part I); pp. 305-308. Presented at the Twelfth International Conference on Amorphous and Liquid Semiconductors, Prague, Czechoslovakia, August 24-28, 1987. Work performed by Department of Physics and Astronomy, University of North Carolina, Chapel Hill, North Carolina, and Ovonic Information Systems, Chapel Hill, North Carolina.

Sinton, R. A.; Swanson, R. M. (1987). "Optimization Study of Si Point-Contact Concentrator Solar Cells." Conference Record of the Nineteenth IEEE Photovoltaic Specialists Conference-1987; May 4-8, 1987; New Orleans, Louisiana. New York: The Institute of Electrical and Electronics Engineers, Inc.; pp. 1201-1208. Work performed by Stanford University, Stanford, California.

Sites, J. R.; Mauk, P. H.; Blake, J. (1987). "Spatial Non-Uniformities in the Photovoltaic Response of CuInSe<sub>2</sub> Solar Cells." Proceedings of the Polycrystalline Thin Film Program Meeting; July 20-22, 1987; Lakewood, Colorado. SERI/CP-211-3171. Golden, CO: Solar Energy Research Institute; p. 135. Work performed by Physics Department, Colorado State University, Fort Collins, Colorado.

Sites, J. R.; Mauk, P. H.; Jacobson, R. D. (1987). "Reflection Losses from Polycrystalline CuInSe<sub>2</sub> Solar Cells." Conference Record of the Nineteenth IEEE Photovoltaic Specialists Conference-1987; May 4-8, 1987; New Orleans, Louisiana. New York: The Institute of Electrical and Electronics Engineers, Inc.; pp. 818-822. Work performed by

Department of Physics, Colorado State University, Ft. Collins, Colorado, and Department of Electrical Engineering, University of New Mexico, Albuquerque, New Mexico.

Spencer, M. G.; Kennedy, T. A.; Magno, R. (March/April 1988). "Chemical Nature and Atomic Structure of Midgap Levels in Molecular-Beam Epitaxially Grown  $\text{Al}_x\text{Ga}_{1-x}\text{As}$ : Summary Abstract." Journal of Vacuum Science & Technology. B, Microelectronics, Processing and Phenomena (6:2); pp. 647-648. Work performed by Department of Electrical Engineering, Howard University, Washington, DC.

Stewart, J. M.; Chen, W. S.; Devaney, W. E.; Mickelsen, R. A. (1987). "Thin Film Polycrystalline  $\text{CuIn}_{1-x}\text{Ga}_x\text{Se}_2$  Solar Cells." Ternary and Multinary Compounds; Proceedings of the 7th International Conference; Snowmass, Colorado, September 10-12, 1986. Pittsburgh, PA: Materials Research Society; pp. 59-64. Work performed by High Technology Center, Boeing Electronics Company, Seattle, Washington.

Stirn, R. J.; Nouhi, A. (1987). "Investigations of Wide Band Gap II-VI Window and Photon Absorber Materials for Cascaded Cells." Proceedings of the Polycrystalline Thin Film Program Meeting; July 20-22, 1987; Lakewood, Colorado. SERI/CP-211-3171. pp. 173-180. Work performed by Jet Propulsion Laboratory, Pasadena, California.

Street, R. A. (July/August 1988). "Origin of Metastable States in a-Si:H." Solar Cells (24:3-4); pp. 211-221. Presented at the 8th Photovoltaic Research and Development Project Review Meeting, Denver, Colorado, November 15-18, 1987.

Street, R. A. (1987). "Density of States in Hydrogenated Amorphous Silicon." Physics of Amorphous Semiconductor Devices; 15-16 January 1987; Los Angeles, California, Proceedings of SPIE - The International Society for Optical Engineering, Volume 763, Adler, D., ed. Bellingham, WA: SPIE - The International Society for Optical Engineering; pp. 10-16. Work performed by Xerox Palo Alto Research Center, Palo Alto, California.

Street, R. A. (1987). "Hydrogen Diffusion and Thermal Equilibrium of Electronic States in a-Si:H." Amorphous Silicon Semiconductors - Pure and Hydrogenated, Materials Research Society Symposia Proceedings, Volume 95, Madan, A., et al., eds. Pittsburgh, PA: Materials Research Society; pp. 13-22. Presented at the MRS Spring Meeting, Anaheim, California, April 21-24, 1987. Work performed by Xerox Palo Alto Research Center, Palo Alto, California.

Street, R. A.; Hack, M.; Jackson, W. B. (15 March 1988). "Mechanisms of Thermal Equilibration in Doped Amorphous Silicon." Physical Review. B, Condensed Matter (37:8); pp. 4209-4224. Work performed by Xerox Palo Alto Research Center, Palo Alto, California.

Street, R. A.; Kakalios, J. (1987). "Thermal Equilibration and Structural Relaxation in Amorphous Silicon." 18th International Conference on the Physics of Semiconductors; Stockholm, Sweden; August 11-15, 1986. Singapore: World Scientific Publishing Co Pte Ltd.; Volume 2, pp. 1045-1048. Work performed by Xerox Palo Alto Research Center, Palo Alto, California.

Street, R. A.; Kakalios, J.; Hack, M. (15 September 1988). "Electron Drift Mobility in Doped Amorphous Silicon." Physical Review. B, Condensed Matter (38:8); pp. 5603-5609. Work performed by Xerox Palo Alto Research Corporation, Palo Alto, California.

Street, R. A.; Kakalios, J.; Hack, M. (1988). "Doping Dependence of the Drift Mobility in n-Type a-Si:H." Amorphous Silicon Technology, Materials Research Society Symposium Proceedings, Volume 118, Madan, A., et al., eds. Pittsburgh, PA: Materials Research Society; pp. 495-500. Presented at the MRS Spring Meeting, Reno, Nevada, April 5-8, 1988. Work performed by Xerox Palo Alto Research Center, Palo Alto, California.

Street, R. A.; Tsai, C. C. (May 1988). "Dependence of Hydrogen Diffusion on Growth Conditions in Hydrogenated Amorphous Silicon." Philosophical Magazine B (57:5); pp. 663-669. Work performed by Xerox Palo Alto Research Center, Palo Alto, California.

Stutzmann, M.; Tsai, C. C.; Street, R. A. (December 1987). "Electronic States in the Gap of Amorphous Silicon-Germanium Alloys." Journal of Non-Crystalline Solids (97&98, Part II); pp. 1011-1014. Presented at the Twelfth International Conference on Amorphous and Liquid Semiconductors, Prague, Czechoslovakia, August 24-28, 1987. Work performed by Xerox Palo Alto Research Center, Palo Alto, California.

Summers, C. J.; Rogahti, A.; Brennan K. F. (1987). "Avalanche Heterostructure and Superlattice Solar Cell." Proceedings of the Polycrystalline Thin Film Program Meeting; July 20-22, 1987; Lakewood, Colorado. SERI/CP-211-3171. pp. 35-39. Work performed by Physical Sciences Division, Georgia Tech Research Institute, Georgia Institute of Technology, Atlanta, Georgia, and School of Electrical Engineering, Georgia Institute of Technology, Atlanta, Georgia.

Taylor, P. C.; Lee, C.; Hautala, J.; Ohlsen, W. D. (1987). "Electron Spin Resonance Studies of Amorphous Semiconductors." Proceedings of the International Workshop on Amorphous Semiconductors; Beijing, China; 13-18 October 1986. Singapore: World Scientific Publishing Co.; pp. 91-101. Work performed by Department of Physics, University of Utah, Salt Lake City, Utah.

Taylor, P. C.; Lee, C.; Ohlsen, W. D. (1987). "ESR and the Density of Deep Gap States in a-Si:H." Physics of Amorphous Semiconductor Devices; 15-16 January 1987; Los Angeles, California, Proceedings of SPIE - The International Society for Optical Engineering, Volume 763, Adler, D., ed. Bellingham, WA: SPIE - The International Society for Optical Engineering; pp. 27-31. Work performed by Department of Physics, University of Utah, Salt Lake City, Utah.

Taylor, P. C.; Vanderheiden, E. D.; Ohlsen, W. D. (1987). "Molecular Hydrogen in a-Si:H and Related Alloys." Proceedings of the International Workshop on Amorphous Semiconductors; Beijing, China; 13-18 October 1986. Singapore: World Scientific Publishing Co.; pp. 53-63. Work performed by Department of Physics, University of Utah, Salt Lake City, Utah.

Thornton, J. A. (1987). "Reactive Sputtered CuInSe<sub>2</sub>: Film Properties and Device Fabrication." Proceedings of the Polycrystalline Thin Film Program Meeting; July 20-22, 1987; Lakewood, Colorado. SERI/CP-211-3171. pp. 71-78. Work performed by Department of Materials Science and Coordinated Science Laboratory, University of Illinois, Urbana, Illinois.

Thornton, J. A. (1987). "Surface Reactions During the Growth of CuInSe<sub>2</sub> Films from Cu, In, and Se Species." Proceedings of the Polycrystalline Thin Film Program Meeting; July 20-22, 1987; Lakewood, Colorado. SERI/CP-211-3171. pp. 117-124. Work performed by Department of Materials Science and Coordinated Science Laboratory, University of Illinois, Urbana, Illinois.

Thornton, J. A.; Lommasson, T. C.; Talieh, H.; Tseng, B. H. (May/June 1988). "Reactive Sputtered CuInSe<sub>2</sub>." Solar Cells (24:1-2); pp. 1-9. Presented at the 8th Photovoltaic Research and Development Project Review Meeting, Denver, Colorado, November 15-18, 1987. Work performed by Department of Materials Science and Coordinated Science Laboratory, University of Illinois, Urbana, Illinois.

Thornton, J. A.; Schiff, E. A.; Milnes, A. G.; Schlesinger, T. E.; Bedair, S. M.; Taylor, P. C.; Williams, G. D.; Ohlsen, W. D.; Dapkus, P. D.; Bube, R. H.; Gerritsen, H. J.; Crisman, E. E. (June 1988). SERI PV AR&D University Participation Program, Annual Subcontract Report, FY 1987. SERI/STR-211-3335. 85 pp. Work performed by University of Illinois; Syracuse University; Carnegie Mellon University; North Carolina State University; University of Utah; University of Southern California; Stanford University; and Brown University. Available NTIS: Order No. DE88001182.

Timmons, M. L.; Chiang, P. K. (1987). "Progress with Germanium Intercell Ohmic Connections for AlGaAs-GaAs, Monolithic Cascade Solar Cells." Conference Record of the Nineteenth IEEE Photovoltaic Specialists Conference-1987; May 4-8, 1987; New Orleans, Louisiana. New York: The Institute of Electrical and Electronics Engineers, Inc.; pp. 102-107. Work performed by Research Triangle Institute, Research Triangle Park, North Carolina.

Timmons, M. L.; Hutchby, J. A.; Lamorte, M. F. (1987). "High Efficiency AlGaAs-GaAs Patterned Tunnel Junction and Point-Contact GaAs Concentrator Cells." Proceedings of the 1987 High-Efficiency Photovoltaic Subcontractors' Review Meeting; May 19-20, 1987; Golden, Colorado. SERI/CP-211-3152. Golden, CO: Solar Energy Research Institute; pp. 23-26. Work performed by Research Triangle Institute, Research Triangle Park, North Carolina.

Timmons, M. L.; Lamorte, M. F.; Chiang, P. K.; Hutchby, J. A.; deLyon, T. (1987). "Single-Junction, Point-Contact, Back-Surface GaAs Concentrator Solar Cell." Conference Record of the Nineteenth IEEE Photovoltaic Specialists Conference-1987; May 4-8, 1987; New Orleans, Louisiana. New York: The Institute of Electrical and Electronics Engineers, Inc.; pp. 76-80. Work performed by Research Triangle Institute, Research Triangle Park, North Carolina.

Tobin, S. P.; Vernon, S. M.; Haven, V. E., Jr.; Bajgar, C.; Sanfacon, M. M.; Pearton, S. J. (1987). "Factors Controlling the Efficiency of GaAs-on-Si Solar Cells." Conference Record of the Nineteenth IEEE Photovoltaic Specialists Conference-1987; May 4-8, 1987; New Orleans, Louisiana. New York: The Institute of Electrical and Electronics Engineers, Inc.; pp. 113-118. Work performed by Spire Corporation, Bedford, Massachusetts.

Tran, N. T.; Epstein, K. A.; Grimmer, D. P.; Vernstrom, G. D. (1987). "Effect of Low Level Doping of Boron and Phosphorous on the Properties of Amorphous Silicon Films." Amorphous Silicon Semiconductors - Pure and Hydrogenated, Materials Research Society Symposia Proceedings, Volume 95, Madan, A., et al., eds. Pittsburgh, PA: Materials Research Society; pp. 137-144. Presented at the MRS Spring Meeting, Anaheim, California, April 21-24, 1987. Work performed by Electronic and Information Sector Laboratories, 3M Company, St. Paul, Minnesota.

Tran, N. T.; Jeffrey, F. R.; Olsen, D. J. (1987). "Effects of Carbon Grading at the p/i Interface of the Open Circuit Voltage of p-i-n and n-i-p Amorphous Silicon Solar Cells." Amorphous Silicon Semiconductors - Pure and Hydrogenated, Materials Research Society Symposia Proceedings, Volume 95, Madan, A., et al., eds. Pittsburgh, PA: Materials

Research Society; pp. 545-548. Presented at the MRS Spring Meeting, Anaheim, California, April 21-24, 1987. Work performed by Electronic and Information Sector Laboratories, 3M Company, St. Paul, Minnesota.

Tsai, C. C. (1987). "Film Growth Mechanisms of Plasma-Deposited Amorphous Silicon Studied by Step Coverage." Proceedings of the International Workshop on Amorphous Semiconductors; Beijing, China; 13-18 October 1986. Singapore: World Scientific Publishing Co.; pp. 43-52. Work performed by Xerox Palo Alto Research Center, Palo Alto, California.

Tsai, C. C.; Shaw, J. G.; Wacker, B.; Knights, J. C. (1987). "Film Growth Mechanisms of Amorphous Silicon in Diode and Triode Glow Discharge Systems." Amorphous Silicon Semiconductors - Pure and Hydrogenated, Materials Research Society Symposia Proceedings, Volume 95, Madan, A. et al., eds. Pittsburgh, PA: Materials Research Society; pp. 219-224. Presented at the MRS Spring Meeting, Anaheim, California, April 21-24, 1987. Work performed by Xerox Palo Alto Research Center, Palo Alto, California.

Tsai, C. C.; Street, R. A. (1987). "'Low' Temperature Hydrogen Diffusion in Amorphous Silicon and Its Relation to Structural Stability." Abstracts of Presentation, International Conference on Stability of Amorphous Silicon Alloy Materials and Devices; January 28-30, 1987; Palo Alto, California. SERI/CP-211-3090. Golden, CO: Solar Energy Research Institute; p. 161. Work performed by Xerox Palo Alto Research Center, Palo Alto, California.

Tsu, D.; Lucovsky, G. (December 1987). "Properties of the Si-H Bond-Stretching Absorption Band in a-Si:H Grown by Remote Plasma Enhanced CVD (RPECVD)." Journal of Non-Crystalline Solids (97&98, Part II); pp. 839-842. Presented at the Twelfth International Conference on Amorphous and Liquid Semiconductors, Prague, Czechoslovakia, August 24-28, 1987. Work performed by Department of Physics, North Carolina State University, Raleigh, North Carolina.

Vecht, A.; Saunders, A.; Tyrrell, G. (1987). "Preparation of Thin Films for Photovoltaic Conversion by Novel MOCVD Techniques." Proceedings of the Polycrystalline Thin Film Program Meeting; July 20-22, 1987; Lakewood, Colorado. SERI/CP-211-3171. pp. 55-59. Work performed by Phosphor Consultants, London, England.

Vernon, S. M.; Tobin, S. P.; Wolfson, R. G. (1987). "Gallium Arsenide Based Ternary Compounds and Multibandgap Solar Cell Research." Proceedings of the 1987 High-Efficiency Photovoltaic Subcontractors' Review Meeting; May 19-20, 1987; Golden, Colorado. SERI/CP-211-3152. Golden, CO: Solar Energy Research Institute; pp. 33-38. Work performed by Spire Corporation, Bedford, Massachusetts.

Viner, J. M.; Lee, C.; Ohlsen, W. D.; Taylor, P. C. (1988). "Metastable Optical Absorption and Paramagnetism in Hydrogenated Amorphous Silicon." Amorphous Silicon Technology, Materials Research Society Symposium Proceedings, Volume 118, Madan, A., et al., eds. Pittsburgh, PA: Materials Research Society; pp. 309-313. Presented at the MRS Spring Meeting, Reno, Nevada, April 5-8, 1988. Work performed by Department of Physics, University of Utah, Salt Lake City, Utah.

Warmsinski, T.; Kwiecinski, M.; Giri, W.; Kazmerski, L. L.; Loferski, J. J. (1987). "Structural Properties of Some Copper Ternary Compounds." Ternary and Multinary Compounds; Proceedings of the 7th International Conference; Snowmass, Colorado, September 10-12, 1986. Pittsburgh, PA: Materials Research Society; pp. 127-131. Work

performed by Instituto Venezolano de Investigaciones Cientificas, Caracas, Venezuela; Solar Energy Research Institute, Golden, Colorado; and Division of Engineering, Brown University, Providence, Rhode Island.

Wiedeman, S.; Bennett, M. S.; Newton, J. L. (1987). "Method for the Reduction of Photothermal Deflection Spectroscopy Data Taken on Amorphous Silicon (a-Si:H)." Amorphous Silicon Semiconductors - Pure and Hydrogenated, Materials Research Society Symposia Proceedings, Volume 95, Madan, A., et al., eds. Pittsburgh, PA: Materials Research Society; pp. 145-150. Presented at the MRS Spring Meeting, Anaheim, California, April 21-24, 1987. Work performed by Solarex Corporation, Newtown, Pennsylvania.

Willing, F.; Bennett, M. S.; Newton, J. L. (1987). "Thermal Stability of Interconnected a-Si:H Solar Modules." Conference Record of the Nineteenth IEEE Photovoltaic Specialists Conference-1987; May 4-8, 1987; New Orleans, Louisiana. New York: The Institute of Electrical and Electronics Engineers, Inc.; pp. 1086-1089. Work performed by Solarex Thin Film Division, Newtown, Pennsylvania.

Winborne, G.; Xu, L.; Silver, M. (1988). "Comparison between Forward Bias Currents in P/I/N and P/C(B/P)/N Hydrogenated Amorphous Silicon Diodes." Amorphous Silicon Technology, Materials Research Society Symposium Proceedings, Volume 118, Madan, A., et al., eds. Pittsburgh, PA: Materials Research Society; pp. 501-506. Presented at the MRS Spring Meeting, Reno, Nevada, April 5-8, 1988. Work performed by Department of Physics and Astronomy, University of North Carolina at Chapel Hill, Chapel Hill, North Carolina.

Wood, R. F.; Westbrook, R. D.; Jellison, G. E., Jr. (1987). "High-Efficiency Intrinsically and Externally Passivated Laser-Processed Silicon Solar Cells." Conference Record of the Nineteenth IEEE Photovoltaic Specialists Conference-1987; May 4-8, 1987; New Orleans, Louisiana. New York: The Institute of Electrical and Electronics Engineers, Inc.; pp. 519-524. Work performed by Solid State Division, Oak Ridge National Laboratory, Oak Ridge, Tennessee.

Xu, L.; Winborne, G.; Silver, M.; Cannella, V.; McGill, J. (June 1988). "Drift Mobility under Single and Double Injection in Hydrogenated Amorphous Silicon." Philosophical Magazine B (57:6); pp. 715-720. Work performed by Department of Physics and Astronomy, University of North Carolina at Chapel Hill, Chapel Hill, North Carolina, and Ovonic Imaging Systems, Troy, Michigan.

Yang, J.; Glatfelter, T.; Ross, R.; Mohr, R.; Fournier, J. P.; Guha, S. (December 1987). "Crucial Parameters and Device Physics of Amorphous Silicon Alloy Tandem Solar Cells." Journal of Non-Crystalline Solids (97 & 98, Part II); pp. 1303-1306. Presented at the Twelfth International Conference on Amorphous and Liquid Semiconductors, Prague, Czechoslovakia, August 24-28, 1987. Work performed by Energy Conversion Devices, Troy, Michigan.

Yang, J.; Ross, R.; Mohr, R.; Fournier, J. P. (1987). "Physics of High Efficiency Multijunction Solar Cells." Amorphous Silicon Semiconductors - Pure and Hydrogenated, Materials Research Society Symposia Proceedings, Volume 95, Madan, A., et al., eds. Pittsburgh, PA: Materials Research Society; pp. 517-525. Presented at the MRS Spring Meeting, Anaheim, California, April 21-24, 1987. Work performed by Energy Conversion Devices, Inc., Troy, Michigan.

Zanio, K. R. (October 1987). CdZnTe as a Wide-Band-Gap Absorber for a Tandem Thin-Film Solar Cell, Final Subcontract Report, 1 April 1986 - 31 August 1987. SERI/STR-211-3217. 14 pp. Work performed by Ford Aerospace and Communications Corporation, Newport Beach, California. Available NTIS: Order No. DE88001114.

Zanio, K. R. (1987). "CdZnTe for a Wide Bandgap Thin Film Solar Cell." Proceedings of the Polycrystalline Thin Film Program Meeting; July 20-22, 1987; Lakewood, Colorado. SERI/CP-211-3171. pp. 157-159. Work performed by Ford Aerospace & Communications Corporation, Newport Beach, California.

### Branch Publications

Annual Report, Photovoltaic Program Branch, FY 1987. (March 1988). SERI/PR-211-3299. 309 pp. Available NTIS: Order No. DE88001155.

Proceedings of the 1987 High-Efficiency Photovoltaic Subcontractors' Review Meeting; May 19-20, 1987; Golden, Colorado. (1987). SERI/CP-211-3152. 85 pp. Available NTIS: Order No. DE88003354.

Ahrenkiel, R. K.; Dunlavy, D. J.; Benner, J.; Gale, R. P.; McClelland, R. W.; Gormley, J. V.; King, B. D. (15 August 1988). "Minority-Carrier Lifetime in GaAs Thin Films." Applied Physics Letters (53:7); pp. 598-599. Work performed by Solar Energy Research Institute, Golden, Colorado, and Kopin Corporation, Taunton, Massachusetts.

Benner, J. P.; Leboeuf, C. M. (1987). "Progress in Crystalline Materials for High Efficiency Solar Cells." Conference Record of the Nineteenth IEEE Photovoltaic Specialists Conference-1987; May 4-8, 1987; New Orleans, Louisiana. New York: The Institute of Electrical and Electronics Engineers, Inc.; pp. 53-57.

Chu, T. L.; Chu, S. S.; Ang, S. T.; Han, K. D.; Siu, Y. Z.; Zweibel, K.; Ullal, H. S. (1987). "High Efficiency Thin Film Cadmium Telluride Solar Cells." Conference Record of the Nineteenth IEEE Photovoltaic Specialists Conference-1987; May 4-8, 1987; New Orleans, Louisiana. New York: The Institute of Electrical and Electronics Engineers, Inc.; pp. 1466-1469. Work performed by Southern Methodist University, Dallas, Texas, and Solar Energy Research Institute, Golden, Colorado.

Hulstrom, R. L.; Ohi, J. M. (September 1988). "Results of the SERI Multijunction Device Efficiency Measurement Task Force." SERI Preprints for the 20th IEEE Photovoltaic Specialists Conference: Solar Electric Research Division. SERI/SP-210-3384. Golden, CO: Solar Energy Research Institute; Late News.

Langford, A. A.; Stafford, B. L.; Tsuo, Y. S. (1987). "Maintaining Window Transparency in Photo-CVD: A Simultaneous Etch/Deposition Method." Conference Record of the Nineteenth IEEE Photovoltaic Specialists Conference-1987; May 4-8, 1987; New Orleans, Louisiana. New York: The Institute of Electrical and Electronics Engineers, Inc.; pp. 573-576.

Leboeuf, C. M.; Kurtz, S. R.; Olson, J. M. (September 1988). "Hydrogen Passivation of AlGaAs and GaInP for High Efficiency Solar Cells." SERI Preprints for the 20th IEEE Photovoltaic Specialists Conference: Solar Electric Research Division. SERI/SP-210-3384. Golden, CO: Solar Energy Research Institute; Session 18.

Luft, W. (September 1988). "Characteristics of Hydrogenated Amorphous Silicon-Germanium Alloys." SERI Preprints for the 20th IEEE Photovoltaic Specialists

Conference: Solar Electric Research Division. SERI/SP-210-3384. Golden, CO: Solar Energy Research Institute; Session 12C.

Luft, W. (February 1988). Hydrogenated Amorphous Silicon-Germanium Alloys. SERI/TR-211-3317. 120 pp. Available NTIS: Order No. DE88001147.

Luft, W. (1987). "High-Rate Deposition of Hydrogenated Amorphous Silicon Films and Devices." Conference Record of the Nineteenth IEEE Photovoltaic Specialists Conference-1987; May 4-8, 1987; New Orleans, Louisiana. New York: The Institute of Electrical and Electronics Engineers, Inc.; pp. 564-568.

Luft, W.; Tsuo, S. (March 1988). "Plasma Deposition of Hydrogenated Amorphous Silicon Films." Applied Physics Communications (8:1); pp. 1-74.

Mitchell, R. L. (February 1988). New Ideas Task: Evaluation of Procurement Trends and Research Results. SERI/MR-211-3244. 130 pp.

Mitchell, R. L.; Surek, T. (May 1988). SERI's Photovoltaic Research Project: A Foundation for Tomorrow's Utility-Scale Electricity. SERI/TP-211-3354. 9 pp. Prepared for the 23rd Intersociety Energy Conversion Engineering Conference, Denver, Colorado, July 31-August 5, 1988. Available NTIS: Order No. DE88001161.

Mitchell, R. L.; Surek, T. (1988). "SERI's Photovoltaic Research Project: A Foundation for Tomorrow's Utility-Scale Electricity." Proceedings of the 23rd Intersociety Energy Conversion Engineering Conference; Denver, Colorado; July 31-August 5, 1988. New York: American Society of Mechanical Engineers; Vol. 3, pp. 107-115.

Ohi, J.; Stafford, B.; Luft, W.; Sabisky, E. (1988). "Overview of Amorphous Silicon Photovoltaic Technology." Solar 88, Proceedings of the 1988 Annual Meeting, American Solar Energy Society, Cambridge, Massachusetts, June 20-24, 1988. Boulder, CO: American Solar Energy Society, Inc.; pp. 47-53.

Sabisky, E. S. (April 1988). "Solar Electric Power: The Birth of a New Industry." Solid State Technology (31:4); pp. 149-150.

Sabisky, E. S.; Annan, R. A. (February 1988). "Government's Role in the Development of Amorphous Silicon." PV International (VI:1); pp. 14-17.

Sabisky, E. S.; Stone, J. L. (September 1988). "Odyssey of Thin-Film Amorphous Silicon Photovoltaics." SERI Preprints for the 20th IEEE Photovoltaic Specialists Conference: Solar Electric Research Division. SERI/SP-210-3384. Golden, CO: Solar Energy Research Institute; Session 1A.

Singh, R.; Radpour, F.; Anandakugan, S.; Chou, P.; Ullal, H. S.; Asher, S. E.; Kazmerski, L. L. (1987). "Rapid Isothermal Processing of Bulk and Thin Film Solar Cells." Conference Record of the Nineteenth IEEE Photovoltaic Specialists Conference-1987; May 4-8, 1987; New Orleans, Louisiana. New York: The Institute of Electrical and Electronics Engineers, Inc.; pp. 1279-1284. Work performed by School of Electrical Engineering and Computer Science, University of Oklahoma, Norman, Oklahoma, and Solar Energy Research Institute, Golden, Colorado.

Sopori, B. L. (September 1988). "Influence of Oxygen on the Performance of Silicon Solar Cells." SERI Preprints for the 20th IEEE Photovoltaic Specialists Conference:

Solar Electric Research Division. SERI/SP-210-3384. Golden, CO: Solar Energy Research Institute; Session 15.

Sopori, B. L. (September 1988). "Influence of Substrate Resistivity on the Degradation of Silicon Solar Cell Performance Due to Crystal Defects." SERI Preprints for the 20th IEEE Photovoltaic Specialists Conference: Solar Electric Research Division. SERI/SP-210-3384. Golden, CO: Solar Energy Research Institute; Session 10A.

Sopori, B. L. (16 May 1988). "Fabrication of Diode Arrays for Photovoltaic Characterization of Silicon Substrates." Applied Physics Letters (52:20); pp. 1718-1720.

Sopori, B. L. (May 1988). "Principle of a New Reflectometer for Measuring Dielectric Film Thickness on Substrates of Arbitrary Surface Characteristics." Review of Scientific Instruments (59:5); pp. 725-727.

Sopori, B. L. (1 January 1988). "Broadband Very Low Reflectance Surface." Applied Optics (27:1); pp. 25-27.

Sopori, B. L. (December 1987). "Spectral Response Measurement System for Large-Area Solar Cells." Solar Cells (22:4); pp. 287-294. Work performed by Solavolt International, Phoenix, Arizona, and Solar Energy Research Institute, Golden, Colorado.

Stafford, B. L.; Sabisky, E. S., eds. (1987). International Conference on Stability of Amorphous Silicon Alloy Materials and Devices; January 28-30, 1987; Palo Alto, California, AIP Conference Proceedings 157. New York: American Institute of Physics; 406 pp.

Stafford, B. L.; Sabisky, E. S.; Wallace, W. L.; Luft, W. (November/December 1987). "DOE/SERI Amorphous Silicon Research Project." Solar Today (1:6); pp. 7-11.

Stafford, B. L.; Sabisky, E. S.; Wallace, W. L.; Luft, W. (1987). "Status of the DOE/SERI Amorphous Silicon Research Project." Solar '87; Proceedings of the 1987 Annual Meeting, American Solar Energy Society, Inc., Solar Energy Society of Canada, Inc.; Portland, Oregon; July 12-16, 1987. Boulder, CO: American Solar Energy Society, Inc.; pp. 59-64.

Surek, T. (November 1987). SERI's Photovoltaic R&D Project: Recent Progress and Future Directions. SERI/TP-211-3272. 13 pp. Presented at a Special Meeting of the Kansai Section of the Japan Solar Energy Society and the Japan Applied Physics Society, November 10, 1987, Osaka, Japan. Available NTIS: Order No. DE88001129.

Surek, T.; Jones, G. J.; Annan, R. H. (September 1988). Overview of the U.S. Experience with Photovoltaics in Developing Countries. SERI/TR-211-3401. 13 pp. Presented at the International Workshop on Renewable Energy in Developing Countries, Kiryat Anavim, Israel, June 12-17, 1988. Available NTIS.

Ullal, H. S. (May 1988). Electronic Structure of Electrodeposited Thin Film CdTe Solar Cells. SERI/TP-211-3361. 15 pp. Available NTIS: Order No. DE88001170.

Ullal, H. S.; Zweibel, K.; Sabisky, E. S.; Surek, T. (August 1988). Solar Photovoltaic Technology: The Thin Film Option. SERI/TP-211-3390. 10 pp. Presented at the AIChE Summer National Meeting, Denver, Colorado, August 21-24, 1988.

Wallace, W. L.; Ohi, J.; Luft, W.; Stafford, B.; Sabisky, E. (September 1988). "Advances in Material/Cell/Submodule Research in the DOE/SERI Amorphous Silicon Research Project." SERI Preprints for the 20th IEEE Photovoltaic Specialists Conference: Solar Electric Research Division. SERI/SP-210-3384. Golden, CO: Solar Energy Research Institute; Session 18C.

Wallace, W. L.; Sabisky, E. S. (1987). "Progress in Stable, High-Efficiency Amorphous Silicon Cells and Submodules." Proceedings of the 22nd Intersociety Energy Conversion Engineering Conference; Philadelphia, Pennsylvania; August 10-14, 1987. New York: American Institute of Aeronautics and Astronautics; Volume 1, pp. 82-87.

Wallace, W. L.; Sabisky, E. S.; Stafford, B. L.; Luft, W. (1987). "Successes and Plans of the SERI/DOE Amorphous Silicon Research Project." Conference Record of the Nineteenth IEEE Photovoltaic Specialists Conference-1987; May 4-8, 1987; New Orleans, Louisiana. New York: The Institute of Electrical and Electronics Engineers, Inc.; pp. 593-598.

Zweibel, K. (May 1988). "Second-Generation Solar Cells." The World and I. pp. 158-166.

Zweibel, K.; Ullal, H. S.; Mitchell, R. L. (September 1988). "DOE/SERI Polycrystalline Thin Film Subcontract Program." SERI Preprints for the 20th IEEE Photovoltaic Specialists Conference: Solar Electric Research Division. SERI/SP-210-3384. Golden, CO: Solar Energy Research Institute; Session 6.

Zweibel, K.; Ullal, H. S.; Mitchell, R. L. (1987). "DOE/SERI Polycrystalline Thin-Film Solar Cell Program." Conference Record of the Nineteenth IEEE Photovoltaic Specialists Conference-1987; May 4-8, 1987; New Orleans, Louisiana. New York: The Institute of Electrical and Electronics Engineers, Inc.; pp. 1322-1328.